Hashemite Kingdom of Jordan

Jordan Journal of Biological Sciences

An International Peer-Reviewed Scientific Journal

Financed by the Scientific Research and Innovation Support Fund

This title is indexed in Scopus

http://jjbs.hu.edu.jo/

المجلة الأردنية للعلوم الحياتية
Jordan Journal of Biological Sciences (JJBS)
http://jjbs.hu.edu.jo

Jordan Journal of Biological Sciences (JJBS) (ISSN: 1995–6673 (Print); 2307-7166 (Online)): An International Peer- Reviewed Open Access Research Journal financed by the Scientific Research and Innovation Support Fund, Ministry of Higher Education and Scientific Research, Jordan and published quarterly by the Deanship of Scientific Research , The Hashemite University, Jordan.

Submission Address
Professor Atoum, Manar F
The Hashemite Universit y
P.O. Box 330127, Zarqa, 13115, Jordan
Phone: +962-5-3903333 ext.4147
E-Mail: jjbs@hu.edu.jo

المجلة الاردنية للعلوم الحياتية
Jordan Journal of Biological Sciences (JJBS)
http://jjbs.hu.edu.jo

International Advisory Board (Arranged alphabetically)

Instructions to Authors

Scopes

Study areas include cell biology, genomics, microbiology, immunology, molecular biology, biochemistry, embryology, immunogenetics, cell and tissue culture, molecular ecology, genetic engineering and biological engineering, bioremediation and biodegradation, bioinformatics, biotechnology regulations, gene therapy, organismal biology, microbial and environmental biotechnology, marine sciences. The JJBS welcomes the submission of manuscript that meets the general criteria of significance and academic excellence. All articles published in JJBS are peer-reviewed. Papers will be published approximately one to two months after acceptance.

Type of Papers

The journal publishes high-quality original scientific papers, short communications, correspondence and case studies. Review articles are usually by invitation only. However, Review articles of current interest and high standard will be considered.

Submission of Manuscript

Manuscript, or the essence of their content, must be previously unpublished and should not be under simultaneous consideration by another journal. The authors should also declare if any similar work has been submitted to or published by another journal. They should also declare that it has not been submitted/ published elsewhere in the same form, in English or in any other language, without the written consent of the Publisher. The authors should also declare that the paper is the original work of the author(s) and not copied (in whole or in part) from any other work. All papers will be automatically checked for duplicate publication and plagiarism. If detected, appropriate action will be taken in accordance with International Ethical Guideline. By virtue of the submitted manuscript, the corresponding author acknowledges that all the co-authors have seen and approved the final version of the manuscript. The corresponding author should provide all co-authors with information regarding the manuscript, and obtain their approval before submitting any revisions. Electronic submission of manuscripts is strongly recommended, provided that the text, tables and figures are included in a single Microsoft Word file. Submit manuscript as e-mail attachment to the Editorial Office at: JJBS@hu.edu.jo. After submission, a manuscript number will be communicated to the corresponding author within 48 hours.

Peer-review Process

It is requested to submit, with the manuscript, the names, addresses and e-mail addresses of at least 4 potential reviewers. It is the sole right of the editor to decide whether or not the suggested reviewers to be used. The reviewers' comments will be sent to authors within 6-8 weeks after submission.
Manuscripts and figures for review will not be returned to authors whether the editorial decision is to accept, revise, or reject. All Case Reports and Short Communication must include at least one table and/ or one figure.

Preparation of Manuscript

The manuscript should be written in English with simple lay out. The text should be prepared in single column format. Bold face, italics, subscripts, superscripts etc. can be used. Pages should be numbered consecutively, beginning with the title page and continuing through the last page of typewritten material.

The text can be divided into numbered sections with brief headings. Starting from introduction with section 1. Subsections should be numbered (for example 2.1 (then 2.1.1, 2.1.2, 2.2, etc.), up to three levels. Manuscripts in general should be organized in the following manner:

Title Page

The title page should contain a brief title, correct first name, middle initial and family name of each author and name and address of the department(s) and institution(s) from where the research was carried out for each author. The title should be without any abbreviations and it should enlighten the contents of the paper. All affiliations should be provided with a lower-case superscript number just after the author's name and in front of the appropriate address.
The name of the corresponding author should be indicated along with telephone and fax numbers (with country and area code) along with full postal address and e-mail address.

Abstract

The abstract should be concise and informative. It should not exceed **350 words** in length for full manuscript and Review article and **150 words** in case of Case Report and/ or Short Communication. It should briefly describe the purpose of the work, techniques and methods used, major findings with important data and conclusions. No references should be cited in this part. Generally non-standard abbreviations should not be used, if necessary they should be clearly defined in the abstract, at first use.

Keywords

Immediately after the abstract, **about 4-8 keywords** should be given. Use of abbreviations should be avoided, only standard abbreviations, well known in the established area may be used, if appropriate. These keywords will be used for indexing.

Abbreviations

Non-standard abbreviations should be listed and full form of each abbreviation should be given in parentheses at first use in the text.

Introduction

Provide a factual background, clearly defined problem, proposed solution, a brief literature survey and the scope and justification of the work done.

Materials and Methods

Give adequate information to allow the experiment to be reproduced. Already published methods should be mentioned with references. Significant modifications of published methods and new methods should be described in detail. Capitalize trade names and include the manufacturer's name and address. Subheading should be used.

Results

Results should be clearly described in a concise manner. Results for different parameters should be described under subheadings or in separate paragraph. Results should be explained, but largely without referring to the literature. Table or figure numbers should be mentioned in parentheses for better understanding.

Discussion

The discussion should not repeat the results, but provide detailed interpretation of data. This should interpret the significance of the findings of the work. Citations should be given in support of the findings. The results and discussion part can also be described as separate, if appropriate. The Results and Discussion sections can include subheadings, and when appropriate, both sections can be combined

Conclusions

This should briefly state the major findings of the study.

Acknowledgment

A brief acknowledgment section may be given after the conclusion section just before the references. The acknowledgment of people who provided assistance in manuscript preparation, funding for research, etc. should be listed in this section.

Tables and Figures

Tables and figures should be presented as per their appearance in the text. It is suggested that the discussion about the tables and figures should appear in the text before the appearance of the respective tables and figures. No tables or figures should be given without discussion or reference inside the text.

Tables should be explanatory enough to be understandable without any text reference. Double spacing should be maintained throughout the table, including table headings and footnotes. Table headings should be placed above the table. Footnotes should be placed below the table with superscript lowercase letters. Each table should be on a separate page, numbered consecutively in Arabic numerals.

Each figure should have a caption. The caption should be concise and typed separately, not on the figure area. Figures should be self-explanatory. Information presented in the figure should not be repeated in the table. All symbols and abbreviations used in the illustrations should be defined clearly. Figure legends should be given below the figures.

References

References should be listed alphabetically at the end of the manuscript. Every reference referred in the text must be also present in the reference list and vice versa. In the text, a reference identified by means of an author's name should be followed by the year of publication in parentheses (e.g.(Brown,2009)). For two authors, both authors' names followed by the year of publication (e.g.(Nelson and Brown, 2007)). When there are more than two authors, only the first author's name followed by "*et al*." and the year of publication (e.g. (Abu-Elteen *et al*., 2010)). When two or more works of an author has been published during the same year, the reference should be identified by the letters "a", "b", "c", etc., placed after the year of publication. This should be followed both in the text and reference list. e.g., Hilly, (2002a, 2002b); Hilly, and Nelson, (2004). Articles in preparation or submitted for publication, unpublished observations, personal communications, etc. should not be included in the reference list but should only be mentioned in the article text (e.g., Shtyawy,A., University of Jordan, personal communication). Journal titles should be abbreviated according to the system adopted in Biological Abstract and Index Medicus, if not included in Biological Abstract or Index Medicus journal title should be given in full. The author is responsible for the sccuracy and completeness of the references and for their correct textual citation. Failure to do so may result in the paper being withdraw from the evaluation process. Example of correct reference form is given as follows:-

Reference to a journal publication:

Bloch BK. 2002. Econazole nitrate in the treatment of *Candida vaginitis*. *S Afr Med J.* , **58**:314-323.

Ogunseitan OA and Ndoye IL. 2006. Protein method for investigating mercuric reductase gene expression in aquatic environments. *Appl Environ Microbiol*., **64**: 695-702.

Hilly MO, Adams MN and Nelson SC. 2009. Potential fly-ash utilization in agriculture. *Progress in Natural Sci.*, **19**: 1173-1186.

Reference to a book:

Brown WY and White SR.1985. **The Elements of Style**, third ed. MacMillan, New York.

Reference to a chapter in an edited book:

Mettam GR and Adams LB. 2010. How to prepare an electronic version of your article. In: Jones BS and Smith RZ (Eds.), **Introduction to the Electronic Age**. Kluwer Academic Publishers, Netherlands, pp. 281–304.

Conferences and Meetings:

Embabi NS. 1990. Environmental aspects of distribution of mangrove in the United Arab Emirates. Proceedings of the First ASWAS Conference. University of the United Arab Emirates. Al-Ain, United Arab Emirates.

Theses and Dissertations:

El-Labadi SN. 2002. Intestinal digenetic trematodes of some marine fishes from the Gulf of Aqaba. MSc dissertation, The Hashemite University, Zarqa, Jordan.

Nomenclature and Units

Internationally accepted rules and the international system of units (SI) should be used. If other units are mentioned, please give their equivalent in SI.

For biological nomenclature, the conventions of the *International Code of Botanical Nomenclature, the International Code of Nomenclature of Bacteria,* and the *International Code of Zoological Nomenclature* should be followed.
Scientific names of all biological creatures (crops, plants, insects, birds, mammals, etc.) should be mentioned in parentheses at first use of their English term.

Chemical nomenclature, as laid down in the *International Union of Pure and Applied Chemistry* and the official recommendations of the *IUPAC-IUB Combined Commission on Biochemical Nomenclature* should be followed. All biocides and other organic compounds must be identified by their Geneva names when first used in the text. Active ingredients of all formulations should be likewise identified.

Math formulae

All equations referred to in the text should be numbered serially at the right-hand side in parentheses. Meaning of all symbols should be given immediately after the equation at first use. Instead of root signs fractional powers should be used. Subscripts and superscripts should be presented clearly. Variables should be presented in italics. Greek letters and non-Roman symbols should be described in the margin at their first use.

To avoid any misunderstanding zero (0) and the letter O, and one (1) and the letter l should be clearly differentiated. For simple fractions use of the solidus (/) instead of a horizontal line is recommended. Levels of statistical significance such as: $^{*}P < 0.05$, $^{**}P < 0.01$ and $^{***}P < 0.001$ do not require any further explanation.

Copyright

Submission of a manuscript clearly indicates that: the study has not been published before or is not under consideration for publication elsewhere (except as an abstract or as part of a published lecture or academic thesis); its publication is permitted by all authors and after accepted for publication it will not be submitted for publication anywhere else, in English or in any other language, without the written approval of the copyright-holder. The journal may consider manuscripts that are translations of articles originally published in another language. In this case, the consent of the journal in which the article was originally published must be obtained and the fact that the article has already been published must be made clear on submission and stated in the abstract. It is compulsory for the authors to ensure that no material submitted as part of a manuscript infringes existing copyrights, or the rights of a third party.

Ethical Consent

All manuscripts reporting the results of experimental investigation involving human subjects should include a statement confirming that each subject or subject's guardian obtains an informed consent, after the approval of the experimental protocol by a local human ethics committee or IRB. When reporting experiments on animals, authors should indicate whether the institutional and national guide for the care and use of laboratory animals was followed.

Plagiarism

The JJBS hold no responsibility for plagiarism. If a published paper is found later to be extensively plagiarized and is found to be a duplicate or redundant publication, a note of retraction will be published, and copies of the correspondence will be sent to the authors' head of institute.

Galley Proofs

The Editorial Office will send proofs of the manuscript to the corresponding author as an e-mail attachment for final proof reading and it will be the responsibility of the corresponding author to return the galley proof materials appropriately corrected within the stipulated time. Authors will be asked to check any typographical or minor clerical errors in the manuscript at this stage. No other major alteration in the manuscript is allowed. After publication authors can freely access the full text of the article as well as can download and print the PDF file.

Publication Charges

There are no page charges for publication in Jordan Journal of Biological Sciences, except for color illustrations,

Reprints

Ten (10) reprints are provided to corresponding author free of charge within two weeks after the printed journal date. For orders of more reprints, a reprint order form and prices will be sent with article proofs, which should be returned directly to the Editor for processing.

Disclaimer

Articles, communication, or editorials published by JJBS represent the sole opinions of the authors. The publisher shoulders no responsibility or liability what so ever for the use or misuse of the information published by JJBS.

Indexing

JJBS is indexed and abstracted by:

DOAJ (Directory of Open Access Journals)	CABI
Google Scholar	EBSCO
Journal Seek	CAS (Chemical Abstract Service)
HINARI	ETH- Citations
Index Copernicus	Open J-Gat
NDL Japanese Periodicals Index	SCImago
SCIRUS	Clarivate Analytics (Zoological Abstract)
OAJSE	Scopus
ISC (Islamic World Science Citation Center)	AGORA (United Nation's FAO database)
Directory of Research Journal Indexing (DRJI)	SHERPA/RoMEO (UK)
Ulrich's	

المجلة الأردنية للعلوم الحياتية
Jordan Journal of Biological Sciences (JJBS)
ISSN 1995- 6673 (Print), 2307- 7166 (Online)
http://jjbs.hu.edu.jo

The Hashemite University

Deanship of Scientific Research

TRANSFER OF COPYRIGHT AGREEMENT

Journal publishers and authors share a common interest in the protection of copyright: authors principally because they want their creative works to be protected from plagiarism and other unlawful uses, publishers because they need to protect their work and investment in the production, marketing and distribution of the published version of the article. In order to do so effectively, publishers request a formal written transfer of copyright from the author(s) for each article published. Publishers and authors are also concerned that the integrity of the official record of publication of an article (once refereed and published) be maintained, and in order to protect that reference value and validation process, we ask that authors recognize that distribution (including through the Internet/WWW or other on-line means) of the authoritative version of the article as published is best administered by the Publisher.

To avoid any delay in the publication of your article, please read the terms of this agreement, sign in the space provided and return the complete form to us at the address below as quickly as possible.

Article entitled:----------

Corresponding author: ----------

To be published in the journal: Jordan Journal of Biological Sciences (JJBS)

I hereby assign to the Hashemite University the copyright in the manuscript identified above and any supplemental tables, illustrations or other information submitted therewith (the "article") in all forms and media (whether now known or hereafter developed), throughout the world, in all languages, for the full term of copyright and all extensions and renewals thereof, effective when and if the article is accepted for publication. This transfer includes the right to adapt the presentation of the article for use in conjunction with computer systems and programs, including reproduction or publication in machine-readable form and incorporation in electronic retrieval systems.
Authors retain or are hereby granted (without the need to obtain further permission) rights to use the article for traditional scholarship communications, for teaching, and for distribution within their institution.

☐ **I am the sole author of the manuscript**

☐ **I am signing on behalf of all co-authors of the manuscript**

☐ **The article is a 'work made for hire' and I am signing as an authorized representative of the employing company/institution**

Please mark one or more of the above boxes (as appropriate) and then sign and date the document in black ink.

Signed:_____ **Name printed:** _____
Title and Company (if employer representative) : _____
Date: _____

Data Protection: By submitting this form you are consenting that the personal information provided herein may be used by the Hashemite University and its affiliated institutions worldwide to contact you concerning the publishing of your article.

Please return the completed and signed original of this form by mail or fax, or a scanned copy of the signed original by e-mail, retaining a copy for your files, to:

Hashemite University
Jordan Journal of Biological Sciences
Zarqa 13115 Jordan
Fax: +962 5 3903338
Email: jjbs@hu.edu.jo

EDITORIAL PREFACE

Jordan Journal of Biological Sciences (JJBS) is a refereed, quarterly international journal financed by the Scientific Research and Innovation Support Fund, Ministry of Higher Education and Scientific Research in cooperation with the Hashemite University, Jordan. JJBS celebrated its 12th commencement this past January, 2020. JJBS was founded in 2008 to create a peer-reviewed journal that publishes high-quality research articles, reviews and short communications on novel and innovative aspects of a wide variety of biological sciences such as cell biology, developmental biology, structural biology, microbiology, entomology, molecular biology, biochemistry, medical biotechnology, biodiversity, ecology, marine biology, plant and animal biology, plant and animal physiology, genomics and bioinformatics.

We have watched the growth and success of JJBS over the years. JJBS has published 11 volumes, 45 issues and 479 articles. JJBS has been indexed by SCOPUS, CABI's Full-Text Repository, EBSCO, Clarivate Analytics- Zoological Record and recently has been included in the UGC India approved journals. JJBS Cite Score has improved from 0.18 in 2015 to 0.7 in 2019 (Last updated on 1 March, 2021) and with Scimago Institution Ranking (SJR) 0.18 (Q3) in 2019.

A group of highly valuable scholars have agreed to serve on the editorial board and this places JJBS in a position of most authoritative on biological sciences. I am honored to have six eminent associate editors from various countries. I am also delighted with our group of international advisory board members coming from 15 countries worldwide for their continuous support of JJBS. With our editorial board's cumulative experience in various fields of biological sciences, this journal brings a substantial representation of biological sciences in different disciplines. Without the service and dedication of our editorial; associate editorial and international advisory board members, JJBS would have never existed.

In the coming year, we hope that JJBS will be indexed in Clarivate Analytics and MEDLINE (the U.S. National Library of Medicine database) and others. As you read throughout this volume of JJBS, I would like to remind you that the success of our journal depends on the number of quality articles submitted for review. Accordingly, I would like to request your participation and colleagues by submitting quality manuscripts for review. One of the great benefits we can provide to our prospective authors, regardless of acceptance of their manuscripts or not, is the feedback of our review process. JJBS provides authors with high quality, helpful reviews to improve their manuscripts.

Finally, JJBS would not have succeeded without the collaboration of authors and referees. Their work is greatly appreciated. Furthermore, my thanks are also extended to The Hashemite University and the Scientific Research and Innovation Support Fund, Ministry of Higher Education and Scientific Research for their continuous financial and administrative support to JJBS.

Professor Atoum, Manar F.
March, 2021

JJBS

Volume 14, Number 3, September 2021
ISSN 1995-6673

Jordan Journal of Biological Sciences

CONTENTS

Original Articles

JJBS

Volume 14, Number 3, September 2021
ISSN 1995-6673
Pages 383- 388

Jordan Journal of Biological Sciences

Molecular Characteristic of *Fusarium oxysporum* from Different Altitudes in East Java, Indonesia

Henik Sukorini[1,*], Erfan Dani Septia[1], Lili Zalizar[2] and Netnapis Khewkhom[3]

[1]*Department of Agrotechnology, Faculty of Agriculture and Animal Science, University of Muhammadiyah Malang, Jl. Raya Tlogomas no 246 Malang 65145, East Java, Indonesia;*[2]*Department of Animal Science, University of Muhammadiyah Malang;* [3]*Department of Plant Pathology, Faculty of Agriculture, Kasetsart University, 50 Thanon Ngamwongwan, Lat Yao, Chatuchak, Bangkok 10900, Thailand*

Received: Feb 20, 2021; Revised: May 28, 2021; Accepted May 29, 2021

Abstract

Tomato (*Solanum lycopersicum* L.) is one of the most economically important vegetable crops in Indonesia. Tomato diseases caused by fungi are transmitted by seed or transplants. Fusarium wilt disease is a cosmopolitan species caused by *Fusarium oxysporum* Schlecht. Emend. Snyder & Hansen. Among this special attention of disease caused by *F. oxysporum* has been given to stem and root rotting. Six selected *Fusarium* samples from previous research were prepared using a single spore method and cultured in the PDB medium, The Research carried out in the Agrotechnology Laboratory of the University of Muhammadiyah Malang. DNA extraction and PCR used ITS 1 and ITS 4, electrophoresis, and data analysis was achieved at the Genetic and Molecular Laboratory of the Biology Department of the Faculty of Science and Technology, Maulana Malik Ibrahim Malang Islamic State University. Isolate code 3313439 originating from Karangploso soil (515 m a.s.l) and code 3313428 derived from the soil of Blitar (156 m a.s.l.) showed species similarity to *F. oxysporum* f. sp *lycopersici* strain CBS249.52. Then for sample 3313426, the roots of Pujon have similarities with the strain of *F. oxysporum* S58. Besides, samples of 3313 422 Blitar roots, 3313 424 Karangploso roots, and 3313 432 Pujon soils (956 m a.s.l.) showed proximity to species *F. oxysporum* f.sp. p*isi* HG423346. The samples were in one clade with the nucleotide base sequences of two other *F. oxysporum* species recorded in the NCBI Genbank database. Differences in species will likely affect the pathogenicity, growth rate, spore production, and disease control management.

Keywords: Fungi, *Fusarium* wilt, Molecular Identification, Plant Pathology, Tomato

1. Introduction

Globally, one of the most economically important crops is the Tomato (*Solanum lycopersicum* L.) (Aydi-Ben-Abdallah et al., 2020). Several economically essential tomato diseases caused by fungi are transmitted by seed or transplants. *Fusarium oxysporum* f. splycopersici Schlecht. Snyder & Hansen (FOL) is the causal agent of fusarium wilt disease on tomatoes. It is a cosmopolitan species that can be found in all types of soil. Ignjatov *et al.* (2012) reported healthy plants could become infected by *F. oxysporum* if the soil in which they are growing is infested with the pathogen. FOL spread through short distances, mainly through irrigation water and contaminated farm equipment, and it can spread long distances through infected transplants, soils, etc. (Agrios, 2005). Special attention to disease has been given to the rotting of stems and roots caused by *Fusarium* sp. Based on the symptoms of the disease caused by *Fusarium* sp. indistinguishable. Control of this disease is ~~also~~ still problematic. The use of chemicals such as methyl bromide is quite effective for disease management but impacts humans and the environment. The use of resistant varieties has also been carried out. This method is environmentally friendly but requires a lot of money. The ease with which pathogens form new strains and break the resistance of varieties causes this disease to be difficult to control (Xie *et al.*, 2015).

Biju *et al*. (2017) reported three known FOL races (Races 1, 2 and 3) pathogens of tomato cultivars are distinguishable by their principle resistance genes. Races 1 and 2 are grown through the tomato-growing regions globally. Race 3 has been reported in countries such as California, Australia, Southwestern Georgia, and Mexico. Most commercial tomato varieties grown through the world are resistant to race 1 and 2, and a few are resistant to race 3. Certainly, once a region becomes contaminated with FOL, the fungus usually remains indefinitely (Animashaun *et al.*, 2017; Prihatna *et al*., 2018). Pathogenic isolates from three different heights, namely low, medium, high altitude, have different colony colors, sporulation power, and growth rate. The ability to survive at high temperatures and resistance to Mancozeb 64 % + Metalaxyl 8 % and Benomil 50 % fungicide also varies even though the growth inhibition value is below 60 % (Henik *et al*., 2021). This, of course, will affect the success of controlling this pathogen. Therefore, molecular identification is required.

Identification can be made in two ways consisting of morphological and molecular character identification. Molecular character identification is based on the similarity of DNA (Alsohaili and Bani-Hasan, 2018)

* Corresponding author e-mail: hsukorini@yahoo.com.

The genus *Fusarium* has often served as a testing ground for new speciation concepts in fungi (Hsuan *et al.* 2011). The use of molecular approaches to differentiate species has been tried with many strains usually considered problematic, i.e. not fitting within a given species but not distinguishable from it. Studies of the grouping patterns resulting from studies with amplified fragment length polymorphisms (AFLPs) and phylogenetic lineages based on multiple-gene genealogies provide new means of evaluating relatedness.

This research is a follow-up study from previous studies, namely the control of *Fusarium* sp wilt in tomato plants and *Alternaria* sp in potato plants. Henik *et al.* (2021) reported earlier studies, *F. oxysporum* from tomatoes originating from different altitude and parts of plants with spore shape and size characters. The same, but has other growth characters, so too has different pathogenicity and virulence. Therefore, it is necessary to reveal more about the differences in isolates from regions with different altitudes with molecular character identification.

2. Method

2.1. Single spore isolation technique for F. oxysporum isolates

Soil and tomato roots samples were taken from tomato growing areas in Blitar (156 m a.s.l.), Karangploso (515 m a.s.l.), and Pujon (956 m a.s.l.). After preparation, isolates were grown on PDA media (Merck). Then the isolates were made suspended and transferred to the water agar media. A suspension of conidia either from a sporodochium or aerial mycelium was prepared in 5 mL sterile water in a sterile vial. The conidial suspension was scraped by an L-shape inoculating needle several times and streaked across the water agar plate. The plate was incubated for 12 h to 24 h at 25 °C; after that, it was examined under a dissecting microscope (Olympus CX43). A lot of germinating conidia appeared on the inoculation, and by following the streaked lines using the low power of the microscope, single germinating conidia could be observed. Finally, identification of *F. oxysporum* cultures was accomplished (Niemeyer and De Andrade, 2016).

Soil and tomato root samples were taken from tomato growing areas in Blitar (156 masl), Karangploso (515 m a.s.l.), and Pujon (956 m.a.s.l.). Isolation was carried out using the method (El-shafey, 2020) with slight modifications in the medium. Isolation was carried out by growing the sample on PDA (Merck) media until pure isolates were obtained. This will be used for further investigations. 0.1uL of *Fusarium* isolates were then grown in water agar media for 24 h, then a single spore from *Fusarium* was cut and grown on new PDA media in Petri dish for 7 d at 25 ^{o}C. The growing isolates were then used for DNA testing and stored in the refrigerator for collection and other purposes. Isolates aged 7 d were then harvested for DNA testing.

2.2. Isolate preparation

Isolates grown on PDA media (Merck) were then developed into PDB media (potato dextrose broth - Merck) and incubated in water bath shakers for 7 d to 9 d until the mycelium grew. The mycelium can be harvested, put into an Eppendorf tube, then added 500 mL Mili Q water and be ready for extraction with centrifuged at 10 000 rpm (1 rpm=1/60 Hz) for 10 min (Hussain *et al.*, 2012).

2.3. Fungi DNA extraction

PCR Preparation Based on isolate preparation, the supernatant was taken with a micropipette and crushed with pastel until it became colloidal. Colloids were added with Reagent 1 as much as 300 mL, then homogenized using tips from the micropipette. Added 3 µL of RNAse, homogenized using tips, and incubated for 30 min at 37 °C in a water bath, then added Reagent 2 for 200 µL, strong shaking for ± 10 min set for 10 min at room temperature, put in the freezer for 20 min. After freezing, added 250 µ of chloroform and 250 µ of phenol. It was homogenized for ± 4 min, centrifuged (DLAB High-Speed Refrigerated Micro-Centrifuge D3024R) at 10 000 rpm for 10 min at the temperature of 14 °C. The supernatant was taken, plus isopropanol, in half of the sample volume (250 µL), then reversed slowly to homogeneous. Centrifuged at 10 000 rpm for 10 min, then the supernatant was removed. Added 50 µL ethanol 99 %, then centrifuged with a speed of 10 000 rpm for 10 min; the supernatant was disposed of by pouring. It was dried up by turning the microtube over the tissue by opening the lid for ± 30 min. Added Nuclease free water as much as 100 µL(lots) and 50µL (a little).

2.4. Polymerase Chain Reaction

The DNA obtained was then multiplied by a polymerase chain reaction. The primers used for this PCR process were ITS 1 and ITS ~~primers~~ 4. The primer ITS1 (5'-TCT GTA GGT GAA CCT GCG G3') and ITS4 (5'-TCC TCC GCT TAT TGA TAT GC-3'). The PCR solution mixture was 1 uL to 2 uL primer, 5 uL DNA samples, and 6 uL PCR mix (Half reaction) (Singha *et al*., 2017). The PCR condition was run in 5 min 94 ^{o}C for pre-denaturation, then followed by 35 cycles where each cycle consisted of 30s, 94 ^{o}C for denaturation, 30s, 50^{o}C for annealing, and 1 min temperature 72 ^{o}C centigrade for extension; then ended with 1 min cycle with a temperature of 72 ^{o}C. The particular annealing temperature was also tested at 48 ^{o}C as the annealing temperature recommended by primer pairs.

2.5. Agarose Preparation

mixed 1 % agarose (0.3 g) with 30 mL TBE 1× (from Tris base and boric acid 10×) in an Erlenmeyer ~~tube~~. Agarose was dissolved by heating it to the microwave for ± 2 min until the solution was dissolved entirely then add ETBR 2 µL and pour it into a gel mold into a gel mold that has been fitted with a comb The gel was allowed to hard for ± 30 min.

2.6. Electrophoresis preparation

After the comb was removed from the mold, then the gel was transferred into the electrophoresis tank. The 3 µL DNA solution was mixed with loading dye 1µL and 2µL on parafilm paper, then the mixture and marker were put into the agarose gel well. Adjust the position of the agarose gel in electrophoresis. After combining DNA loading, dye and water were inserted into the well. The electrophoresis device has adjusted the electrophoresis with 100 V and 25 min later running. Electrophoresis was complete. The agarose gel lifted in the agarose gel was brought into the doc gel illuminated with a UV-

Transilluminator and gel photographed with the gel documentation to visualize the results.

2.7. Measurement of concentration and purity of extracted DNA

The concentration and purity of DNA extracted using NanoDrop with two different wavelengths, wavelengths 260 and 280. The purity of DNA can be determined by dividing the results of the NanoDrop measurements of both wavelengths (Srinivas *et al.*, 2019), while the DNA concentration was obtained directly from the NanoDrop.

2.8. Analyzing the results of reading Gel Doc

Analyzing the results of reading Gel Doc was done qualitatively by observing and determining the band's size that comes out with PCR-electrophoresis results compared to the marker. This information was then compared with the literature to ascertain whether the target DNA location obtained was precisely the location of ITS (Adame-García, 2015).

2.9. Sequencing the results of amplification of DNA samples

The results of the DNA sample amplification obtained were then sent to PT. Indonesian Science Genetics for sequencing. The 1st Base company carried out the sequencing process, Axil Scientific Pte Ltd., Based in Singapore. The material used for DNA sequencing is BigDye® Terminator v3.1 Cycle Kit Chemistry.

2.10. Data Analysis of Sequencing Results

Sequencing results based on ITS 1 or ITS 4 primers for each isolate were aligned and then edited using Mega v.10 software by referring to the chromatogram and being converted to fasta. The data in the form of fasta were further analyzed by looking for similarities using the basic local alignment search tool (BLAST) program from the GeneBank Gen database owned by the National Center of Biotechnology Information / NCBI.

BLAST was used to determine which species has the closest homology. Ambiguous areas in parallel sequences were omitted from the analysis. The gap was considered missing data (Pinaria, *et al.*, 2015). The phylogeny tree's evolutionary history was inferred based on the Neighbor-Joining method (Cañizares *et al.*, 2015). The evolutionary distance was calculated using the Maximum Composite Likelihood method (Chala, *et al*., 2019). And it was in units of base substitution per site. Evolution analysis was carried out with the MEGA X version application (Nirmaladevi, *et al.* 2016). Preparation of the genetic distance matrix *F. oxysporum* Karangploso sample with several species genes recorded in GenBank was also carried out using the MEGA X version application.

3. Result and Discussion

The isolates used in this research had the highest sporulation and growth rates from previous studies, namely those from roots and soil from three high, medium. and low land altitudes. (Henik *et al.*, 2021). Morphologically, Fusarium species are identified by several morphological characteristics. One of the notable features is the development of various shapes and sizes of macro and microconidia. Other structures that they form are called chlamydospores spores (El Kichaoui *et al*., 2017; Raghu *et al*. 2016), and also identified based on the growth rate and their pigmentations on agar media (Leslie *et al*., 2008).

Moreover, morphological identification can be quite difficult among the Fusarium species (Lievens *et al*., 2008). The sequence information using ITS regions has been immensely used in the phylogeny and taxonomy of Fusarium species (Menezes *et al*., 2010) as ITS regions have successfully identified them (Chen *et al*., 2004). ITS is differentiated into ITS1 and ITS2 (genes 18S to 5.8S and 5.8S to 28S, respectively) (Hillis and Dixon, 1991). There are more than 172 000 fungal ITS sequences present in Genbank. The result showed the thickness of DNA bands that varied from those showing thin bands to thick bands (Figure 1). The thickness of the tape is related to the concentration of DNA isolation results. The thin ribbon shows that the DNA concentration produced from the extraction process is low, while the thick band indicates the low concentration of DNA from extraction (Menu, *et al.*, 2018).

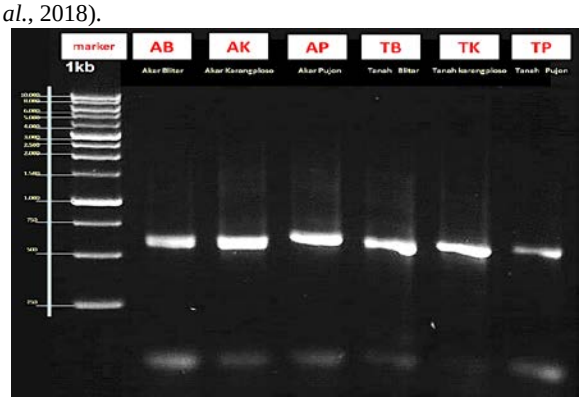

Figure 1. The amplification of Fusarium DNA samples using primary pairs ITS 1 and ITS 4 with an annealing temperature of 50 oC at three different altitudes (156 m a.s.l, 515 m a.s.l. and 956 m a.s.l.). AB= Blitar root, AK= Karangploso root, AP= Pujon root, TB= Blitar soil, TK= Karangploso soil, TP= Pujon soil .

Electrophoresis results show a band with a smear (Figure 1.). Smear is the remainder of the solutions that are still carried during the isolation process and can also be degraded DNA during the isolation process (González-Mendoza, *et al*., 2015). The process of DNA degradation at the stage of isolation can be caused by mixing the solution using a vortex, which aims to help cell lysis so that some DNA comes out and is fragmented and causes smears when electrophoresed (Campbell *et al*., 2010).

The results of *Fusarium* sample DNA amplification with a temperature of 48 ^{o}C annealing in the Polymerase Chain Reaction (PCR) process showed no amplification in each sample DNA testedThe thin bands below show a size that is much smaller than 250 bp. Allegedly, these bands are a visual form of primers' formation during polymerized Chain Reaction (PCR). Primers-dimers are not the result of the desired target DNA amplification. It can be seen from the size of the resulting tape that it is between 500 bp and 750 bp, but there are still smears.

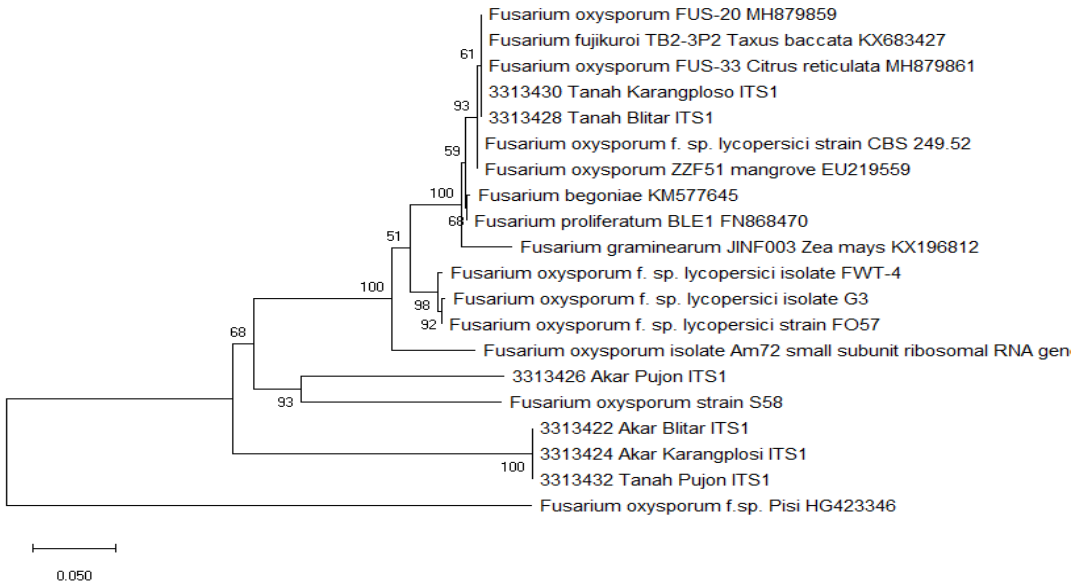

Figure 2. Phylogeny tree of *Fusarium oxysporum* at three different altitudes.

Based on the results of the evolution of tree evolution (phylogeny tree) and the similarity of nucleotide base sequences originating from the Internal Spacer (ITS) region, *F. oxysporum* from six samples consisting of soil samples and roots of tomato plants at three different altitudes (156 m a.s.l., 515 m a.s.l. and 956 m a.s.l.), it was found that code 3313439 derived from Karangploso soil and code 3313428 originating from Blitar soil showed similarity of species with *Fusarium oxysporum* f.sp. *lycopersici* strain 249.52. A sample of 3313426 pujon roots has similarities with *Fusarium oxysporum* strain S58. Besides, samples of 3313422 Blitar roots, 3313424 roots of Karangploso, and 3313432 Pujon soil showed closeness to the species *Fusarium oxysporum* f.sp. *pisi* HG423346. That sample is in one clade with a nucleotide base sequence; other *Fusarium oxysporum* species have been recorded in the NCBI Genbank database. This third sample forms a monophyletic group with each other. In other parts of the branching, all groups incorporated in the *F. oxysporum* taxon species are polyphyletic with taxon members of Genus *Fusarium* sp. others. Knowledge of Fusarium wilt symptoms as a result of in depth is required. Tomato plants at the same altitudes have different closeness to Fusarium species or forma species in one area. It might affect the resistance of heat, fungicides, and different pathogenicity (Henik, *et al*., 2021) and show variations in pathogenicity, response to management systems, environment, and host differences (Hami *et al*., 2021).

Campbell *et al*., (2014) reported that a taxon is monophyletic if its single ancestor produces a whole derivative species in the taxon and not a species in another taxon, polyphyletic. If its members come from several ancestors that are not the same for all members, and paraphyletic if the taxon does not include species with grandmothers, the same ancestor in a member of a species towards another species. Branching like this can occur when two types of molecular characters specific to different homologous DNA species over time change due to various conditions (Nath, *et al*., 2017). The situation is like a point mutation that removes a nucleotide from the specific DNA sequences and inserts three adjacent nucleotides (Edel-Hermann and Lecomte, 2019). As a result of this situation, DNA sequences that are initially very similar have different lengths and sequences.

At the end of the branching of these three samples, a figure of 100 % shows the high bootstrap value of this branching group. Bootstrap value is one of the measures introduced by (Fredricks, Smith, and Meier, 2005), which offers the stability value of a topology tree. The higher the bootstrap value in a branching, the more fulfilling the topology's validity level requirements. In other words, a high boost value (close to 100 %) does not mean showing the accuracy of a topology tree but rather indicates that each character information of each individual in the branching group "agrees" that a branching member is a group.

3313422_Root_Blitar_ITS1																
3313424_Root_Karang_ploso_ITS1	0.000															
3313426_Root_Pujon_ITS1	0.329	0.329														
3313428_Soil_Blitar_ITS1	0.324	0.324	0.281													
3313430_Soil_Karang_ploso_ITS1	0.234	0.324	0.281	0.00												
3313432_Soil_Pujon_ITS1	0.000	0.00	0.329	0.324	0.324											
Fusarium_circinatum_361_Pinus_pinaster_FJ74410	0.322	0.322	0.281	0.007	0.007	0.322										
Fusarium_circinatum_SF1_KX276593	0.322	0.322	0.281	0.007	0.007	0.322	0.00									
Fusarium_fujikuroi_dmV_MF567510	0.322	0.322	0.279	0.002	0.002	0.322	0.005	0.005								
Fusarium_graminearum_KCS7e_MG182681	0.326	0.326	0.283	0.046	0.046	0.326	0.041	0.041	0.043							
Fusarium_oxysporum_BRM004946_MG461603	0.324	0.324	0.281	0.000	0.000	0.324	0.007	0.007	0.002	0.046						
Fusarium_oxysporum_C5-2_KT876656	0.324	0.324	0.281	0.000	0.000	0.324	0.007	0.007	0.002	0.046	0.000					
Fusarium_oxysporum_EF-382_MF992182	0.324	0.324	0.281	0.000	0.000	0.324	0.007	0.007	0.002	0.046	0.000	0.000				
Fusarium_oxysporum_MR43-1_myricaria_laxiflora_KU324799	0.324	0.324	0.281	0.000	0.000	0.324	0.007	0.007	0.002	0.046	0.000	0.000	0.000			
Fusarium_sambucinum_CBS_187.34_MH855483	0.322	0.322	0.281	0.007	0.007	0.322	0.000	0.000	0.005	0.041	0.007	0.007	0.007	0.007		
Fusarium_solani_DOS_Dendrobium_officinale_Kimura_et_Migo_KY644557	0.322	0.322	0.279	0.002	0.002	0.322	0.005	0.005	0.000	0.043	0.002	0.002	0.002	0.002	0.005	
Fusarium_Verticilioides_05007_MG274298	0.324	0.324	0.279	0.009	0.009	0.324	0.002	0.002	0.007	0.043	0.009	0.009	0.009	0.009	0.002	0.007

Figure 3. Genetic distance analysis of *F. oxysporum* at three different altitudes

Based on genetic distance analysis results, *F. oxysporum* from six sample-consisted soil samples and tomato plant roots at three different altitudes. Genetic distance matrix *F. oxysporum* with several specific Genes recorded from GenBank between 0.00 to 0.32. The closest genetic distance is 0.00 for the sample. On the other hand, the genetic distance of the DNA sample *F. oxysporum* has a value of 0.32, which is the farthest distance. which is of the genus Fusarium from other F. oxysporum species and then widens to other species.

In contrast, phylogeny's opening results show various levels of kinship between one species and another. The bootstrap value of the phylogeny tree is available between 51 % and 100 % the highest. According to Hafizi *et al*. (2013), the lower the genetic distance of species with other species, the closer the kinship distance.

According to Dharmayanti (2011), the farther the genetic distance of an individual or group from other individuals or groups, the more distant the kinship of the organism. Vice versa, the closer the genetic distance, the more closely related. Although the targeted gene's location is the same, differences in several nucleotide points in the gene sequence are prevalent mutations that cause this matter. Mutations are changes in genetic material that can be inherited and give rise to alternative forms of any gene. The more changes occur, the farther the genetic distance is from other species that share a common ancestor. Mutations result in a new variation of alleles, genes with the same location on the chromosome but whose properties vary (Stansfield et al., 2006).

4. Conclusion

From the results of molecular tests, information was obtained that all isolates found from different plant parts and from different altitudes were *Fusarium oxysporum.*

analysis shows *Fusarium oxysporum* f. sp. *Lycopersici* CBS 249.52 strain has the closest relationship in code 3313439 from Karangploso soil and code 3313428, which comes from Blitar soil. Besides, *Fusarium oxysporum* strain S58 has the closest relationship with the isolate 3313426 Pujon roots. Then samples of 3313422 Blitar roots, 3313424 Karangploso roots, and 3313432 Pujon soils showed proximity to the *Fusarium oxysporum* f.sp. *pisi* HG423346

References

Adame-García J., Rodriguez-Guerra R., Iglesias-Andreu LG, Ramos-Prado JM and Luna-Rodríguez M. 2015. Molecular identification and pathogenic variation of fusarium species isolated from *Vanilla planifolia* in Papantla Mexico. *Bot. Sci.* **93(3)**: 669–678.

Agrios G, 2005. **Plant Pathology,** fifth ed. Elsevier Academic Press, Burlington, MA, USA.

Animashaun BO, Popoola AR, Enikuomehin OA, Aiyelaagbe IOO, Imonmion J E. 2017. Induced resistance to Fusarium wilt (*Fusarium oxysporum*) in tomato using plant growth activator, Acibenzolar-S-methyl. *Niger J Biotechnol* **32:**83–90

Aydi-Ben-Abdallah, Jabnoun-Khiareddine H and Daami-Remadi M. 2020. Fusarium wilt biocontrol and tomato growth stimulation, using endophytic bacteria naturally associated with *Solanum sodomaeum* and *S. bonariense* plants. *Egypt J Biol Pest Co* **30:**1–13.

Biju VC, Fokkens L, Houterman PM, Rep M and Cornelissen BJC. 2017. Multiple evolutionary trajectories have led to the emergence of races in *Fusarium oxysporum* f. sp. *lycopersici. Appl Environ Microbiol* **83(4):**e02548-16: 1–20.

Campbell NA, Reece JB, Urry LA, Cain M L, Wasserman SA, Minorsky P V and Jackson RB. 2010. Campbell biology. In: **Campbell Biology** (11th ed.). Pearson, London, UK

Cañizares MC, Gómez-Lama C, García-Pedrajas MD and Pérez-Artés E. 2015. Study of phylogenetic relationships among *Fusarium oxysporum* f. sp. *dianthi* Isolates: Confirmation of intrarace diversity and development of a practical tool for simple population analyses. *Plant Dis*. **99(6)**:780–787.

Chala A, Degefu T and Brurberg MB. 2019. Phylogenetically diverse Fusarium species associated with sorghum (*Sorghum bicolor* L. Moench) and finger millet (*Eleusine coracana* L. Garten) grains from Ethiopia. *Diversity*, **11(93):**1–11

Chen CA, Chang CC, Wei NV, Chen C, Lein YT, Lin HE, Dai CF and Wallace C. 2004. Secondary structure and phylogenetic utility of the ribosomal internal transcribed spacer 2 (ITS2) in Scleractinian corals. *Zool Stud* **43(4)**: 759–771.

Dharmayanti, I., 2011. Filogenetika molekuler: Metode taksonomi organisme berdasarkan sejarah evolusi [Molecular phylogenetics: The taxonomic method of organisms based on evolutionary history]. *Wartazoa*. **21 (1):**1–10. [in Bahasa Indonesia]

Edel-Hermann V and Lecomte C. 2019. Current status of *Fusarium oxysporum* formae speciales and races. *Phytopathology*, **109(4):**512–530.

Fredricks DN, Smith C and Meier A. 2005. Comparison of six DNA extraction methods for recovery of fungal DNA as assessed by quantitative PCR. *J. Clin. Microbiol*, **43(10)**: 5122–5128.

González-Mendoza D, Adame-García J, Rodriguez-Guerra R, Iglesias-Andreu LG, Ramos-Prado JM and Luna-Rodrígue M. 2010. A rapid method for isolation of total DNA from pathogenic filamentous plant fungi. *Genet. Mol. Res*, **9(1)**:162–166.

Hafizi R, Salleh B and Latiffah Z. 2013. Morphological and molecular characterization of *Fusarium. solani* and *F. oxysporum* associated with crown disease of oil palm. *Braz. J. Microbiol*. **44(3)**: 959–968.

Henik S, Erfan DS and Netnapis K. 2021. Variability of *Fusarium oxysporum* f. sp. *lycopersici* from different altitudes in East Java, Indonesia. *E3S Web of Conf*., **226(00023)**:1–9.

Hillis DM and Dixon MT.1991. Ribosomal DNA: Molecular evolution and phylogenetic inference. *Q RevBiol*. **66(4):**411–453.

Hsuan HM, Salleh B and Zakaria L. 2011. Molecular identificationn of Fusarium species in *Gibberella fujikuroi* species complex from rice, sugarcane and maize from Peninsular Malaysia. *Int. J. Mol. Sci*. **12(10):** 6722–6732.

Hussain MZ, Rahman MA, Islam MN, Latif MA and Bashar MA. 2012. Morphological and molecular identification of *Fusarium oxysporum* Sch. isolated from guava wilt in Bangladesh. *Bangladesh J. Bot*., **41(1):**49–54.

Ignjatov M, Milosevic D, Nikolic Z, Gvozdanovic-Varga J, Jovicic D and Zdjelar G. 2012. *Fusarium oxysporum* as causal agent of tomato wilt and fruit rot. *Pestic. Fitomed*., **27(1)**: 25–31.

Kichaoui AE, Elnabris K, Shafie A, Fayyad N, Arafa M, and El Hindi M. 2017. Development of *Beauveria bassiana* based bio-fungicide against *Fusarium* wilt pathogens for *Capsicum annuum*, a promising approach toward vital biocontrol industry in Gaza Strip. *IUG Journal of Natural Studies*. **25(2)**:183–190.

Leslie JF and Summerell BA. 2006. **Handbook Fusarium**. Blackwell Publishing Professional. New Jersey, USA

Leslie JF and Summerell BA. 2008. **The Fusarium Laboratory Manual**. Wiley, New York.

Lievens B, Rep M and Tomma BP. 2008. Recent developments in the molecular discrimination of formae speciales of *Fusarium oxysporum*. *Pest Manag Sci*. **64(8):**781–788.

Menezes JP, Lupatini M, Antoniolli' ZI, Blume' L, Junges E, Manzoni CG. 2010. Genetic variability in rDNA ITS region of Trichoderma spp. (Bio controle agent) and Fusarium oxysporum f. sp. chrysanthemi isolates. Cienc. e Agrotecnologia **34(1):**132–139.

Menu E, Mary C, Toga I, Raoult D, Ranque S. and Bittar F. 2018. Evaluation of two DNA extraction methods for the PCR-based detection of eukaryotic enteric pathogens in fecal samples. *BMC Res Notes*, **11(1)**:4–9.

Nath N, Ahmed AU and Aminuzzaman FM. 2017. Morphological and physiological variation of *Fusarium oxysporum* f. sp. ciceri isolates causing wilt disease in chickpea. *Int. J. Agric. Environ. Biotechnol*., **2(1):**202–212.

Nirmaladevi D, Venkataramana M, Srivastava RK, Uppalapati SR, Gupta VK, Yli-Mattila T, Chandra NS. 2016. Molecular phylogeny, pathogenicity, and toxigenicity of *Fusarium oxysporum* f. sp. Lycopersici. *Sci. Rep*, **6(21367**): 1–14.

Pinaria AG, Laurence MH, Burgess LW and Liew ECY. 2015. Phylogeny and origin of *Fusarium oxysporum* f. sp. vanillae in Indonesia. *Plant Pathol*., **64(6)**:1358–1365.

Prihatna C, Barbetti MJ, and Barker SJ. 2018. A novel tomato *Fusarium* wilt tolerance gene. *Front. Microbiol*. **9(1226)**: 1–11.

Raghu S, Benagi, V and Nargund, V. 2016. Cultural, morphological and pathogenic variability among the isolates of *Fusarium solani* causing wilt disease of Chilli (*Capsicum annuum* L.). *J. Pure Appl. Microbiol*. **10(1):**599–604.

Singha IM, Kakoty Y, Unni BG, Das J and Kalita MC. 2016. Identification and characterization of Fusarium sp. using ITS and RAPD causing fusarium wilt of tomato isolated from Assam, North East India. *J Genet Eng Biotechnol*. **14(1)**: 99–105.

Sohail A. Alsohaili and Bayan M. Bani-Hasan. 2018. Morphological and molecular identification of fungi isolated from different environmental sources in the Northern Eastern desert of Jordan. *Jordan J. Biol. Sci*. **11(3):** 329–337**.**

Srinivas C, Nirmala DD, Narasimha MK., Mohan CD, Lakshmeesha TR, Singh BP and Chandra NS. 2019. *Fusarium oxysporum* f. sp. *lycopersici* causal agent of vascular wilt disease of tomato: Biology to diversity– A review. *Saudi J Biol Sci*., **26(7)**:1315–1324.

Stansfield, William D., Jaime S., Raul J., 2006. **Biologi Molekuler dan Sel** [Molecular and Cell Biology]. Penerbit Erlangga, Jakarta, Indonesia [in Bahasa Indonesia].

Teixeira LM, Coelho L, and Tebaldi TD. 2015. Characterization of *Fusarium oxysporum* isolates and resistance of passion fruit genotypes to fusariosis. *Rev. Bras. Frutic*. **39(3):** e-415:1–11.

JJBS

Volume 14, Number 3, September 2021
ISSN 1995-6673
Pages 389 - 393

Jordan Journal of Biological Sciences

The Characteristics and Predicted of Glycemic Index of Rice Analogue from Modified Arrowroot Starch (*Maranta arundinaceae* L.)

Damat Damat[1,*], Roy Hendroko Setyobudi[2], Joko Susilo Utomo[3], Zane Vincēviča-Gaile[4], Anas Tain[1] and Devi Dwi Siskawardani[1]

[1]*Department of Food Technology, Faculty of Agriculture and Animal Science, University of Muhammadiyah Malang, Jl. Raya Tlogomas No 246, Malang 65144, East Java, Indonesia;*[2]*Department of Agriculture Science, Postgraduate Program, University of Muhammadiyah Malang, East Java Indonesia;*[3]*Indonesian Legumes and Tuber Crops Research Institute, Jl. Raya Kendalpayak No.66, Malang 65162, East Java, Indonesia;*[4]*Department of Environmental Science, University of Latvia, Jelgavas Street 1, Room 302, Riga LV-1004, Latvia*

Received: Feb 20, 2021; Revised: May 28, 2021; Accepted May 29, 2021

Abstract

The modification of arrowroot starch is able to increase its resistant starch (RS) levels, as the result improve the functional characteristic of rice analogue for healthy diabetics. Therefore, the purpose was to determine the physical characteristics, digestibility, hydrolysis index (HI) and predicted glycemic index (PGI) of rice analogue obtained from modified arrowroot starch. The completely randomized design using single factor was conducted. The proportions of the modified arrowroot starches used were 0 %, 25 %, 50 %, 75 %, and 100 %. The procedure consisted of formulation, extrusion, and analysis parameter. According to the results, the proportions of the modified arrowroot starch had a significant effect on the microscopy as well as the rice analogue digestibility. The amount of rice analogue obtained from the 100 % modified arrowroot starch was 649 µm, which was the highest, the digestibility value at 180 min was 14.23 % ± 0.17 %, HI values at 32.14 ± 0.20 and PGI 56.79 ± 0.14, which was the smallest when compared with other treatments. It can be concluded that higher proportions of the modified arrowroot starch, resulted in higher grain size, but lower digestibility, hydrolysis index and predicted glycemic index of gluten-free rice analogue.

Keywords: Digestibility, Food diversification, Functional rice, Gluten-free rice, Healthy diabetics, Hydrolysis Index

1. Introduction

Arrowroot (*Maranta arundinaceae* L.) is a type of tuber, which is cultivated in some areas in Indonesia (Deswina and Priadi, 2020; Sholichah *et al*., 2019). Carbohydrate is the main component of this plant and various studies have been conducted to examine its starch constituents (Charles *et al*., 2016; Damat *et al*., 2017; Villas-Boas and Franco, 2016). However, the focus of this research was generally on the physical and chemical characteristics of arrowroot starch. Also, research has been conducted on the modification of arrowroot starch through esterification (Damat *et al*., 2008), cross-linking (Maulani *et al*., 2013), acetylation (Abba *et al*., 2014), gelatinization-retrogradation (Damat *et al*., 2019b; Pepe *et al*., 2015) as well as through physical modification methods (Astuti *et al*., 2018).

In addition, the previous research was conducted to the application of arrowroot starch as raw material of rice analogue (Damat *et al*., 2019b). However, there was not research on the modification of arrowroot starch through gelatinization-retrogradation and its application for functional rice analogue. Moreover, there was not research on the digestibility and predictions of the glycemic index of functional rice analogue obtained modified arrowroot starch.

According to Damat *et al*. (2019a), the modification of arrowroot starch through gelatinization-retrogradation increased its resistant starch (RS) levels. Consequently, the rice analogue resulting was rich in RS and low in GI. Damat *et al*. (2008); Damat *et al*. (2020) reported the importance of food products, which are rich in RS in controlling blood glucose since they had slower digestion rates. Control of blood glucose level was one goal of a healthy diet plan for diabetes sufferers (Al-Jamal and Alqadi, 2011; Bhaskar and Ajay, 2009); therefore, the rice analogues were usually consumed (Budijanto and Yuliana, 2015; Wahjuningsih *et al.*, 2018). The metabolism of RS occurred 5 h to 7 h after eating (Lestari *et al*., 2017); hence, it had the ability to reduce the postprandial glucose levels (Setyobudi *et al.*, 2019). This research aimed to evaluate the microscopic physical properties, in vitro digestibility, hydrolysis index (HI) and the predicted glycemic index (PGI) of the functional rice analogue from modified arrowroot starch.

2. Materials and Methods

The arrowroot starch was obtained from the farmers in Malang Regency, East Java. This research was

* Corresponding author e-mail: damatumm@gmail.com

conducted in two stages, i) the production of the modified arrowroot starch through gelatinization-retrogradation method (Damat *et al*., 2018) and ii) the production of the rice analogue. The Completely Randomized Design (CRD), with one factor, which included K0 (Control), K1 (100 % Natural Arrowroot Starch); K2 (75 % Natural Arrowroot Starch: 25 % Modified Arrowroot Starch); K3 (50 % Natural Arrowroot Starch: 50 % Modified Arrowroot Starch); K4 (25 % Natural Arrowroot Starch: 75 % Modified Arrowroot Starch); and K5 (100 % Modified Arrowroot Starch) were applied. The result expected was to increase the resistant starch, followed to reduce the degree of hydrolysis and predict the glycemic index of rice analogue.

2.1. Formulation

The ingredient formulation consisted of cornstarch, modified cassava flour, natural arrowroot starch, modified arrowroot starch, and water. Moreover, GMS (glycerol monostearate) as an emulsifier was added. The exact formula is presented in Table 1.

Table 1. Formula of rice analogue

Raw material	Ko	K1	K2	K3	K4	K5
Cornstarch (g)	250	0	0	0	0	0
Modified cassava flour (g)	250	0	0	0	0	0
Natural arrowroot starch (g)	0	500	375	250	125	0
Modified arrowroot starch (g)	0	0	125	250	375	500
Water (mL)	110	110	110	110	110	110
Emulsifier: GMS (g)	5	5	5	5	5	5

2.2. Extrusion

The ingredients were mixed and steamed for 30 min at 80 °C. The steamed materials were directly inserted into an extruder in order to form the analogue rice. After analogue, rice granules were formed; they were dried in a dryer cabinet at 50 °C for 20 h.

Then, analyses of the microscopic properties of the rice analogue was carried out using the modified version of Scanning Electron Microscope by Han *et al.* (2018), the resistant starch levels (Fabbri *et al*., 2016), and those of the digestibility, hydrolysis index (HI) and predicted glycemic index (PGI) conducted in vitro in accordance to Ratnaningsih *et al*. (2017). The research data were expressed as mean ± deviation standards in triplicate independent analyzes. One-way ANOVA was conducted on the data using SPSS version 17.

3. Results and Discussion

Arrowroot starch with different granule morphology were scanned used SEM (Figure 1). Unmodified arrowroot starch resulted round to elliptical granules with a size 9 µm to 36 µm. The starch granules had a smooth surface, and it was consistent with the granular shape of arrowroot starch reported by Charles *et al.* (2016). While, in the modified arrowroot starch granules showed different, it had a rough and irregular surface (Figure 1).

Modified arrowroot starch granules had a size of 88 µm to 591 µm, which is larger than natural arrowroot starch. Majzoobi *et al.* (2016) suggested that the increase in grain size might be related to the absorption of acid, causing some internal transformation in the granules. The alteration in the size of starch granules can cause starch digestibility and increase resistant starch level (Damat *et al*., 2019b). Modification of starch through gelatinization-retrogradation accompanied by cooling changed in the surface of the starch grains becomes uneven. Starch retrogradation generate the granules are difficult to swell and strengthen the grains, to be more heat and shear resistant leading to a lower viscosity. Changes in the structure, size and shape of starch grains induced alteration in the regularity structure of short distances, viscosity, solubility and swelling (Lin *et al*., 2015).

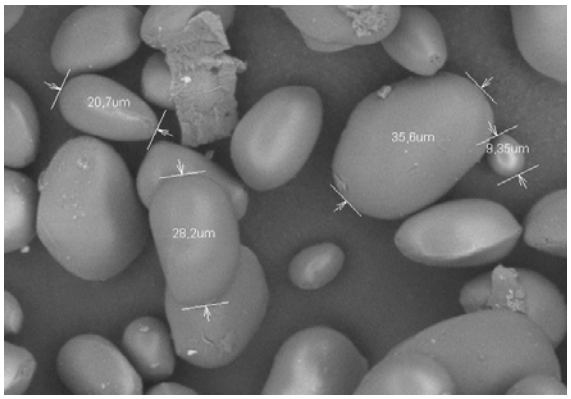

Natural arrowroot starch granules

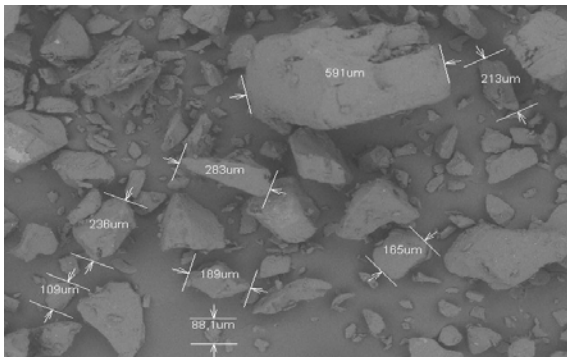

Modified arrowroot starch granules

Figure 1. Granules of natural arrowroot starch and modified arrowroot starch

The sizes and the shapes of starch granule rice analogue produced were shown in Figure 2. The K1 treatment (100 % natural arrowroot starch) was almost the same as K0, with the size was smaller ranging from 136 µm to 229 µm. Furthemore, enhancement of modified arrowroot starch induced more irregular and larger size of rice analogue granule. This was due to the incorporation of amylose in the cooling process to form crystals, which different to natural starch. The granule size of rice analogue ranged from 175 µm to 649 µm, with the biggest size ranging from 334 µm to 649 µm, found in the K5 treatment (100 % modified arrowroot starch).

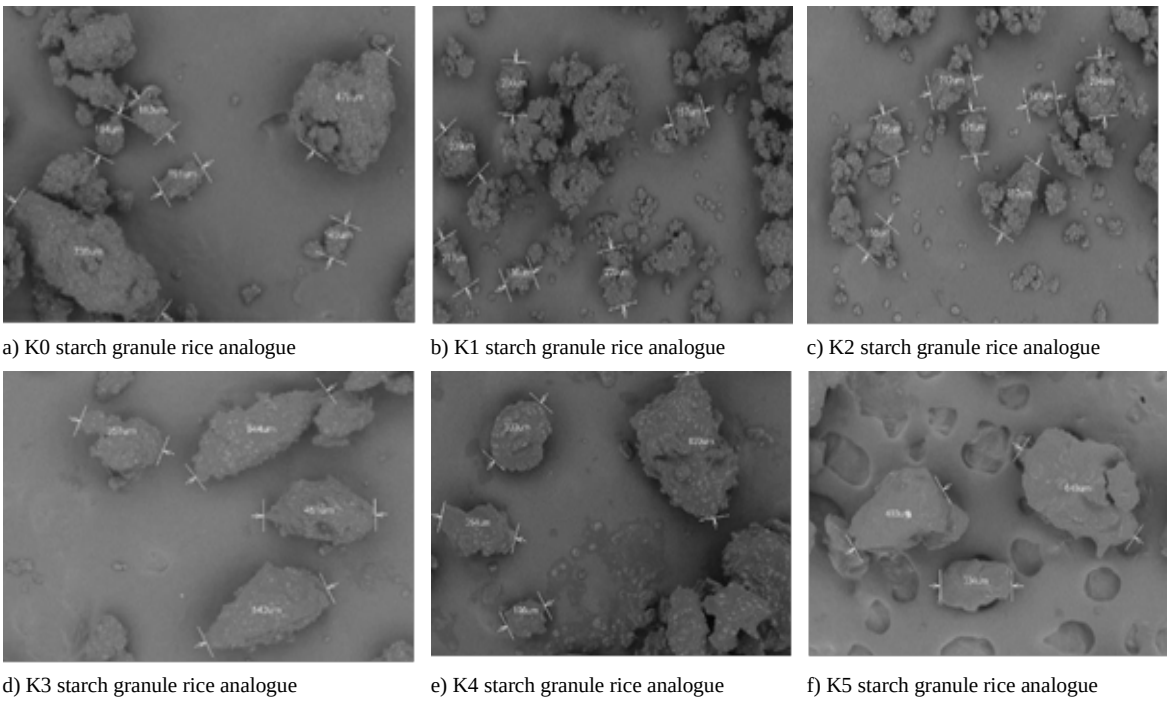

a) K0 starch granule rice analogue b) K1 starch granule rice analogue c) K2 starch granule rice analogue

d) K3 starch granule rice analogue e) K4 starch granule rice analogue f) K5 starch granule rice analogue

Figure 2. Starch Granule Rice analogue under the Scanning Electron Microscope (SEM) at 100× magnification

The highest starch resistant rice analogue was found in the treatment K5, which was 16.71 % ± 0.40 %. The rice analogue with the lowest hydrolysis index and predicted glycemic index obtained this treatment were 32.14 ± 0.20 and 56.79 ± 0.14 respectively (Table 2). The results showed that the higher amount of modified arrowroot starch added produced higher levels of the resistant starch in rice analogue. However, there was a positive correlation between the resistant starch content enhancement, to the decreasing degree of hydrolysis (HI) and predicted glycemic index (PGI). According to Figure 3, the rice analogue with the lowest total hydrolyzed starch was found in treatment K5, which was 7.80 % at 30 min and 14.23 % at 180 min.

Table 2. The Resistant Starch (RS), Hydrolysis Index (HI), and Predicted Glycemic Index (PGI) of Rice Analogue

F Treatment	RS level (%)	Hydrolysis Index (HI)	Predicted Glycemic Index (PGI)
K0 (Control)	3.92 ± 0.31a	66.15 ± 0.12f	76.03 ± 0.32f
K1 (NAS 100 %, MAS 0 %)	5.81 ± 0.23b	65.68 ± 0.17e	75.77 ± 0.19e
K2 (NAS 75 %, MAS 25 %)	8.36 ± 0.35c	44.79 ± 0.23d	64.30 ± 0.24d
K3 (NAS 50 %, MAS 50 %)	11.22 ± 0.27d	40.81 ± 0.20c	62.11 ± 0.20c
K4 (NAS 25 %, MAS 75 %)	14.21 ± 0.24e	35.37 ± 0.19b	59.13 ± 0.22b
K5 (NAS 0 %, MAS 100 %)	16.71 ± 0.40f	32.14 ± 0.20a	56.79 ± 0.14a

Note: Number followed by the same letter is not significantly different according to Duncan's Test α= 5 %,

This is due to the differences in granule size and the levels of resistant starch in the rice analogue. In addition, Dundar and Gocmen (2013) stated that the increased level of the resistant starch was caused by modification through gelatinization-retrogradation method. The results obtained were similar to those of Ratnaningsih *et al.* (2017), the ability of enzymes to hydrolyze starch was strongly influenced by amylose content, resistant starch content and granule size. In accordance with Damat *et al*. (2008) and Damat *et al*. (2020), food products with high contents of resistant starch (RS) had a hypoglycemic effect as well as a low glycemic index. Resistant starch included to food fiber.

Supparmaniam *et al.* (2019) described that increasing levels of food fiber from starch were able to reduce the glycemic index of the product. In addition, resistant starch, ratio of amylose-amylopectin, the interaction between starch, and other components contained in the product also influenced the glycemic index (Bakar *et al*., 2019). Moreover, starchy foods with low glycemic index are very good for diabetic and hypertriglyceridemia patients. Ratnaningsih *et al*. (2017) reported that functional ~~such~~ food products provide a longer feeling of satiety and increase the fermentation process in the colon.

In vitro, analogue rice starch hydrolysis was presented in Figure 3. The analogue rice starch hydrolysis speed and bread as a control increased with time. Analogue rice produced from modified arrowroot starch (MAS) had a lower starch hydrolysis speed than plain bread and natural arrowroot starch at all observation times. Analogue rice made from 100 % MAS has the lowest hydrolysis rate. The analogue rice starch hydrolysis speed was similar to raw green bean starch (Kaur *et al*., 2015), but it was lower than that reported by Ambaigapalan *et al*. (2014) on black bean, and pinto bean starch, also on field pea starch (Liu *et al*., 2015). The analogue rice digestibility of modified arrowroot starch was influenced by the absence of pores on the starch granule surface and the strong interaction between amylose chains due to the gelatinization-retrogradation process. The low digestibility of analogue rice starch was considered related to high amylose content and starch granule size (Hoover *et al*., 2010; Liu *et al*., 2015).

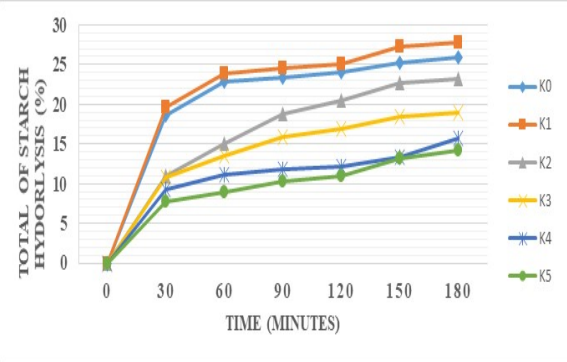

Figure 3. Starch hydrolysis pattern

4. Conclusion

The modified arrowroot starch's proportion had a significant effect on the microscopy and digestibility of rice analogue. The modified arrowroot starch enhancement resulted in larger granule size and resistant starch (RS) of rice analogue produced. Moreover, the increasing levels of RS and digestibility, the hydrolysis index (HI), and predicted glycemic index (PGI) of the rice analogue decreased, and rice analogue with low PGI is recommended for healthy diabetics.

Acknowledgements

The authors wish to thank the Ministry of Research and Technology, Republic of Indonesia, for funding for this research (E.5c/092/DPPM/L/IV/2019).

References

Abba H, Ibrahim A, Shalllangwa GA, Uba S and Dallatu YA. 2014. Effect of acetylation on stability to retrogradation of starch extracted from wild polynesian arrowroot (*Tacca leontopetaloides* (L.) Kuntze) for utilization as adhesive on paper. *J. Polym.* **732174**:1–9.

Al-Jamal A, and Alqadi T. 2011. Effects of rosemary (*Rosmarinus officinalis*) on lipid profile of diabetic rats. *Jordan J Biol Sci* **4(4):** 199–204.

Ambigaipalan P, Hoover R, Donner E, and Liu Q. 2014. Starch chain interactions within the amorphous and crystalline domains of pulse starches during heat-moisture treatment at different temperatures and their impact on physicochemical properties. *Food Chem.* **143**:175–184.

Astuti RM, Widaningrum, Asiah N, Setyowati A and Fitriawati R. 2018. Effect of physical modification on granule morphology, pasting behavior, and functional properties of arrowroot (*Marantha arundinacea* L) starch. *Food Hydrocoll*, **81**:23–30.

Bakar NAFA, Rashid AAA, Ishak MF and Jalil AMM. 2019. Glycemic index of starch-based foods commonly consumed in Terengganu, Malaysia. *Malays Appl Biol*, **48(4)**:129–138.

Bhaskar VH and Ajay SS. 2009. Antihyperglycemic and antihyperlipidaemic activities of root extracts of *Calotropis procera* (Ait.) R.Br on streptozotocin induced diabetic rats. *Jordan J Biol Sci* **. 2(4):** 177–180.

Budijanto S and Yuliana ND. 2015. Development of rice analog as a food diversification vehicle in Indonesia. *J. Sustain. Agric.* **10**: 7–14.

Charles AL, Cato K, Huang T, Chang Y, Ciou J, Chang J and Lin H. 2016. Functional properties of arrowroot starch in cassava and sweet potato composite starches. *Food Hydrocoll.* **53**:187–191.

Damat D, Marsono Y, Haryadi and Cahyanto MN. 2008. Hypocholesterolemic and hypoglicemic effects of butyrylated arrowroot starch on Sprague Dawley rats. *Indones. J. Pharm.* **19(3)**:109–116.

Damat D, Tain A, Handjani H and Chasanah U. 2017. Microscopy and organoleptic properties of functional pastries form modified arrowroot starch (*Maranta arundinaceae* L.). *Jurnal Aplikasi Teknologi Pangan*, **6(4)**:161–166.

Damat D, Tain A, Handjani H, Chasanah U and Putri DN. 2018. **Modified Starch Technology and it's Benefits for Health**. UMM Press, Malang, Indonesia.

Damat D, Anggriani R, Setyobudi RH and Soni P. 2019a. Dietary fiber and antioxidant activity of gluten-free cookies with coffee cherry flour addition. *Coffee Sci*, **14(4)**: 493–500.

Damat D, Tain A, Handjani H, Chasanah U and Siskawardani DD. 2019b. Functional cake characteristics of modified arrowroot starch (MAS) with the gelatinization-retrograde method. *IOP Conf. Ser.: Mater. Sci. Eng.* **532 (012017)**: 1–6.

Damat D, Setyobudi RH, Soni P, Tain A, Handjani H and Chasanah U. 2020. Modified arrowroot starch and glucomannan for preserving physicochemical properties of sweet bread. *Cienc. e Agrotecnologia* **44(e014820)**: 1–9.

Deswina and Priadi D. 2020. Development of arrowroot (*Maranta arundinacea* L.) as functional food based of local resource. *IOP Conf. Series: Earth and Environ. Sci.* **439 (012041)**: 1–11.

Dundar AN and Gocmen D. 2013. Effects of autoclaving temperature and storing time on resistant starch formation and its functional and physicochemical properties. *Carbohydr Polym*, **97(2)**:764–771.

Fabbri ADT, Schacht RW and Crosby GA. 2016. Evaluation of resistant starch content of cooked black beans, pinto beans, and chickpeas. *NFS Journal.* **3:** 8–12.

Han W, Jiao H and Fox D. 2018. Scanning electron microscopy. In: Wang R, Wang C, Zhang H, Tao J and Bai X. (Eds.) **Progress in Nanoscale Characterization and Manipulation.** *Springer Tracts in Modern Physics.* **272**: 35–68. Springer Singapore.

Hoover R, Hughes T, Chung HJ, and Liu Q. 2010. Composition, molecular structure, properties, and modification of pulse starches: A review. *Food Res. Int.* **43(2)**: 399–413.

Kaur M, Sandhu KS, Ahlawat R and Sharma S. 2015. *In vitro* starch digestibility, pasting and textural properties of Mung Bean: Effect of different processing methods. *J Food Sci. Technol.* **52(3)**:1642–1648.

Lestari LA, Huriyati E and Marsono Y. 2017. The development of low glycemic index cookie bars from foxtail millet (*Setaria italica*), arrowroot (*Maranta arundinacea*) flour, and kidney beans (*Phaseolus vulgaris*). *J. Food Sci. Technol.* **54(6)**:1406–1413.

Lin L, Huang J, Zhao L, Wang J, Wang Z and Wei C. 2015. Effect of granula size on the properties of lotus rhizome C-type starch. *Carbohydr. Polym.* **134**: 448–457.

Liu C, Wang S, Copeland L and Wang S. 2015. Physicochemical properties and *in vitro* digestibility of starches from field peas grown in China. *LWT Food Sci Technol.* **64(2)**:829–836.

Majzoobi M, Kaveh Z and Farahnaky A. 2016. Effect of acetic acid on physical properties of pregelatinized wheat and corn starch gels. *Food Chem.* **196**:720–725.

Maulani RR, Fardiaz D, Kusnandar F and Sunarti TC. 2013. Characterization of chemical and physical properties of hydroxypropylated and cross-linked arrowroot *(Marantha arundinacea*) starch. *J. Eng. Technol.Sci.* **45(3)**:207−221.

Pepe LS, Moraes J, Albano KM, Telis VRN and Franco CML. 2015. Effect of heat-moisture treatment on the structural, physicochemical, and rheological characteristics of arrowroot starch. *Food Sci. Technol. Int.* **22(3)**:256–265.

Ratnaningsih N, Suparmo, Harmayani E and Marsono Y. 2017. In vitro starch digestibility and estimated glycemic index of Indonesian cowpea starch (*Vigna unguiculata*). *Pak. J. Nutr.* **16(1)**:1–8.

Setyobudi RH, Zalizar L, Wahono SK, Widodo W, Wahyudi A, Mel M, Prabowo B, Jani Y., Nugroho YA, Liwang T, and Zaebudin A. 2019. Prospect of Fe non-heme on coffee flour made from solid coffee waste: Mini review. *IOP Conf. Series: EES.* **293(012035)**:1–24.

Sholichah E, Deswina P, Sarifudin A, Andriansyah CE and Rahman N. 2019. Physicochemical, structural and morphological properties of some arrowroot (*Maranta arundinacea*) accessions growth in Indonesia. *AIP Conf. Proc.* **2175(020008)**:1–9.

Supparmaniam H, Hussin N and Jalil AMM. 2019. Glycaemic index, palatability, acceptability and perceived satiety of cookies prepared with durian (*Durio zibethinus* Murr.) and β-glucan. *Malays Appl Biol.* **48(4)**:89–99.

Villas-Boas F and Franco CML. 2016. Effect of bacterial β-amylase and fungal α-amylase on the digestibility and structural characteristics of potato and arrowroot starches. *Food Hydrocoll*. **52**: 795–803.

Wahjuningsih SB, Haslina H and Marsono M. 2018. Hypolipidaemic effects of high resistant starch sago and red bean flour- based analog rice on diabetic rats. *Mater. Sociomed.* **30(4)**: 232–239.

JJBS

Volume 14, Number 3, September 2021
ISSN 1995-6673
Pages 395 - 401

Jordan Journal of Biological Sciences

Genotype Distribution and Prevalence of Human Papillomavirus Among Russian Women in Rostov, Southern Federal District of Russia

Abbas Hadi AlBosale[1,3,*], Konstantin Alekseevich Kovalenko[2], Elena Vladimirovna Mashkina[1]

[1] Southern Federal University, Rostov-on-Don, Russia; [2] Laboratory "Nauka", Rostov-on-Don, Russia.Southern Federal University, Rostov-on-Don, Russia; [3]Northern Technical University, mosul, Iraq

Received: June 22, 2020; Revised: October 16, 2020; Accepted: October 31, 2020

Abstract

HPV burden is a marker for cervical neoplasms and cancer. Prevalence of HPV infection and HPV genotypes varies amongst different regions. This research was aimed to investigate the age distribution patterns and prevalence of high-risk HPV genotypes among Rostov-on-Don women. Scrapings of epithelial cells obtained from the urogenital tract of 5655 women. Total DNA was extracted by the sorbent method; Real-Time PCR was used to investigate the HPV load and HPV genotyping. HPV was found in 40% of the DNA samples. The HPV infection was most prevalent among women age ≤ 20 years (55,26%) compared to 27,34% of women older than 40 years (p = 0,001). The prevalence of HPV 16/18 types was almost the same in all age groups. More 50% of women with a high HPV load were women at age group 20-30 years old. Among 254 women, 79,13% had single HPV type infection, and 20,86% had multiple HPV infection. The most frequent of high-risk HPV types were 16, 51 and 31 types. The most common variant of genotypes co-exist for multiple HPV infections were genotypes of A7 + A9 phylogenetic groups (30,18 %). Multiple HPV infections were the most prevalent (67,92%) in women at age group 20-30 years old. We concluded the prevalence of HPV infection among younger women was the highest and declined gradually with age among Rostov-on-Don women.

Keywords: Human Papillomavirus, HPV Genotypes, Multiple HPV Infections, Rostov-on-Don, Russia.

1. Introduction

Human papillomavirus (HPV) is one of the most common sexually transmitted viruses in the world. Anogenital HPV is the most predominant infection (Suligoi et al., 2017). Genital HPV types were subdivided into high-risk and low-risk types, based on the risk of infection-induced malignant neoplasms. The high-risk HPV genotypes identified to date (HPV 16, 18, 31, 33, 35, 39, 45, 51, 52, 56, 58, 59, 68, 73 and 82) are the main causative agents for various cancers types, most oropharyngeal and anal cancers, some cancers of the vagina and vulva. Also, low-risk types (HPV 6, 11, 40, 42, 43, 44, 54, 61, 70, 72, 81, and 89) cause different clinical symptoms of lesions of the skin and mucous membranes, including anogenital warts (Muñoz et al., 2003; Bihl et al., 2017). Other types of HPV are under review and may be categorized in the near future as high-risk or low-risk types (Chan et al., 2019). HPV 16 is the most prevalent and carcinogenic type worldwide, followed by HPV 18. In many regions, the HPV 16 and HPV 18 contribute to more than 70% of all cervical cancer cases (Li et al., 2011). The distribution of HPV genotypes varies geographically around the world. HPV 31 and 33 are predominant in Brazil. HPV 16 and HPV 52 are the most common types in Africa (Silva et al., 2009; Omar et al., 2017). The most common three HPV genotypes in Asian are 52, 58 and 16 (Vinodhini et al., 2012; Nah et al., 2017; Niyazmetova et al., 2017; Aimagambetova and Azizan, 2018; Wang et al., 2019a). The HPV 16 type prevails in the population of Russia, while the HPV genotypes 31, 39, 52 and 18 are less frequent (Sirotkina and Smith, 2012). In addition, the distribution of different HPV genotypes changes significantly according to age, race, economic situation, and sexual behaviors (Mitchell et al., 2014). The probability infection with HPV rises shortly after teenagers beginning sexual activity, but in most instances, the infection has a transient character and does not contribute to pathological changes (Boda et al., 2018). The frequencies of HPV-infection reach the maximum level among females between 20 to 25 years old, after which it decreases in the third decade of life (Gravitt and Winer, 2017). The HPV disappears in most cases during 1-2 years after infected. Nonetheless, the persistent infection with specific HPV genotypes can cause cellular changes and induce cervical intraepithelial neoplasia and cervical cancer (Radley et al., 2016). Several studies have demonstrated that mixed HPV infection and high viral load were associated with persistent HPV infection. They are regarded as critical risk factors for developing cervical lesions and predicting the progress of the HPV infection

* Corresponding author e-mail: abbashammadi4@gmail.com.

(Sun et al., 2001; Bello et al., 2009). Over the past years, in many countries, the incidence of cervical cancer has decreased. At the same time, Russia has a high incidence of cervical cancer per 100,000 people. In 2018, about 18,164 new cervical cancer cases were diagnosed in the Russian Federation. Cervical cancer is the fourth-largest cause of women's cancer and the second-most common cause of women's cancer in aged between 15 and 44 years in Russian Federation (ICO/IARC Information Centre on HPV and Cancer, 2019). The studies about HPV distribution and prevalence provide important information on the epidemiology of HPV infection and as basic data for determining the changes in the prevalence of specific HPV genotypes that may direct potential screening applications in different regions to the identification and prevention of the predominant HPV genotypes related-cervical carcinogenesis; consequently reducing the health burdens and helping assess the possible benefits of immunization against HPV types. In Rostov-on-Don, by the beginning of 2018, more than half of the region's population was women - 53.6%. The proportion of women in the total population by age group were 48,5% for (10-19) years old, 49,7% for (20-34) years old, 50,9% for (35-44) years old and 68,6% for (45 – 70) years old (Federal State Statistics Service, 2018). The high level of the cervical cancer occurrence, high prevalence of HPV infection and the differences of HPV genotypes prevalence across geographical. So, our study aimed to analyze data for HPV virus load, genotypes and to assess rates of co-infection among women in Rostov-on-Don (Russia, Southern Federal District of Russia).

2. Material and methods

2.1. Materials study

The materials used in our study were DNA samples collected from epithelial cells of the urogenital tract of women. A total number was 5655 DNA samples from women who underwent a screening examination at the “Nauka” clinical diagnostic laboratory (Rostov-on-Don, Russia) during the period: September 2016 to November 2019. All individuals had previously signed forms of informed consent and the laboratory questionnaire. The study was approved by the Bioethics Committee of the Academy of Biology and Biotechnology of the Southern Federal University (Protocol No. 2 of March 29, 2016) according to the standards and ethical guidelines of the World Medical Association (Declaration of Helsinki) for human experiments.

2.2. DNA extraction from epithelial cells

The total DNA was extracted from epithelial cells of cervical canal scrapings according to the protocol of DNA-sorb-AM kit (NextBio, Russia).

2.3. HPV Genotyping analysis

High carcinogenic risk HPV genotypes were analyzed according to the AmpliSense HPV HCR genotype-FL reagent kit (Interlabservice, Russia) protocol by polymerase chain reaction (PCR) with hybridization-fluorescence detection. The method relies on the simultaneous amplification (multiplex-PCR) of HPV DNA regions and the β-globin gene region used as an endogenous internal control. PCR analyses were conducted in real-time in a single tube on a 4-channel RotorGene amplifier. The four major phylogenetic groups were analyzed: A9 group (16, 31, 33, 35, 52 and 58 types), A7 group (18, 39, 45 and 59), as well as HPV DNA 51 (group A5) and HPV DNA 56 (group A6) types.

2.4. HPV Quantitative analysis

DNA quantification of high carcinogenic risk HPV types (16, 18, 31, 33, 35, 39, 45, 51, 52, 56, 58, 59) in biological materials was analyzed according to the protocol of the AmpliSense HPV HCR screen-titer-FL reagent kit (Interlabservice, Russia). It should be mentioned that the risk of developing epithelial cells dysplasia depends on the concentration of HPV. The viral load of less than 3 lg of HPV genomes per 100 thousand human cells has low clinical significance because the probability of virus elimination from the human organism is high. A viral load, more than 3 lg of HPV genomes per 100 thousand human cells, is a clinically significant threshold where the risk of cell dysplasia and the probability of malignant cell transformation is increased (Federal Budget Institute of Science, 2018).

2.5. Statistical analysis

The percentages and standard deviation were determined. Comparison of frequencies of discrete variables was performed using Student's t-test. P values of <0,05 were assumed as statistically significant. All the statistical calculations were performed using Excel (version 2016) and SPSS software (version 25,0).

3. Results

A total of 5655 DNA samples were examined to detect the presence of human papillomavirus. (Table 1) shows the distribution of women according to the age groups. The majority of the women belong to the age groups from 20 to over 40 years old. Our analysis revealed the frequency of HPV-positive women was 40% (95% CI 38,72-41,27) (2262 from 5655 women). The frequencies of HPV-positive samples, depending on age, are shown in (Table 2). The maximum frequency of HPV-positive samples was observed among women under 20 years old. In this age group, more than half of the individuals were carriers of the human papillomavirus (55,26%). The lowest frequency of HPV positive samples (27,34%) was found in the women group for over 40 years. Analysis of the HPV 16/18 types was conducted for 2262 women among different age groups. The identification frequency of the most carcinogenic dangerous types HPV was almost the same in all age groups. It showed that 57 women from 215 HPV-positive in the age group less 20 years old were diagnosed with 16/18 HPV types; 404 women from 1446 with HPV16/18 were revealed at the age group 20-30 years old, 141 women from 534 at the age group 31-40 years old were found with HPV 16/18 and revealed 13 women infected with HPV16/18 types from 67 in the age group over 40 years old. The frequency of the detected HPV 16 /18 types in women from the Rostov region is shown in (Table 3). We conducted a quantitative analysis of the HPV DNA level for 2262 HPV-positive women. According to the HPV DNA content, 3 groups were identified. The first group included women with less than 3 lg of HPV genomes per 100 thousand human cells

(clinically insignificant). The second group included DNA samples with HPV load 3 - 5 lg, and the third group included women with HPV level more than 5 lg of HPV genomes per 100 thousand human cells which is a clinically significant threshold where a high probability of cell dysplasia and development to cervix cancer can arise. 42,79% of HPV-positive women had a viral load between 3 to 5 lg. The lowest percentage of women was (26,55%) infected by HPV in the viral load above 5 lg. Viral load distributions among HPV-positive women groups are shown in (Table 4). Among women with a high concentration of human papillomavirus (more than 5 lg HPV per 100 thousand cells) above 50% were women at age group 20-30 years old. The lowest quantity (4,64 %) women with high HPV load observed at the age group over 40 years old (Table 5). Our genotype analysis for 12 different types of high carcinogenic risk HPV types was performed for 254 women. Single HPV type infection was observed in 201 samples (79,13%), and co-infection with two or more types of HPV was observed in 53 samples (20,86%). The most common types of HPV were 16 and 51 (Table 6). 31 and 56 types of HPV were detected with a frequency of about 10%. 58 and 59 types of HPV were detected less often. We have analyzed 53 samples with co-infection and determined HPV genotypes depending on the four main phylogenetic groups A9, A7, A5 and A6. Two women had more than one HPV type from A7 phylogenetic group 3,77% (95% CI -1,35-8,90). The simultaneous presence of HPV types of A7 and A5/6 phylogenetic groups was detected in 11,32 % cases (95% CI 2,79-19,85). 13,20 % (95% CI 4,09-22,32) of women carrying HPV types from the A9 phylogenetic group. However, in 30,18 % (95% CI 17,82-42,54) of cases, virus types from A7 and A9 phylogenetic groups were detected. Co-infection of HPV types from A9 and A5/6 phylogenetic groups was detected in 26,41% (95% CI 14,5-38,28). Eight women have HPV types from all phylogenetic groups A7, A9 and A5/6 (15,09 %, 95% CI 5,45-24,73). Among women infected with several types of human papillomavirus, 15,09% (95% CI 5,45- 24,73) was from group less 20 years old. 67,92%, (95% CI 55,35-80,49) are young women at age group 20-30 years old. This age group is characterized by high sexual activity, possibly a frequent change of sexual partners, which contributes to HPV infection. Women with mixed HPV infection between the 30 and 40 account for only 11,32% (95% CI 2,79-19,85). 5,66 % of women (95% CI -0,56-11,88) were in the age group of over 40 years old.

4. Discussion

In this study of Rostov-on-Don women, the frequency of HPV-positive samples among residents of the Rostov region was 40,0%. According to the literature, infection of the population in the world with human papillomavirus is from 40 to 80% (Forman et al., 2012; Guan et al., 2012; Bruni et al., 2019). In Western European countries, Russian Federation, the Western countries of the former Soviet Union(Republic of Moldova, Belarus, Ukraine), the Central Asia and Caucasus region, high-risk HPV prevalence ranged to 48.4% (Rogovskaya et al., 2013; Belyaeva et al., 2018; Zykova et al., 2018). Several studies were conducted around the world and in different regions in Russia, but prevalence ratios were always different (Clifford et al., 2005; Sanjosé et al., 2007; Kulmala et al., 2007; Shipitsyna et al., 2011). The estimates of hr-HPV prevalence vary across regions, partially due to the different demographics and ages groups included in studies, utilization various methods for HPV identification, different screening programs implemented, or variability in test and study designs. We observed a significant association between age and HPV prevalence. In women under 20 to 30 years old, the prevalence was greater than in women over 40 years. Younger women had an HPV infection most frequently. Our data correspond to the results of other studies, according to which the peak of HPV detection occurs in age groups of women younger than 30 years old who have the highest sexual activity and change of sexual partners (Zeng et al., 2016; Roik et al., 2018). In the United States population, the prevalence range of HPV positive was in young women under 30 years old, between 41-51%(Karuri et al., 2017). Among women of the Rostov region in the older age groups, the proportion of HPV-positive people is steadily decreasing. But our analysis for 2262 women demonstrated that the frequency of the most carcinogenic dangerous high-risk HPV 16/18 prevailed almost all age groups. About a third of people over 30 years are carriers of the high-risk HPV, which increases the risk of malignant neoplasms development. HPV 16/18 types are associated with the largest contribution to the incidence of precancerous and cancerous lesions (Ahmed et al., 2017). Risk degree is higher among high carcinogenic HPV types 16/18 carriers. Our analysis for determining the viral load among HPV-positive women of the Rostov region demonstrated that about a third of HPV-positive individuals have a low viral load (less 3lg). That level of HPV is associated with a high probability of spontaneous disappearance of the human papillomavirus. More than 40% of the HPV-positive women demonstrate HPV load of 3 - 5 lg, at which cell dysplasia is possible. In 26,55% of cases, a high HPV load of the virus is observed, which is associated with a high risk of developing a malignant process. Certain studies showed that cells of HPV-positive women with higher viral load are more likely to progress to high-grade cervical intraepithelial neoplasia (Moberg et al., 2005; Cricca et al., 2007; Xi et al., 2011). Their own study showed that among women with a high human papillomavirus viral load (above 5 lg HPV per 100 thousand cells), young women under 30 years are 66 %. However, women older than 30 years (33% from total women with high HPV level) should thoroughly require constant medical monitoring. Most likely, in this case, the virus persists for a long time in the body; that is, the virus has not been eliminated, and a high viral load indicates active reproduction of the virus (Rodríguez et al., 2008, 2010). Long-term persistence of the virus leads to the integration of virus DNA into the human genome, expression of oncogenic proteins E6 and E7, and the development of cancer(Gupta and Mania-Pramanik, 2019). At the next stage of our work, using the AmpliSense HPV HCR genotype FRT test system, we analyzed the frequency of 12 different types of HPV with high carcinogenic risk (the test system uses type-specific primers located in the E6-E7 region of HPV genes). Genotyping of HPV was performed for 254 women. 79,13% HPV positive of women in Rostov Region population are carriers one of high carcinogenic risk HPV

type. Our findings indicate that 16, 51 and 31 (15,42%, 11,94% and 9,95% respectively) are the most common HPV genotypes in women in Rostov region. The HPV 18, 58 and 59 genotypes were less frequent. Our data are consistent with literature data on the dominance of 16, 39, 31 HPV genotypes in Russia (Marochko and Artymuk, 2017; Mkrtchyan et al., 2018). In the Russian Federation, HPV 16 had been confirmed as the most common type with a prevalence range of (2.7–14.1%) and Belarus, (4.0–7.1%), while in Georgia, (16.1%) (Samoylova et al., 1995; Kleter et al., 1999; Zumbach et al., 2000; Alibegashvili et al., 2011). In 20,86% of cases, co-infection with two or more types of HPV was observed. The most prevalent variant of genotypes co-existing for multiple HPV infections were genotypes of A7 + A9 phylogenetic groups (30,18 %) and A9 and A5/6 phylogenetic groups (26,41%). Our data are consistent with other studies, the most of high-risk HPV genotypes appear in the Co-infection infections (Oliveira et al., 2008; Conesa-Zamora et al., 2009; Wang et al., 2019b). Among women infected with several types of human papillomavirus, nearly 83% are young women at age 20 to 30 years. This age group is characterized by high sexual activity, possibly a frequent change of sexual partners, which contributes to mixed HPV infection. The prevalence of multiple infections among women with various lifetime sex partners was significantly higher, consistent with the sexual transmission of genital HPV infections (Widdice et al., 2010). Immunological mechanisms can also determine multiple infection prevalence. The prevalence of mixed infections among immunosuppressed women infected with HIV is still high(Massad et al., 2016). Women with HPV Co-infection between the ages of 30 to 40 account for only 11,32%. About 5,66 % are in the age group over 40 years old. However, people over 30 years infected with multiple types of HPV high oncogenic risk are highly likely to develop malignant neoplasms(Brot et al., 2017). Determining the epidemiology of mono and co-infections of HPV is essential to develop suitable preventive strategies according to each population. For some countries, co-infection with HPV is less frequent than mono-infection (Li et al., 2016), but in others, co-infection incidence is higher (Gallegos-Bolaños et al., 2017). In this analysis, there are many limitations. First, our analysis may not reflect the whole population. Our study represents only the women infected with high-risk HPV without men, HPV DNA tests unable to determine if the HPV detected was for a participant or a partner, Demographic nature of the population from either urban or rural areas is not specified. Our data reflected only three years of data for a particular subset of the population, and over the years, the distribution of HPV types may change. Second, we did not study the possible effect of social and sexual behaviors on the infection. Third, the absence of follow-up data for each patient in this study is a limitation. Finally, we recommend further studies among women and male populations in Rostov-on-Don. These studies are of considerable significance in terms of the effects of the vaccine program and in determining the transmission rate of the most prevalent of HPV types.

Table 1. The distribution of women among the age groups.

Age groups	≤ 20 years	20-30 years	31-40 years	> 40 years
Frequency, abs. (%) (95% CI)	389 (6,87%) (6,21-7,53)	3236 (57,22%) (55,93-58,51)	1785 (31,56%) (30,35-32,77)	245 (4,33%) (3,80-4,86)

Table 2. The frequency of HPV-positive women among the age groups.

Age groups	**≤ 20 years**	**20-30 years**	**31-40 years**	**> 40 years**
Cases / Total	215/389	1446/3236	534/1785	67/245
Frequency, %	55,26%	44,68% ***	29,91% ***	27,34% ***
(95% CI)	(50,32-60,21)	(42,97-46,39)	(27,79-32,04)	(21,76-32,92)

Note: ***-Significant differences compared with the first age group at P<0,001

Table 3. The frequency of HPV 16 / 18 types among HPV-positive women depending on the age.

Age groups	**≤ 20 years**	**20-30 years**	**31-40 years**	**> 40 years**
Frequency, abs. (%) (95% CI)	57 (26,51%) (20,61-32,41)	404 (27,55%) (25,27-29,84)	141 (26,40 %) (22,66-30,14)	13 (19,40 %) (9,93-28,87)

Table 4. Quantitative level of human papillomavirus among HPV-positive individuals.

Viral loads groups	**HPV level (lg HPV per 100 thousand cells)**		
	≤3 lg	**3 - 5 lg**	**> 5 lg**
Frequency, abs. (%)	691 (30,54 %)	968 (42,79 %)	603 (26,65 %)
(95% CI)	(28,64-32,44)	(40,75-44,83)	(24,83-28,48)
Average concentration of DNA HPV lg	1,89	4,17	5,98

Table 5. The frequency of women with high HPV load (≥5 lg HPV per 100 thousand cells) depending on the age groups.

Age groups	**≤ 20 years**	**20-30 years**	**31-40 years**	**> 40 years**
Cases/Total	86/603	313/603	176/603	28/603
Frequency, %	14,26 %	51,90 %	29,18 %	4,64 %
(95% CI)	(11,47-17,05)	(47,91-55,89)	(25,55-32,81)	(2,96-6,32)

Table 6. Prevalence (%) of HPV genotype distribution in HPV-infected women.

HPV types	Abs. cases / Total	% (95% CI)
HPV 16	31/201	15,42 % (10,42-20,41)
HPV 18	10/201	4,97 % (1,96-7,98)
HPV 31	20/201	9.95 % (5,81-14,08)
HPV 33	16/201	7,96 % (4,21-11,70)
HPV 35	17/201	8,45% (4,61-12,30)
HPV 39	16/201	7,96 % (4,21-11,70)
HPV 45	17/201	8,45% (4,61-12,30)
HPV 51	24/201	11,94 % (7,45-16,42)
HPV 52	17/201	8,45% (4,61-12,30)
HPV 56	19/201	9,45 % (5,40-13,49)
HPV 58	5/201	2,48 % (0,33-4,64)
HPV 59	9/201	4,47 % (1,61-7,33)

5. Conclusions

Based on these study results, we hypothesized that besides HPV 16, the genotypes 51 and 31 are of public health issues and could contribute to cervical carcinogenesis in Rostov-on-Don population due to their high frequency. Moreover, the correlation of various HPV genotypes, especially high-risk HPV genotypes, most likely represents a synergistic interaction in the development of certain carcinogenesis. These results call for our research efforts to focus on the clinical effects of interaction between the different HPV genotypes, and to establish new preventive and therapeutic approaches based on HPV types-prevalence trends in Russia.

Conflict of interest:

None.

References

Ahmed HG, Bensumaidea SH, Alshammari FD, Alenazi FSH, ALmutlaq BA, Alturkstani MZ, Aladani IA. 2017. Prevalence of human papillomavirus subtypes 16 and 18 among Yemeni patients with cervical cancer. *Asian Pacific J cancer Prev APJCP*, **18**(6):1543-1548.

Aimagambetova G, Azizan A. 2018. Epidemiology of hpv infection and hpv-related cancers in Kazakhstan: a review. *Asian Pacific J cancer Prev APJCP* ,**19**: 1175-1180.

Alibegashvili T, Clifford GM, Vaccarella S, Baidoshvili A, Gogiashvili L, Tsagareli Z, Kureli I, Snijders PJF, Heideman DAM, Kemenade FJ van. 2011. Human papillomavirus infection in women with and without cervical cancer in Tbilisi, Georgia. *Cancer Epidemiol*, **35**:465–470.

Bello BD, Spinillo A, Alberizzi P, Cesari S, Gardella B, D'Ambrosio G, Roccio M, Silini EM. 2009. Cervical infections by multiple human papillomavirus (HPV) genotypes: prevalence and impact on the risk of precancerous epithelial lesions., *J Med Virol*, **81**:703–712.

Belyaeva E, Tokarskaya O, Bairova T. 2018. Features of the spread of human papillomavirus infection in various regions of the Russian Federation (literature review)., *Acta Biomed Sci* **3**(3):127.

Bihl MP, Tornillo L, Kind AB, Obermann E, Noppen C, Chaffard R, Wynne P, Grilli B, Foerster A, Terracciano LM. 2017. Human Papillomavirus (HPV) detection in cytologic specimens: similarities and differences of available methodology. *Appl Immunohistochem Mol Morphol*, **25** (3):184-189.

Boda D, Docea AO, Calina D, Ilie MA, Caruntu C, Zurac S, Neagu M, Constantin C, Branisteanu DE, Voiculescu V. 2018. Human papilloma virus: Apprehending the link with carcinogenesis and unveiling new research avenues. *Int J Oncol*, **52**:637–655.

Brot L De, Pellegrini B, Moretti ST, Carraro DM, Soares FA, Rocha RM, Baiocchi G, Cunha IW da, Andrade VP de. 2017. Infections with multiple high-risk HPV types are associated with high-grade and persistent low-grade intraepithelial lesions of the cervix. *Cancer Cytopathol*,**125**:138–143.

Bruni L, Albero G, Serrano B, Mena M, Gómez D, Muñoz J, Bosch FX, Sanjosé S de. 2019. ICO/IARC information centre on HPV and cancer (HPV information centre). Human papillomavirus and related diseases in the world. available at: *https://www.hpvcentre.net/statistics/reports/XWX.pdf* **22**.

Chan CK, Aimagambetova G, Ukybassova T, Kongrtay K, Azizan A. 2019. Human papillomavirus infection and cervical cancer: epidemiology, screening, and vaccination—review of current perspectives., *J Oncol*, **10;**2019:3257939.

Clifford GM, Gallus S, Herrero R, Munoz N, Snijders PJF, Vaccarella S, Anh PTH, Ferreccio C, Hieu NT, Matos E. 2005. Worldwide distribution of human papillomavirus types in cytologically normal women in the International Agency for Research on Cancer HPV prevalence surveys: a pooled analysis. *Lancet*, **366**:991–998.

Conesa-Zamora P, Ortiz-Reina S, Moya-Biosca J, Doménech-Peris A, Orantes-Casado FJ, Pérez-Guillermo M, Egea-Cortines M. 2009. Genotype distribution of human papillomavirus (HPV) and co-infections in cervical cytologic specimens from two outpatient gynecological clinics in a region of southeast Spain. *BMC Infect Dis*, **9**:124.

Cricca M, Morselli-Labate AM, Venturoli S, Ambretti S, Gentilomi GA, Gallinella G, Costa S, Musiani M, Zerbini M. 2007. Viral DNA load, physical status and E2/E6 ratio as markers to grade HPV16 positive women for high-grade cervical lesions. *Gynecol Oncol.*, **106**:549–557.

Federal Budget Institute of Science. 2018. AmpliSens HPV HCR genotype-titre-FRT PCR kit Manual Instruction. available at:*https://interlabservice.ru/upload/iblock/77b/HPV%2016-18-FRT_130218.pdf*.

Federal State Statistics Service. 2018. Analytic note on the age and sex composition of the population Rostov region. available at: *https://www.donland.ru/upload/uf/5c8/26_04_2019_Prilozhenie.pdf*.

Forman D, Martel C de, Lacey CJ, Soerjomataram I, Lortet-Tieulent J, Bruni L, Vignat J, Ferlay J, Bray F, Plummer M. 2012. Global burden of human papillomavirus and related diseases. *Vaccine*, **30**:F12–F23.

Gallegos-Bolaños J, Rivera-Domínguez JA, Presno-Bernal JM, Cervantes-Villagrana RD. 2017. High prevalence of co-infection between human papillomavirus (HPV) 51 and 52 in Mexican population. *BMC Cancer*, **17**:531.

Gravitt PE, Winer RL. 2017. Natural history of HPV infection across the lifespan: role of viral latency., *Viruses* **9**(10):267.

Guan P, Howell-Jones R, Li N, Bruni L, Sanjosé S de, Franceschi S, Clifford GM. 2012. Human papillomavirus types in 115,789 HPV-positive women: a meta-analysis from cervical infection to cancer. *Int J cancer.*, **131**:2349–2359.

Gupta SM, Mania-Pramanik J. 2019. RETRACTED ARTICLE: Molecular mechanisms in progression of HPV-associated cervical carcinogenesis. *J Biomed Sci*,**26**:1–19.

ICO/IARC Information Centre on HPV and Cancer. 2019. Human Papillomavirus and Related Diseases Report.Russian Federation. available at: *https://hpvcentre.net/statistics/reports/RUS.pdf.*

Karuri AR, Kashyap VK, Yallapu MM, Zafar N, Kedia SK, Jaggi M, Chauhan SC. 2017. Disparity in rates of HPV infection and cervical cancer in underserved US populations., *Front Biosci (Schol Ed)* **9**: 254-269.

Kleter B, Doorn L-J Van, Schrauwen L, Molijn A, Sastrowijoto S, Schegget J ter, Lindeman J, Harmsel B ter, Burger M, Quint W. 1999. Development and clinical evaluation of a highly sensitive PCR-reverse hybridization line probe assay for detection and identification of anogenital human papillomavirus. *J Clin Microbiol*, **37**:2508–2517.

Kulmala SA, Shabalova IP, Petrovitchev N, Syrjänen KJ, Gyllensten UB, Syrjänen SM. 2007. Prevalence of the most common high-risk HPV genotypes among women in three new independent states of the former Soviet Union. *J Med Virol*, **79**:771–781.

Li N, Franceschi S, Howell-Jones R, Snijders PJF, Clifford GM. 2011. Human papillomavirus type distribution in 30,848 invasive cervical cancers worldwide: Variation by geographical region, histological type and year of publication. *Int J cancer*, **128**:927–935.

Li Z, Liu F, Cheng S, Shi L, Yan Z, Yang J, Shi L, Yao Y, Ma Y. 2016. Prevalence of HPV infection among 28,457 Chinese women in Yunnan Province, southwest China. *Sci Rep*, **6**:21039.

Marochko KV, Artymuk NV. 2017. Features of Papillomavirus Infection in Human Immunodeficiency Virus-Infected Women. *Fundam Clin Med*, **2**:35–41.

Massad LS, Keller MJ, Xie X, Minkoff H, Palefsky J, D'Souza G, Colie C, Villacres MC, Strickler HD. 2016. Multitype infections with human papillomavirus: Impact of HIV coinfection. *Sex Transm Dis*, **43**(10):637-641.

Mitchell SM, Sekikubo M, Biryabarema C, Byamugisha JJK, Steinberg M, Jeronimo J, Money DM, Christilaw J, Ogilvie GS. 2014. Factors associated with high-risk HPV positivity in a low-resource setting in sub-Saharan Africa. *Am J Obstet Gynecol*, **210**:81-e1.

Mkrtchyan L, Kaprin A, Ivanov S, Kiseleva V, Minakova J V., Lyubina L V., Bezyaeva G, Panarina L V., Zamulaeva I, Krikunova L. 2018. Prevalence of high-risk carcinogenic human papillomavirus types in women with proved neoplastic lesions in the cervix. *Radiat Risk (Bulletin Natl Radiat Epidemiol Regist.*,**27**:55–64.

Moberg M, Gustavsson I, Wilander E, Gyllensten U. 2005. High viral loads of human papillomavirus predict risk of invasive cervical carcinoma. *Br J Cancer*, **92**:891–894.

Muñoz N, Bosch FX, Sanjosé S De, Herrero R, Castellsagué X, Shah K V, Snijders PJF, Meijer CJLM. 2003. Epidemiologic classification of human papillomavirus types associated with cervical cancer. *N Engl J Med*, **348**:518–527.

Nah E-H, Cho S, Kim S, Cho H-I. 2017. Human papillomavirus genotype distribution among 18,815 women in 13 Korean cities and relationship with cervical cytology findings. *Ann Lab Med*, **37**:426–433.

Niyazmetova L, Aimagambetova G, Stambekova N, Abugalieva Z, Seksembayeva K, Ali S, Azizan A. 2017. Application of molecular genotyping to determine prevalence of HPV strains in Pap smears of Kazakhstan women. *Int J Infect Dis.*, **54**:85–88.

Oliveira LHS, Rosa MLG, Cavalcanti SMB. 2008. Patterns of genotype distribution in multiple human papillomavirus infections. *Clin Microbiol Infect*, **14**:60–65.

Omar VE, Orvalho A, Nália I, Kaliff M, Lillsunde-Larsson G, Ramqvist T, Nilsson C, Falk K, Nafissa O, Vindorai JI. 2017. Human papillomavirus prevalence and genotype distribution among young women and men in Maputo city, Mozambique. *BMJ Open*, **7(7)**: e015653.

Radley D, Saah A, Stanley M. 2016. Persistent infection with human papillomavirus 16 or 18 is strongly linked with high-grade cervical disease. *Hum Vaccin Immunother* **12**:768–772.

Rodríguez AC, Schiffman M, Herrero R, Hildesheim A, Bratti C, Sherman ME, Solomon D, Guillén D, Alfaro M, Morales J. 2010. Longitudinal study of human papillomavirus persistence and cervical intraepithelial neoplasia grade 2/3: critical role of duration of infection. *J Natl Cancer Inst*, **102**:315–324.

Rodríguez AC, Schiffman M, Herrero R, Wacholder S, Hildesheim A, Castle PE, Solomon D, Burk R, Group PEG. 2008. Rapid clearance of human papillomavirus and implications for clinical focus on persistent infections. *J Natl Cancer Inst*, **100**:513–517.

Rogovskaya SI, Shabalova IP, Mikheeva I V, Minkina GN, Podzolkova NM, Shipulina OY, Sultanov SN, Kosenko IA, Brotons M, Buttmann N. 2013. Human papillomavirus prevalence and type-distribution, cervical cancer screening practices and current status of vaccination implementation in Russian Federation, the Western countries of the former Soviet Union, Caucasus region and Central Asia. *Vaccine*, **31**:H46–H58.

Roik E, Sharashova E, Kharkova O, Nieboer E, Postoev V, Odland JØ. 2018. Sociodemographic characteristics, sexual behaviour and knowledge about cervical cancer prevention as risk factors for high-risk human papillomavirus infection in Arkhangelsk, North-West Russia. *Int J Circumpolar Health.*, **77**:1498681.

Samoylova E V, Shaikhaiev GO, Petrov S V, Kisseljova NP, Kisseljov FL. 1995. HPV infection in cervical-cancer cases in Russia. *Int J cancer*, **61**:337–341.

Sanjosé S De, Diaz M, Castellsagué X, Clifford G, Bruni L, Muñoz N, Bosch FX. 2007. Worldwide prevalence and genotype distribution of cervical human papillomavirus DNA in women with normal cytology: a meta-analysis. *Lancet Infect Dis*, **7**:453–459.

Shipitsyna E, Zolotoverkhaya E, Kuevda D, Nasonova V, Romanyuk T, Khachaturyan A, Orlova O, Abashova E, Kostyuchek I, Shipulina O. 2011. Prevalence of high-risk human papillomavirus types and cervical squamous intraepithelial lesions in women over 30 years of age in St. Petersburg, Russia. *Cancer Epidemiol*, **35**:160–164.

Silva MB Da, Chagas BS, Guimarães V, Katz LM, Felix PM, Miranda PM, Lima AA, Arraes LC, Martins DB, Lima Filho JL. 2009. HPV31 and HPV33 incidence in cervical samples from women in Recife, Brazil. *Genet Mol Res.*, **8**:1437–1443.

Sirotkina I, Smith R. 2012. Russian Federation. *In D. B. Baker (Ed.), Oxford library of psychology. The Oxford handbook of the history of psychology: Global perspectives. Oxford University Press.* (p. 412–441)**.**

Suligoi B, Vittori G, Salfa MC, Timelli L, Corsini D, Fattorini G, Mariani L. 2017. Prevalence and incidence of external genital warts in a sample of Italian general female population. *BMC Infect Dis*, **17**:126.

Sun C-A, Lai H-C, Chang C-C, Neih S, Yu C-P, Chu T-Y. 2001. The significance of human papillomavirus viral load in prediction of histologic severity and size of squamous intraepithelial lesions of uterine cervix. *Gynecol Oncol*, **83**:95–99.

Vinodhini K, Shanmughapriya S, Das BC, Natarajaseenivasan K. 2012. Prevalence and risk factors of HPV infection among women from various provinces of the world. *Arch Gynecol Obstet*, **285**:771–777.

Wang J, Tang D, Wang J, Zhang Z, Chen Y, Wang K, Zhang X, Ma C. 2019a. Genotype distribution and prevalence of human papillomavirus among women with cervical cytological abnormalities in Xinjiang, China. *Hum Vaccin Immunother*, **15**:1889–1896.

Wang Y, Meng Y, Li W, Zhang X, Deng Z, Hu M, Shen P, Xu S, Fu C, Jiang W. 2019b. Prevalence and Characteristics of hrHPV Infection among 414,540 Women: A Multicenter Study in Central and Eastern China. *J Cancer*, **10**(8):1902-1908.

Widdice LE, Breland DJ, Jonte J, Farhat S, Ma Y, Leonard AC, Moscicki A-B. 2010. Human papillomavirus concordance in heterosexual couples. *J Adolesc Heal*, **47**:151–159.

Xi LF, Hughes JP, Castle PE, Edelstein ZR, Wang C, Galloway DA, Koutsky LA, Kiviat NB, Schiffman M. 2011. Viral load in the natural history of human papillomavirus type 16 infection: a nested case–control study. *J Infect Dis*, **203**:1425–1433.

Zeng Z, Yang H, Li Z, He X, Griffith CC, Chen X, Guo X, Zheng B, Wu S, Zhao C. 2016. Prevalence and genotype distribution of HPV infection in China: analysis of 51,345 HPV genotyping results from China's largest CAP certified laboratory. *J Cancer*, **7** (9):1037-1043.

Zumbach K, Kisseljov F, Sacharova O, Shaichaev G, Semjonova L, Pavlova L, Pawlita M. 2000. Antibodies against oncoproteins E6 and E7 of human papillomavirus types 16 and 18 in cervical-carcinoma patients from Russia. *Int J cancer*, **85**:313–318.

Zykova T, Nerodo G, Bogomolova O, Duritsky M, Sustretov V, Nikitina V, Menshenina A, Shevchenko A, Khomutenko I, Kruse P. 2018. Prevalens, viral load and types diversity of high-risk HPV in patients with infl ammatory and tumor diseases. *Med Her South Russ*, **9**:42–50.

JJBS

Volume 14, Number 3, September 2021
ISSN 1995-6673
Pages 403 - 412

Jordan Journal of Biological Sciences

Production of Chemotherapeutic agent L-asparaginase from Gamma-Irradiated *Pseudomonas aeruginosa* WCHPA075019.

Amany, B. Abd El–Aziz[1,*]; Wesam, A. Hassanein[2]; Zakaria, A. Mattar[1]; and Rabab, A. El-Didamony[2]

[1]*Microbiology Department, National Center for Radiation Research and Technology, Atomic Energy Authority, Nasr City, Cairo, Egypt;*[2]*Department of Botany and Microbiology, Faculty of Science, Zagazig University, Zagazig, Egypt.*

Received: June 24, 2020; Revised: October 28, 2020; Accepted: November 10, 2020

Abstract

Because of the dangers and painful effects of chemotherapeutic drugs, the need for therapeutic agents with less adverse effects will increase several times in the coming years. L-asparaginase enzyme is an effective antitumor agent, especially acute lymphoblastic leukemia, with no side effects compared to other chemotherapeutic agents. Microorganisms are emerging as a safer source of L-asparaginase. Therefore, the findings of new L-asparaginase-producing bacterial strains with high yield for therapeutic applications become necessary. From twenty bacterial isolates tested for their L-asparaginase activity, 16S rRNA sequencing for the most potent isolate showed that the selected isolate had 100% identity to *pseudomonas aeruginosa* strain (accession number: WCHPA075019). In the presence of L-asparagine (1%) and glucose (1%) as nitrogen and carbon sources at a low dose of gamma radiation (0.75 kGy), the maximum productivity of L-asparaginase was reached after 2 days at 35 ° C, pH 7.6 under shaking at 200 rpm. Purification of L-asparaginase with 70% ammonium sulphate, followed by Sephadex G100 increases enzyme purity by 1.5-fold after gel filtration. Pure L-asparaginase had a molecular weight of 123 kDa by SDS- PAGE. The maximum activity of the enzyme against L-asparagine was detected at 35°C and pH 9.0 after 30 min and 200 mM substrate. L-asparaginase activated in the presence of metal ions such as K+, and Na+, not affected when exposed to EDTA and strongly inhibited in the presence of Ba2+, and Cd2+. The anticancer activity of the purified enzyme was tested in vitro against three types of cell line carcinoma. The growth inhibition of L-asparaginase for HEPG2 carcinoma cell line (IC50 value of 3.5 µg/ml) was greater than the inhibition of HCT and MCF-7 carcinoma cell lines with IC50 value of 3.8 and 12.5 µg/ml, respectively relative to the growth of the untreated control cells.

Keywords: *pseudomonas aeruginosa*, 16s rDNA analysis, L-asparaginase, Optimization, Gamma radiation, Purification, Enzyme activity, Anti-cancer.

1. Introduction

Microbial-source enzymes are potential biocatalysts used in various reactions and are part of the most essential products required to meet human needs in many fields (Olukunle and Ajayi, 2018). Approximately, 40% of global enzyme sales are L-asparaginase, which considered as one of the major important biomedical and biotechnological groups of therapeutic enzymes (Qeshmi *et al*., 2018). L-asparagine is an essential amino acid used in normal and cancer cell nutritional requirements. The enzyme L-asparaginase converts L-asparagine to ammonia and aspartic acid (Chand *et al*., 2020). The major medical use of L-asparaginase is L-asparagine elimination from the blood of acute lymphoblastic leukemia (ALL) treated patients in order to prevent a recurrence (Gutierrez *et al*., 2006).

In the 19th WHO list of specific medicinal products, L-asparaginase enzyme is listed as a cytostatic adjuvant to acute lymphoblastic leukemia, as well as in the WHO model list of essential medicinal products for children (WHO, 2015).

The enzyme is commonly used as an anticancer agent because it is non-toxic biodegradable, cheap, and can be easily supplied at the local site. Recent clinical trials have shown that this enzyme is also a promising agent in the treatment of certain forms of human's neoplastic cells (Alrumman *et al*., 2019).

Because of immeasurably useful medical applications, L- asparaginase biotechnological production has become the subject of extensive research by many researchers worldwide. L-asparaginase activity was frequently reported in plants, micro-organisms (bacteria, fungi, and actinomycetes), animals, and in the serum of certain rodents but was not isolated from a human source (Lalitha and Ramanjaneyulu, 2016). Many genera of bacteria, *Bacillus circuans* (Prakasham *et al*., 2010), *Bacilus brevis* (Narta *et al*., 2011), *Pseudomonas flurescens* (Sinha *et al*., 2015), *Pseudomonas aeruginosa* (Saeed *et al*., 2018), and *Escherichia coli* (Kante *et al*., 2019) are reported as L-asparaginase producers.

* Corresponding author e-mail: abdelazizamany@gmail.com.

Optimizing research conditions aiming to repeatedly increase L-asparaginase yield is the goal of many studies (Pallem, 2019). Among all the fermentation parameters tested, Prakasham *et al*. (2007) found that the inoculum volume incubation temperature and medium pH are the main effective parameters at a single level. These factors account for more than 60% of enzyme total yield. Furthermore, Arumugam and Senthil (2017) tested the effect of the nitrogen source on enzyme production under various conditions using the one factor at a time method (OFAT). Different studies indicated that low doses of gamma radiation can improve the growth and metabolism of microorganisms. Abdelrazek *et al*. (2019) use gamma rays to increase the productivity of L-asparaginase.

Specific purification steps were applied to the crude culture filtrate to obtain a pure enzymatic preparation. Various purifying steps, including ammonium sulfate fractionation, were followed by separation on Sephadex G-100 and CM-Sephadex C50 (El-Bessoumy *et al*., 2004) or partial purification of the ammonium sulfate precipitation and dialysis (Arumugam and Senthil, 2017). Obtained results demonstrated an increase in treated L-asparaginase activity relative to the crude enzyme.

Some L-asparaginase preparations are currently approved for ALL treatment (Horvath *et al*., 2019). Asparaginase from *Escherichia coli* and *E. chrysanthemi* was considered for therapeutic purposes. Due to their serious side effects, such as liver dysfunction, allergies, and central nervous system disorders, it did not achieve complete remission, (Egler *et al*., 2016). To overcome these defects, further studies are required to find new bacterial strains that produce L-asparaginase without these effects (Fatima *et al*., 2019).

The aim of this research is to optimize the culture conditions for l-asparaginase production by a selected local bacterial isolate and to investigate the effect of various gamma irradiation low-doses on the production. Extraction and characterization of the purified enzyme and determination for the purified enzyme therapeutic efficacy as an anti-cancer in vitro against standard cancer cell lines were also evaluated.

2. Materials and Methods

2.1. Materials

2.1.1. Chemicals and media.

Analytical grade reagents and other chemicals were obtained from El-Gomhoria Company, Cairo, Egypt. From Sigma Aldrich (St. Louis, Missouri, USA), media and L-asparagine were bought.

2.1.2. Samples

Samples were collected from various asparagine rich sources and screened for isolation of bacteria-producing L-asparaginase. Bacterial samples have been isolated from fish, meat, cheese, rice, yellow lentils, asparagus, black lentils, potatoes, soybeans, eggs, milk, and beans. All sources were refined and exposed to the air for a day to activate bacterial growth.

2.2. Methods

2.2.1. Isolation, purification, and screening of bacterial isolates for L- asparaginase production

For each sample taken, 10g sample was inoculated in 90 ml nutrient broth. The samples were serially diluted (10^{-1}: 10^{-8}) and from each dilution, 0.1 ml was streaked over solid modified M9 medium (Gulati *et al*., 1997). After 24h of incubation at 37°C, the pink color of the plate indicated L-asparaginase production. A single colony of each isolate was collected and streaked on nutrient agar medium several times until single pure colonies were obtained. Pure cultures were reserved at 4°C on slants of nutrient agar medium for further studies (Atlas and Parks, 1993).

2.2.2. Screening of bacterial isolates for L- asparaginase production A. Qualitative assay of L –asparaginase

Screening procedure based on the principle that the pH indicator Phenol red was incorporated. It is yellow at pH below 7 (acidic pH), and above pH 7 it turns pink (alkaline pH).

Primary screening using agar well diffusion (Magaldi et al., 2004).

Fifty ml of modified M9 broth medium was taken in conical flasks, inoculated with 1 ml of 24 h aged bacterial culture suspension, and incubated for 24 h at 37 °C. After that, 30 min centrifugation for the culture broth was carried out at 4 °C and 5000 rpm. For each isolate, cell-free supernatant (100 µl) was poured into a well (8 mm diameter) in a modified M9 agar plate. At 4 °C for 12 h, the inoculated plate was left to diffuse the filtrate into the medium and then incubated for 24 h at 37 °C. Diameters measuring of the pink area with a yellow background around the hole (mm) stating L-asparaginase activity. The cultures with high enzyme production were selected for further studies.

Disc diffusion technique (Balouiri et al., 2016***).***

The isolated bacteria were inoculated in Erlenmeyer flasks of modified M9 broth medium and incubated for 24 h at 37 °C. On sterilized filter paper discs (6mm) 25µl from cell-free supernatant was suspended. Then saturated discs were placed on the solid modified M9 medium surface and kept for 12 h at 4°C to allow diffusion of the filtrate and then the plates incubated for 24h at 37°C. Diameters of the pink zone around discs were measured, and the more L- asparaginase producer was selected for further studies.

B. Quantitative assay of L –asparaginase (Imada et al., 1973***).***

The modified M9 medium (50 ml) has been inoculated with a 24-h old bacterial cell suspension (2 ml), and the un-inoculated medium has been used as a control. The flask was incubated at 37°C with shaking (250 rpm) for 48 h. Centrifugation of the bacterial culture was carried out at 6000 rpm for 20 min.

2.2.3. Estimation of L-asparaginase enzyme activity in culture filtrates

Nesslerization determined the culture filtrate enzyme activity. From the cell-free supernatant or enzyme solution, 0.1 ml of the sample was combined with 0.9 ml 0.1 M Tris-HCl buffer (pH 8.5), and then 1 ml 0.04 M L-asparagine substrate was added. After incubating at 37°C

for 30 minutes, the reaction was terminated with 0.5 ml of tri-chloro-acetic acid (TCA) 1.5 M.

Dilution of 0.1 ml of supernatant to 8 ml using distilled water after centrifugation for protein precipitation occurred before treatment with Nessler's reagent (1.0 ml). For 15 minutes, the brown reaction was allowed to proceed, and the ammonia release was estimated at 500 nm. A typical ammonium-sulfate graph at different concentrations (1.5-11.8 µg / ml) was used for evaluating the liberated ammonia.

2.2.4. Determination of enzyme activity

The released quantity of NH_3 from asparagine is used to calculate the activity of the L-asparaginase enzyme (Peterson and Ciegler, 1969).

The International Unit (IU) identified the activity of the L-asparaginase enzyme as the quantity of enzyme needed to release one micromole of ammonia from L-asparagine per ml per minute (µmole / ml/min) at pH 8.5 and 37 ° C (Manna *et al*., 1995).

Bovine serum albumin (BSA) was used for the determination of protein contents (Lowery *et al*., 1951).

The amount of enzyme required for releasing 1µ mole of the product/min /mg of protein was considered as specific activity (Lalitha and Ramanjaneyulu, 2016).

2.2.5. Characterization and identification of the most potent L-asparaginase producing strain.

According to the standard biochemical and physiological identification test described in Bergey's Manual for Systematic Bacteriology, the most active isolate was identified (Brenner *et al*., 2005), and 16S rRNA gene sequencing was used for confirmation of the identification.

Extraction of DNA

On a rotary shaker (120 rpm), the selected bacterial strain was cultivated (on nutrient broth) overnight at 30°C. Bacterial DNA has been extracted using the Bacterial Genomic DNA Mini-Prep Kit (Axygen cat. No. V110440-05).

Polymerase chain reaction (PCR)

The specificity of primers is revised by the ribosome database (PROBE CHECK function) and BLAST search tool. In the Perkin Elmer 2400 (Nowalk, CT) thermo cycler, DNA amplification is performed on a pure 2 µl to 3µl sample, each 1µl sample contains approximately 150 ng DNA. The final volume of PCR amplification reaction was 100µl; 0.2µM from each primer (F1 and R1), 200µM dNTPs, 2.0 mM MgCl2 and 2.5 units of Maxima® Hot start Taq DNA polymerase (Fermentas, www. fermentas.com) mixed by PCR buffer (1X). The thermal cycle (PCR) steps were applied as follows; 5 min initial denaturation at 95°C, followed by 35 cycles of denaturation at 94°C for 1 min, primer annealing for 1 min at 55°C, 2min extension at 72°C. DNA was extended for 10 min at 72 °C after the last cycle (Khan *et al*., 2018).

DNA Sequencing

The amplification has been confirmed by analysis of 5 µl of the PCR product on 1% agarose gel (Promega) by electrophoresis. The size of the resulting PCR product ranged from 1450 to 1500 bp (Yamamoto and Harayama, 1998).

The PCR purification kit (Fermentas, Germany) was used for purification of the PCR products. Using the same PCR primers, the 16S rDNA amplicon was sequenced using an ABI377 DNA automatic sequencer (Perkin Elmer, Applied Bio-system Div., Waltham, USA).

2.2.6. One variable at a time method for Optimization of L-asparaginase production

Optimization of the experiments was carried out using a one factor at a time (OFAT) strategy. The effect of different nutritional and physiological parameters was evaluated by changing just one factor at a time and leaving the other factors stable. The physiological parameters that were investigated included initial pH (4.0-9.0), incubation time (18, 24, 48, 60, 72, 84, and 96 h), and incubation temperature (from 25 to 60 °C), with temperatures increasing by 5 °C each time. In order to test the impact of different sources of carbon and nitrogen (nutritional parameters), maltose, starch, fructose, lactose, xylose, sucrose, and mannitol (1% w / v) were added separately to the M9 fermentation medium by replacing the glucose, and various sources of nitrogen (L-arginine, yeast, peptone, NH_4Cl, $NaNO_3$, Glutamine, and NH_4SO_4) were added separately at final concentration equimolecular to locate in 5 g of L- asparagine. Under static and shaking conditions at various speeds of 100, 150, and 200 rpm, M9 basal liquid media were inoculated and incubated for 48 h at 35 ° C to study the effect of static and shaking conditions on the enzyme production.

2.2.7. Influence of different gamma radiation doses on L-asparaginase production

At the National Center for Radiation Research and Technology in Nasr City, Cairo, Egypt, using an experimental ^{60}Co Russian gamma chamber, the M9 broth medium from the 24h test bacteria was exposed to various low doses of gamma radiation (0.25, 0.5, 0.75 and 1.5 kGy). At the time of the experiment, the average dose rate was 1 kGy / 50 min. The irradiated samples were grown on flasks containing M9 medium at pH 7.6 under shaking conditions at 200 rpm and 35 ° C for 48 h (Abdelrazek *et al*., 2019).

The cell free filtrate was used at the end of each test period for measuring protein (mg / ml) and the activity of the enzyme (U / ml) as previously mentioned.

2.2.8. Purification of L-Asparaginase Crude enzyme preparation

The experimental strain was grown in the modified production medium (M9 medium) under optimal condition. The cell-free filtrate obtained after the culture fermentation was harvested, centrifuged (10,000 rpm) for 30 min and considered as the crude enzyme (Gulati *et al*., 1997).

Ammonium sulphate precipitation

A slow addition of ammonium sulphate to the crude enzyme by stirring was submitted at 4 °C until the desired saturation (70%) of ammonium sulphate was achieved (Bollag *et al*., 1996). The mixture was kept at 4 ° C overnight, and then the protein precipitation was carried out by centrifugation (10,000 rpm) for 15 min at 4°C. The

precipitate protein pellet was immediately dissolved at a minimal volume of 0.1 M buffer (citrate phosphate: pH 7). The protein content and enzyme activity of the dissolved fractional precipitate were tested.

Dialysis

Precipitated pellets were introduced into cellulose bag for dialysis against distilled water and then were dialyzed against phosphate buffer pH7.0 (Bhargavi and Jayamadhuri, 2016). The enzyme preparation was concentrated against polyethylene glycol crystals (PEG).

Sephadex gel filtration

The concentrated elution fractions were combined and applied to a Sephadex G-100 column (2.5x45cm) pre-equilibrated with the same buffer at a flow rate of 20 ml/h. Combine the active fractions, concentrate, and examined for protein (mg/ml) content and enzyme activity (U/ml). The fraction with a sharp peak was pooled and concentrated by the dialysis membrane and used for further study (Bhargavi and Jayamadhuri, 2016).

SDS- PAGE protein electrophoresis

SDS-polyacrylamide gel electrophoresis (SDS-PAGE) was performed at the Regional Center for Mycology and Biotechnology Azhar University Cairo, Egypt. SDS-PAGE was made in accordance to the method of Laemmli (1970), using a 10% separating gel and 5% stacking gel containing 0.1% SDS. The gel was strained with coomassie brilliant blue R-250. Then distained with methanol, acetic acid and water in the ratio of 4:1:5.

Determination of molecular weight

The molecular weight of the purified L-asparaginase was determined in comparison with standard molecular weight markers phosphorylase b (97.4 kDa), Bovine serum albumin (66.2kDa), Ovalbumin (45 kDa), carbonic anhydrase (25 kDa) and lactoglobulin (18.4 kDa). Standard curve for protein marker was drawn based on the electrophoretic mobility (Rf) of proteins against their log10 molecular weights.

2.2.9. Biochemical Properties of the purified L-asparaginase enzyme

Effect of pH: The purified enzyme and asparagine reaction mixture were adjusted to different pH values (4.0-9.0) at 35°C for 30 min.

Effect of different incubation temperature: The purified enzyme and asparagine reaction mixture has been incubated for 30 min at various temperatures (25, 30, 35, 40, 45, 50, 55 and 60 °C).

Effect of reaction time: The reaction mixture incubated for 5, 10, 15, 20, 25, 30, 35, 40, 45, 50, 55, and 60 min.

Effect of substrate different concentrations (L-asparagine): Different concentrations of L-asparagine (50, 100, 150, 200, 250 and 300 mM) were used.

Effect of Metal ions (activator / inhibitor): Purified enzymes were separately pre-incubated with different metal ions (Cu^{+2}, Fe^{+2}, Zn^{+2}, $EDTA^{+2}$, Co^{+2}, Ba^{+2}, Ca^{+2}, Mn^{+2}, Mg^{+2}, K^{+}, Na^{+} & Cd^{+2}) for 30 minutes prior to the addition of asparagine (40 mM). At the end of the incubation period, the enzyme activity was measured by using the cell-free filtrate, as previously mentioned.

2.2.10. Anticancer activity

Cell Viability Assay for three cell lines: human hepatocarcinoma hepG2 cell line, colon cancer HCT, and human breast adenocarcinoma (MCF-7), which were from the American Model Culture Collection (ATC Collection, Minisota, United States) have been performed by the Cairo National Cancer Institute in Egypt using MTT (3-(4, 5-dimethyl-2)-2, 5-diphenyltetrazolym bromide. The viability of MTT cells was determined according to Vichai and Kirtikara (2006).

Percentage of cell viability = Optical Density for the treated cells / control cells Optical Density * 100.

Sigmoidal dose-response curve-fitting models (Graphpad Prizm Software, version 3) were used to detect L- asparaginase as an anticancer against three human cell lines.

2.2.11. Statistics and calculations

For each analysis, results have been expressed as a mean ± SD (standard deviation). All tests have been conducted in triplicates, n=3.

3. Results and Discussion

3.1. Screening of isolated bacteria for production of L-asparaginase.

Twenty bacterial isolates were randomly isolated from fish, meat, cheese, rice, yellow lentils, asparagus, black lentils, potatoes, soybeans, eggs, milk, and beans. The data showed that the majority of the isolates are gram-positive, rod-shaped and spore-forming. Modified M9 with a sole source of nitrogen (asparagine, 1%) was the medium used for screening the activity of all isolated bacteria for L-asparaginase production. The change of yellow color of media to pink is a positive indicator for the enzyme production. The plate culture assay indicated that all bacterial isolates exhibited positive production for L-asparaginase with different zone diameter, which provides an assay for L-asparaginase activity. L-asparaginase efficacy was tested spectrophotometrically. Table 1 results show the activity of L-asparaginase in U / ml, and the pink zone (mm) diameter. L-asparaginase activity of the isolates was observed to range from 12.0 to 44 U / ml and the diameter to range from 12 to 37 mm using both agar-well and disk diffusion methods. It is in agreement with Gulati *et al*. (1997), who proved that the transformation of medium color to pinkish was triggered by the production of L-asparaginase.

Table 1. Screening of isolated bacteria for production of L-asparaginase

Isolate no	Sample source	Agar well diffusion (mm) Pink zone diameter	Protein (mg/ml)	Activity (U/ml)	Specific activity (U/mg)
1	Fish	17	0.160	15.0	93.16
2	Fish	16	0.173	18.0	104.0
3	Fish	15	0.158	15.0	94.90
4	Meat	13	0.251	14.7	58.48
5	Cheese	12	0.160	12.0	75.00
6	Rice	18	0.190	10.5	55.63
7	Yellow lentil	29	0.240	32.6	135.0
*8	Asparagus	36	0.320	44.0	137.7
9	Black lentil	28	0.280	34.4	122.8
10	Black lentil	26	0.252	31.8	126.3
11	Potato	18	0.280	15.53	55.40
12	Potato	19	0.220	14.5	65.90
13	Potato	19	0.250	16.6	66.40
14	Soybeans	30	0.260	32.0	123.0
15	Soybeans	28	0.270	30.0	111.1
16	Egg	18	0.216	21.21	69.09
17	Milk	23	0.200	27.20	105.7
18	Milk	20	0.231	26.0	112.1
19	Beans	22	0.190	30.0	120.8
20	Beans	21	0.232	29.2	125.3

*Out of twenty isolates, isolate no 8 was selected as the most L-asparaginase producer.

3.2. Identification and characterization of the most potent isolate

The isolate number (8) was identified using the tests of systematic bacteriology guided by Bergey`s Manual, and the results indicated that it belonged to the genus pseudomonas (Paul and Sinha, 2014). For confirming the identification, isolate No 8 DNA was extracted directly from the organism. Based on the alignment of 16s rDNA available in the gene bank, two primer set was used. 1kb DNA product was obtained in confirmation genus identification. On the other hand, BLAST searches were performed to investigate whether high homology of tested strain exits to other Pseudomonas. The genomic DNA for the bacterial isolates was used as a template for the amplification of rRNA using the forward and reverse primers for 16S rDNA (Figure 1). After running of PCR and agarose gel (Figure 2), the purified PCR products from *P. aeruginosa* were sequenced and the sequence obtained was deposited with the accession number WCHPA075019 in the bank of gene (Figure 3). BLAST studies have shown that the strain tested has a 100% identity with *pseudomonas aeruginosa* and it was identified as *pseudomonas aeruginosa* WCHPA075019.

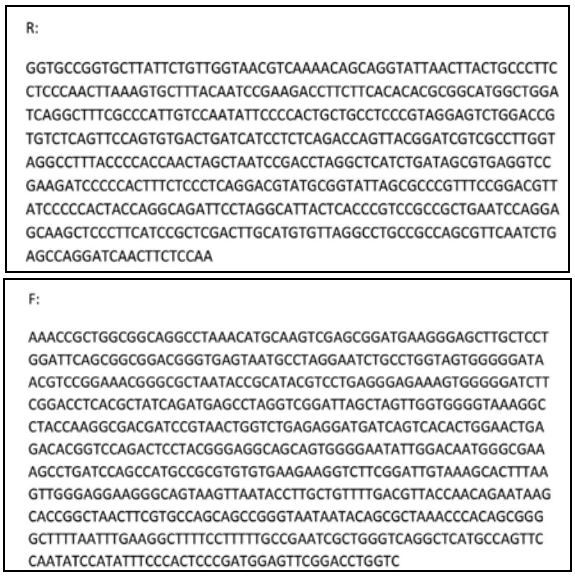

Figure 1. DNA sequences of *pseudomonas aeruginosa.*

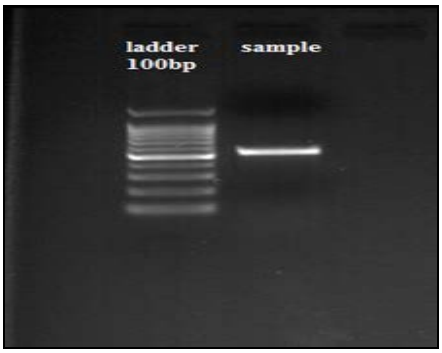

Figure 2. PCR product of 16S *rRNA* of *pseudomonas aeruginosa*.

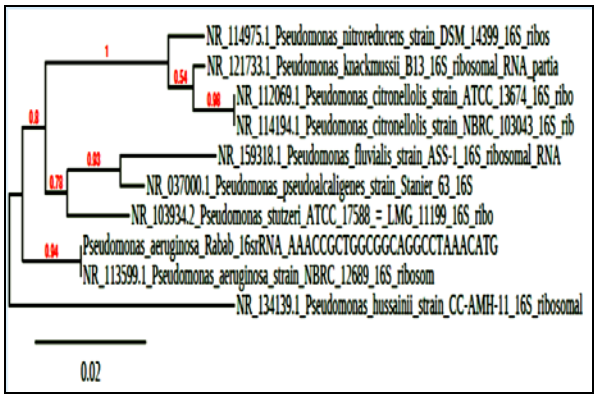

Figure 3. Phylogenetic tree analysis of *pseudomonas aeruginosa* WCHPA075019 obtained after performing 16S *rRNA* sequencing

This is in accordance with Badoei-Dalfard (2015) and Jois *et al*. (2013) who reported that *P. aeruginosa* is a good L-asparaginase producer.

3.3. Optimization of P. aeruginosa WCHPA075019 L-asparaginase production

To optimize *Pseudomonas aeruginosa* L-asparaginase production, many cultural and nutritional parameters were examined. The maximum enzyme production was exhibited at 35°C for 2 days and pH 7.6 in presence of 1% glucose and L-asparagine under shaking condition at 200 rpm (Figure 4). Such findings are in accordance with Komathi *et al*. (2013) who stated that the maximum

enzyme production by *P. aeruginosa* was after 48 h of incubation at 35°C and pH 7.6.

Badoei-Dalfard (2016) revealed that with L-asparaginase and glucose as nitrogen and carbon sources, the largest amount of L-asparaginase by *P. pseudoalcaligens* JHS-71 was obtained at pH 7.0 and 37°C after 48 h. This result was consistent with the data recorded by Badoei-Dalfard (2015), which showed that *P. aeruginosa* strain SN004 maximum production was achieved when glucose was used as carbon source. Various sources of organic and inorganic nitrogen have been tested. The present data showed that *P. aeruginosa* WCHPA075019 was capable of using both organic and inorganic nitrogen sources. L-asparagine was the ideal nitrogen source for the L-asparaginase production (170.7 Umg-1), which indicates that L-asparagine is an L-asparaginase inducer. This results in accordance with Badoei-Dalfard (2015), who confirmed that (0.5%) L-asparagine is the best source of nitrogen for *P. aeruginosa* strain SN004 L-asparaginase maximum production (785 U / ml). Shukla and Mandal (2013) reported that the use of L-asparagine followed by peptone and yeast extract can achieve *Bacillus subtilis* L-asparaginase maximum yield. The maximum enzyme production by *P. aeruginosa* WCHPA075019 occurred at 200 rpm. Also, Kuwabara *et al*. (2015) reported that at 200 rpm *P. aeruginosa* PAO1 L-asparaginase maximum production took place.

3.4. Influence of different gamma radiation doses on L-asparaginase production

Numerous studies have shown that low gamma irradiation doses can improve metabolic activities and microbial development. *P. aeruginosa* was exposed to gamma rays at doses from 0.25 to 1.5 kGy using an experimental ^{60}Co Russian gamma chamber, (dose rate 1kGy/50min). Results showed that enzyme activity increased gradually from 0.25 to 0.75 kGy and maximum activity at 0.75 kGy and decreased sharply at 1.0 kGy dose and had no activity at 1.5 kGy (Figure 5). This result is in agreement with Abd EI-Aziz and Hassan (2010) who showed that radiation dose level 0.75kGy resulted in an increase in the elastase yield of *Bacillus subtilis* by 7.94% and in the final dry weight when compared with non-irradiated control. The inhibitory effect of radiation on a microbial enzyme may be due to the action of ionizing radiation on either of the two components of which the enzymes are made up, i.e. the protein or the prosthetic group. When acting on protein moiety they may oxidize reactive groups, amino groups or double bonds or may act by or precipitation, when acting on the prosthetic group they may produce chemical changes that alter the biological activity of the enzyme (Reisz *et al*., 2014). On the other hand, the improvement by gamma radiation may either be due to an increase in gene copy or gene expression or both (Rajoka *et al*., 1998) and by inducing mutagenesis in the microbial cell to enhance its activity for enzyme production (Awan *et al*., 2011).

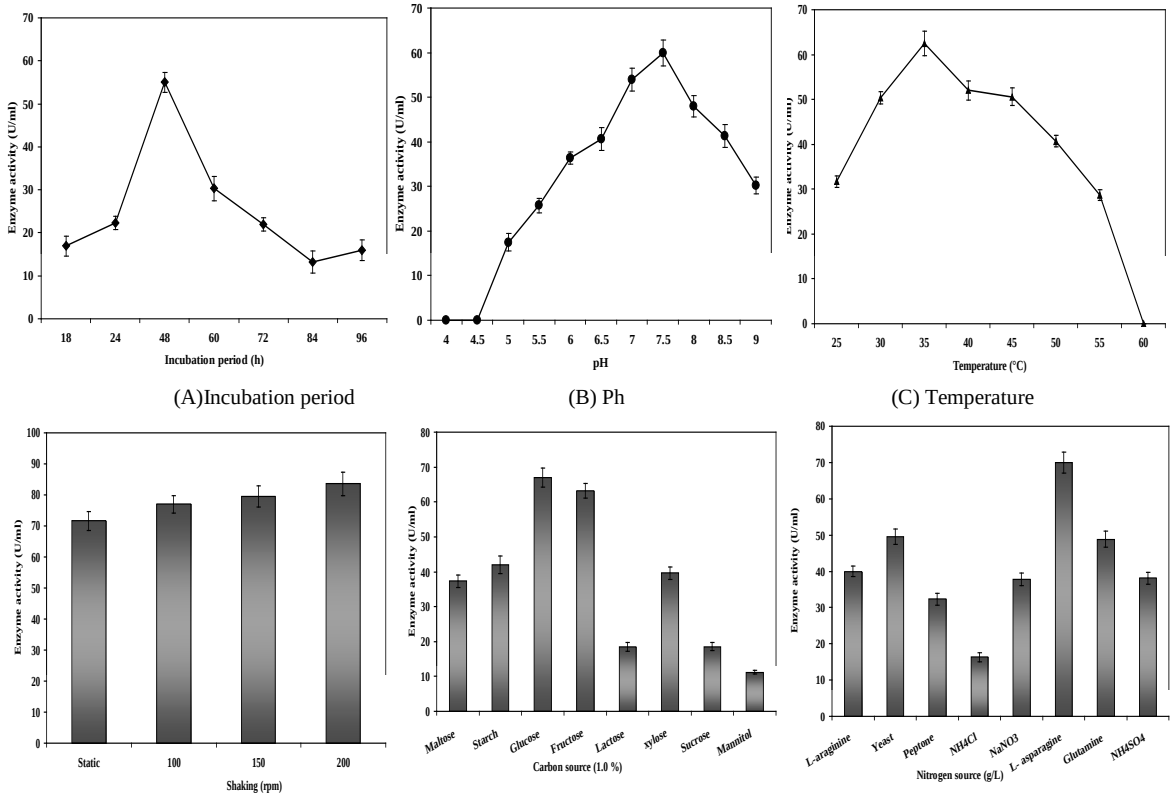

(A)Incubation period (B) Ph (C) Temperature

(D) Static and Shaking (E) Carbon source (F) Nitrogen source

Figure 4. Optimization of the production of *P. aeruginosa* L-asparaginase

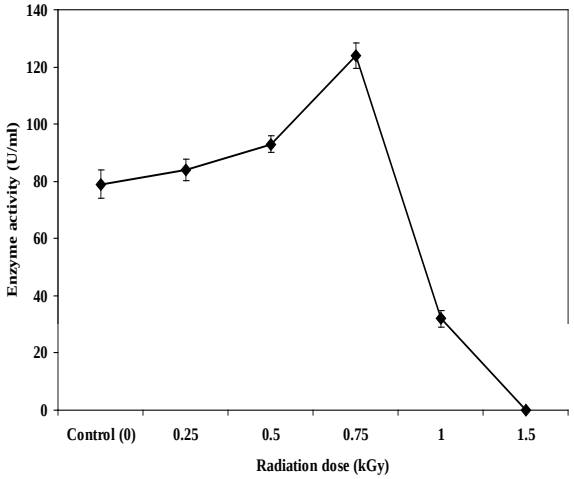

Figure 5. Effect of gamma radiation on *P. aeruginosa* L-asparaginase activity.

3.5. Enzyme Purification

L-asparaginase produced by *P. aeruginosa* in liquid media was purified by Ultra-filtration and combination of gel filtration and ion-exchange chromatography to obvious homogeneity with varying recovery and purification yield.

Results in Table 2 revealed that the final specific enzyme activity was 366 Um/g with 1.5 fold and 6.6% yield. When El-Bessoumy *et al*. (2004) grown *P. aeruginosa* 50071 on solid-state fermentation, the purified enzyme final specific activity was 1900 IU / mg, the purification rate was 106 -fold and the yield was 43 %.

L- asparaginase fractional purification by Sephadex G-100 column chromatography. As a result of gel filtration chromatography on Sephadex, G-100 the specific activity increased to 1.5 fold with a 6.6% yield. Fractions with the highest activity were pooled and dialyzed at 4.0 °C against distilled water (Figure 6).

Table 2. L-asparaginase purification profile.

Purification Steps	Volume (ml)	Enzyme activity (U/ml)	Protein content (mg/ml)	Total activity (U)	Total protein (mg)	Specific activity U/mg	Yield %	Purification fold
Culture filtrate (crude extract)	2730	124	0.48	338520	1310	245.8	100	1
Precipitation by amm.Sulphate (70%)	901	129	0.45	111711	405	287	33	1.17
Sephadex G100	160	139	0.38	22240	60.8	366	6.6	1.5

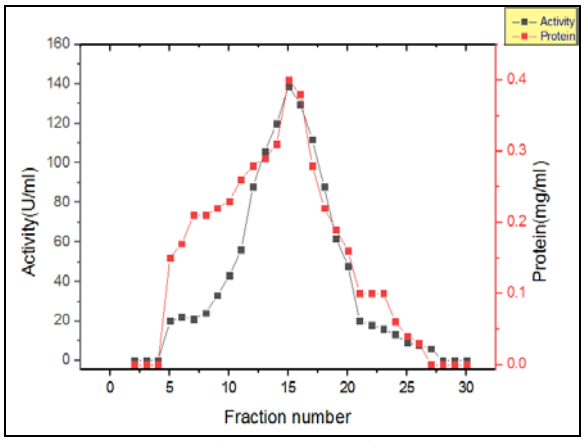

Figure 6. Fractional purification pattern of the L- asparaginase produced by *P. aeruginosa* applying Sephadex G-100 column chromatography.

In addition to demonstrating the purity of the enzyme, the molecular weight was measured. *Pseudomonas aeruginosa* L-asparaginase purified enzyme molecular weight was 123 KDa **(**Figure 7).

The L-asparaginase sizes vary from one organism to another in terms of genus and species. The Pseudomonas L-asparaginase molecular size and subunits vary from a single subunit of 34–33 kDa under non-denaturing and denaturing conditions respectively (Shakambari *et al*., 2019). The molecular weight of *Pseudomonas aeruginosa* pure and crude enzyme samples are found to be 75KDa by Jois *et al*. (2013). Also, *Pseudomonas aeruginosa* L-asparaginase exists as a monomer with a size of 160 kDa as reported by (El-Bessoumy *et al*., 2004). Thus, L-asparaginase shows a wide structural variation in the subunits of the above-mentioned bacteria.

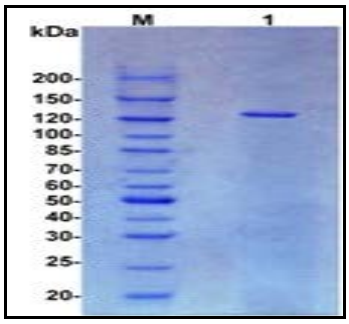

* Lane M =marker protein, Lane 1= purified enzyme.

Figure 7. SDS- PAGE of *P. aeruginosa* purified L-asparaginase.

3.6. Properties of P. aeruginosa L- asparaginase purified enzyme

Clearly, after a 30 min incubation period, the maximum L-asparaginase enzyme activity was achieved (Figure 8A). This finding is consistent with (Komathi *et al*., 2013) who observed the maximum *P. aeruginosa* enzyme activity after 30 min. The maximum recorded activity was also 30 min for *Streptomyces noursei* asparaginase enzyme (Kumar *et al*., 2011). The optimal pH value for *P. aeruginosa* purified L-asparaginase was pH 9 (Figure 8B). El-Bessoumy *et al*. (2004) recorded comparable results for *P. aeruginosa* 50071. Moreover, Shukla and Mandal (2013) recorded maximum activity of *Bacillus subtilis* purified L-asparaginase at pH 9. For every enzyme, there is a specific optimal temperature beyond which there has been a decrease in activity (Kumar *et al*., 2011). In the current study, the optimum incubation temperature was reported at 35 °C (Figure 8C) for maximum activity of *P. aeruginosa* L-asparaginase. Also, the optimal temperature

for the maximum activity of *P. aeruginosa* asparaginase enzyme was observed at 35ºC by Komathi *et al*. (2013).

The findings in (Figure 8D) indicate that by increasing the L-asparagine concentration, the activity of L-asparaginase gradually increases. L-asparaginase maximum activity was determined at asparagine concentration of 200 mM (167 U/ml). *P. aeruginosa* SN004 L-asparaginase maximum production (785 U / ml) was achieved with 0.5% L-asparagine on an optimized medium as defined by Badoei-Dalfard (2015).

The activity of the enzyme decreased when of Mg^{2+}, Cu^{2+}, Zn^{2+}, Ba^{2+}, CO^{2+}, $Mn^{2+}$and Cd^{2} were present by 110, 70, 85, 80, 100, 98 and 60 U/ml, respectively (Figure 8E). However, K^{+} exerted a highly stimulatory effect to occupy the first rank among all tested compounds followed by Na^{+}, Ca^{2+}, and Fe^{2+} with increase in activity by 210, 194, 184, and 177 U/ml, respectively. L-asparaginase activity was not affected by the EDTA chelator agent which indicated that the enzyme was not a metalloprotein. The enzyme reached its maximum activity in optimizing media containing magnesium ions (Shukla and Mandal, 2013).

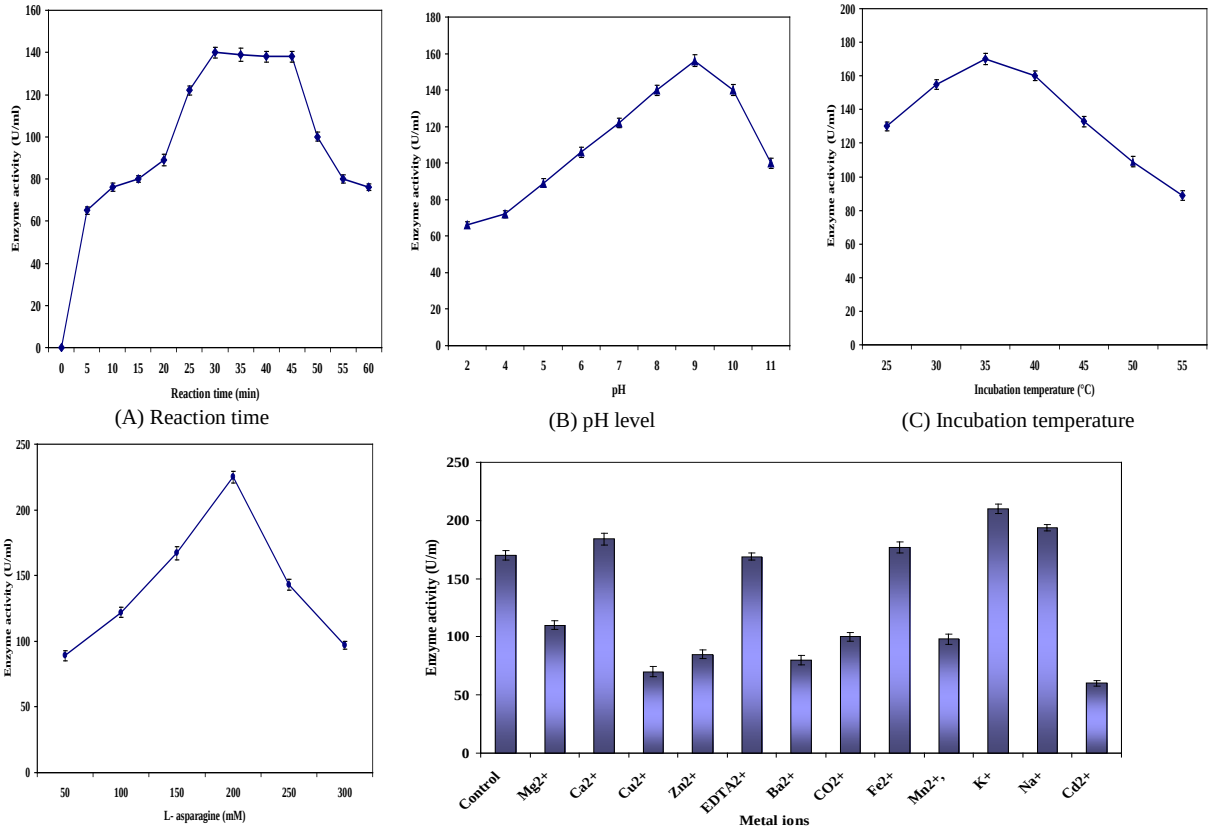

(A) Reaction time (B) pH level (C) Incubation temperature

(D) substrate concentration (E) Metal ions

Figure 8. Characteristics of *P. aeruginosa* L- asparaginase purified enzyme.

3.7. Anticancer activity

In the present study, three tumour cell lines were used to investigate the in vitro antitumor activity of *P. aeruginosa* L-asparaginase enzyme (Figure 9). Incubation of HEPG2-116 with progressive doses of the *P. aeruginosa* asparaginase enzyme causes progressive cell growth inhibition, as indicated by its IC_{50} value of 3.5 µg/ml. The enzyme anti-tumour activity against the breast adenocarcinoma MCF-7 was IC_{50} 12.5 µg /ml. The tested enzyme was found to have activity against HCT-116 cells (IC_{50}, 3.8 µg/ml) compared to the growth of the control (untreated cells). The in vitro cytotoxicity of *Helicobacter pylori* CCUG 17874 new L-asparaginase against a variety of cells has been studied by Cappelletti *et al*. (2008), they stated that gastric epithelial cells AGS and MKN 28 are most affected. When Moharam *et al*. (2010) examined the antioxidant and antitumor activities of *Bacillus sp* R36 asparaginase; they found two human cell lines were inhibited by the enzyme, including colon carcinoma (HCT-116) and hepatocellular carcinoma (HEPG2-116) with IC_{50} value of 218.7 µg/ml and 112.19 µg/ml, respectively.

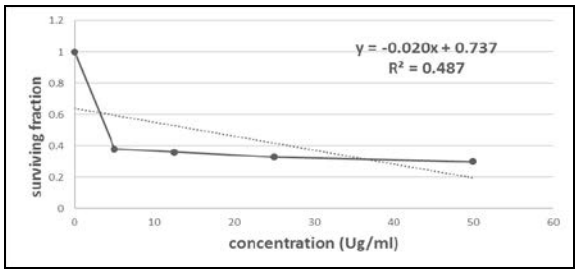

(A) HCT-116 IC_{50}=3.8µg/ml

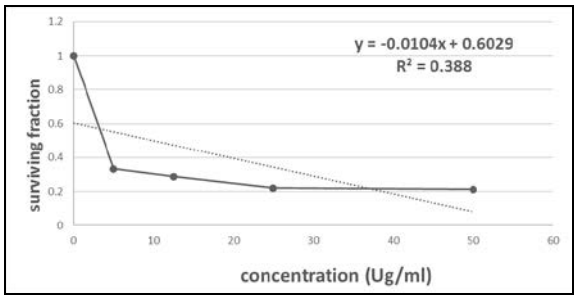

(B) HEPG2-116 IC50=3.5 µg/ml

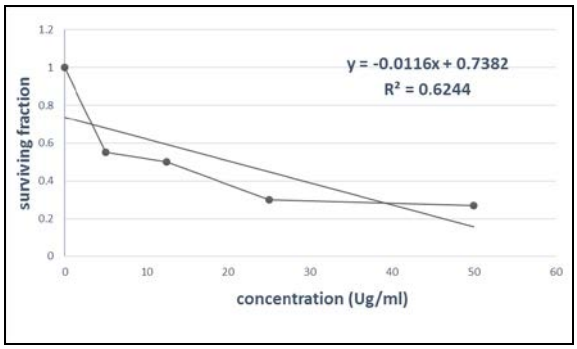

(C) MCF-7 IC_{50}=12.5 µg/ml

The diagram represents the relation between the concentration (horizontal axis) and surviving fraction (vertical axis).

Figure 9. *P. aeruginosa* L-asparaginase toxic effect on cancer cells.

4. Conclusion

L-asparaginase is considered one of the therapeutic enzymes used in the treatment of blood cancer (ALL) in children. Using enzymes developed by these commercial strains causes adverse side effects for patients in the long run. So, finding new bacterial strains that can be used for L-asparaginase commercial production is essential. In this study, the most potent local bacterial isolate *P. aeruginosa* WCHPA075019 isolated from asparagus was selected for the production of L-asparaginase. The culture conditions, nutritional requirements, and low doses of gamma radiation were optimized to reach maximum l-asparaginase productivity. The study was, moreover, extended to purify L- asparaginase and investigate its physicochemical properties. The purified enzyme preparation showed anti-cancer activity against 3 human cell lines. From the results, *P. aeruginosa* WCHPA075019 L-asparaginase may be evaluated clinically as an anticancer pharmaceutical agent for the tested cancer cell lines.

Declaration of competing interests:

None

References

Abd EI-Aziz A B and Hassan A A. 2010. Optimization of Microbial Elastase Production. *Radiation Res appl Sci*., **3 (4B)**: 1237-1257.

Abdelrazek N A, Elkhatib W F, Raafat M M and Aboulwafa M M. 2019. Experimental and bioinformatics study for production of L-asparaginase from *Bacillus licheniformis*: a promising enzyme for medical application. *AMB Express*., **9 (1)**: 39.

Alrumman S, Mostafa Y, Al-izran K, Alfaifi M, Taha T and Elbehairi S. 2019. Production and Anticancer Activity of an L-Asparaginase from *Bacillus licheniformis* Isolated from the Red Sea, *Saudi Arabia*. *Scientific Rep*., **9(1)**:3756.

Arumugam T and Senthil K P. 2017. Optimization of media components for production of antimicrobial compound by *Brevibacillus brevis* EGS9 isolated from mangrove ecosystem. *Microbiol Methods*., **142**: 83-89.

Atlas R M and Parks L C. 1993. Handbook of microbiological media. Boca Raton: CRC Press.

Awan M S, Tabbasam N, Ayub N, Babar M E, Rana S M and Rajoka M I. 2011. Gamma radiation induced mutagenesis in *Aspergillus niger* to enhance its microbial fermentation activity for industrial enzyme production. *Molecular biology reports*., **38(2)**: 1367–1374.

Badoei-Dalfard A. 2015. Purification and characterization of l-asparaginase from *Pseudomonas aeruginosa* strain SN004: Production optimization by statistical methods. *Biocatalysis and agricultural biotechnol*., **4**: 388-397.

Badoei-Dalfard A. 2016. L-asparaginase production in the *pseudomonas pseudoalcaligenes* strain JHS-71 isolated from Jooshan Hot-spring. *Molecular biology Res communications*., **5(1)**: 1–10.

Balouiri M, Sadiki M and Ibnsouda S. 2016. Methods for in vitro evaluating antimicrobial activity: A review. *Pharm analy*., **6(2)**: 71-79.

Bhargavi M and Jayamadhuri R. 2016. Isolation and Screening of Marine Bacteria Producing Anti-Cancer Enzyme L-Asparaginase. *Am J Marine Sci*., **4(1)**: 1-3.

Bollag D M, Rozyeki MD and Edelstein S J. 1996. Protein Methods 2nd ed. Wiley Liss., New York. p. 110.

Brenner D J, Krieg N R, Staley J T and Garrity G M (Eds.). 2005. Bergey's Manual® of Systematic Bacteriology: Volume Two: The Proteobacteria, Part A Introductory Essays. Springer-Verlag US.

Cappelletti D, Chiarelli LR, Pasquetto MV, Stivala S, Valentini G and Scotti C. 2008. *Helicobacter pyloril*-asparaginase: a promising chemotherapeutic agent. *Biochem Biophys Res Communications*., **377(4)**: 1222-1226.

Chand S, Mahajan R, Prasad J, Sahoo D, Mihooliya K, Dhar M and Sharma G. 2020. A comprehensive review on microbial l -asparaginase: Bioprocessing, characterization, and industrial applications. Biotechnol Appl Biochem., **67(4)**: 619-647.

Egler R A, Ahuja S P and Matloub Y. 2016. L-asparaginase in the treatment of patients with acute lymphoblastic leukemia. *Pharm and pharmacotherapeutics.*, **7(2)**: 62-71.

El-Bessoumy A, Sarhan M and Mansour J. 2004. Production, Isolation, and Purification of L-Asparaginase from *Pseudomonas aeruginosa* 50071 Using Solid-state Fermentation. *BMB Reports*., **37(4)**: 387-393.

Fatima N, Khan M M and Khan I A. 2019. L-asparaginase produced from soil isolates of *Pseudomonas aeruginosa* shows potent anti-cancer activity on HeLa cells. *Saudi J Biol sci*., **26(6)**: 1146-1153.

Gulati R, Saxena R and Gupta R. 1997. A rapid plate assay for screening L-asparaginase producing micro-organisms. *Lett Appl Microbiol.*, **24(1)**: 23-26.

Gutierrez J, Pan Y, Koroniak L, Hiratake J, Kilberg M and Richards N. 2006. An Inhibitor of Human Asparagine Synthetase Suppresses Proliferation of an L-Asparaginase-Resistant Leukemia Cell Line. *Chem and Biol.*, **13(12)**: 1339-1347.

Horvath T D, Chan W K, Pontikos M A, Martin L A, Du D, Tan L, Konopleva M, Weinstein N J and Lorenzi L P. 2019. Assessment of l-asparaginase pharmacodynamics in mouse models of cancer. *Metabolites*., **9(1)**: 10.

Imada A, Igarasi S, Nakahama K and Isono M. 1973. Asparaginase and Glutaminase Activities of Micro-organisms. *General Microbiol*., **76(1)**: 85-99.

Jois S, Lakshmikantha RY and Rai P S. 2013. Study On Production, Purification And Characterisation Of L-Asparaginase From *Escherichia Coli* And *Pseudomonas Aeruginosa*. *Int J Pharm, Chem Biol Sci*., **3(3)**: 565-570

Kante R, Somavarapu S, Vemula S, Kethineni C, Mallu M and Ronda S. 2019. Production of Recombinant Human Asparaginase from *Escherichia coli* under Optimized Fermentation Conditions: Effect of Physicochemical Properties on Enzyme Activity. *Biotechnol Bioprocess Eng*., **24(5)**: 824-832.

Khan I, Jahan P, Hasan Q and rao P. 2019. Genetic confirmation of T2DM meta-analysis variants studied in gestational diabetes mellitus in an Indian population. *Diabetes and metabolic syndrome*., **13 (1)**: 688-694.

Komathi S, Rajalakshmi G, Savetha S and Balaji S. 2013. Isolation, production and partial purification of l-asparaginase from P*seudomonas aeruginosa* by solid state fermentation. *Scholars Academic J Pharm*., **2(2)**:55-59.

Kumar S, Dasu V V and Pakshirajan K. 2011. Studies on pH and thermal stability of novel purified L-asparaginase from *Pectobacterium carotojorum* MTCC 1428. *Mikrobiologiia*., **80(3)**: 349–355.

Kuwabara T, Prihanto A, Wakayama M and Takagi K. 2015. Purification and Characterization of *Pseudomonas aeruginosa* PAO1 Asparaginase. *Procedia Environ Sci*., **28**: 72-77.

Laemmli U K. 1970. Cleavage of Structural Proteins during the Assembly of the Head of Bacteriophage T4. *Nature.*, **227**: 680–685.

Lalitha Devi AS and Ramanjaneyulu R. 2016. Isolation of L-Asparaginase Producing Microbial Strains from Soil Samples of Telangana and Andhra Pradesh States, India. India. *Int J Current Microbiol Appl Sci.*, **5(10)**: 1105-1113.

Lowery O H, Rosebrough N J, Farr A L and Randall R J. 1951. Protein measurement with the Folin phenol reagent. *Biological Chem*., **139**: 265-275.

Magaldi S, Mata-Essayag S, Hartung de Capriles C, Perez C, Colella M, Olaizola C and Ontiveros Y. 2004. Well diffusion for antifungal susceptibility testing. *Int J infectious diseases.,* **8(1)**: 39-45.

Manna S, Sinha A, Sadhukhan R and Chakrabarty S.1995. Purification, characterization and antitumor activity of l-asparaginase isolated from *Pseudomonas stutzeri* MB-405. *Current Microbiol.,* **30(5)**: 291-298.

Moharam M E, Gamal-Eldeen A M and El-Sayed S T. 2010. Production, Immobilization and Anti-tumor Activity of L-Asparaginase of *Bacillus sp* R36. *Am Sci*., **6(8)**:131-140.

Narta U, Roy S, Kanwar S and Azmi W. 2011. Improved production of l-asparaginase by *Bacillus brevis* cultivated in the presence of oxygen-vectors. *Bioresource Technol*., **102(2)**: 2083-2085.

Olukunle O F and Ajayi O E. 2018. Screening Wild and Mutant Strains of *Aspergillus flavus* and *Aspergillus niger* Isolated from Plantain Stalks for Amylase Production. *Jordan J Biol Sci.,* **11(5)**: 557 - 562.

Pallem C. 2019. Solid-state fermentation of corn husk for the synthesis of Asparaginase by *Fusarium oxysporum*. *Asian J Pharm Pharm.,* **5(4)**:678-681.

Paul D and Sinha S N. 2014. Extracellular Synthesis of Silver Nanoparticles Using *Pseudomonas aeruginosa* KUPSB12 and Its Antibacterial Activity. *Jordan J Biol Sci.,* **7(4)**: 245 - 250.

Peterson R E and Ciegler A. 1969. L–Asparaginase production by *Erwinia aroideae*. *Appl Microbiol*., **17(6)**: 929–930.

Prakasham R, Hymavathi M, Ch Rao C, Arepalli S, Venkateswara Rao J, Kennady P K, Nasaruddin K, Vijayakumar J B and Sarma P N. 2010. Evaluation of Antineoplastic Activity of Extracellular Asparaginase Produced by Isolated *Bacillus circulans*. *Appl Biochem Biotechnol*., **160(1)**: 72-80.

Prakasham R, Rao C, Rao R, Lakshmi G and Sarma P. 2007. L-asparaginase production by isolated *Staphylococcus sp*.? 6A: design of experiment considering interaction effect for process parameter optimization. *Appl Microbiol.,* **102(5)**: 1382-1391.

Qeshmi F I, Homaei A, Fernandes P and Javadpour S. 2018. Marine microbial L-asparaginase: Biochemistry, molecular approaches and applications in tumor therapy and in food industry. *Microbiol Res.,* **208**: 99-112.

Rajoka M I, Bashir A, Hussain S R S and Malik K A. 1998. γ-ray induced mutagenesis of Cellulomonas biazotea for improved production of cellulases. *Folia Microbiol.*, **43**: 15-22.

Reisz J, Bansal N, Qian J, Zhao W and Furdui C. 2014. Effects of Ionizing Radiation on Biological Molecules—Mechanisms of Damage and Emerging Methods of Detection. *Antioxidants and Redox Signaling*., **21(2)**: 260-292.

Saeed H, Soudan H, El-Sharkawy A, Farag A, Embaby A and Ataya F. 2018. Expression and Functional Characterization of *Pseudomonas aeruginosa* Recombinant l. Asparaginase. *Protein J*., **37(5)**: 461-471.

Shakambari G, Ashokkumar B and Varalakshmi P. 2019. L-asparaginase – A promising biocatalyst for industrial and clinical applications. *Biocatalysis and agricultural biotechnol*., **17**: 213-224.

Shukla S and Mandal S K. 2013. Production optimization of extracellular L-asparaginase through solid- state fermentation by isolated *Bacillus subtilis*. *Int Appl Biol Pharm Technol.,* **4 (1)**: 219-226.

Sinha R K, Singh H R and Jha S K. 2015. Production, purification and kinetic characterization of l-asparaginase from *Pseudomonas fluorescens. Int J Pharm Pharm Sci.,* **7(1)**: 135-138.

Vichai V and Kirtikara K. 2006. Sulforhodamine B colorimetric assay for cytotoxicity screening. *Nature protocols*., **1(3)**: 1112–1116.

World Health Organization. 2015. The selection and use of essential medicines: report of the WHO expert committee, 2015 (including the 19th WHO model list of essential medicines and the 5th WHO model list of essential medicines for children) (Vol. **994**). World Health Organization.

Yamamoto S and Harayama S.1998. Phylogenetic relationships of Pseudomonas putida strains deduced from the nucleotide sequences of gyrB, rpoD and 16S rRNA genes. *Int J Systematic and Evolutionary Microbiol.*, **48(3)**: 813-819.

JJBS

Jordan Journal of Biological Sciences

Volume 14, Number 3, September 2021
ISSN 1995-6673
Pages 413 - 416

Parasite Survey in *Rastrelliger brachysoma* (Short Mackerel) from Selected Fish Markets in Zamboanga City, Philippines

Romenick Alejandro Molina*

Senior High School Department, Zamboanga City State Polytechnic College

Received: June 25, 2020; Revised: September 28, 2020; Accepted: November 7, 2020

Abstract

Rastrelliger brachysoma (short mackerel) or locally known as kabalyas is one of the most commercially important small pelagic fish because of its low price in the market and a good source of protein. However, like other fish, *R. brachysoma* are also prone to parasites. Thus, this study aimed to conduct a parasite survey in *R. brachysoma* sold in selected public markets in Zamboanga City. This study provides a baseline data about parasites in *R. brachysoma* and promote public health awareness with the locals in Zamboanga City. The researcher collected a total of 60 *R. brachysoma* using purposive sampling. In the laboratory, gills, stomach and intestines were removed from the samples and subjected for microscopic examination. Images were taken and used for identification of parasites and verified by experts. Prevalence and mean intensity were computed for parasites. There were eight genera, and three of which were identified to the species level. Among which, the most prevalent were *Dermocystidium sp.* and *Amyloodinium sp.* while *Cryptocaryon irritans*, *Schistosoma sp.* and *Echinorhynchus sp.* were least prevalent. In terms of intensity, *Dermocystidium sp.* has the highest mean intensity while *Schistosoma sp.* has the lowest mean intensity.

Keywords: Mean Intensity, Parasites, Prevalence, *Rastrelliger brachysoma*

1. Introduction

Rastrelliger brachysoma (short mackerel) or locally known as kabalyas, is a species of mackerel in the family Scombridae. It is widely spread in the shallow waters of Southeast Asia (Collette *et al*., 2011). It is one of the most commercially important small pelagic fish because of its low price, serving as a high protein source and contributing significantly to the total income of families engaged in it (Ghazali *et al*., 2012).

In spite of the direct value of short mackerel, most people do not focus so much attention on the health status of *R. brachysoma*. *R. brachysoma* plays an important ecological role as host to a range of taxonomically diverse parasites that exhibit a wide variety of life cycle strategies (Indaryanto *et al*., 2015). Like other fishes, *R. brachysoma* is prone to parasitism, which is a common phenomenon in marine environments (Ruiz, 1991).

Parasites are used increasingly as indicators for the differentiation of marine ecology because parasitic fauna might show a distribution parallel to the host (Madhavi and Lakshmi, 2012). Parasites in fish have been a great concern since they often produce disease conditions in fish which will lead to reduced growth, increase in the fishes' susceptibility to other diseases as well as fish loss (Raissy and Ansari, 2012). Effects of parasitism in fish range from mild to severe depending upon the intensity and pathogenicity of the parasites. As a result, there is a great threat to the fish industry which may result in the failure of production, and some infected fish could be unsuitable for human consumption.

Figure 1. *Rastrelliger brachysoma* (Short Mackerel)

There were several studies conducted in investigating of fish parasites, and in the Philippines, it is being carried in freshwater fish. For instance, Salcedo *et al*. (2009), investigated the presence of parasites in *Oreochromis niloticus* (tilapia), *Osphomenus olfax* (gourami), *Clarias batrachus* (catfish), *Ophiociphalus striatus* (snakeheadfish), and *Anabas testudineus* (climbing perch) which were sold in Kabacan, Cotabato Public Markets.

In the case of R. brachysoma, the only studies on describing *Lecithocladium angustiovum (*Digenea: Hemiuridae*) and the community of helminths were conducted (Indaryanto, 2014; Indaryanto et al., 2015).* Thus, this study aimed to conduct a parasite survey present in R. brachysoma sold in selected fish markets in

* Corresponding author e-mail: molina.romenick17@gmail.com.

Zamboanga City. Thus, it will serve as a baseline data about fish parasites and promote public health awareness with the locals of Zamboanga City. This study focused on parasites which could be found in the gills, stomach and intestines of R. brachysoma.

2. Material and Methods

2.1. Collection of Samples

A total of 60 *R. brachysoma* were purchased from selected fish markets in Zamboanga City and used in this study. Purposive sampling was employed, wherein only freshly caught *R. brachysoma* were selected. The samples were placed in a plastic bag with labels and placed in an ice chest. Samples were brought to the Biology Laboratory, College of Science and Mathematics, Western Mindanao State University, Zamboanga City.

2.2. Microscopic Examination in Fish Samples

To examine the internal organs for the presence of parasites, the fish were dissected by opening the abdominal cavity from the anus and anteriorly using dissecting tools. The gills of the fishes were scraped using scalpel and mixed with 10 drops of 0.8% saline water in a petri dish. A drop of the mixture was placed in a slide for microscopic examination. Prepared slides were examined under high power objective and low power objective using Photomicrograph. For the stomach and intestines of the fishes, they were removed and dissected for inspection. The stomach and intestines were scrapped with 10 drops of 0.8% saline water in petri dish. A drop of mixture was placed in a slide for microscopic examination under low and high power objectives using Photomicrograph.

2.3. Staining and Identification

Samples were preserved in Alcohol Formalin Acetic Acid (AFA). AFA was prepared by adding 5 ml glacial acetic acid and 5 ml formalin to 90 ml 70% ethyl alcohol. Samples on slides were stained with 1 drop of eosin solution. Eosin solution was prepared by adding 1 gram of Eosin Y, 5 ml of glacial acetic acid to 1 liter of 70% ethyl alcohol (Echem at al., 2018). Images of the parasites were documented and were brought to Dr. Evelyn Campos of Zamboanga State College of Marine Sciences and Technology and Paul K. Aranton a Registered Medical Technologist for identification.

2.4. Analysis of Data

Prevalence and mean intensity of the parasites were computed using the formulas by Bush *et al*. (1997):

$$\text{Prevalence} = \frac{\text{Total Number of Fish Infected with Specific Parasite}}{\text{Total Number of Fish Examined}} \times 100$$

$$\text{Mean Intensity} = \frac{\text{Total Number of Specific Parasite in the Sample}}{\text{Number of Infected Fish}}$$

3. Results

3.1. Identification of Parasites

There were 8 parasites isolated and identified in *R. brachysoma* which include: *Dermocystidium sp*., *Myxosporidia truttae*, *Amyloodinium sp*., *Cryptocaryon irritans*, *Encephalitozoon sp*., *Schistosoma sp*., *Kudoa thyrites* and *Echinorhynchus sp*.

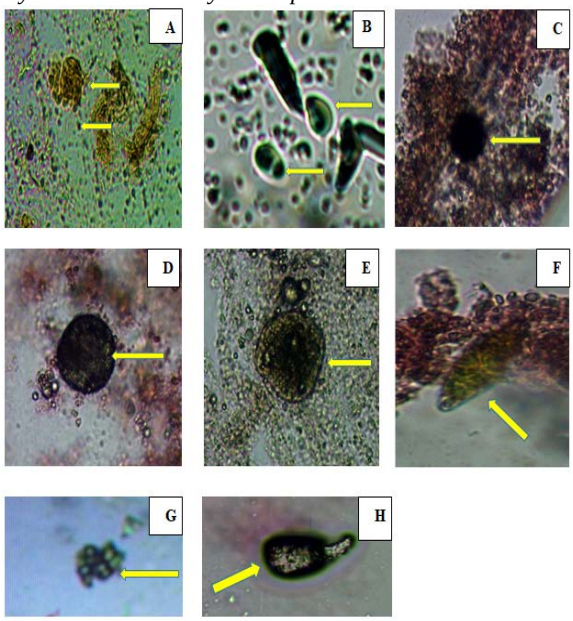

Figure 2. Identified Parasites in R. brachysoma at 100x magnification (A. *Dermocystidium sp*., B. *Myxosporidia truttae*, C. *Amyloodinium sp*., D. *Cryptocaryon irritans*, E. *Encephalitozoon sp*., F. *Schistosoma sp*., G. *Kudoa thyrites* and H. *Echinorhynchus sp*.)

3.2. Prevalence and Mean Intesity of the Parasites

Table 1 shows the computed prevalence of parasites in *R. brachysoma*. Result revealed that *Dermocystidium sp.* and *Amyloodinium sp.* were the most prevalent parasite with a prevalence value of 16.67%. The second most prevalent parasite is *Myxosporidia truttae* with a prevalence value of 13.33%, followed by *Encephalitozoon sp.* and *Kudoa thyrsites* with a prevalence value of 8.33% and 6.67%, respectively. *Cryptocaryon irritans*, *Schistosoma sp.* and *Echinorhynchus sp.* were the least prevalent with a prevalence value of 5.00%. Hence, there were only three (3) *R. brachysoma* where these parasites were spotted.

Table 1. Prevalence of Parasites in *Rastrelliger brachysoma*

Parasites	Total Number Examined	Total Number of Infected *R. brachysoma*	Prevalence (%)
Dermocystidium sp.	60	10	16.67
Myxosporidia truttae	60	8	13.33
Amyloodinium sp.	60	10	16.67
Cryptocaryon irritans	60	3	5.00
Encephalitozoon sp.	60	5	8.33
Schistosoma sp.	60	3	5.00
Kudoa thyrsites	60	4	6.67
Echinorhynchus sp.	60	3	5.00

Table 2 shows the computed mean intensity of parasites in *R. brachysoma*. Results revealed that *Dermocystidium sp.* has the highest mean intensity of 17.80. *Myxosporidia truttae* has the second highest mean intensity of 11.25, followed by *Echinorhynchus sp.* (6.00), *Cryptocaryon*

irritans (4.33), *Kudoa thyrsites* (3.50), *Encephalitozoon sp.* (2.80) and *Amyloodinium sp.* (2.70). *Schistosoma sp.* has the lowest mean intensity, with a value of 1.33.

Table 2. Mean Intensity of Parasites in *Rastrelliger brachysoma*

Endoparasites	Total Number of Parasite	Total Number of Infected *R. brachysoma*	Mean Intensity
Dermocystidium sp.	178	10	17.80
Myxosporidia truttae	90	8	11.25
Amyloodinium sp.	27	10	2.70
Cryptocaryon irritans	13	3	4.33
Encephalitozoon sp.	14	5	2.80
Schistosoma sp.	4	3	1.33
Kudoa thyrsites	14	4	3.50
Echinorhynchus sp.	18	3	6.00

4. Discussion

The parasites isolated and identified in *R. brachysoma* were classified to their taxonomic groups into: fungi (n = 1), protozoans (n = 5), trematode (n = 1) and acanthocephalans (n = 1).

Among the organs examined, the existence of parasites were found in gills and intestines only. In gills, *Amyloodinium sp.*, *Dermocystidium sp.* and *Cryptocaryon irritans* were present. *Amyloodinium sp.* is a dinoflagellate that can be found on gills and skin of infected marine and estuarine fish that causes a powdery or velvety appearance. This kind of parasite can cause devastating disease which is known as marine velvet or amyloodiniosis that can lead to mortality of fish (Floyd and Floyd, 2011). *Dermocystidium sp.* contains a small spherical spore with a nucleus in the periphery and a prominent rectile body in the centre (Fujimoto *et al*., 2017). This can be found in gills, skin and cornea of the eye causing visible cysts of different sizes and shapes (El-Mansy, 2008). *Cryptocaryon irritans* is an obligate parasitic ciliate protozoan that causes white spot disease in marine fish. Furthermore, the presence of this protozoan can cause significant loses for aquarists and marine cultures in the world (Cardoso *et al*., 2019). The exposure of gills to the external water due to their respiratory activities causes the presence of these parasites (Bichi and Ibrahim, 2009).

In intestines, *Myxosporidia truttae*, *Encephalitozoon sp.*, *Schistosoma sp.*, *Kudoa thyrsites* and *Echinorhynchus sp.* were found. *Myxosporidia truttae* is a multicellular organism that is known for invading the tissues and organs of a fish, particularly the gall bladder. A normal gall bladder is characterized by a greenish hue. Infected gall bladder by *Myxosporidia truttae* turns its color into light pink (Fujita, n.d.). If the fish ingests the spores of *Encephalitozoon sp.*, then the fish is infected. *Encephalitozoon sp.* are intracellular parasites with unicellular spores with an imperforate chitinous wall containing 1 sporoplasm and an elaborate hatching apparatus (Bruno, Nowk and Elliott, 2006). *Schistosoma sp.* or blood flukes live inside the blood vessels and are the only trematodes with separate sexes (Skelly, 2008). In this study, eggs of *Schistosoma sp.* were seen with terminal spines. *R. brachysoma* might ingested the eggs accidentally. Hence, fishes are not ordinary hosts in any of *Schistosoma* species' life cycle. The typical life cycle of *Schistosoma* treamatode or its related species involves only two hosts, (a) a freshwater snail intermediate host and (b) either a mammalian or bird definitive hosts (Nelwan, 2019). *Kudoa thyrsites* is a microscopic parasite present in marine fish species worldwide. It produces an enzyme that can make fish flesh soft, commonly known as soft flesh (Whitaker and Kent, 1991). *Echinorhynchus sp.* are endoparasitic worms found in both freshwater and marine fishes worldwide that has a retractable probscis armed with rows of hooks used to attach in the intestines of fish. Infected fish is associated with irreversible damage on intestinal tract and tissue necrosis in areas where the worm is attached (Sakthivel *et al*., 2014).

Among the parasites, the most prevalent were *Dermocystidium sp.* and *Amyloodinium sp.* while *Cryptocaryon irritans*, *Schistosoma sp.* and *Echinorhynchus sp.* were least prevalent. In terms of intensity, *Dermocystidium sp.* has the highest mean intensity while *Schistosoma sp.* has the lowest intensity. Prevalence and intensity depends on many factors such as feeding habits of host and physical parameters such as salinity, quality of water, pH and temperature (Velasquez, 1984; Indaryanto *et al*., 2015).

5. Conclusion

There were eight parasites isolated and identified in *R. brachysoma* which can be found in the gills and intestines. In terms of prevalence, *Dermocystidium sp.* and *Amyloodinium sp.* were the most prevalent parasites while *Cryptocaryon irritans*, *Schistosoma sp.* and *Echinorhynchus sp.* were least prevalent. In terms of intensity, *Dermocystidium sp.* was the highest while *Schistosoma sp.* was the lowest.

Conflict of Interest

The author declares that there is no conflict of interest with this work and the preparation of the paper.

References

Bichi A and Ibrahim A. 2009. A survey of ecto and intestinal parasites of *Tilapia zillii* (Gervas) in Tiga Lake, Kano, Northern Nigeria. *Bayero Journal of Pure and Applied Science*, **2(1)**: 79-82.

Bruno D, Nowak B and Elliott D. 2006. Guide to the identification of fish protozoan and metazoan parasites in stained tissue sections. *Diseases of Aquatic Organisms*, **70**: 1-36

Bush A, Lafferty K, Lotz J and Shostak W. 1997. Parasitology meets ecology on its own terms: Margolis *et al*. re-visited. *J. Parasitol*, **83**:575–583.

Cardoso P, Soares H, Martins M and Balian S. 2019. *Cryptocaryon irritans*, a ciliate parasite of an ornamental reef fish yellowtail tang *Zebrasoma xanthurum*. *Rev. Bras. Parasitol. Vet*., 28: 4.

Collette B, Di Natale A, Fox W, Juan Jorda M, Nelson R. 2011. *Rastrelliger brachysoma*. The IUCN Red List of Threatened Species 2011: e.T170318A6745895.

Echem R, Barba H, Guangyao L, Peng F, Buenaventura N. 2018. Endoparasites in *Chanos chanos* (Forsskal, 1775) from the wetlands of Zamboanga City, Western Mindanao, Philippines. *J Aquac Res Development*, **9**: 535.

El-Mansy A. 2008. A new finding of Dermocystidium- like spores in the gut of cultured *Oreochromis niloticus*. *Global Veterinaria*, **2**: 369–371.

Floyd R and Floyd M. 2011. *Amyloodinium ocellatum*, an Important Parasite of Cultures Marine Fish. *Southern Regional Aquaculture Center*, **4705**; 1-12.

Fujimoto R, Sousa N, Diniz D, Diniz J, Madi R, Martin, M, *et al*. 2017. *Dermocystidium sp.* infection in farmed hybrid fish *Colossoma macropomum* x *Piaractus brachypomus* in Brazil. *Journal of Fish Diseases*, 1-4

Fujita T. nd. Studies on Myxosporidia of Japan. *Journal of the College of Agriculture, Hokkaido Imperial University, Sapporo, Japan*, **10(7)**: 191-248.

Ghazali A, Abidin D, Nor S and Nalm D. 2012. Genetic variation of Indian Mackerel (*Rastrelliger kanagurta*) of Sabah water based on Mitochondrial D-loop Region: A Preliminary Study. *Asian Journal of Biology and Biotechnology*, **1(1)**: 1-10.

Indaryanto F. 2014. Community Structure of Helminth Parasites of Mackerel (*Rastrelliger* spp.) from Banten Bay and Pelabuhan Ratu Bay. *Jurnal Ilmu Pertanian Indonesia*, **19(1)**: 1-8.

Indaryanto F, Abdullah M, Wardiatno Y, Tiuria R and Imai H. 2015. A description of *Lecithocladium angustiovum* (Digenea: Hemiuridae) in Short Mackerel, *Rastrelliger brachysoma* (Scombridae) of Indonesia. *Tropical Life Sciences Research*, **26(1)**: 31-40.

Madhavi R and Lakshmi T. 2012. Metazoan parasites of the Indian Mackerel, *Rastrelliger kanagurta* (Scombridae) of Visakhapatnam Coast, Bay of Bengal. *Journal of Parasitic Diseases*, **35(1)**: 66-74.

Nelwan M. 2019. Schistosomiasis: Life cycle, diagnosis and control. *Current Therapeutic Research*, **91**: 5-9.

Raissy M and Ansari M. 2012. Parasites of some freshwater fish from Armand River, Chaharmal va Bakhtyari Province, Iran. *Iran Journal Parasitology*, **7(1)**: 73-79.

Ruiz, G. 1991. Consequences of parasitism to marine invertebrates host evolution?. *The American Society of Zoologists*, **31(6)**: 831-893.

Sakthivel A, Selvakumar P and Gopalakrishnan. 2014. Acanthocephalan (*Echinorhynchus sp*.) infection of yellowfin tuna (*Thunnus albacares*) from Nagapattinam, south east coast of India. *Journal of Coastal Life Medicine*, **2(8)**: 596-600.

Salcedo N, Gonzaga E, Garduque R, Jimenez V and Panes T. 2009. Detection of common parasites in freshwater fish sold at the public market, Kabacan, Cotabato, Philippines. *USM R&D*., **17(2)**: 147-149.

Skelly P. 2008. Sex and the Single Schistosome. *Natural History*, **117(5)**: 22-27

Velasquez C. 1984. Fish Parasitology and Aquaculture Management in the Philippines. National Academy of Science and Technology. 105-159.

Whitaker D and Kent M. 1991. Myxosporean *Kudoa thyrsites*: a cause of soft flesh in farm-reared Atlantic salmon. *Journal of Aquatic Animal Health*, **3**: 291–294.

JJBS

Volume 14, Number 3, September 2021
ISSN 1995-6673
Pages 417 - 422

Jordan Journal of Biological Sciences

Cypermethrin-Induced Alterations in Serum Calcium and Phosphate of Rats: Protective Role of Jamun Seed and Orange Peel Extracts

Babita D. Srivastava[1], Manish Srivastava[2], Sunil K. Srivastav[1], Makoto Urata[3, 4], Nobuo Suzuki[4] and Ajai K. Srivastav[1,*]

[1]*Department of Zoology, DDU Gorakhpur University, Gorakhpur 273009, India;*[2]*Department of Chemistry, Digvijai Nath P.G. College, Gorakhpur, India;*[3]*Institute of Noto SATOUMI Education Research, Noto-cho, Ishikawa 927-0553, Japan;*[4]*Noto Marine Laboratory, Institute of Nature and Environmental Technology, Division of Marine Environmental Studies, Kanazawa University, Noto-cho, Ishikawa 927-0553, Japan*

Received: July 6, 2020; Revised: September 27, 2020; Accepted: October 4, 2020

Abstract

The present study investigated alterations in serum calcium and phosphate levels induced by cypermethrin (trade name Basathrin) exposure to rats and aimed to evaluate protecting role of jamun (*Syzygium cumini*) seed (JSE) and orange (*Citrus sinensis)* peel (OPE) extracts.

Wistar rats were treated as - Group A: Control; Group B: cypermethrin (CY); Group C: cypermethrin and jamun seed extract (CY+JSE); Group D: cypermethrin and orange peel extract (CY+OPE); Group E: orange peel extract (OPE); Group F: jamun seed extract (JSE). Cypermethrin dose was 25 mg/ kg body wt/day whereas orange peel and jamun seed extract dose was 200 mg/kg body wt/day. Serum calcium and phosphate were analyzed after 15 days and 30 days following the treatment.

Serum calcium of rat treated with cypermethrin decreased after 15 and 30 days. In-group C, serum calcium decreased on day 15 and 30. In-group D serum calcium decreased at day 15 but on day 30 level increased. Calcium levels in-group C increased on day 15 and 30 as compared to group B. Moreover, levels in-group D is not significant on day 15 and 30.

In cypermethrin exposed rats, serum phosphate declined from day 15 to 30. In-group C, serum phosphate decreased at day15, which continued till day 30. Serum phosphate in-group D treated rats decreased on day 15 and 30. In groups E and F, there is no change in serum phosphate of rats on day 15; however, on day 30 levels decreased.

It can be concluded that cypermethrin treatment (25 mg/ kg body wt/day) caused alterations in the serum calcium and phosphate of the rats. The changes in these electrolytes could be protected by supplementation of extracts of jamun seed and orange peel at 200 mg/kg body wt/day. It is suggested that the cypermethrin exposed organisms should be given dietary supplement of these botanical extracts, which would reverse the toxic symptoms.

Keywords: Cyprmethrin; Serum calcium; Serum phosphate; Jamun seed; Orange peel

1. Introduction

Pests have always been a nuisance, and they damage crops in the field as well in stores. For the increased yield of crops, human beings use pesticides for the noxious arthropods and pests (Tripathi and Srivastav, 2010). Pesticides, being important for controlling injurious pests, also cause hazards to non-target organisms including humans (Bhusan *et al*., 2013; Chrustek *et al*., 2018; Tewari *et al*., 2018; Mahat *et al*., 2020). Pyrethroids have potent insecticidal properties and are potentially non-toxic to most non-target species, especially mammals. Cypermethrin is a non-systemic, light stable synthetic pyrethroid which is used mostly as residual treatment for the control of flies, ectoparasite infestation of animals, mosquitoes, cockroaches and for the control of range of insects on crops (Nair *et al*., 2011; Sharma *et al*., 2018; Mahat *et al*., 2020). The widespread use of cypermethrin caused several health hazards to non-target animals (including humans) such as toxicological alterations in liver and kidney (Grewal *et al*., 2010; Mossa *et al*., 2015; Bhusan *et al*., 2013; Das *et al*., 2017; Hamid *et al*., 2017; Srivastava *et al*., 2018), hematological (Saxena and Saxena, 2010; Das *et al*., 2017), genotoxic and neurotoxic effects (Sharma *et al*., 2014; Mhadhbi *et al*., 2020), generation of ROS (reactive oxygen species) (Yousef *et al*., 2019) and reproductive toxicity (Grewal *et al*., 2010; Das *et al*., 2017; Simon *et al*., 2018; Sharma *et al*., 2018; Singh *et al*., 2020; Zhang *et al*., 2020).

Phytonutrients/phytochemicals have been reported to be present in fruits, vegetables, spices and herbs. These phytochemicals have antioxidant properties as they scavenge free radicals (Mossa *et al*., 2015; Attia *et al*., 2017 a, b; Srivastava and Srivastav, 2017; Srivastava *et al*., 2018; Ahmed *et al*., 2019; Bashandy *et al*., 2019). *Syzygium cumini* (Jamun) has antidiabetic, antibacterial, antimalarial, free radical scavenging property, anti-

* Corresponding author e-mail: ajaiksrivastav@hotmail.com.

ulcerogenic and anti-fertility activities (Nair *et al*., 2013; Kumari *et al*., 2017; Srivastava and Srivastav, 2017; Chagas *et al*., 2018; Srivastava *et al*., 2018). These properties of jamun have been attributed to antioxidant compounds present in jamun namely flavonoids, phenolic acids and anthocyanins (Raza *et al*., 2007; Srivastava and Srivastav, 2017; Srivastava *et al*., 2018). Orange (*Citrus sinensis*) also possess vitamin C, flavonoids, acridone alkaloids, carotenoids, limonoids etc. (Hegazy and Ibrahim, 2012; Srivastava and Srivastav, 2017; Srivastava *et al*., 2018; Ahmed *et al*., 2019). Bashandy *et al*. (2019) reported that *Citrus* peel contain hespiridin which has anti-inflammatory, antioxidant, anti-cancer and anti-lipedemic activities. Naringen and naringenin have been found in *Citrus* peels which have antimicrobial, antidiabetic and toxicity protecting activities (Ahmed *et al*., 2019).

Calcium, particularly its ionic form, plays a vital role in several physiological processes of vertebrates – hormone synthesis and release, neuronal excitability, blood clotting, cell adhesion, permeability of cell membranes to ions, muscle contraction, reproduction, etc. (Srivastav *et al*., 2008). These physiological processes are severely affected if there is a minor change in ionic calcium. Phosphate is required for intermediary metabolism (phosphorylated intermediates), genetic information (DNA and RNA), enzyme/protein components (phosphohistidine, phosphoserine), phospholipids and membrane structure (Norman and Litwack, 1987).

There exists no report regarding the protective effects of jamun seed extract and orange peel extract on the blood parameters (calcium and phosphate) in vertebrates. Therefore, the present study was aimed to investigate the changes in serum calcium and phosphate levels induced by cypermethrin exposure to male rats and to evaluate the possible protecting role of jamun (*Syzygium cumini*) seed and orange (*Citrus sinensis)* peel extracts.

2. Materials and methods

Male Wistar rats (115-130 g) were housed in polypropylene cages and acclimatized for 2 weeks in the laboratory under natural photoperiod (Light -11:46 to 12:08 hour) and provided standard laboratory feed and water *ad libitum.* Animal care and sacrifice were carried out according to the guidelines provided by Ethics Committee of the University.

The animals were randomly divided into six groups -- A, B, C, D, E, and F, each consisting of 20 animals (5 rats per cage). During experiment, rats were maintained under natural photoperiod (Light -11:46 to 12:08 hour) and on the standard laboratory feed and water *ad libitum.* Dose of cypermethrin used in this study has been selected considering the doses used earlier by other investigators—(i) 40-120 mg/kg b wt (Nair *et al.*, 2011), (ii) 30 mg/ kg b wt (Hamid *et al.*, 2017 and (iii) 21.2-85 mg/kg b wt (Madu, 2015). The dose of jamun seed extract used in this study has been selected on the basis of doses used by earlier workers – (i) 250 mg/kg b wt (Behera *et al*., 2014), (ii) 200-800 mg/kg b wt (Vihan and Brashier, 2017) and (iii) 200 and 400 mg/kg b wt (Kumar and Thakur, 2018). Dose of orange peel extract used in this study has been selected considering the doses used earlier by other investigators—(i) 125, 250 and 500 mg/kg b wt (Muhtadi *et* al., 2015), (ii) 100, 200 and 400 mg/kg b wt (Selmi *et al.*, 2017) and 200 mg/kg b wt (Bashandy *et al*., 2019). Following treatments were given daily to these groups at 08:00 each day throughout the experiment:

- Group A: Control
- Group B: CY-treated: Rats received daily cypermethrin (25 mg/ kg body wt)
- Group C: CY+JSE: These rats were given daily cypermethrin (25 mg/ kg body wt) and jamun seed extract (200 mg/kg body wt) simultaneously
- Group D: CY+OPE: These rats were given daily cypermethrin (25 mg/ kg body wt) and orange peel extract (200 mg/kg body wt) simultaneously
- Group E: OPE: Rats received daily orange peel extract (200 mg/kg body wt)
- Group F: JSE: Rats received daily jamun seed extract (200 mg/kg body wt)

Cypermethrin (trade name Basathrin) used in the present study was manufactured by BASF India Limited, Mumbai, India. Every day fresh cypermethrin dose was prepared. Jamun (*Syzygium cumini*) seeds were obtained from M/S SVM Naturals, Tamilnadu, India. *Citrus sinensis* fruits were obtained locally and peels were separated. Seeds and peels were thoroughly washed with water and dried at 40 °C. The dried materials were powdered and mixed with ethanol (90%) in 1:20 ratio (w/v) and kept on an orbital shaker for 48 h. The solution was filtered with Whatman grade No.1 filter paper and filtrates were dried at 40 °C. The dried residue was weighed and kept at -20 °C for further use. For experiment, the residues were reconstituted with ethanol to provide desired dose to be given to rats (Srivastava *et al*., 2018).

Rats (from each group, under light ether anesthesia) were sacrificed 24 h after last dose on 15^{th} and 30^{th} day following the start of the experiment. Animals were fasted overnight before sacrifice. Blood samples (n=5 from each group at each interval) were collected by cardiac puncture and allowed to clot at room temperature. Sera were separated and kept at -20 ºC until analyzed for serum calcium (Calcium kit, Sigma-Aldrich) and inorganic phosphate (Pointe Scientific, USA). Analysis was performed in duplicates for each sample.

Data are presented as mean ± S.E. of five specimens. For multiple group comparisons, Two-way analysis of variance (ANOVA) was used. Differences between groups were determined by the *post hoc* Duncan test.

3. Results

Serum calcium level of cypermethrin (group B) treated rat exhibits a decrease after 15 ($P < 0.0001$) and 30 day ($P < 0.0001$) (Fig. 1). In group C (cypermethrin and JSE), the serum calcium level decreased on 15 day ($P < 0.0001$) and on 30 day ($P < 0.014$) as compared to group A. However, the levels at day 30 in group C are slightly increased as compared to value of group C at day 15. In group D (CY+OPE), the serum calcium level shows a decrease ($P < 0.0006$) at 15 day as compared to group A but on 30 day the level increases (not significant as compared to group A). The calcium levels in group C is increased on day 15 ($P < 0.008$) and day 30 ($P<0.002$) as compared to group B. Moreover, the levels in group D are not significant on day 15 and day 30 as compared to group B This indicates that

orange peel extract is not effective in recovering the decrease in calcium levels caused by cypermethrin. In group E (OPE) and group F (JSE), there is no change in serum calcium levels on 15 and 30 day. Analysis of Variance (ANOVA) indicates that the treatment is significant (15 day -- F=12.004, P< 0.0001; 30 day – F=2.658, P< 0.041).

Serum phosphate levels of cypermethrin (group B) exposed rats decrease progressively from 15 day (P< 0.0008) to 30 day (P< 0.0001) (Fig. 2). In group C, the serum phosphate level displays a decline at 15 day (not significant) which continued till 30 day (P< 0.0004). Serum phosphate levels in group D treated rats show decreased value on day 15 (P< 0.009) and day 30 (P< 0.033). In group E and group F, there is no change in serum phosphate levels of rats on day 15 as compared to control (group A); however, on day 30 the levels show significant decrease (group E (P< 0.04) as compared to group A. ANOVA indicates that the treatment is significant (15 day -- F=4.014, P< 0.006; 30 day – F=10.125, P< 0.0001).

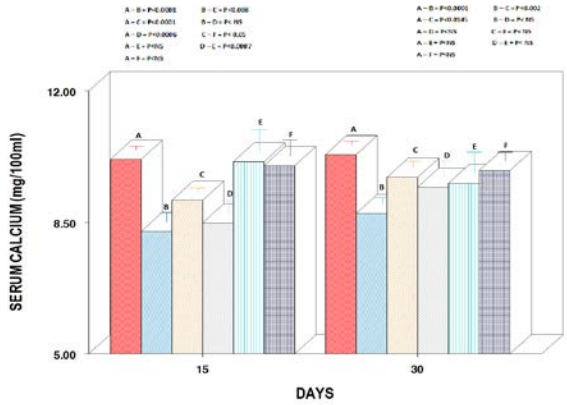

Figure 1: Serum calcium levels (mg/100 ml) of Wistar rat. Control (, Group A), CY (, Group B), CY+JSE (, Group C), CY+OPE (, Group D), OPE (, Group E) or JSE (, Group F). All values indicate mean ± SE of five specimens.

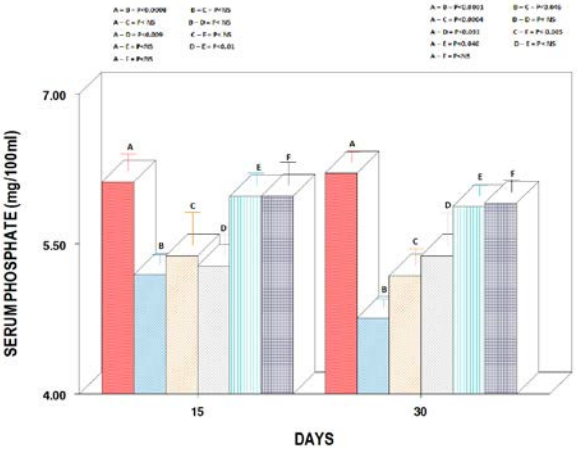

Figure 2: Serum phosphate levels (mg/100 ml) of Wistar rat. Control (, Group A), CY (, Group B), CY+JSE (, Group C), CY+OPE (, Group D), OPE (, Group E) or JSE (, Group F). All values indicate mean ± SE of five specimens.

4. Discussion

Cypermethrin treatment to rats provoked hypocalcemia. This is in agreement with the studies of earlier researchers who have observed hypocalcemia in rats after exposure to toxicants — mipcin (Rangoonwala *et al.*, 2007), microcystin LR (Moreno *et al.*, 2003), diazinon (Rangoonwala *et al.*, 2005), heroin (Barai *et al.*, 2009), heptachlor (Rangoonwala *et al.*, 2004), cadmium (Tripathi and Srivastav, 2011) and chlorpyrifos (Tripathi *et al.* 2013). Agarwal *et al.* (2009) have reported hypocalcemia from chicken after exposure to gamma benzene hexachloride and quinalphos. Toxicants-induced hypocalcemia has also been reported from amphibian – chlorpyrifos (Srivastav *et al.*, 2018) and fish-- cadmium (Rai and Srivastav, 2003; Chowdhury *et al.*, 2004), deltamethrin (Srivastav *et al.*, 1997 b, 2010), cypermethrin (Mishra *et al.*, 2010), malachite green (Srivastava *et al.*, 1995), aldrin (Singh *et al.*, 1996), formothion (Singh *et al.*, 1997), botanical pesticides (Prasad *et al.*, 2011 a, b; Kumar *et al.*, 2011 a, b), microcystin LR (Prakash *et al.*, 2015, 2016) and combination of dimethoate, chlorpyrifos and malathion (Rani *et al.*, 2017). Ghelichpour and Mirghaed (2019) have noticed an increase in plasma calcium levels after lufenuron and flonicamid exposure to common carp after 24 h, however, with elongation of exposure the levels decrease. Andjelkovic *et al.* (2019) have recorded an insignificant decrease in serum calcium levels after exposure of cadmium to rats. In the present study, the calcium levels in group C are increased on day 15 and day 30 as compared to group B. This indicates that jamun seed extract is effective in recovering the calcium levels which were decreased by treatment with cypermethrin. Moreover, the levels in group D are not significant on day 15 and day 30 as compared to group B. This indicates that orange peel extract is not effective in recovering the decrease in calcium levels caused by cypermethrin.

Rats exposed to cypermethrin exhibited hypophosphatemia. Contradictory reports have been given by other investigators regarding the effects of toxicants on phosphate levels of rats – hypophosphatemia (microcystin – Moreno *et al.*, 2003; cadmium --Tripathi and Srivastav, 2011 ; Andjelkovic *et al.*, 2019; chlorpyrifos --Tripathi *et al.*, 2013), hyperphosphatemia (heroin – Barai *et al.*, 2009), intermittent effect (microcystin LR –Hooser *et al.*, 1989) and no effect (mipcin –Rangoonwala *et al.*, 2007; diazinon-- Rangoonwala *et al.*, 2005; heptachlor-- Rangoonwala *et al.*, 2004). Several workers have noticed hypophosphatemia in fish after treatment with toxicants such as -- pyrethroids (deltamethrin, Srivastav *et al.*, 1997 b; cypermethrin, Mishra *et al.*, 2001), cadmium (Rai and Srivastav, 2003), organophosphate (chlorpyrifos, Srivastav *et al.*, 1997 a), botanical pesticides (Kumar *et al.*, 2011 a, b; Prasad *et al.*, 2011 a, b) and microcystin LR (Prakash *et al.*, 2015, 2016). Ghelichpour and Mirghaed (2019) have recorded an initial increase in plasma phosphate levels after 24 h exposure of common carp to pesticide – lufenuron and flonicamid. Later, these authors noticed a decrease in phosphate levels after elongation of exposure. The observed decrease in blood electrolytes of cypermethrin exposed rats could be attributed to the degeneration of kidney tubules (our unpublished work)

which might have caused decreased reabsorption of these electrolytes.

5. Conclusion

It can be concluded that cypermethrin treatment at 25 mg/kg body wt/day caused alterations in the serum calcium and phosphate of the rats. The changes in these electrolytes could be protected by supplementation of extracts of jamun seed and orange peel at 200 mg/kg body wt/day. It is suggested that the cypermethrin exposed organisms should be given dietary supplement of these botanical extracts which would reverse the toxic symptoms.

Acknowledgments

Ajai Kumar Srivastav is thankful to University Grants Commission, New Delhi, India for providing financial assistance for this study. The present study was also partly supported by the cooperative research program of the Institute of Nature and Environmental Technology, Kanazawa University, Japan (Accept No. 20007).

References

Agarwal S, Batra M and Chauhan S. 2009. Effects of gamma benzene hexachloride and quinalphos on serum calcium and phosphorus levels in experimentally fed broiler chickens. *J Immunology Immunopathol.*, **11**: ISSN 0973-9149.

Ahmed OM, Fahim HI, Ahmed HY, Al-Muzafar HM, Ahmed RR, Amin KA, El-Nahass E and Abdelazeem WH. 2019. The preventive effects and the mechanisms of action of navel orange peel hydroethanolic extract, naringin, and naringenin in N-acetyl-p-aminophenol-induced liver injury in Wistar rats. *Oxidative Med Cellular Long.*, 2019: 2745352.

Andjelkovic M, Buha Djordjevic A, Antonijevic E, Antonijevic B, Stanic M, Kotur-Stevuljevic J, Spasojevic-Kalimanovska V, Jovanovic M, Boricic N, Wallace D and Bulat Z. 2019. Toxic effect of acute cadmium and lead exposure in rat blood, liver, and kidney. *Int J Environ Res Public Health*, **16**: 274.

Attia YA, Hamed RS, Bovera F, Abd El-Hamid AE, Al-Harthi MA and Shahba HA. 2017a. Semen quality, antioxidant status and reproductive performance of rabbits bucks fed milk thistle seeds and rosemary leaves. *Anim Reprod Sci.*, **184**:178-186. doi: 10.1016/j.anireprosci.2017.07.014.

Attia YA, Al-Harthi MA and Hassan SS. 2017b. Turmeric (*Curcuma longa* Linn.) as a phytogenic growth promoter alternative for antibiotic and comparable to mannan oligosaccharides for broiler chicks. *Rev Mex Cienc Pecu*, **8 (1):**11-21.

Bashandy SAE, Ahmad-Farid OAH, Omara EA, El-Toumy SA and Salib JY. 2019. Protective effects of *Citrus reticulata* peel extract against potassium dichromate-induced reproductive toxicity in rats. *Asian Pac J Reprod*., **8:** 267-275.

Barai SR, Suryawanshi SA and Pandey AK. 2009. Responses of parathyroid gland, C cells, and plasma calcium and inorganic phosphate levels in rat to sub-lethal heroin administration. *J Environ Biol.*, **30:** 917-922.

Behera SR, Sckkizhar M and Babu KS. 2014. Hepatoprotective activity of aquous extract of *Syzygium cumini* seed on streptozotocin induced diabetes in rats. *Inter J Ayurvedic Herbal Med.*, **4:**1470-1477.

Bhusan B, Saxena PN and Saxena N. 2013. Biochemical and histological changes in rat liver caused by cypermethrin and beta-cyfluthrin. *Arhiv za Higijenu Rada i Toksikologiju.*, **64:** 57-67.

Chagas VT, Coelho RMRS, Gaspar RS, Silva SA, Mastrogiovanni M, Mendoca CJ, Ribeiro MNS, Paes AMA and Trostchansky A. 2018. Protective effects of a polyphenol-rich extract from *Syzygium cumini* (l.) skeels leaf on oxidative stress-induced diabetic rats. *Oxidative Med Cellular Lon.,*. **2018:** Article ID 5386079.

Chowdhury MJ, Pane FF and Wood CM. 2004. Physiological effects of dietary cadmium acclimation and waterborne cadmium challenge in rainbow trout: respiratory, ionoregulatory, and stress parameters. *Comp Biochem Physiol. C,* **139:** 163-173.

Chrustek A, Holynska-Iwan I, Dziembowska I, Bogusiewicz J, Wroblewski M, Cwynar A and Olszewska-Slonina D. 2018. Current research on the safety of pyrethroids used as insecticides. *Medicina,* **54:** 61

Das T, Ghosh R, Paramanik A, Pradhan A, Dey SK, Roy T, Chatterjee D and Choudhary SM. 2017. Dose-dependent hematological, hepatic and gonadal toxicity of cypermethrin in Wistar rats. *Toxicol Forensic Med.*, **2:** 74-83.

Ghelichpour M and Mirghaed AT. 2019. Effects of sublethal exposure to new pesticides lufenuron and flonicamid on common carp, *Cyprinus carpio*, hydromineral balance to further saltwater exposure. *Int J Aquat Bio.*, **7:** 195-201.

Grewal KK, Sandhu GS, Kaur R, Brar RS and Sandhu HS. 2010. Toxic impacts of cypermethrin on behavior and histology of certain tissues of albino rats. *Toxicol Intern.*, **17:** 94-98.

Hamid MA, Moustafa N, Asran AEMAA and Mowafy L. 2017. Cypermethrin-induced histopathological, ultrastructural and biochemical changes in liver of albino rats: The protctive role of propolis and curcumin. *Beni-Suef Univ J Basic Appl Sci.*, **6:** 160-173.

Hegazy AE and Ibrahim MI. 2012. Antioxidant activities of orange peel extract. *World Appl Sci J*., **18:** 684-688.

Hooser SB. Beasley VR, Lovell RA, Carmichael WW and Haschek WM. 1989. Toxicity of microcystin-LR , a cyclic hepatopeptide hepatotoxin from *Microcystis aeruginosa* to rats and mice. *Vet Pathol.*, **26:** 246-252.

Kumar A, Prasad M, Mishra D, Srivastav SK and Srivastav Ajai K. 2011 a. Botanical pesticide, azadirachtin attenuates blood electrolytes of a freshwater fish *Heteropneustes fossilis*. *Pest Biochem Physiol.*, **99:** 170-173.

Kumar A, Prasad M, Mishra D, Srivastav SK and Srivastav Ajai K. 2011 b. Effects of *Euphorbia tirucalli* latex on blood electrolytes (calcium and phosphate) of a freshwater air-breathing catfish *Heteropneustes fossilis. Toxicol Environ Chem.*, **93:** 585-592.

Kumar M and Thakur R. 2018. *Syzygium cumini* seed extract ameliorates arsenic-induced blood cell genotoxicity and hepatotoxicity in Wistar albino rats. *Reports Biochem Molec Biol.*, **7:**110-118.

Kumari B, Sharma V and Yadav S. 2017. The therapeutic potential of *Syzygium cumini* seeds in diabetes mellitus. *J Med Plant Stud.*, **5:** 212-218.

Madu EP. 2015. Teratogenic and embryotoxic effects of orally administered cypermethrin in pregnant albino rats. *J Toxicol Environ Hlth Sci*., **7:** 60-67.

Mahat S, Jha CB, Shrestha S and Koirala S. 2020. Effcets of vitamin E on cypermethrin induced toxicity in cerebral cortex of Wistar albino rats: A histological study. *J Karnali Acad Health Sci.*, **3:** 1-10.

Mhadhbi L, Khazri A, Sellami B, Dellali M, Mahmoudi E and Beyrem H. 2020. The protective effect of *Hibiscus sabdariffa*

calyxes extract against cypermethrin induced oxidative stress in mice. *Pesticide Biochem Physiol.,* **165:** 104463.

Mishra D, Srivastav S, Srivastav SK and Srivastav Ajai K. 2001. Plasma calcium and inorganic phosphate levels of a freshwater catfish *Heteropneustes fossilis* in response to cypermethrin treatment. *J Ecophysiol Occup Hlth*., **1:** 131-138.

Mishra D, Tripathi S, Srivastav SK, Nobuo S and Srivastav Ajai K. 2010. Corpuscles of Stannius of a teleost *Heteropneustes fossilis* following intoxication with a pyrethroid (cypermethrin). *North-Western J Zool.,* **6:** 203-208.

Moreno IM, Mate A, Repetto G, Vázquez CM and Cameán AM. 2003. Influence of microcystin-LR on the activity of membrane enzymes in rat intestinal mucosa. *J Physiol Biochem.,* **59:** 293–300.

Mossa AH, Ibrahim FM, Mohafrash SMM, Baker DHA and Gengaihi SE. 2015. Protective effect of ethanolic extract of grape pomace against the adverse effects of cypermethrin on weanling female rats. *Evidence-Based Complem Alt Med.,* **2015:** 381919. doi:10.1155/2015/381919

Muhtadi, Haryolo, Azizah T, Suhendi A and Yen KH. 2015. Antidiabetic and antihypercholesterolemic activities of *Citrus sinensis* peel: in vivo study. *Nat J Physiol Pharma Pharmacol.,* **5:** 382-385. doi: 10.5455/njppp.2015.5.2807201561

Nair LK, Begum M and Geetha S. 2013. In Vitro antioxidant activity of the seed and leaf extracts of *Syzygium cumini. IOSR J Environ Sci Toxicol Food Technol.,* **7:** 54-62.

Nair RR, Abraham MA, Lalithakunjamma CR and Nair ND. 2011. A pathomorphological study of the sublethal toxicity of cypermethrin in Sprague Dawley rats. *Intern J Nutrition Pharmacol Neurolo Diseases,* **1:**179-183.

Norman AW, Litwack G. 1987. Hormones. pp. 355-396, Academic Press Inc., New York.

Prakash C, Kumar A, Prasad M, Srivastav SK and Srivastav Ajai K. 2015. Microcystin-LR attenuates blood calcium and phosphate levels in stinging catfish *Heteropneustes fossilis. Int J Pharm Bio Sci.,* **6:** 1147- 1153.

Prakash C, Prasad M, Kumar A, Mishra D, Chaudhary A and Srivastav SK. 2016. Protective effect of $ZnCl_2$ on toxicity produced by Microcystin-LR on serum calcium and phosphate levels of freshwater catfish *Heteropneustes fossilis. Int J Pure App Biosci.,* **4:** 111-117.

Prasad M, Kumar A, Mishra D, Srivastav SK and Srivastav Ajai K. 2011 a. Alterations in blood electrolytes of a freshwater catfish *Heteropneustes fossilis* in response to treatment with a botanical pesticide, *Nerium indicum* leaf extract. *Fish Physiol Biochem.,* **37:** 505-510.

Prasad M, Kumar A, Mishra D, Srivastav SK and Srivastav Ajai K. 2011 b. Blood electrolytes of a freshwater catfish *Heteropneustes fossilis* in response to treatment with a botanical pesticide, *Euphorbia royleana* latex. *Integ Zool.,* **6:** 150-156.

Rangoonwala SP, Suryawanshi SA and Pandey AK. 2007. Responses of serum calcium and inorganic phosphate levels as well as parathyroid gland and calcitonin producing C cells of *Rattus norvegicus* to mipcin ad ministration. *J Environ Biol.,* **28:** 475-481.

Rangoonwala SP, Suryawanshi SA and Pandey AK. 2004. Responses of serum calcium and inorganic phosphate levels, parathyroid gland and C cells of *Rattus norvegicus* to heptachlor administration. *J Environ. Biol.,* **25:** 75-480.

Rangoonwala SP, Kazim M and Pandey AK. 2005. Effects of diazinin on serum calcium and inorganic phosphate levels as well as ultrastructures of parathyroid and calcitonin cells of *Rattus norvegicus.*. *J Environ Biol.,* **26:** 217-221.

Rai R and Srivastav Ajai K. 2003. Effects of cadmium on the plasma electrolytes of a freshwater fish *Heteropneustes fossilis*. *J Ecophysiol Occup Hlth.,* **3:** 63-70.

Rani M, Gupta RK, Kumar S, Yadav J and Rani S. 2017. Pesticides' induces alterations in blood serum ions of Indian major carps. *The Bioscan,* **12:** 847-850.

Raza A, Butt MS, Ul-Haq I and Suleria HAR. 2017. Jamun (*Syzygium cumini*) seed and fruit extract attenuate hyperglycemia in diabetic rats. *Asian Pac J Trop Biomed.,* **7:** 750-754.

Saxena P and Saxena AK. 2010. Cypermethrin induced biochemical alterations in the blood of Albino rats. *Jordan J Biol Sci.,* **3:** 111-114.

Selmi S, Rtibi K, Grami D, Sebai H and Marzonki L. 2017. Protective effects of orange (*Citrus sinensis* L.) peel aquous extract and hesperidin on oxidative stress and peptic ulcer induced by alcohol in rat. *Lipids Hlth Disease,* **16:** 152.

Sharma A, Yadav B, Rohtagi S and Yadav B.,2018. Cypermethrin toxicity: A review. *J Forensic Sci Criminal Invest.,* **9:** 1-3

Sharma P, Firdous S and Singh R. 2014. Neurotoxic effect of cypermethrin and protective role of resveratrol in wistar rats. *Intern. J Nutrition Pharmacol Neurol Diseases,* **4:** 104-111.

Simon U, David O, Peter R, Joseph R, Ijeoma C and Celestine N. 2018. Pathological effects of cypermethrin on the testes and accessory sexual glands of Yankasa rams. *Arch Pathol Clinical Res.,* **2:** 6-12.

Singh D, Irani D, Bhagat S and Vanage G. 2020. Cypermethrin exposure during perinatal period affects fetal development and impairs reproductive functions of F1 female rats. *Sci Total Environ.,* **707:** 135945. doi:10.1016/j.scitotenv.2019.135945

Singh NN, Das VK and Singh S. 1996. Effect of aldrin on carbohydrate, protein and ionic metabolism of a freshwater catfish, *Heteropneustes fossilis. Bull Environ Contam Toxicol*., **57:** 204-210.

Singh NN, Das VK and Srivastava AK. 1997. Formothion and propoxur induced ionic imbalance and skeletal deformity in a catfish, *Heteropneustes fossilis. J Environ Biol*., **18:** 357-363.

Srivastav Ajai K, Srivastav S, Srivastav SK and Suzuki N. 2018. Alterations in the serum electrolytes of the Indian skipper frog *Euphlyctis cyanophlyctis* caused by an organophosphate pesticide: chlorpyrifos. *Jordan J Biol Sci.,* **11:** 395-399.

Srivastav Ajai K, Srivastava SK and Srivastava AK. 1997 a. Response of serum calcium and inorganic phosphate of freshwater catfish, *Heteropneustes fossilis*, to chlorpyrifos. *Bull Environ Contam Toxicol.,* **58:** 915-921.

Srivastav Ajai K, Srivastava SK and Srivastav SK. 1997 b. Impact of deltamethrin on serum calcium and inorganic phosphate of freshwater catfish *Heteropneustes fossilis*. *Bull Environ Contam Toxicol*., **59:** 841-846.

Srivastav Ajai K, Srivastava SK, Mishra D and Srivastav SK. 2010. Deltamethrin-induced alterations in serum calcium and prolactin cells of a freshwater teleost, *Heteropneustes fossilis*. *Toxicol Environ Chem.,* **92:** 1857-1864.

Srivastav Ajai K, Yadav S, Srivastav SK and Suzuki N. 2008. The ultimobranchial gland in poikilotherms: Morphological and functional aspects. In "Experimental Endocrinology and Reproductive Biology", eds.: Haldar C, Singaravel M, Pandi-Perumal SR, Cardinali DP, Science Publishers, U.S.A. pp. 269-296.

Srivastava BD and Srivastav Ajai K. 2017. Hepatoprotective effects of extracts of *Syzygium cumini* seeds and *Citrus sinensis* peels against microcystin LR-induced toxicity in rat. *Intern J Zool Invest.,* **3:** 95-105.

Srivastava BD, Srivastava M, Srivastav SK, Suzuki N and Srivastav Ajai K. 2018. Cypermethrin-induced liver histopathology in rat: Protective role of jamun seed and orange peel extracts. *Iranian J Toxicol.,* **12:** 25-30.

Srivastava SJ, Singh ND, Srivastava AK and Sinha R. 1995. Acute toxicity of malachite green and its effect on certain blood parameters of a catfish *Heteropneustes fossilis*. *Aquat Toxicol.,* **31:** 241-247.

Tewari A, Banga HS and Gill JPS. 2018. Sublethal chronic effects of oral dietary exposure to deltamethrin in Swiss albino mice. *Toxicol Indust Health,* **34:** 423-432.

Tripathi S and Srivastav Ajai K. 2010. Liver profile of rats after long-term ingestion of different doses of chlorpyrifos. *Pesticide Biochem Physiol.,* **97:** 60-65.

Tripathi S and Srivastav Ajai K. 2011. Alterations in the serum electrolytes, calcitonin cells and parathyroid gland of Wistar rat in response to administration of cadmium.. Proc. Intern. Con. Environ. Pollution Remediation Ottawa, Ontario, Canada, 17-19 August 2011 Paper No. 126.

Tripathi S. Suzuki N and Srivastav Ajai K. 2013. Response of serum minerals (calcium, phosphate and magnesium) and endocrine glands (calcitonin cells and parathyroid gland) of Wistar rat after chlorpyrifos administration. *Microscopy Res Technique,* **76:** 673-678.

Vihan S and Brashier DBS. 2017. A study to evaluate the antidiabetic effect of *Syzygium cumini* Linn. Seed extract in high fructose diet induced diabetes in albino rats. *Int J Basic Clin Pharmacol.,* **6:** 1363-1366.

Yousef DM, El-Fatah SSA and Hegazy AA. 2019. Protective effect of ginger extract against alterations of rat thyroid structure induced by cypermethrin administration. *J Exper Med Biol.,* **1:** 19.

Zhang Y, Kong C, Chi H, Li J, Xing J, Wang F, Shao L and Zhai Q. 2020. Effect of a beta-cypermethrin and emamectin benzoate pesticide mixture on reproductive toxicity in male mice in a greenhouse environment. *Toxicol Mech Methods,* **30:** 100-106.

JJBS

Volume 14, Number 3, September 2021
ISSN 1995-6673
Pages 423 - 431

Jordan Journal of Biological Sciences

Acacia auriculiformis Cunn. Ex Benth As Phytoextraction Agent: A Growth Response, Physiological Tolerance and Lead Removal Capability Evaluation

Abderrahmane Zerkout, Muskhazli Mustafa*, Hishamuddin Omar, Mohd Hafiz Ibrahim and Rusea Go

Department of Biology, Faculty of Science, Universiti Putra Malaysia, 43400 UPM Serdang Selangor, Malaysia

Received: July 9, 2020; Revised: October 15, 2020; Accepted: November 14, 2020

Abstract

This study was conducted to determine *A. auriculiformis* capability to tolerate elevated Pb concentration. The uptake, distribution, and the capability of *A. auriculiformis* plant to remove lead (Pb) Pb from the soil was assessed, as well as the growth performance, and some physiological parameters of the plant. The results revealed that Pb toxicity has no effect on *A. auriculiformis* plant growth up to 1 g/kg of soil, with the maximum amount of Pb absorbed in soil treated with 1 g/kg of Pb. The bioconcentration factor (BCF), and translocation factor (TF) values were 0.78 and 3.55 respectively, indicating that *A. auriculiformis* is an ideal phytoremediator for soils containing 1 g/kg Pb. In conclusion, *A. auriculiformis* exposed to high Pb concentration (1 g/kg of soil) showed good growth and development, thereby a high tolerance capacity, so it is a suitable candidate for Pb phytoremediation over the short or medium term.

Keywords: Proline, Catalase, transpiration rate, net photosynthesis, bioconcentration factor, translocation factor

1. Introduction

The exploitation of various types of deposits in the underground lead (Pb) to the accumulation of Pb on the surface which has an effective effect on plant growth and development (Adhikari *et al.,* 2014). Extensive researches have been conducted on the early stages of plants' growth and how they can be affected by heavy metals in order to help distinguish species that are heavy metal-tolerant which is crucial for this field of study as with nowadays pollution, the phytoremediation of polluted sites from toxic heavy metals is unescapable (Ali *et al.,* 2013). The high concentration of Pb intervenes various plant physiological process and development such as photosynthesis, mineral nutrition, sugar transport, seedling growth and seed germination (Zerkout *et al.* 2018).

It has been reported that plants are able to manipulate the heavy metal from the soil by restoring it in their roots (Masvodza *et al.,* 2013; Majid *et al.*, 2012; Ochonogor and Atagana, 2014). Phytoremediation has become the way out to extract heavy metal properly without affecting the environment and potentially cost-effective (Illié *et al.*, 2015), especially the phytoextraction technique. Phytoextraction is an important aspect of phytoremediation; it consists especially of the extraction of heavy metals from soil and storing them in roots, shoots and leaves (Souza *et al.,* 2013). One disadvantage of using this technique is that it takes a longer time than other treatments, due to plant limitation, where in most cases high contaminant concentration can reduce the speed of plant growth (Meriem *et al.*, 2015; Ali *et al.*, 2013; Moosavi and Seghatoleslami, 2013). However, fast growing and high heavy metal tolerance plant has been used, which requires an intensive search to identify the potential plant. The choice of phytoremediation candidates is important. Some plants can be short-lived, too small to be significant as pool to contain heavy metals or serve as food for herbivores. Ideal phytoremediation agents should be a hardy plant, long-lived, fast growing, big and inedible.

Acacia plants fit the above description perfectly, they are adapted to a wide range of environments, both tropical and temperate, and this adaptability has made them popular for planting on degraded lands in Asia and elsewhere (Turnbull *et al.,* 1997). *Acacia* spp. have the potential to rehabilitate the soil through absorption and storage of heavy metals their leaves, shoots and roots which makes them the best phytoremediation candidates (Veronica *et al.*, 2011). *Ex-situ* studies using seedling have shown that *Acacia sp.* is able to tolerate and accumulate heavy metals in a different part of the plant (Majid *et al.,* 2012; Mahdavi *et al.*, 2014). *In situ* studies using *Acacia sp.* have also been reported, such as the use of *A. saligna* and *A polyacantha* at the gold mine area in Zimbabwe (Masvodza *et al.,* 2013). In Malaysia, several studies using *Acacia mangium* in ex-tin mine (Ahmad Zuhaidi and Jeyanny, 2018), gold mine (Ahmad Zuhaidi *et al.,* 2018) and sewage disposal site (Mohd *et al.,* 2013) had shown a positive response, especially in translocation of Aluminium (Pb), Ferum (Fe), Zinc, (Zn) Copper (Cu) and Cadmium (Cd). However, *A. auriculiformis* has not been

* Corresponding author e-mail: muskhazli@upm.edu.my.

tested or reported as phytoremediation agent. Therefore, it is necessary to study other *Acacia* plants that can resist higher concentrations and have similar phytoremediation properties.

Acacia auriculiformis can be a potential candidate in this matter as it produces high biomass yield and well adapts to degraded or poor soil conditions (Sofea *et al.*, 2017). It is a fast-growing multipurpose tree species in the Leguminosae family that can reach 30 m of height and 30 cm of diameter (Turnbull *et al.*, 1997). However, phytoremediation using *A. auriculiformis* species on Pb contaminated soils has never been reported. Based on the attributes mentioned, theoretically, *A. auriculiformis* should be able to tolerate, absorb and accumulate a large amount of Pb from the soil providing a perfect remediation technique to clean up Pb from the soil.

Therefore, the current study was conducted:

I. to examine the capability of A. auriculiformis plants to tolerate elevated Pb concentration,
II. to evaluate the uptake and distribution of Pb in different parts of the plant, and;
III. to determinate the capability of A. auriculiformis plant to remove Pb from the soil.

2. Materials and Methods

2.1. Growth parameters measurement

Germinated seeds were planted in plastic polybags containing a mixture of topsoil and sand, which were artificially spiked with different Pb concentrations (ranging from 0 to 3 g/kg soil) under ambient conditions (Srinivas *et al*., 2013). The pants were arranged in a completely randomised design, and normal watering was performed every 2 days. Physical growth parameters such as shoot height, leaves number, basal diameter, and root length were measured every 3 weeks for a period of 90 days.

2.2. Physiological parameters measurement

Several selected different physiological parameters were measured to determine the plant's physiological response to Pb occurrence in soil. Net photosynthesis, total chlorophylls, internal CO_2 concentration, transpiration rate and water use efficiency (WUE) were measured directly from the plant leaves using a portable photosynthesis system LI-6400 according to Liu *et al.,* (2014) and Sinclair *et al.,* (1984).

Cell membrane integrity was estimated by measuring the electrolytic conductivity using a conductometer (Pike *et al.,* 1998) by comparing the electrolytic conductivity of fresh leaves submerge in stirred distilled water (EC1) and the electrolytic conductivity of the same sample after heated for 1 hour at 95 °C ± 0.5 °C (EC2). Membrane integrity (%) was based on the ratio between EC1 and EC2.

The relative water content (RWC) was determined based on method by Scippa *et al.,* (2004) following the formula:

$$RWC\ (\%) = [(FW - DW) / (TW - DW)] \times 100$$

Where FW is the leave fresh weight; TW is the turgescence weight (TW) and DW is the dry weight (DW).

2.3. Proline and Catalase enzyme activities

The proline or pyrrolidine 2-carboxylic acid was measured using Troll and Lindsay's (1955) method modified by Magné and Larher (1992). This technique is based on the proline's ability to react in acid and hot environments with ninhydrin to give a pink-coloured compound soluble in organic solvents such as toluene. The optical density of the samples was determined by spectrophotometry at a length of 520 nm. The standard curve was constructed using the series of proline concentrations prepared from a stock solution of 10 µg/ml.

Catalase activity (CAT) was determined as previously described by Weydert and Cullen (2009). Catalase activity was measured by monitoring the decrease in absorbance at 240 nm resulting from the decomposition of hydrogen peroxide (H_2O_2). One unit of catalase activity was defined as the amount of enzyme necessary to decompose 1 µmol/min H_2O_2 in 60 s at 25 °C ± 0.5 °C. The quantity of CAT is calculated based on the molar extinction coefficient $\Sigma = 40\ mM^{-1}.cm^{-1}$.

2.4. Quantification of Pb in plant parts.

The direct aqua regia method by McGrath and Cunliffe (1995) was used for the analyses of Pb concentrations in the samples. The Pb concentration in the sample was determined by using an air/acetylene (2.5: 15.0 L/min) flame atomic absorption spectrophotometer (AAS) at wavelengths of 283.31 nm (Lakshmi *et al.,* 2015).

2.5. Quantification of macronutrients in Acacia auriculiformis plants

Root sample solution was prepared as recommended by Abuye *et al.,* (2003) and quantification of macronutrient in the solution was then analysed by using air/acetylene (2.5: 15.0 L/min) flame atomic absorption spectrophotometer (AAS) at wavelengths of 239.856 nm for *Calcium* (Ca), 202.588 nm for *Magnesium* (Mg), 404.414 nm for *Nitrogen* (N), 213.618 nm for (P), and 766 nm for *Potassium* (K) (Silvana *et al.,* 2010).

2.6. Determination of Pb removal factor

To examine the ability of the plant to accumulate Pb with respect to its concentration in the soil and plant potential to transfer metals from the roots to shoots and leaves, the bioconcentration factor (BCF) and the translocation factor (TF) were calculated based on the following equations 1 and 2, respectively (Majid *et al.,* 2012):

$$BCF = \frac{[\text{Pb concentration in plant tissue}]}{[\text{Initial concentration of Pb in soil}]} \quad \text{(Equation 1)}$$

$$TF = \frac{\text{Pb concentration (stems + leaves)}}{\text{Pb concentration (roots)}} \quad \text{(Equation 2)}$$

3. Results

3.1. The effect of Pb on A. auriculiformis growth parameters

Figure 1 shows the effect of Pb concentrations on the growth parameters of *A. auriculiformis* plants after twelve weeks of growth. The growth parameters of *A. auriculiformis* seedlings in different treatments varied significantly compared to the control during the whole

period of growth. There was no significant difference between the control treatment and the plants treated with 1 g/kg Pb. However, plants grown in 2 and 3 g/kg Pb-treated soil had more yellow and wilted leaves with smaller buds in comparison to the control.

After 3 weeks, plants grown in 1 g/kg Pb-treated soil showed no significant difference compared to the control for all the measured parameters. Increasing the Pb concentration up 2 g/kg Pb-treated soil had led to a decrease in the shoot height, basal diameter, leaves number and root length by 52%, 16%, 31% and 65%, respectively compared to the control (Figure 2).

Figure 1. The effect of different Pb concentrations on shoot height, basal diameter, leaves numbers and root length of *A. auriculiformis* plants after twelve weeks of growth.

Lead had no effect on *A. auriculiformis* plant growth up to a concentration of 1 g/kg Pb-treated soil, as there was no significant difference in the growth performance of *A. auriculiformis* seedlings between the control treatment and plants grown in 1 g/kg Pb-treated soil.

3.2. The effect of Pb on A. auriculiformis physiological parameters

The effect of different Pb concentrations on some physiological parameters such as the net photosynthesis, total chlorophylls, transpiration rate, the internal CO_2 concentration, water use efficiency (WUE) and the relative water content (RWC) in *A. auriculiformis* is shown in Table 1. The Pb stress at 1 g/kg and 2 g/kg Pb-treated soil showed a reduction on net photosynthesis, total chlorophylls, transpiration rate and the internal CO_2 concentration in *A. auriculiformis* compared to the control. The plant showed Pb stress at 1 g/kg Pb-treated soil with decreased in WUE by 12% and the RWC by 15% significantly compared to the control. However, *A. auriculiformis* showed no significant difference between 1 g/kg and 3 g/kg Pb-treated soil for WUE and between 2 g/kg and 3 g/kg Pb-treated soil for RWC, thus indicating that the effect of Pb on *A. auriculiformis* physiological properties may vary depending on the concentration.

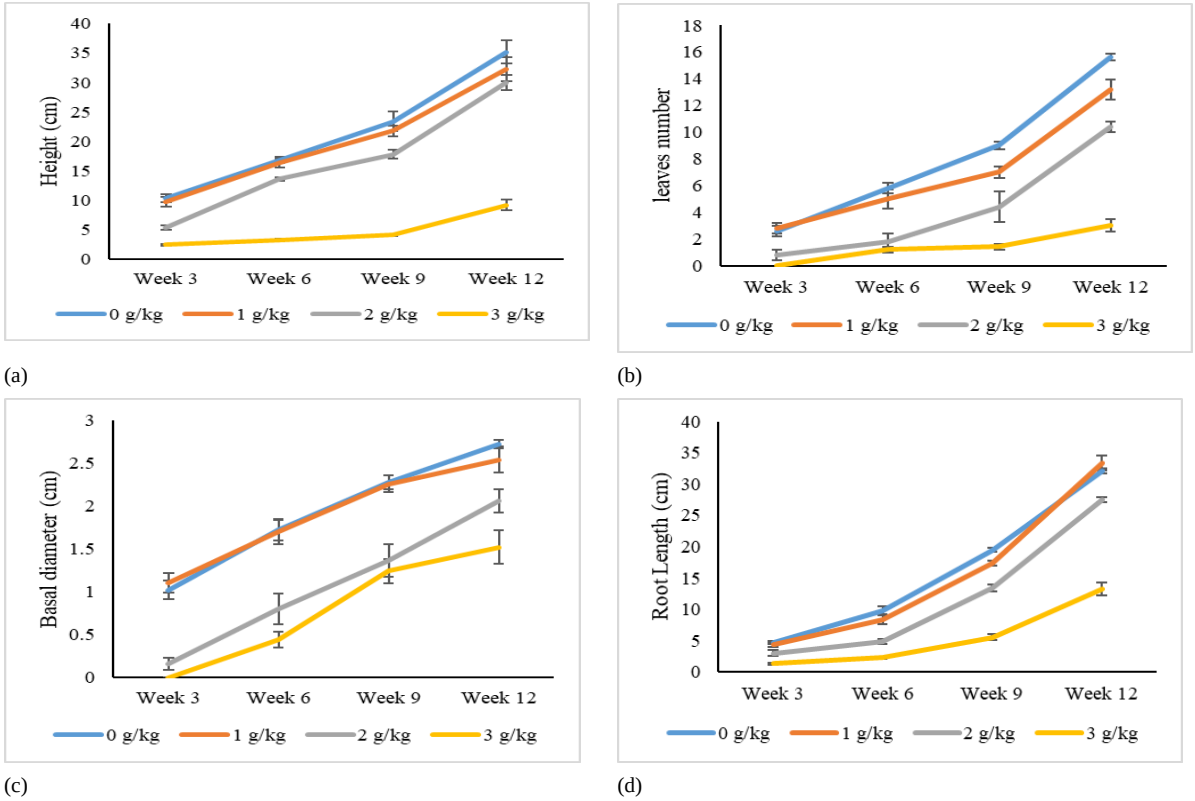

Figure 2. The effect of Pb on (a) the shoot height; (b) the leaves number; (c) the basal diameter and (d) the root length of *A. auriculiformis* plants.

Table 1. The effect of Pb on selected physiological properties in *A. auriculiformis* leaves after 90 days planted in soil supplemented with Pb

Pb (g/kg)	Net Photosynthesis ($Mmol/M^2/S$)	Total Chlorophylls	Internal CO_2 Concentration (mol/mol)	Transpiration Rate ($Mmol/M^2/S$)	WUE	RWC
0	5.60 ± 0.34^a	54.66 ± 1.6^a	217.83 ± 4.6^a	2.66 ± 0.17^a	2.40 ± 0.08^a	68.95 ± 1.5^a
1	3.59 ± 0.19^b	43.48 ± 0.2^b	169.83 ± 6.6^b	1.55 ± 0.11^b	2.11 ± 0.25^b	58.39 ± 1.8^b
2	2.60 ± 0.18^c	41.83 ± 0.3^b	169.17 ± 4.5^b	1.33 ± 0.08^b	2.00 ± 0.24^b	55.67 ± 2.8^c
3	1.71 ± 0.15^d	35.81 ± 0.8^c	146.67 ± 2.6^c	1.11 ± 0.46^c	1.55 ± 0.15^c	55.83 ± 0.8^c

3.3. Proline and Catalase response towards Pb

The results related to Pb effect on proline content in *A. auriculiformis* plant are shown in Figure 3a. The highest proline content was recorded in *A. auriculiformis* plant treated with 2 g/kg Pb-treated soil (1.40 mg/ml) followed by 1 g/kg Pb-treated soil (0.87 mg/ml). Increasing Pb concentration up to 3 g/kg of soil had significantly decreased proline content to 0.13 mg/ml. Proline accumulation in *A. auriculiformis* plants treated with 1 g/kg and 2 g/kg Pb-treated soil explained the high water content relatively close to the control (Table 4.1).

The effect of Pb on the catalase (CAT) activity in *A. auriculiformis* plant (Figure 3b), indicating that the Pb caused a significant overproduction of the CAT enzyme in *A. auriculiformis* plants grown in 1 g/kg Pb-treated soil, which was the highest (24.45 $\mu mol.min^{-1}.mg^{-1}$ protein), followed by plants grown in 2 g/kg Pb-treated soil (22.35 $\mu mol.min^{-1}.mg^{-1}$ protein). The lowest production of CAT enzyme was observed in plants grown in 3 g/kg Pb-treated soil (13.71 $\mu mol.min^{-1}.mg^{-1}$ protein).

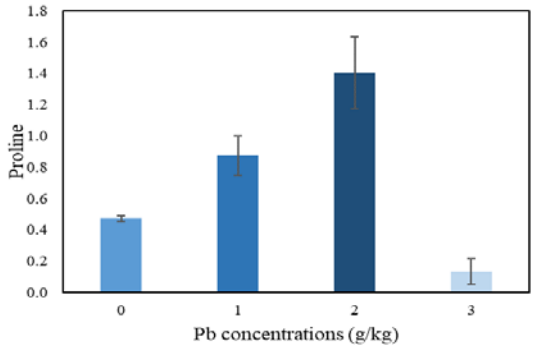

(a)

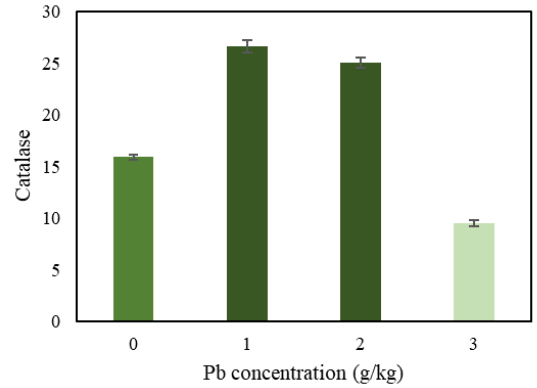

(b)

Figure 3. The effect of Pb on the (a) Proline and (b) Catalase activities in *A. auriculiformis* leaves.

3.4. Pb storage capability in different part of plant

Lead concentrations in the soil before and after planting *A. auriculiformis* were significantly influenced by Pb concentration (Figure 4a). Comparison of Pb concentration in soil between before and after *A. auriculiformis* planting showed that the lowest Pb reduction in soil was 0.28 g by control treatment, while the highest Pb concentration reduction was noted in the plants grown in 2 g/kg Pb-treated soil followed by 1 and 3 g/kg Pb-treated soil at 1.12 g, 0.95 g and 0.36 g, respectively Lead was detected in all plant parts of *A. auriculiformis*, but its distribution was not equal across parts as illustrated in Figure 4b. Roots contained the highest Pb concentration compared to other parts, followed by shoots and leaves. In roots, plants grown in 2 g/kg Pb-treated soil showed the highest Pb accumulation (0.97 g) followed by plants grown in 1 g/kg and 3 g/kg Pb-treated soil at 0.64 g and 0.60 g, respectively.

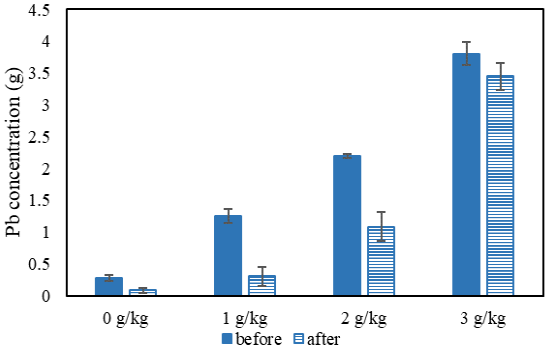

(a)

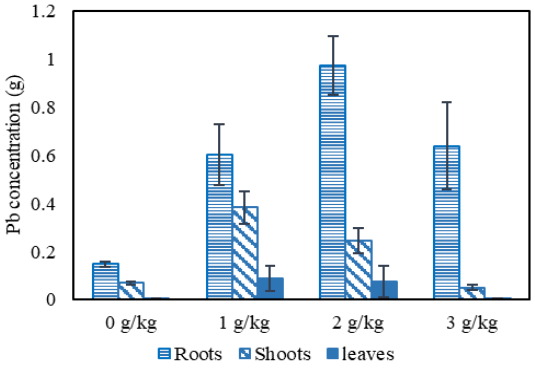

(b)

Figure 4. The concentration of Pb (a) in the soil before and after planting *A. auriculiformis* plant, and (b) in the different part of the plant.

3.5. Impact of Pb on the distribution of macronutrients

The effect of Pb on the distribution of selected macronutrients in *A. auriculiformis* plant is shown in Figure 5. It is clearly presented that Pb induced changes in the uptake of macronutrients by *A. auriculiformis* plant. Where in general, an increase in Pb concentration on soil

had produced declined pattern in the distribution of micronutrient in *A. auriculiformis*. The results showed no significant difference in the macronutrients concentrations in plants grown in 1g/kg Pb-treated soil and the control treatment. The concentration of 2 g/kg Pb-treated soil reduced the concentrations of N, P and K by 77%, 60% and 48%, respectively compared to the control, while Ca and Mg were relatively stable. The high concentration of Pb (3g/kg) affects all macronutrients content in *A. auriculiformis* plant as the concentration of all macronutrient had been decreased compared to the control (88% N, 86% P, 48% K, 19% Ca and 80% Mg).

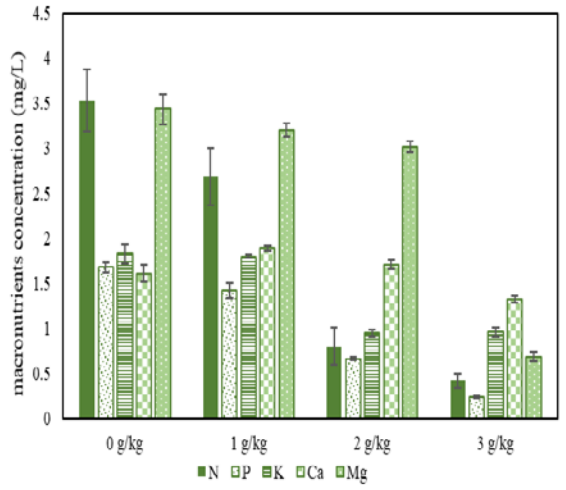

Figure 5. The effect of Pb toxicity on the absorption of macronutrients in *Acacia auriculiformis* plants.

3.6. Evaluation on potential to absorb and accumulate Pb

The bioconcentration factor decreased gradually from 3.55 to 1.20 with increasing Pb concentration from 1g/kg to 2 g/kg respectively (Figure 6). The bioconcentration factor was greater than one in all treatments (BCF > 1) indicating the plant's capability to translocate Pb from the soil to the roots which suggests that *A. auriculiformis* is a potential candidate for Pb phytoremediation. The translocation factor (TF) in A. auriculiformis plant is shown in Figure 6. Plants grown in 1 g/kg Pb-treated soil showed highest TF value (1.28) followed by plants grown in 2 g/kg Pb-treated soil (0.33), whereas the lowest TF value was observed in plant grown in 3 g/kg Pb-treated soil (0.08).

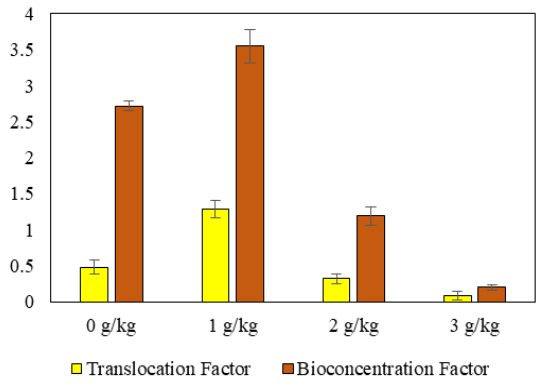

Figure 6. Values of the bioconcentration factor (BCF), and translocation factor (TF) in *A. auriculiformis* under different Pb concentration.

4. Discussion

Acacia auriculiformis seedlings grown in 1 g/kg Pb-treated soil showed high tolerance toward Pb toxicity, and this tolerance is ensured by various defence systems responsible for capturing and neutralizing the metal, and for eliminating and replacing damaged molecules (Pan *et al.*, 2011). These defence systems are usually present in the cytosol, and in different organelles, such as chloroplasts, mitochondria and peroxisomes (Del Rio *et al.*, 2006). Plants grown in 2 g/kg and 3 g/kg Pb-treated soil showed symptoms of Pb toxicity, which was observed in a reduction of plant height, leaves number, basal diameter, and root length. These results are concurring with Kanwal *et al.*, (2014) who found that high Pb doses reduced plant height and biomass, and long-term Pb exposure, even at non-lethal doses, led to necrosis at the root apex and leaves, as well as leaf chloroses. In the present study, all observed disturbances could be the result of Pb interaction with different cellular components and macromolecules, disrupting many physiological processes such as water status regulation, mineral nutrition, respiration, or photosynthesis (Ali *et al.*, 2012). According to Muhammad *et al.*, (2008) the reason for seedlings' high decrement could be the reduction in meristematic cells present in the shoot and some enzymes contained within the cotyledon and endosperms. When a metal is present in assimilable form and in very large quantities, the plant will be enriched with this metal, and above a certain rate, the plant metabolism will be reduced, the yield of the crop decreases and in extreme cases the death of the plant can occur (Ochonogor and Atagana, 2014).

The reduction in the selected physiological parameters had been observed in this study. The Pb toxicity had caused significant disruption on the biochemical pathway of the photosynthesis by distorting the chloroplast ultrastructure by either, (i) directly disrupting chlorophyll synthesis, plastoquinone and carotenoids via the inhibition of δ-aminolevulinic acid dehydratase and protochlorophyllide reductase (Pereira *et al.*, 2006; Tang *et al.*, 2008), or (ii) acting on the transport of electrons and enzymes in Calvin cycle (Rubisco in particular) causing a reduction in the chlorophyll content (Chatterjee and Chatterjee, 2003). Subsequently, Pb can also be the main cause of deterioration of thylakoid and chloroplast structure and composition, leading to photosystems damage (Ali *et al.*, 2012; Huang *et al.*, 2013).

By closing the stomata, Pb considerably affects the electron transport chain, restricting gases exchange between the leaves and the atmosphere and leads to significant reduction in CO_2 flow and fixation (Pourrut *et al.*, 2011). Decreasing the fixation of CO_2 and the transpiration rate of the stomata by Pb led to a decrease in the water use efficiency (WUE), which refers to the ratio of water used in plant metabolism to water lost by the plant through transpiration. The present study showed that Pb stress applied at 1 g/kg Pb-treated soil had caused drop in WUE and RWC. Sharma and Dubey (2005) reported the same response on WUE and RWC in *Lathyrus sativus L.* due to Pb exposure. RWC decrement indicates that the excess concentrations of Pb affect root growth by decreasing the formation of root hairs and causing structural changes thus affecting water flow into and

within roots, which reduces water uptake and its transport to the shoot (Kastori et al. 1992). The limited effect of Pb on WUE and RWC (up to 1 g/kg of soil) indicated that *A. auriculiformis* tolerates the presence of Pb by controlling water loss (15% compared to the control). This effect may result from effective stomatal regulation in cells turgidity (Chandra *et al.*, 2016). To maintain this turgidity, plants trigger other tolerance mechanisms that contribute to the adaptation of osmotic and ionic stress caused by metals, and allow the internal osmotic pressure to be adjusted due to electrolytes and organic solutes mainly from soluble sugars and amino acids, such as proline (Taji *et al.*, 2004; Denden *et al.*, 2005).

When the oxidative stress is too high and outstrips the antioxidant capacity, excess radicals cause damage to plant molecules leading to a disruption of many physiological processes such as photosynthesis and respiration (Cecchi, 2008; Agati *et al.*, 2012). At this point, the appearance of visible symptoms take place, such as browning of the roots, as well as chlorosis and necrosis on the leaves, leading to a disruption of growth that can even lead to the death of the organism. Proline is the most important amino acid that accumulates under heavy metals stress. Hence, proline accumulations in plants grown in 1 g/kg and 2g/kg Pb-treated soil proves that *A. auriculiformis* has a high tolerance potential against Pb toxicity because proline plays three major roles under metal stress; (i) acting as an excellent osmolyte, (ii) as a metal chelator (Ashraf and Foolad, (2007), and (iii) inhibitor of lipid peroxidation, thus protecting plants from oxidative stress and plays a key role in heavy metal tolerance (Ullah *et al.* 2019). Even though proline is not the only defences involve since total antioxidant activities were not correlated to their phenolic and flavonoid contents (Hamli *et al.* 2017), plants with high proline accumulation were able to tolerate or accumulate a higher concentration of metals (Ahmad *et al*., 2015). In the present study, the phytoremedial potential of *A. auriculiformis* plants was assessed by the CAT enzyme content, which is considered as a defence mechanism that allows the plant to combat this damage. The increment in the CAT enzyme in the plants are grown in 1 and 2 g/kg Pb-treated soil provides a piece of evidence that *A. auriculiformis* has a good antioxidant defence system to tolerate Pb stress, which is a powerful tool for the survival of metal accumulating plants (Habiba *et al.,* 2015). Catalase enzyme acts as an antioxidant against the reactive oxygen species (Nayana and Malode, 2012). Hence, when cells are in stress condition, they will generate H_2O_2 through emergency catabolic processes, but CAT will degrade H_2O_2 and result in a net gain of reducing equivalents (Afshan *et al.,* 2015).

However, when the capacity of antioxidant processes and detoxification mechanisms are lower than the reactive oxygen species (ROS) production, which was noted in *A. auriculiformis* seedlings grown in 3 g/kg Pb-treated soil, plant damage occurs. High levels of ROS cause inactivation of certain enzymes, decrease enzyme synthesis or change the assembly of enzyme subunits resulting in a reduction in CAT activity, thereby longer H_2O_2 action, which leads to cell disturbances and DNA damage (Lo *et al.,* 2011). *Acacia auriculiformis* showed high accumulation in proline and CAT enzyme content in plants grown in 1 g/kg and 2 g/kg Pb-treated soil to face the overproduction of ROS and the oxidative stress induced by the metal. This finding gave strong evidence of *A. auriculiformis* plant tolerance characteristic, which makes it a potential phytoremediation agent to resist and absorb Pb from the soil. Still, *A. auriculiformis* plant exposed to 3 g/kg Pb resulted in a lower accumulation in proline and CAT enzyme which adversely affect the plant resistance to oxidative stress by the inhibition of cytoplasmic enzymes and damage the structures of a cell (Asati *et al.*, 2016).

The Pb concentration in the soil had appreciable effects on Pb accumulation in *A. auriculiformis* plant tissues, and as the concentration of Pb increased, the transport of Pb from the root to different plant parts decreased in the following order: root > shoot > leaves. The findings pertaining to the Pb uptake in this study agree with John *et al.* (2009) study on *Brassica juncea* roots, as roots are directly subjected to Pb contamination and act as barriers to apoplastic and symplastic Pb transport. Hence, Pb translocation to the aerial part of the plant is disturbed (Page and Fuller, 2015). This may be due to a decrement in lignified cells and xylem vessels, which can be explained by occlusion of the xylem vessels (Dugé de Bernoville, 2009). The phenomena of vascular occlusion are the deposition of a fibrous polysaccharide material, which is the origin of the formation of plugs in the xylem, preventing water supply and consequently, reduction in the vessel's lumen diameter. This obstruction is a defensive reaction of the plant to prevent the flux of Pb which follows the water movement in the plant (Dugé de Bernoville, 2009) and that explains the reduction in the water content observed in Table 4.1. Vessel occlusion has been reported as plant response under metal stress in *Vicia sativa* (Pérez-de-Luque *et al.*, 2006).

According to Wierzbicka, (1987) only a small fraction of Pb presented in the root will be transferred to the aerial parts because more than 90% is found in insoluble form and strongly bound to the outer cellular envelopes. In the present study, 20% and 14% of Pb absorbed by *A. auriculiformis* plants were translocated to the areal parts in 1g/kg and 2 g/kg Pb-treated soil, respectively. This limited transport from roots to leaves was caused by the barrier formed by the root endoderm where casparian strip bands is the major factor restricting the movement of Pb from the endoderm to the central cylinder (Sharma and Dubey 2005),. This restriction of transport to aerial parts represents a tolerance factor for some plants to the presence of contaminants in their growing medium, and it is important for their survival where only a small portion of Pb absorbed and transferred to the leaves, as Pb is a toxic element for photosynthetic activity, chlorophyll and antioxidant enzymes synthesis (Kim *et al.,* 2003).

The competition on the sorption place between Pb ions and the macronutrients in the roots surface especially those with the same valency such as N, P, and K which affects their absorption (Küpper and Kochian, 2010). Therefore, Pb will interfere with nutrient uptake by affecting membrane transport processes and altering the permeability of the plasma membrane (Dong *et al.*, 2006). When Pb attaches to membrane wall components in large quantities, it changes the physical and chemical properties of the wall, and its plasticity. This plasticity reduction affects many cellular mechanisms such as cell division and elongation, which affects the proper functioning of plant cells (Pourrut, 2008). As shown in Figure 2, the symptoms

of high Pb toxicity in *A. auriculiformis* plants were expressed by growth inhibition, particularly root growth, by reducing the absorption of water and similarly the absorption of essential nutrients, such as N, P, and K which play a significant role in the metabolism of plants including chlorophyll synthesis, protein analysis, stem and root growth, and enzyme cofactors associated with metabolites transport (Tripathi *et al.*, 2014).

The crucial factors determining *A. auriculiformis* phytoremediation either as phytostabilisation or phytoextraction may lie in the translocation process of Pb from the roots to the areal parts. According to Bongoua-Devisme *et al.* (2019), TF and BFC value will determine the type of phytoremediation agent either as phytoextraction (TF and BCF > 1) or phytostabilisation (TF and BCF <1) or phytostabiliser but act as phytoextract at lower concentrations (BCF > 1 and TF < 1). Oseni *et al.* (2018) reported herbaceous plant, *Sida acuta* and *Chromolaena odorata* only managed to exhibit TF value at 0.9 and 0,7 respectively with most of extracted Pb stored in the roots system. Thus, both plants can only be considered as phytostabilisations agent since the Tf value was less than 1. In the present study, the BCF and TF in 1 g/kg Pb treatments were higher than 1. The high tolerance of *A. auriculiformis* shown previously in growth result, with the BCF and TF greater than 1 makes it an excellent candidate to phytoextract Pb from the soil. However, BCF and TF decreased with the increment of Pb concentration as increasing the concentration of Pb to 2 g/kg and 3g/kg Pb-treated soil hampered normal physiological and metabolic activities. Subsequently *A. auriculiformis* avoids translocation of this metal by the implementation of several mechanisms to reduce the transfer of Pb to the aerial part of the plant. This is an important protective mechanism against the spread of this toxic metal to green tissue (Sinha *et al.*, 2013). Majid *et al.*, (2012) observed a BCF of 1.02 and a TF of 1.89 in *A. mangium* grown in a sewage sludge containing only 19.2 ppm of Pb. However, the concentrations of metals experimented in the media are very low compared to the present study, where *A. auriculiformis* plants grown in 1 g/kg Pb-treated soil showed high tolerance, absorbed 0.64 g in their roots and translocated 0.38 g to the shoots. With the BCF and TF more than 1, *A. auriculiformis* could be a perfect phytoremediation candidate as a Pb phytoextractor in a contaminated soil with no more than 1 g/kg Pb. Although increasing Pb concentration to 2 g/kg of soil reduced and hampered different plant morphological and physiological functions, *A. auriculiformis* plants were able to grow and absorb 0.97 g of Pb in its roots; thus it can be used as a phytostabilizer in a 2 g/kg Pb contaminated soil.

5. Conclusion

Lead accumulation induced both physiological and biochemical changes in *A. auriculiformis* with Pb tolerance proportional to the increased of Pb concentrations and significantly increased level of antioxidative enzymes (catalase). The results demonstrated that *A. auriculiformis* can tolerate Pb toxicity up to 2 g/kg Pb of soil, and hyper–accumulate a significant amount of Pb content in roots and shoots through phyto stabilisation and phyto-extraction.

Acknowledgment

The authors would like to thank the Ministry of Higher Education, Malaysia and Universiti Putra Malaysia for the financial support through FRGS Grant no. FRGS/1/2016/STG03/UPM/202/8 and all staff of the Plant Systematic and Microbe Laboratory, Biology Department, Universiti Putra Malaysia for all their continuous efforts and contributions. in one way or another.

References

Abuye C, Urga K, Knapp H, Selmar D, Omwega AM, Imungi JK, and Winterhalter P. 2003. A compositional study of *Moringa stenopetala* leaves. *J. East Afr. Med*, **80:** 247–252.

Adhikari T, Kumar A, Singh MV and Rao AS. 2014. Phytoaccumulation of lead by selected wetland plant species. *Commun. Soil Sci. Plant Anal*. **41**: 2623-2632.

Afshan S. Ali S, Bharwana SA, Rizwan M, Farid M, Abbas M, Ibrahim F, Mehmood MA and Abbasi GH. 2015. Citric acid enhances the phytoextraction of chromium, plant growth and photosynthesis by alleviating the oxidative damages in *Brassica napus* L. *Environ. Sci. Pollut. Res.* **22**: 11679-11689.

Agati G, Azzarello E, Pollastri S and Tattini M. 2012. Flavonoids as antioxidants in plants: location and functional significance. *Plant Sci*. **196**: 67–76.

Ahmad A, Hadi F and Ali N. 2015. Effective phytoextraction of cadmium (Cd) with increasing concentration of total phenolics and free proline in *Cannabis sativa (L)* plant under various treatments of fertilizers, plant growth regulators and sodium salt. *Int J Phytoremediation.* **17**: 56-65.

Ahmad Zuhaidi Y and Jeyanny V. 2018. Phytoremediation of heavy metals using *Acacia mangium* in Rahman Hydraulic Tin (RHT) tailings, Klian Intan, Malaysia. *Adv. Plant Agri. Res.* **8**: 247-249

Ahmad Zuhaidi Y, Jeyanny Y, Fakhri MI and Wan Rasidah K. 2018. Reversing soil degradation via phytoremediaton techniques in an ex-tin mine and gold mine in Peninsular Malaysia. Pp 686-691 *Proceeding Global Symposium of Soil Pollution*, 2-4 May 2018. Rome, Italy

Ali A, Iqbal N, Ali F, Afzal B and Nicholson G. 2012. *Alternanthera bettzickiana* (Regel) a potential halophytic ornamental plant. *Growth Physiol. Adapt. Flora.* **20**: 318–321.

Ali H, Khan E and Sajad MA. 2013. Phytoremediation of Heavy Metals-Concepts and Applications. *Chemosphere*. **91**: 869-881.

Asati S, Pichhode M and Nikhil K. 2016. Effect of Heavy Metals on Plants: An Overview. *Int J App Inno Engin Management*. **5**: 2319-4847.

Ashraf M and Foolad MR. 2007. Roles of glycine betaine and proline in improving plant abiotic stress resistance. *Environ. Exp. Bot.* **59**: 206-216.

Bongoua-Devisme AJ, Akotto OF, Guety T, Kouakou SAAE, Ndoye F and Diouf D. 2019. Enhancement of phytoremediation efficiency of Acacia mangium using earthworms in metal-contaminated soil in Bonoua, Ivory Coast. *African J Biotech* **18**: 622-631.

Chatterjee J, and Chatterjee C. 2003. Management of phytotoxicity of cobalt in tomato by chemical measures. *Plant Sci.* **64:** 793-801.

Cecchi M. (2008). Devenir du plomb dans le système Sol-Plante: Cas d'un sol contaminé parune usine de recyclage du plomb et de deux plantes potagères (Fève et Tomate). PhD thesis. Institut National Polytechnique de Toulouse. France

Chandra R. and Kang H. 2016. Mixed heavy metal stress on photosynthesis, transpiration rate, and chlorophyll content in poplar hybrids. *Forest Sci. Technol*. **12**: 55–61.

Del Rio CM, Font R, Moreno-Rojas R and De Haro-Bailon A. 2006. Uptake of lead and zinc by wild plants growing on contaminated soils. *Ind Crop Prod*. **24:** 230-237.

Denden M, Bettaieb T, Salhi A and Mathlouthi M. 2005. Effet de la salinité sur la fluorescence chlorophyllienne, la teneur en proline et la production florale de trois espèces ornementales, *Tropicultura*, **23:** 220-225.

Dong J, Wu F and Zhang G. 2006. Influence of cadmium on antioxidant capacity and four microelement concentrations in tomato seedlings (*Lycopersicon esculentum*). *Chemosphere*. **64:** 1659–1666.

Dugé de Bernonville, T. 2009. Caractérisations histologique, moléculaire et biochimique des interactions compatible et incompatible entre Erwinia amylovora, agent du feu bactérien, et le pommier (*Malus x domestica*). PhD Thesis. University of Angers, Fance.

Habiba U, Ali S, Farid M, Shakoor MB, Rizwan M, Ibrahim M, Abbasi GH, Hayat T and Ali B. 2015. EDTA enhanced plant growth, antioxidant defense system and phytoextraction of copper by *Brassica napus* L. *Environ. Sci. Pollut. Res*. **22** : 1534–1544.

Hamli S, Kadi K, Addad D and Bouzerzour H. 2017. Phytochemical Screening and Radical Scavenging Activity of Whole Seed of Durum Wheat (*Triticum durum* Desf.) and Barley (*Hordeum vulgare* L.) Varieties. *Jordan J Bio Sci.* **10**: 323-327

Huang J, Qin F, Zang G, Kang Z, Zou H, Hu F, Yue C, Li X and Wang G. 2013. Mutation of OsDET1 increases chlorophyll content in rice. *Plant Sci* **210**: 241-249.

Illié ZS, Mirecki N, Trajkovic R, Kapoulas N, Milenkovic L and Sunic L. 2015. Effect of Pb on germination of different seed and his translocation in bean seed tissues during sprouting. *Fresenius Environ Bull*. **24**: 670–75.

John R, Ahmad P, Gadgil K and Sharma S. 2009. Heavy metal toxicity: Effect on plant growth, biochemical parameters and metal accumulation by *Brassica juncea L. Int J Plant Prod*. **3**: 65-76.

Kanwal U, Ali S, Shakoor MB, Farid M, Hussain S, Yasmeen T, Adrees M, Bharwana SA and Abbas F. 2014. EDTA ameliorates phytoextraction of lead and plant growth by reducing morphological and biochemical injuries in *Brassica napus* L. under lead stress. *Environ. Sci. Pollut. Res*. **21**: 9899–9910.

Kastori R, Petrović M and Petrović N. 1992. Effect of excess lead, cadmium, copper, and zinc on water relations in sunflower. *J Plant Nut* **15**: 2427-2439

Kim YY, Yang YY and Lee Y. 2003. Pb and Cd uptake in rice roots. *Physiol Plant*. **116:** 368-372.

Küpper H and Kochian LV. 2010. Transcriptional regulation of metal transport genes and mineral nutrition during acclimatization to cadmium and zinc in the Cd/Zn hyperaccumulator, *Thlaspi caerulescens* (Ganges population). *New Phytol*. **185:** 114–129.

Liu X, Mak M, Babla M, Wang F, Chen G, Veljanoski F, Wang G, Shabala S, Zhou M and Chen Z. 2014. Linking stomatal traits and expression of slow anion channel genes HvSLAH1 and HvSLAC- 1with grain yield for increasing salinity tolerance in barley. *Front Plant Sci*. **5**:1–12

Lo IMC, Tsang DCW, Yip TCM, Wang F and Zhang W. 2011. Influence of injection conditions on EDDS-flushing of metal-contaminated soil. *J Hazard Mater*. **192**: 667-675.

Magné C and Larher F. 1992. High sugar content of extracts interferes with colorimetric determination of amino acids and free proline. *Anal. Biochem*. **200**:115–118.

Mahdavi A, Khermandar K, Asbchin SA and Tabaraki R. 2014. Lead Accumulation Potential in *Acacia victoria*. *Int J Phytomerediation*. **16**: 582-592

Majid NM, Islam MM and Mathew L. 2012. Heavy metal uptake and translocation by mangium (*Acacia mangium*) from sewage sludge contaminated soil. *Aust J Crop Sci* **6**:1228- 1235.

Masvodza DR, Dzomba P, Mhandu F and Masamha B. 2013. Heavy Metal Content in *Acacia saligna* and *Acacia polyacantha* on Slime Dams: Implications for Phytoremediation. *Am J Exp Agri.* **3**: 871-883.

McGrath SP and Cunliffe CH. 1995. A simplified method for the extraction of the metals in sewage sludge on soils, microorganisms and plants. *J. Ind. Microbiol*. **14:** 94-104.

Meriem L, Baghdad B, El Hadi D and Bouabdli A. 2015. Phytoremediation Mechanisms of Heavy Metal Contaminated Soils: A Review. *Open J Ecol.* **5**:375–88.

Mohd SN, Majid N M, Shazili N A M and Abdu A. 2013. Growth performance, biomass and phytoextraction efficiency of *Acacia mangium* and *Melaleuca cajuputi* in remediating heavy metal contaminated soil. *Am J Environ Sci* **9**: 310-316.

Moosavi SG and Seghatoleslami MJ. 2013. Phytoremediation: A Review. *Adv Agri Biol* **1**: 5–11

Muhammad S, Iqbal MZ and Mohammad A. 2008. Effect of lead and cadmium on germination and seedling growth of *Leucaena leucocephala*. *J. Appl. Sci. Environ.* **12:** 61 - 66.

Nayana S and Malode SN. 2012. Phytoremediation Potential of *Cassia Tora* (L.), Roxb. to remove heavy metals from Waste soil, collect from sukali compost and landfill depot, amravati (M.S.). Global J Bio-Sci Biotech **1**: 104-109

Ochonogor RO and Atagana HI. 2014. Phytoremediation of Heavy Metal Contaminated Soil by *Psoralea pinnata*. *Int J Environ Sci Dev*. **5**: 440-443.

Oseni OM, Dada OE, Okunlola GO and Ajo AA. 2018. Phytoremediation Potential of *Chromolaena odorata* (L.) King and Robinson (Asteraceae) and *Sida acuta* Burm. f. (Malvaceae) Grown in lead-Polluted Soils. *Jordan J Bio Sci.* **11**: 355-360

Page V and Feller U. (2015). Heavy Metals in Crop Plants: Transport and Redistribution. *Agronomy*. **5**: 447-463.

Pan X, Zhang D, Chen X, Bao A and Li L. 2011. Antimony accumulation, growth performance, antioxidant defense system and photosynthesis of *Zea mays* in response to antimony pollution in soil. *Water Air Soil Pollut*. **21:** 517-523.

Pereira LB, Tabaldi LA, Goncalves JF, Jukoski JO and Pauletto MM. 2006. Effect of aluminium on inolevulinic acid dehydratase (ALAD) and the development of cucumber (*Cucumis sativus*). *Environ Exp Bot*. **57:** 106-115.

Pérez-de-Luque A, Lozano-Baena MD, Prats E, Moreno MT and Rubiales D. 2006. Medicago truncatula as a Model for Nonhost Resistance in Legume-Parasitic Plant Interactions. *Plant Physiol*. **145:** 2437-449.

Pike S M, Ádám A L, Pu X A, Hoyos ME, Laby R, Beer SV and Novacky A. 1998. Effects of Erwinia amylovora harpin on tobacco leaf cell membranes are related to leaf necrosis and electrolyte leakage and distinct from perturbations caused by inoculated *E. amylovora*. *Physiol Mol Plant Pathol*. **53:** 39-60.

Pourrut B, Shahid M, Dumat C, Winterton P and Pinelli EB. 2011. Lead uptake, toxicity, and detoxification in plants. *Rev Environ Contam Toxicol*. **213**:113-36.

Pourrut B, Perchet G, Silvestre J, Cecchi M, Guiresse M and Pinelli E. 2008. Potential role of NADPH-oxidase in early steps of lead-induced oxidative burst in *Vicia faba* roots. *J Plant Physiol*. **165:** 571–579

Scippa G, Di-Michele M, Onelli NE, Patrignani G, Chiatante D. and Bray E. 2004. The histone-like protein H1-S and the response of tomato leaves to water deficit. *J Exp Bot.* **55**: 99-109.

Sharma P and Dubey RS. 2005. Lead toxicity in plants. *Braz J Plant Physiol*. **17**:35-52.

Sofea A, Zerkout A, Nor Azwady AA, Rusea G and Muskhazli M. 2017. Assessment of *Acacia auriculiformis* Cunn. Ex Benth. Seed Germination and Growth Resistance towards Arsenic Toxicity. *Annu Res Rev Biol.* **18**: 1-10.

Souza LA, Fernando AP, Roberta CN and Ricardo AA. 2013. Use of Non-Hyperaccumulator Plant Species for the Phytoextraction of Heavy Metals Using Chelating Agents. *Sci. Agric.* **4:** 290–95.

Sinclair TR, Tanner CB and Bennett JM. 1984. Water use efficiency in crop production. *BioScience*. **34**: 36-40.

Sinha S, Mishra RK, Sinam G, Mallick S and Gupta AK. 2013. Comparative Evaluation of Metal Phytoremediation Potential of Trees, Grasses and Flowering Plants from Tannery Wastewater Contaminated Soil in Relation with, Physico-Chemical Properties. *Soil Sediment Contam.* **22**: 958-983.

Silvana RO, José AGN, Joaquim AN and Bradley TJ. 2010. Determination of macro- and micronutrients in plant leaves by high-resolution continuum source flame atomic absorption spectrometry combining instrumental and sample preparation strategies. *Spectrochim Acta Part B.* **65**: 316–320.

Srinivas TNR, Kailash TB and Anil KP. 2013. *Silanimonas mangrovi* sp. nov., a member of the family *Xanthomonadaceae* isolated from mangrove sediment, and emended description of the genus *Silanimonas*. *Int. J. Syst. Evol. Microbiol*. **63**: 274-279.

Taji T, Seki M, Satou M, Tetsuya S, Masatomo K, Kanako I, Yoshihiro N, Mari N, Jian-Kang Z and Kazuo S. 2004. Comparative genomics in salt tolerance between Arabidopsis and aRabidopsis-related halophyte salt cress using Arabidopsis microarray. *Plant Physiol*. **135:**1697-1709.

Tang Q, Lin LX, Yu ZX, Yi H and Hua Y. 2008. Effects of plumbum and chromium stress on the growth of tea plants. *Southwest China J Agri Sci*. **21**:156-162.

Tripathi DK, Singh VP, Chauhan DK, Prasad SM and Dubey NK. 2014. Role of macronutrients in plant growth and acclimation: recent advances and future prospective. In: Ahmad P, Wani MR, Azooz MM and Tran LSP (Eds.). Improvement of crops in the era of climatic changes. Springer, New York, pp 197–216

Troll W and Lindsey J. 1955. A photometric method for the determination of proline. *J Biol Chem* **215**: 655-660

Turnbull JW, Midgley SJ and Cossalter C. 1997. Tropical *Acacias* planted in Asia: an overview of recent developments in *Acacias* planting. In: Turnbull, J.W., et al. (Eds.) Proceedings of Recent Developments in Acacia Planting. Australia Center of International Agriculture Research. Hanoi.

Ullah R, Hadi F, Ahmad S, Jan AU and Rongliang Q. 2019. Phytoremediation of Lead and Chromium Contaminated Soil Improves with the Endogenous Phenolics and Proline Production in *Parthenium*, *Cannabis*, *Euphorbia*, and *Rumex* Species. *Water Air Soil Poll.* **230**: 40

Veronica J, Majid NM, Islam MM and Arifin A. 2011. Assessment of heavy metal uptake and translocation in *Acacia mangium* for phytoremediation of cadmium contaminated soil. *J Food Agric Environ*. **9:** 588-592.

Weydert CJ and Cullen JJ. 2009. Measurement of superoxide dismutase, catalase, and glutathione peroxidase in cultured cells and tissue. *Nat Protoc*. **5**: 51–66.

Wierzbicka M. (1987). Lead translocation and localization in *Allium cepa* roots. *Can J Bot.* **65:** 1851-1860.

Zerkout A, Omar H, Ibrahim MH and Muskhazli M. 2018. Influence of Lead on *In vitro* Seed Germination and Early Radicle Development of *Acacia auriculiformis* Cunn. Ex Benth Species. *Annu Res Rev Biol.* **28**: 1-12.

JJBS

Jordan Journal of Biological Sciences

Volume 14, Number 3, September 2021
ISSN 1995-6673
Pages 433 - 440

Ovicidal, Larvicidal and Pupicidal Efficacy of Crude Methanol and Hexane Extract of *Urtica massaica* Mildbri on *Anopheles gambiae* Giles

Khatoro R.T[1], Yugi, J.O.[2,*] and Sudoi V[1]

[1] School of Environmental Studies, University of Eldoret, P. O. Box 1125-30100, Eldoret, Kenya;[2]School of Science and Technology, University of Kabianga P.O Box 2030 -20200. Kericho, Kenya.

Received: March 11, 2020; Revised: September 13, 2020; Accepted: September 13, 2020

Abstract

This study was designed to evaluate ovicidal, larvicidal and pupicidal potency of methanol and hexane extracts of leaves, stems and roots of *Urtica massaica* Mildbr. against aquatic stages of *Anopheles gambiae* Giles. The effectiveness of the extracts was evaluated using the WHO protocol. One-way analysis of variance was performed for statistical justifications of the insecticidal property of the extracts with *p* considered significant at $p < 0.05$. It was found that potency of extracts was dose dependent. Extracts from the stem were more potent than the roots or leaves. Mortalities of the aquatic stages were however, significantly different ($p < 0.05$) irrespective of stage. Third larval instars (L3s) were more susceptible than eggs or pupae. Doses of 80 cm^3/100ml (s/w) and above matched the WHO > 80% mortality for an effective insecticide. It was concluded that higher doses of the crude extracts of *U. massaica* were potent against *An. gambiae.*

KeyWords: *Urtica massaica*, Extracts, Methanol, Hexane, *Anopheles gambiae*, *Bacillus thurigiensis*

1. Introduction

Mosquitoes serve as vectors of several diseases, causing serious health problems and death in humans (Alayo *et al.*, 2015). Among diseases transmitted by mosquitoes is malaria whose causative agent is *Plasmodium* parasites. Malaria is responsible for morbidity, mortality, low birth weight, stillbirths, and early infant death mainly in tropical and subtropical areas (Karunamoorthi *et al.*, 2014). About 3.2 billion people are at risk of malaria (WHO, 2017) infection.

Presently, protection against mosquito bites is through vector control from the use of insecticide treated nets (ITNs) and larval source reduction. This approach has greatly reduced the frequency of contact between mosquitoes and humans and is considered a big win towards the fight against vector borne diseases since the current lack of effective prophylactic vaccine or well-established preventive measure (Soonwera, 2015) at the moment would mean escalation in the current sorry state of such disease burden. Moreover, the continual application of synthetic insecticides in the management of insect vectors is disadvantageous as it is non target specific (Sanghong *et al.*, 2015; Soonwera, 2015; Govindarajan *et al.*, 2016), bringing about disturbance of natural ecosystems, leading to development of resistance in vector population and in some cases resulting in resurgence of vector borne diseases.

To mitigate these challenges, scientists have turned their attention to the use of natural products as an alternative strategy to the control of insect vector population. This is because the natural products are not only a rich source of bioactive phytochemicals but are also safe, biodegradable and non-toxic (Asadollahi *et al.*, 2019). These products are, therefore, an excellent source of green insecticides that are eco-friendly and also seen as the solution to the inevitable environment and human health challenges.

Urtica massaica Mildbr, commonly known as stinging nettle, is a perennial herb (Ayan *et al.*, 2006) from the family of *Urticaceae.* It grows naturally in the borders of fields, roads and forests and is mostly found in the wet parts of the highlands in Kenya. It is a vegetable (Grubben, 2004) among other uses. Leaf and root extracts of this plant are rich in proteins, vitamins, minerals, amino acids (Westfall, 2001) and polyphenols that have found use as food and in the pharmaceutical industries (Kregiel *et al.*, 2018). Though the extracts are toxic (Oloro *et al.*, 2015) and with potential for teratogenicity (Wabai *et al.*, 2018), they have been known to cure stomach aches, malaria, bruises, injuries, fractures, venereal diseases, rheumatism, urethral leak, hepatic diseases (Grubben, 2004) as well as manage diabetes (Ketera and Mutiso, 2012; Kamau *et al.*, 2017). Methanolic extracts of *U. massaica* have also been demonstrated to have antimicrobial (Ko¨rpe *et al.*, 2013) as well as fungal potential (Kamalakannan *et al.*, 2012; Kipruto *et al.*, 2019).

* Corresponding author e-mail: jowiti@kabianga.ac.ke; yugijared@gmail.com.

It is believed that there are a lot of other potential benefits of this wonder herb that have not been exposed, and the present study was designed to enlighten us on this. In this study, potency of methanolic and hexane extracts of leaves, stems and roots of *U. massaica* is evaluated against *An. gambiae* Giles aquatic stages under laboratory conditions. This is to generate and inform on effect on mosquitocidal effect of these extracts and avail this information that is presently unknown.

2. Materials and Methods

2.1. Study area, experimental mosquitoes and study design

Eggs, third larval instars (L3s) and pupae of *An. gambiae* mosquitoes kept at the insectary of the Entomological laboratory at the Centre for Global Health Research and reared following standard techniques as describe by Das *et al.* (2007) and Yugi *et al.* (2014) were used in the experiments described in this study. A completely randomized informal 'after-only with control' experimental design (Kothari, 2004) was used to investigate the ovicidal, larvicidal and pupicidal effect of crude methanol and hexane extracts of *U. massaica* on the aquatic stages. Solvent, dose and *U. massaica* extracts were taken as independent while observed mortalities as dependent variables respectively. *Bacillus thurigiensis israelensis* (Bti) was taken as positive while dimethyl sulfoxide (DMSO) and distilled water were taken as negative control.

2.2. Plant materials

Fresh leaves, stem and roots of *U. massaica* were collected from Kambi Somali in Eldoret on May 2017. The site is at an altitude of (35^0 16' 46'' E, 0^0 31' 41'' N) and an elevation of 2118 meters above sea level. The plant was identified and a voucher specimen number JOY2017/001 issued. The voucher was later deposited at the School of Biological Sciences, University of Nairobi herbarium.

2.3. Methanol and hexane extracts of Urtica massaica

Two hundred grams of ground powdered leaves of *U. massaica* were soaked in 400ml of absolute methanol for 1hr after which the suspension was filtered using Whatman No. 1 filter paper and the filtrates freeze-dried using the Edwards Modulyo Freeze-drying machine to remove the solvent. The derived paste was stored as freeze-dried stock for later use. The procedure was repeated for stem and root grounded powders respectively. Hexane extracts of the respective plant parts was also derived following a similar procedure.

2.4. Preparation of stocks solution

One (1) g of crude methanol stock's extracts of *U. massaica* leaves was weighed and dissolved in 100ml of dimethyl sulfoxide (DMSO). Eighty milliliters (ml) of this solution was obtained and topped up with 20 ml of distilled water to make 100 ml. This solution made a 80 ml/100ml of distilled water. A second quantity of 80ml of the stock's solution was prepared but toped up with 120 ml of distilled water. This solution was then apportioned in two beakers of equal capacity (100ml) each with a concentration of 40 ml/100ml (s/w). One of this was picked and 100ml distilled water added and later apportioned in two beakers of equal capacity with each having 20ml/100ml (s/w). This procedure was repeated until serial dilution of 80, 40, 20, 10, 5 and 2.5 ml /100 ml distilled water was obtained. A similar procedure was used to prepare stock's and serially dilute solution for stems and roots as well as for crude hexane extracts of similar parts of *U. massaica*

2.5. Baccillus thurigiensis israeliensis (Bti)

Baccillus thurigiensis israeliensis (Bti) used in this study was obtained from CGHR/KEMRI. 80 mg of it was dissolved in 1l of distilled water to make a stock's solution. Bti has demonstrated efficacy as larvicide against mosquitoes (Uragayala *et al.*, 2018; Derua *et al.*, 2019), and it is on this basis that it was used as a positive control to compare to that of the test botanical extracts from *U. massaica.*

2.6. Empirical activities

Three bioassay experiments were conducted to evaluate ovicidal, larvicidal and pupicidal potency of crude methanol and hexane extracts of leaf, stem and root of *U. massaica* against *An. gambiae* aquatic stages. In each experimental arrangement, three sets of plastic containers measuring 6 cm × 5.7 cm × 3.5 cm were used. To each container, approximately 33ml of a particular solution of either crude methanol or hexane extracts of leaf, stem or root of *U. massaica* was added. Four replicates for each concentration including appropriate controls were used. Standard WHO procedures and thresholds were used to assess effectiveness of the extracts as insecticides at a mortality rate of > 80% (WHO, 2005).

2.6.1. Ovicidal, Larvicidal and Pupicidal Bioassays

Freshly laid eggs of *An. gambiae* were collected from adult culturing cages, counted in batches of 10 under a dissecting microscope (Leica Zoom 2000) at × 10 magnification using fine tipped painting brushes and placed in smaller Whatman No. 1 filter papers. Each of such filter paper was then gently placed in containers. Mortality of the eggs was assessed 48 hrs post treatment by observing the eggs under dissecting microscope (Leica Zoom 2000) at × 10 magnification and noting if the egg was dead or alive. A dead egg was one that was non-hatched and with unopened opercula and a live egg was one that had hatched or with open operculum. Abbot's formula (1925) was employed to correct percentage viability of eggs if control inhibition of egg hatching was between 5 % and 20 %. Egg mortality was calculated using the formula;

$$\% \text{ egg mortality} = \frac{\text{Number of hatched laevae}}{\text{Total number of eggs exposed}} \times 100$$

Batches of ten freshly transformed third larval instars (L3) were collected and transferred by means of a dropper to plastic containers. The larvae were left exposed overnight. Moribund and dead larvae were put in a pail of hot water and dispensed in a septic tank. Larval mortality was registered 24 hours post exposure and mortality calculated using the formula;

$$\% \text{ Larval mortality} = \frac{\text{Number of dead larvae}}{\text{Total number of exposed larvae}} \times 100$$

Ten early stage pupae (pupae metamorphosing from L4 larvae within a two-hour window) were randomly picked from a tray containing such pupae using a dropper and placed individually in plastic containers**.** The mouth of each container was covered with mosquito netting to prevent emerged adult from escape. The pupae were exposed overnight and mortality rate determined 24 h later. This experiment was replicated four times. Mortality was calculated as well as corrected using Abbott's formula (Abbott, 1925) as shown below;

$$\%\ \text{Mortality} = \frac{\text{Number of dead pupae}}{\text{Total number of pupae introduced}} \times 100$$

$$\%\ \text{Corrected mortality} = \frac{\text{Percent mortality in test} - \text{Percent mortality in control}}{100 - \text{Percent in control}} \times 100$$

2.7. Statistical Analysis

Data was entered in excel spreadsheets and the relationship between the effect of the crude methanol and hexane extracts of *U. massaica* on exposed eggs, larvae and pupae of *An. gambiae* were determined. Descriptive statistics was used to express the effect of the solvent of extraction, dose and part of plant used on exposed mosquito stages. One-way analysis of variance (ANOVA) was used to determine the level of significance of the impact of the extracts on the exposed mosquitoes. Student's t test was used to compare effect of solvent on potency of extracts. All statistical analysis was performed using statistical package for social scientists (SPSS) version 22.

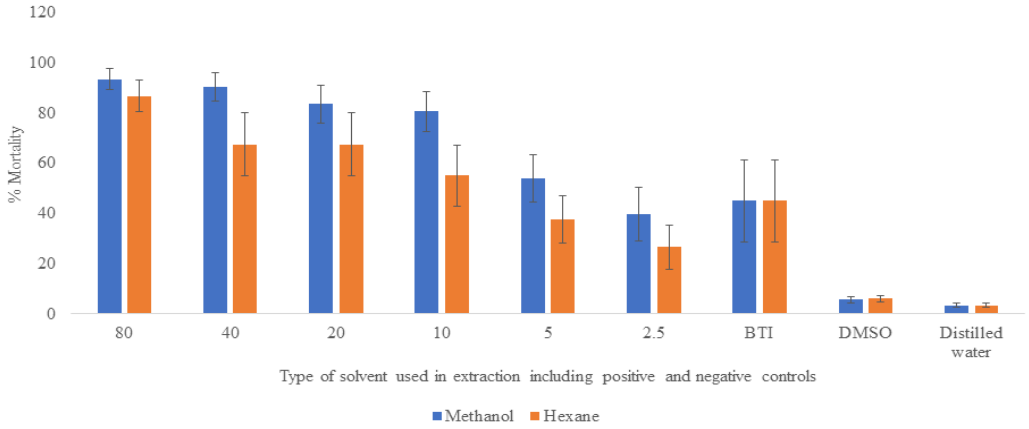

Figure 1: Effects of solvent of extraction on mortality of *An. gambiae* aquatic stages: Bti= *Bacillus thurigiensis israelensis* and **DMSO=** Dimethyl sulfoxide

Table 1: Effects of crude extracts from different parts of *U. massaica* on mortality of exposed *An. gambiae* eggs, larvae and pupae [% mortality is expressed as mean ± standard error of mean (SEM)]

Dose (ml/100ml)	Parts of Plant extracted for botanicals			df	F	p
	Leaves	Stem	Roots			
80	86.92 ± 7.97	99.96 ± 0.04	83.75 ± 7.29	2	1.899	0.184
40	70.96 ± 17.16	98.38 ± 1.58	76.38 ± 8.38	2	1.723	0.212
20	64.21 ± 18.02	93.21 ± 4.87	69.25 ± 10.68	2	1.558	0.243
10	53.17 ± 17.20	86.04 ± 7.93	64.29 ± 11.54	2	1.705	0.215
5	31.33 ± 9.53	49.00 ± 12.38	56.88 ± 12.35	2	1.294	0.303
2.5	22.50 ± 12.81	34.33 ± 13.83	42.58 ± 9.27	2	0.693	0.515
BTI	50.67 ± 20.45	34.67 ± 19.89	49.83 ± 20.97	2	0.194	0.826
DMSO	6.83 ± 1.68	4.67 ± 0.80	6.00 ± 1.77	2	0.542	0.592
Distilled water	4.17 ± 0.87	2.00 ± 0.86	4.00 ± 0.86	2	1.958	0.176

Notes: df = degree of freedom; F = the F statistical factor; *P* = probability for the level of significance. P was taken as significant at $p < 0.05$. BTI = *Bacillus thurigiensis israelensis*; DMSO = dimethyl sulfoxide.

Table 2: Effects of dose of methanolic or hexane crude extracts of *U. massaica* on mortality of *An. gambiae* eggs, larvae and pupae [% mortality is expressed as mean ± standard error of mean (SEM)]

Dose (ml/100ml)	Exposed aquatic stages of *Anopheles gambiae*			df	F	p
	Eggs	Larval Instar 3 (L3)	Pupae			
80	88.13 ± 7.16^{b}	100.00 ± 0.00^{b}	82.50 ± 7.93^{b}	2	2.097	0.157
40	76.54 ± 10.10^{b}	100.00 ± 0.00^{b}	69.17 ± 15.67^{b}	2	2.236	0.141
20	61.67 ± 9.75^{a}	100.00 ± 0.00^{a}	65.00 ± 16.82^{a}	2	3.578	0.054
10	51.00 ± 7.54^{b}	100.00 ± 0.00^{b}	62.92 ± .80^{b}	2	2.616	0.106
5	40.13 ± 7.85^{a}	70.00± 12.37^{a}	27.08 ± 7.54^{a}	2	5.350	0.018
2.5	28.58 ± 2.96^{b}	54.58 ± 16.58^{b}	16.25 ± 6.73^{b}	2	3.493	0.057
BTI	81.33 ± 15.67^{a}	35.67 ± 19.10^{a}	18.17 ± 15.80^{a}	2	3.710	0.049
DMSO	6.00 ± 1.63^{b}	7.50 ± 1.59^{b}	4.00 ± 0.82^{b}	2	1.581	0.238
Distilled water	3.00 ± 0.82^{b}	3.33 ± 1.05^{b}	3.83 ± 0.98^{b}	2	0.193	0.827

Notes: df = degree of freedom; F = the F statistical factor; *P* = probability for the level of significance. P was taken as significant at $p < 0.05$. Bti = *Bacillus thurigiensis israelensis*; DMSO = dimethyl sulfoxide. Rows having mean percentage mortality superscripted with letter "**a**" indicate a significant influence of dose on exposed *An. gambiae* aquatic stages

Table 3: Comparative performance of hexane and methanol crude extracts of *U. massaica* leaves on *An. gambiae* eggs, larvae and pupae [% mortality is expressed as mean ± standard error of mean (SEM)]

Part of plant	Mosquito stage	Solvent	N	Mean ± SEM	t	df	P (2-tailed)
Leaves	eggs	Methanol	6	68.71 ± 9.84^{a}	6.983	5	0.001
		Hexane	6	25.79 ± 7.05^{a}	3.656	5	0.015
	L3	Methanol	6	87.50 ± 9.44^{a}	9.266	5	0.000
		Hexane	6	61.67 ± 17.93^{a}	3.439	5	0.018
	Pupae	Methanol	6	73.33 ± 17.17^{a}	4.271	5	0.008
		Hexane	6	12.08 ± 10.62^{b}	1.138	5	0.307

Notes: df = degree of freedom; t = the t statistical factor for student t test; *P* = probability for the level of significance. *P* was taken as significant at $p < 0.05$ for a two tailed test. N = total number of considered samples for the t test; Rows having mean percentage mortality superscripted with letter "**a**" indicate a significant influence of *U. massaica* leaf extracts on exposed *An. gambiae* aquatic stages

Table 4: Comparative performance of hexane and methanol crude extracts of *U. Massaica* stems on *An. gambiae* eggs, larvae and pupae [% mortality is expressed as mean ± standard error of mean (SEM)]

Part of plant	Mosquito stage	Solvent	N	Mean ± SEM	t	df	P (2-tailed)
Stem	eggs	Methanol	6	74.13 ±11.00^{a}	6.740	5	0.001
		Hexane	6	62.21 ±12.37^{a}	5.029	5	0.004
	L3	Methanol	6	98.33 ±1.31^{a}	75.173	5	0.000
		Hexane	6	80.42 ±12.89^{a}	6.241	5	0.002
	Pupae	Methanol	6	69.17 ±19.51^{a}	3.545	5	0.016
		Hexane	6	75.00 ±15.26^{a}	4.914	5	0.004

Notes: df = degree of freedom; t = the t statistical factor for student t test; *P* = probability for the level of significance. *P* was taken as significant at $p < 0.05$ for a two tailed test. N = total number of considered samples for the t test; Rows having mean percentage mortality superscripted with the same letter indicate a significant influence of *U. massaica* stem extracts on exposed *An. gambiae* aquatic stages

Table 5: Comparative performance of hexane and methanol crude extracts of *U. Massaica* roots on *An. gambiae* eggs, larvae and pupae [% mortality is expressed as mean ± standard error of mean (SEM)]

Part of plant	Mosquito stage	Solvent	N	Mean ± SEM	t	df	P (2-tailed)
Roots	eggs	Methanol	6	52.17 ± 7.00^{a}	7.455	5	0.001
		Hexane	6	63.04 ± 10.40^{a}	6.062	5	0.002
	L3	Methanol	6	86.67 ± 11.45^{a}	7.569	5	0.001
		Hexane	6	97.92 ± 2.08^{a}	47.000	5	0.000
	Pupae	Methanol	6	50.83 ± 4.22^{a}	12.056	5	0.000
		Hexane	6	42.50 ± 5.16^{a}	8.230	5	0.000

Notes: df = degree of freedom; t = the t statistical factor for student t test; *P* = probability for the level of significance. *P* was taken as significant at $p < 0.05$ for a two tailed test. N = total number of considered samples for the t test; Rows having mean percentage mortality superscripted with the same letter indicate a significant influence of *U. massaica* root extracts on exposed *An. gambiae* aquatic stages

3. Results

Solvent of extraction had an impact on potency of extracts as ovicides, larvicides as well as pupicides. Methanol extracts were more potent than hexane extracts regardless of the dose. Potency of extracts reduced with reduced dose irrespective of solvent of extraction. Doses of 80 ml/100ml killed >80% of exposed *An. gambiae* immature stages (Figure 1). Both methanol and hexane extracts were more potent than *Bacillus thurigiensis israelensis* (Bti); however, none of the observed mortalities were significantly different ($p > 0.05$) regardless of dose or solvent of extraction. Similarly, stem extracts were more potent than root or leaf regardless of dose though the observed mortalities did not differ significantly ($p > 0.05$), irrespective of dose (Table 1).

Larvae (L3) were more susceptible to *U. massaica* crude extracts than either eggs or pupae. Mortalities were, however, dose dependent with doses of 10 ml and above killing all exposed L3. Interestingly, preparations of Bti were more effective on eggs than L3 or pupae. Observed mortalities for 20 ml were significantly different ($p < 0.05$), while the rest were not ($p > 0.05$) (Table 2).

Methanol extracts of leaves were more potent than hexane extracts of the same part for exposed eggs and L3 in all observed cases. Mortalities from exposure to methanol extracts of leaves were significantly different for all stages at $p < 0.05$, while that of exposure to hexane extracts were significantly different for eggs and L3 but not for pupae (Table 3). A similar trend was observed for extracts of stem albeit with slight difference (Table 4).

Hexane extracts of roots were more potent than methanol extracts for the same part to exposed eggs and L3. The trend, however, was different for pupae where methanol extracts were more potent than those of hexane. Observed mortalities were, however, significantly different at $p < 0.05$ (Table 5) irrespective of solvent of extraction or stage used.

4. Discussion

Aquatic mosquito stages (eggs, larvae and pupae) are "sitting ducks" as they are unlikely to escape from the habitat and, therefore, easy to control than the highly mobile winged adults. A control program focused on eliminating mosquito eggs; larvae or pupae is likely to be more effective in reducing mosquito population (Chung *et al.,* 2009; Conti *et al.,* 2010). If such a strategy employs the use of botanicals, then it may not only be used to mitigate the problem of vector resistance, but also help to reduce the undesirable effect on human health and environment resulting from the use of synthetic insecticides (Govindarajan *et al.,* 2016). By virtue of the fact that growing of plants universally encourages as a strategy to increase vegetation on planet earth, the plant-based insecticides will not only be readily available in many areas, but the product can be easily and cheaply acquired.

In this study the most vulnerable aquatic stage to the toxic effect of *U. massaica* was the larvae (L3). This is because they were totally annihilated, especially when exposed to high doses. This finding was consistent with that of *Plectranthus glandulosus* and *Callistemon rigidus* leaves extracts against fourth larval instars (L4s) of *Ae. aegypti, An. gambiae* and *Cx. Quinquefasciatus* (Pierre *et al.,* 2014) and ethanol and water extracts of *Phytolacca dodecandra* against all larval stages of *An. gambiae* (Yugi *et al.,* 2015).

It was observed that high doses of the extracts were even more lethal to the L3. Indeed doses higher than 10 ml killed all exposed L3. Of the exposed aquatic stages, only L3 feed. Eggs and pupae do not feed. It is safe to say that the mode of action of the toxic extracts was due to gut poisoning and that the toxic effect of the extracts was delivered most effectively through the gut. It could be said that the L3 might have accumulated (through ingestion) large doses of the poison in their gut while feeding, and that the higher doses were responsible for the observed fatalities (Nathan *et al.,* 2005; Akinkurolere *et al.,* 2011; Ileke and Ogungbite, 2015). This finding was similar to that observed for *Terminalia chebula* against larvae and eggs of *An. stephensi*, *Ae. aegypti* and *Cx quinquefasciatus* (Thangapandi *et al.,* 2017) where it was noted that higher doses of the botanicals yielded better mortality rates on mosquito immatures. In this study, doses of 80ml and above met WHO threshold for an effective insecticide (>80% mortality) irrespective of solvent used in the extraction.

It was also observed that exposed *An. gambiae* eggs and pupae failed to hatch or eclode to adults respectively. *An. gambiae* eggs as well as pupae are non-feeding and could not ingest toxic *U. massaica* extracts. The fact that the eggs failed to hatch or pupae to moult to adults demonstrate that the mode of action of the toxicants was not only enteric but topical as well. This finding was similar to that of *Phytolacca dodecandra* plant extracts against *An. gambiae* eggs (Yugi and Kiplimo, 2017) and pupae (Yugi et al., 2017).

Interestingly, solutions of *Bacillus thurigiensis israelensis* (Bti), inhibited more eggs from hatching than it killed exposed L3. Bti has proven bioefficacy against mosquito larvae (Uragayala *et al.,* 2018; Derua *et al.,* 2019). It affects the midgut epithelium of affected larvae (de Barjac 1978) by enhancing swelling and busting of cells herein causing severe damage to the gut wall (de Barjac 1978; Kalfon *et al.,* 1984) and death to the larvae. Earlier, it had been shown that though Bti had effect on oviposition behaviour of mosquitoes, it had no effect on either the adults or their eggs (Futami *et al.,* 2011). The observation made herein of Bti on *An. gambiae* eggs is, therefore, unique and is neither finding support nor given meaning by the demonstrations mentioned above.

Indeed, extracts of plants, prepared using specific solvents had been shown to influence bioactivity, probably because of the concentration of active components present therein (Oliveira *et al.,* 2010). This was also reported for crude benzene, hexane, ethyl acetate, chloroform and methanol extracts of leaf of *T. chebula* against A. *stephensi, A. aegypti, and C. quinquefasciatus* (Thangapandi *et al.,* 2017). In the current study, methanol extracts were more potent than hexane extracts, an observation that was similar to that made by Munusamy *et al.* (2016) on ovicidal and larvicidal activities of some plant extracts on *Aedes aegypti* L. and *Culex quinquefasciatus* Say (Diptera: Culicidae). It

would seem here that methanol facilitated optimal extraction of the botanicals due to its high polarity.

In the current study, it was found that extracts from the stem were more potent followed by roots and then leaves though mortalities arising from the exposures were not significantly different irrespective of dose. For some time, it had been known that different parts of plants (leaves, fruits, seeds, roots and bark) contained polyphenols or secondary metabolites (flavanols, anthocyanins and phenolic acids). The polyphenols are the components responsible for free radical scavenging activity (Mathew and Abraham 2006) as well as unique biological activity (Govindarajan *et al.,* 2008) including mosquitocidal properties (Niraimathi *et al.,* 2010; Ramkumar *et al.,* 2015).

Concentrations of botanicals have been known to be differentially distributed within plant parts, with parts of plants with higher concentrations demonstrating high bioassay potency (Yugi and Kiplimo, 2017). In the present study, extracts from the stem killed a higher percentage of exposed aquatic stages than extract from leaves or roots irrespective of solvent or dose. It would be correct to assume that stems of *U. massaica* contain a higher concentration of botanicals than either leaves or roots. If this be true, then the findings of this study are consistent with that of Mgbemena, (2010), Anupam *et al*., (2012) and Yugi and Kiplimo, (2017) that reported on differential vertical distribution of polyphenols commensurate with the reported levels of bio-potency of extracts from different plant parts. This however was inconsistent with the findings by Rafajlovska *et al.* (2013) that showed that the concentration of botanicals in stinging nettles did indeed differ in distribution vertically along the length of stinging nettles but that the leaves and not the stem had higher quantities of the polyphenols followed by stems and then roots. This was confirmed by Pinelli *et al.* (2008) who demonstrated in their study that roots of stinging nettles indeed contained the least concentration of botanicals.

The present study clearly proves, therefore, that crude extracts of *U. massaica* has impressive ovicidal, larvicidal and pupicidal properties against *An. gambiae*, and that methanol and hexane extracts of leaves, stem and roots of this herb have insecticidal ability. This puts *U. massaica* in the same category with plants with insecticidal properties such as *Anacardium occidentale, Afromomum melegueta,Garcina kola and Citrus sinensis* (Ileke *et al.,* 2014) and a few others with ovicidal, larvicidal and pupicidal potential against *Anopheles gambiae* and *Aedes aegypti* mosquitoes (Raveen *et al.,* 2017). Although the effects of pure samples of *U. massaica* were never experimented on either singly or synagestically against *An. gabiae* aquatic stages, it may be postulated that the complex mixtures of active components of crude methanol and hexane extracts (Oliveira *et al.,* 2010) of different parts of *U. massaica* acted synergistically to show greater overall bioactivity compared to the individual constituents (Sumroiphon *et al.,* 2006).

It is, therefore, our submission that although the findings of this study proves the mosquitocidal potential of *U. massaica* extracts on aquatic stages of *An. gambiae* mosquitoes, we recommend that extracts be isolated to pure compounds to determine their impacts before the development of natural mosquitocidal products to complement synthetic insecticides is done.

Authors' contributions

YJO conceived the concept, conducted the statistical analysis and wrote the manuscript. YJO and SV designed, supervised and guided the experiments. KRT cultured the experimental mosquitoes and conducted the experiments.

Competing interests

The authors declare that they have no competing interests and that *U. massaica* and *Bacillus thurigiensis israelensis* (Bti) were used purely for experimental purposes only.

Acknowledgements

We thank Dr. Eric Ochomo for providing technical insights and supervising laboratory experimentation for the study, Richard Amito, Jackline Koskei and Antony Odera for processing and culturing the experimental mosquitoes, Centre for Global Health Research/Kenya Medical Research Institute (CGHR/KEMRI) for providing laboratory space, mosquitoes and equipment for conducting the experiments and the, University of Eldoret, through Chemistry laboratory for personnel and equipment for the extraction of the phytochemicals.

References

Abbot WS. 1925. A method of computing the effectiveness of an insecticide. *Journal of Economic Entomology*, **18**: 256 – 257.

Akinkurolere RO, Adedire CO, Odeyemi OO, Raji J and Owoeye JA. 2011. Bioefficacy of Extracts of some Indigenous Nigerian Plants on the developmental stages of mosquito (*Anopheles gambiae*). *Jord J Biol Sci*, **4**: 237-242.

Alayo M, Femi-Oyewo M, Bakre L and Fashina A. 2015. Larvicidal potential and mosquito repellent activity of Cassia mimosoides extracts. *Southeast Asian J Trop Med Public Health*, 46: 596–601.

Anupam G, Nandita C and Goutam C. 2012. Plant extracts as potential mosquito larvicides. *Ind J Med Res*, **135**: 581-598.

Asadollahi A, Khoobdel M, Zahraei-Ramazani A, Azarmi S and Mosawi SH. 2019. Effectiveness of plant-based repellents against different *Anopheles* species: *A syst rev*, **18**: 436.

Ayan AK, Alıs C, Kan O¨ C and Irak C. 2006. Economic importance of stinging nettle (*Urtica* spp.) and its cultivation. *J Fac Agric OMU*, **21**: 357–363.

Chung IM, Seo SH, Kang EY, Park SD, Park WH and Moon HI. 2009. Chemical composition and larvicidal effects of essential oil of *Dendropanax morbifera* against *Aedes aegypti* L. *Biochem Syst Ecol*, **37(4):** 470-473.

Conti B, Canale A, Bertoli A, Gozzini F and Pistelli L. 2010. Essential oil composition and larvicidal activity of six Mediterranean aromatic plants against the mosquito *Aedes albopictus* (Diptera: Culicidae). *Parasitol. Res*, **107(6):** 1455-1461.

Das NG, Goswami, D and Rabha B. 2007. Preliminary evaluation of mosquito larvicidal efficacy of plant extracts. *J Vect Bor Dis*, **44:** 145-148.

de Barjac H, 1978. A new variety of Bacillus thuringinesis very toxic to mosquitoes: B. thuringiensis var. israelensis serotype 14. *C R Acad Hebd Seances Acad Sci D.* 13; **286(10):** 797-800.

Derua YA, Kweka EJ, Kisinza WN, Githeko AK and Mosha FW. 2019. Bacterial larvicides used for malaria vector control in sub-Saharan Africa: review of their efectiveness and operational feasibility. *Parasit Vect*. **12**: 426.

Futami K, Kongere JO, Mwania MS, Lutiali PA, Njenga, SM and Minakawa N. 2011. Effects of *Bacillus thuringiensis israelensis* on *Anopheles arabiensis. J Amer Mos Contr Assoc.* **27(1):** 81-83.

Govindarajan M, Jebanesan A, Pushpanathan T and Samidurai K. 2008. Studies on effect of *Acalypha indica* L. (Euphorbiaceae) leaf extracts on the malarial vector, *Anopheles stephensi* Liston (Diptera: Culicidae). *Parasitol Res*, **103(3):** 691–695.

Govindarajan M, Rajeswary M, Arivoli S, Tennyson S and Benelli G. 2016. Larvicidal and repellent potential of *Zingiber nimmonii* (J. Graham) Dalzell (Zingiberaceae) essential oil: an eco-friendly tool against malaria, dengue, and lymphatic filariasis mosquito vectors? *Parasitol Res*, **115**: 1807–1816.

Grubben GJ. 2004. *Plant Resources of Tropical Africa* (PROTA). PROTA;

Ileke KD and Ogungbite OC. 2015. *Alstonia boonei* De Wild oil extract in the management of mosquito (*Anopheles gambiae*), a vector of malaria disease. *J Coast Life Med*, **3**: 557-563.

Ileke KD, Afolabi OJ, Ogungbite OC, Olagunju JO and Akanbi OM. 2014. Mosquitocidal activity of *Anacardium occidentale*, *Afromomum melegueta*, *Garcina kola* and *Citrus sinensis* against the developmental stages of mosquito, *Anopheles gambiae* Giles. *J Mosq Res*, **4**: 21-26.

Kalfon A, Charles JF, Bourgouin C and De Barjac H. 1984. Sporulation of Bacillus sphaericus 2297: An Electron Microscope Study of Crystal-like Inclusion Biogenesis and Toxicity to Mosquito Larvae. *J. Gen Micro*. **130**: 893-900.

Kamalakannan P, Kavitha R, Elamathi R, Deepa T and Sridhar S. 2012. Study of phytochemical and antimicrobial potential of methanol and aqueous extracts of aerial parts of *Elephantopus scaber* L. *Inter J Curr Pharm Res*, **4(1):** 18-21.

Kamau LN, Mbaabu PM, Karuri PG, Mbaria JM and Kiama SG. 2017. Medicinal plants used in the management of diabetes by traditional healers of Narok County, Kenya. *Tang*, **7**(2): e10. Karunamoorthi K, Girmay A and Hayleeyesus SF. 2014. Mosquito repellent activity of essential oil of Ethiopian ethnomedicinal plant against Afro-tropical malarial vector *Anopheles arabiensis. J King Saud Uni Sci*, **26**: 305–310.

Karunamoorthi K. 2014. The counterfeit anti-malarial is a crime against humanity: a systematic review of the scientific evidence. *Mal J*, **13**: 209.

Ketera LK and Mutiso PC. 2012. Ethnobotanical studies of medicinal plants used by Traditional Health Practitioners in the management of diabetes in Lower Eastern Province, Kenya. *J Ethnopharm*, **139:** 74 – 80.

Kipruto A, Mwamburi L, BII C and Kipngetich B. 2019. The antimicrobial activity of the leaves of *Urtica massaica* on *Staphylococcus aureus*, *Escherichia coli*. *J Med Plants Stud*, **7(2):** 21-24.

Ko¨rpe DA, Iseri OD, Ffet Sahin FI, Cabi E and Haberal M. 2013. High-antibacterial activity of *Urtica* spp. seed extracts on food and plant pathogenic bacteria. *Inter J Food Sci Nutr*, **64(3):** 355–362

Kothari CR. 2004, *Research design: research methodology, methods and techniques*. 2nd edition. New Age International Publishers, New Delhi, India.

Kregiel D, Pawlikowska E and Antolak H. 2018. Urtica spp.: Ordinary Plants with Extraordinary Properties. *Mol*, **23**: 1664.

Mathew S and Abraham TE. 2006. Studies on the antioxidant activities of Cinnamon (*Cinnamomum verum*) bark extracts through in vitro models. *Food Chem*, **94**: 520–528.

Mgbemena IC. 2010. Comparative evaluation of larvicidal potentials of three plant extracts on *Aedes aegypti*. *J Amer Sci*, **6**: 435-440.

Munusamy RG, Appadurai DR, Kuppusamy S, Michael GP and Savarimuthu I. 2016. Ovicidal and larvicidal activities of some plant extracts against *Aedes aegypti* L. and *Culex quinquefasciatus* Say (Diptera: Culicidae). *Asian Pac J Trop Dis*, **6(6):** 468 – 471.

Nathan SS, Kalaivani K and Murugan K. 2005. Effects of neem limonoids on the malaria vector *An. stephensi* Liston (Diptera: Culicidae). *Acta Trop*, **96**: 47-55.

Niraimathi S, Balaji N, Venkataramanan N and Govindarajan M. 2010. Larvicidal activity of alkaloid from Sida acuta against *Anopheles subpictus* and *Culex tritaeniorhynchus*. *Inter J Curr Res*, **11**: 034–038.

Oliveira PV, Ferreira JC Jr, Moura FS, Lima GS, de Oliveira FM and Oliveira PES, Conserva LM, Giulietti AM and Lemos RPL. 2010. Larvicidal activity of 94 extracts from ten plant species of northeastern of Brazil against Aedes aegypti L. (Diptera: Culicidae). *Parasitol Res*, **107**: 403–407.

Oloro J, Tanayen JK, Barbra K, Lawrence I, Paul W, Francis B and Amon AG. 2015. Toxicity of four herbs used in erectile dysfunction;*Mondia whiteii*,*Cola acuminata*,*Urtica massaica*, and *Tarenna graveolens*in male rats. *Afri J Pharm Pharmacol*, **9(30):** 756-763.

Pierre DYS, Okechukwu EC, Lame Y and Nchiwan NE. 2014. Larvicidal and Pupicidal Activities of *Plectranthus glandulosus* and *Callistemon rigidus* Leaf Essential Oils against Three Mosquito Species. *J Mosq Res*, **4(2):** 5-14.

Pinelli P, Ieri F, Vignolini P, Bacci L, Baroni S and Romani A. 2008. Extraction and HPLC analysis of phenolic compounds in leaves, stalks, and textile fibers of *Urtica dioica* L. *J Agri Food Chem*, **56**: 9127–9132.

Rafajlovska V, Kavrakovski Z, Simonovska J and Srbinoska M. 2013. Determination of protein and mineral contents in stinging nettle. *Quality Life*, **4**: 26–30.

Ramkumar G, Karthi S, Muthusamy R, Natarajan D and Shivakumar MS. 2015. Adulticidal and smoke toxicity of *Cipadessa baccifera* (Roth) plant extracts against *Anopheles stephensi*, *Aedes aegypti*, and *Culex quinquefasciatus*. *Parasitol Res*, **114(1):** 167–173.

Raveen R, Ahmed F, Pandeeswari M, Reegan D, Tennyson S, Arivoli S and Jayakumar M. 2017. Laboratory evaluation of a few plant extracts for their ovicidal, larvicidal and pupicidal activity against medically important human dengue, chikungunya and Zika virus vector, *Aedes aegypti* Linnaeus 1762 (Diptera: Culicidae). *Inter J Mosq Res*, **4(4):** 17-28.

Soonwera M. 2015. Efficacy of essential oil from *Cananga odorata* (Lamk.) Hook. f. & Thomson (Annonaceae) against three mosquito species *Aedes aegypti* (L.), *Anopheles dirus* (Peyton and Harrison), and *Culex quinquefasciatus* (Say). *Parasitol Res*, **114:** 4531–4543.

Sumroiphon S, Yuwaree C, Arunlertaree C, Komalamisra N and Rongsriyam Y. 2006. Bioactivity of citrus seed for mosquito borne diseases larval control. *Southeast Asian J Trop Med Pub Health*, **37(3):** 123–127.

Thangapandi V, Thambusamy P and Jeyaraj M. 2017. Larvicidal and ovicidal activity of *Terminalia chebula Retz*. (Family: Combretaceae) medicinal plant extracts against *Anopheles stephensi*, *Aedes aegypti* and *Culex quinquefasciatus*. *J Par Dis,* **41(3):** 693–702.

Uragayala S, Kamaraju R, Tiwari S, Ghosh SK and Valecha N. 2018. Field testing & evaluation of the efficacy & duration of effectiveness of a biolarvicide, Bactivec® SC (*Bacillus thuringiensis* var. *israelensis* SH-14) in Bengaluru, India. *Indian J Med Res.* **147(3):** 299–307.

Wabai WY, Mwonjoria JKM and Njagi EM. 2018. Teratogenic potential of *Urtica massaica* (Mildbr.) and *Croton megalocarpus* (Hutch) in mice. *The J Phytopharm*, **7(6):** 460-463

Westfall RE. 2001. Herbal Medicine in Pregnancy and Childbirth. *Adv. Ther*, **18**: 47-55.

WHO. 2005. Guidelines for laboratory and field testing of mosquito larvicides. WHO/CDS/WHOPES/ GCDPP/2005: 13.

WHO. 2017. World malaria report. Geneva: World Health Organization (WHO).

Yugi JO and Kiplimo JJ. 2017. Inhibitory effect of crude ethanol and water extracts of *Phytolacca dodecandra* (L'Herit) on embryonic development of *Anopheles gambiae* (Diptera: Culicidae). *Jord J Biol Sci*, **10(3):** 177 – 183.

Yugi JO, Kiplimo JJ and Misire C. 2017. Pupicidal activity of ethanol and water extracts of *Phytolacca dodecandra* (L' Herit) on *Anopheles gambiae* (Diptera: Culicidae) pupae, *J Mosq Res*. **7(13):** 104-110.

Yugi JO, Okeyo-Owour JB, Atieli F, Amito R and Vulule JM. 2014. Knockdown effect of crude ethanol extracts of *Phytolacca dodecandra* on *Anopheles gambiae* adults. *J Mosq Res*, **4(18):** 1-7

Yugi JO, Okeyo-Owour JB, Awiti CA, Juma JI, Were-Kogogo P and Vulule MJ. 2015. Larviciding potency of water and ethanol extracts of *Phytolacca dodecandra* (L' Herit) on *Anopheles gambiae* (Diptera: Culicidae), *J Mosq Res*, **5(2):** 1-6.

JJBS

Volume 14, Number 3, September 2021
ISSN 1995-6673
Pages 441 - 451

Jordan Journal of Biological Sciences

Molecular and Phenotypic Characterization of Novel *Streptomyces* Species Isolated from Kurdistan Soil and its Antibacterial Activity Against Human Pathogens

Bayan Kakamand Jalal, Ayad H. Hasan*

[1] Department of Medical Microbiology, Faculty of Science and Health, Koya University, Koya KOY45, Kurdistan Region - F.R. Iraq

Received: July 14, 2020; Revised: October 27, 2020; Accepted: November 7, 2020

Abstract

The rise in antibiotic resistance globally has expedited the search for novel antibiotics. Streptomycetaceae are the producer of more than 70% of clinical antibiotics; researchers have been shedding light on the genus *Streptomyces* in hope of discovering novel species with the ability to produce effective and efficient molecules against superbugs. This study aims to investigate different sources of Kurdistan soil for the existence of novel *Streptomyces* species that possess bioactive compounds. So, twenty soil samples were obtained from agricultural soil, house garden soil, cave soil, and soil contaminated with petroleum. Selective media combined with morphological characterisation, biochemical tests and molecular techniques were used for species identification. Only fifty-eight bacterial samples were given a positive PCR product in which thirty-one 16S rDNA sequences were compared with previously existed prokaryotic DNA sequences using the EzTaxon database. Twenty-nine out of thirty-one samples showed >99% similarity to previously cultured *Streptomyces* spp. and two isolates from house garden soil samples were candidates to be novel species, and they have shown antibacterial activity against *E. coli* (ATCC 25218) and *Staphylococcus aureus* (ATCC 25923) by inhibiting their growth on Mueller-Hinton agar plate using cross streak method.

Keywords: *Streptomyces*, Soil, 16S rDNA, Phylogenetic tree

1. Introduction

The genus *Streptomyces* is well-known for producing plenty of bioactive specialized metabolites with advantageous applications in clinical, veterinary, and agriculture settings (Li *et al.,* 2019), such as antifungal, antibacterial, anticancer, and anthelmintic drugs (Janardhan *et al.,* 2014; Chen *et al.,* 2018).

This enormous resource of diverse compounds puts *Streptomyces* at the top of medically important microbial genera (George *et al.,* 2010). In addition, it has a number of important functions, including degradation/ decomposition of all sorts of organic substances such as cellulose, polysaccharides, protein fats, and organic acids, they have a great role in the subsequent decomposing of humus (resistant material) in soil (Anandan *et al.,* 2016). It is also responsible for the distinctive earthy odor of freshly ploughed soil caused by geosmin production (Adegboye and Babalola, 2012).

The rapid emergence of antimicrobial resistance in bacterial and fungal pathogens is a public health crisis (Chevrette *et al.,* 2019). For instance, the clinical bacterial strain methicillin-resistant *Staphylococcus aureus* (MRSA) has been designated as one of the major hazardous pathogens associated with the development of antimicrobial resistance (AMR), along with the other clinical strain vancomycin-resistant *Enterococcus faecium* (VRE) (Yücel and Yamaç, 2010; Walker *et al.,* 2019) and *Pseudomonas aeruginosa* that are resistant to even last resort antibiotics (Murray *et al.,* 2019). Novel antibacterial molecules are necessary to fight against pathogens that have advanced resistance against current antibiotics (Fatima *et al.,* 2019; Sottorff *et al.,* 2019). So, researchers are eagerly searching for a novel, sustainable, potent, and broad-spectrum antimicrobial compounds from various sources, including microbes in natural soil habitats. Many known species of *Streptomyces* with antibacterial and antifungal activities were identified in the past decade during Iraqi soil investigation for novel species of actinomycetes (Al-Hulu *et al.,* 2011; Laidi *et al.,* 2013). However, to the best of our knowledge, no one targeted Kurdistan soil to isolate *Streptomyces* spp. So, based on that and considering, *Streptomyces* as prolific producers of useful bioactive compounds (Singh *et al.,* 2016), this study was aimed to isolate and identify new species of *Streptomyces* from the soil of Kurdistan Region in Iraq then test its secondary metabolites activities toward exemplary of gram positive and negative pathogenic bacteria.

2. Materials and Methods

2.1. Sample Collection

Several diverse habitats in Kurdistan Region-Iraq (36.4103°N, 44.3872°E) were chosen to increase the chances of finding new species. Between October and November 2018 twenty samples from each of the

* Corresponding author e-mail: : ayad.hasan@koyauniversity.org.

following locations were collected; Jgila-Kirkuk (35.869°N, 44.552°E)/ agricultural soil, Taqtaq-Irbil (35.915°N, 44.490°E)/ house garden soil, Kanylala (35.886°N, 44.583°E)/ cave soil, and Barhushtr-Irbil (36.350°N, 43.888°E)/ petroleum soil. The samples were collected from down to 15 cm depth after discarding 3.0 cm of soil surface. Polyethylene bags were used to collect about 5gm of the soil samples then sealed and immediately transported to the laboratory. Then, the soil was kept at 4°C until the time of processing. To provide a pH condition similar to the original habitat of the taken samples, the soil's pH was measured as follows; 50 gm of soil from each location was suspended in 100 ml of distilled water and vortexed and incubated for 30 min at 20°C then filtrated using Whatman filter paper No. 1. Then the supernatant pH was measured by pH meter (HI 22 11 Ph/ ORP Meter, Italy) (Massadeh and Mahmoud., 2019).

2.1.1. Isolation of Streptomyces spp.

The collected soil samples were prepared as follows: 5 gm of soil from each sample was added to 45 ml distilled water in a 250 ml Pyrex bottle under sterile condition and incubated at room temperature for 30 min with shaking (120 rpm) (shaker incubator GFL, Germany). 1 ml from each sample supernatant was serially diluted up to 10^{-3} dilutions, then aliquot of 100 µl from each dilution was spread over International *Streptomyces* project medium No. 4 (ISP4) agar plates contain ampicillin and nystatin at a final concentration of 25 µg/ml and 50 µg/ml, respectively (Chen *et al.,* 2018). All the cultured plates were incubated at 28°C in aerobic condition for 5 days. After incubation, *Streptomyces* look alike colonies were selected according to their phenotype and subjected to pure culture technique (George *et al.,* 2010; Maleki *et al.,* 2013).

2.1.2. Cultural Purification and Spore Stocks Preparation:

A single colony from each grown plate in section 2.1.1 was streaked on ISP4 agar plates and incubated at 28°C for 5 days. Then the single isolated colonies were characterised based on the colony pigmentation and *Streptomyces* morphological appearance (Arifuzzaman *et al.,* 2010). To store the bacterial strains for long term and be used when needed, a Mannitol Soya Flour medium (MSF) was used for this purpose. Then 20% glycerol spore stocks of suspected *Streptomyces* spp. were prepared according to Kim *et al.* (2015) and stored at -80°C which can remain viable for several years even after multiple freeze-thaw cycles (Shepherd *et al.,* 2010).

2.1.3. Gram Stain and Biochemical Tests

Standard Gram stain was carried out on the bacterial isolates and visualized under a compound microscope at X100. At the same time, they were subjected to the following biochemical tests: catalase test, citrate utilization test, indole production test, and melanin production. *Streptomyces coelicolor* M15 was used as a positive control.

2.1.4. Phenotypic Characterisation

40 ml of Yeast Extract-Malt Extract medium (YEME) supplemented with 50 µg/ml ampicillin in 250 ml Pyrex bottle was inoculated with the bacterial isolate to be examined; all the inoculated bottles were incubated for 3 to 5 days with shaking at 220 rpm 20 µl from each cultured strain was spotted onto Tryptone Soya Agar (TSA). All plates were incubated for 5 days before being photographed at this point every 24 hrs for the next 120 hrs. Morphological observations through macromorphology were based on the growth pattern on the TSA medium. The colour of *Streptomyces* colonies and soluble pigment was observed by the naked eye.

2.2. Molecular identification

2.2.1. Strain Preparation for Genomic DNA Extraction

To extract genomic DNA from each bacterial isolate individually, 40 ml of YEME supplemented with 50 µg/ml ampicillin in a Pyrex bottle (250 ml volume) was inoculated with an appropriate amount of certain *Streptomyces* spores. The Pyrex bottle was fitted with glass beads for better aeration and to break up mycelium clump. All bottles were incubated at 28°C with shaking at 220 rpm for 72 hrs or up to 96 hrs for the slow growing isolate (Minas *et al.,* 2000).

After the incubation period, the 40 ml culture was transferred into a 50 ml Falcon tube, centrifuged at 13000 rpm (Cooling Centrifuge 3-30K Sigma 147101, Germany) for 10 min The cell pellet was washed with 10 ml sterilised D.W and re-harvested then subjected to DNA extraction according to Romero *et al.* (2014). The cell pellet was re-suspended in 10 ml of 1 M TE buffer (pH 8) containing 20 mg/ml lysozyme then incubated at 37°C for 1 hr. SDS and NaCl were added to final concentrations of 0.5% [w/v] and 150 mM, respectively. The tube was added to a boiling-water bath for 1 min after brief vortexing and then placed in ice to cool down. An equal volume of phenol pH 8 (buffer-saturated) was added, and the mixture was vortexed. The cell debris was separated from the cell lysate at room temperature by centrifugation at 13000 rpm for 10 min For further extraction as described for the phenol, the supernatant was moved to a new Eppendorf tube containing an equal volume of phenol (pH 8): chloroform: isoamyl alcohol (25:24:1) extraction. The extraction was then repeated using chloroform: isoamyl alcohol (49:1). The resulting aqueous phase was transferred to new tubes and a 2.5 volume of absolute ethanol was added to each. Sodium chloride was added to its final concentration (150 mM) and the tube was incubated for 30 min at -20°C. The precipitate genomic DNA was collected at 4°C by centrifugation for 30 min at 13000 rpm The harvested pellet was washed with 70% (v/v) ethanol then re-suspended in nuclease free D.W to be stored at -20°C.

2.2.2. Standard PCR Amplification of 16S rRNA Genes

Partial amplification of 16S rRNA genes was performed using Prime Taq premix PCR Master Mix (2X) kit. All amplification reactions were performed in a final volume of 40 µl of PCR reaction mixture which included 20 µl of 2X prime Taq premix, 10 pmol (2 µl) of forward (FWD) and reverse (REV) primers. StrepB (FWD) and StrepF (REV) primers were used to amplify the 16S rRNA gene partially with an end product size of 1074bp (see Table 1), 100 ng (1 µl) template DNA, and 15 µl DEPC treated D.W or nuclease-free water were added for each reaction. The PCR process was performed using BIO RAD T100TM Thermal Cycler (UK) and programmed as follows: 5 min of initial denaturation at 98°C, followed by 25 cycles of reaction with 30s of denaturing at 98°C, 30s of annealing at 59°C, 45s of extension at 72°C, and the final extension was performed for 5 min at 72°C.

Table 1. Names, target gene, sequences, size, binding site, and annealing temperature of primers used in this study.

Primer Name	Target Gene	Sequence (5' >>>>>> 3') *	Size (bp)	Position**	Tm
StrepB (FWD)	16S rRNA	ACAAGCCCTGGAAACGGGGT	1074	139–158	58
StrepF (REV)		ACGTGTGCAGCCCAAGACA		1194–1212	

* The 16S RNA gene primers sequence were taken from (Rintala *et al.,* 2001). ** Reference to the 16s rRNA genes in *Streptomyces coelicolor*.

2.2.3. Gel Electrophoresis Analysis

To confirm that a correct size of the targeted gene was amplified, an aliquot of 2 µl of PCR reaction products was electrophoresed on a 1% agarose gel containing ethidium bromide (0.5 µg/ml) along with 100bp DNA marker (Amresco DNA MW Marker 100bp) and ran in 1X TBE buffer at 85 V for 1:15 hrs. After the course of running, the DNA bands were visualized and photographed using (UV Gel Imager SynGene 1409) (Abdullah *et al.,* 2017).

2.3. Sequencing of The 16S rRNA Gene Amplicons

The resulted PCR products were sent out for sequencing, after size confirmation. The sequencing was carried out by (Macrogen Inc, a South Korean company) using StrepF for partial 16S rRNA gene sequencing.

2.3.1. Sequence Quality and Length

Sequence analysis and editing were performed using DNA Baser Assembler. In order to perform quality trimming, the start and end of the sequences were trimmed when more than 80% good bases in a 20 bases window were found. After trimming, the sample was counted as low quality when less than 90% of the bases with less than 25 quality values (QV) were detected. The sequence samples were considered good when over 90% of the bases have QV over 25. When the size of the remaining DNA segment after trimming was shorter than 600bp, the sample was discarded.

2.3.2. Novel Species Identification

To identify the isolated bacterial samples individually, the 16S rRNA genes query sequence was compared with previously existed prokaryotic DNA sequences using the EzTaxon database (Yoon *et al.,* 2017). In order to detect novel strains of *Streptomyces* the following criteria were applied: candidate for uncultured species (similarity threshold between 98.7% and 99.0%), genera (95.3-90.0%) or family (<90.0%), >99% similarity considered as same species (Stackebrandt and Ebers, 2006; Schlaberg *et al.,* 2012). For strains with no similar sequences, the data were deposited in the GenBank database using the following website "http://www.ncbi.nlm.nih.gov/BankIt".

2.4. Phylogenetic Analysis

The sequences of new *Streptomyces* spp. candidate were aligned against the sequence of all species of *Streptomyces* that came up after comparison search using Clustal W (Thompson *et al.,* 1994). The Neighbor-joining (NJ) method was used to find out the phylogenetic tree using Molecular Evolutionary Genetics Analysis (MEGA-X) software (Saitou and Nei, 1987; Tamura *et al.,* 2011).

2.5. Antibacterial Activity of Secondary Metabolites

In order to screen the antibacterial activities of *Streptomyces* spp. secondary metabolites, a straight line was drawn by a loopful of certain *Streptomyces* bacterial colony from one side of Mueller-Hinton agar plate to the other side across the center (Alabi *et al.,* 2019). After seven days of incubation at 28°C, one side of the grown line was inoculated by a single streak of *E. coli* (ATCC 25218) and the other side was inoculated by *Staphylococcus aureus* (ATCC 25923) at a 90-degree angle toward the grown line of *Streptomyces* spp. then the plates were incubated at 37°C for 24 hrs. For comparison, positive and negative controls were set up using *Streptomyces coelicolor* L646 strain and *Streptomyces* spp. free Mueller-Hinton agar plate inoculated with *E. coil* and *Staphylococcus aureus*, respectively. This experiment was performed in triplicate and the antimicrobial activity was observed by the naked eye.

3. Results and Discussion

3.1. Sample Collection, Bacterial Isolation and Purification

In total, 68 bacterial entities were detected from 80 soil samples that were collected from different areas of Kurdistan Region-Iraq. The soil samples were collected specifically from agricultural and house garden soil where a great component of roots organic compounds exudate is available, which in turn can promote differential recruitment of actinomycetes (Massenssini *et al.,* 2014), cave soil with manure where the composition of manure such as carbon and other organic materials increases the rate of soil respiration and microbial activity which lead to increase the functional diversity of microbial biomass (Adebola *et al.,* 2017) and petroleum soil where petroleum inhibits and reduces species member of a microbial community; thus few of them govern the community such as *Pseudomonas* and *Streptomyces* (Xu *et al.,* 2018).

The pH of the soil was between (7.5 – 7.8) for all the locations that have been examined. As known, soil provides a suitable environment for many bacterial genus and fungi to grow, so in order to inhibit their growth ISP4 media was used which is a selective media supplemented with nystatin that inhibits fungal growth and ampicillin that suppresses the growth of a wide range of bacteria (Awad and Germoush, 2017).

In general, *Streptomyces* colonies show powdery consistency and stick firmly to the ISP4 agar surface, producing hyphae and conidia/ sporangia-like fungi (Anandan *et al.,* 2016). Colonies were relatively smooth surfaced, but later they developed a weft of aerial mycelium that appeared floccose, granular, powdery, and

velvety coloured white or grey with a white ring (Ambarwati *et al.*, 2012).

Although every grown single colony on ISP4 may be counted as *Streptomyces*, only those that expressed typical *Streptomyces* morphology have been isolated from the collected samples and subjected to pure culture technique (Hasani *et al.*, 2014). So, a colony with *Streptomyces* look alike morphology was re-streaked out on the ISP4 agar plate contains nystatin and ampicillin. After 5 days of incubation, they produced a wide variety of pigments such as white, grey with a white ring, grey, red, yellow, blue, purple, and pink, which are responsible for the colour of the vegetative and aerial mycelia (see Lane A in Figures 1, 2, 3 and 4) (Flärdh and Buttner, 2009). The spores were grown on MSF with different colour characteristics such as grey with various shades, white, dark green, pink, yellow, brown, purple, purple-red, a black centered colony with a white edge, and pale blue after five days of incubation at 28°C (see Lane B in Figures 1, 2, 3 and 4). Some strains had slow growth properties that took more than 10 days to produce spores and pigmentation; those were AS18-3, HGS5-3, HGS5-5, HGS7-2, HGS8-3, HGS13-2, HGS14-1, CS12, PS5-2, and PS13. Observed growth status appeared to be in the scope of *Streptomyces* slow growing properties with their limited resource of nutrition (Westhoff *et al.*, 2020). For future work, these strains can be compared with the reported from the literature to check if this behavior (slow growth) is common. The most dominant colours in the population of sporulation process have been assigned to two groups: grey with different shades and brown; however, unique pigments were detected as well such as green, blue and purple. *Streptomyces* spp. spore pigmentation is the result of polyketide synthesis regulated by *whi* genes that are responsible for the production of polyketide type II components such as tetracenomycin, granaticin, oxytetracycline, and actinorhodin (Kelemen *et al.*, 1998; Salerno *et al.*, 2013).

3.2. Bacterial Identification

3.2.1. Microscopic Characterisation and Biochemical Tests

Streptomyces isolates were found as long filamentous gram-positive bacteria when examined by compound microscope at X1000 magnification. According to the biochemical tests that were carried out to identify the isolated strains, all the isolates including *S. coelicolor* M145 were found to be positive for catalase and citrate utilization tests and negative for indole and melanin productions.

3.2.2. Phenotypic Characteristics

Streptomyces is well known for its ability to produce a wide range of pigments that colour the aerial spore mass and vegetative and aerial mycelia. This ability has been used to identify the genus of *Streptomyces*, and in fact, it was the only character used in many early descriptions (Al-Saadi *et al.*, 2013). So, in this study pigment production during isolation (on ISP4), sporulation, and vegetative stage were adopted as a primitive method to determine the phenotype of certain bacterial strains after being cultured on MSF agar for sporulation and TSA agar for mycelial growth. Spore's colour was determined during spore stock preparation on MSF, which was mentioned previously.

Actinomycetes produce many types of antibiotics that have pigments and can be detected in artificial media; these pigments are commonly defined in different colours (Kheiralla *et al.*, 2016). The colours and nature of the pigments are varied depending on the type of nitrogen and carbon sources present in the media (Reddy and Umamaheshwara, 2016) and are also affected by incubation temperature, aeration, and initial medium pH (Kheiralla *et al.*, 2016). In order to examine the ability of purified bacterial samples to produce secondary metabolite (SM), 20 µl of fresh bacterial culture in YEME was spotted as a patch on TSA agar in triplicate and incubated for five days at 28°C. The bacterial isolates were assigned to six colour series: white, pink, yellow, grey, pale grey, and brown. Surprisingly, a group of four bacterial isolates did not grow on TSA agar plates which can be due to the limitation of some crucial nutrients and elements or inadequate incubation temperatures or pH conditions or the growth might have been inhibited by antibacterial substances present within the medium. For future work, we will try to change these conditions and check for growth (see Lane C in Figures 1, 2, 3 and 4) (Vartoukian *et al.*, 2010).

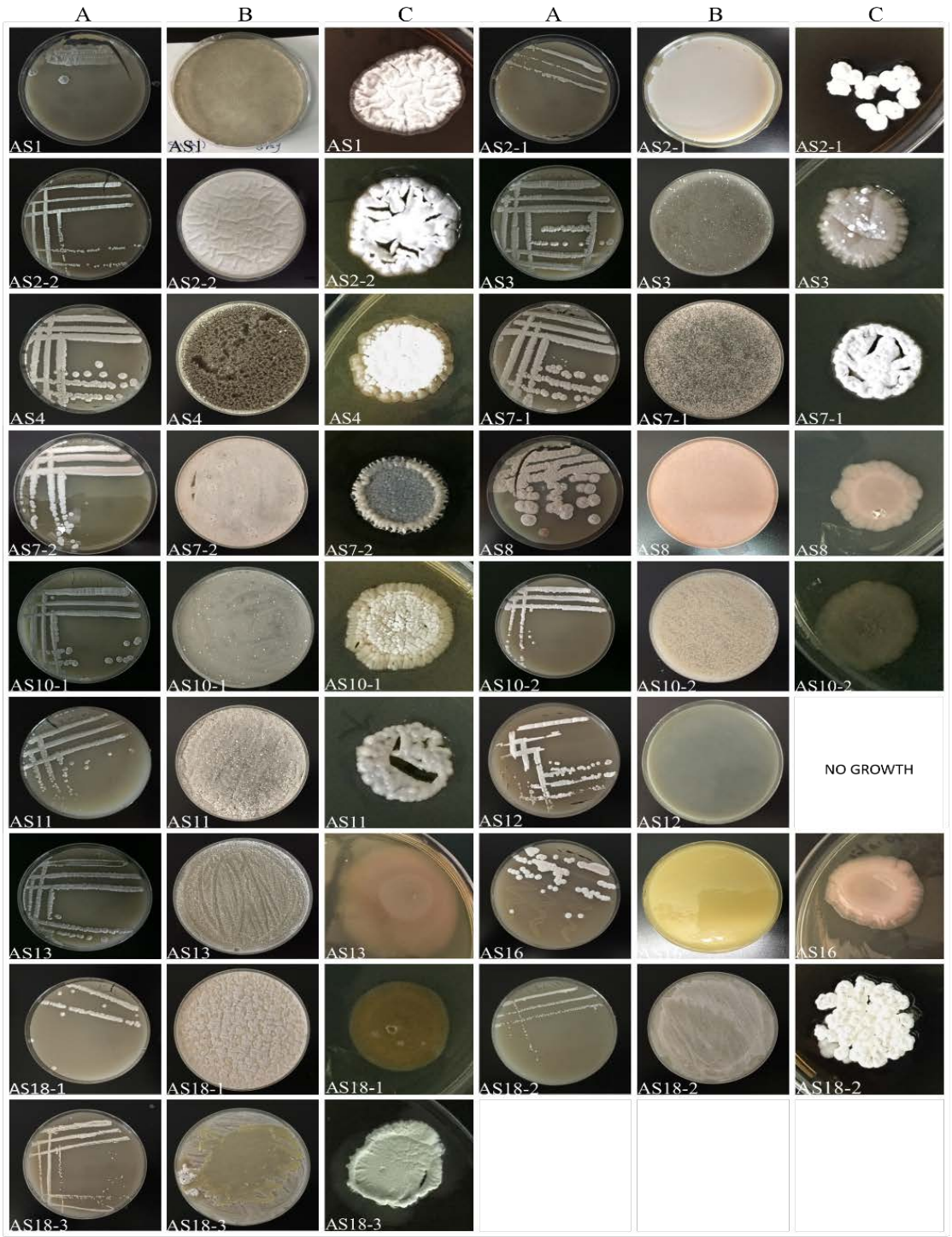

Figure 1. Colour and morphology of *Streptomyces* spp. that are isolated from agricultural soil. The names have been abbreviated to include A (agriculture) S (soil) followed by the sample number. Lane A shows a pure culture process. A single bacterial colony from the original soil sample was streaked on ISP4 agar plates. Lane B shows spore formation on MSF agar plates. Lane C shows patches of colour for each bacterial isolate on TSA plates. All the plates were incubated at 28°C for five days.

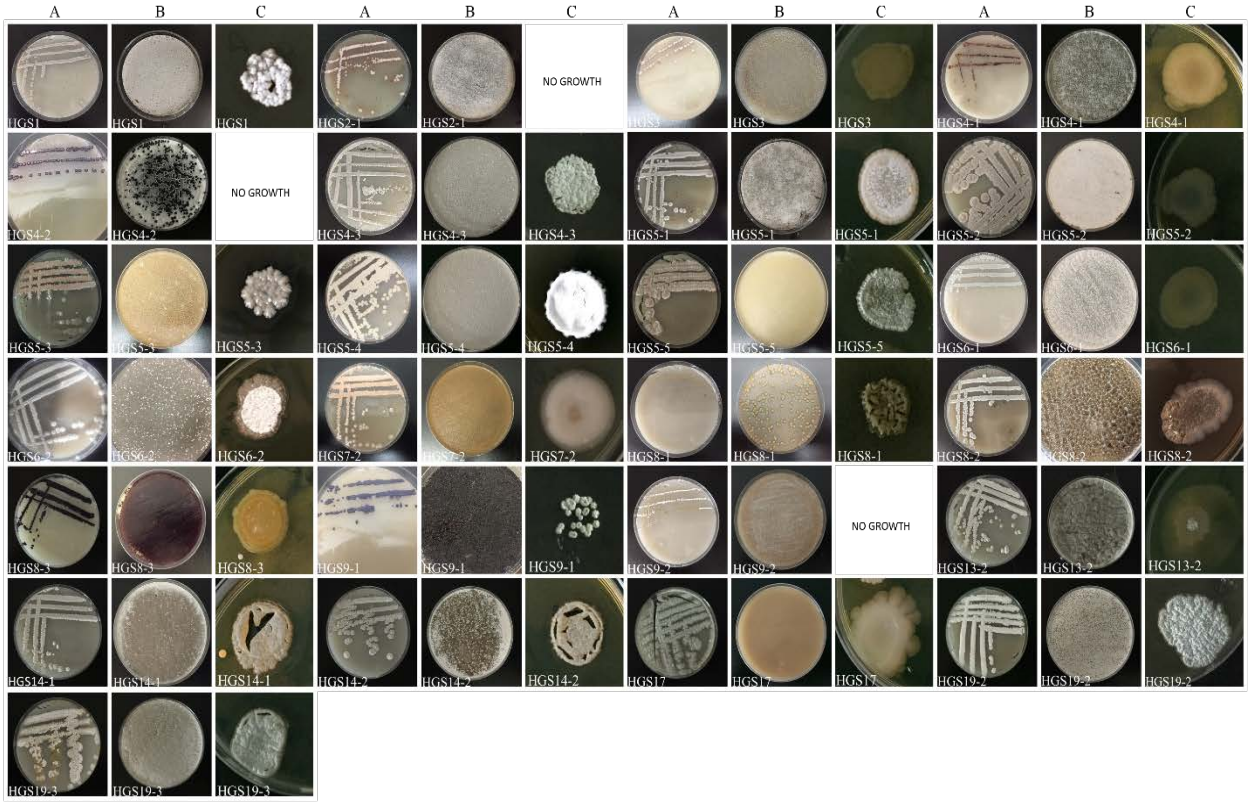

Figure 2. Colour and morphology of *Streptomyces* spp. that are isolated from house garden soil. The names have been abbreviated to include HG (house garden) S (soil) followed by the sample number. Lane A shows a pure culture process. A single bacterial colony from the original soil sample was streaked on ISP4 agar plates. Lane B shows spore formation on MSF agar plates. Lane C shows patches of colour for each bacterial isolate on TSA plates. All the plates were incubated at 28°C for five days.

Figure 3. Colour and morphology of *Streptomyces* spp. that isolated are from cave soil. The names have been abbreviated to include C (cave) S (soil) followed by the sample number. Lane A shows a pure culture process. A single bacterial colony from the original soil sample was streaked on ISP4 agar plates. Lane B shows spore formation on MSF agar plates. Lane C shows patches of colour for each bacterial isolate on TSA plates. All the plates were incubated at 28°C for five days.

Figure 4. Colour and morphology of *Streptomyces* spp. that are isolated from petroleum contaminated soil. The names have been abbreviated to include P (petroleum) S (soil) followed by the sample number. Lane A shows a pure culture process. A single bacterial colony from the original soil sample was streaked on ISP4 agar plates. Lane B shows spore formation on MSF agar plates. Lane C shows patches of colour for each bacterial isolate on TSA plates. All the plates were incubated at 28°C for five days.

3.2.3. Molecular Characteristics

The expected size of DNA fragment (1074bp) was amplified successfully from template DNA isolated from the positive control *Streptomyces coelicolor* M145 and 58 out of 68 bacterial isolates. No PCR products were detected in the negative control and the remaining 10 bacterial samples (see Figure 5).

To track down each bacterial isolate to its exact species, the 16S rRNA gene PCR amplicons of each isolate were sent out for sequencing using the reverse primer StrepF.

3.3. Partial Sequencing of 16S rRNA Gene and its Quality

Based on the validity of the DNA sequencing, just 31 samples were considered for further investigation. The samples were AS1, AS3, AS7-1, AS7-2, AS10-1, AS10-2, AS11, AS12, AS13, AS18-1, AS18-3, HGS3, HGS4-1, HGS4-3, HGS5-1, HGS5-3, HGS5-5, HGS6-1, HGS9-1, HGS14-1, HGS19-3, CS2, CS7-1, CS8-1, CS12, CS13-1, CS16-4, CS17, CS19, PS5-2, and PS13.

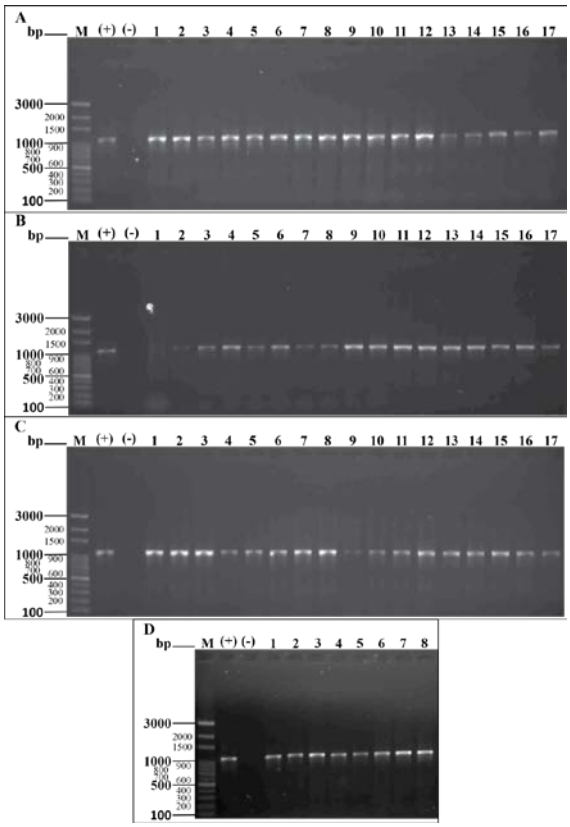

Figure 5. Genomic DNA amplification using StrepB and StrepF primer pairs that target 16S rRNA gene (1074bp). Lanes M, +V, and –V corresponds to the 100bp DNA ladder (Amresco DNA MW Marker 100bp), positive control that contained DNA template from *Streptomyces coelicolor* M145 and negative control that has been run without any DNA template, respectively. The bands are showing 1074bp of PCR amplicons. **Panel A** Lanes 1 to 17 contain PCR products from AS1, AS2-2, AS3, AS4, AS7-1, AS7-2, AS10-1, AS10-2, AS11, AS12, AS13, AS18-1, AS18-3, HGS1, HGS3, HGS4-1, and HGS4-3, respectively. **Panel B** Lanes 2 to 17 contain PCR products from HGS5-1, HGS5-2, HGS5-3, HGS5-4, HGS5-5, HGS6-1, HGS6-2, HGS7-2, HGS8-1, HGS8-2, HGS8-3, HGS9-1, HGS13-2, HGS14-1, HGS14-2, and HGS19-2, respectively. **Panel C** Lanes 1 to 17 contain PCR products from HGS19-3, CS1, CS2, CS3, CS5-1, CS5-2, CS6, CS7-1, CS8-1, CS8-2, CS9, CS11, CS12, CS13-1, CS13-2, CS14, and CS15, respectively. **Panel D** Lanes 1 to 8 contain PCR products from CS16-2, CS16-4, CS17, CS19, PS5-1, PS5-2, PS13, and PS18, respectively.

3.4. Uncultured Species

To analyse the taxonomic position of the 31 good quality 16S rDNA samples, individual automated alignment was conducted using EZBioCloud (Yoon *et al.*, 2017) against available bacterial 16S rDNA sequences. The samples were identified through sequence pairwise-similarity based on the criteria mentioned in section (2.3.2). A total of 29 samples showed >99% similarity to previously cultured *Streptomyces* spp., so no further investigation was conducted on them. The remaining two isolates from house garden soil HGS6-1 and HGS19-3 showed 98.8% and 98.9% similarity to their top hit, which were *Streptomyces nigra* and *Streptomyces albogriseolus*, respectively. This percentage of similarity and mismatches candidate HGS6-1 and HGS19-3 isolates as uncultured species because the sequence identity value of their shared gene is located between 98.7% and 99% (Stackebrandt and

Ebers, 2006). So, HGS6-1 and HGS19-3 isolates are considered to serve as novel species for which the name *Streptomyces nigra* strain BA1 and *Streptomyces albogriseolus* strain BA2 proposed, respectively.

Online multiple alignments (Huang and Miller, 1991) between *S. nigra* strain BA1 and *S. nigra* showed one gap and 7 mismatches at nucleotide positions 155, 166, 17, 193, 202, 08, 328, and 502 based on *S. nigra* 16S rDNA sequence (Data not shown). The same approach of multiple alignments was applied to *S. albogriseolus* strain BA2 and *S. albogriseolus* which showed 9 nt mismatches located at potions 185, 193, 199, 202, 249, 308, 328, 522, and 930 based on the 16S rDNA sequence of *S. albogriseolus* (Data not shown).

The sequence identity of the two proposed novel species *S. nigra* strain BA1 and *S. albogriseolus* strain BA2 fell within the specified cutoff of 98.7%–99.0%, in which *S. nigra* strain BA1 showed 98.8% similarity to *S. nigra 452* and *S. albogriseolus* strain BA2 showed 98.9% similarity to *S. albogriseolus* NRRL B-1305 based on the query sequence length during comparison against other prokaryotic species in EzBiocloud. In addition to molecular evidence above, *S. nigra* strain BA1 (HGS6-1) can be differentiated from its closely related species *S. nigra* by morphological characteristics in which it gave pale blue pigmented spores on MSF and yellow pigmented mycelia on TSA against greyish blue spores and white mycelia for *S. nigra*. On the other hand, *S. albogriseolus* strain BA2 (HGS19-3) showed pale brown spores on MSF and grey mycelia on TSA compared with its closely related species *S. albogriseolus* which gives grey spores on MSF and white mycelia on TSA. Both proposed new species were isolated from house garden soil and incubated for 5 days at 28°C during morphological characteristics.

3.5. GenBank accession number

The nucleotide sequence of *S. nigra* strain BA1 and *S. albogriseolus* strain BA2 were deposited in GenBank with accession numbers MT239403 and MT239401, respectively.

3.6. Phylogenetic tree analysis

To coin a phylogenetic tree of *Streptomyces nigra* strain BA1, 16S rRNA gene sequence was aligned with homologous of fifty different species of *Streptomyces* using multiple sequence alignment command in MEGA X software. The resulting file was used to build up a neighbor-joining tree (see Figure 6).

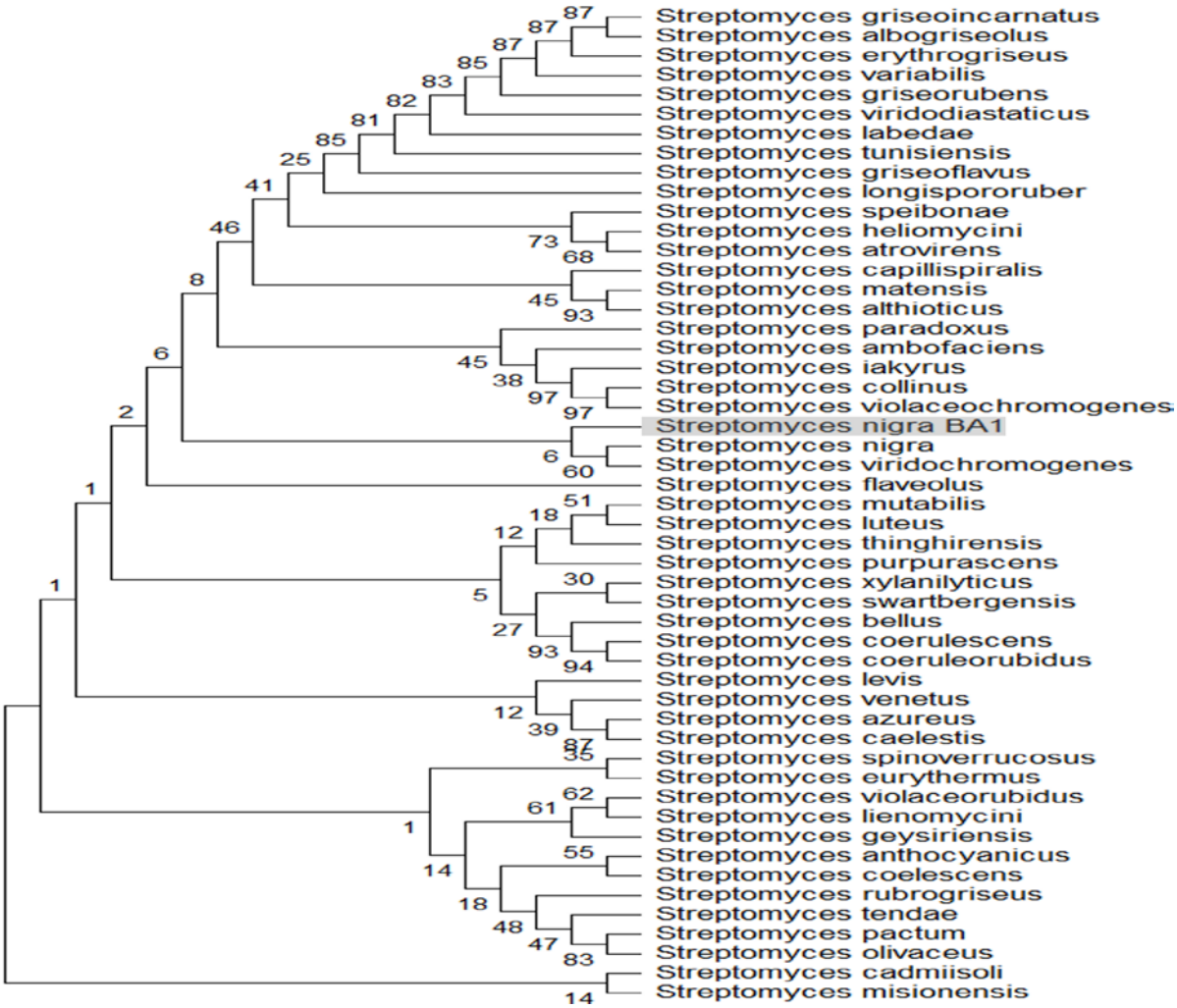

Figure 6. Phylogenetic tree represents relationships among fifty *Streptomyces* spp. and *Streptomyces nigra* strain BA1 (highlighted in grey) with based on 682bp nucleotide of 16S rRNA gene that positioned 154-836 based on *S. nigra* 16s rRNA. Numbers above nodes represent bootstrap values, the greater values give stronger support for the nodes. The proposed new species are highlighted in grey.

The partial sequence of the 16S rRNA gene of *S. nigra* strain BA1 was found to be reasonably in strong relation with *S. nigra* and *S. viridochromogenes* which was supported by 60% bootstrap replicates. These results support what has been detected from the 16S-based ID database (Yoon *et al.,* 2017), which revealed that the closest species to *S. nigra* strain BA1 is *S. nigra* in terms of nucleotide sequence similarity (98.8%) followed by *S. viridochromogenes* with 98.5% similarity. *S. nigra* strain BA1 has seven unique nucleotides at the following positions of its 16S rDNA sequence compared to *S. nigra*: 155 (A→gap), 166 (C→T), 173 (A→G), 193 (C→T), 202 (C→T), 308 (C→G), 328 (C→T) and 502 (A→C). A weaker relationship was found between *S. nigra* strain BA1 and the last thirteen species which were *S. coelescens*, *S. atrovirens*, *S. speibonae*, *S. thinghirensis*, *S. luteus*, *S. xylanilyticus*, *S. venetus*, *S. geysiriensis*, *S. heliomycini*, *S. anthocyanicus*, *S. mutabilis* and *S. capillispiralis* with 97.5% similarity to *S. nigra* strain BA1 16S rDNA sequence.

A neighbor-joining tree was carried out between *Streptomyces albogriseolus* strain BA2 and homologous of fifty different species of *Streptomyces* using MEGA X software to obtain the taxonomic position of *S. albogriseolus* strain BA2 (Figure 7).

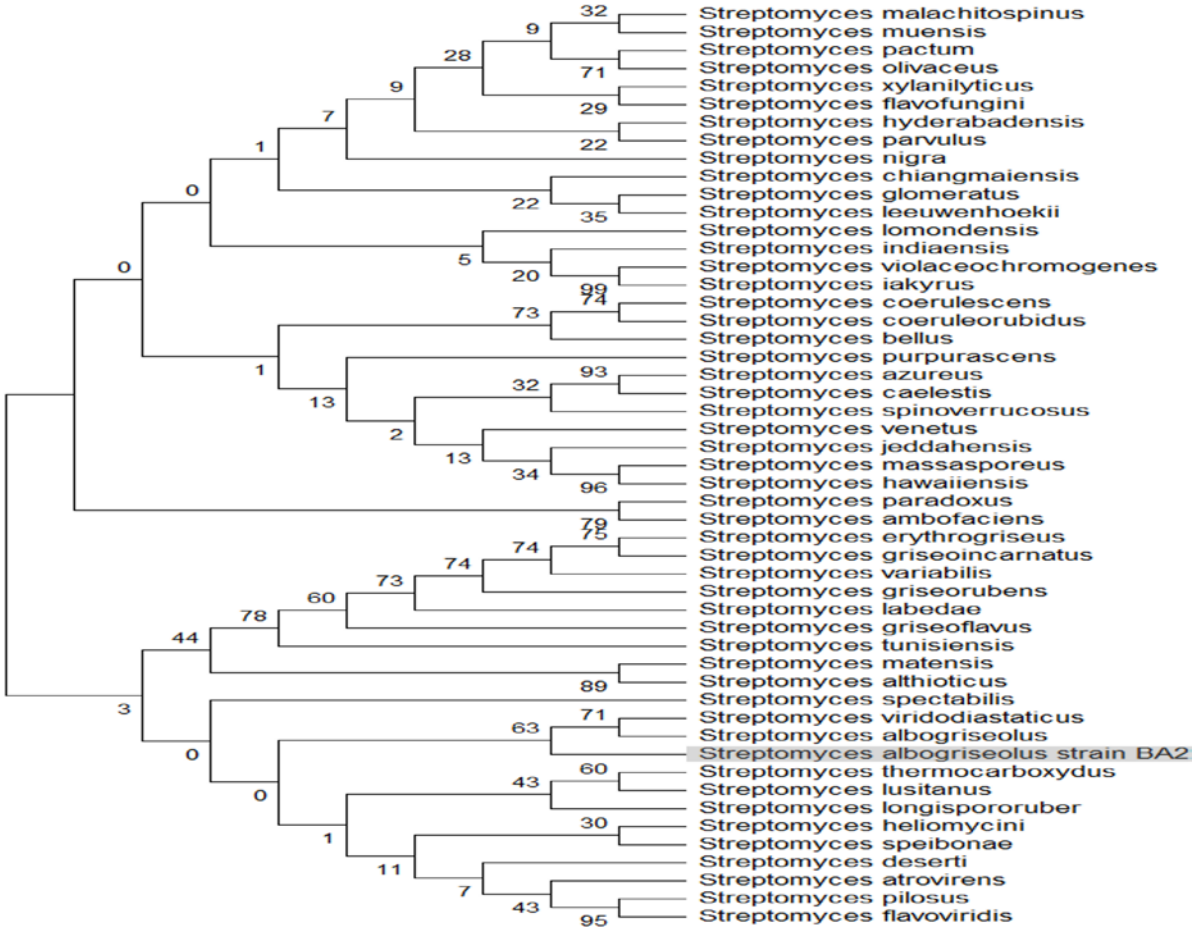

Figure 7. Phylogenetic tree shows relationships among fifty *Streptomyces* spp. and *Streptomyces albogriseolus* strain BA2 (highlighted in grey) based on 856bp nucleotide of 16S rRNA gene that positioned 167-1022 based on *S. albogriseolus* 16S rRNA. Numbers above nodes represent bootstrap values, the greater values give stronger support for the nodes.

It was found through comparing the 16S rDNA partial sequence of *S. albogriseolus* strain BA2 with its homologous that the strongest relation formed with *S. albogriseolus* and *S. viridodiastaticus* supported by 63% bootstrap. A weaker association was shaped with *S. caelestis*, *S. azureus*, *S. malachitospinus*, *S. chiangmaiensis*, *S. jeddahensis* and *S. paradoxus* with a bootstrap of 0%. These results are in line with what has been detected from the 16S-based ID database (Yoon *et al.*, 2017), which revealed that the closest species to *S. albogriseolus* strain BA2 is *S. albogriseolus* and *S. viridodiastaticus* with 98.9% similarity and less similarity (97%) was found with last six *Streptomyces* spp. that mentioned above. *S. albogriseolus* strain BA2 has nine unique nucleotides at the following positions compared to the closest species of *Streptomyces* (*S. albogriseolus*) based on the phylogenetic tree position and percentage of 16s rDNA similarity: 185 (A→C), 193 (C→T), 199 (C→T), 202 (C→T), 249 (A→T), 308 (C→G), 328 (C→T), 522 (C→T) and 930 (C→T).

3.7. Antibacterial Activity of S. nigra strain BA1 and S. albogriseolus strain BA2 Secondary Metabolites

Secondary metabolites of *S. nigra* strain BA1 and *S. albogriseolus* strain BA2 showed antimicrobial activity against *staphylococcus aureus* and *E.coli* (Figure 8, Panels C and D); however, *S. coelicolor* strain L646 showed less inhibition ability against *E.coli* (Figure 8, Panel A).

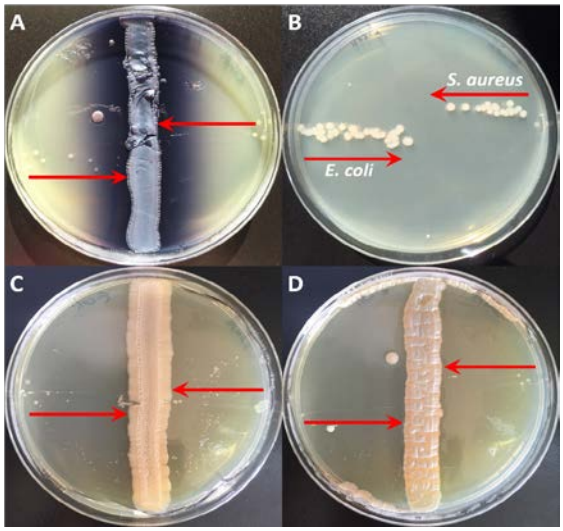

Figure 8. Antibacterial activity of *Streptomyces* spp. Panels A and B serve as positive and negative controls, respectively. *S. coelicolor* strain L646 was used in panel A and no *Streptomyces* spp. were used in panel B, it just streaked out with the tested bacteria as shown. **Panels C and D** represent the antibacterial activity of *S. nigra* strain BA1 and *S. albogriseolus* strain BA2 against *E. coli* (left-hand side) and *Staphylococcus aureus* (right-hand side), respectively. The red arrows indicate the direction of inoculated bacteria toward the midline of grown *Streptomyces* spp.

The antibacterial inhibition activities of current *Streptomyces* spp. isolates can be identified by doing mode of action studies on purified or semi-purified extracts (Imai *et al.*, 2015).

4. Conclusion

Morphological characterisation, biochemical test, partial 16S rDNA sequencing and phylogenic analysis were pronounced as two new candidate species of *Streptomyces* which were distinctive from their most closely related species. Therefore, HGS6-1 and HGS19-3 isolates are considered to serve as novel species for which the name *Streptomyces nigra* strain BA1 and *Streptomyces albogriseolus* strain BA2 proposed, respectively. Inhibition of *E. coli* and *Staphylococcus aureus* growth by secondary metabolites produced by the proposed novel *Streptomyces* species introduced strong evidence that they possess small molecules of medically important activity. Further work needs to be done on these two proposed novel species to identify their bioactive compounds then use them in the development of new therapeutic agents.

Acknowledgements

The authors would like to thank the Department of Medical Microbiology/ Faculty of Science and Health/ Koya University and Science and Health Research center (where the work was done) for their support.

References

Abdullah BS, Khailany RA, Muhammad HH and Hamad MI. 2017. Molecular Identification and Evolutionary Relationship of the New Record Callistethus sp. 7VF-2014 (Coleoptera: Scarabaeidae: Reutelinae) in North of Iraq. *Jordan J Biol Sci*., **10(1)**: 33-36.

Adebola A, Ewulo B and Arije D. 2017. Effects of Different Animal Manures on Soil Physical and Microbial Properties. *Appl Trop Agric*., **22(1)**: 128-133.

Adegboye MF and Babalola OO. 2012. Taxonomy and ecology of antibiotic producing actinomycetes. *Afr J Agric Res.*, **7(15)**: 2255-2261.

Alabi OS, Koleoso OB and Abiala AM. 2019. Antimicrobial screening and GC-MS analysis of bioactive compounds from strains of *Pseudomonas aeruginosa* isolated from poultry fecal littered soil in Ibadan, Nigeria. *Nig J Pure & Appl Sci.*, **32(1)**: 3347- 3357.

AL-Hulu SM, AL-Charrakh AH and Jarallah EM. 2011. Antibacterial activity of *Streptomyces gelaticus* isolated from Iraqi soils. *Med J Babylon,* **8(3):** 404-411.

Al-Saadi A, Majid N and Jaralla E. 2013. Isolation and Identification of *Streptomyces* from different sample of soils. *JBMS*, **1**: 31-36.

Ambarwati A, Sembiring L and Soegihardjo C. 2012. Antibiotic produced by *streptomycetes* associated with rhizosphere of purple nutsedge (Cyperus rotundus L.) in Surakarta, Indonesia. *Afr J Microbiol Res.*, **6(1)**: 52-57.

Anandan R, Dharumadurai D and Manogaran G. 2016. An Introduction to Actinobacteria. In: Dharumadurai D and Yi J (Eds). **Actinobacteria - Basics and Biotechnological Applications**.IntechOpen Publishers, India pp.1-37.

Arifuzzaman M, Khatun M and Rahman H. 2010. Isolation and screening of *actinomycetes* from Sundarbans soil for antibacterial activity. *Afr J Biotechnol.*, **9(29)**: 4615-4619.

Awad HM and Germoush MO. 2017. Molecular and morphological identification of *Streptomyces sp*. NRC-88 nova species as β-lactamase inhibitor for pharmaceutical application. *Asian J Pharm Clin Res.*, **10(10)**: 376-383.

Chen Y, Zhou D, Qi D, Gao Z, Xie J and Luo Y. 2018. Growth promotion and disease suppression ability of a Streptomyces sp. CB-75 from banana rhizosphere soil. *Front Microbiol*., **8**: 2704.

Chevrette MG, Carlson CM, Ortega HE, Thomas C, Ananiev GE, Barns KJ, Book AJ, Cagnazzo J, Carlos C and Flanigan W. 2019. The antimicrobial potential of *Streptomyces* from insect microbiomes. *Nat Commun*., **10(1)**: 516-527.

Fatima A, Aftab U, Shaaban KA, Thorson JS and Sajid I. 2019. Spore forming Actinobacterial diversity of Cholistan Desert Pakistan: Polyphasic taxonomy, antimicrobial potential and chemical profiling. *BMC Microbiol.*, **19(1)**: 1-17.

Flärdh K and Buttner MJ. 2009. *Streptomyces* morphogenetics: dissecting differentiation in a filamentous bacterium. *Nat Rev Microbiol.*, **7(1)**: 36-49.

George J, Arunachalam R, Paulkumar K, Wesely E, Shiburaj S and Annadurai G. 2010. Characterization and phylogenetic analysis of cellulase producing *Streptomyces noboritoensis* SPKC1. *Interdiscip Sci.*, **2(2)**: 205-212.

Hasani A, Kariminik A and Issazadeh K. 2014. *Streptomycetes*: characteristics and their antimicrobial activities. *Int J Adv Biol Biom Res.*, **2(1)**: 63-75.

Huang X and Miller W. 1991. Lalign-find the best local alignments between two sequences. *Adv Appl Math*, **12**: 373-381.

Imai Y, Sato S, Tanaka Y, Ochi K. and Hosaka T. 2015. Lincomycin at subinhibitory concentrations potentiates secondary metabolite production by *Streptomyces spp*. *Appl Environ Microbiol.*, **81(11):** 3869-3879.

Janardhan A, Kumar AP, Viswanath B, Saigopal D and Narasimha G. 2014**.** Production of bioactive compounds by *actinomycetes* and their antioxidant properties. *Biotechnol Res Int.*, **2014**: 1-8.

Kelemen GH, Brian P, Flardh K, Chamberlin L, Chater KF and Buttner MJ. 1998. Developmental regulation of transcription of *whiE*, a locus specifying the polyketide spore pigment in *Streptomyces coelicolor* A3 (2). *J Bacteriol.*, **180(9)**: 2515-2521.

Kheiralla ZH, Hewedy MAH, Mohammed HR and Darwesh OM. 2016. Isolation of pigment producing *actinomycetes* from rhizosphere soil and application it in textiles dyeing. *Res J Pharm Biol Chem Sci*., **7(5):** 2128-2136.

Kim SH, Traag BA, Hasan AH, McDowall KJ, Kim B-G and van Wezel GP. 2015. Transcriptional analysis of the cell division-related ssg genes in *Streptomyces coelicolor* reveals direct control of ssgR by AtrA. *Antonie Van Leeuwenhoek*, **108(1)**: 201-213.

Laidi RF, Abderrahmane A and Norya AH. 2013. Identification and Antibiosis of a Novel *Actinomycete* Strain RAF-11 Isolated From Iraqi Soil. *Int J Sci: Basic Appl Res.*, **12(1):** 141-159.

Li Y, Liu J, Díaz-Cruz G, Cheng Z and Bignell DR. 2019. Virulence mechanisms of plant-pathogenic *Streptomyces species*: an updated review. *Microbiology*, **165:** 1025–1040.

Maleki H, Dehnad A, Hanifian S and Khani S. 2013. Isolation and molecular identification of *Streptomyces spp*. with antibacterial activity from northwest of Iran. *BioImpacts*, **3(3)**: 129-134.

Massadeh MI and Mahmoud SM. 2019. Antibacterial Activities of Soil Bacteria Isolated from Hashemite University Area in Jordan. *Jordan J Biol Sci*., **12(4)**: 503-511.

Massenssini A, Bonduki V, Melo C, Totola M, Ferreira F and Costa M. 2014. Soil microorganisms and their role in the interactions between weeds and crops. *Planta Daninha*, **32(4):** 873-884.

Minas W, Bailey JE and Duetz W. 2000. *Streptomycetes* in micro-cultures: Growth, production of secondary metabolites, and storage and retrieval in the 96–well format. *Antonie Van Leeuwenhoek*, **78(3-4)**: 297-305.

Murray J, Salih T and Tucker N. 2019. The emergent properties of *streptomyces* observed during co-culture and the genomic and morphological characterisation of a *Streptomyces lydicus* strain. *Access Microbiology*, **1(1A)**: 115-120.

Reddy P and Umamaheshwara RV. 2016. Mycelial and Pigmentation studies of Dibenzothiophene desulfurizing *Streptomyces species* isolated from oil contaminated sites. *Int J Pharm Biol Sci.*, **11(5)**: 143-146.

Rintala H, Nevalainen A, Rönkä E and Suutari M. 2001. PCR primers targeting the 16S rRNA gene for the specific detection of Streptomycetes. *Mol Cell Probes*, **15(6)**: 337-347.

Romero DA, Hasan AH, Lin Yf, Kime L, Ruiz-Larrabeiti O, Urem M, Bucca G, Mamanova L, Laing EE and van Wezel GP. 2014. A comparison of key aspects of gene regulation in *Streptomyces coelicolor* and *Escherichia coli* using nucleotide-resolution transcription maps produced in parallel by global and differential RNA sequencing. *Mol Microbiol.*, **94(5)**: 963-987.

Salerno P, Persson J, Bucca G, Laing E, Ausmees N, Smith CP. and Flardh K. 2013. Identification of new developmentally regulated genes involved in *Streptomyces coelicolor* sporulation. *BMC Microbiol.*, **13(1):** 281-299.

Saitou N and Nei M. 1987. The neighbor-joining method: a new method for reconstructing phylogenetic trees. *Mol Biol Evol.*, **4(4)**: 406-425.

Schlaberg R, Simmon KE and Fisher MA. 2012. A Systematic Approach for Discovering Novel, Clinically Relevant Bacteria. *Emerg Infect Dis*., **18 (3)**: 422-430.

Shepherd MD, Kharel MK, Bosserman MA and Rohr J. 2010. Laboratory maintenance of *Streptomyces species*. *Curr Protoc Microbiol.*, **18(1)**: 10E.1.1-10E.1.8.

Singh V, Haque S, Singh H, Verma J, Vibha K, Singh R, Jawed A and Tripathi C. 2016. Isolation, screening, and identification of novel isolates of *Actinomycetes* from India for antimicrobial applications. *Front Microbiol.*, **7**: 1921.

Sottorff I, Wiese J, Lipfert M, Preußke N, Sönnichsen FD and Imhoff JF. 2019. Different secondary metabolite profiles of phylogenetically almost identical *Streptomyces griseus* strains originating from geographically remote locations. kim*Microorganisms*, **7(6)**: 166.

Stackebrandt E. and Ebers J. 2006. Taxonomic parameters revisited: tarnished gold standards. *Microbiol Today*, **8(4)**: 6-9.

Tamura K, Peterson D, Peterson N, Stecher G, Nei M and Kumar S. 2011. MEGA5: molecular evolutionary genetics analysis using maximum likelihood, evolutionary distance, and maximum parsimony methods. *Mol Biol Evol.*, **28(10)**: 2731-2739.

Thompson JD, Higgins DG and Gibson TJ. 1994. CLUSTAL W: improving the sensitivity of progressive multiple sequence alignment through sequence weighting, position-specific gap penalties and weight matrix choice. *Nucleic Acids Res*., **22(22)**: 4673-4680.

Vartoukian SR, Palmer RM and Wade WG. 2010. Strategies for culture of 'unculturable' bacteria. *FEMS Microbiol Lett.*, **309(1)**: 1-7.

Walker T, Stapleton P and Gibbons S. 2019. Identification of novel antimicrobial-producing bacteria from an ancient water source by Oxford Nanopore Whole Genome Sequencing and Natural Product Chemistry. *Access Microbiology*, **1(1A)**.

Westhoff S, Otto SB, Swinkels A, Bode B, van Wezel GP and Rozen DE. 2020. Spatial structure increases the benefits of antibiotic production in *Streptomyces**. *Evolution*, **7(1)**: 179-187.

Xu X, Liu W, Tian S, Wang W, Qi Q, Jiang P, Gao X, Li F, Li H and Yu H. 2018. Petroleum hydrocarbon-degrading bacteria for the remediation of oil pollution under aerobic conditions: a perspective analysis. *Front Microbiol.*, **9:** 2885.

Yoon S-H, Ha S-M, Kwon S, Lim J, Kim Y, Seo H and Chun J. 2017. Introducing EzBioCloud: a taxonomically united database of 16S rRNA gene sequences and whole-genome assemblies. *Int J Syst Evol Microbiol.*, **67(5)**:1613-1617.

Yücel S and Yamaç M. 2010. Selection of *Streptomyces* isolates from Turkish karstic caves against antibiotic resistant microorganisms. *Pak J Pharm Sci*, **23(1)**:1-6.

JJBS

Volume 14, Number 3, September 2021
ISSN 1995-6673
Pages 453 - 461

Jordan Journal of Biological Sciences

Phytochemical, Chemical and Biomedical Characterization of Crude Extracts of *Macrosphyra longistyla* (DC.) Hiern

Ernest U. Durugbo [1,*], James O. Ogah [2], Nwankwo Chukwuemeka [1], Peter G. Sename [1], Adedayo T. Olukanni [3, 4], Kafayat O. Yusuf [2], Isioma C. Awuzie [2] Olumide D. Olukanni [3], and Simbo O. Aboaba[2]

[1]*Department of Biological Sciences, Redeemer's University, P.M.B. 230, Ede, Osun State, Nigeria.*[2]*Department of Microbiology, University of Lagos, Akoka-Yaba, Lagos, Nigeria;*[3]*Department of Biochemistry, Redeemer's University, P.M.B. 230, Ede, Osun State, Nigeria;*[4]*Department of Cell Biology and Genetics, University of Lagos, Akoka-Yaba, Lagos, Nigeria.*

Received: April 17, 2020; Revised: August 30, 2020; Accepted: September 15, 2020

Abstract

Phytochemical analysis of *Macrosphyra longistyla* leaf, stem bark, and root extracts revealed different constituents. The GC-MS analyses of their ethanolic extracts showed the presence of bioactive compounds: the stem bark yielded 9 compounds, such as squalene, vitamin E, and fatty acids; the root extract revealed 10 different compounds, especially morpholine, isophorone and fatty acids. The extracts demonstrated high proteinase inhibition potentials. The aqueous, ethanol and ethyl acetate extracts of the leaf, stem bark, and root were tested against *Methicillin-Resistant Staphylococcus aureus (MRSA) 144m, Escherichia coli ATCC11229, Salmonella typhimurium ATCC13311, Enterococcus faeciumATCC700221, Shigella flexneri ATCC12012* and laboratory strain of *Streptococcus mutans* with the diameter of zone of inhibitions ranging from 10 to 40 mm. The study revealed a marked susceptibility pattern of the test organisms to the ethanol and ethyl-acetate extracts showing varied diameter of zones of inhibitions. The aqueous extract was ineffective against the pathogens.. The minimum inhibitory concentrations (MIC) ranged from 25-100mg/ml. All the test organisms except *S. mutans* were susceptible to control antibiotic (streptomycin 10µg).. The presence of arrays of bioactive ingredients implicated in the treatment of specific ailments has provided a scientific justification for *Macrophyla longistyla* as an alternative remedy for the treatment of bacterial infections.

Keywords: *Macrosphyra longistyla*, DPPH scavenging, isophorone, plants alkyne, antibacterial agents.

1. Introduction

Numerous medicinal herbal plants have been associated with the treatment and the prevention of different diseases for thousands of years (Wang *et al.* 2012). This association, however, diminished with the discovery of antibiotics. As resistant pathogens develop and spread, the effectiveness of the antibiotics also diminished. In recent years, clinically relevant bacteria with multiple drug-resistant (MDR) strains had been reported globally (Andersson and Levin, 1999; Davies and Davies, 2010; Odumosu *et al.* 2017).

Bouyahaya *et al.* (2017) reported that numerous research works had demonstrated the potential of medicinal plants used in different traditional, complementary, and alternative disease treatments. Jaiswal and Sharma (2020) further added that in the last two decades, different parts of the plant such as leaves, stem, seeds, flowers, fruits, and roots of many medicinal plants and weeds had been documented to exert antibacterial potentials. They together with (Belakhdar *et al.* 2015; Maffo *et al.* 2015; Al-Jadidi and Hossain, 2016; Bouyahya *et al*, 2016; Lopez-Rubalava and Estrada-Camarena, 2016; Karthikeyan *et al.* 2009; Saranraj and Sivasakthi, 2014) had attributed this ability to various secondary metabolites such as tannins, terpenoids, alkaloids, flavonoids, phenols, glycosides, saponins, fatty acids, gums, resins, and steroids, present in these medicinal plants. Recently, interest in plant extracts exhibiting antimicrobials and pharmacological applications has been increasing (; Sacan 2018; Singh and Sharma, 2019; Jaiswal and Sharma, 2020; Mak *et al*. 2013; Yigit, 2018).

Macrosphyra longistyla (DC.) Hiern is a popular medicinal plant in West Africa (Burkill, 1995; Govaerts *et al*. 2003; Arbonnier, 2000). It belongs to the family Rubiaceae. The plant parts used include the fruit, leaf, and also flower. Generally, the flower is used for healing; the young leaves are boiled and eaten as vegetables. The leaves are excellent treatments for cutaneous, subcutaneous parasitic infections, abortifacients, embolic, and leprosy. The roots are diuretic and useful for treating kidney problems (Arbonnier, 2000).

Since the main antimalarial drug quinine is of Rubiaceae origin, researchers tend to infer that similar compounds with similar properties may occur in other genera of the family Rubiaceae (Karou *et al.* 2011). Singh and Sharma (2019) had reviewed the therapeutic potentials of plant-based natural compounds used for malaria

* Corresponding author e-mail: durugboe@run.edu.ng.

treatment. From the available literature, reports on *M. longistyla* are scarce (Odugbemi, 2008; Elufioye *et al.* 2019). Hence, this study was set out to investigate the phytochemical components and antibacterial activities of ethanolic, aqueous and ethyl acetate of the leaf, stem bark, and root extracts of *M. longistyla* on selected bacteria.

2. Material and Methods

2.1. Collection of plant materials

The fresh stem-bark, leaves, and roots of *Macrosphyra longistyla* were collected from within the premises of Redeemer's University Ede, Osun State, Nigeria, in March 2018. The plant specimen was identified by Dr. Ernest Durugbo of the Department of Biological Sciences Redeemer's University and later authenticated by Dr. George Nodza at the University of Lagos Herbarium and a voucher number LUH 8194 assigned. The plant materials were air-dried for two weeks at room temperature crushed and grounded into powder, using mortar and pestle ready for extraction.

2.2. Preparation of crude extracts

The extraction of powdered plant material was carried out by maceration, as previously described (Ogah and Osundare, 2015). Thirty grams (30 g) of dry powdered materials percolated in 300 ml of absolute ethanol, ethyl-acetate, and distilled water in 500 ml conical flasks were stoppered and kept for 48 hours at room temperature (28±2ºC). The extracts were filtered with Whatman No. 1 filter paper, concentrated at 40^{o}C using a rotary evaporator (REL200, Bibby Sterlin, England, Agyare *et al.* 2014), and the concentrated extracts were used for the antibacterial assay and further analysis.

2.3. Selection of Bacteria culture

The pure typed bacteria cultures of Methicillin-Resistant *Staphylococcus aureus* (MRSA)144m, *Escherichia coli* ATCC11229, *Salmonella typhimurium* ATCC13311, *Enterococcus faecium* ATCC700221, *Shigella flexneri* ATCC12012 and Laboratory strain of *Streptococcus mutans* used for the antibacterial assay were obtained from the pure culture laboratory of Microbiology Department of the University of Lagos, Akoka-Yaba, Lagos, Nigeria. They were maintained in glycerol-peptone water at 4^{o}C before use.

2.4. Antibacterial Study

The bacterial cultures were inoculated in Mueller-Hinton Broth to obtain a fresh 18-h old culture for the assay. The leaf, stem bark and root extracts of *M. longistyla* were tested using the well-diffusion method described by CLSI. A stock solution of extract consists of 0.4g of plant material in 1ml of water. A loopful of bacterial colonies from overnight culture was inoculated into sterile Mueller-Hinton Broth (MHB). Broth inoculums were incubated at 37°C for 16-20 h. Broth inoculums were standardized to 0.5 McFarland standards using dilution with sterile MHB and measuring the optical density t at 625 nm wavelengths. Absorbance readings were fixed within the range of 0.08 - 0.13 (equivalent to approximately 1.5 x 10^{8} CFU/mL). Standardized broth inoculums were lawned onto sterile Muller Hinton Agar by swabbing with sterile cotton swabs and allowed to sit for 10 minutes. Wells (6 mm in diameter) were bored into the solidified and well-seeded agar equidistant to each other with a cork borer. Streptomycin, a standard antibiotic, was used as the positive control for the test organisms, while 1% DMSO was the negative control. Each plant extract (100 µl) was dispensed into the wells in triplicates. The agar plates were kept at room temperature for 10 min before incubation at 37°C for 18-24 h. The diameter zones of inhibition were measured using a ruler in millimeters, and the average zone was taken.

2.4.1. Minimum Inhibitory Concentration of M. longistyla on the selected Bacterial Isolates

The minimum inhibitory concentrations (MIC) of the extracts of *M. longistyla* were determined by the double dilution technique (Ochei and Kolhatkar, 2004). Known weights of plant extracts were diluted with physiological saline (0.85%) into four different concentrations (100, 50, 25 and 12.5 mg/ml). One hundred microliters (100 µl) of different dilutions were inoculated (Cheesbrough, 2013), and incubated at 37^{o}C for 24 h. After the overnight incubation, the lowest concentrations of the extract that inhibited the organisms' growth were taken as the minimum inhibitory concentration.

2.5. Qualitative phytochemical analysis

Ethanol extracts of the various parts of *M. longistyla* were screened for the presence of bioactive chemicals such as alkaloids using Mayer's reagents, flavonoids with sodium hydroxide test as described by Trease and Evans (2002). Tannins and saponins were detected using ferric salt and frothing tests, respectively, according to the standard procedures described by Parekh and Chanda (2007) while Steroids, terpenoids, and phlobatannins were screened as documented by Harborne (1998).

2.6. Quantitative phytochemicals analysis

2.6.1. Determination of total phenolic content

The total phenolic compounds in the various extracts of the plant were determined with Folin-Ciocalteu reagent using the method of Ebrahimzadeh *et al.* (2008). To 0.5 mL of each sample (in triplicates) of plant extract in methanol solution (1 mg/mL), 2.5 mL of 10 % Folin-Ciocalteu reagent and 2 mL of Na_2CO_3 (2 % w/v) was added. The mixture was incubated at 50°C for 30 min, and the absorbance was measured at 765 nm using a U.V./visible spectrophotometer. Concentrations of the phenolic compounds in the extracts were extrapolated from a calibration curve of Gallic acid. Results were expressed as mg Gallic acid equivalent/ g of extract.

2.6.2. Determination of total flavonoids content

Total flavonoids content was determined using the colorimetric method of Singleton and Rossi (1965) to extract and estimate flavonoids with some modifications. Flavonoids react with vanillin to produce a colored product, which can be measured spectrophotometrically. According to the procedure, 250 µl of the extract was added to 1.25 ml of distilled water and 75 µl of 5% $NaNO_2$. After 5 min, 150 µl of 10% $AlCl_3.H_2O$ was added, followed by 500 µl of 1 M NaOH and 275 µl of distilled water after 6 min. The solution was adequately mixed, and the color intensity of the mixture read at 510 nm. The standard used was Gallic acid.

2.6.3. Estimation of antioxidant activity

The antioxidant activity was measured using the DPPH assay. This spectrophotometric assay uses the stable radical 1, 1-diphenyl-1- picrylhydrazyl (DPPH) as a reagent (Amarowicz *et al.* 2004). The DPPH free radical is commercially available, and it was prepared at a 0.1 mM concentration (25 mg/L) in methanol (Sánchez-Moreno *et al.* 1998; Larrauri *et al.* 1999; Sasidharan *et al.* 2011). The absorbance at 518 nm was monitored in the presence of different concentrations of extracts. The blank experiment was carried out to determine the absorbance of DPPH before interacting.

2.6.4. Proteinase inhibition assay

The method of Kunitz (1947) was used for the proteinase inhibition study. One mL aliquot of trypsin [EC 3.4.21.4, SRL, India (1000 units/mg)] (0.5 mg/mL prepared in 0.1 M phosphate buffer pH 7) was pre-incubated with 1 mL of varied concentration of the plant extracts and aspirin (standard) at 37° C for 15 min. To the mixture, 2 mL of 1% casein (S.R.L., India) (prepared in 0.1 M phosphate buffer) was added and incubated at 37° C for 30 min. The reaction was terminated with 2.5 mL of 0.44 M trichloroacetic acid (TCA) solution. The reaction mixture was centrifuged to remove the precipitated protein at 10,000 rpm for 15 min (Eppendorf, Germany). The absorbance of the clear supernatant was measured at 280 nm in a UV–Visible spectrophotometer (Shimadzu, Japan) against appropriate blanks. The formula below gave percentage inhibition:

$$\%\ Inhibition = \frac{Absorbance\ of\ control - Absorbance\ of\ test}{Absorbance\ of\ control} X\ 100\%$$

2.7. GC-MS Analysis

Gas Chromatography-Mass Spectrometry (GC-MS) Analysis of Crude Extracts of *M. longistyla*

GC-MS analysis was carried out on the extracts according to the protocol previously described by Odumosu *et al.* (2017) using a 7890A Gas Chromatography system (Agilent Technology HP5MS), with a mass spectrometer (5975C VLMSD) as a detector. The column has a length of 30 m, the internal diameter of 0.32 mm, and thickness of 0.25 µm; volume injected was 1 µL, and the injector temperature was 250°C, Helium was the carrier gas, and oven temperature initially programmed at 80°C for 2 min, increased at 10°C per min to 240°C, and held for 6 min. Interpretation of the mass spectrum of GC-MS was conducted using the National Institute Standard and Technology (NIST) database. Unknown spectra were compared with those of the known ones stored in the NIST library.

3. Results and Discussions

Qualitative phytochemical screening of the ethanolic extract of *M. longistyla* revealed that the leaf extract contained almost all the tested phytochemicals except alkaloids. The stem bark had only alkaloids, flavonoids, saponins, steroids, and tannins. In contrast, the root contained flavonoids, saponins, steroids, and carbohydrates (Table 1). Some of these compounds are known to possess antimicrobial activities.

Table 1. Phytochemical content of ethanolic extracts of *Macrosphyra longistyla*

Group	Plant parts		
	Stem bark	Leaf	Root
Alkaloids	+	-	-
Flavonoids	+	+	+
Saponins	+	+	+
Steroids	+	+	+
Tannins	+	+	-
Terpenoids	-	+	-
Phobatannin	-	+	-
Carbohydrate	-	+	+
Amino acids and proteins	-	+	-

The quantitative phytochemical contents (total polyphenols and total flavonoids) of the various parts of *Macrosphyra longistyla* are shown in Table 2. The leaves presented the highest content of total polyphenols (226.69 ± 4.53 mg/g gallic acid equivalents (GAE). Although the root extract has the lowest content of total polyphenols, it demonstrated high flavonoid content (254.25 ± 4.75).

Table 2. Total phenols, total flavonoids and DPPH scavenging activities of extracts

Plant extract	Total polyphenols (G.A.E./g extract)	Total flavonoids (G.A.E./g extract)	DPPH Assay (IC50 (µg/mL)
GA.	-	-	16.78± 1.14[a]
MLS	226.60 ± 4.53	180.29 ± 5.61	43.33± 1.83[b]
MLL	271.27 ± 19.88	287.10 ± 5.83	73.07± 2.86[c]
MLR	115.13 ± 13.74	254.25 ± 4.75	114.87± 3.13[d]

The DPPH assay is a spectrophotometric measurement of the color changes, from violet to yellow, when an antioxidant substance scavenges the radical, reducing it to hydrazine. The ML leaf extract showed relatively high antioxidant capacity with an IC50 of 43.33 ± 1.83µg/mL while the standard had an IC50 of 16.78 ±1.14 µg/mL (Figure 1 and Table 2). The ML root and stem fractions showed high IC50 values comparable to those of plants with low antioxidant activities. These results agreed with the content of polyphenols found in the fractions (MLL> MLR> MLS) and were significantly different from those of the total flavonoids; thus, it is impeccable to attribute the antioxidant capacity of the various ML parts to the polyphenol and/or flavonoid contents. This relationship has been described by many authors using various plants species (Schubert *et al.* 2007; Zadra *et al.* 2012) (Fig. 1).

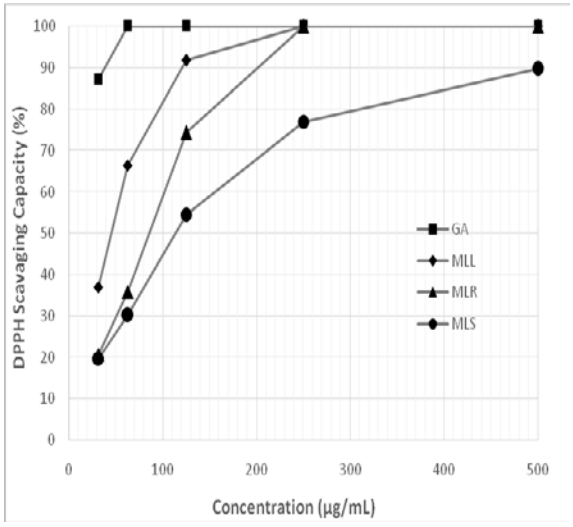

Figure 1. Antioxidant capacity of methanol extracts of various parts of M. longistyla using DPPH assay (n=3)

Figure 2 shows the reducing power potentials of the ethanol extracts of ML compared to the gallic acid standard at 700 nm. The reducing capacity of the extracts, a significant indicator of antioxidant activity, was found to be appreciable. The results showed that there were increases in the reductive capability of the extracts from ML. The leaf (MLL), and stem extracts (MLS) showed a comparable high reducing ability of 1.49 and 1.46 at 0.2 mg/mL when compared with the ascorbate control (1.67). This reducing activity is higher than that reported by Atolani *et al.* (2011), who worked on *Kigelia pinnata*, even at a high concentration of 0.4 mg/mL. However, the findings are in tandem with recent works of Kudumula *et al.* (2018), who did an extensive survey on selected medicinal plants used in the treatment of bacterial infections in South Africa (Fig. 2).

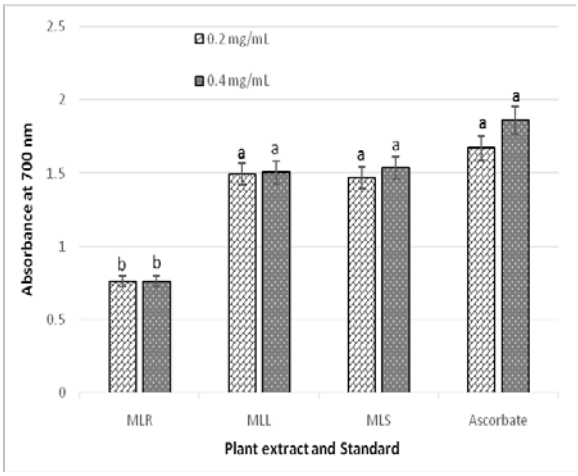

Figure 2. The reducing power potential of the selected plant extracts and ascorbic acid, with absorbance increasing with increasing concentration (values with different alphabets are significantly different at p =0.05, t-test).

Similarly, the extracts demonstrated high proteinase inhibition potential competing effectively with the Aspirin standard, as shown by their inhibition effect on trypsin (Figure 3). Trypsin inhibitors are serine based inhibitors and are of high pharmaceutical importance (Bejina *et al.* 2011). Proteinase inhibitors are generally good anti-inflammatory drugs, suggesting that ML will be a good candidate for drug development and direct consumption for locals as a pain-killer.

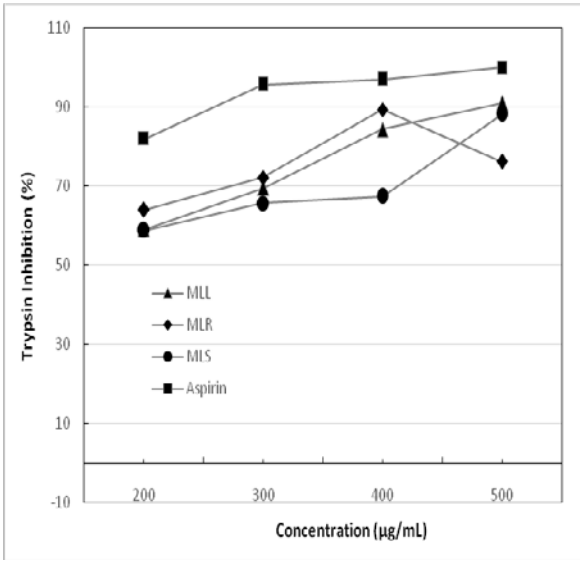

Figure 3. Trypsin inhibitory activities of extracts from various parts of Macrosphyra longistyla

The antibacterial activities of the crude extracts of stem-bark, leaves, and roots of *M. longistyla* showed zones of inhibition in millimetres against the clinical isolates ranging from 10 to 40 mm (Table 3) with minimum inhibitory concentration (MIC) ranging from 25 – 100 mg/ml (Table 4). GC- MS analyses showed a significant presence of bioactive compounds from ethanolic crude extracts and their characteristics (Tables 5 and 6). The chromatograms of the ethanolic extracts of the root and stem are shown in Figures 4 and 5, respectively.

Table 3. Antibacterial Activity of Extracts of *Macrosphyra longistyla* against Bacterial Isolates

Bacterial Isolates	The diameter of the zone of inhibition in millimeter (mm)									
	A	B	C	D	E	F	G	H	I	J
MRSA (144m)	-	-	-	40	35	26	-	14	23	27
E. coli ATCC11229	-	-	-	27	23	33	22	15	24	11
S. typhimurium ATCC13311	-	-	-	-	39	-	32	31	-	15
E. faecium ATCC700221	-	-	-	24	36	-	19	26	20	12
S. flexneri ATCC12012	-	-	-	12	39	-	-	17	-	10
S. mutans	-	-	-	19	32	18	-	19	15	-

Zone of inhibition included 8mm cork-borer, - resistance, **A**=Aqueous stem extract, **B**=Aqueous leaf extract, **C**=Aqueous root extract, **D**=Ethanol stem extract, **E**=Ethanol leaf extract, **F**=Ethanol root extract, **G**=Ethyl-acetate stem extract, **H**=Ethyl-acetate leaf extract, **I**=Ethyl-acetate root extract, **J**=Streptomycin (10µg).

Table 4. Minimum Inhibitory Concentration of Extracts of *Macrosphyra longistyla* against Bacterial Isolates

Bacterial Isolates	Minimum inhibitory concentration (MIC) in mg/ml								
	A	B	C	D	E	F	G	H	I
MRSA (144m)	-	-	-	25	25	50	-	50	50
E. coli ATCC11229	-	-	-	25	100	50	25	25	25
S. typhimurium ATCC13311	-	-	-	-	50	-	25	50	-
E. faecium ATCC700221	-	-	-	100	50	-	50	25	100
S. flexneri ATCC12012	-	-	-	100	50	-	-	100	-
S. mutans	-	-	-	25	25	50	-	100	100

Zone of inhibition included 8mm cork-borer, - resistance, **A**=Aqueous stem extract, **B**=Aqueous leaf extract, **C**=Aqueous root extract, **D**=Ethanol stem extract, **E**=Ethanol leaf extract, **F**=Ethanol root extract, **G**=Ethyl-acetate stem extract, **H**=Ethyl-acetate leaf extract, **I**=Ethyl-acetate root extract, **J**=Streptomycin (10µg).

The ability of the stem, leaf and root extracts of *M. longistyla* in this study to inhibit both Gram-positive and Gram-negative bacteria is an indication of its broad-spectrum activity; hence, a potential source of drugs for the treatment of dental caries, diarrhoea, skin and wound infections, typhoid and non-typhoid fever, gastroenteritis, urethritis, otitis media, septicemia, osteomyelitis and any other infections caused by these pathogenic bacterial strains. Aqueous extracts could not inhibit any of the isolates used, whereas ethanol extracts of stem-D inhibited *MRSA* (40), *E. coli* (27), *E. faecium* (24), *S. flexneri* (12) and *S. typhimurium* (R); leaf-E all tested organisms (23-39) and root-F *MRSA* (26), *E. coli* (33), *S. mutans* (15), *S. typhimurium* (R), *S. flexneri* (R) and *E. faecium* (R) millimetre zones of inhibitions. However, ethyl acetate extracts of stem-G inhibited *E. coli* (22), *S. typhimurium* (32), *E. faecium* (19), others resistance (R); Leaf-H all isolates (14-31) and root-I *MRSA* (23), *E. coli* (24), *E. faecium* (20), *S. mutans* (15), others resistance (R). Streptomycin-J inhibited all except *S. mutans* between 10-27 millimetre diameters. Results showed that the leaf extract of *M. longistyla* was more potent than extracts of other parts of the plant. Hence, *M. longistyla* leaf contains more active ingredients than the stem and root (Table 1). The inability of aqueous extracts to inhibit the growth of the bacterial strains may be due to its low extraction ability. The findings agreed with Ogah and Osundare's (2015) report, which observed that aqueous extract showed little or no activity against tested strains, suggesting that water may have a low penetration and extraction ability compared to organic solvents. Other researchers had also supported this view that organic solvent extracts exhibited higher antibacterial activity than aqueous extracts. The antibacterial principles may be either polar or non-polar since extraction can be with organic solvents or aqueous media (Britto, 2001). Odeleye *et al*. (2016) reported that aqueous extracts' poor inhibition ability might be due to the weak solubility nature of the plants' active components in water.

Minimum inhibitory concentration (MIC) of the plant extracts (Table 4) showed the following range against *MRSA* (25-50), *E. coli* (25-100), *S. typhimurium* (25-50), *S. flexneri* (25-100) and *S. mutans* (25-100) milligram per millimetre. The MICs implied that the extracts had some substantial effects on the test organisms.

The result of the GC-MS analysis revealed certain bioactive compounds such as fatty acids, amino acids, vitamin E, and their derivatives, which were shown to have medicinal properties. It showed that isophorone is prevalent in the three parts of the plant studied; it is the most prevalent in the MLL and MLR, and the second most prevalent in MLS (Table 5). Besides, the isophorone, which is common to the three parts, the leaf (MLL) has 1-methoxymethoxy-oct-2-yne, 7-chloro-3-heptyne, 11-dodecyn-1-ol acetate as prominent components. The root (MLR) also presented linoleic acid ethyl ester, 3-eicosene, octadecanoic, n-hexadecanoic acid, and their ester derivatives as prominent components. The stem (MLS), however, has 5H,6H,7H-cyclopenta[d]pyrimidin-2-amine as the most prominent compound alongside hexadecanoic ethyl ester, Vitamin E and Squalene. Other bioactive components identified include 3-ethyl-1-pyrroline and morpholines.

Table 5. Bioactive Compounds identified in the *Macrosphyra longistyla* ethanol extract of the leaf (MLL), root (MLR) and stem (MLS) and their characteristics

Peak #	RT (Min)	Compound name	Molecular formulae	Molecular Weight ($gmol^{-1}$)	% Peak Area
MLL					
1	4.191	Aziridine, 1-(2-buten-1-yl)-, (Z)-	$C_6H_{11}N$	97.16	2.76
2	4.775	3-Methyl-3-hexene	C_7H_{14}	98.19	3.16
3	5.204	Propanenitrile, 3-amino-2,3-dihydroxymino)-	$C_3H_4N_4O_2$	128.09	2.32
4	8.351	Isophorone*	$C_9H_{14}0$	138.21	33.54
5	13.043	4-Cyclopentene-1,3-diol, trans-	$C_5H_8O_2$	100.12	1.06
6	13.861	2-Azatricyclo[4.3.1.1(4,8)]undecane	$C_{10}H_{17}N$	151.25	1.20
7	14.805	Benzaldehyde, 2-nitroso-	$C_7H_5NO_2$	135.12	1.58
8	15.486	Octadecane, 1-(ethenyloxy)-	$C_{20}H_{40}O$	296.50	1.21
9	16.127	Oxirane, 2,2'-(1,4-butanediyl)bis-	$C_8H_{14}O_2$	142.20	1.15
10	17.684	2-Hexyn-1-ol	$C_6H_{10}O$	98.14	1.46
11	18.313	3-Heptyne, 7-chloro-	$C_7H_{11}CL$	130.61	9.10
12	21.672	Paromomycin	$C_{23}H_{45}N_5O_{14}$	615.60	1.45
13	22.427	1-Pyrroline, 3-ethyl-	$C_{16}H_{15}N$	97.16	1.56
14	22.707	7-Oxabicyclo[4.1.0]heptane, 1,5-dimethyl-	$C_8H_{14}O$	126.20	2.48
15	22.851	11-(2-Cyclopenten-1-yl)undecanoic acid, (+)-	$C_{16}H_{28}O$	252.39	1.41
16	23.451	1-Methoxymethoxy-oct-2-yne**	$C_{10}H_{18}O_2$	170.25	27.02
17	23.583	11-Dodecyn-1-ol acetate	$C_{14}H_{24}O_2$	224.34	3.85
18	25.105	4-Acetoxy-3-methylbut-2-enoic acid, methyl ester	$C_8H_{12}O_4$	172.18	1.07
19	25.397	8-Nonynoic acid	$C_9H_{14}O_2$	154.21	1.08
20	26.318	Trichloroacetic acid, 2-methyloct- 5-yn-4-yl ester	$C_{11}H_{15}Cl_3O_2$	285.60	1.54
MLR					
1	4.730	2(5H)-Furanone, 5-methyl-	C5H6O2	98.10	2.49
2	5.001	Morpholine	C4H9NO	87.12	4.05
3	8.268	Isophorone*	C9H14O	138.21	30.35
4	18.75	(5-Carbamoyl-2,4-dioxo-3H-pyrimidin-1-yl) acetic acid	C7H7N3O5	213.15	0.40
5	19.562	Pentadecanoic acid, 14-methyl	C16H32O2	256.42	2.29
6	20.493	n-Hexadecanoic acid	C16H32O2	256.42	10.24
7	20.629	Octadecanoic acid	C18H36O2	284.48	10.90
8	23.452	Linoleic acid ethyl ester **	C20H36O2	308.50	17.12
9	23.522	3-Eicosene, (E)-	C20H40	280.53	15.15
10	23.918	Octadecanoic acid, ethyl ester	C20H40O2	312.53	3.729
11	28.651	Benzene, 1-isothiocyanato-2-methyl	C8H7NS	149.21	1.02
12	30.856	2-Buten-1-ol, (E)-, TBDMS derivative	C10H22OSi	186.37	0.21
13	31.056	2,6,10-Dodecatrien-1-ol, 3,7,11-trimethyl	C15H260	222.37	2.05
MLS					
1	5.078	Propanoic acid, 2-methylpropyl ester	$C_7H_{14}O_2$	130.18	1.26
2	8.271	Isophorone**	$C_9H_{14}O$	138.21	18.37
3	18.118	Cyclohexanone, 2,2-dimethyl-5-(ethyloxiranyl)	$C_{12}H_{20}O_2$	196.29	1.24
4	18.49	5H,6H,7H-Cyclopenta[d]pyrimidin-2-amine*	C_7H_9N3	135.17	30.93
5	20.625	Hexadecanoic acid, ethyl ester	$C_{18}H_{36}O_2$	284.48	16.46
6	23.451	Linoleic acid ethyl ester	$C_{20}H_{36}O_2$	308.50	12.64
7	31.044	Squalene	$C_{30}H_{50}$	410.72	4.90
8	33.585	Vitamin E	$C_{29}H_{50}O_2$	430.71	14.20

***** most prevalent phytochemical in each plant's part

** the second most prevalent

Isophorone, the phytochemical, which is common to the three parts, is a well-known plant metabolite that has been used as an industrial solvent. It is used as a carrier of pesticide for plants, and when partly hydrogenated, it forms a derivative, trimethylcyclohexanone, a common raw material for polycarbonates production. Polycarbonate can further be reacted with phenol to give an analogue of bisphenol A with potent antimicrobial properties; the antimicrobial is usually used to disinfect skin or wound. The high level of this solvent may suggest exogenous sources from pesticide applications.

The long-chain fatty acids, which are the major components of the root extracts, linoleic acid ethyl ester and octadecanoic acid, are well known for their nutritional values. Besides, octadecanoate is a potent antifungal and antibacterial compound; the antioxidant, hypo-cholesterolemic, and nematicide, activities of n-hexadecanoic acid is also well known (Elaiyaraja and

Chandramohan, 2018). The stem, however, has 5H,6H,7H-cyclopenta[d]pyrimidin-2-amine as its prominent compound; pyrimidin-2-amine is presently being considered as an anticancer drugs and H3 receptor antagonist (Tadesse et al. 2018; Wagner et al. 2019). H3 receptor antagonists are principal in allergy prevention and autoimmune response suppression. The presence of vitamin E and squalene in stem bark collaborated the presence of flavonoid in the previous analysis, so did the lowest DPPH scavenging IC50 recorded by MLS extract in that study. Squalene has a role in topical skin lubrication and protection against pathogens (Pappas, 2009); in addition to the aforementioned, vitamin E has been reported to demonstrate antioxidant, anti-aging and anti-inflammatory activities (Saliha *et al.,* 2014). It was also observed that the plant extracts had particular alkyne groups such as 1-methoxymethoxy-oct-2-yne, 7-chloro-3-heptyne, and 11-dodecyn-1-ol acetate and some bioactive ring structure (Figure 4). These alkyne groups are known with rare bioactivities such as antiprotozoal and nematocidal activities (Jorgensen et al., 1996).

The presence of a 3-ethyl-1-pyrroline suggests that the compound could be responsible for the scent (aroma) of the plant leaf. A similar compound, 2-acetyl-1-pyrroline, has been implicated in aromatic rice and other plants (Routray and Rayaguru, 2018). Also, propanenitrile, 3-amino-2,3-di (hydroxymino)- has been reported in the volatile compounds identified from root exudates of chilli seedling primed with 6% *Bacillus amyloliquefaciens* (Sathya et al. 2016). Morpholines are widely used in organic synthesis. They serve as -building blocks in the preparation of the antibiotic linezolid, the anticancer agent gefitinib (Iressa), and the analgesic dextromoramide (Wikipedia, 2019). Recently, some studies have shown that morpholines derivative, 1-[4-(morpholin-4-yl) phenyl]-5-phenylpenta-2,4- dien-1- one, is a potent monoamine oxidase inhibitor (Maliyakkal et al. 2020). Monoamine oxidase inhibitors are effective antidepressant drugs that have found usage in social phobia and panic disorder.

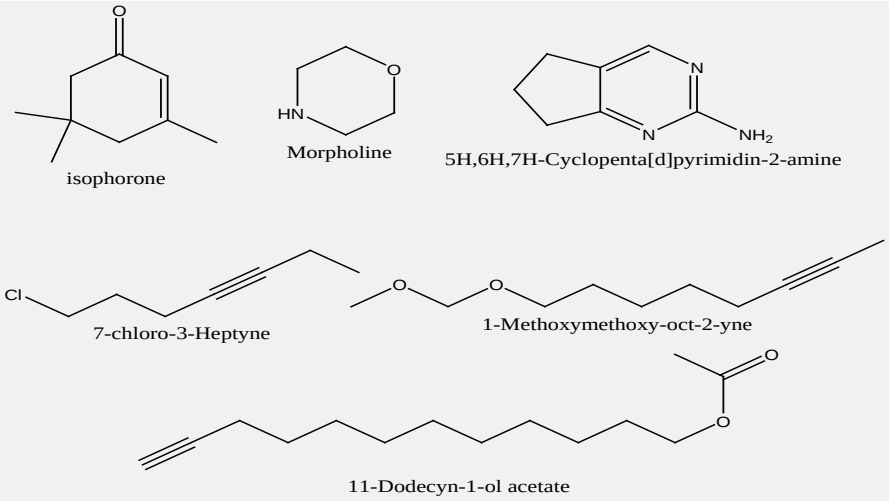

Figure 4. Prominent bioactive compounds and rare alkyne groups identified from the GCMS analysis of *Macrosphyra longistyla* extracts

4. Conclusion

The presence of arrays of phytochemicals or bioactive ingredients such as alkaloids, saponins, tannins, flavonoids, phlobatanins, isophorone, squalene, morpholine, vitamin E and host of others revealed in this study, which were implicated in the treatment of certain ailments, has provided a scientific justification for the use of *Macrophyla longistyla* as an alternative remedy for the treatment of bacterial infections, hence acting as a potential source of drugs with broad-spectrum activity. Furthermore, the GCMS identified plants alkynes, and pyrimidin-2-amine suggested the possible anticancer and antihistamine potentials of the plant. These, however, need to be verified through further studies. In the meantime, -studies are also ongoing on the toxicity, pharmacological evaluation, and structural elucidation of the plant's active principles since this will enhance the plant materials' potency at lower concentrations.

References

Agyare C, Owusu-Ansah A, Ossei PPS, Apenteng JA and Boakye YD. 2014. Wound Healing and Anti-Infective Properties of *Myrianthus arboreus* and *Alchornea cordifolia*. *Medicinal Chemistry*, 4:533-539.

Al-Jadidi HSK, and Hossain AM. 2016. Determination of the total phenols, flavonoids, and antimicrobial activity of the crude extracts from locally grown neem stems. *Asian Pacific Journal of Tropical Disease*, 6: 376-379.

Amarowicza R, Peggb RB, Rahimi-Moghaddamc P, Barld B and Weilc JA. 2004. Free-radical scavenging capacity and antioxidant activity of selected plant species from the Canadian prairies. *Food Chem*, **84:** 551–562.

Andersson DI and Levin BR. 1999. The biological cost of antibiotic resistance, *Curr. Opin. Microb.* **2**:489–493.

Arbonnier M. 2000. Arbres, arbustes et lianes des zones sèches d'Afrique de l'Ouest. CIRAD, MNHN, UICN. 541 pp.

Atolani O, Adeyemi SO, Akpan E, Adeosun CB and Olatunji GA. 2011. Chemical Composition and Antioxidant Potentials of *Kigelia pinnata* Root Oil and Extracts *Excli Jour*, **10**: 264-273.

Bejina F, Bystricky M and Ingrin J. 2011. Experimental Deformation of Polyphase Aggregates at Pressures and Temperatures of the Upper Mantle. American Geophysical Union, Fall Meeting 2011, *abstract id*. MR11B-2173.

Belakhdar G, Benjouad A, Abdennebi EH.2015. Determination of some bioactive chemical constituents from *Thesium humile* Vahl. *J Mater Environ Sci*, **6:** 2778-83.

Bouyahya A, Abrini J, El-Baabou A, Bakri Y, and Dakka N.2016. Determination of phenol content and antibacterial activity of five medicinal plants ethanolic extracts from north-west of Morocco. J Plant Pathol Microbiol, **7:** 107-111.

Britto JS. 2001. Comparative Antibacterial Activity Study of *Solanum incanum* Lam. *Jour Swamy Bot Club*, **18**:81-82.

Burkill HM. 1995. The useful plants to West tropical Africa, Ed 2, vol.3, Royal Botanic Gardens. Kew. 274pp.

Cheesbrough M. 2004. Microscope. In: District Laboratory Practice in Tropical Countries. Part 1, Low price Egyptian edition 2013. The Anglo-Egyptian Bookshop & Cambridge University Press, pp: 110.

Davies J and Davies D. 2010. Origins and evolution of antibiotic resistance, *Microbiology, and Molecular. Biology Reviews*, **74**: 417–433.

Ebrahimzadeh MA, Pourmorad F and Hafezi S. 2008. Antioxidant activities of Iranian corn silk. *Turkish Journal of Biology*, **32**:43-49.

Elaiyaraja A, Chandramohan G, 2018. Comparative Phytochemical Profile of Crinum Defixum Ker-Gawler Leaves Using GC-MS, *Journal of Drug Delivery and Therapeutics*, 8(4): 365-380

Elufioye TO, Chinaka CG and Oyedeji AO. 2019. Antioxidant and Anticholinesterase Activities of *Macrosphyra Longistyla* (DC) Hiern Relevant in the Management of Alzheimer's Disease. *Antioxidants*, 8 (9), 400. doi:10.3390/antiox8090400

Govaerts B, Schum FT, Benith A and Hook F. 2003. Word checklist of selected Plant Families Database in Access. The Board of Trustees of the Royal Botanic Gardens Kew (http://powo.science.kew.org/taxon/urn:lsid:ipni.org:names:34870-1#source-FTEA), Accessed on the 5th of May, 2019.Harborne JB. 1998. *Phytochemical Methods A Guide to Modern Techniques of Plant Analysis*, London: Springer. 64 pp.

Jaiswal J and Sharma B. 2020. A Comparative Study of Antimicrobial and Pharmacological Properties of *Argemone mexicana*, *Solanum xanthocarpum* and *Thevetia peruviana. Acta Scientific Microbiology*, **3(3):**1-5. Doi: 10.31080/ ASMI. 2020.03.0524

Jorgensen, T., Montresor, A., and Savioli, L., 1996. Effectively controlling strongyloidiasis. *Parasitol. Today*, **12:**164.

Karou SD, Tchacando T, Ilboudo DP and Simpore J. 2011. Sub-Saharan Rubiaceae: A Review of Their Traditional Uses, Phytochemistry, and Biological Activities. *Pakistan Journal of Biological Sciences*, **14(3):** 149-169.

Karthikeyan A, Shanti V and Nagasathaya A. (2009). Preliminary phytochemical and antibacterial screening of crude extracts of the leaf of *Adhatoda vasica* L. *International Journal of Green Pharmacy*, (3):78-80.

Kudumela RG and Masoko P. 2018. In Vitro Assessment of Selected Medicinal Plants Used by the Bapedi Community in South Africa for Treatment of Bacterial Infections. *Journal of Evidence-based Integrative Medicine*, **23**:1-10

Kunitz M. 1947. *Journal of General Physiology*, **30**: 291.

Larrauri JA, Sanchez-Moreno C, Rupérez P and Saura-Calixto F. 1999. Free Radical Scavenging Capacity in the Aging of Selected Red Spanish Wines. *Journal of Agricultural and Food Chemistry*, **47(4):**1603-1606.

Lopez-Rubalava C and Estrada-Camarena E. 2016. Mexican medicinal plants with anxiolytic or antidepressant activity: focus on preclinical research. *J Ethnopharmacol*,186: 377-391.

Maffo T, Wafo P, Teoua Kamdem RS, Melong R, Uzor PF, Mkounga P, Ali, Z and Ngadjui, BT 2015. Terpenoids from the stem bark of *Neoboutonia macrocalyx* (Euphorbiaceae). *Phytochem Lett*, **12:** 328-331.

Mak, Y.W., Chuah, L.O., Ahmad, R., Bhat, R., 2013. Antioxidant and antibacterial activities of hibiscus (*H. rosa-sinensis* L.) and *Cassia* (*Senna bicapsularis* L.) flower extracts. *Journal of King Saud University- Science*, 25:275-282.

Maliyakkal N, Eom BH, Heo JH, Almoyad MAA, Parambi DGT, Gambacorta N, Nicolotti O, Beeran AA, Kim H, Mathew B. 2020. A New Potent and Selective Monoamine Oxidase-B Inhibitor with Extended Conjugation in a Chalcone Framework: 1-[4-(Morpholin-4-yl)phenyl] -5-phenylpenta-2,4- dien-1-one, ChemMedChem, 10.1002/cmdc.202000305, **0**, 0.

Ochei J and Kolhatkar A. 2004. Medical Laboratory Science; Theory and Practice. McGraw-Hill Publishing Company Limited, New Delhi.

Odeleye OF, Okunye OL, Kesi C and Abatan TO. 2016. Study of the Anticaries Activity of Three Common Chewing Sticks and Two Brands of Toothpaste in South West Nigeria" *British Journal of Pharmacological Research*, **11(5)**: 1-7. Article no. BJPR 26004.

Odugbemi T. (2008). (Ed) *A Textbook Medicinal Plant from Nigeria*. University of Lagos press. Lagos, Nigeria. 628 pp.

Odumosu TB, Olanike MB, Okeke CJ, Ogah JO and Michel FC. Jr 2017. Antimicrobial activities of the *Streptomyces coelicolor* strain AOB KF977550 isolated from a tropical estuary. *Journal of Taibah University for Science*, **11**: 836-841.

Ogah JO and Osundare FA. 2015. Evaluation of Antibacterial Activity and Preliminary Phytochemical Screening of *Moringa oleifera* on Pathogenic Bacteria. *International Journal of Pharmacology Research*, **5(11):** 310-315.

Pappas A. 2009. "Epidermal surface lipids". Dermato-endocrinology. **1(2):** 72–76. doi:10.4161/derm.1.2.7811. PMC 2835894. PMID 20224687.

Parekh J and Chanda S. 2007. Antibacterial and phytochemical studies on twelve species of Indian medicinal plants. *African Journal of Biomedical Research*, **10**: 175 – 181.

Routray W and Rayaguru K. 2018. 2-Acetyl-1-pyrroline: A key aroma component of aromatic rice and other food products, *Food Reviews International*, **34**:6, 539-565,

Sacan O. 2018. Antioxidant Activity, Total Phenol and Total Flavonoid Contents of *Trachystemon orientalis* (L.) G. Don. *European Journal of Biology*, 77(2): 70-75.

Saliha R, Syed T, Faizal A, Absar A, Shania A and Farzana M, 2014. The Role of Vitamin E in Human Health and Some Diseases. *Qaboos Univ Med J*. 14(2): e157–e165.

Sanchez-Moreno C, Larrauri JA and Saura-Calixto F. 1998. A procedure to measure the antiradical efficiency of polyphenols. *Journal of the Science of Food and Agriculture*, **76**: 270-276.

Sathya S Lakshmi, S., and Nakkeeran S. 2016. Combined effect of biopriming and polymer coating against chilli damping off. *International Journal of Agricultural Science and Research*,**6(3):** 45-54.

Saranraj P and Sivasakthi S. 2014. Medicinal plants and its antimicrobial properties: A review. *Global Journal of pharmacology*, **8(3):**316-327.

Sasidharan S, Chen Y, Saravanan D, Sundram KM and Yoga Latha L. 2011. Extraction, Isolation, and Characterization of Bioactive Compounds from Plants' Extracts. *African Journal Traditional, Complementary Alternative Medicine*, **8(1)**: 1–10.

Schubert A, Pereira DF, Zanin FF, Alves SH, Beck RCR and Athayde ML. 2007. Comparison of antioxidant activities and total polyphenolic and methylxanthine contents between the unripe fruit and leaves of *Ilex paraguariensis* A. St. Hil. *Pharmazie*, **62:** 876–880.

Singh R. and Sharma B. 2019.'Therapeutic Potential of Plant-Based Natural Compounds for Malaria-Recent Advances and Future Perspectives". *EC Pharmacology and Toxicology*, **7(10):**1078-1089.

Singh N, Jaiswal J, Tiwari P and Sharma B. 2020. Phytochemicals from *Citrus Limon* Juice as Potential Antibacterial Agents. *The Open Bioactive Compounds Journal*, **8:***1-6*.

Singleton, V.L. and Rossi, J.A.1965. Colorimetry of Total Phenolics with Phosphomolybdic-Phosphotungstic Acid Reagents. *American Journal of Enology and Viticulture*, **16**:144-158.

Tadesse S, Yu M, Mekonnen LB, Lam F, Islam S, Tomusange K, Rahaman MH, Noll B, Basnet SKC, Teo T, Albrecht H, Milne R and Wang S. **2017.** Highly Potent, Selective, and Orally Bioavailable 4-Thiazol-N-(pyridin-2-yl) pyrimidin-2-amine Cyclin-Dependent Kinases 4 and 6 Inhibitors as Anticancer Drug Candidates: Design, Synthesis, and Evaluation *Journal of Medicinal Chemistry*, **60 (5),** 1892-1915

Trease GE and Evans WC. 2002. *Pharmacognosy, Univ. Press, Aberdeen, Great Britain*. Pp 161-163.

Wang H, Khor TO, Shu L, Su Z, Fuentes F, Lee, J and Kong AT. 2012.*Plants Against Cancer: A Review on Natural Phytochemicals in Preventing and Treating Cancers and Their Druggability". *Anticancer Agents in Medicinal Chemistry*, 12 (10): 1281-1305.

Wágner G, Mocking T, Arimont M, Provensi G, Rani B, Silva-Marques B, and Leurs R. 2019. 4-(3-Aminoazetidin-1-yl) pyrimidin-2-amines as high-affinity non-imidazole histamine H3 receptor agonists within vivo central nervous system. *Journal of Medicinal Chemistry*, **62(23),** 10848-10866.

Yigit D. 2018. Antimicrobial and Antioxidant Evaluation of Fruit Extract from *Cornus mas* L. *Aksaray University Journal of Science and Engineering*, ***2*(1):** 41-51.

Zadra M, Piana M, Faccim de Brum T, Boligon AA, Borba de Freitas R, Machado MM, Stefanello ST, Soares FAA and Athayde ML. 2012. Antioxidant Activity and Phytochemical Composition of the Leaves of *Solanum guaraniticum* A. St.-Hil. *Molecules*, **17**: 12560-12574.

JJBS

Volume 14, Number 3, September 2021
ISSN 1995-6673
Pages 463 - 469

Jordan Journal of Biological Sciences

Vernonia amygdalina Leaf Extract Abates Oxidative Hepatic Damage and Inflammation Associated with Nitrobenzene in Rats

Johnson O. Oladele[1,*], Oyedotun M. Oyeleke[1], Blessing O. Akindolie[1], Boyede D. Olowookere [1], and Oluwaseun T. Oladele [2]

[1]*Department of Chemical Sciences, Faculty of Science, Kings University, Ode-Omu, Osun State, Nigeria;*[2]*Phytomedicine and Toxicology Laboratories, Department of Biochemistry, Faculty of Basic and Applied Sciences, Osun State University, Osogbo, Nigeria.*

Received: March 30, 2020; Revised: September 16, 2020; Accepted: September 17, 2020

Abstract

Liver diseases have been documented to have great influence on the global burden of mortality and morbidity. This study was conducted to investigate the ability of *Vernonia amygdalina* to protect against hepatic damage and inflammation in nitrobenzene rat model of hepatotoxicity. Thirty male Wistar strain albino rats were used for this study. Rats were exposed to 100 mg/kg body weight (BW) of nitrobenzene via oral administration and treated with 200 and 400 mg/kg BW of methanol leaf extract of *Vernonia amygdalina* (MLVA) and 400 mg/kg BW of Vitamin E for 14 consecutive days. Nitrobenzene significantly ($P<0.05$) induced hepatic damage with marked serum level of aspartate aminotransferase (AST), alanine aminotransferase (ALT), acid phosphatase (ACP) and alkaline phosphatase (ALP). Furthermore, nitrobenzene mediated oxidative stress and lipid peroxidation with a significant increase in hepatic level of malondialdehyde (MDA), hydrogen peroxide (H_2O_2), with concomitant decrease in level of reduced glutathione (GSH), Catalase (CAT) and Superoxide dismutase (SOD). Similarly, inflammation was observed in nitrobenzene-treated rats with elevated level of nitric oxide (NO) and myeloperoxidase (MPO). However, treatment with the chosen doses of MLVA and Vitamin E significantly reversed all the nitrobenzene-associated hepatic damage, oxidative stress, lipid peroxidation, inflammation and altered antioxidant defence system. Taken together, MLVA exhibited hepatoprotection which may be beneficial for the treatment and management of liver diseases or other related disorders via protecting the structural integrity of the liver, antioxidant, anti-inflammatory mechanisms.

Keywords: Hepatotoxicity, oxidative stress, Inflammation, Nitrobenzene, *Vernonia amydalina*

1. Introduction

Liver diseases have been reported to have huge impact on the global burden of mortality and morbidity (Lozano *et al.*, 2010; Murray *et al.*, 2010). In 2010, Global Burden of Disease (GDB) documented that liver cirrhosis caused more than one million deaths (1,030,800 deaths representing 2.0% of all deaths, 1.4% of all deaths of women and 2.4% of all deaths of men) and 31,027,000 Disability Adjusted Life Years (DALYs) (1.2% of all DALYs, 0.8% of all DALYs for women, 1.6% of all DALYs for men). Systematic analysis of Mokdad *et al.*, (2014) also documented that about 2 million deaths annually are caused by liver diseases. In the study, hepatocellular carcinoma and viral hepatitis caused about 1 million deaths while complications of cirrhosis were responsible for about 1 million deaths globally. The Middle East, Caribbean, Latin America and North Africa are the regions that showed the highest percentage of deaths due to liver related diseases (Briggs, 2003).

Among other factors, exposure to toxic chemicals from industrial and occupational sources has been implicated to play a pivotal role in the aetiology and pathogenesis of liver diseases (Briggs, 2003). Hepatotoxins are toxic foreign compounds capable of damaging the liver structural and physiological functions leading to severe adverse effects on the liver. Nitrobenzene is an example of such hepatotoxicants; it is an important chemical material widely applied in national defence and the industries of printing and dyeing, plastics, pesticide and pharmaceutical. Nitrobenzene is considered a dangerous air pollutant and has proven to be an animal carcinogen. According to the 1986 Cancer guide lines, nitrobenzene has been classified as a group B2 chemical, i.e. a likely human carcinogen (Cattley *et al.*, 1994). Intermediates such as nitrosobenzene and phenylhydroxylamine (PH) are produced during metabolism of nitrobenzene. These intermediates have been documented to play a pivotal role in the process of nitrobenzene carcinogenesis (Howard *et al.*, 1983). Following accidental nitrobenzene poisoning in humans, the highest concentration was found in the liver, brain, blood and stomach (International Programme on Chemical Safety, 2003). Akinloye *et al* (2014) have documented the hepatotoxicity effects of nitrobenzene.

Phytochemicals are naturally occurring compounds regarded as one of the important origins of biologically active natural products (Koksal *et al.*, 2009). The reported biological and pharmacological activities such as anticarcinogenic, anti-inflammatory, and antioxidant, and

* Corresponding author e-mail: oladelejohn2007@gmail.com, jo.oladele@kingsuniversity.edu.ng.

antimutagenic activities of these isolated active compounds from plants have awaken research interest towards development of more potent drugs to combat various diseases (Wu *et al.,* 2008; Yang *et al.,* 2006). The bioactive compounds that have been recorded to be present in a number of plants may produce medicinal effects for in treatment of reproductive related disorders.

Vernonia amygdalina, commonly known as bitter leaf, is a medicinal plant with several health benefits. The documented phytochemical constituents of various fractions of *Vernonia amygdalina* includes epivernodalol, sesquiterpene lactones, elemanolide (Erasto *et al.,* 2006), edotides (Izeybigie, 2003), terpenes, steroids, coumarins, flavonoids, phenolic acids, lignans, xanthones and anthraquinone (Cimanga *et al.,* 2004), saponins and alkaloids (Muraina *et al.,* 2010). These phytochemical constituents have been reported to be responsible for a number of medicinal valves of the plant such as antimicrobial activities (Iwu *et al.,* 1999), antioxidant properties (Adesanoye and Farombi, 2010), and anti-inflammatory (Ibrahim *et al.,* 2010). The anti-malarial activity of *Vernonia amygdalina* essentially against *P. falciparum* was reported to be due to the presence of sesquiterpenes lactones compounds which include *vernolide, vernodalin, hydroxy vernolides* and the steroid related constituents, *vernoniosid* B1 and *vernonoid* B1 (Magboul *et al.,* 2008).

Therefore, the aim of this study is to investigate the cytotoxic effects of nitrobenzene in the liver of Wistar albino rats via evaluation of liver function tests, oxidative hepatic damage markers histopathological indices and cytoarchitecture of the hepatic cells. Moreover, to investigate the protective effect of methanol leaf extract of *Vernonia amygdalina* against the nitrobenzene-induced hepatic damage. Vitamin E, a standard clinical medicine, is used to compare the protective activities of the extract.

2. Materials and methods

2.1. Chemicals/ Reagents

High purity (> 99.7%) Nitrobenzene was obtained from BDH chemical Poole England. Vitamin E (Alpha Tocopherol) is a product of Embassy pharmaceuticals, Nigeria. Aspartate aminotransferase (AST), alanine aminotransferase (ALT), acid phosphatase (ACP) and alkaline phosphatase (ALP) enzyme diagnostic kits were obtained from Randox. Potassium iodide, Copper sulphate, hydrogen peroxide, KCl, phosphate buffer salts: Na_2HPO_4 $12H_2O$ and 1.19g NaH_2PO_4 $2H_2O$ are of analytical grade and were obtained from Analar BDH Limited, Poole, England. Bovine Serum Albumin (standard), 5′, 5′ – dithiobis - (2-nitrobenzoic acid) (Ellman's reagent), epinephrine, reduced glutathione, 2 – nitro-5-thiobenzoic acid are products of Sigma-Aldrich Co. St Louis, Missouri, USA.

2.2. Collection of Plant Material and Preparation of Extract

Fresh leaves of *Vernonia amygdalina* were collected at the staff quarters in Kings University, Odeomu, Osun State. The leaf has been identified at IFE-Herbarium of Botany Department, Obafemi Awolowo University, Ile-Ife with voucher number. The *Vernonia amygdalina* leaves were washed and air-dried at room temperature in the Biochemistry laboratory, Kings University, Nigeria and pulverized using an electric blender. The powdered leaf was defatted in n-hexane using Soxhlet apparatus. Thereafter, methanolic extract was prepared by soaking the defatted leaf in 90% methanol for 72 hours. The resulting mixture was then filtered, and the filtrate was concentrated on water bath. The concentrated extract was lyophilized using Bosch freeze drying machine. The full chemical identification and bioactive compounds of *Vernonia amygdalina* have been earlier reported by Oladunmoye *et al* (2019) using gas chromatography-mass spectrometry (GC-MS). The technique reveals methyl-2-O-benzyl-d-arabinofuranoside, phytol, hexadecanoic acid, ethyl ester, squalene and 9, 12, 15, octadecatrienoic acid as the more abundant compounds (>85% abundance) while N-[2-(dimethylamino)-5-pyrimidinyl] benzene sulfonamide, 9, 12, 15 and octadecatrien-1-ol, p-Menth-4(8)-en-9-ol has the less abundance (<12% abundance) compounds.

2.3. Experimental animals

Thirty matured 4-5 months old male Wistar strain albino rats were used in the study. The rats were sourced and raised at the Biochemistry breeding colony of the Biochemistry unit, Department of Chemical Sciences, Kings University, Ode-Omu, Osun state, Nigeria. Animals were kept under ambient standard conditions (25 ± 2 ^oC and relative humidity of 50 ± 15 %) in stainless steel cages, and metabolic wastes were cleaned twice daily. The rats were allowed to acclimatize to these conditions for fourteen days and were exposed to 12 hrs daylight and darkness cycle, fed with commercially available rat pellet and water *ad libitum.* The experiment was carried out in accordance with current rules and guidelines that have been established for the care of the laboratory animals (NRC, 2011). The rats were randomised into five groups containing six rats each.

Group A: received distilled water daily and serve as the Control.

Group B: received 100 mg/kg Nitrobenzene orally.

Group C: received 100 mg/kg Nitrobenzene and 200 mg/kg *Vernonia amygdalina*

Group D: received 100 mg/kg Nitrobenzene and 400 mg/kg *Vernonia amygdalina*

Group E: Received 100 mg/kg Nitrobenzene and 400 mg/kg Vitamin E

Treatments were administered to the rats orally for 14 consecutive days.

2.4. Preparation of Serum

The rats were sacrificed 24hrs after the last treatment and blood sample collected into clean, dry centrifuge tube. The blood was left for 10 min at room temperature to clot after which it was centrifuged at 4,000 rpm for 20 min in an MSC (Essex, UK) bench centrifuge. The clear supernatant (serum) was aspirated using a Pasteur pipette into clean, dry sample bottles and then stored at 4 °C for biochemical analyses.

2.5. Preparation of liver homogenates

The livers were immediately excised and blotted to remove blood stains. They were cleansed and rinsed in 1.15% KCl on ice to remove haemoglobin, then weighed. They were then chopped into bits and homogenized in four volumes of the homogenizing buffer (10 mM potassium phosphate buffer, pH 7.4) using a Teflon homogenizer.

The homogenates were centrifuged at 12,500 g for 15 minutes in a cold centrifuge (4 ℃) to obtain the post mitochondrial fractions which were collected and used for biochemical analyses.

2.6. Measurement of biochemical markers

AST, ALT, ACP and ALP were measured by following the enzymes kits manufacturer's instructions (Randox). The protein content of the homogenates was determined using BSA as a standard in the protocol described by Lowry *et al.* (1951). Nitric oxide (NO) level was assessed by procedure reported by Green *et al.* (1982). Myeloperoxidase (MPO) activity in the homogenate was quantified following the method of Granell *et al.* (2003). Superoxide dismutase (SOD) activity was evaluated following the inhibition of adrenaline auto-oxidation in a basic milieu as described by Misra and Fridovich, (1972). Lipid peroxidation was evaluated by monitoring the level of MDA using procedure reported by Varshney and Kale (1990). The reduced GSH content in the brain samples was determined using the protocol reported by Buetler *et al.* (1963). Catalase (CAT) activity was determined following the protocol documented by Clairborne (1995) using hydrogen peroxide (H_2O_2) as a substrate. Hydrogen peroxide generation was assayed oxidation of ferrous ions and sorbitol colour amplification system using the method of Wolff (1994).

2.7. Histological Examination

The livers were immediately fixed in 10% formalin and embedded in paraffin wax. Fine sections (7–9 mm thickness) of the livers were then dewaxed in xylene, hydrated in decreasing percentage of alcohol and stained with hematoxylin and eosin. The stained sections were observed under a Leitz microscope and their photomicrograph taken at X 100 with a Canon (Meville, NY) Power Shot G2 Digital Camera (Oladele *et al.*, 2017).

2.8. Statistical Analysis

Results obtained were expressed as mean ± standard deviation (mean ± SD) and analysed using one-way analysis of variance (ANOVA) with the aid of SPSS 22.0 computer software package (SPSS Inc; Chicago, U.S.A) to compare the experimental groups followed by Bonferroni's post-hoc test. Valves at $P<0.05$ were considered significant.

3. Results

3.1. MLVA enhances hepatic enzymes activities in nitrobenzene-induced hepatotoxicity in rats

Figures 1 and 2 show that rats exposed to 100 mg/kg body weight of nitrobenzene (group B) showed a significant increase ($P<0.05$) serum concentration levels of ALT, AST, ACP and ALP as compared to the control (group A). This suggests injury to the liver membrane and alteration to liver physiological activities. These altered valves were reverted significantly ($P<0.05$) toward normal in a dose dependent manner in rats treated with 200 and 400mg/kg body weight of MLVA or vitamin E (group C, D & E respectively).

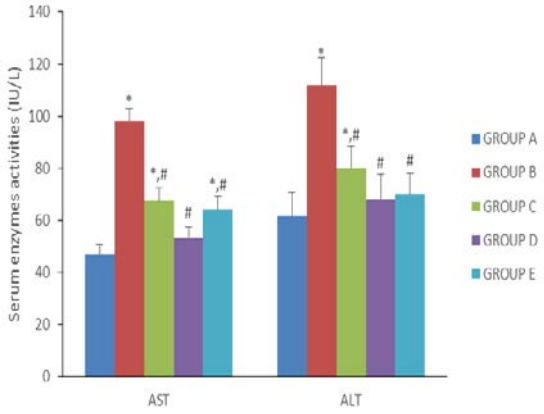

Figure 1: Effect of MLVA on aspartate aminotransferase (AST) and alanine aminotransferase (ALT) activities in rats treated with nitrobenzene.

Data are given as mean ± SD of rats per group. n=6. MLVA: methanol leaf extract of *Vernonia amygdalina*, *: Values differ significantly from group A (control) ($P < 0.05$). #: Values differ significantly from group B.

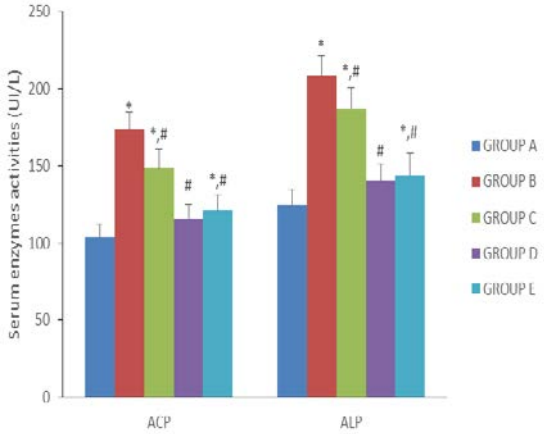

Figure 2: Effect of MLVA on acid phosphatase (ACP) and alkaline phosphatase (ALP) activities in rats treated with nitrobenzene.

Data are given as mean ± SD of rats per group. n=6. MLVA: methanol leaf extract of *Vernonia amygdalina*, *: Values differ significantly from group A (control) ($P < 0.05$). #: Values differ significantly from group B.

3.2. MLVA inhibits inflammatory activity in liver of rats treated with nitrobenzene

The effects of MLVA on inflammation in liver of the experimental rats was evaluated by measuring MPO activities and NO concentration level. Rats administered nitrobenzene alone demonstrated a marked increase in NO level and MPO activities when compared with the control (Figure 3 and 4). However, treatment with of 200 and 400 mg/kg of MLVA or Vitamin E significantly attenuated both NO and MPO levels in the liver when compared with control.

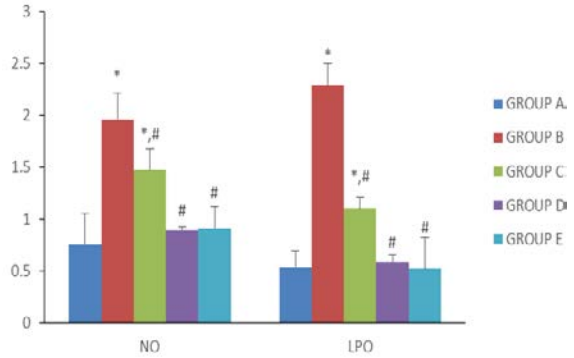

Figure 3: Effect of MLVA on nitric oxide (NO) and Lipid peroxidation (LPO) level in rats treated with nitrobenzene.

Lipid peroxidation (µmol MDA/mg protein); NO level (Unit/mg protein). Data are given as mean ± SD of rats per group. n=6. MLVA: methanol leaf extract of *Vernonia amygdalina*, *: Values differ significantly from group A (control) ($P < 0.05$). #: Values differ significantly from group B.

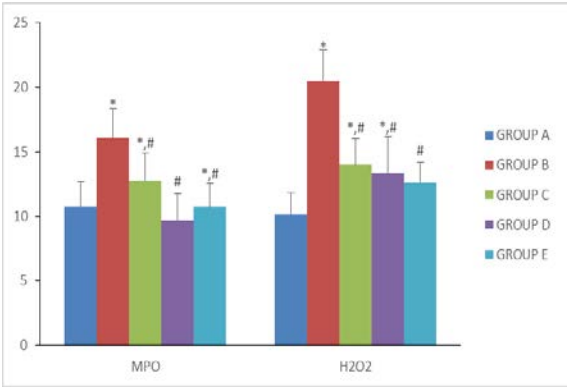

Figure 4: Effect of MLVA on myeloperoxidase (MPO) and hydrogen peroxide generation (H_2O_2) levels in rats treated with nitrobenzene.

MPO activity (Units/mg protein); H_2O_2 (µmole/mg protein). Data are given as mean ± SD of rats per group. n=6. MLVA: methanol leaf extract of *Vernonia amygdalina*, *: Values differ significantly from group A (control) ($P < 0.05$). #: Values differ significantly from group B.

3.3. MLVA suppressed lipid peroxidation and oxidative stress in liver of rats treated with nitrobenzene

Fig. 3 and 4 showed the results of hepatic oxidative stress biomarkers carried out in the experimental rats. There was a marked increase in MDA level (an index of lipid peroxidation) and H_2O_2 generation in rats administered nitrobenzene only when compared with the control group. Upon treatment with 200 and 400 mg/kg of MLVA or Vitamin E, there was a significant decrease ($p < 0.05$) in both MDA and H_2O_2 generation levels in the livers.

3.4. MLVA influenced reduced glutathione level and antioxidant enzymes activities in liver of rats treated with nitrobenzene

Fig. 5-7 show the glutathione level and antioxidant activities of CAT and SOD in the liver of experimental rats. Administration of rat with nitrobenzene alone showed a significant decrease ($p < 0.05$) in GSH level and decline in activities of CAT and SOD when compared with the control. However, treatment with 200 and 400 mg/kg of MLVA or Vitamin E significantly increased the GSH level and enhanced all the enzymes.

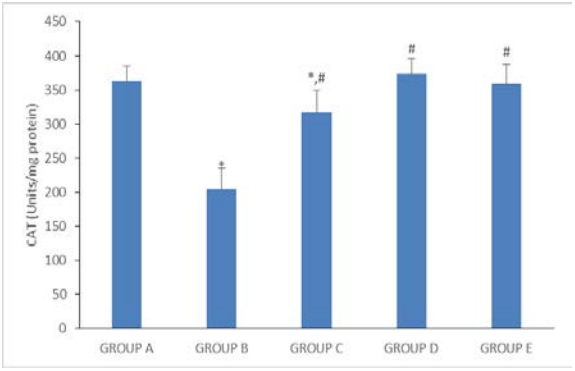

Figure 5: Effect of MLVA on catalase (CAT) activities in rats treated with nitrobenzene.

MPO activity (Units/mg protein); H_2O_2 (µmole/mg protein). Data are given as mean ± SD of rats per group. n=6. MLVA: methanol leaf extract of *Vernonia amygdalina*, *: Values differ significantly from group A (control) ($P < 0.05$). #: Values differ significantly from group B.

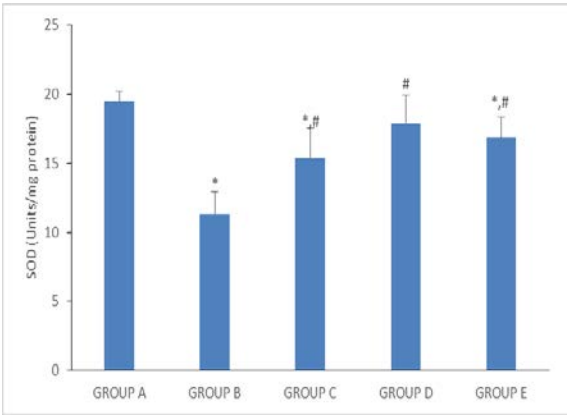

Figure 6: Effect of MLVA on superoxide dismutase (SOD) activities in rats treated with nitrobenzene.

MPO activity (Units/mg protein); H_2O_2 (µmole/mg protein). Data are given as mean ± SD of rats per group. n=6. MLVA: methanol leaf extract of *Vernonia amygdalina*, *: Values differ significantly from group A (control) ($P < 0.05$). #: Values differ significantly from group B.

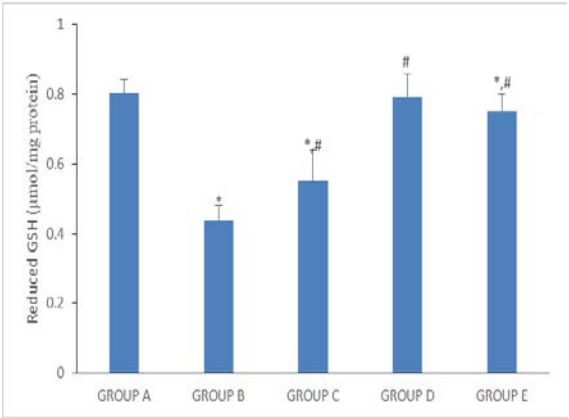

Figure 7: Effect of MLVA on reduced glutathione (GSH) content in rats treated with nitrobenzene.

Data are given as mean ± SD of rats per group. n=6. MLVA: methanol leaf extract of *Vernonia amygdalina*, *: Values differ significantly from group A (control) ($P < 0.05$). #: Values differ significantly from group B.

3.5. Ameliorative effects of MLVA on histological alterations in liver sections of nitrobenzene-induced hepatotoxicity in rats

Fig. 8 shows the histological alterations seen with the light microscope in the liver sections of the experimental rats. The cytoarchitecture and morphology of liver of rats from control group appeared normal. However, obvious pathological lesions were observed in the liver sections of nitrobenzene group characterized by a mild loss of liver parenchyma, some mild derangement in the cellular profiles, haemorrhage and presence of inflammatory red cells within and around the central vein including the sinusoids as well as distorted hepatic vessels (red arrows). A, C and E group showed no altered panoramic morphological presentation accompanied by well outlined cellular profile as well as distinct hepatic structures.

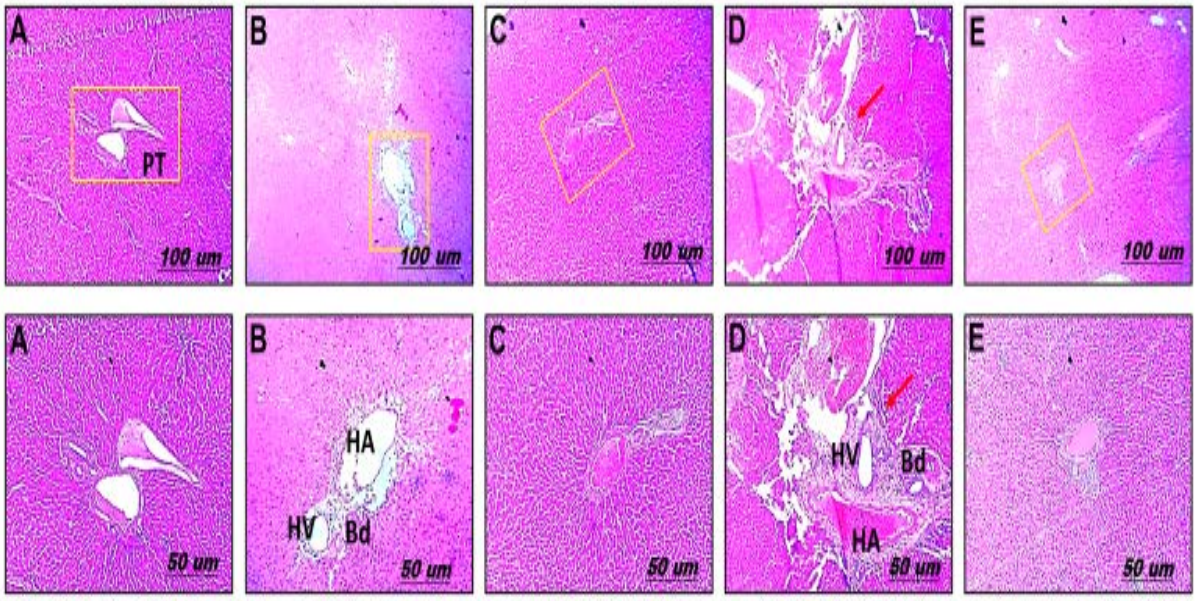

Figure 8: Photomicrographs of the panoramic views of liver general micromorphological presentations in Adult Wistar rats across the study groups. Hematoxylin and Eosin stain. The hepatic duct, Portal triad (PT) composed of the hepatic vein (HV) and artery (HA) as well as the bile duct (BD), the well distributed hepatocytes across the general cytoarchitecture are demonstrated across study groups A-E.

4. Discussions

Nitrobenzene is an industrial chemical widely used in the synthesis of aniline and other products such as dyes, analgesics, pesticides, pyroxylin compounds and shoes polishes. However, it has been reported to induce tumour in vital organs (including liver) in experimental animals (Cattley *et al.*, 1994), thus classified as a group B2 toxicants which is likely to be human carcinogen (US EPA, 1996). *Vernonia amygdalina* is a medicinal plant with potential chemo-preventive activities. This study is designed to investigate the protective ability of methanol leaf extract of *Vernonia amygdalina* against nitrobenzene-induced toxicities. The efficacy of the extract is compared with vitamin E.

In this study, we demonstrated that exposure of rats to nitrobenzene resulted in a marked increase in the serum levels of ALT, ACP, AST and ALP which is indicative of hepatocellular damage, as previously documented (Oladele and Oyewole, 2017; Oladele *et al.*, 2017; Oyewole *et al.*, 2017). The significant increase in the hepatic markers in the serum of the experimental rats could be as a result of release of these compartmentalized enzymes into the blood circulatory system due to rupture of the membrane and cellular damage caused by nitrobenzene (Oladele *et al.*, 2020a; Essawy *et al.*, 2019). Treatment with graded doses of methanol leaf extract of *Vernonia amygdalina* or Vitamin E significantly reversed the elevated activities of these enzymes. This effect might be due to the extract's ability to mitigate free radical mediated oxidative damage in the hepatocytes (Alamoudi, 2019). Also, Vitamin E has been reported to have antioxidant and cyto-protective activities (Oladele *et al.*, 2020c).

Biotransformation of nitrobenzene has been reported to generate free radicals and reactive oxygen species which, in turn, alters the antioxidant system and finally results into oxidative stress and macromolecule damage (Akinloye *et al.*, 2014). In this study, exposure of rats to nitrobenzene caused a marked increase in the level of hepatic hydrogen peroxide (H_2O_2). H_2O_2 can be rapidly decomposed into oxygen and water, and this may produce hydroxyl radicals ($^{\bullet}OH$) that can initiate lipid peroxidation and cause DNA damage (Sahreen *et al.*, 2011). However, treatment with graded doses of methanol leaf extract of *Vernonia amygdalina* or Vitamin E significantly mitigated the hydrogen peroxide generation in the liver. This can be attributed to the antioxidant and free radical scavenging effects of the extract.

Lipid peroxidation has been reported to play a critical role in cancer development (carcinogenesis) (Banakar *et al.*, 2004). The process produces some byproducts which are highly toxic to the cells. These toxic byproducts include malondialdehyde (MDA) and 4-hydroxynonenal. They can easily attack cellular targets such as proteins and DNA leading to genetic mutations and ultimately to carcinogenicity (de Zwart *et al.*, 1999). In this study, administration of nitrobenzene into rats caused a significant increase in lipid peroxidation as indicated by marked level of malondialdehyde (MDA) in the liver. However, groups treated with graded doses of methanol leaf extract of *Vernonia amygdalina* or Vitamin E showed

a significant reduction in level of malondialdehyde when compared to the animals treated with nitrobenzene only. The observed decrease in lipid peroxidation in rats treated with methanol leaf extract of *Vernonia amygdalina* could be due to its ability to scavenge the hydroxyl and peroxyl radicals.

Similarly, nitrobenzene induced inflammation in the liver of the experimental rats with evidence of marked increase in the level of nitric oxide (NO) and myeloperoxidase (MPO) activity. This observation indicates involvement of aggravated inflammatory response in nitrobenzene-induced hepatotoxicity. NO is a toxic defense molecule synthesized by inducible nitric oxide synthase (iNOS) in many cell types involved in immunity and inflammation. Treatment the various doses of methanol leaf extract of *Vernonia amygdalina* or Vitamin E significantly inhibited the inflammatory process in the hepatic cells. This agrees with the previous report that the extract has anti-inflammatory properties.

One of the primary functions of antioxidant and free radical scavenging enzymes such as CAT, and SOD is to protect biological cells against free radical attacks and oxidative stress. This study revealed that administration of nitrobenzene to rats caused a significant decrease in these enzymes activities. The observed reduction in these enzymes activities may have been a result of overwhelming detoxification activities of the enzymes by conjugating with the free radicals/ROS and other toxic by-products to enhance their excretion. However, there was a marked increase in CAT, and SOD in rats treated with graded doses of methanol leaf extract of *Vernonia amygdalina* or Vitamin E. Many scientific reports have proven that one of the protective mechanism of actions of plant extracts is via upregulation of these endogenous antioxidant enzymes (Farombi *et al.,* 2019, Oladele *et al.,* 2020b).

Similarly, a depletion in the GSH level was observed in the nitrobenzene treated rats. This significant decrease in GSH level might have been due to GSH usage by the detoxifying enzyme (GST) and may be responsible for increase in lipid peroxidation (Bansal *et al.,* 2005; Mohamed *et al.,* 2018). Free radical mediated tissue damage can be inhibited or alleviated by ensuring the redox balance to decrease the oxidative stress status. On the other hand, rats treated with *Vernonia amygdalina* or Vitamin E display a marked increase in GSH level. This agrees with previous report of Oladele *et al* (2020c) who documented that *Vernonia amygdalina* caused a reversal to decreased GSH level induced by nitrobenzene. This suggests that the protective effect of *Vernonia amygdalina* extract involves the maintenance of antioxidant capacity in preventing the hepatic cells against oxidative damage.

5. Conclusion

This study demonstrated that nitrobenzene induced liver injury which was followed by significant increase in serum activities level of ALT, AST, ACP. Also, inflammation was observed in the liver with increased level of NO and MPO with concomitant increased level of MDA confirming lipid peroxidation. Furthermore, there is a significant decreased in reduced GSH level, CAT and SOD activities indicating oxidative stress in the liver tissue. However, treatment with graded doses of methanol leaf extract of *Vernonia amygdalina* reversed all the nitrobenzene-associated hepatic damage, oxidative stress, lipid peroxidation, inflammation and altered antioxidant defence system. Similarly, histological observations showed that the extract was capable of not only preventing but actually reversing the patho-morphological changes of nitrobenzene-induced liver injury such as changes in fat deposition, mild loss of liver parenchyma, haemorrhage and inflammatory cell infiltration. Taken together, methanol leaf extract of *Vernonia amydalina* exhibited hepatoprotection which may be beneficial for the treatment and management of liver diseases or other related disorders via protecting the structural integrity of the liver, antioxidant, anti-inflammatory mechanisms.

References

Adesanoye OA, and Farombi EO. 2010. Hepatoprotective effects of *V. amygdalina* (*Astereaceae*) in rats treated with carbon tetrachloride. *Exp. Toxicol. Pathol.*, **62**: 197-206.

Akinloye OA, Somade OT, Akindele AS, Adelabu KB, Elijah FH, and Adewumi OJ. 2014. Anticlastogenic and hepatoprotective Properties of ginger (*zingiber officinale*) Extract against nitrobenzene-induced Toxicity in rats. *Rom. J. Biochem.*, **51:** *3–15*

Alamoudi WM. 2019. An Evaluation of the Antioxidant Properties of Propolis against Fenvalerate-induced Hepatotoxicity in Wistar Rats. *Jordan Journal of Biological Sciences.* 12: 581 – 588

Banakar MC, Paramasivan SK, Chattopadhyay MB. 2004. 1alpha, 25-dihydroxyvitamin D3 prevents DNA damage and restores antioxidant enzymes in rat hepatocarcinogenesis induced by diethylnitrosamine and promoted by phenobarbital. *World J Gastroenterol.* **10**: 1268-75.

Bansal AK, Bansal M, Soni G. 2005. Protective role of Vitamin E pre-treatment on N-nitrosodiethylamine induced oxidative stress in rat liver. *Chem Biol Interact.* **156**: 101-11.

Briggs D. 2003. Environmental pollution and the global burden of disease. *British Med. Bulletin*. **68**:1-24

Buetler E, Duron O and Kelly BM. 1963. Improved method for the determination of blood glutathione. *Journal of Laboratory and Clinical Medicine,* **61**: 882–888.

Cattley RC, Everitt JI, and Gross EA. 1994. Carcinogenicity and toxicity of inhaled nitrobenzene in B6C3F1mice and F344 and CD rats. *Toxicol. Sci.*, **22**: 328–340.

Cimanga RK, Tona L, Mesia K, Musuamba CT, De Bruyne T, Apers S, Hernan N, Miert VS, Pieters L, Totte J, and Vlietink, AJ. 2004. *In vitro* antiplasmodia acivity of extravts and fractions of seven medicinal plants used in the democratic republic of Congo. *J. Ethnopharmacol.* **93**: 27–32.

Clairborne A. 1995. Catalase activity. Handbook of Methods for Oxygen Radical Research. CRC Press, Florida.

de Zwart LL, Meerman JH, Commandeur JN, et al. 1999. Biomarkers of free radical damage applications in experimental animals and in humans. *Free Radic Biol Med* **26**: 202-26.

Erasto P, Grierson DS, Afolayan AJ. 2006. Bioactive sesquiterpenes lactones from the leaves of *V. amygdalina. J. Ethnopharmacol.*, **106**: 117-120.

Essawy AE, Lamfon HA, Al Harbi AB, Ali AM and Lamfon NA. 2019. The Effect of Salvia officinalis Extract on Alleviating Oxidative Stress and Hepatic Dysfunction Induced by Carbon Tetrachloride in Mice. *Jordan Journal of Biological Sciences.* **12**: 403 – 408

Farombi EO, Awogbindin IO, Farombi TH, Oladele JO, Izomoh ER, Aladelokun OB, Ezekiel IO, Adebambo OI, and Abah VO. 2019. Neuroprotective role of kolaviron in striatal redo-inflammation associated with rotenone model of Parkinson's disease. *Neurotoxicology*. **73**:132–141.

Granell S, Gironella M, Bulbena O, Panes J, Mauri M, Sabater L, Aparisi L, Gelpi E, and Closa D. 2003. Heparin mobilizes xanthine oxidase and induces lung inflammation in acute pancreatitis. *Crit. Care Med.,* **31**: 525–530.

Green LC, Wagner DA, Glogowski J, Skipper PL, Wishnok JS, and Tannenbaum SR. 1982. Analysis of nitrate, nitrite, and [15N] nitrate in biological fluids. *Anal. Biochem.*, **126**: 131–138.

Howard PC, Beland FA, and Cerniglia CE. 1983. Reduction of the carcinogen 1-nitropyrene to1-aminopyrene by the rat intestinal bacteria. *Carcinogenesis,* **4**: 985–990.

Ibrahim G, Abdurahman EM, Ibrahim H, and Ibrahim NO. 2010. Comparative cytomormological studies on the studies of V. *amygdalina* Del. and V. Kotschyama. *Nig. J. Botany,* **23** (1): 133-142.

International Programme on Chemical Safety (IPCS). Nitrobenzene environmental health criteria 230. Geneva: WHO; 2003

Iwu MW, Duncan AR, and Okunji CO. 1999. New Antimicrobials of Plant Origin. In Perspectives on New Crops and New Uses. J. Janick (Ed). ASHS Press, Alexandria, VA.

Izeybigie EB. 2003. Discovery of water soluble anticancer agent (Edotides) from a vegetable found in Benin City, *Nigeria. Exper. Bio. Med.*, **228**: 293-299.

Koksal E, Gulcin I, Beyza S, Sarikaya O, Bursal E. 2009. In vitro antioxidant activity of silymarin. *Journal of Enzyme Inhibition and Medicinal Chemistry* **24**(2): 395–404.

Lowry OH, Rosenbrough NJ, Farr AL, and Randall RJ. 1951. Protein measurement with the Folin phenol reagent. *Journal of Biological Chemistry* **193**: 265–275.

Lozano R, Naghavi M, Foreman K, Lim S, Shibuya K, Aboyans V. 2012. Global and regional mortality from 235 causes of death for 20 age groups in 1990 and 2010: a systematic analysis for the Global Burden of Disease Study 2010. *Lancet,* **380**: 2095–2128.

Magboul AZI, Bashir AK, Khalid SA, Farouk A. 1997. Anti-microbial activity of vernolein and vernodalin. *Fitoterapia* **68**: 83-84.

Misra HP, and Fridovich I. 1972. The role of superoxide anion in the autoxidation of epinephrine and a simple assay for superoxide dismutase. *J. Biol. Chem.* **247**: 3170–3175.

Mohamed NA, Shehata MI, El-Sawaf AL., Hussein KH, and Michel TN. 2018. The Ameliorating Effect of Erythropoietin on Diabetic Neurodegeneration by Modulating the Antioxidant-Oxidant Imbalance and Apoptosis in Diabetic Male Rats. *Jordan Journal of Biological Sciences*. **11**: 339 – 345

Mokdad AA, Lopez AD, Shahraz S, Lozano R, Mokdad AH, Stanaway J, et al. 2014. Liver cirrhosis mortality in 187 countries between 1980 and 2010: a systematic analysis. *BMC Med.* **12**: 145.

Muraina IA, Adaudi AO, Mamman M, Kazeem HM, Picard J, McGaw LJ, and Eloff JN. 2010. Antimycoplasmal activity of some plant species from northern Nigeria compared to the currently used therapeutic agent. *Pharm. Biol.* **48**: 1103-1107.

Murray CJL, Vos T, Lozano R, Naghavi M, Flaxman AD, Michaud C, et al. 2012. Disability-adjusted life years (DALYs) for 291 diseases and injuries in 21 regions, 1990–2010: a systematic analysis for the Global Burden of Disease Study 2010. *Lancet.* **380**: 2197–2223.

National Research Council (NRC), 2011. Guide for the care and use of laboratory animals 8th Edition. The National Academies Press.

Oladele JO, Oladele OT, Ademiluyi AO *et al*. 2020a. Chaya (*Jatropha tanjorensis*) leafs protect against sodium benzoate mediated renal dysfunction and hepatic damage in rats. *Clin Phytosci*, **6**: 13.

Oladele JO, Oyeleke OM, Awosanya OO, Oladele TO. 2020b. Effect of *Curcuma longa* (Turmeric) Against Potassium Bromate-induced Cardiac Oxidative Damage, Hematological and Lipid Profile Alterations in Rats. *Singapore Journal of Scientific Research, **10**: 8-15*.

Oladele JO, Oyeleke OM, Oladele OT. *et al*. 2020c. Nitrobenzene-induced hormonal disruption, alteration of steroidogenic pathway, and oxidative damage in rat: protective effects of *Vernonia amygdalina*. *Clin Phytosci,* **6**: 15.

Oladele JO, Oyewole OI, Bello OK, Oladele OT. 2017. Hepatoprotective Effect of Aqueous Extract of *Telfairia occidentalis* on Cadmium Chloride-Induced Oxidative Stress and Hepatotoxicity in Rats. *Journal of Drug Design and Medicinal Chemistry*. **3**(3): 32-36.

Oladunmoye MK, Afolami OI, Oladejo BO, Amoo IA, Osho BI. 2019. Identification and Quantification of Bioactive Compounds Present in the Plant *Vernonia amygdalina* Delile using GC-MS Technique. *Nat Prod Chem Res* **7**: 356.

Oyewole OI, and Oladele JO. 2017. Changes in Activities of Tissues Enzymes in Rats Administered *Ficus exasperata* Leaf extract. *Int. J. Biol. Chem. Sci.* **11**(1): 378-386.

Oyewole OI, Oladele JO, and Oladele OT. 2017. Methanolic leaf extract of *Ficus Exasperata* Leaf attenuates Arsenate-Mediated hepatic and renal oxidative stress in rats. *Res. J. of Health Sci.* **5**(2): 115- 123.

Sahreen S, Khan MR, Khan RA. 2011. Phenolic compounds and antioxidant activities of Rumex hastatus D. Don. Leaves. *J Med Plants Res*. **5**:2755–2765.

US EPA (1996) "Proposed guidelines for carcinogen risk assessment" Federal Register, **61**: 17960 - 8011.

Varshney R, and Kale RK. 1990. Effect of calmodulin antagonist on radiation induced lipid peroxidation in microsomes. *International Journal of Radiation Biology* **58**: 733–743.

Wolff SP. 1994. Ferrous ion oxidation in the presence of ferric ion indicator xylenol orange for measurement of hydroperoxides. *Methods Enzym.* **233**: 182–189.

Wu SJ, Lin YH, Chu CC, Tsai YH, Jane CJ. 2008. Curcumin or saikosaponin a improves hepatic antioxidant capacity and protects against CCl4-induced liver injury. *Journal of Medicinal Food* **11**(2): 224–229.

Yang HL, Chen SC, Chang NW, Chang JM, Lee ML, Tsai PC, and Hseu YC. 2006. Protection from oxidative damage using Bidens pilosa extracts in normal human erythrocytes. *Food and Chemical Toxicology* **44**: 1513–1521.

JJBS

Volume 14, Number 3, September 2021
ISSN 1995-6673
Pages 471 - 475

Jordan Journal of Biological Sciences

AFLP Primer Selection for the Analysis of Genetic Diversity in Persimmon (*Diospyros kaki* L.) Originated From Central and East Java, Indonesia

Marshelina Noor Indah Delfianti[1], Endang Yuniastuti[2,*] and Vita Ratri Cahyani[2]

[1]*Master Program of Agronomy, Graduate Program, University of Sebelas Maret, St. Sutami 36A Kentingan Surakarta Central Java 57126, Indonesia;*[2]*Department of Agrotechnology, Faculty of Agriculture, University of Sebelas Maret, St. Sutami 36A Kentingan Surakarta Central Java 57126, Indonesia*

Received: March 17, 2020; Revised: September 13, 2020; Accepted: September 19, 2020

Abstract

Persimmon (*Diospyros kaki* L.) belongs to the family Ebenaceae known as the Japanese persimmon kaki. This crop was introduced in the Highlands in Central and East Java-Indonesia. A genetic analysis of a small sample of accessions was conducted using the *Amplified Fragment Length Polymorphism* (AFLP) method with IRDye700 labelled *Pst*1 (P11-700) and *Mse*1 restriction enzymes and seven primers combinations (M48, M49, M50, M51, M53, M55, and M58). The analysis resulted in a set of 441 bands, of which 117 were monomorphic and 324 polymorphic. The average percentage of polymorphic bands was 73.4%. The four persimmon accessions were genetically distinguished into three groups, with a high genetic diversity among them, while accessions B (Batu) and D (Dampit) show little differences in their profiles.

Keywords: *Diospyros kaki* L., AFLP markers, *Pst*1, *Mse*1, genetic diversity.

1. Introduction

Persimmon (*Diospyros kaki* L.) belongs to the family of Ebenaceae and is known as Japanese foot Persimmon. This plant is native to Central China and has been introduced in Korea, Japan as well as other subtropical countries (Ikegami *et al.*, 2009). In the early 20th century, this crop began to enter Southeast Asia including Indonesia (Java and Sumatra), Malaysia and Thailand (Butt *et al.*, 2015).

In Indonesia, this plant is widely grown in highlands such as Selo-Boyolali (Delfianti *et al.*, 2019), Magetan (Wardani *et al.*, 2019b), Junggo-Batu (Baswarsiati *et al.*, 2006), Dampit-Malang, Garut; Majalengka (Setiawan, 2017), Brastagi; Karo-Sumatera Utara (Hanafiah *et al.*, 2018). Persimmon can grow well at an altitude of 1,000 - 1,500 m above sea level according to Delfianti *et al.*, (2019) where plants require a mild and humid climate for survival.

Persimmon is classified in astringent and non astringent types. According to Butt *et al.*, (2015); Drahansky *et al.*, (2016); Min *et al.*, (2012) astringent persimmon tastes bitter. It is a fruit intended for cooking and requires to overripe to have the astringency removed , while the non astringent persimmon can be eaten immediately after the harvest and does not require to overripe. Persimmon cultivated in Indonesia is an astringent type and is harvested by farmers although they prefer to grow more profitable horticultural crops such as vegetables and citrus. Accordings to Delfianti *et al.*, (2019) and Ridwan & Iskandar Ishaq (2005) in Indonesia persimmon is propagated by rooted cuttings although the percentage of plants obtained is relatively small. To increase the interest of farmers in cultivating persimmons breedingprograms might be developed to produce new varieties of good quality and quantity.

There are two basic methods to study the genetic diversity: the phenotypic and the genotypic ones. According to Hanafiah *et al.* (2018), the phenotypic method uses morphological characters, but is often influenced by environmental factors so that differences between genotypes are difficult to analyze especially if they do not have a simple genetic control system. The genotypic methods are supported by molecular analysis (Syam *et al.*, 2012).

According to Jones *et al.* (1997), there are several kinds of DNA markers, namely *Random Amplified Polymorphic DNA* (RAPD), *Restriction Fragment Length Polymorphism* (RFLP), *Amplified Fragment Length Polymorphism* (AFLP), *Simple Sequence Repeat* (SSR) or DNA microsatellites.

Amplified Fragment Length Polymorphism (AFLP) is a study technique of genetic diversity based on DNA fragments obtained by restriction enzymes and selective amplification of these fragments (Makful et al., 2010; Vos et al., 1995). The basic principle of AFLP technique is to detect the difference in fragment length polymorphism among compared samples (Saunders et al., 2001).

* Corresponding author. e-mail: : yuniastutisibuea@staff.uns.ac.id.

2. Materials and Methods

2.1. Sample collection

Persimmon (*D. kaki* L.) leaves were collected from a single tree in the following locations:

- Central Java Province, which consisted of two villages: Jrakah (coded J), located at 07^o 29' 05.641"S - 110^o 25' 27.815"E dan 1,400 m above sea level and Gebyok (coded G), located at 7°29’57.4”S - 110°28’16.1”E dan 1,499 m above sea level
- East Java Province, which consisted of two villages: Batu (coded B), located at 07°80’18.370”S - 112°52’47.787”E dan 1,318 m above sea level and Dampit (D), located at 08°14’92.001”S - 112°85’90.381”E dan 1,130 m above sea level

The distance between the two villages in Central Java province is 6.8 km from each other. The distance between villages of East Java province is 53.4 km.

2.2. DNA Isolation and quantification

DNA of leaves taken from the field was isolated using a genomic DNA Mini Kit (Plant) following the manufacturer’s instructions.

DNA was quantifyed using a spectrophotometry and concentration, and purity of DNA at λ260 nm and λ280 nm (Sambrook *et al.*, 1989; Witkowski, 1995) was recorded.

2.3. AFLP Analysis

AFLP analysis used the method of Vos *et al.*, (1995) modified on primer labeling with IRD 700. The steps were:

Restriction and ligation: The DNA was treated with the *Pst*1 and *Mse*1 restriction enzymes (Suryati et al., 2013). The reaction mixture included 5 µl of DNA (100 ng/µl); 0.25 µl restriction enzymes *Pst*1 and *Mse*1; 0.5 µl *Pst*1 adapter and *Mse*1 adapter; 0.5 µl ATP 10 mM; 2.5 µl NEB buffer 10 X; 0.2 µl T4 ligase; and 15, 8 µl dH_2O. The mixture was incubated for 24 hours at 37°C.

Pre-amplification: Pre-amplification process required 10 µl of RL plus 1.2 µl primer Pst1 (P00), 1.2 primer µl Mse1 (Mo2), 0.8 µl 10 mM dNtp, 0.4 Taq Polimerase 5 U/µl. Pre-Amplification was carried out with the following PCR profile: denaturation at 94 °C for 30 sec, 56 ° C for 30 seconds and extension of 72 °C for 60 seconds for 24 cycles. Pre-amplification product was diluted 10x and 10 µl as a DNA template was used for further selective amplifications. AFLP primer for the pre-amplification were *Pst*1 (5' GACTGCGTACATGCAG3') and *Mse*1 (5'GATGAGTCCTGAGTAAC3').

Selective Amplification: Selective amplification used seven primer combinations (Muluvi et al., 1999), the *Pst*1 primer 5' GACTGCGTACATGCAGAA3' was labeled with I IRDye 700 (P11-700) ; while *Mse*1 primer sequences are reported in Table 2.

Fragment separation and visualization: The electrophoresis of the products of selective amplification was carried out using the LI-COR 4300 DNA analyzer equipment and the acrylamide gel at 6.5%. The gel for electrophoresis was made by mixing 20 ml of KB plus 6.5% gel matrix; 12.5 µl Tetramethilenediamine (TEMED) and 150 µl ammonium Persulfat (APS) 10% (b/V). The mixture was then inserted into the glass plates and allowed to solidify. The gel was run with the TBE buffer 1X. Pre-electrophoresis was performed for 20 minutes with 20 watt to raise the temperature up to 50ºC. As much as 10 µl of DNA sample, coupled with 10 µl of loading buffer, formamid 98% (b/V), EDTA 10 mM, blue bromophenol 0.1% (b/V) with the same volume (10 µl) so that the mixture becomes 20 µl. All the samples were denatured at 94 °C for 10 minutes and then moved into the ice for approx. 5 minutes. The electrophoresis was run for a. 3 hours with 40 watt and 1500 voltage.

2.4. Data Analysis.

The DNA bands were scored and converted into binary data (1 = presence, 0 = absence). The differences between samples were analysed using a similarity matrix from which a UPGMA (unweighted pair group method with arithmetic mean) dendrogram was constructed (Rohlf 1988).

3. Result and Discussion

3.1. DNA Isolation and Quantity and QualityTest

Data on concentration and purity of persimmon DNA are reported in Table 1.

Table 1. Result of Persimmon DNA Quantification

No.	Sample	Concentration (ng/ µl)	λ 260/280
1.	Jrakah	80.5	1.94
2.	Gebyok	85.2	1.91
3.	Batu	90.3	1.95
4.	Dampit	82.4	1.97

DNA quality of the four samples of persimmon ranged between 1.91 and 1.97. According to Sambrook *et al.*, (1989); Sundari (2018); Wardani *et al.*, (2019) the absorbancy ratio of a DNA of good quality ranges from 1.8 to 2.0.

The DNA concentration was in the range of 80.5 – 90.3 ng/µl.

3.2. The AFLP analysis

The study used 7 primer combinations, including P11-M48; P11-M49; P11-M50; P11-M51; P11-M53; P11-M55; and P11-M58. The primers combination produced the number of bands reported in table 2.

Table 2. Primers combinations and number of AFLP bands produced in four persimmon accessions

No.	Primer	Sequence (5'-3')	Amplicons (n)	Polymorphic bands (n)	Polymorphism (%)
1.	P11-M48	GATGAGTCCTGAGTAA**CAC**	64	49	76
2.	P11-M49	GATGAGTCCTGAGTAA**CAG**	50	35	70
3.	P11-M50	GATGAGTCCTGAGTAA**CAT**	55	43	78
4.	P11-M51	GATGAGTCCTGAGTAA**CCA**	73	51	69
5.	P11-M53	GATGAGTCCTGAGTAA**CCG**	45	19	42
6.	P11-M55	GATGAGTCCTGAGTAA**CGA**	84	70	83
7.	P11-M58	GATGAGTCCTGAGTAA**CGT**	70	57	81
Total or average			441	324	73.4

The amount of bands obtained from the seven primer combinations and four samples were as many as 441. The largest number of bands was produced by the P11-M55 primers pair with as much as 84 bands, while the lowest number of bands was produced by the primers pair P11-M53 with only 45 bands.

The size of the AFLP bands obtained ranged from 50 to 700 bp (Figure 1).

Based on the pattern of the AFLP bands, it can be concluded that there is polymorphism on the four persimmon samples in the seven primer combinations used. Of the total of 441 bands, 117 were monomorphic and present in all samples and 324 were polymorphic. The polymorphic bands ranged from 42 to 83% according to the primers combination.

The sample clustering produced the dendrogram of Figure 2.

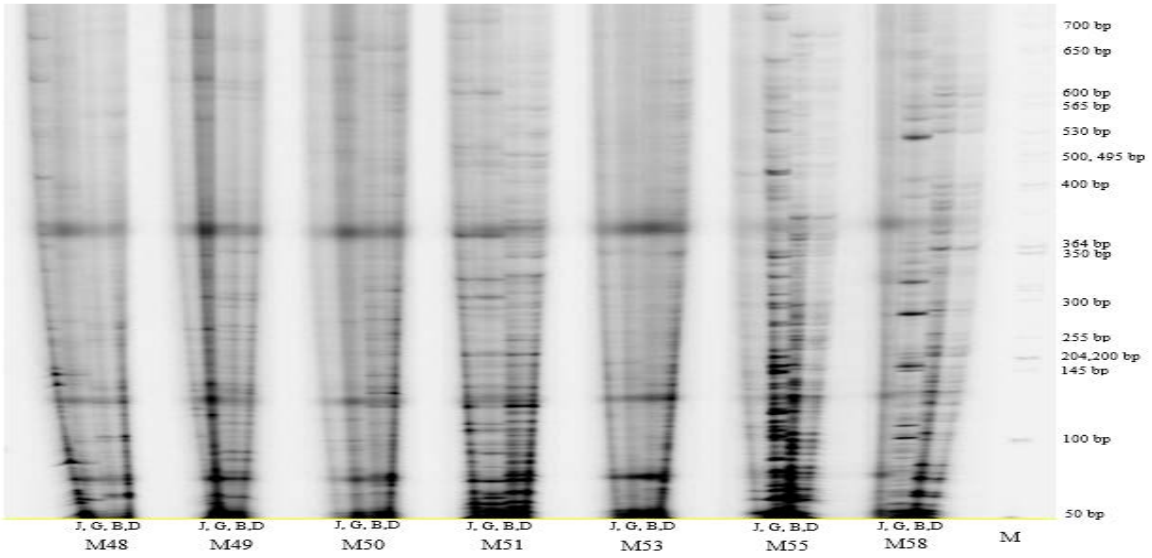

Figure 1. AFLP fragment profile of four persimon (*Diospyros kaki* L.) genotypes amplified using 7 primer combinations (P11-M48; P11-M49; P11-M50; P11-M51; P11-M53; P11-M55; P11-M58). On the right the standard size marker 50 – 700 bp.

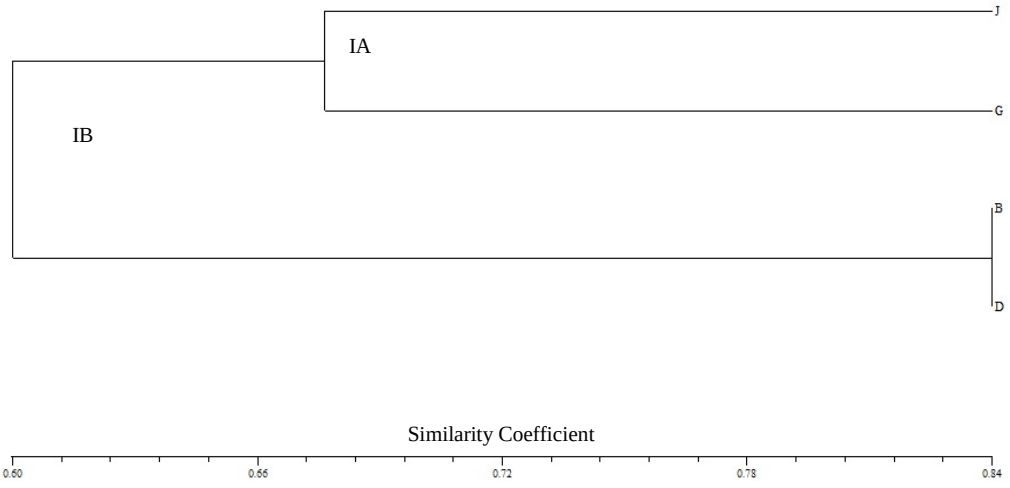

Figure 2. UPGMA cluster analysis of four persimmon samples with seven AFLP primers pairs.

Genetic relationships between persimmon individuals are grouped based on the value of the similarity coefficient on the dendogram. Persimmon samples formed two groups namely IA and IB. IA group consists of Jrakah and Gebyok accessions that had a similarity coefficient of around 0.675. The IB subclaster shows that Batu accession is genetically very close to Dampit accession with a similarity coefficient of 0.84. IA and IB groups are clustered at a similarity coefficient around 0.60.

4. Conclusion

The AFLP markers were successfully used to analyze the genetic diversity of four persimmon samples scattered in Central and East Java, Indonesia based on the number of polymorfisms generated by the AFLP markers. Of the seven primers combinations used, the three most suitable ones for the analyzsis of persimmon genetic diversity were P11-M48; P11-M49; and P11-M51. The clustering procedure generated three main branches that clearly separated the genotypes Jrakah (J) and Gebyok (G) and these two from the third group that included the genotypes Batu (B) and Dampit (D), which resulted being very similar to each other at the AFLP markers profile.

Acknowledgement

Author declare thanks to the University of Sebelas Maret-Indonesia for funding this research from PUT-UNS (PNBP).

References

Badenes ML and Byrne DH. 2012. **Fruit breeding**. In *Fruit Breeding* (Handbook o). https://doi.org/10.1007/978-1-4419-0763-9

Baswarsiati N, Suhardi N and Rahmawati D. 2006. Potential and Development Area Persimmon Junggo. *Buletin Plasma Nutfah*, **12(2)**: 56.

Bruno L. 2000. Simplified AFLP Protocol: Replacement of Primer Labeling by the Incorporation of α-Labeled Nucleotides during PCR. *BioTechniques*, ***28*(4)**: 622–623.

Butt MS, Sultan T, Aziz M, Naz A, Ahmed W, Kumar N, Imran M. 2015. Persimmon (Diospyros kaki) Fruit: Hidden Phytochemicals and Health Claims. *EXCLI Journal*, **14**: 542–561.

Das M, Banerjee S, Topdar N, Kundu A, Sarkar D, Sinha MK, Gupta PK. 2011. Development of large-scale AFLP markers in jute. *Journal of Plant Biochemistry and Biotechnology*, **20(2)**: 270–275.

Delfianti MNI, Yuniastuti E and Cahyani VR. 2019. Propagation and growth of persimmon (Diospyros kaki L.) in Indonesia. *IOP Conference Series: Earth and Environmental Science*, **250(1)**: 1–5.

Drahansky M, Paridah M, Moradbak A, Mohamed A, Owolabi F, abdulwahab taiwo, Asniza M and Abdul Khalid SH. 2016. Genetic Diversity and Breeding of Persimmon. In *Intech*: *Vol. i* (2nd ed., p. 13).

Du XY, Zhang QL, and Luo ZR. 2009. Comparison of four molecular markers for genetic analysis in Diospyros L. (Ebenaceae). *Plant Systematics and Evolution*, **281(1–2)**: 171–181.

Guan C, Chen W, Mo R, Du X, Zhang Q and Luo Z. 2016. Isolation and characterization of DkPK genes associated with natural deastringency in C-PCNA Persimmon. *Frontiers in Plant Science*, ***7***: 1–11.

Hanafiah DS, Sangita S and Lubis K. 2018. The phenotypic appearance of Japanese persimmon (Diospyros kaki L.f.) in Karo district, North Sumatra, Indonesia. *Biodiversitas*, **19(2)**: 509–514.

Hess CM, Wang Z and Edwards SV. 2007. Evolutionary genetics of Carpodacus mexicanus, a recently colonized host of a bacterial pathogen, Mycoplasma gallisepticum. *Genetica*, **129(2)**: 217–225.

Ikegami A, Akagi T, Potter D, Yamada M, Sato A, Yonemori K, Inoue K. 2009. Molecular identi W cation of 1-Cys peroxiredoxin and anthocyanidin / X avonol 3 -O- galactosyltransferase from proanthocyanidin-rich young fruits of persimmon (Diospyros kaki Thunb .). *Planta*, **230**: 841–855.

Jing Z, Ruan X, Wang R and Yang Y. 2013. Genetic diversity and relationships between and within persimmon (Diospyros L.) wild species and cultivated varieties by SRAP markers. *Plant Systematics and Evolution*, **299(8)**: 1485–1492.

Jones CJ, Edwards KJ, Castaglione S, Winfield MO, Sala F. 1997. Reproducibility testing of RAPD, AFLP and SSR markers in plants by a network of European laboratories. *Molecular Breeding*, **(3)**: 381–390.

Kanzaki S, Yonemori K, Sato A, Yamada M, and Sugiura A. 2000. Analysis of the Genetic Relationship Among Pollination-Constant and Non-Astringent (PCNA) Cultivars of Persimmon (Diospyros kaki Thunb.) from Japan and China Using Amplified Fragment Length Polymorphism (AFLP). *J. Japan. Soc. Hort. Sci.*, **69(6)**: 665–670. https://doi.org/10.2503/jjshs.69.665

Kanzaki S, Yamada M, Sato A, Mitani N, Ustunomiya N and Yonemori K. 2009. Conversion of RFLP markers for the selection of pollination-constant and non-astringent type persimmons (Diospyros kaki Thunb.) into PCR-based markers. *Journal of the Japanese Society for Horticultural Science*, **78(1):** 68–73.

Kim CS, Lee CH, Shin J S, Chung YS and Hyung NI. 1997. A simple and rapid method for isolation of high quality genomic DNA from fruit trees and conifers using PVP. *Nucleic Acids Research*, **25(5)**: 1085–1086.

Loh JP, Kiew R, Hay A, Kee A, Gan LH and Gan YY. 2000. Intergeneric and interspecific relationships Araceae tribe Caladieae and development of molecular markers using amplified fragment length polymorphism (AFLP). *Annals of Botany*, **85(3)**: 371–378.

Makful, Purnomo SS. 2010. Analysis of Genetic Diversity of Mangosteen Based on the Amplified Fragment Length Polymorphism (AFLP) Technique. *Jurnal Hortikultura*, **20(4)**: 313–320.

Mba C and Tohme J. 2005. Use of AFLP markers in surveys of plant diversity. *Methods in Enzymology*, **395**: 177–201.

Min T, Yin Xue-ren, Shi Yan-na, Luo Zheng-rong, Yao Yun-cong, Grierson D, Ferguson IB and Chen K. 2012. Ethylene-responsive transcription factors interact in with In Posidonia oceanica cadmium induces changes DNA promoters of ADH and PDC patterning involved in persimmon methylation and (Diospyros kaki) fruit de-astringency. *Journal of Experimental Botany*, **63(18)**: 6393–6405.

Muluvi GM, Sprent JI, Soranzo N, Provan J, Odee D, Folkard G, McNicol JW, Powell W. 1999. Amplified fragment length polymorphism (AFLP) analysis of genetic variation in Morнga oleifera Lam. *Moleculer Ecology*, **8**: 463–470.

Mustafa H, Rachmawati I and Udin Y. 2016. Genomic DNA Concentration and Purity Measurement of Anopheles barbirostris. *Jurnal Vektor Penyakit*, **10(1)**: 7–10.

Naval MM, Zuriaga E and Badenes ML. 2013. AFLP analysis of mutations induced by gamma irradiation in "rojo brillante" persimmon. *Acta Horticulturae*, **996**: 117–122.

Parfitt DE, Yonemori K, Honsho C, Nozaka M, Kanzaki S, Sato A and Yamada M. 2015. Relationships among Asian persimmon cultivars, astringent and non-astringent types. *Tree Genetics & Genomes*, **51(2)**: 1–9.

Qi X and Lindhout P. 1997. Development of AFLP markers in barley. *Molecular and General Genetics*, **254(3)**: 330–336.

Quagliaro G, Vischi M, Tyrka M and Olivieri M. 2001. Identification of Wild and Cultivated Sunflower for Breeding Purposes by AFLP Markers. *Journal of Heredity*, **92(1)**: 38–42.

Ridwan H and Ishaq I. 2005. Kajian Sistem Usaha Tani Buah Kesemek (Diosphyros kaki L.f) dan Permasalahannya Di Kabupaten Garut-Jawa Barat. *Jurnal Pengkajian Dan Pengembangan Teknologi Pertanian*, **8(1**): 94–110.

Rohlf F. 1988. NTSYS-pc - Numerical Taxonomy and Multivariate Analysis System. Applied Biostatistics Inc. New York. 2.1.

Sambrook J, Fritsch EF and Maniatis T. 1989. Moleculer Cloning: A Laboratory Manual. Cold Spring Harbor Laboratory Press. New York.

Saunders Ja, Mischke S and Hemeida AA. 2001. The use of AFLP techniques for DNA fingerprinting in plants. *Beckman Coulter Application Notes A1910A*, 1–9. Retrieved from http://citeseerx.ist.psu.edu/viewdoc/download?doi=10.1.1.134.699&rep=rep1&type=pdf

Setiawan E. 2017. Effecttiveness of IAA, IBA, NAA, and Root-up Application on Persimmon Seedling. *Jurnal Hortikultura Indonesia*, **8(2)**: 97–103.

Sundari. 2018. DNA Isolation Technique of Clove Plant Genomes Using Buffer CTAB Modification. *Jurnal Biologi Edukasi*, **10(2)**: 21–26.

Suparningtyas JF, Pramudyawardhani OD, Purwoko D and Tajuddin T. 2018. Phylogenetic Analysis of Rubber Tree Clones using AFLP (Amplified Fragment Length Polymorphism) Marker Juniza. *Jurnal Bioteknologi & Biosains Indonesia (JBBI)*, **5(1)**: 8–19.

Suryati E, Puspaningtyas L and Widyastuti U. 2013. Genetic Characteriztics Kappapycus alvarezii Healthy and Infected Disease Ice-Ice by Amplified Fragment Length Polymorphism Methods (AFLP). *J.Ris.Akuakultur*, **8(1)**: 21–30.

Syam R, Sadimantara GR and Muzuni. 2012. Genetic Variation Analysis of Cashew Trees (Anacardium accidentale L.). *Penelitian Agronomi*, **1(2)**: 164–173.

Vos P, Hogers R, Bleeker M, Reijans M, Lee T. Van De, Hornes M, Zabeau M. 1995. AFLP: A new technique for DNA fingerprinting. *Nucleic Acids Research*, ***23*(21)**: 4407–4414.

Wardani NC, Yuniastuti E and Sulandjari. 2019a. Genetic identification and micropropagation of distributed persimmons (Diospyros kaki) in Indonesia. *Pertanika Journal of Tropical Agricultural Science*, **42(4)**: 1343–1359.

Wardani NC, Yuniastuti E and Sulandjari. 2019b. Micropropagation protocol of juvenile buds derived from mature persimmon (Diospyros kaki L.) tree. *AIP Conference Proceedings*, *2120*(July).

Weising K, Nybom H, Wolff K and Kahl G. 2005. DNA Fingerprinting in Plants (Principles, Methods, and Applications). In M. Hollingsworth (Ed.), *Annals of Botany* (Second edi, Vol. 97).

Witkowski JA. 199). Biological Laboratory: Cold Spring Harbor Laboratory. *Molecular Medicine (Cambridge, Mass.)*, **1(7)**: 715–717.

Yamagishi M, Matsumoto S, Nakatsuka A and Itamura H. 2005. Identification of persimmon (Diospyros kaki) cultivars and phenetic relationships between Diospyros species by more effective RAPD analysis. *Scientia Horticulturae*, **105(2)**: 283–290.

JJBS

Volume 14, Number 3, September 2021
ISSN 1995-6673
Pages 477 - 484

Jordan Journal of Biological Sciences

Prevalence and Risk Factors Associated with *Aeromonas hydrophila* infection in *Clarias gariepinus* and Pond Water from Fish Farms in Kaduna State, Nigeria.

Deborah A. Adah [1,*], Lawal Saidu[2], Sonnie J. Oniye[3],Haruna M. Kazeem[4], Sylvanus A. Adah[5]

[1]*Department of Veterinary Medicine, University of Ilorin, Ilorin, Nigeria;*[2]*Veterinary Teaching Hospital, Ahmadu Bello University Zaria, Nigeria;*[3]*Department of Zoology, Ahmadu Bello University, Zaria;*[4]*Department of Veterinary Microbiology, Ahmadu Bello University Zaria, Nigeria;*[5]*Department of Veterinary Physiology and Biochemistry, University of Ilorin, Ilorin. Nigeria.*

Received: March 17, 2020; Revised: September 18, 2020; Accepted: September 22, 2020

Abstract

Clarias gariepinus remains important among fish species, and its farming in Africa has contributed immensely to fast growth in pisciculture. However, the successful rearing of fish is hampered by the occurrence of disease. The study was carried out to establish the prevalence, risk factors associated with, and antibiotic susceptible patterns of *Aeromonas hydrophila* isolates from *C. gariepinus* obtained from fish farms in the study area in Kaduna state, Nigeria. Two hundred and fifty-five (255) fish samples with their respective pond water from 30 randomly selected fish farms in Kaduna state were examined for the prevalence of *Aeromonas hydrophila*. The prevalence of *A. hydrophila* was 19.6% (50/255) and 53.3% (16/30) in fish and pond water respectively. *A. hydrophila* infected fish exhibited erosions and haemorrhages on the skin and fin and degeneration of the fin and barbell. The age, weight, and holding facilities were significantly associated with the prevalence of *A. hydrophila*. Multidrug resistance (MDR) ability ranging from two to seven commonly used antibiotics and twelve resistant patterns was also displayed by the isolates. The presence of *A. hydrophila* with associated MDR characteristics portends public and aquatic health hazards and, therefore, needs active surveillance and monitoring.

KeyWords: Aquaculture, Antibiotics, *Clarias gariepinus*, management practise, multi-drug resistance

1. Introduction

Wild fish stock is declining worldwide mainly due to overfishing and climate change, paving the way to the rapid development of fish farming. Fish farming is the world's fastest thriving sector of animal production, involving the use of water (FAO, 2017). Fish takes a prominent place as a source of protein compared to other protein sources and is estimated to provide at least 50% of total animal protein intake in developing countries (Ugwem *et al*., 2011; Obiero *et al*., 2019). However, the successful rearing of *Clarias gariepinus (C. gariepinus)* is hampered by the occurrence of disease, which at any stage of the fish culture will have a great consequence on the economic viability of fish farms and the yield of protein for human consumption (Babek *et al*., 2015; Opiyo *et al*., 2018).

Aeromonas hydrophila (A. hydrophila) is known to be one of the most important bacteria associated with disease in marine, freshwater and cultured fish (Pękala-Safińska, 2018), and infection by *A. hydrophila* has been recognized for many years and has been associated with brown patch skin disease, tail and fin rot, motile aeromonad septicaemia and haemorrhagic septicaemia which can lead to huge mortality among wild and cultured fishes (Plumb and Hanson, 2011; Bebak *et al*., 2015).

Aeromonas hydrophila is a ubiquitous Gram-negative bacterium, facultatively anaerobic, oxidase-positive, and glucose-fermenting bacteria belonging to the family *Aeromonadaceae* (Hussain *et al*.,2014; Stratev and Odeyemi, 2015), which is commonly isolated from freshwater ponds and inhabits the gastrointestinal tract and are considered to be emerging bacterial pathogens (Igbinosa *et al*., 2012). More so, *A. hydrophila* has also been reported to cause zoonotic diseases leading to intestinal and extra-intestinal diseases in humans such as septic arthritis, diarrhoea (traveller's diarrhoea), gastroenteritis, skin and wound infections, meningitis, and fulminating septicaemia (Salunke *et al*.,2015).

Diseases associated with *A. hydrophila may have led to an increase in antibiotics application in the fish farms* to manage infections and mixtures of antibiotics in feeds resulting in antibiotic resistance among pathogenic bacteria. This is a more challenging problem in developing countries (Wegener and Frimodt-Moller, 2000). Reports on the prevalence of *A. hydrophila* from *C. gariepinus* and pond water in Kaduna state, Nigeria are scanty. Hence, this study is undertaken to ascertain the prevalence, risk factors associated with, and antibiotic susceptible patterns of *A. hydrophila* isolates from *C. gariepinus* and pond water from fish farms in the study areas.

* Corresponding author e-mail: adah.ad@unilorin.edu.ng.

2. Materials and method

2.1. Study Location

The study was conducted in Kaduna State, where 4 Local Government Areas (LGAs) including Sabo-Gari, Kaduna-South, Kaduna North, and Zaria LGAs were chosen by random sampling.

Kaduna State is situated in the North -Central region of Nigeria (with Kaduna town as its capital) and shares common borders with Zamfara, Katsina, Niger, Kano, Bauchi, and Plateau States and to the South-West, the Federal Capital Territory, and Abuja. The global location of the State is 10°20′N, 7° 45′E 10.333°N. The State occupies an area of approximately 48,473.2 square kilometres and has a population of more than 6 million people (KSGC, 2017).

2.2. Sample Collection

A stratified random sampling method was employed, in which four Local Government Areas (LGAs) and thirty fish farms were selected comprising 40 concrete ponds, 26 earthen ponds, and 22 plastic tanks making a total of 88 holding facilities within which fish and water were selected. A range of 5-15 fish/ponds were selected based on the stocking density and water samples were collected from 2-6 holding facilities based on the number of holding facilities on the farms (Table 1). A total of two hundred and fifty-five fish samples were conveyed in a plastic receptacle with a cover having the pond water. Also 88 water samples each measuring 500 ml were collected from ponds using sterile bottles and transported under the cold chain to the Veterinary Microbiology laboratory of Ahmadu Bello University Zaria for analyses.

Table 1. Distribution of selected fish holding facilities in 4 LGAs in Kaduna State.

LGA	NO OF FARMS	EARTHEN POND	CONCRETE POND	PLASTIC TANK
Sabo Gari	5	0	16	3
Kaduna North	11	14	0	10
Kaduna South	8	5	12	6
Zaria	6	7	12	3
TOTAL	30	26	40	22

Clarias gariepinus samples were examined clinically, by taking history and conducting antemortem, and post-mortem procedures after which each fish was tagged (Kwaga *et al.,* 1988; (Kwaga *et al.,* 1988; Austin and Austin, 2012). The age, sex, and gross lesions were observed and recorded. Each live fish was sacrificed (by brain spiking to minimise suffering) and placed on a clean stainless tray dorsally, and swab (sterile cotton wool soaked in 70% alcohol) was used to clean the fish from the operculum to the abdominal area to reduce bacterial load.

2.3. Bacterial culture and isolation of Aeromonas hydrophila

The isolation of *Aeromonas hydrophila* followed the standard procedure described by Cowan and Steel (1974). For each fish, the gastrointestinal tract was excised and macerated, and 10% of it was inoculated into a test tube containing enrichment broth (Alkaline peptone water) pH, 8.6. The glass tubes were incubated at 37^0C for 18-24 hours. This was then subcultured onto MacConkey agar. Also, water samples collected from each farm were pooled and centrifuged at 3,000 rpm for 10 minutes. The sediment was inoculated into alkaline peptone water and incubated at 37^0C for 18-24 hours and later subcultured onto MacConkey agar (Buchanan and Gibbons, 1974).

Biochemical tests were carried out ~~for~~ on the isolated Gram-negative bacteria (non-lactose fermenters) included catalase test, citrate utilization test, haemolysis of sheep Red Blood cells, hydrogen sulphide production, indole test, methyl red test, oxidase test, sugar fermentation tests (glucose, sorbitol, sucrose, lactose, rhamnose, and galactose), urease test, and Voges -Proskauer test.

All the chemicals used for biochemical tests were set according to manufacturer instructions (Difco®, Laboratories, USA and Oxoid®, London, UK) and the results were interpreted using the manual for bacteria identification (Cowan and Steel, 1974) and online ABIS Advanced Bacteriological Identification Software (ABIS, 2017).

2.4. Antibiotic sensitivity of the bacterial isolates

The antimicrobial susceptibility of 50 and 16 *Aeromonas hydrophila* isolates from fish and pond water, respectively, were ascertained using the disc diffusion method. The antibiotics were selected based on their common use in the fish farms and these included Ampicillin (10 µg), Chloramphenicol (10 µg) Gentamycin (10 µg), Oxacillin (5µg), Penicillin (10 units), Streptomycin (10 µg), Tetracycline (30 µg), and Vancomycin (5 µg). The susceptibility test was carried out on Muller Hinton agar using antibiotic-impregnated discs. Zones of inhibition were compared with reference strain (ATCC 646) and interpreted as sensitive, intermediate, and resistant (CLSI, 2011).

2.5. Statistical Analysis

Data from this study were loaded into Microsoft Office Excel version 2016 for establishing the frequencies and percentages (%). Chi-square test was used to assess the discrete variables at a 95% confidence interval at $p < 0.05$ was considered to ascertain the associations of potential risk factors with the isolate on of *A. hydrophila in the study area.* The Statistical Package for the Social Sciences (SPSS, Chicago, Illinois, USA) for windows version 22.0 was used for all analysis, and p-value < 0.05 was considered significant in all the analyses.

3. Results

3.1. Clinical manifestations and prevalence rate of Aeromonas hydrophila in C. gariepinus

The *Clarias gariepinus* samples comprised of 200 clinically sick and 55 apparently healthy ones aged between 4 -24 weeks and measuring 15-42 cm in length, 3.8-12 cm in width, and 200-1000g in weight. Among the sick *Clarias gariepinus*, observations such as anorexia and sluggish movements were observed. On physical examination, one or more of the following were observed, which include: exophthalmia (protrusion of the eyeball), erosions, and severe haemorrhages on the skin, eyes, barbels, and fin. Fin rot, white spot, oedema petechiation, and hyperemia of the abdomen. Post-mortem examination

of the sick fish revealed pale gills, congestion of liver, kidney, and spleen, distended gallbladder, and yellowish-green mucoid in the intestine.

The highest isolation rate of *A. hydrophila* was 33.3 % (9/27) obtained from sick fish in Sabo Gari LGA, while the least isolation rate of 13.4 % (9/67) was obtained from Kaduna South LGA. More so, among the apparently healthy fish, the isolation rate was up to 23.1 % (3/13) in Kaduna South LGA. However, there was no significant difference ($P > 0.05$) within the different locations sampled. The prevalence of *A. hydrophila* was 28.1 %, 20.7 %, 20 %, and 15 % obtained from *C. gariepinus* gotten from Sabo Gari (9/32), Zaria (12/58), Kaduna North (17/85), and Kaduna South (12/80) respectively (Table 2). A total of 50 *A. hydrophila*, 43 (21.5 %) from sick (n= 200) and 7 (12.7 %) from apparently healthy (n= 50) were obtained from *Clarias gariepinus* respectively given a total prevalence rate of 19.6 % (50/255), but there was no significant difference ($P > 0.05$) between the fish sampled (Table 2).

The prevalence of *A. hydrophila* infection increases with the age, weight, and length of *C. gariepinus*. The likelihood of infection with *A. hydrophila* in female *C. gariepinus* was 1.41 times when compared to their male counterpart. *C gariepinus* managed semi-intensively were 1.46 times more likely to be infected with *A. hydrophila* when compared to *C. gariepinus* raised in the intensive system, while sick *C. gariepinus* were 1.87 times likely to be infected with *A. hydrophila* when compared with the healthy ones. There was a higher infection tendency of 2.98 of *A. hydrophila* among *C. gariepinus* raised in earthen ponds and 2.70 times likely to occur in fish raised in a concrete tank. There was no significant difference in the prevalence of *A. hydrophila* from the different sampled Local Government Areas.

However, the prevalence was higher in *C. gariepinus* sampled in Sabo Gari LGA. The association between age, (1-3, 4-6, and 7-9months), weight (201-400g and 401-600g), and holding facilities (concrete and earthen ponds) with the prevalence of *A. hydrophila* was statistically significant at $p < 0.05$. The prevalence rate of 24 %, 22.2 %, and 9.5 % was obtained from *C. gariepinus* in earthen ponds, concrete ponds, and plastic tanks, respectively, although there was no significant difference $p > 0.05$ (Table 3).

Table 2. Prevalence of *Aeromonas hydrophila* in sick, apparently healthy fish and pond water obtained from four LGAs in Kaduna State.

LGA	NFS	No. of *A. hydrophila* isolate (%)	*P*-Value (NFS)	NFS	No. of *A. hydrophila* isolate (%)	NPWS	No. of *A. hydrophila* isolate (%)	*P*-Value (NPWS)
Sabo Gari				32	9 (28.1)	5	2 (40.0)	
Apparently healthy	5	0 (0.0)	0.16					
Sick	27	9 (33.3)						
Kaduna North				85	17 (20.0)	11	7 (63.7)	
Apparently healthy	22	3 (13.6)	0.39					0.56
Sick	63	14 (22.2)						
Kaduna south				80	12 (15.0)	8	5 (62.5)	
Apparently healthy	13	3 (23.1)	0.37					
Sick	67	9 (13.4)						
Zaria				58	12 (20.7)	6	2 (33.3)	
Apparently healthy	15	1 (6.7)	0.12					
Sick	43	11 (25.6)						
Total NFS								
Apparently healthy	55	7 (12.7)	0.14					
Sick	200	43 (21.5)						
Total	255	50 (19.6)		255	50 (19.6)	30	16 (53.3)	

Key: NFS: Number of fish sampled; NPWS: Number of pooled pond water sample

Table 3. Prevalence and risk factors associated with *A. hydrophila* infection in *C. gariepinus* from 4 LGAs in Kaduna State.

Risk Factors	N	Prevalence (%)	OR (95% CI)	*P*-Value
Sex				
Female	105	24 (22.86)	1.41 (0.75 - 2.64)	0.28
Male [a]	150	26 (17.33)	1.00	
Weight(g)				
0-200	44	8 (18.18)		
201-400	96	10 (10.42)	0.08 (0.02 - 0.34)	<0.01*
401-600	53	12 (22.64)	0.20 (0.04 - 0.85)	0.03*
601-800	35	9 (25.71)	0.24 (0.05 -1.07)	0.06
801-1000	12	5 (41.67)	0.49 (0.08 -2.81)	0.43
> 1000 [a]	10	6 (60.00)	1.00	
Total Length (cm)				
< 20	20	2 (10.00)	0.31 (0.04- 1.38)	0.14
21-30	45	7 (15.56)	0.52 (0.18 - 1.41)	0.20
31-40	72	14 (19.44)	0.67(0.29-1.59)	0.66
41-50	65	13 (20.00)	0.70 (0.29- 1.67)	0.42
51-60 [a]	53	14 (26.42)	1.00	
Age (months)				
1-3	70	8(11.43)	0.07(0.02- 0.23)	0.0001*
4-6	85	9(10.59)	0.07 (0.02- 0.21)	0.0001*
7-9	56	10(17.86)	0.12 (0.04-0.38)	0.0001*
10-12	23	10(43.48)	2.36(0.68- 8.59)	0.18
>12 [a]	20	13(65.00)	1.00	
Management system				
Semi- intensive	75	18 (24.00)	1.46 (0.75 -2.80)	0.2624
Intensive [a]	180	32 (17.78)	1.00	
Health Status				
Sick	200	43 (21.50)	1.87 (0.82 - 4.77)	0.14
Apparently healthy [a]	55	7 (9.09)	1.00	
Local Government Areas				
Sabo Gari	32	9 (28.13)	1.49 (0.53 - 4.11)	0.44
Kaduna North	85	17 (20.00)	0.96 (0.42 - 2.25)	0.92
Kaduna South	80	12 (15.00)	0.68 (0.28 - 1.67)	0.40
Zaria [a]	58	12 (20.69)	1.00	
Holding facilities				
Concrete ponds	117	26 (22.22)	2.70 (1.08 - 7.60)	0.03*
Earthen ponds	75	18 (24.00)	2.98 (1.13 - 8.73)	0.03*
Plastic tanks [a]	63	6 (9.52)	1.00	

[a] = Reference category; OR = Odds Ratio; CI = Confidence Interval; * = Significant $P < 0.05$

3.2. Prevalence of A. hydrophila in Pond Water collected from the sampled location

Aeromonas hydrophila isolation rates of 63.7 %, 62.5 %, 40.0 %, and 33.3 % were obtained from pond water gotten from Kaduna North (7/11), Kaduna South (5/8%), Sabo Gari (2/5), and Zaria LGAs (2/6), respectively. The total isolation rate was 53.3% (16/30) from the pooled pond water (Table 2). The isolation rate of 60% (6/10) was obtained from pooled pond water collected from concrete and earthen ponds while 40% (4/10) was obtained from pooled pond water collected from plastic tanks (Table 2).

The prevalence of *A. hydrophila* was higher in pond water sampled from Kaduna North LGA when compared to Sabo Gari, Kaduna South, and Zaria LGAs. The prevalence was higher and was 2.16 likely to occur in pond water sampled from the earthen and concrete pond when compared to pond water samples from plastic tanks. Consequently, ponds semi intensively managed was 1.48 likely for *A. hydrophila* to occur when compared with ponds intensively managed. There was no significant difference ($p > 0.05$) in the prevalence of *A. hydrophila* from water samples (Table 4).

Table 4. Prevalence and risk factors associated with *A. hydrophila* infection in pond water from 4 LGAs in Kaduna State.

Risk	N	Prevalence (%)	OR (95% CI)	*P*-Value
Local Government Areas				
Sabo Gari	5	2 (40.00)	1.30 (0.09 - 19.43)	0.85
Kaduna North	11	7 (63.63)	3.24 (0.39 - 35.49)	0.29
Kaduna South	8	5 (62.50)	3.04 (0.32 - 37.36)	0.35
Zaria [a]	6	2 (33.33)	1.00	
Holding facilities				
Concrete ponds	10	6 (60.00)	2.16 (0.35 - 14.71)	0.42
Earthen ponds	10	6 (60.00)	2.16 (0.35 - 14.71)	0.42
Plastic tanks [a]	10	4 (40.00)	1.00	
Management system				
Semi- intensive	10	6 (60.00)	1.48 (0.31- 7.70)	0.63
Intensive [a]	20	10 (50.00)	1.00	

OR=Odds Ratio, CI=Confidence Interval, a Reference category;

3.3. Antibiotic susceptibility of the Aeromonas hydrophila *isolates.*

The susceptibility test of *Aeromonas hydrophila* indicated that gentamicin had the highest sensitivity (66.7 %, 44/66) followed by chloramphenicol (48.5 %, 32/66), streptomycin (15.2 %, 10/66), oxytetracycline and tetracycline (6.1 % 4/66), respectively, and none to vancomycin, penicillin, and ampicillin. All the *A. hydrophila* isolates were found to be resistant to penicillin (100 %, 66/66), oxytetracycline (93.9 %, 62/66), vancomycin (92.4 % ,61/66) ampicillin (69.7 %, 46/66) tetracycline (60.6%, 40/66), chloramphenicol (36.4 %, 24/66), streptomycin (30.3 %, 20/66) and gentamicin (9.1 %, 6/66) respectively. There was a statistical significance p < 0.01 between the sensitive, resistant, and intermediate *A. hydrophila* (Table 5). Multidrug resistance (MDR) was displayed *by A. hydrophila* isolates to the antibiotics mostly used in pisciculture in Kaduna state, Nigeria. Multidrug resistance of *A. hydrophila* isolates ranged between 2 – 7 different antibiotics used, twelve different MDR patterns were observed and the prevalence of MDR among the *A. hydrophila* ranged between 3.0 % - 15.2 % (Table 6).

Table 5. Antibiotics susceptibility of *Aeromonas hydrophila* isolated from fish and pond water

Antibiotic	Sensitive (%)	*P*-Value	Intermediate (%)	*P*-Value	Resistant (%)	*P*-Value
Ampicillin	0 (0.0)		20 (30.3)		46 (69.7)	
Chloramphenicol	32 (48.5)		10 (15.2)		24 (36.4)	
Gentamycin	44 (66.7)		16 (24.2)		6 (9.1)	
Oxytetracycline	4 (6.1)		0 (0.0)		62 (93.9)	
Penicillin	0 (0.0)	<0.01*	0 (0.0)	<0.01*	66 (100.0)	<0.01*
Streptomycin	10 (15.2)		36 (54.5)		20 (30.3)	
Tetracycline	4 (6.1)		22 (33.3)		40 (60.6)	
Vancomycin	0 (0.0)		5 (7.6)		61 (92.4)	
Total	94 (17.8)		108 (20.5)		326 (61.7)	

* = Significant $P < 0.05$

Table 6. Multidrug resistance patterns of *Aeromonas hydrophila* isolated from fish and pond water

Resistance patterns	Number of *Aeromonas hydrophila* isolates	Prevalence (%)	*P*-Value
PEN, OXA,	5	7.6	
PEN, OXA, VAN, TET	10	15.2	
PEN, OXA, VAN, AMP,	4	6.1	
PEN, OXA, VAN, STR, AMP	5	7.6	
PEN, OXA, VAN, GEN, STR	2	3.0	
PEN, OXA, VAN, TET, CHL	3	4.5	
PEN, OXA, VAN, TET, AMP	10	15.2	0.25
PEN, VAN, GEN, AMP, CHL	4	6.1	
PEN, OXA, VAN, TET, AMP	6	9.1	
PEN, OXA, VAN, TET, AMP, CHL	4	6.1	
PEN, OXA, VAN, STR, AMP, CHL	6	9.1	
PEN, OXA, VAN, TET, STR, AMP, CHL	7	10.6	

PEN: Penicillin; AMP: Ampicillin; CHL: Chloramphenicol; GEN Gentamycin; OXA: Oxacillin STR: Streptomycin; TET: Tetracycline; VAN: Vancomycin

4. Discussion

In this present study, the prevalence rate in *C. gariepinus* was higher than that of Mailafia (2003), who reported a prevalence of 11.6 % in fish from wild sources. These differences could be due to different geographical locations, seasons of the year, species of fish, isolation methods, quality of water, and management practices. Isolation and identification of *A. hydrophila* in apparently healthy *C. gariepinus* were similar to the report of Omeje and Chukwu (2014), where *A. hydrophila* was isolated in both healthy and diseased fish. Consequently, the isolation in apparently healthy *Clarias gariepinus* may lead to the outbreak of disease when the water quality and management practices of fish farms become unfavorable for production. The variation of the prevalence rates in the different locations may have been contributed by the differences in the interaction of the pathogen, host, and the environment (Raman *et al.*, 2013). Isolation of *A. hydrophila* in ponds water and *C. gariepinus* in this study showed that it is a natural inhabitant of the culture system in the selected fish farms (Shiranee *et al.*, 1993). The isolation of *Aeromonas species* in pond water has been described to be an indication of the presence of fish disease on a farm (Noga, 2000). The higher prevalence of *A. hydrophila* in the earthen ponds could be because most of the farms sourced their water from the natural water bodies' that are already contaminated with animal and human activities especially the dumping of refuse which invariably get into the ponds. This development is suitable for the propagation and multiplication of several microorganisms including *A. hydrophila*. More so, *A. hydrophila* is saprophytic and thus their prevalence of *A. hydrophila* is ensuing upon environmental fluctuations and changes (Okpokwasili and Ogbulie, 1999).

It has been documented that A. hydrophila causes disease in both cultured and wild fish and can cause clinical signs to the host tissue. Which may be in the form of haeamorrhages and inflammation (Goharriz *et al.*, 2015; Stratev *et al*., 2015). Our findings were similar to the clinical manifestation of *A. hydrophila* found in *Clarias gariepinus* and other fish species (Omeje and Chukwu, 2014; Kumar *et al*., 2016). Anyanwu *et al* (2014) and El-Bouhy *et al. (2015)* reported earlier that motile Aeromonads are associated with erosive and heamorrhagic ulcerative skin lesions observed in the present study. Damage to the fish skin has been recognized as a portal of entry for many bacterial pathogens (Long *et al*., 2014). The different patterns of clinical and pathological manifestations expressed in diseased fish caused by *A. hydrophila* as observed in this study may be due to the difference in individual *C. gariepinus* susceptibility to *A. hydrophila* (Baumgartner *et al*., 2017; Mohamed, 2018). The prevalence of *A. hydrophila* in *C. gariepinus* in our study was less compared to the 30.5 % prevalence rate reported by Omeje and Chukwu (2014), and 31.7 % by Omeje and Chukwu (2012).

There was no bias in the infection of *A. hydrophila* among the *C. gariepinus* based on sex, weight, and length. It has been documented that *Aeromonas* species affects fishes of all ages and sizes (Camus *et al*., 1998), but in our study, the isolation rate was in older fish when compared with younger fish. This is contrary to the reports by Mzula *et al.*, 2019 who opined that the infection of *A. hydrophila* was higher in fingerlings than in older fish, our observation could be attributed to the fact that older fish have stayed longer in the different holding facilities increased the exposure to the *A. hydrophila*. More so, they are bigger in size and this provides a larger surface area for the infection to multiply in number than smaller ones.

Management practise of the fish farms seems to contribute significantly to the isolation of *A. hydrophila* from *C. gariepinus*. In line with this, it was observed that *C gariepinus* raised in earthen ponds, which are semi intensively managed were more prone to the infection than those raised in concrete and plastic tanks intensively managed. Our findings could be attributed to the high presence of elevated pollution levels and anthropogenic activities in earthen ponds which often causes the *A. infections* in *C. gariepinus*, and so the vulnerability of *C. gariepinus* to pathogenic infections is enhanced (Dar *et al*., 2016).

A. hydrophila isolates in this study showed a high level of multidrug resistance and were resistant to oxytetracycline, vancomycin, ampicillin, and tetracycline in which Gentamicin had the highest sensitivity. The result obtained in this present study is similar to that reported by Nahar *et al*. (2016) and Odeyemi and Ahmad (2017). Antibiotic application on fish farms is often practiced as a means of managing diseases on fish farms (Chitmanat *et al*., 2016), and this practice leads to the increased development of resistance of *A. hydrophila* infection against the antibiotics used (Nahar *et al*., 2016). This resistance of *A. hydrophila* to routinely used antimicrobial agents is a budding problem in pisciculture (Dias *et al.*, 2012), and the spread of antibiotics resistance is of great concern because *A. hydrophila* is also a zoonotic pathogen (Janda and Abbott, 2010). The excessive and indiscriminate use of penicillin, amoxicillin, oxytetracycline, and vancomycin may have predisposed this current finding. Nahar *et al*. (2016), reported that *Aeromonas hydrophila* showed marked levels of resistance against chloramphenicol, penicillin, amoxicillin, metronidazole, sulphamethoxazole-trimethoprim, and amikacin.

The diversity of antibiotic resistance pattern exhibited by *A. hydrophila* encountered in this present study reflects the diversity among the isolates and the challenge of multidrug resistance (MDR) seems to affect many pets, livestock, and aquatic animals and its consequence might be detrimental (Lee and Wendy, 2011; Igbinosa *et al.*, 2012; Daodu *et al.*, 2017). MDR might also reflect the consequence of the irrational use of antibiotics used in fish farms.

5. Conclusion

Aeromonas hydrophila is present in pond water and *C. gariepinus* from selected fish farms in Kaduna state harboring multidrug-resistant *Aeromonas hydrophila* which constitute a potential public health risk and may affect aquatic health. The unregulated antibiotic usage in the aquatic industry in Nigeria has to be keenly scrutinized and monitored from time to time to determine the spread and increase of bacterial resistance. The detection of *A. hydrophila* in fish suggests that strict hygiene procedures

and proper cooking before consumption of fish is essential to safeguard consumers.

Acknowledgment

The authors want to appreciate the assistance of all fishermen and laboratory technologists who contributed to the realization of this work.

Statement of Animal Right

All regulations and international standard involved in the use of animal were duly followed.

Conflict of interest

The Authors hereby declare that there was no conflict of interest.

References

ABIS(Advanced Bacteriological Identification Software). 2018. (http://www.tgw1916.net/bacteria_logare_desktop.html). Accessed 12, March 2019.

Anyanwu MU, Chah KF and Shoyinka VS. 2014. Antibiogram of aerobic bacteria isolated from skin lesions of African catfish cultured in South East Nigeria. *Int. J. Fish. Aquat. Stud* ., **2**:134-141.

Austin B and Austin DA. 2012. Bacterial fish pathogens: Disease of farmed and wild fish 3rd edition. pp: 112-115.

Baumgartner WA, Ford L and Hanson L. 2017. Lesions caused by virulent Aeromonas hydrophila in farmed catfish (*Ictalurus punctatus* and *I. punctatus* × *I. furcatus*) in Mississippi. *J. Vet. Diagnostic Investig*.**, 29**(5): 747–751.

Bebak J, Wagner B, Burnes B and Hanson T. 2015. Farm size, seining practices, and salt use: risk factors for *Aeromonas hydrophila* outbreaks in farm-raised catfish, Alabama, USA, *Prev. Vet. Med*.., **118**: (1)161–168.

Buchanan RE and Gibbons NE. 1974. Manual of determinative bacteriology, In: ed Bergey's 8th Edition.Williams and Wilkins, Baltimore. pp. 1268.

Camus AC, Durborow RM, Hemstreet WG, Thune RL and Hawke JP. 1998. *Aeromona*s bacterial infections - motile Aeromonad septicemia. *South. Reg. Aquacult. Cent.*, 478 (1) 1-4.

Chitmanat C, Lebel C, Whangchai C and Lebel L. 2016. **Tilapia diseases and management in river-based cage aquaculture in northern Thailand** *J. Appl. Aquac.*, **28** (1): 9-16.

Clinical and Laboratory Standards Institute (CLSI), 2011. Performance standards for antimicrobial susceptibility testing; twenty-second informational supplements. CLSI document M100-S22. Wayne, Pennsyslvania, 32: 3.

Cowan ST and Steel KJ. 1974. Cowan and steel manual for identification of Medical Bacteria 2nd Edition Cambridge University Press. Cambridge, UK. pp 28-106.

Daodu OB, Elizabeth EA and Oluwayelu DO. 2017. Antibiotic resistance profiling and microbiota of the upper respiratory tract of apparently, South West Nigeria. *Afr J Infect Dis*., **11** (1): 1-11.

Dar GH, Kamili AN, Chishti MZ, Dar SA, Tantry TA and Ahmad F. 2016. Characterization of *Aeromonas sobria* isolated from fish Rohu (*Labeo rohita*) collected from polluted pond. *J Bacteriol Parasitol.*, **7:** 273 doi:10.4172/2155-9597.1000273.

Dias C, Mota V, Martinez-Murcia A and Saavedra MJ. 2012. Antimicrobial Resistance Patterns of *Aeromonas* spp. Isolated from Ornamental Fish. *J Aquacult Res Dev*, **3**:131

El-Bouhy ZM, El-Nobi G, Reda RM and Ali SA. 2015. Prevalence of Septicemia and Red Mouth Disease Caused by Aeromonas sobriaatSahl El-Housinia Fish Farm Zag. Vet. J., **43**(3): 53-63.

FAO. 2017. Regional review on status and trends in aquaculture development in subSahran Africa -2015 . FAO Fisheries and Aquaculture circular No.1135/4,Rome, Italy.

Goharrizi LY, Zorriehzahra MEJ and Adel M. 2015. The study on effect of temperature stress on occurrence of clinical signs caused by *Aeromonas hydrophila* in *Capoeta damascina* in in vitro condition. *Adv. Anim. Vet. Sci*.**, 3**(7): 406-412.

Hussain IA, Jeyasekaran G, Shakila RJ, Raj KT and Jeevithan E. 2014. Detection of hemolytic strains of *Aeromonas hydrophila* and *A . sobria* along with other *Aeromonas* spp. from fish and fishery products by multiplex PCR. *Int J Food Sci Tech*., **51**(2),401–407.

Igbinosa IH, Igumbor EU, Aghdasi F, Tom M and Okoh AI. 2012. Emerging *Aeromonas* species Infections and Their Significance in Public Health. *Sci. World J*., Janda JM and Abbott SL. 2010.The genus Aeromonas: taxonomy, pathogenicity, and infection. *Clin Microbiol Rev*., **23**: 35-73.

KDGC (Kaduna state geographical center), 2017. www.kadunastate.gov.ng Accessed 11 March, 2019.

Kumar R, Pande V, Singh L, Sharma L and Saxena N. 2016. Pathological findings of experimental *Aeromonas hydrophila* infection in golden mahseer (*Tor putitora*) *Fish Aquacult. J.,* **7**:160-165

Kwaga KJ, Kwanashie CN, Dusai DHM and Oni OO. 1988. Occurrence and antimicrobial susceptibility of *Pleisiomonas shigelliodes*, *Aeromonas hydrophila* and *Edwardsiella tarda* in healthy fish in Zaria. Nigerian Journal of Food and Agriculture., **2**:176-181.

Long A, Fehringer TR, LaFrentz BR, Call DR, and Cain KD. 2014. Development of a waterborne challenge model for *Flavobacterium psychrophilum*. *FEMS Microbiol Lett*., **359**:154–60.

Lee SW and Wendy W. 2011. Antibiogram and Heavy Metal Resistance Pattern of Salmonella spp. Isolated from Wild Asian Sea Bass (*Lates calcarifer*) from Tok Bali, Kelantan, Malaysia , *Jordan J. Biol. Sci* 4(3) :125 – 128.

Mailafia, S., 2003. Studies on *Aeromonas* species isolated from fishes in Zaria, Nigeria. M.Sc.Thesis, Ahmadu Bello University, Zaria, pp.23-34.

Mohamed M. 2018. *Aeromonas hydrophila* in fish and humans; prevalence, virulotyping and antimicrobial resistance. *Slov Vet Res.*, **55:** 636- 9

Mzula A, Philemon NW, Robinson H, Mdegela G and Shirima M. 2019. Phenotypic and molecular detection of Aeromonads infection in farmed Nile tilapia in Southern highland and Northern Tanzania. *Heliyon..*, **5(8)**:02220.

Nahar S, Rahman M, Ahmed G, and Faruk M. 2016. Isolation, identification, and characterization of *Aeromonas hydrophila* from juvenile farmed pangasius (Pangasianodon hypophthalmus). *Int. J. Fish. Aquat. Stud.*, **4**: 52-60.

Noga EJ. 2000. Fish disease diagnosis and treatment. Iowa State University, Iowa, USA.

Obiero O, Herwig W, Bryan ON, Jonathan MM, Julius OM and Boaz KA. 2019. Predicting uptake of aquaculture technologies among smallholder fish farmers in Kenya *Aquac Int.*, **27**:1689–1707.

Odeyemi OA and Ahmad A. 2017. Antibiotic resistance profiling and phenotyping of *Aeromonas* species isolated from aquatic sources. *Saudi J. Biol. Sci.*, 24(1): 65–70.

Okpokwasili, GC. and Ogbulie L. 1999. Haematological and histological responses of *Clarias gariepinus* and *Heterobranchus bidosalis* to some bacterial disease in River state *Nigeria. J. Nat. Sci. Res.*, 27: 1-16.

Omeje VO and Chukwu C. 2012. A relative prevalence of *Oreochromis niloticus*, *Clarias gariepinus* and *Heterotis niloticus* to *Aeromonas hydrophila* in an integrated fish farm.*Niger. Vet. J.*, **33** (2):492 – 498.

Omeje VO and Chukwu CC.2014. Prevalence of *Aeromonas hydrophila* Isolates in cultured and Feral *Clarias gariepinus* of the Kainji Lake Area, Nigeria. *Niger. Vet. J.*, **35** (1)9-8· 955.

Opiyo MA, Marijani, E, Muendo, P, Odede R, Leschen W and Charo-Karisa H. 2018. **A review of aquaculture production and health management practices of farmed fish in Kenya .***Int. J. Vet. Sci. Med..*, **6:** 141-148.

Pękala-Safińska A. 2018. Contemporary Threats of Bacterial Infections in Freshwater Fish. .J *Vet* Res., **62**(3), 261–267.

Plumb JA, Larry A and Hanson LA. 2011. Health maintenance and principal microbial diseases of cultured fishes: In 3rd edition Blackwell Publishing Ltd, Iowa. Pp 492 John Wiley & Sons.

Raman R, Prakash C, Marappan, M, and Pawar NA.2013. Environmental stress mediated diseases of fish: an overview. In: Advances in Fish Research, Vol.-V, Publisher: Narendra Publishing House, Delhi, India, pp.141-158.

Salunke G, Namshikar V, Gaonkar Rand Gaonkar T. 2015. A case of *Aeromonas hydrophila* meningitis in septic shock. *Trop J Med Res.*, **18**:54-7.

Shiranee P, Natarajan P and Dherendran R..1993. The role of gut and sediment bacterial flora in the nutrition of cultured pearl spot (Etroplussaratensis, *Bloch*). *Isr J Aquac.*, **45**(2): 45-58.

Stratev D and Odeyemi OA . 2015. Antimicrobial Resistance of Aeromonas hydrophila Isolated from Different Food Sources: A Mini-Review.*J Infect Public Heal.*, **9:**535-544.

Stratev D, Stoev S, Vashin I, Daskalov H. 2015.Some varieties of pathological changes in eximentalper infection of carps (*Cyprinus carpio*) with *Aeromonas hydrophila*. J. *Aquacult. Eng. Fish. Res.*, **1**:191–2.

Ugwem UG , Ojo A A and Funkeye E. 2011Haematological Responses of Wild Nile Tilapia Oreochromis niloticus after Acclimation to Captivity. *Jordan J. Biol. Sci* **4**: 225 – 230.

Wegener HC and Frimodt-Moller N. 2000. Reducing the use of antimicrobial agents in animals and man. *J. Med. Microbiol.*, 49:111–115.

JJBS

Jordan Journal of Biological Sciences

Volume 14, Number 3, September 2021
ISSN 1995-6673
Pages 485 - 491

The Correlation between Excess Weight and Duration of COVID-19 Symptoms in a Tertiary Hospital in Amman, Jordan

Laith Khasawneh* , Duaa Shaout, Sara Abu-Ghazal, Tishreen Fazza and Mohammad Abdelmajid

Department of Surgery, Faculty of Medicine, Hashemite University

Received: Dec 13, 2020; Revised: Jan 25, 2020; Accepted: Feb 2, 2021

Abstract

Overweight and obesity have several negative pathophysiological consequences on the human body during COVID-19 infection. These pathophysiological consequences have a synergistic effect on disease prognosis and outcome. The association between excess weight and COVID-19 outcome has not been investigated before in Jordan. The objective of this study is to evaluate the correlation between excess body weight and the duration and severity of symptoms in patients affected by the novel corona virus in a tertiary hospital in Amman, Jordan. This is a single-center retrospective cross-sectional study of adult patients with confirmed positive COVID-19 who were admitted to a tertiary academic hospital between April and August 2020. Data were collected by telephone interviews and by the review of medical records. One hundred and seventy patients participated in the current study. Around two-thirds of the participants were female patients. Mean BMI for study participants was 27.6 ± 5.4. BMI was statistically significantly correlated with COVID-19 symptoms duration (p-value = 0.003). The mean duration of COVID-19 symptoms for obese patients was 16.0 ±7.3 days compared to a mean duration of 11.9 ±6.4 days for overweight patients and a mean duration of 12.0 ±6.1 days for patients with normal BMI. Multivariate analysis showed that higher BMI was significantly associated with increased symptom duration after controlling other variables. There is a need to increase public health efforts in fighting overweight and obesity. The Jordanian authorities are advised to develop focused awareness messages for overweight and obese individuals to have strict social distancing and other prevention measures against COVID-19. People with increased BMI are a vulnerable group for this respiratory infection and they deserve advanced and tailored efforts to protect them from its adverse outcomes.

Keywords: COVID-19, SARS-COV-2, Body Mass Index, Excess weight

1. Introduction

The new coronavirus (2019-nCov) infection, which is thought to have a zoonotic origin, appeared first in the Chinese province of Wuhan back in December 2019 (Cornejo-Pareja et al., 2020; Curtin et al., 2020). In 2020, towards the end of the first quarter, the World Health Organization (WHO) declared an emergency state: the virus had become a global pandemic (Cuthbertson et al., 2020). Affecting over 216 countries or territories by August 2020, with around 20 million infected cases, the death toll has reached over 700 thousand deaths (Huang et al., 2020). The first case of COVID-19 was reported in Jordan on March 2, 2020 (Samrah et al., 2020b). By July 2020, the total number of active cases in Jordan reached 1,209 and 10 confirmed deaths have been reported (Akour et al., 2020).

Overweight and obesity are major health challenges, as they might raise the risk of other diseases considerably. With prevalence stages on the steady increase globally for almost half a century, it has reached a pandemic level, thus contributing to a deterioration in individuals' quality of life and longevity (Blüher, 2019). Previous estimates showed that more than two billion people are overweight globally and more than 650 million people are obese (Khan and Moverley Smith, 2020; Magdy Beshbishy et al., 2020). In Jordan, obesity rates have been in constant increase. It has been reported as being among the highest in the region. A recent study estimated that three-quarters of Jordanian adults suffer from obesity or overweight according to their body mass index (BMI) measurement (Ajlouni et al., 2020). BMI is a widely used, low-cost tool to assess patients' weight status. It is a useful predictor for poor health outcomes in overweight and obese patients (Hall and Cole, 2006; Klatsky et al., 2017).

The first suspicions about the association between poor COVID-19 outcomes and obesity came from China in April 2020 (Dyett, 2020). However, obesity prevalence in China is in general lower than in western countries. Therefore, this association was not fully observed until the pandemic reached western hemisphere countries that suffer from higher obesity prevalence, such as the USA, Spain, Italy and other developed countries (Holly et al., 2020; Kwok et al., 2020; Rancourt et al., 2020). Although age remains the most single independent risk factor for poor COVID-19 prognosis (Lockhart and O'Rahilly, 2020), the current literature identified overweight and obesity as another strong independent and significant risk factor for COVID-19 mortality, Intensive Care Unit (ICU)

* Corresponding author e-mail: L.Khasawneh80@gmail.com.

admission, intubation for mechanical ventilation, and other severity or poor prognosis indicators (Caussy et al., 2020; Huang et al., 2020; Liu et al., 2020; Smati et al., 2020).

Overweight and obesity have several negative pathophysiological consequences on the human body during COVID-19 infection. These pathophysiological consequences have a synergistic effect on disease prognosis and outcome (Caci et al., 2020; Kimura and Namkoong, 2020). For example, Fedele et al. and Holly et al. reported that obese COVID-19 patients tend to have hyper- coagulopathy status and inadequate immune response. Besides, overweight has been linked to specific co-morbidities that are very concerning, such as hypertension, type 2 diabetes mellitus, coronary artery diseases, sleep apnea among others (Fedele et al., 2021; Holly et al., 2020; Magdy Beshbishy et al., 2020; Popkin et al., 2020).

Adipose tissue was identified as a reservoir for SARS-CoV-2 virus (Kruglikov et al., 2020; Ranjan et al., 2020). It also creates a microenvironment with several hormonal and metabolic effects that worsen the infection. Excessive fat tissue was linked with the upregulation of Angiotensin-Converting Enzyme 2 (ACEII) receptors, which are used by the SARS-CoV-2 virus to infect host cells at several organs (Kang et al., 2020; Magdy Beshbishy et al., 2020). Moreover, the low inflammatory status of the obese body could lead to cytokine storm, elevated interleukin levels and, eventually, excessive inflammatory response after COVID-19 infection (Biscarini et al., 2020; Seidu et al., 2020; Soeroto et al., 2020). It is well-known that adipose tissue secretes leptin and adiponectin and those two hormones play a major pro-inflammatory and anti-inflammatory roles (Gunturiz Albarracín and Forero Torres, 2020). However, what has been discovered recently is the association between COVID-19 complications and inflammatory effects of leptin and adiponectin (Méry et al., 2020). Another possible explanation for poor COVID-19 infection outcomes in obese and overweight patients is the mechanical consequences of excessive fat tissue on the respiratory system (Curtin et al., 2020). Visceral fat limits diaphragmatic movement, especially in the prone position. Also, obesity decreases the expiratory reserve volume of the lungs, affects the pulmonary perfusion, increase the chances for lung fibrosis and excise neck fat tissue affects the intubation process (Kwok et al., 2020; Malik et al., 2020; Soeroto et al., 2020).

Unfortunately, the lockdown measures that aimed to flatten the curve have led to not only negative economic consequences but also it was associated with reports about extra food consumption, very limited exercises opportunities, stress-related eating disorders and all of these behaviors would eventually increase the risk for overweight, which would deteriorate COVID-19 management efforts (Cornejo-Pareja et al., 2020; Khan and Moverley Smith, 2020; Singh et al., 2020). This association between obesity and poor respiratory infection outcome has been observed before during the H1N1 epidemic, and it is a recurrent observation with seasonal flu, among other viral pneumonia infections (Michalakis et al., 2020; Shaka et al., 2020).

To the best of our knowledge, the association between overweight and COVID-19 outcome has not been investigated before in Jordan and there is only one published article that examined this association on patients from Arab ethnicity (Al-Sabah et al., 2020). The objective of the current study was to evaluate the correlation between excess weight and the duration and severity of symptoms in patients affected by the novel corona virus in a tertiary hospital in Amman, Jordan.

2. Materials And Methods

This is a single-center retrospective cross-sectional study of patients with confirmed positive COVID-19 diagnosis, who were admitted to a tertiary academic hospital between April and August 2020. At the time of data collection, all patients in Jordan with COVID-19 positive tests were under mandatory hospital quarantine regardless if they were symptomatic or asymptomatic (Samrah et al., 2020a).

A convenience sample of admitted COVID-19 cases was selected. Data were collected through reviewing patients' records and by a short telephone interview. All telephone interviews were conducted in July and August 2020. This study was reviewed and approved by the Hashemite University Institutional Review Board (IRB). After explaining the study purpose and details, verbal consent was obtained from all study participants during the telephone interview. For data protection purposes, all collected data in this study were de-identified data.

Inclusion criteria were any adult patient (18+ years old) with confirmed COVID-19 PCR test who was admitted to Prince Hamza Hospital. Included cases were diagnosed with SARS-CoV-2 infection based on the World Health Organization's interim guidance (Ravi et al., 2020). The confirmation of SARS-CoV-2 infection was done by Real-Time Polymerase Chain Reaction (RT-PCR) assay using a nasal or a pharyngeal swab. Exclusion criteria were patients without a confirmed test, patients with missing anthropometric measurement data at the medical record and pregnant women.

The dependent variables of this study were the duration of symptoms, defined here as those patients complaining of any coronavirus associated symptoms and ICU admission.

Several covariates of interest were collected in the current study, such as age, sex, weight, height, and comorbidities. BMI was calculated in kilograms per meter squared on admission through standardized measurements of weight and height. The patient was considered overweight when the BMI result was between 25 and 29.9 and considered obese when the BMI was 30 or more (Hijona Elósegui et al., 2020). Comorbidities were identified if the patient had a medical record with an established diagnosis, or was on medications known to treat these comorbidities.

3. Statistical Analysis

Means and Standard Deviation (SD) were calculated for age and BMI. Categorical patient characteristics were summarized with counts and percentages. Pearson correlation was used to measure the correlation between study variables. Multivariable logistic regression analysis was performed to examine the association between ICU Admission adjusting for the potential effects of BMI, age, sex and comorbidities. Results were presented as odds

ratios (OR) with 95% confidence intervals (C.I.s). A p-value of less than 0.05 was considered statistically significant. Data were analyzed using Statistical Package for Social Science (SPSS) software (IBM Corp. Released 2017. IBM SPSS Statistics for Windows, Version 25.0. Armonk, NY: IBM Corp).

4. Results

One hundred and seventy patients participated in the current study. Around two-thirds of the participants were female patients. The mean age of study participants was 41.8 ± 14.4 years. The main characteristics of the included COVID-19 participants are described in Table 1. Around one-quarter of the participants had one or more non-communicable diseases (NCDs). The most frequent reported NDCs were type 2 Diabetes mellitus (DM) and hypertension, 11.8% and 7.6%, respectively (Table 1).

Mean BMI for study participants was 27.6 ± 5.4. Six out of ten patients were either overweight or obese. The prevalence of overweight between hospitalized COVID-19 patients was 34.1% and the prevalence of obesity was 29.4%. Only 4.1% of the participants required ICU admission for COVID-19 management (Table 1).

Around half of the participants were symptomatic (56.5%). The symptoms lasted for almost two weeks (mean 13.1 ± 6.8 days). The three most common reported symptoms were cough, loss of smell and loss of taste, 25.9%, 31.8%, and 25.9%, respectively (Table 1).

Table 1 Characteristics of included COVID-19 cases (n=170)

Variable	Number	Percent
Age (years) (mean ± SD = 41.8 ± 14.4) range (18 – 83)		
Sex		
Male	58	34.1
Female	112	65.9
Comorbidities		
Type 2 DM	20	11.8
Hypertension	13	7.6
Other comorbidities	12	8.1
On chronic medications		
No	136	80.0
Yes	34	20.0
Received seasonal flu vaccine in 2019		
No	157	92.4
Yes	13	7.6
BMI (mean ± SD = 27.6 ± 5.4) range (17.6 – 45.5)		
Underweight (<18.5)	3	1.8
Normal (18.5-24.9)	59	34.7
Overweight (25.0 – 29.9)	58	34.1
Obese (≥ 30.0)	50	29.4
Requiring ICU admission for COVID-19 management		
No	163	95.9
Yes	7	4.1
Treated with an Oxygen mask	13	7.6
Treated with Hydroxychloroquine	81	47.6
Symptomatic		
No	74	43.5
Yes	96	56.5
Reported symptoms*		
Cough	44	25.9
Shortness of breath	24	14.1
Fever	46	27.1
General weakness	32	18.8
Loss of smell	54	31.8
Loss of taste	44	25.9
Headache	21	12.4
Gastrointestinal symptoms	23	13.5
Flu like symptoms	12	7.1
Symptoms duration (days) (n=96) (mean ± SD = 13.1 ± 6.8)		

* Percentages do not add up to 100% due to multiple symptoms.

On correlation analysis, BMI was statistically significantly correlated with COVID-19 symptoms duration (p-value = 0.003). Similarly, a significant correlation was identified between symptoms duration and ICU admission (p-value < 0.001), and a significant correlation was identified between symptoms duration and male gender (p-value = 0.044). On the other hand, the correlation analysis failed to identify an association between the presence of comorbidities and symptoms duration, p-value 0.174 (Table 2).

Table 2. Correlation of study variable with Symptoms Duration (n=96)

		Gender	Comorbidities	Requiring ICU admission for COVID-19 management	BMI
Symptoms Duration	Pearson Correlation	0.155*	0.105	0.314**	0.230**
	p-value	0.044	0.174	<0.001	0.003
	N	170	170	170	170

* Correlation is significant at the 0.05 level (2-tailed).

** Correlation is significant at the 0.01 level (2-tailed).

Meanwhile, multivariate analysis was used to examine the adjusted effect of the study variable on ICU admission. The only variable that was a significantly associated factor with ICU admission was the age of 60+ years, after controlling for other variables (odds ratio 9.0, 95% C.I. 1.5 – 55.9) (Table 3).

Table 3. Adjusted Odd Ratio of Study Variables on ICU Admission for COVID-19 Management in Logistic Regression Analysis (n=170)*

Variable	Adjusted OR	95% C.I.	p-value
Age			
60+ years	9.0	(1.5 – 55.9)	0.018*
< 60 years	Reference	-	
Gender			
Male	1.0	(0.2 – 5.6)	0.978
Female	Reference	-	
Comorbidity			
Yes	1.6	(0.3 – 9.8)	0.613
No	Reference	-	

* Significant at $\alpha<0.05$ level

5. Discussions

SARS-CoV-2 infection presentation could range from asymptomatic to severe shortness of breath, lung fibrosis, multi-organ failure and eventually death of the patients (Holly et al., 2020; Zhu et al., 2020). The current study revealed that half of the hospitalized Jordanian patients were asymptomatic. This percentage of asymptomatic patients is higher than the previously reported prevalence of asymptomatic SARS-CoV-2 infection in a Korean sample (Kim et al., 2020). However, due to the study methodology of telephone interviews, survival bias could explain this higher asymptomatic prevalence in the current study cohort. On the other hand, the prevalence of asymptomatic cases in the current study is in line with reported 40 to 45% prevalence in Oran & Topol review of the current literature (Oran and Topol, 2020).

The main finding of the current study was the significant association between increased BMI and longer COVID-19 symptoms in a group of Jordanian patients. A similar significant association was reported in a group of Kuwaiti patients where obesity was associated with significant poor COVID-19 outcomes (Al-Sabah et al., 2020). In addition, in five recent meta-analysis and review studies, a significant association between body weight and poor COVID-19 outcome were identified (Chang et al., 2020; Cornejo-Pareja et al., 2020; Du et al., 2020; Malik et al., 2020; Peres et al., 2020). For example, Rodríguez-Molinero et al. revealed that obesity was an independent risk factor for poor COVID-19 prognosis in a group of Spanish patients (Rodríguez-Molinero et al., 2020). Similarly, Fresán et al reported that obesity was an independent risk factor for hospitalization and COVID-19 severity, especially in young patients; Peters et al. reported that obesity increase the odds for COVID-19 mortality for both genders (Fresán et al., 2020; Peters et al., 2020). Even though some studies identified increased BMI risk on COVID-19 poor outcome among certain groups, such as young people, women or people of black and Asian ethnic backgrounds, it seems that obesity is considered an independent risk factor for poor COVID-19 outcome across all patients groups, and even sometimes preceding the age as the main risk factor for poor prognosis of this novel infection (Caci et al., 2020; Fresán et al., 2020; Magdy Beshbishy et al., 2020; Moussa et al., 2020; Popkin et al., 2020).

The synergistic effects of overweight and obesity pandemic on COVID-19 pandemic made some researchers invent a new pandemic term, which is Covibesity, to emphasize the daring effects of these two pandemics when they interact with each other (Khan and Moverley Smith, 2020). In the current study, six out every ten COVID-19 confirmed cases in Jordan were obese or overweight. Currently, there is emerging evidence about the increased susceptibility of obese patients of acquired COVID-19 infection in community settings. However, this is an area that requires further investigation (Kimura and Namkoong, 2020).

The current cohort included seven patients who required an ICU admission after COVID-19 infection. This would limit the measurement of factors associated with ICU admission. However, it is not surprising that age was identified as an independent risk factor for ICU admission in the current study, after adjusting for other factors. Biscarini et al. conducted a larger study on Italian patients to explore the risks of ICU admission after COVID-19 infection, and they found that obesity was significantly associated with ICU admission after controlling for other variables (Biscarini et al., 2020). In addition, Popkin and colleagues revealed that obesity and overweight are both independent risk factors for ICU, IMV and mortality after SARS-CoV-2 infection (Popkin et al., 2020).

Although there is still not enough evidence about the efficacy of Hydroxychloroquine in COVID-19 management, from our medical records review, it seems

that half of the hospitalized COVID-19 patients in Jordan were treated with Hydroxychloroquine (Table 1). This might require further review from health authorities about the need for applying and monitoring the local standard operating procedure (SOPs) in hospital settings (Das et al., 2020; Dragojevic Simic et al., 2020).

According to the current study findings, the average duration for COVID-19 symptoms was 13.1 ±6.8 days. This is longer than Shah et al. findings, who reported a median duration of seven days in a cohort of American patients. However, Shah et al. study was conducted in an emergency department settings, while the current study was conducted in inpatients settings, and this could explain this difference in symptoms duration (Shah et al., 2020). On the other hand, Gupta et al. reported much shorter symptoms durations (two days), but their study sample was composed of only 21 Indian patients who were identified in February and March 2020 (Gupta et al., 2020). It seems that the focus of most COVID-19 studies is on mortality and severe outcomes, and there is a gap in the current literature about symptoms duration, especially in mild and moderate cases (Älgå et al., 2020).

The most common identified symptoms in this study were cough, loss of smell and loss of taste. This is slightly different from Kwok et al. findings who reported fever and cough as the most common symptoms of SARS-CoV-2 infection (Kwok et al., 2020). This difference in symptoms prevalence could be explained by the difference in study methodology, with recall biased of telephone interviews and with incomplete data documentation at the medical records.

In addition to BMI association with longer duration of COVID-19 symptoms, the current study revealed an independent significant association between gender and symptoms duration. Seidu and colleagues reported a similar association between male gender and poor COVID-19 outcome (Seidu et al., 2020). Several physiological and behavioral factors could explain this association such as the increased prevalence of tobacco product consumption between male patients, the effect of testosterone hormone and immune response differences (Howard, 2021; Salah and Mehta, 2020; Womersley et al., 2020).

Finally, the main limitations of the current study are the cross-sectional nature of the study, which does not allow for the measurement of causality between BMI and symptoms duration. In addition, this study was conducted with survivors of this novel infection; therefore, the survival bias cannot be avoided. Finally, the small sample size and having a sample from a single center in the capital city would limit the generalization of study results on the entire Jordanian population. Meanwhile, the main strength of this study is having a sample of both symptomatic and asymptomatic patients, in addition to collecting the data in a hybrid methodology that involved telephone interviews and medical records review. Lastly, the current study is one of the very first studies to explore the effects of SARS-CoV-2 infection on sample of patients of Arab ethnicity.

6. Conclusions

Increased BMI is significantly associated with more prolonged symptoms duration after SARS-CoV-2 infection. Likewise, the male gender was an independent significant factor associated with longer symptoms duration. The Jordanian authorities are advised to develop and share focused awareness messages for overweight and obese individuals so they can have strict social distancing and other prevention measures against COVID-19. Obese and overweight persons are a vulnerable group for this respiratory infection and they deserve advanced and tailored efforts to protect them from its adverse outcomes.

Declaration of Interest

No conflicting interests.

References

Ajlouni, K., Khader, Y., Batieha, A., Jaddou, H., El-Khateeb, M., 2020. An alarmingly high and increasing prevalence of obesity in Jordan. Epidemiol Health **42**: e2020040.

Akour, A., Al-Tammemi, A.B., Barakat, M., Kanj, R., Fakhouri, H.N., Malkawi, A., Musleh, G., 2020. The Impact of the COVID-19 Pandemic and Emergency Distance Teaching on the Psychological Status of University Teachers: A Cross-Sectional Study in Jordan. The American Journal of Tropical Medicine and Hygiene.

Älgå, A., Eriksson, O., Nordberg, M., 2020. Scientific Publications During the Early Phase of the COVID-19 Pandemic: A Topic Modeling Study. J Med Internet Res.

Al-Sabah, S., Al-Haddad, M., Al-Youha, S., Jamal, M., Almazeedi, S., 2020. COVID-19: Impact of obesity and diabetes on disease severity. Clin Obes.

Biscarini, S., Colaneri, M., Ludovisi, S., Seminari, E., Pieri, T.C., Valsecchi, P., Gallazzi, I., Giusti, E., Cammà, C., Zuccaro, V., Mondelli, M.U., 2020. The obesity paradox: Analysis from the SMAtteo COvid-19 REgistry (SMACORE) cohort. Nutrition, Metabolism and Cardiovascular Diseases **30**: 1920–1925.

Blüher, M., 2019. Obesity: global epidemiology and pathogenesis. Nat Rev Endocrinol **15**: 288–298.

Caci, G., Albini, A., Malerba, M., Noonan, D.M., Pochetti, P., Polosa, R., 2020. COVID-19 and Obesity: Dangerous Liaisons. JCM **9**: 2511.

Caussy, C., Wallet, F., Laville, M., Disse, E., 2020. Obesity is Associated with Severe Forms of COVID-19. Obesity **28**: 1175–1175.

Chang, T., Chou, C., Chang, L., 2020. Effect of obesity and body mass index on coronavirus disease 2019 severity: A systematic review and meta-analysis. Obesity Reviews 21.

Cornejo-Pareja, I.M., Gómez-Pérez, A.M., Fernández-García, J.C., Barahona San Millan, R., Aguilera Luque, A., Hollanda, A., Jiménez, A., Jimenez-Murcia, S., Munguia, L., Ortega, E., Fernandez-Aranda, F., Fernández Real, J.M., Tinahones, F., 2020. Coronavirus disease 2019 and obesity. Impact of obesity and its main comorbidities in the evolution of the disease. Eur Eat Disorders Rev **28**: 799–815.

Curtin, K.M., Pawloski, L.R., Mitchell, P., Dunbar, J., 2020. COVID-19 and Morbid Obesity: Associations and Consequences for Policy and Practice. World Medical & Health Policy wmh3.361. 1

Cuthbertson, D.J., Alam, U., Tahrani, A., 2020. COVID-19 and obesity: an opportunity for change. Therapeutic Advances in Endocrinology **11**: 204201882094974.

Das, R.R., Behera, B., Mishra, B., Naik, S.S., 2020. Effect of chloroquine and hydroxychloroquine on COVID-19 virological outcomes: An updated meta-analysis. Indian J Med Microbiol **38**: 265–272.

Dragojevic Simic, V., Miljkovic, M., Stamenkovic, D., Vekic, B., Ratkovic, N., Simic, R., Rancic, N., 2020. An overview of antiviral strategies for coronavirus 2 (SARS-CoV-2) infection with special reference to antimalarial drugs chloroquine and hydroxychloroquine. Int J Clin Pract e13825.

Du, Y., Lv, Y., Zha, W., Zhou, N., Hong, X., 2020. Association of Body mass index (BMI) with Critical COVID-19 and in-hospital Mortality: a dose-response meta-analysis. Metabolism 154373.

Dyett, J., 2020. Possible link between obesity and severe COVID-19. Medical Journal of Australia **213**: 380.

Fedele, D., De Francesco, A., Riso, S., Collo, A., 2021. Obesity, malnutrition, and trace element deficiency in the coronavirus disease (COVID-19) pandemic: An overview. Nutrition **81**: 111016.

Fresán, U., Guevara, M., Elía, F., Albéniz, E., Burgui, C., Castilla, J., Working Group for the Study of COVID-19 in Navarra, Martín, C., Navascués, A., Eugenia Portillo, M., Polo, I., Ezpeleta, C., Albéniz, E., Elía, F., Gorricho, J., Ardanaz, E., Ascunce, N., Arriazu, M., Barricarte, A., Barriuso, L., Burgui, C., Casado, I., Díaz, J., Ederra, M., Egüés, N., Fresán, U., Garde, C., Gómez-Ibáñez, C., García Cenoz, M., García, V., Guevara, M., Iriarte, N., Martínez-Baz, I., Moreno-Iribas, C., Sayón, C., Vidán, J., Castilla, J., 2020. Independent role of morbid obesity as a risk factor for COVID-19 hospitalization: a Spanish population-based cohort study. Obesity oby.23029.

Gunturiz Albarracín, M.L., Forero Torres, A.Y., 2020. Adiponectin and Leptin Adipocytokines in Metabolic Syndrome: What Is Its Importance? Dubai Diabetes Endocrinol J **26**: 93–102. https://doi.org/10.1159/000510521

Gupta, N., Agrawal, S., Ish, P., Mishra, S., Gaind, R., Usha, G., Singh, B., Sen, M.K., Covid Working Group, S.H., 2020. Clinical and epidemiologic profile of the initial COVID-19 patients at a tertiary care centre in India. Monaldi Arch Chest Dis 90. https://doi.org/10.4081/monaldi.2020.1294

Hall, D.M.B., Cole, T.J., 2006. What use is the BMI? Arch Dis Child **91**: 283–286.

Hijona Elósegui, J.J., Carballo García, A.L., Fernández Risquez, A.C., 2020. New evidences that discard the possible vertical transmission of SARS-CoV-2 during pregnancy. Medicina Clínica (English Edition) **155**: 313–314.

Holly, J.M.P., Biernacka, K., Maskell, N., Perks, C.M., 2020. Obesity, Diabetes and COVID-19: An Infectious Disease Spreading From the East Collides With the Consequences of an Unhealthy Western Lifestyle. Front. Endocrinol. **11**: 582870.

Howard, M.C., 2021. Gender, face mask perceptions, and face mask wearing: Are men being dangerous during the COVID-19 pandemic? Pers Individ Dif **170**: 110417.

Huang, Y., Lu, Y., Huang, Y.-M., Wang, M., Ling, W., Sui, Y., Zhao, H.-L., 2020. Obesity in patients with COVID-19: a systematic review and meta-analysis. Metabolism **113**: 154378.

Kang, Z., Luo, S., Gui, Y., Zhou, H., Zhang, Z., Tian, C., Zhou, Q., Wang, Q., Hu, Y., Fan, H., Hu, D., 2020. Obesity is a potential risk factor contributing to clinical manifestations of COVID-19. Int J Obes.

Khan, M.A., Moverley Smith, J.E., 2020. "Covibesity," a new pandemic. Obesity Medicine **19**: 100282.

Kim, G.-U., Kim, M.-J., Ra, S.H., Lee, J., Bae, S., Jung, J., Kim, S.-H., 2020. Clinical characteristics of asymptomatic and symptomatic patients with mild COVID-19. Clin Microbiol Infect **26**: 948.e1-948.e3.

Kimura, T., Namkoong, H., 2020. Susceptibility of obese population to COVID-19. International Journal of Infectious Diseases.

Klatsky, A.L., Zhang, J., Udaltsova, N., Li, Y., Tran, H.N., 2017. Body Mass Index and Mortality in a Very Large Cohort: Is It Really Healthier to Be Overweight? Perm J **21:** 16–142.

Kruglikov, I.L., Shah, M., Scherer, P.E., 2020. Obesity and diabetes as comorbidities for COVID-19: Underlying mechanisms and the role of viral–bacterial interactions. eLife **9:** e61330.

Kwok, S., Adam, S., Ho, J.H., Iqbal, Z., Turkington, P., Razvi, S., Le Roux, C.W., Soran, H., Syed, A.A., 2020. Obesity: A critical risk factor in the COVID-19 pandemic. Clin Obes.

Liu, M., Deng, C., Yuan, P., Ma, J., Yu, P., Chen, J., Zhao, Y., Liu, X., 2020. Is there an exposure–effect relationship between body mass index and invasive mechanical ventilation, severity, and death in patients with COVID-19? Evidence from an updated meta-analysis. Obesity Reviews 21.

Lockhart, S.M., O'Rahilly, S., 2020. When Two Pandemics Meet: Why Is Obesity Associated with Increased COVID-19 Mortality? Med S2666634020300106.

Magdy Beshbishy, A., Hetta, H.F., Hussein, D.E., Saati, A.A., C. Uba, C., Rivero-Perez, N., Zaragoza-Bastida, A., Shah, M.A., Behl, T., Batiha, G.E.-S., 2020. Factors Associated with Increased Morbidity and Mortality of Obese and Overweight COVID-19 Patients. Biology **9:** 280.

Malik, P., Patel, U., Patel, K., Martin, M., Shah, C., Mehta, D., Malik, F.A., Sharma, A., 2020. Obesity a predictor of outcomes of COVID-19 hospitalized patients—A systematic review and meta-analysis. J Med Virol jmv.26555.

Méry, G., Epaulard, O., Borel, A.-L., Toussaint, B., Le Gouellec, A., 2020. COVID-19: Underlying Adipokine Storm and Angiotensin 1-7 Umbrella. Front. Immunol. **11**: 1714.

Michalakis, K., Panagiotou, G., Ilias, I., Pazaitou-Panayiotou, K., 2020. Obesity and COVID-19: A jigsaw puzzle with still missing pieces. Clin Obes.

Moussa, O., Zakeri, R., Arhi, C., O'Kane, M., Snowdon-Carr, V., Menon, V., Mahawar, K., Purkayastha, S., 2020. Impact of COVID-19 on Obesity Management Services in the United Kingdom (The COMS-UK study). OBES SURG.

Oran, D.P., Topol, E.J., 2020. Prevalence of Asymptomatic SARS-CoV-2 Infection : A Narrative Review. Ann Intern Med **173**: 362–367.

Peres, K.C., Riera, R., Martimbianco, A.L.C., Ward, L.S., Cunha, L.L., 2020. Body Mass Index and Prognosis of COVID-19 Infection. A Systematic Review. Front. Endocrinol. **11**: 562.

Peters, S.A.E., MacMahon, S., Woodward, M., 2020. Obesity as a risk factor for COVID-19 mortality in women and men in the UK biobank: Comparisons with influenza/pneumonia and coronary heart disease. Diabetes Obes Metab.

Popkin, B.M., Du, S., Green, W.D., Beck, M.A., Algaith, T., Herbst, C.H., Alsukait, R.F., Alluhidan, M., Alazemi, N., Shekar, M., 2020. Individuals with obesity and COVID-19: A global perspective on the epidemiology and biological relationships. Obesity Reviews 21.

Rancourt, R.C., Schellong, K., Plagemann, A., 2020. Coronavirus disease 2019 and obesity: one pandemic meets another. Am J Obstet Gynecol.

Ranjan, P., Kumar, A., Chowdhury, S., Pandey, S., Choudhary, A., Bhattacharya, A., Singh, A., Pandey, R.M., Wig, N., Vikram, N.K., 2020. Is excess weight a risk factor for the development of COVID 19 infection? A preliminary report from India. Diabetes & Metabolic Syndrome: Clinical Research & Reviews **14:** 1805–1807.

Ravi, N., Cortade, D.L., Ng, E., Wang, S.X., 2020. Diagnostics for SARS-CoV-2 detection: A comprehensive review of the FDA-EUA COVID-19 testing landscape. Biosens Bioelectron **165:** 112454.

Rodríguez-Molinero, A., Gálvez-Barrón, C., Miñarro, A., Macho, O., López, G.F., Robles, M.T., Dapena, M.D., Martínez, S., Milà Ràfols, N., Monaco, E.E., Hidalgo García, A., on behalf of the COVID-19 Research Group of CSAPG, 2020. Association between COVID-19 prognosis and disease presentation, comorbidities and chronic treatment of hospitalized patients. PLoS ONE **15**: e0239571.

Salah, H.M., Mehta, J.L., 2020. Hypothesis: Sex-Related Differences in ACE2 Activity May Contribute to Higher Mortality in Men Versus Women With COVID-19. J Cardiovasc Pharmacol Ther 1074248420967792.

Samrah, S.M., Al-Mistarehi, A.-H., Aleshawi, A.J., Khasawneh, A.G., Momany, S.M., Momany, B.S., Abu Za'nouneh, F.J., Keelani, T., Alshorman, A., Khassawneh, B.Y., 2020a. Depression and Coping Among COVID-19-Infected Individuals After 10 Days of Mandatory in-Hospital Quarantine, Irbid, Jordan. Psychol Res Behav Manag **13**: 823–830.

Samrah, S.M., Al-Mistarehi, A.-H.W., Ibnian, A.M., Raffee, L.A., Momany, S.M., Al-Ali, M., Hayajneh, W.A., Yusef, D.H., Awad, S.M., Khassawneh, B.Y., 2020b. COVID-19 outbreak in Jordan: Epidemiological features, clinical characteristics, and laboratory findings. Annals of Medicine and Surgery (2012) **57:** 103–108.

Seidu, S., Gillies, C., Zaccardi, F., Kunutsor, S.K., Hartmann-Boyce, J., Yates, T., Singh, A.K., Davies, M.J., Khunti, K., 2020. The impact of obesity on severe disease and mortality in people with SARS-CoV-2: A systematic review and meta-analysis. Endocrinol Diab Metab.

Shah, S.J., Barish, P.N., Prasad, P.A., Kistler, A., Neff, N., Kamm, J., Li, L.M., Chiu, C.Y., Babik, J.M., Fang, M.C., Abe-Jones, Y., Alipanah, N., Alvarez, F.N., Botvinnik, O.B., Castaneda, G., CZB CLIAhub Consortium, Dadasovich, R.M., Davis, J., Deng, X., DeRisi, J.L., Detweiler, A.M., Federman, S., Haliburton, J., Hao, S., Kerkhoff, A.D., Kumar, G.R., Malcolm, K.B., Mann, S.A., Martinez, S., Mary, R.K., Mick, E., Mwakibete, L., Najafi, N., Peluso, M.J., Phelps, M., Pisco, A.O., Ratnasiri, K., Rubio, L.A., Sellas, A., Sherwood, K.D., Sheu, J., Spottiswoode, N., Tan, M., Yu, G., Kangelaris, K.N., Langelier, C., 2020. Clinical features, diagnostics, and outcomes of patients presenting with acute respiratory illness: A retrospective cohort study of patients with and without COVID-19. EClinicalMedicine **27**: 100518.

Shaka, H., Raghavan, S., Trelles-Garcia, V.P., Trelles-Garcia, D., Abusalim, A.I., Parfieniuk, A., Ojemolon, P.E., Azubuike, C., 2020. Predicting COVID-19 Using Retrospective Data: Impact of Obesity on Outcomes of Adult Patients With Viral Pneumonia. Cureus.

Singh, S., Bilal, M., Pakhchanian, H., Raiker, R., Kochhar, G.S., Thompson, C.C., 2020. Impact of Obesity on Outcomes of Patients With Coronavirus Disease 2019 in the United States: A Multicenter Electronic Health Records Network Study. Gastroenterology S0016508520350678.

Smati, S., Tramunt, B., Wargny, M., Caussy, C., Gaborit, B., Vatier, C., Vergès, B., Ancelle, D., Amadou, C., Bachir, L.A., Bourron, O., Coffin-Boutreux, C., Barraud, S., Dorange, A., Fremy, B., Gautier, J., Germain, N., Larger, E., Laugier-Robiolle, S., Meyer, L., Monier, A., Moura, I., Potier, L., Sabbah, N., Seret-Bégué, D., Winiszewski, P., Pichelin, M., Saulnier, P., Hadjadj, S., Cariou, B., Gourdy, P., for the CORONADO investigators, 2020. Relationship between obesity and severe COVID-19 outcomes in patients with type 2 diabetes: Results from the CORONADO study. Diabetes Obes Metab dom.14228.

Soeroto, A.Y., Soetedjo, N.N., Purwiga, A., Santoso, P., Kulsum, I.D., Suryadinata, H., Ferdian, F., 2020. Effect of increased BMI and obesity on the outcome of COVID-19 adult patients: A systematic review and meta-analysis. Diabetes & Metabolic Syndrome: Clinical Research & Reviews **14**: 1897–1904.

Womersley, K., Ripullone, K., Peters, S.A., Woodward, M., 2020. Covid-19: Male disadvantage highlights the importance of sex disaggregated data. BMJ m2870.

Zhu, Z., Hasegawa, K., Ma, B., Fujiogi, M., Camargo, C.A., Liang, L., 2020. Association of obesity and its genetic predisposition with the risk of severe COVID-19: Analysis of population-based cohort data. Metabolism **112**: 154345.

JJBS

Volume 14, Number 3, September 2021
ISSN 1995-6673
Pages 493 - 501

Jordan Journal of Biological Sciences

Correlation of Chemerin with some Immunological Parameters in Type II Diabetes Mellitus Patients on Hemodialysis in Ramadi General Hospital

Salahaldin M. Fahad[1,*], Rashied M. Rashied[2], and Waleed N. Jaffal[3]

[1] Department of Biology, College of Sciences, University Of Anbar. Iraq. [2] Department of Biotechnology, College of Sciences, University Of Anbar. Iraq. [3]Department of Surgery, College of Medicine, University Of Anbar. Iraq.

Received: July 7, 2020; Revised: November 13, 2020; Accepted: December , 2020

Abstract

Diseases of kidney are among the most important causes of death in many countries. The major causes of chronic kidney disease include diabetes mellitus and chronic hypertension. This study was designed to evaluate some hematological and inflammation aspects in 95 patients, divided into (35) hemodialysis patients with diabetes, (35) hemodialysis patients without diabetes and (25) diabetes patients, and who attended at Ramadi General Hospital, in addition to (25) samples as control subject. Chemerin, Interleukin-18 (IL-18) and high sensitive C-reactive protein (hs-CRP) were established by ELISA. The results showed serum chemerin, interleukin-18 and hs-CRP were significantly higher in HD patients with diabetes (230.13±78.26 ng/ml at P=0.034, 677.23±99.14 pg/mL at P=0.026, and 15.77±2mg/L at P=0.048), respectively compared with control (110±20.42ng/ml, 143.68±35.78pg/mL, and 4.64±1.27mg/L), respectively. The results showed the significant and positive correlations between chemerin and hs-CRP or chemerin and IL-18 (r=0.149 at P=0.004 or r=0.123 at P=0.0325 in control), (r=0.165 at P=0.007 or r =0.190 at P=0.024 in diabetic patients), (r=0. 237 at P=0.0036 or r =0.263 at P= 0.038 in HD patients with diabetic) and (r=0. 0.235 at P = 0.0081or r=0.248 at P = 0.041in HD patients without diabetic) respectively. The mean of hemoglobin (Hb), Packed Cells Volume (PCV), Red Blood cells (RBC), White Blood Cells (WBC) and Lymphocytes were significantly decreased in HD patients without diabetes (8.55±0.63g/L (at p=0.0423), 27.63±1.31%(at p=0.028), 3.12±0.56 $\times 10^{12}$\ L (at p=0.035), 6.7±0.53 $\times 10^{9}$/L (at p=0.021) and 30.23±5.84%(at p= 0.046), respectively compared with control. The mean of Monocytes% (17.23±7.28% at p=0.031) and Granulocyte% (59.31±9.45 % at p=0.042) were significantly higher in HD patients with diabetes, while mean of Mononocytes% was significant lower in diabetic patients. This study suggests a significant role of chemerin, hs-CRP and IL-18 in the pathogenesis and progression of diabetic complications, and we can use these parameters for predicting the progression of diabetic nephropathy in the early stages of CKD.

Keywords: Chronic kidney disease (CKD), Chemerin, Type II Diabetes mellitus (T2DM), Hemodialysis (HD), Interleukin-18.

1. Introduction

Chronic kidney disease is a progressive loss of kidney function over a period of months or years through five stages. Therefore, CKD is a major global public health problem (George et al., 2015). The single most common of CKD is diabetic nephropathy (DN), which occurs as a result of microangiopathy caused by diabetes, where approximately one-third of all diabetic patients are affected by DN (Franz et al., 2012). In addition, renal involvement is a major cause of morbidity and mortality in the diabetic population (Donate-Correa et al., 2015). Persistent inflammation is a risk factor of CKD progress, thereby inflammation reduction is very significant in the treatment of kidney disease (Kurts et al., 2013). Interleukin-18 (IL-18) is a pro-inflammatory protein that acts as an immunoregulatory agent involved in the reactions of both innate and acquired immunity (Kraydaschenko et al., 2016). Recently, IL-18 has been suggested to play a crucial role in the initiation, development, and progression of DN inT2DM patients (Abid Hammed, 2019). Accordingly, plasma IL-18 may reflect insulin-resistance not only in patients with established T2DM, but also in non-diabetic controls(Fischer et al., 2005). Among inflammatory biomarkers, the best evidence to date supports the use of hs-CRP as an independent predictor of increased cardiovascular disease (CVD) risk in diabetic and non-diabetic patients(Pfützner et al., 2007). HsCRP is a well-known marker of systemic inflammation and a most frequently used inflammation marker(Ali et al., 2019). These characteristics make hsCRP a reliable marker of inflammation(Thaha et al., 2018). In CKD, IL-18 has been proposed to be a marker for early detection and outcome prediction in patients with acute myocardial infraction, and nephropathy(Chang et al., 2015). Adipose tissue produces a variety of proteins called adipokines, one of which is chemerin, which modulates the function of innate immune cells and may be a potential candidate in the pathogenesis of cardiovascular complications (Salama et al., 2016). Chemerin positively correlated with inflammatory markers

* Corresponding author e-mail: salahalden615@gmail.com.

such as hs-CRP(Blaszak et al., 2015). Interestingly, it has been previously reported that kidney function is inversely related to circulating chemerin in HD patients, chemerin features anti-microbial as well as chemotactic properties, plays a regulatory role for immune response including regulation of specific immune cell migration, and anti-inflammatory effects on macrophages (Leiherer et al., 2016; Haddad et al., 2018). Anemia is a common feature in patients with CKD and is mainly attributable to the relative decrease in erythropoietin (EPO) production by the kidneys(Vanholder et al., 2016). Anemia is defined as Hb level lower than (12)g/dL in humans according to WHO (Latiweshob et al, 2017). Stanifer et al., (2014) reported that mean of RBCs, Hb, and PCV are significantly lowered in CKD patients, which occurs earlier in these patients and tends to be of greater severity by CKD stages. Elevated total WBC and granulocyte counts are correlated with the raised progression of CKD (Kuo et al., 2018). Therefore, this study aimed to determine the association between immunological markers such as chemerin, IL-18, and hsCRP and diabetic nephropathy diagnosis in hemodialysis patients.

2. 2. Materials and Methods

2.1. Time and Location of collection

The Specimens collection were started from April, 2019 till the end of June 2019. HD patients with diabetes and HD patients without diabetes samples were collected from the Industrial Renal department and T2DM patients from the Diabetes Center for Treatment at Ramadi General Hospital.

2.2. Study design

The study is designed on 95 patients at age rang (30-70) years. The patients in this study included (35) hemodialytic patients with diabetes and (35) hemodialytic patients without diabetes and (25) T2DM patients without any other complications. The diagnosis was performed by specialist doctors. And (25) samples as control group were included in the study. The controls were selected among subjects who were healthy in terms of non-diabetic, non-hypertensive, no other endocrine disorders at the time of sampling.

2.3. Blood Samples Collection

Before the collection of samples, all patients provided written informed consent prior to participation in this study, which was approved by institutional ethics committees (university Of Anbar\ ethical approval committee). From each patient and control, 5 ml of blood was obtained. The blood samples were divided into two aliquots; 2 ml was dispensed in tube containing ethylene diamine tetracetic acid (EDTA). This blood was used for CBC estimation such as white blood cells (WBC), WBC differentiation, red blood cells (RBC), hemoglobin (Hb) and packed cell volume (PCV). While 3ml was dispensed in a gel plain tube to collect serum, the serum was used to estimate the Chemreine, interleukin-18, and Hs-CRP by using ELISA technique.

2.4. Anthropometric Measurements

Patients and controls are characterized in terms of age, gender, smoking and body mass index (BMI). The BMI is calculated by dividing weight (kilogram)/ the squared height (meter), BMI= Kg/m2 (Abid Hammed, 2019).

2.5. laboratory investigation

Concentrations of serum chemrein was estimated by commercially available chemerin ELISA assays kit provided from Elabscience Company / U.S.A. The IL-18 level was estimated by the direct ELISA kit method provided from Elabscience Company / U.S.A. The concentrations of serum HsCRP was measured by the ELISA direct kit method which provided from Shanghai company / China. All ELISA procedures were carried out according to the manufacturer's instructions.

2.6. Determination of hematological parameters

Hematological parameters in whole blood of all study groups are determined by using an automated hematology analyzers XT 2000i (from sysmex, Japan).

2.7. Statistical Methods:

The data were translated into a computerized database structure, and the statistical analyses were carried out using SPSS version 25. One way ANOVA test was used to find means and standard deviation (SD) for all variables of the study. The difference of significances in proportions was analyzed by LSD test. The correlations between variables was confirmed by Pearson correlation analysis. P-value less than 0.05 was considered to be significant.

3. Results

3.1. Characteristics of controls and patients:

These results showed no significant difference at level ($p \leq 0.05$) in mean of age, smoking, gender and BMI among patients and healthy control, as shown in table (1).

Table 1. Characteristics of controls and patients:

Factor	Control	T2DM	HD patients with diabetes	HD patients without diabetes	P
Age(Y)	52.6±6.01	54.12±7.83	55.94±11.2	53 ±12.47	0.065^{NS}
Gender (M/F)	12M/13F	12M/13F	16M/19F	15M20F	0.507^{NS}
Smoking (S/no S)	10/15	14/11	17/18	22/13	0.113^{NS}
BMI	24.61±0.35	28.97±0.4	28.71±0.54	27.03±0.62	0.777^{NS}

Results were expressed as mean ± SD, ANOVA test was used for the purpose of comparison between the four groups. *** NS:** Mean non-significant differences at $P \leq 0.05$.
HD= hemodialysis, **BMI**=body mass index, **M**=Male, **F**=female, **S**= Smokers, **no S**= no smokers, **T2DM**= Type II diabetes mellitus.

3.2. Determination of Chemrein between the four study groups

As shown in the table (2), the mean of serum Chemerin was significantly higher in HD patients with diabetes (230.13±78.26) ng/ml, followed by HD patients without diabetes (221.90±65.17)ng/ml compared with control (110±20.42) ng/ml. Also, mean of serum chemerin significant increased in diabetic patients (212.29±70.88)ng/ml when compared with control.

Table 2. The difference in chemerin level between the four study groups:

Chemerin (30-190) ng/ml			
Groups	N	Mean±SD	Range
Control	25	110±20.42a	(95-175)
Diabetes	25	212.29±70.88b	(142-275)
HD patients with diabetes	35	230.13±78.26c	(172-297)
HD patients without diabetes	35	221.90±65.17d	(152-273)
Total	120	183.66±21.68	(95-297)

*Different Letters (a, b, c, d): Mean significant difference at P =0.034.

SD= Stander Deviation.

3.3. Human IL-18(Interleukin 18) level between the four study groups

As demonstrated in table (3), the IL-18 level was significantly higher in HD patients with diabetes (677.23±99.14)pg/mL followed by HD patients without diabetes (589±44.77) pg/mL compared with control group(143.68±35.78) pg/mL, also IL-18 level was significantly increased in diabetic patients (245.18±87.45) pg/mL when compared with control group.

Table 3. The difference in IL-18 level between the four study groups:

IL-18 (20-800) pg/mL			
Groups	N	Mean±SD	Range
Control	25	143.68±35.78[a]	(110- 178)
Diabetes	25	245.18±87.45[b]	(168-332)
HD patients with diabetes	35	677.23±99.14[c]	(578-776)
HD patients without diabetes	35	589±44.77[d]	(545-633)
Total	120	413.12±76.58	(312- 524)

*Different Letters (a, b, c, d): Mean significant difference at P =0.026.

SD= Stander Deviation, **IL-18=** Interleukin 18**.**

3.4. Human high sensitivity C-Reactive Protein (hs-CRP) level in four study groups

As shown in the table (4), the mean of hs-CRP was significantly higher in HD patients with diabetes (15.77±2) mg/L followed by HD patients without diabetes was (14.61±7.13) mg/L compared with control (4.64±1.27) mg/L, also mean of serum hs-CRP was significant increase diabetic patients (8.06±2.28) mg/L when compared with control.

Table (4): The difference in hsCRP level between the four study groups:

Hs-CRP (0.05-12)mg/L			
Groups	**N**	**Mean±SD**	**Range**
Control	25	4.64±1.27[a]	(3.44-5.8)
Diabetes	25	8.06±2.28[b]	(5.78-10.3
HD patients with diabetes	35	15.77±2[c]	(13.7-17.7)
HD patients without diabetes	35	14.61±7.13[c]	(7.3-21.7)
Total	120	10.42±4.40	(4.4-20.6)

***Different Letters (a, b, c):** Mean significant difference at P =0.048.

SD= Stander Deviation, **hs-CRP=** high sensitivity C-Reactive Protein.

3.5. Correlation between Chemerin and hs-CRP or Chemerin and IL-18 between the four study groups.

As shown in Figures (1) and (2), there were significant and positive correlations between chemerin and hs-CRP (r =0.149, P =0.004; Figure A1) or chemerin and IL-18 (r=0.123, P= 0.0325; Figure B1) in control group. The correlations between chemerin and hs-CRP were (r=0.165, P=0.007; Figure A2) and (r=0. 237, P=0.0036; Figure A3) or chemerin and IL-18 were (r =0.190, P=0.024; Figure B2) and (r =0.263, P=0.038; Figure B3) in diabetic patients group and HD patients with diabetic group respectively. Figure A4 indicates the correlation of chemerin with hs-CRP (r=0. 0.235, P = 0.0081) and chemerin with IL-18 (r=0.248, P = 0.041; Figure B4) in HD patients without diabetic group.

3.6. Determination of Hb, PCV and RBC in the four study groups.

The result indicates the significant difference in mean of Hb, PCV, and RBC in groups of the study. The levels of Hb, PCV, and RBC were significantly decreased in HD patients with diabetes group and HD patients without diabetes group (8.76±0.78 and 8.55±0.63)g/L, (28.29±1.62 and 27.63±1.31)%, and (3.27±0.40 and 3.12±0.56) ×1012\ L respectively, compared with control group (13.32±1.70)g/L, (41.88±2.90)% and (4.81±0.60)*10^{12}\L, while Hb, PCV, and RBC showed non-significant difference in diabetic patients group: (13.1±1.41) g/L, (41.78±1.33)%, and (4.651±0.70) ×10^{12}\ L compared with control, as shown in the table (5).

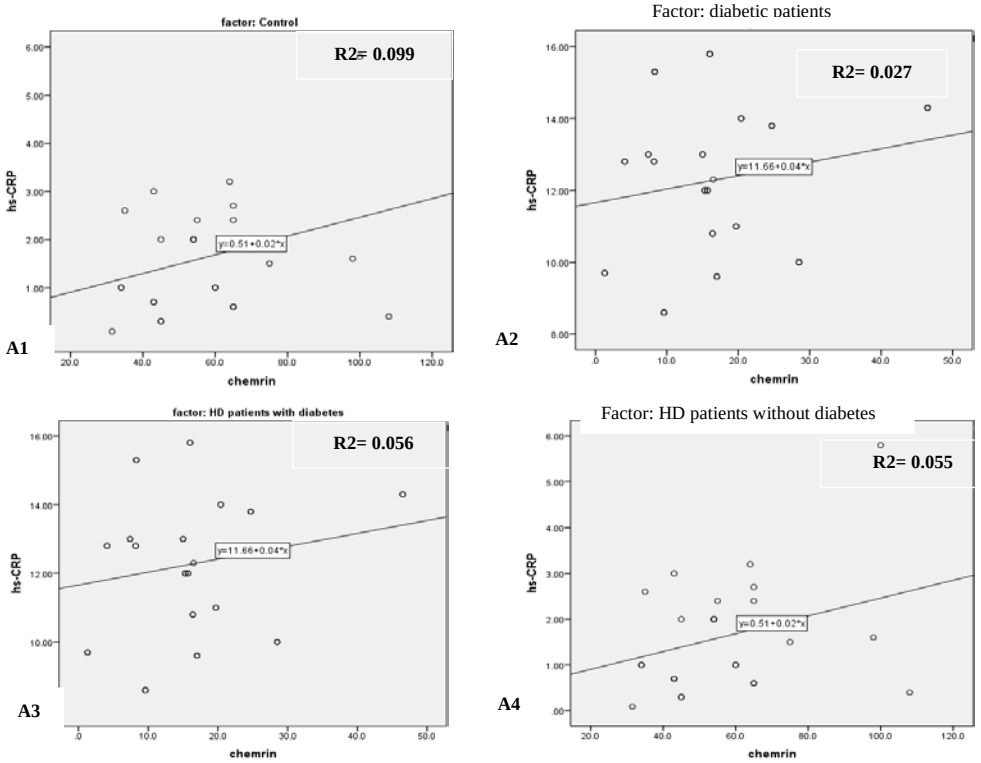

Figure1. Correlation determine between serum Chemerin and high sensitivity C-Reactive Protein (hs-CRP): Figure A1: In control at P =0.004.Figure A2: In diabetic patients at P=0.007.Figure A3: HD patients with diabetes at P=0.0036.Figure A4: HD patients without diabetes at P = 0.0081.

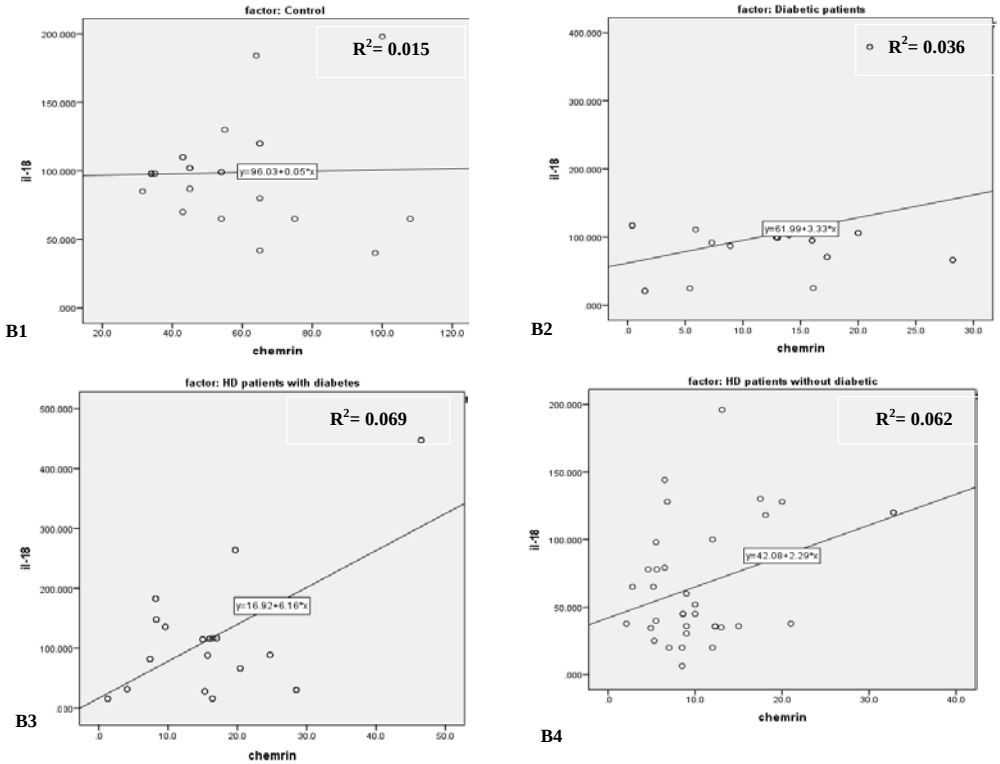

Figure 2. Correlation between serum Chemerin and Interleukin-18 (IL-18): Figure B1: In control at P= 0.0325.Figure B2: In diabetic patients at P=0.024.Figure B3: In HD patients with diabetes at P= 0.038. Figure B4: In HD patients without diabetes at P = 0.041.

Table (5): The difference in Hb, PCV and RBC in the four study groups.

Groups	N.	Mean±SD Hb (12-16) g\L	Mean±SD PCV % (36 – 50)%	Mean±SD RBCs (3.8–5.5) $\times 10^{12}$\ L
Control	25	13.32±1.70[a]	41.88±2.90[a]	4.81±0.60[a]
Diabetes	25	13.1±1.41[a]	41.78±1.33[a]	4.651±0.70[a]
HD patients with diabetes	35	8.76±0.78[b]	28.29±1.62[b]	3.27±0.40[b]
HD patients without diabetes	35	8.55±0.63[b]	27.63±1.31[c]	3.12±0.56[b]
Total	120	10.76±2.40	34.43±7.69	3.55±0.86
P Value		0.0423	0.028	0.035

***Different Letters (a, b, c):** Mean significant difference at P ≤0.05.

SD= Stander Deviation**, Hb=** Hemoglobin**, PCV=** packed cell volume**, RBC=** Red Blood Cell.

3.7. The difference in WBC and WBC differentiation between the four study groups.

This study indicates the significant difference in mean of WBC, Lymphocytes, Monocytes and granulocytes of the study, where the mean of WBC and Lymphocytes were significantly lower in HD patients without diabetes group and HD patients with diabetes group (6.7±0.53 and 6.8±0.65) $\times 10^9$\ L and (31.47±4.59 and 30.23±5.84)% respectively, compared with control (7.14±1.37) $\times 10^9$/L and (35.76±4.21)%. While there were no significant differences in mean Lymphocytes between HD patients with a diabetes group and HD patients without a diabetes group. Also, the level of WBC and Lymphocytes showed a significant decrease in diabetic patients (7.12±0.59) $\times 10^9$/L and (32.34±3.02)% when compared with control. The mean of Mono % was significantly higher in HD patients with diabetes and HD patients without diabetes (17.23±7.28and 16.61±9.17)% respectively followed by in diabetic patients (11.17±1.45)% compared with control (11.16±1.53)%. Whereas mean of Granulocyte% was significantly higher in HD patients with diabetes (59.31±9.45)%, while no significant difference among diabetic patients, control group and HD patients without diabetes group in mean granulocyte % were (52.71±4.18, 53.19±4.16 and 53.21±14.16)% respectively, as shown in the table (6).

Table (6): The difference in WBC, Lympho%, Mono% and Granulocyte% between the four study groups.

Groups	N	Mean±SD WBC (4-10) $\times 10^9$/L	Mean±SD Lympho. % (20-40)%	Mean±SD Mono. % (3-15)	Mean±SD Granulocyte% (50-70)
Control	25	7.14±1.37[a]	35.76±4.21[a]	11.16±1.53[a]	53.19±4.16[a]
Diabetes	25	7.12±0.59[a]	32.34±3.02[b]	11.17±1.45[a]	52.71±4.18[a]
HD patients with diabetes	35	6.8±0.65[b]	31.47±4.59[b]	17.23±7.28[b]	59.31±9.45[b]
HD patients without diabetes	35	6.7±0.53[b]	30.23±5.84[b]	16.61±9.17[b]	53.21±14.16[a]
Total	120	6.22±2.02	32.02±8.82	14.52±6.95	54.88±9.90
P Value		0.021	0.046	0.031	0.042

***Different Letters (a, b, c):** Mean significant difference at P ≤0.05.

SD=Stander Deviation**, WBC=**White Blood Cell**, Lympho=** Lymphocyte**, Mono=** Monocyte**.**

4. Discussion:

4.1. Determination of Chemrein between the four study groups

The results in (Table 2) agreed with (Salama et al., 2016) who showed a significant difference in levels of chemerin in HD patients (332.1±21.54) ng/ml compared to healthy (278.6±10.02) ng/ml, and who found that the chemerin level increased in HD patients with diabetes (354.1±1.4)ng/ml compared with HD patients without diabetes (329±19.9) ng/ml.

These results were consistent with (Ali and Al Hadidi, 2013, Coimbra et al., 2014, Ahmed and Tahir, 2015) who recorded that the chemerin level significant increase in T2DM patients compared with control. These results were inconsistent with (Alissa et al., 2016) who recorded that the chemerin level non-significantly increased in control compared with diabetic patients. In this study, chemerin level increased in diabetic patients compared with control, and this may be due to taking anti-diabetic drugs by a proportion of their T2DM study subjects(Ali and Al Hadidi, 2013).

This adipokine is known to act on glucose metabolism in the liver, skeletal muscle and adipose tissue, promoting regulation of glucose absorption and modulating insulin secretion and sensitivity(Fontes et al., 2018). These results showed that the chemerin level increased in HD patients compared with control may due to decrease of renal function, which has a significant impact on serum chemerin concentration(Salama et al., 2016). The increased circulating chemerin concentration observed in HD patients is not a consequence of the adipose tissue excess, and there is no reason to assume that these medications relevantly impacted the presented results, as mentioned (Mathew and Corso, 2009, Salama et al., 2016). While circulating chemerin level is closely related to renal function, its high serum concentration found in CKD patients is probably a result of a renal failure-associated with decrease of GFR rate and impaired chemerin urine excretion(Blaszak et al., 2015). Chemerin is predictive of renal impairment and patients with high chemerin levels are at a significantly higher CVD risk, independent from their renal function. From a clinical point of view, the treatment of excessive chemerin levels to prevent the onset of diabetes or renal diseases might be a future task to be addressed by researchers (Leiherer et al., 2016).

4.2. Human IL-18(Interleukin 18) level between the four study groups

The results in (Table 3)agreed with (Shi et al.,2012, Abid Hammed,2019) who recorded that the mean IL-18 was significantly higher among HD patients with diabetes and diabetic patients compared to control. Patients with T2DM recently diagnosed appeared to have an essentially higher IL-18 level in contrast with non-diabetic subjects(Aso et al., 2003). IL-18 levels were raised by acute hyperglycemia in humans through an oxidative mechanism(Abid Hammed,2019). The increased IL-18 in HD patients is due to many reasons: firstly, CKD diagnosis, which is responsible for decreased renal clearances of IL-18, was probably the major sites of cytokine elimination, the primary factor that could affect these results. IL-18 is a mid-molecule and protein-bound uremic toxin which is difficult to extract by any of the currently available dialytic strategies(Vanholder et al., 2008), hence the reported IL-18 accumulation in HD patients. Secondly, activating the monocyte and macrophage network discovered during dialysis session produces multiple inflammatory cytokines, which may also demonstrate the serum's increase in IL-18(Formanowicz et al., 2015). Thirdly, serum IL-18 is a marker of tubulo-interstitial kidney tissue lesion, so level of serum IL-18 directly correlated with necrotic and dystrophic changes in epithelial tubules and interstitial fibrosis in kidney of HD patient (Kraydaschenko et al., 2016). This study found that the elevated serum IL-18 levels in diabetic patients may result from kidney tissue from DN patients. IL-18 is increasingly secreted from tubular cells through acute ischemic kidney failure. It is mainly expressed in tubular kidney epithelium so that IL-18 levels of tubular cells may also be increased in diabetes cases and that the cytokine expect an unsafe activity in DN.

4.3. Human high sensitivity C-Reactive Protein (hs-CRP) level in four study groups

The findings in (Table 4) were symmetrical with (Shelbaya et al.,2012, Lachine et al., 2016) who recorded that the hsCRP levels were increased in the diabetic patients and decreased in the control group, with statistically significant difference between them ($p < 0.05$). And these findings were symmetrical with (Abd Rabo et al., 2016, Salama et al., 2016, Leiherer et al., 2016) who recorded that the mean of hsCRP levels was increased in HD patients compared with control group. These results were unsymmetrical with (Shi *et al*., 2012) who found that the mean of hs-CRP was decreased in HD patients. This study showed that the inflammatory marker in HD patients is the presence of proinflammatory state as evidenced by significant increase in hsCRP concentration caused by a synergism of different mechanisms, such as malnutrition, oxidative stress, genetic factors and chronic inflammation(Panichi et al., 2001); in addition, underlying etiology of CKD, such as diabetes or hypertension is by itself a major contributory factor to the existing inflammation(Amanullah et al., 2010; Gowda et al., 2015). Alterations in the immune system in CKD by uremia are associated with a state of immune dysfunction characterized by immune-depression that contributes to the high prevalence of infections among HD patients(Lagrand et al., 1999). Furthermore, vascular calcification in more advanced CKD stage may be another explanation for higher hs-CRP levels(Panichi et al., 2001). Also, this study recorded an increase of mean hs-CRP levels in T2DM patients compared with control, because a possible mechanism by which T2DM patients might induce inflammation by increasing advanced glycation end products that may activate macrophages and increase oxidative stress and IL-6 synthesis, leading to the high production of hsCRP, these results suggest a concomitant action of T2DM in the occurrence of an increase in the inflammatory process that is reflected by an increase in hs-CRP levels (Lima et al., 2007).

Correlation coefficient between Chemerin with hs-CRP and Chemerin with IL-18:

These results agreed with (Alissa et al., 2016, Lachine et al.,2016) who recorded positive correlation between levels of chemerin and hs-CRP among T2DM patients compared with control. And these results agreed with (Blaszak et al., 2015) who showed a significant positive correlation between concentration of chemerin and CRP in HD patients compared to the control. These results disagreed with (Shukla et al.,2016) who found no difference in the concentrations of IL-18 in HD patients compared to the control group. The presence of sustained inflammation in adipose tissue is an initial signal for increased chemerin formation and production, and adipose tissue regulates the ratio of active to total chemerin acting within adipose tissue thus affecting the inflammatory functions induced by immune cells recruitment(Lachine et al., 2016). The elevated chemerin levels in HD patients correlated with adipose tissue infiltration by macrophages and production of well-established inflammatory mediators such as CRP, IL 18, and tumor necrosis factor-alpha (TNF-α) (Salama et al., 2016).

These results showed that chemerin level was positively correlated to the IL-18 and hs-CRP in study groups, which are considered inflammatory markers. This may be explained because chemerin has a dual nature as an adipokine and a chemokine (Fontes et al., 2018). Chemerin showed positive correlation with markers of inflammation in previous study (Lehrke et al., 2009) and the positive association between baseline chemerin and hs-CRP here suggests that serum chemerin is associated with inflammation in T2DM patients and indicating a relationship mainly with systemic inflammation (Kim et al., 2014). In this study, there is a positive correlation between chemerin concentration levels and hs-CRP index in HD patients. This fact suggests a key role of the ChemR23/ chemerin axis in directing plasmacytoid dendritic cell trafficking, which can play a significant role in regulating the immune response by enhancing chemoattraction of the cells of the immune response toward sites of pathological inflammation(Abd Rabo et al., 2016). HsCRP is a sensitive marker of tissue damage, inflammation and infection reflecting the degree of underlying inflammatory response and being a beneficial measure of immune injury to tissues (Formanowicz et al., 2015). Hyperglycemia actuate inflammatory mediators, for example, IL-18 in kidney tissue, and since IL-18 receptors are present mainly in proximal renal tubules and increment with renal tissue damage, so the microalbuminuria will increment as long as serum IL-18 increment. IL-18 can be considered as great indicators for DN; consequently it could be recommended that IL-18 is considered as a

predictive factor for checking the early DN and, furthermore, the likelihood of having a therapeutic methodology impact on DN improvement(Abid Hammed, 2019). Therefore, serum IL-18 levels present in T2DM as result of the predominant viscous deposition of lipids related with the disorder. IL-18 levels were gradually increased in DN to reach the highest level in the micro-albumin phase.

4.4. The difference in Hb, PCV, RBC, WBC and WBC type in the four study groups.

The results in Tables (5 and 6) agreed with results by Abd Rabo et al (2016) who found that significantly decreased of CBC indices in HD patients compared with control. These results agreed with (Shukla et al., 2016) who recorded that no significant in Hb, PCV, RBC and WBCs between T2DM patients and control. These results disagreed with (George et al., 2015, Iyawe and Adejumo, 2018) who recorded increased of WBCs in HD patients compared with control. Hematological investigations, especially full blood counts, are good indicators in health and disease states, helping to understand the real disease presentation juxtaposed to the clinical features in the patients(George et al., 2015). This study showed decrease in Hb, PCV and RBC in HD patients compared with diabetic patients and control; this decrease is due to hematuria and gastrointestinal blood loss or due to a decrease in the production of erythropoietin by the kidney, leading to decreased production of RBC in the bone marrow, and anemia that causes hypoxia; Hypoxia will increase hepsidin that causes functional iron deficiency through inhibition of iron absorption in the intestine and inhibition of Fe distribution in blood circulation as more is stored in macrophages or spleen(Abd Rabo et al.,2016, Thaha et al., 2018).

Kidney function decline will result in a decline in EPO production and, as a consequence, result in decreased Hb synthesis, leading to a fall in total RBC count; clotting of blood during dialysis is also responsible for low Hb level in CKD patients(Kutuby et al., 2015). Uremia interferes with erythropoiesis, granulocyte and immune functions. As a result, uremic patients are almost invariably anemic, and have a high incidence of infections and hemorrhagic complications(George et al., 2015). This study showed decreased WBC count in HD patients. The possible mechanism in which CKD leads to a slight decrease in total leukocyte count may be explained by complement activation in vivo due to exposure of blood to artificial dialyzer membranes in patients undergoing dialysis. The complement is typically C3a or C5a, produced by the classic complement activation pathway. Complement activation induces neutrophil aggregation and adherence to endothelial surface with resultant fall in total leukocyte count. In patients undergoing hemodialysis, the incidence of this affect may be as high as 20% (Latiweshob et al., 2017, Iyawe and Adejumo, 2018). This study showed that CKD was associated with higher monocyte and lower lymphocyte counts; both of which are independently associated with the promotion of cardiovascular outcomes(George et al., 2018). Granulocyte is associated with rapid progression to ESRD, cardiovascular morbidity, and mortality. This may, therefore, imply that our patients with CKD are at increased risk of developing CVD; hence, there is a need for aggressive CVD factor modification and treatment (Jabbar et al., 2015, Iyawe and Adejumo, 2018). Also, this study show that non-significant decreased of Hb, PCV and RBCs in diabetic patients group and control group, where chronic inflammatory state in DM due to insulin action on the adipose tissue, muscles and liver promote differentiation and maturation of WBC via pro-inflammatory cytokines. Possible mechanisms for decreased RBC indices in T2DM are structural modifications of erythrocytes membrane, changes of surface electric charge, erythrocyte aggregation, that could lead to the shorter lifespan of RBC(Milosevic and Panin, 2019).

5. Conclusion

The higher levels of hs-CRP, chemerin and IL-18 in HD patients than control are a circulating inflammatory marker. This finding suggests that patients with two associated diseases have a more active inflammatory state. While raised hs-CRP, chemerin and, IL-18 in diabetic patients are prone to increase the future relative risk of cardiovascular events and other complications. Hence raised these markers indicates the role of ongoing inflammation in the management of diabetes. This study appeared that HD Patients have abnormal hematological parameters. It has been suggested that in CKD, weaken production of EPO is the major reason for the reduction in RBC count, Hb concentration, PCV and, WBC.

Declaration of Competing Interests

None

Acknowledgements

Our special thanks go to all the staff of the industrial renal department, diabetes center, department of Chemistry Laboratory and Blood Laboratory at Ramadi General Hospital for helping us in the collection and analysis of the samples. Our profound thanks go to all patients and healthy people who accepted to participate in the study.

References

Abd Rabo SA, Mohamed NA, Tawfik NA and Hamed MM. 2016. Serum chemerin level in chronic kidney disease. *Egypt J Intern Med*., **28(3)**:99.

Abid Hammed SM. 2019. Study of Relationship between Several Interleukins and Some Biochemical Parameters in Type II Diabetics Patients. Ph. Thesis. College of Science, University of Anbar.

Ahmed HS and Tahir NT. 2015. Chemerin as a New Marker in Iraqi Newly Diagnosed Type 2 Diabetes Mellitus. *AJPS*., **15(1)**:6-13.

Ali TM and Al Hadidi K. 2013. Chemerin is associated with markers of inflammation and predictors of atherosclerosis in Saudi subjects with metabolic syndrome and type 2 diabetes mellitus. *BJBAS*., **2(2)**:86-95.

Ali Z, Ridha MR and Bahar E. 2019. Serum C-Reactive Protein in chronic kidney disease patients undergoing hemodialysis and correlation with dialytic age. *In J Phy*: Conference Series., 1246 (1). IOP Publishing.

Alissa EM, Helmi SR, Alama NA and Ferns GA. 2016. Serum Chemerin and Cardiovascular Risk Factors in Diabetic Subjects without Established Vascular Disease. *J Adv Med Medical Res.*, 1-7.

Amanullah S, Jarari A and Govindan M. 2010. Association of hs-CRP with diabetic and non-diabetic individuals. *Jordan J Biol Sci*. **147(612)**:1-1.

Aso Y, Okumura KI, Takebayashi K, Wakabayashi S and Inukai T. 2003. Relationships of plasma interleukin-18 concentrations to hyperhomocysteinemia and carotid intimal-media wall thickness in patients with type 2 diabetes. *Diabetes care*., **26(9):**2622-7.

Blaszak J, Szolkiewicz M, Sucajtys-Szulc E, Konarzewski M, Lizakowski S, Swierczynski J and Rutkowski B. 2015. High serum chemerin level in CKD patients is related to kidney function, but not to its adipose tissue overproduction. *Renal failure*., **37(6)**:1033-8.

Chang CH, Fan PC, Lin CY, Yang CH, Chen YT, Chang SW, Yang HY, Jenq CC, Hung CC, Yang CW and Chen YC. 2015. Elevation of interleukin-18 correlates with cardiovascular, cerebrovascular, and peripheral vascular events: a cohort study of hemodialysis patients. *Medicine*., 94(42).

Coimbra S, Brandão Proença J, Santos-Silva A and Neuparth MJ. 2014. Adiponectin, leptin, and chemerin in elderly patients with type 2 diabetes mellitus: a close linkage with obesity and length of the disease. *BioMed research international*.

Donate-Correa J, Martín-Núñez E, Muros-de-Fuentes M, Mora-Fernández C and Navarro-González JF. 2015. Inflammatory cytokines in diabetic nephropathy. *JDR*.

Fischer CP, Perstrup LB, Berntsen A, Eskildsen P and Pedersen BK. 2005. Elevated plasma interleukin-18 is a marker of insulin-resistance in type 2 diabetic and non-diabetic humans. *Clin. Immunol*., **117(2)**:152-60.

Fontes VS, Neves FS and Cândido AP. 2018. Chemerin and factors related to cardiovascular risk in children and adolescents: a systematic review. *Rev. Paul. Pediatr*., **36(2)**:221-9.

Formanowicz D, Wanic-Kossowska M, Pawliczak E, Radom M and Formanowicz P. 2015. Usefulness of serum interleukin-18 in predicting cardiovascular mortality in patients with chronic kidney disease–systems and clinical approach. *Sci Rep*., **5**:18332.

Franz MJ, Bantle JP, Beebe CA, Brunzell JD and Chiasson JL. 2012. Evidence-based nutrition principles and recommendations for the treatment and prevention of diabetes and related complications. Diabetes Care, **26**: 51-61.

George C, Matsha TE, Erasmus RT and Kengne AP. 2018. Haematological profile of chronic kidney disease in a mixed-ancestry South African population: a cross-sectional study. *BMJ open.*, 8(11).

George SV, Pullockara JK, Kumar SS and Mukkadan JK. 2015. A study to assess changes in the hematological profile in chronic kidney disease. *TPI*., 4(6, Part A):1.

Gowda BH, Meera KS and Mahesh E. 2015. Serum levels of high sensitivity C reactive protein and malondialdehyde in chronic kidney disease. *IJMRHS*., **4(3)**:608-615.

Haddad NI, Nori E and Hamza SA. 2018. Correlations of Serum Chemerin and Visfatin with other Biochemical Parameters in Iraqi Individuals with Metabolic Syndrome and Type Two Diabetes Mellitus. *Jordan J Biol Sci*, **11(4)**:4369.

Iyawe IO andAdejumo OA. 2018. Hematological profile of predialysis chronic kidney disease patients in a tertiary hospital in Southern Nigeria. *J Med Trop*., **20(1)**:36.

Kim SH, Lee SH, Ahn KY, Lee DH, Suh YJ, Cho SG, Choi YJ, Lee DH, Lee SY, Hong SB and Kim YS. 2014. Effect of lifestyle modification on serum chemerin concentration and its association with insulin sensitivity in overweight and obese adults with type 2 diabetes. *Clin Endocrinol*., **80(6)**:825-33.

Kraydaschenko O, Berezin A, Dolinnaya M and Swintozelsky A. 2016. Serum Interleukin-18 as a Biomarker of Tubular Kidney Damage in Patients with Chronic Glomerulonephritis. *Biol Markers Guid Ther*., **3(1)**:185-91.

Kuo IC, Lin HY, Niu SW, Lee JJ, Chiu YW, Hung CC, Hwang SJ and Chen HC. 2018. Anemia modifies the prognostic value of glycated hemoglobin in patients with diabetic chronic kidney disease. *PloS one*., **13(6)**:e0199378.

Kurts C, Panzer U, Anders HJ and Rees AJ. 2013. The immune system and kidney disease: basic concepts and clinical implications. *Nat. Rev. Immunol*., **13**: 738-753.

Kutuby F, Wang S, Desai C and Lerma EV. 2015. Anemia of chronic kidney disease. *Dis Mon*: *DM.*, **61(10)**:421.

Lachine N, ElSewy FZ, Megallaa MH, Sadaka M, Khalil G, Rohoma K and Amin NG. 2016. Association between serum chemerin level and severity of coronary artery disease in Egyptian patients with type 2 diabetes. *J Diabetol*., 2:3.

Lagrand WK, Visser CA, Hermens WT, Niessen HW, Verheugt FW, Wolbink GJ and Hack CE. 1999. C-reactive protein as a cardiovascular risk factor: more than an epiphenomenon. *Circul*., **100(1)**:96-102.

Latiweshob OB, Elwerfaly HH and Sheriff DS.2017. Haematological changes in predialyzed and hemodialyzed chronic kidney disease patients in libya. *IOSR J Dent Med Sci*., **16**:106-112.

Lehrke M, Becker A, Greif M, Stark R, Laubender RP, von Ziegler F, Lebherz C, Tittus J, Reiser M, Becker C and Goke B. 2009. Chemerin is associated with markers of inflammation and components of the metabolic syndrome but does not predict coronary atherosclerosis. *Eur J Endocrinol*., **161(2)**:339.

Leiherer A, Muendlein A, Kinz E, Vonbank A, Rein P, Fraunberger P, Malin C, Saely CH and Drexel H. 2016. High plasma chemerin is associated with renal dysfunction and predictive for cardiovascular events—Insights from phenotype and genotype characterization. *Vascul pharmacol*., **77**: 60-68.

Lima LM, Carvalho MD, Soares AL, Sabino AD, Fernandes AP, Novelli BA and Sousa MO. 2007. High-sensitivity C-reactive protein in subjects with type 2 diabetes mellitus and/or high blood pressure. *Arq Bras Endocrinol Met.*, **51(6)**:956-9560.

Mathew T and Corso O. 2009. Early detection of chronic kidney disease in Australia: which way to go. *Nephrol*., **14(4)**: 367-373.

Milosevic D and Panin VL. 2019. Relationship between hematological parameters and glycemic control in type 2 diabetes mellitus patients. *J Med Biochem*., **38(2)**:164-71.

Panichi V, Migliori M, De Pietro S, Taccola D, Bianchi AM, Norpoth M, Metelli MR, Giovannini L, Tetta C and Palla R. 2001. C reactive protein in patients with chronic renal diseases. *Ren. Fail*., **23(3-4)**:551-62.

Pfützner A, Schöndorf T, Hanefeld M and Forst T. 2010. High-sensitivity C-reactive protein predicts cardiovascular risk in diabetic and nondiabetic patients: effects of insulin-sensitizing treatment with pioglitazone. *J Diabetes sci technol*., **4(3)**:706-16.

Salama FE, Anass QA, Abdelrahman AA and Saeed EB. 2016. Chemerin: A biomarker for cardiovascular disease in diabetic chronic kidney disease patients. *Saudi J Kidney Dis Transpl*., **27(5)**:977.

Shelbaya S, Amer H, Seddik S, Allah AA, Sabry IM, Mohamed T and El Mosely M. 2012. Study of the role of interleukin-6 and highly sensitive C-reactive protein in diabetic nephropathy in type 1 diabetic patients. *Eur. Rev. Med. Pharmacol. Sci*., **16(2):**176-182.

Shi B, Ni Z, Cao L, Zhou M, Mou S, Wang Q, Zhang M, Fang W, Yan Y and Qian J. 2012. Serum IL-18 is closely associated with renal tubulointerstitial injury and predicts renal prognosis in IgA nephropathy. *Med Inflam*., 2012.

Shukla DK, Chandra KP and Pawah AK. 2016. Study of hematological indices in patients with diabetes mellitus and hypertensive diabetes mellitus. *Indian J Med Res*., **1(4)**:28-31.

Stanifer JW, Jing B, Tolan S, Helmke N, Mukerjee R, Naicker S, Patel U. 2014. The epidemiology of chronic kidney disease in sub-Saharan Africa: a systematic review and meta-analysis. *Lancet Glob Health*, **2(3)**:e174-81.

Thaha M, Imroati TA, Widodo S and Pranawa S. 2018. Comparison of High-sensitivity C-reactive Protein Level between Chronic Kidney Disease Stages. *Bio Heal Sci J*., 1(1):1-9.

Vanholder R, Fouque D, Glorieux G, Heine GH, Kanbay M, Mallamaci F, Massy ZA, Ortiz A, Rossignol P, Wiecek A and Zoccali C. 2016. Clinical management of the uraemic syndrome in chronic kidney disease. *Lancet Diabetes Endocrinol*., **4(4)**:360-3673.

Vanholder R, Van Laecke S and Glorieux G. 2008. What is new in uremic toxicity?. *Pediatric nephrol*., **23(8)**:1211-1221.

JJBS

Jordan Journal of Biological Sciences

Volume 14, Number 3, September 2021
ISSN 1995-6673
Pages 503 - 511

A Review on Reliability and Validity of CRISPR/Cas9 Technology for Gene Editing

Bishnu Dev Das[1] and Niroj Paudel [2,3,*]

[1]Department of Botany, Mahendra Morang Aadarsh Multiple Campus Biratnagar (Tribhuvan University), Nepal;[2]Department of Applied Plant Science, Kangwon National University, Chuncheon 24341, Republic of Korea. [3]National Institute of Horticultural and Herbal Science, Rural Development Administration, Wanju 55365, Republic of Korea

Received: July 24, 2020; Revised: October 3, 2020; Accepted: October 18, 2020

Abstract

Genome engineering is one of the worldwide fast growing field of biotechnology which involves designed programmable DNA-binding nucleases such as homing endonucleases, zinc finger nucleases (ZFNs), transcriptions activator like effector nucleases (TALENs) and clustered regularly interspaced short palindromic repeats (CRISPR)/Cas9 (CRISPR-associated 9) nucleases. These technologies utilize manipulated nucleases which are the complex of sequence-specific DNA binding domains and nonspecific DNA cleavage modules. CRISPR)/Cas9 technology lets scientists accurately cut and paste genes into DNA which can be applied to edit the individual gene or even entire chromosomes from an organism at any point in its development, become a magical tool due to its simplicity. Here we review the four basic pieces of information on the genome editing technologies with their reliability and discuss the applications and their therapeutic potential as well as future prospects.

Key words: Gene editing, CRISPR/Cas9 technology, endonucleases mechanism, transcription.

1. Introduction

In 1905, in a letter to his colleague Adam Sedgwick, the English biologist William Bateson used the word 'genetics' to designate 'the science of heredity and variation' (Gayon, 2016). Onwards 1970s, Genome Editing (GE) technologies establish a new revolution in modern research in genetics or biology. The recent advance technology CRISPR/Cas9 technology are used systematic interrogation of mammalian function of genome (Hsu *et al*., 2014) (Fig. 1). In life science research, genome editing can delete, insert, and modify the DNA sequences of cells that enable the function of specific genes. The biotechnologies used for gene editing are, (1) homing endonucleases or meganucleases), (2) zinc-finger nucleases (ZFNs), (3) transcription activator-like effector nucleases (TALENs and (4) clustered regularly interspaced short palindromic repeats (CRISPR)-CRISPR-associated protein 9 (Cas9). Out of these fours, CRISPRCas9 and TALENs are new genomic sequences that have driven a revolution in genome editing that has accelerated scientific breakthroughs and discoveries in multiple practices such as synthetic biology, human gene therapy, disease modeling, drug discovery, neuroscience, and the agricultural sciences (Gaj *et al*., 2016).

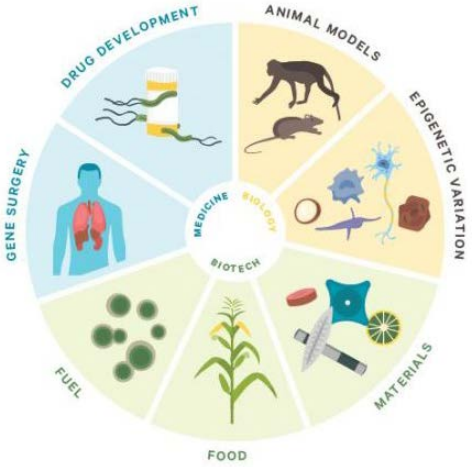

Figure 1. Applications of Genome Engineering (Hsu *et al*., 2014)

2. Homing endonucleases or meganucleases

Endonuclease enzymes are involved in genomic modification, rearrangement, protection, and repair. They specify at least nine orders of magnitude, ranging from nonspecific degradative enzymes up to a variety of gene-specific endonucleases, and most specific enzymes are called homing endonucleases that produce double-strand breaks at individual loci in their host genomes and drive site-specific gene conversion events. The first observation of homing dates to experiments conducted at the Pasteur Institute in the early 1970s, and investigators noted the dominant inheritance of a genetic marker, termed 'omega,'

* Corresponding author e-mail: nirojjirauna@gmail.com.

during yeast mating experiments (mitochondrial genes are passed on biparentally in such studies and are thus related to Mendelian laws of inheritance). Omega was located inside the mitochondrial gene that encodes the large ribosomal RNA subunit (LSrRNA) (Bolotin *et al*., 1971) and was inherited about 100% frequency in experimental processes of homozygous 'omega-plus' and ''omega-minus'' yeast strains (Netter *et al*., 1974). In subsequent experiments, omega was found to correspond to an intervening sequence (recognized as a self-splicing group I intron) (Faye *et al*., 1979).

Mega-nuclease two enzyme such as intron endonuclease and intein endonuclease. Homing endonucleases (meganucleases) are the final member of the targeted nuclease family which have been reviewed at length elsewhere (Silva *et al*., 2011; Stoddard, 2014). But endonuclease bind amino acid present of the enzymes that recognize and cleave long DNA sequence (Figure 2).

The intron is driven by a site-specific endonuclease (now termed I-SceI) that is encoded by an open reading frame harbored within the intron sequence (Jacquier and Dujon, 1985), which generates a DNA double-strand break within a long DNA target sequence in the LSrRNA gene that contains the eventual intron insertion site. Improvement through homologous recombination using the intron containing allele as a corrective template leads to a duplication of the intron and its endonuclease gene into the target site (Figure 3). Homing is a process in which microbial self-splicing intervening sequences group I or group II introns or inteins are specifically duplicated into recipient alleles of their host gene that lack such a sequence (Chevalier and Stoddard, 2001).

Families and Structures of homing endonucleases are universal and are found in microbes from all biological kingdoms, corresponding phage and viruses. Despite the closeness and the frequent symbiotic relationship between multicellular eukaryotes and various microbial species, no examples have been reported of homing endonuclease genes within genomes of those more complex organisms. There are five different families of homing endonucleases recognized and initially associated with a specific biological host range (Stoddard, 2005).

3. Zinc-finger nucleases (ZFNs)

The recent advancements in genome editing include site-specific nucleases, usage of which for genome editing began with the arrival of zinc-finger nucleases (ZFNs) in 2002. The ZFNs were the first specific protein reagents that revolutionized the field of genome manipulation. ZFNs are DNA binding domains and specifically recognize three base pairs at the target site (Rai *et al*., 2019).ZFNs are formed by the combination between Cys_2-His_2 zinc-finger protein and the cleavage domain of the FokI restriction endonuclease (Kim *et al*. 1996) that are the first targeted gene to achieve universal use (Urnov *et al*., 2010).ZFNs behaves as dimers, with each monomer observing a specific "half site" sequence typically nine to 18 base pairs (bps) of DNA via the zinc-finger DNA-binding domain (Fig. 2).

The FokI cleavage domain regulates the dimerization of ZFN which cuts DNA within a five to seven-bp spacer sequence that separates two flanking zinc-finger binding sites (Smith *et al*., 2000). Primarily, each ZFN is made up of three or four zinc-finger domains, with each individual domain composed of 30 amino acid residues that are organized in a bba (beta beta alpha) motif (Pavletich and Pabo, 1991). The residues that facilitate DNA recognition are located within the a-helical domain and typically interact with three bps of DNA, with occasional overlap from an adjacent domain (Wolfe *et al*., 2000). Using methods such as phage display (Wu *et al*., 1995), a large number of zinc finger domains recognizing distinct DNA triplets have been identified (Dreier *et al*., 2005). These domains can be merged in tandem using a canonical linker peptide to produce polydactyl zinc-finger proteins that can target a wide range of possible DNA sequences (Kim *et al*., 2009). Besides this "modular assembly" approach to zinc-finger construction, selection-based methods for constructing zinc-finger proteins have also been reported (Magnenat *et al*., 2004), including those that consider context-dependent interactions between adjacent zinc-finger domains, such as oligomerized pool engineering (OPEN) (Maeder *et al*., 2008). Moreover, particular sets of validated two-finger, zinc-finger modules have been used to gather zinc finger arrays (Kim *et al*., 2009; Bhakta *et al*., 2013), including those which take context-dependent effects into account (Gupta *et al*., 2012).

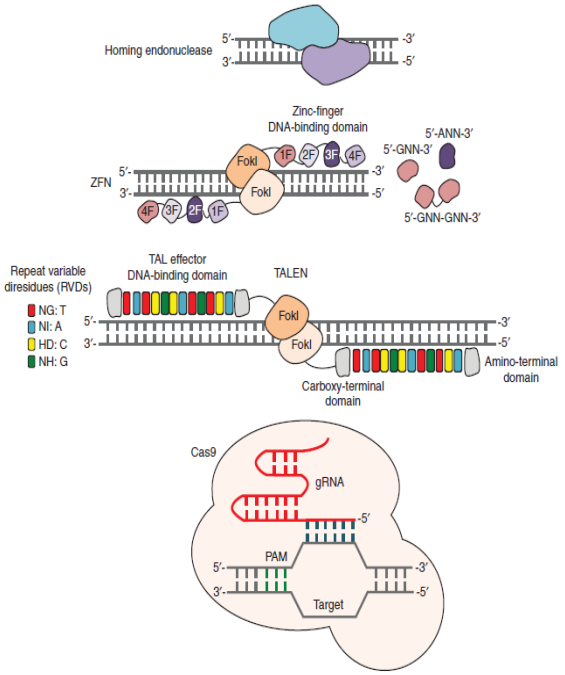

Figure 2. Genome editing technologies. Cartoons showing the mechanisms of targeted nucleases. From top: homing endonucleases, zinc-finger nucleases (ZFNs), transcription activator-like effector (TALE) nucleases (TALENs), and clustered regularly interspaced short palindromic repeats (CRISPR)-CRISPR-associated protein 9 (Cas9). Homing endonucleases cleave their DNA substrates as dimers, and do not have distinct binding and cleavage domains. ZFNs observe target sites that consist of two zinc-finger binding sites that flank a 5- to 7-base pair (bp) spacer sequence recognized by the FokI cleavage domain. TALENs notice target sites that consist of two TALE DNA-binding sites that flank a 12- to 20-bp spacer sequence recognized by the FokI cleavage domain. The Cas9 nuclease is targeted to DNA sequences complementary to the targeting sequence within the single guide RNA (gRNA) located instantly upstream of a compatible proto-spacer adjacent motif (PAM). DNA and protein are not peaked to scale (Gaj *et al*., 2016).

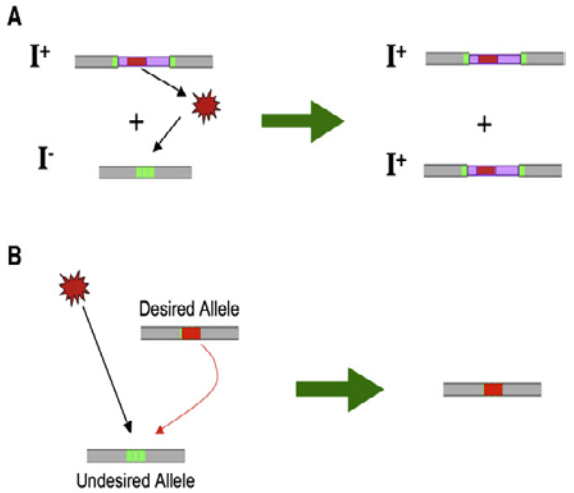

Figure 3. Homing Endonucleases and Genetic Homing (A) Motile element with a homing endonuclease gene (red bar) which is attached within a self-splicing intron or intein (blue bars) resides within a host gene (gray bars). The homing endonuclease (red star) is expressed and cleaves a target site (green bar) which is found in a homologous allele of the host gene lacking the entire element. The arising double-strand break is repaired by cellular machinery, generally leading either to repair via non-homologous end-joining (not shown) or via homologous recombination (HR). If HR successfully uses the intron containing host allele (I^+) as a corrective template, then the original uninterrupted allele (intron-minus [I^-]) is converted to an allele that now contains the intron and homing endonuclease gene (intron-plus [I^+]). (B) Properties homing endonuclease introduced for gene expression. Based on the presence or absence (as well as the sequence)of a corrective DNA template for break repair, and on the catalytic properties of the endonuclease, such applications can lead to mutation, knockout, modification, or insertion of exogenous coding DNA into the gene target (Stoddard, 2011).

The use of ZFNs for gene editing (in addition to all targeted nucleases) is off-target mutations (Gabriel *et al*., 2011). Therefore, several approaches have been undertaken to increase their specificity. For creation of obligate heterodimer ZFNs engineering depends upon the Charge-Charge repulsion for prevent the unwanted homodimof the FokI cleavage domain (Doyon *et al*., 2011), although the minimizing potential for ZFNs to dimerize at off-target sites. The methods of protein engineering have also been used to boost the cleavage efficiency of the FokI cleavage domain (Guo *et al*., 2010). The major approach for improving ZFN specificity is to pass them into cells as protein. Due to the peculiar cell-penetrating activity of zinc-finger domains (Gaj *et al*.,2014), ZFN proteins are naturally cell-permeable and can facilitate the gene editing with fewer off-target effects when tested upon the cells as refined protein compared to when expressed within cells from nucleic acids (Gaj *et al*., 2012). Afterwards, converted ZFN proteins equipped with enhanced cell-penetrating activity have been described (Liu *et al*., 2015).

4. Transcription activator-like effector nucleases (TALENs)

Transcription activator-like effector nucleases (TALENs) are restriction enzymes or restrictase which can be applied to cut specific sequence of DNA. TALENs provide precise insertion, deletion, or substitutions of specific genes alter the genome. TALENs possess a designed TALE domain that mimics the natural transcription activator-like effector proteins and a nuclease that can cleave DNA in cells. TALENs have emerged as a magical genome editing tools in numerous species and cell types.

4.1. TALE Nucleases

TALE proteins are bacterial effectors. The code used by TALE proteins to recognize DNA was discovered in 2009 (Boch *et al*., 2009). Sooner, this discovery approved the creation of custom TALENs capable of modifying nearly any gene. ZFNs and TALENs are flexible in shape and function, comprised of an amino-terminal TALE DNA-binding domain fused to a carboxy- terminal FokI cleavage domain (Christian *et al*., 2010; Miller *et al*., 2011). Dimerization of TALEN proteins is mediated by the FokI cleavage domain like ZFNs which cuts within a 12- to 19-bp spacer sequence that separates each TALE binding site (Fig. 2) (Miller *et al*., 2011). TALEs are gathered to recognize between 12- to 20-bps of DNA, with more bases typically leading to higher genome-editing specificity (Guilinger *et al*., 2014). The TALE binding domain consists of a series of repeat domains, each 34 residues in length. All repeat touches DNA via the amino acid residues at positions 12 and 13, known as the repeat variable diresidues (RVDs) (Boch *et al*., 2009).

Unalike zinc fingers, that verify DNA triplets, each TALE repeat recognizes only a single bp, with little to no target site overlap from adjacent domains (Mak *et al*., 2012). The most generally used RVDs for assembling synthetic TALE arrays are: NI for adenine, HD for cytosine, NG for thymine, and NN or HN for guanine or adenine (Streubel *et al*., 2012). TALE DNA-binding domains can be composed using a different method, with the most straightforward approach being Golden Gate assembly (Cermak *et al*., 2011). TALE assembly methods have also been developed, including FLASH assembly (Reyon *et al*., 2012), iterative capped assembly (Briggs *et al*. 2012), and association independent cloning (Schmid-Burgk *et al*., 2013). Transformation in TALEN assembly have focused on the improvement of methods that can promote their performance, including specificity profiling to uncover nonconventional RVDs that improve TALEN activity (Miller *et al*., 2015), directed evolution as means to refine TALE specificity (Hubbard *et al*., 2015), and even combining TALE domains to homing endonuclease differing to produce chimeric nucleases with extended targeting specificity (Boissel *et al*., 2014).

TALENs proposes two distinct advantages for genome editing compared to ZFNs; first , no directed evolution is necessary to engineer TALE arrays, reducing the amount of time and practice needed to assemble a functional nuclease, whereas, second, TALENs have been reported to show upgraded specificity and minimized toxicity compared to some ZFNs (Mussolino *et al*., 2014) because of their increased closeness for target DNA (Meckler *et al*., 2013) or perhaps a greater energetic penalty for associating with base mismatches. However, TALENs are substantially larger than ZFNs, and have a highly repetitive structure, making their energetic delivery into cells through the use of lentivirus (Holkers *et al*., 2012) or a single adenoassociated virus (AAV) challenged the single particle. Approach for reducing the limitations has

emerged as TALENs can be easily brought into cells as mRNA (Mahiny *et al*., 2015) and even protein (Cai *et al*., 2014), even though other codon usage and amino acid deterioration can also be influenced to precise RVD arrays that might be less susceptible to recombination (Kim *et al*., 2013). Adenoviral vectors are also useful for mediating TALEN delivery to hard-to-transfect cell types (Maggio *et al*., 2016).

5. CRISPR-Cas9

The discovery of CASPR-Cas9 technique dates back to 1987 identified by Atsuo Nakata and colleagues, who discovered a peculiar locus in *Escherichia coli* K12 strain with five identical sequences of 29 nucleotides spaced by 32 nucleotides downstream of the *iap* gene (Ishino *et al*., 1987).The notable characteristics of repeating spacers and direct repeats make CRISPRs easily noticeable in long sequences of DNA, as the number of repeats decreases the likelihood of a false positive match (Sorek *et al*., 2008). In biological research, CRISPR is becoming an indispensable tool. The programmable capacity of the Cas9 enzyme is now revolutionizing different fields of medicine, biotechnology, and agriculture. The CRISPR-Cas based genome editing approach has become a choice of technique and magical tool due to its simplicity, ease of access, cost, and flexibility whereas previous methods were difficult and expensive to design (Doudna and Charpentier, 2014).

It has brought a revolution in life sciences since their development as an experimental tool in 2012. The technology depends on the formation of sequences called as spacers in the CRISPR region of the host genome. Spacer sequences are identical to sections of invading foreign nucleic acids, commonly from phases. These spacers regions are transcribed into noncoding CRISPR-RNA (crRNA), which acts as guide to direct an effort nuclease to make targeted cuts in invading genetic material. The desired cleavage of invading DNA prevents expression of viral elements, which prevents successful infection of the bacterium. In *Streptococcus pyogenes*, CRISPR-II system requires only one effector protein, Cas9, which can be targeted to make a double-stranded break in DNA at a specific nucleotide sequence (Jinek *et al*., 2012). CRISPR-associated protein 9 (Cas9) genes are present in approximately 40% bacterial species such as *Streptococcus pyogenes, Staphylococcus aureus, Neisseria meningitides, Staphylococcus epidermidis, Streptococcus mutans, Streptococcus thermophilus, Escherichia coli, Corynebacterium diptheriae* and around 90% archeal species such as *Sulfolobussolfataricus, Methanocaldococcus jannaschii, Methanothermobacter thermoautotrophicum, Pyrococcusfuriosus, Haloferax mediterranei, Archaeoglobus fulgidus* (Horvath and Barrangou, 2010). CRISPR/Cas9 technology is doing boast of a promising future due to transformed and metamorphosed for potential modify and regulate the prokaryotic and eukaryotic genomes (Das and Paudel, 2020).

5.1. Mechanism of CRISPR-Cas9 system

The main function of CRISPR-Cas9 system is to make a double-stranded break into the target DNA where a new gene of interest can be manipulated. In comparison to random mutagenesis like radiation, ethyl methane suffocate (EMS), Zinc finger nucleases (ZFNs) and Transcription activator like effector nucleases (TALENs) genome editing by targeting, CRISPR-Cas9 is more precise and efficient at a specific site. CRISPR-Cas9 possesses specificity towards a particular sequence because of Cas9 protein's unique structural conformation (Figure 4) (Song *et al*., 2016) and a restricted core, nucleic acid sites and is a bi-lobed structure protein. The nucleic acid sites form recognition (REC) lobe connected with nuclease (NUC) lobe by helix bridge (Doudna and Charpentier, 2014). Cas9 was statically analyzed to be multifaceted crystal structured protein having two nuclease domains that protect the organism (first found in *Staphylococcus aureus*) from infection by cleaving the assaulting genome from phage and viruses (Stemberg *et al*., 2014).The Cas9 protein manifested from the host's genomic sequence goals and splits DNA in natural as well as the artificial system of CRISPR-Cas. Cas9 protein is synthesized by the combination of six domains: recognizing domain-1 (REC-I), REC-II, Protospacers adjacent motif(PAM) sequence, RuvC, Bridge helix and a conserved amino acid sequence of His-Asn-His (HNH). The REC-I, PAM, bridge helix, nuclease domains (RuvC and HNH) acts as binding to guide RNA, initiating binding of DNA, initiating cleavage on target DNA, cleaving the DNA (HNH cleaving complementary and RuvC cleaving non-complementary strand), respectively (Sternberg *et al*., 2014). Cas9 becomes excited when bound to SgRNA, i.e. Single guide RNA at REC lobe and conversion of Cas9 into DNA nickase occurs if nucleases get mutated (Ran *et al*., 2013). Many other different Cas protein including Cas9 inside the host bind to genomic DNA (those having CRISPR sequence), which makes this system so versatile. The total functioning Cas protein has a similar mechanism mediated by RNA, therefore called sgRNA mechanism (Wang *et al*., 2016).

In this figure, the steps are 1: The entry of foreign DNA into the bacterial cell, step 2: Detection of the foreign DNA and activation of bacterial genome, step 3: Fusion of pre-crRNA, step 4: Ligation of pre-crRNA and trans activating crRNA (tracrRNA) to form the guide RNA, step 5: Binding of inactive Cas9 protein with guide RNA to form Active Cas9 complex, step 6: Detection and binding of Cas9 complex with foreign DNA, step 7: Fragmentation and lysis of foreign DNA. Step A: illustrate the isolation of activated guide RNA-Cas9 complex, Step B: Insertion of target gene sequence and activated guide RNA-Cas9 complex into a suitable vector, Step C: Fragmentation of DNA or at specific locus, Step D: Genome editing with Non-Homologous End Joining (NHEJ) method, Step E: Involvement of homologous pair and Homology Directed Repair (HDR) method of gene editing (Mohanty *et al*., 2019).

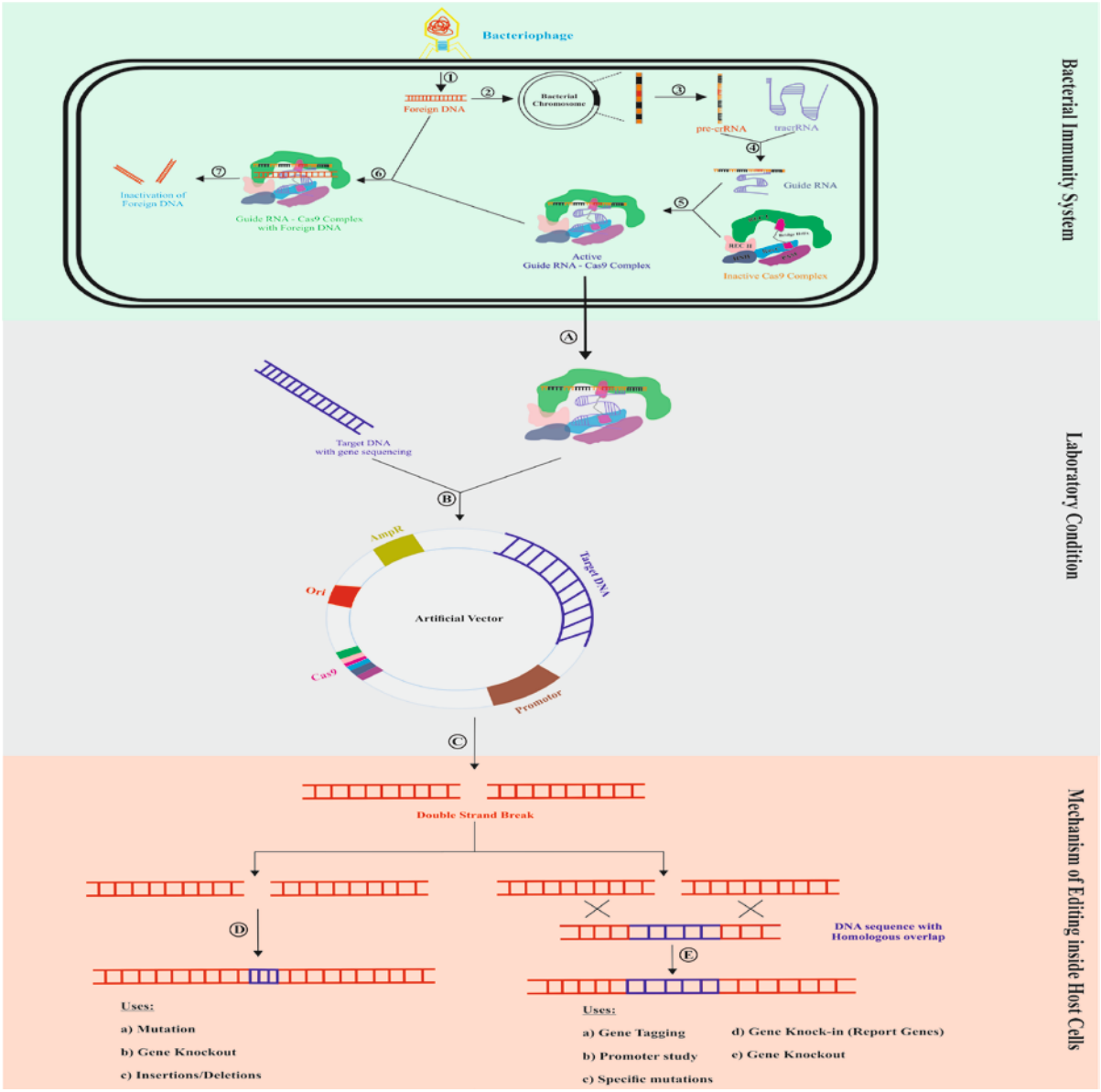

Figure 4. Mechanism of CRISPR-Cas9 system with its uses (Mohanty *et al*., 2019)

5.2. Cas Variants and Other Nucleases for Plant Genome Editing

Streptococcus pyogenes (SpCas9) variant carrying random mutation in to the domain HNH and RuvC which identified that increased the editing efficiency. Cas9 can be modified into a nickase, capable of producing a single strand cleavage by mutating either the HNH or the RuvC-like domain (Xie *et al*., 2014). Cas9 can also be changed into a DNA binding protein, dead Cas9 (dCas9) by mutating both the domains (dCas9; Asp^{10} →Ala, His^{840} →Ala). The SpCas9 uses a 5'-NGG-3' protospacer adjacent motif (PAM), and even though 5'-NGG-3' sequence takes place approximately 5–10 times in every 100 bp in model plant species (Xie *et al*., 2014). The PAM requirement is still a hold up for the Cas9 targetable sites. To get the better of this issue, many Cas9 variants and Cas9 orthologs with various PAM preferences have been applied to get the same results as the wild type CRISPR/Cas9 system. One of that system is CRISPR from Prevotella and Francisella (Cpf1) that is recently cited as Cas12a is a nuclease of class II type V and lacks the HNH domain, possessing only the RuvC-like domain naturally. Cpf1 yields break sites with staggered cuts rather than blunt ends as Cas9 (Zetsche *et al*., 2015). Cpf1 requires a T rich PAM that increases the number of possible plant genetic manipulations and a shorter crRNA than Cas9 (Stella *et al*., 2017). However, short crRNAs raise the possibility of having a secondary structure in the RNA. Cpf1 edited lines need accurate genomic evaluation as Cpf1 has been shown to cause genomic rearrangements in regions surrounding the target sites (Bernabé *et al*., 2019).

Nonetheless, Cpf1 has already been used in many plant species such as rice (Begemann *et al*., 2017; Tang *et al*., 2018) and Arabidopsis (Tang *et al*., 2017) and offers a great alternative to Cas9 and a wider range of targetable genes in addition to the ones offered by Cas9. Recently, a new class II system encoding a miniature (529 amino acids) effector, Cas14a1, has been identified. (Karvelis *et al*., 2019). This Cas variant functions as a PAM-independent single stranded DNA nuclease. Many more Cas variants and orthologs are being discovered (Makarova *et al*., 2015) and exploited for gene editing purposes since the CRISPR/Cas system is a general

immune system present in bacteria and archaea for protection against bacteriophages.

Generally, CRISPR/Cas9 technology can be applied to target multiple genes (or multiple sites within a gene) to generate small or large deletions in the genome and provide practical applications in basic and applied biological research. There are two approaches that have been used for expressing multiple gRNA. First, each gRNA is expressed with an individual promoter, and second multiple gRNAs expressed by one promoter as a single transcript which is further processed to release individual gRNAs (Minkenberg *et al*., 2017).

Transfer-RNAs (tRNAs) are the basic cellular components found in all organisms, and the production and processing are guided by RNA-processing systems. With this concept, Xie *et al* (2015) developed an endogenous RNA-processing system to obtain multiple gRNA from a single transcript (Figure 5). According to them, a synthesized DNA fragment having tRNA–gRNAin a tandemly arrayed fashion can be processed into gRNAs having the desired 50 targeting sequences, which accurately directed Cas9 protein for editing multiple chromosomal targets. The tRNA-processing system includes RNaseZ and RNaseP, inherently present in a cell, precisely cleaves 50 and 30 ends of the tRNAs, thereby releasing individual gRNAs. By the application of this approach in rice plants, stably inherited mutations were easily achieved with up to 100% efficiency, and since tRNA processing machinery is nearly conserved in all the organisms, similar efficiency in mutation can be justified in a variety of organisms. The tRNA-based multiple target editing system is preferred over other methods due to several advantages, including the specificity of RNaseP and RNaseZ for tRNA. Only D-loop arm, acceptor stem and T C-loop arm of tRNA are compulsory for the detection by RNase (Osakabe *et al*., 2010). The tRNAs also contain an internal Pol III promoter site; therefore, tRNA sequences can also bestrike into as an enhancer system for Pol III.

In case, to explore the synthetic poly-tRNA-gRNA(PTG) DNA fragment would be transcribed, processed, and function as anticipated, they manufacture PTG with the structures, tRNA-gRNA (PTG1 and PTG2) or tRNA-gRNA-tRNA (PTG1.1 and PTG2.1), and as a proof, the qRT-PCR analysis declared that the level of PTG was 3 to 31 times higher than the simple sgRNA in rice protoplasts. Furthermore, the full tRNA-gRNA transcripts were not noticed by qRT-PCR, further confirming the efficient cleavage of gRNAs from the tRNA-gRNA transcripts by the tRNA processing system (Figure 3). The Pol III promoters (e.g., U3p) transcribe the PTGs as the SgRNA genes but, PTGs are not obligated to begin with a specific nucleotide as is the case with SgRNAs. Therefore, the vectors used in CRISPR/Cas9 for the expression of SgRNAs can be used accurately to manifest PTGs for the multiplexing approach (Figure 5).

The PTG technology can also be practiced for the enhancement of induction of mutations simultaneously in multiple genomic loci, or for deletion of short fragments of chromosomes. For example, PTG could be used with Cas9 nickase to increase targeting fidelity (Petolino *et al*., 2010) or with dCas9 transcriptional activator or repressor to manipulate multiple gene expression (Shukla *et al*., 2009).

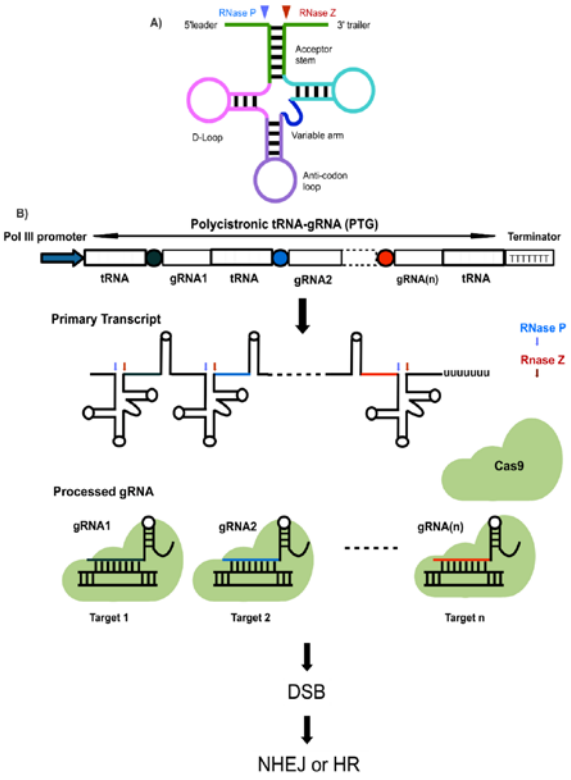

Figure 5. Multigene targeting via CRISPR/Cas9 using PTG/Cas9 method. (A) A eukaryotic pre-tRNAwith a depiction of post-transcriptional processing by RNaseP and RNaseZ (depicted as blue and red arrows respectively), splicing out 50 leader and 30 trailer respectively. (B) Each gRNA with target-specific sequence (labeled here as circles of different colors) and conserved gRNA sequence (blank rectangle) is fused to a tRNA coding sequence (rectangles with boxes), that is cleaved after transcription by RNaseP and RNaseZ to release mature tRNAs and gRNAs (with lines of same colors as the circles). These processed gRNAs direct Cas9 to the target site, which then causes a double-strand break (DSB) repaired by NHEJ or Homologous recombination (HR) (Vats *et al*., 2019).

6. Conclusion

Many attractive features such as simplicity, efficiency, high specificity and amenability to multiplexing, gene editing technologies transforming the way for the next generation breeding. CRISPR/Cas based genome editing system emerged as an evolution in recent years due to its enormous potential to make targeted modifications in the genome and also for versatile diagnostic purposes. Many advancements such as DNA free genome editing systems (RNPs), multiple Cas9 variants, many multi-gene targeting approaches, precise base editing, and measures to increase the frequency of HDR have been achieved very soon. However, crop breeders still need to make significant efforts to implement technological advances in crop improvement programs.

Different from zinc-finger nucleases (ZFNs) and transcription activator like effector nucleases (TALENs), CRISPR/Cas9 takes benefit of an RNA-guided DNA endonuclease enzyme, Cas9, which can generate double-strand breaks (DSBs) at specific genomic locations. It activates cellular endogenous DNA repair pathways, contributing to the generation of desired modifications in the genome. The capacity of the system has opened up a new pathway in the understanding of amyotrophic lateral

sclerosis (ALS) pathogenesis and the development of new therapeutic approaches.

Acknowledgements

Authors are grateful to Swaraj Mohanty for providing his original figure (figure 4). Authors are also thankful to Patrick D. Hsu (figure 1), Thomas Gaj (figure 2), Barry L. Stoddard (figure 3) and Rupesh Deshmukh (figure 5) for the permission to use their figures in this manuscript. Finally, authors are grateful for the reviewer who suggested good comments for the improvement of the manuscript.

Conflict of interest

We declare that there are no conflicting interests.

References

Begemann MB, Gray BN, January E, Gordon GC, He Y, Liu H, Wu X, Brutnell TP, Mockler TC and Oufattole M. 2017. Precise insertion and guided editing of higher plant genomes using Cpf1 CRISPR nucleases. *Sci. Rep*. **7**:11606.

Bernabé-Orts JM, Casas-Rodrigo I, Minguet EG, et al. 2019. Assessment of Cas12a-mediated gene editing efficiency in plants. *Plant Biotechnol J*. **17**(10):1971-1984.

Bhakta MS, Henry IM, Ousterout DG, Das KT, Lockwood SH, Meckler JF, Wallen MC, Zykovich A, Yu Y, Leo H, Liferg XU, Gersbach CA and Segal D. 2013. Highly active zinc-finger nucleases by extended modular assembly. *Genome Res* **23**: 530-538.

Boch J, Scholze H, Schornack S, Landgraf A, Hahn S, Kay S, Lahaye T, Nickstadt A and Bonas U. 2009. Breaking the code of DNA binding specificity of TAL-type III effectors. *Science* **326**: 1509-1512.

Boissel S, Jarjour J, Astrakhan A, Adey A, Gouble A, Duchateau P, Shendure J, Stoddard BL, Certo MT, Baker D and Scharenberg AM. 2014. megaTALs: A rare-cleaving nuclease architecture for therapeutic genome engineering. *Nucleic Acids Res* **42**: 2591-2601.

Briggs AW, Rios X, Chari R, Yang L, Zhang F, Mali P and Church GM. 2012. Iterative capped assembly: rapid and scalable synthesis of repeat-module DNA such as TAL effectors from individual monomers. *Nucleic Acids Res* **40**: e117.

Bolotin M, Coen D, Deutsch J, Dujon B, Netter P, Petrochilo E, and Slonimski PP. 1971. La recombinaison des mitochondries chez *Saccharomyces cerevisiae*. *Bull Inst Pasteur*, **69**:215-239.

Cai Y, Bak RO and Mikkelsen JG. 2014. Targeted genome editing by lentiviral protein transduction of zinc-finger and TALeffector nucleases. *eLife* **3**: e01911.

Cermak T, Doyle EL, Christian M, Wang L, Zhang Y, Schmidt C, Baller JA, Somia NV, Bogdanove AJ, and Voytas DF. 2011. Efficient design and assembly of custom TALEN and other TAL effector-based constructs for DNA targeting. *Nucleic Acids Res* **39**: e82.

Chevalier BS and Stoddard BL. 2001. Homing endonucleases: structural and functional insight into the catalysts of intron/intein mobility. Nucleic Acids Res. **29**:3757-3774.

Das BD and Paudel N. 2020. CRISPR/Cas9 applications and future prospectus in crop genetic improvement. *J Multidiscip Sci*, **2(2)**: 56-66.

Doudna JA and Charpentier E. 2014. The new frontier of genome engineering with CRISPR-Cas9. *Science*, **346**:1077-1087.

Doyon Y, Vo TD, Mendel MC, Greenberg SG, Wang J, Xia DF, Miller JC, Urnov FD, Gregory PD and Holmes MC. 2011. Enhancing zinc-finger-nuclease activity with improved obligate heterodimeric architectures. *Nat Methods*, **8**:74-79.

Dreier B, Fuller RP, Segal DJ, Lund CV, Blancafort P, Huber A, Koksch B and Barbas CF III. 2005. Development of zinc finger domains for recognition of the 50-CNN-30 family DNA sequences and their use in the construction of artificial transcription factors. *J Biol Chem*, **280**: 35588– 35597.

Faye G, Dennebouy N, Kujawa C and Jacq C. 1979. Inserted sequence in the mitochondrial 23S ribosomal RNA gene of the yeast *Saccharomyces cerevisiae*. *Mol. Gen. Genet*. **168**:101-109.

Gabriel R, Lombardo A, Arens A, Miller JC, Genovese P, Kaeppel C, Nowrouzi A, Bartholomae CC, Wang J, Friedman G, *et al*. 2011. An unbiased genome-wide analysis of zinc-finger nuclease specificity. *Nat Biotechnol*, **29**:816-823.

Gaj T, Guo J, Kato Y, Sirk SJ and Barbas CF III. 2012. Targeted gene knockout by direct delivery of zinc-finger nuclease proteins. *Nat Methods*, **9**:805-807.

Gaj T, Liu J, Anderson KE, Sirk SJ and Barbas CF III. 2014. Protein delivery using Cys2-His2 zinc-finger domains ACS. *Chem Biol*, **9**:1662-1667.

Gaj T, Sirk SJ, Shui S, and Liu J. 2016. Genome-Editing Technologies: Principles and Applications. *Cold Spring Harb Perspect Biol*, **8**:a023754.

Gayon, J. 2016. From Mendel to epigenetics: History of genetics. *Comptes Rendus Biologies*. **339**:225-230.

Guilinger JP, Thompson DB and Liu DR. 2014. Fusion of catalytically inactive Cas9 to FokI nuclease improves the specificity of genome modification. *Nat Biotechnol* **32**:577-82.

Guo J, Gaj T and Barbas CF III. 2010. Directed evolution of an enhanced and highly efficient FokI cleavage domain for zinc finger nucleases. *J Mol Biol*, **400**: 96-107.

Gupta A, Christensen RG, Rayla AL, Lakshmanan A, Stormo GD and Wolfe SA. 2012. An optimized two-finger archive for ZFN-mediated gene targeting. *Nat Methods*, **9**: 588-590.

Holkers M, Maggio I, Liu J, Janssen JM, Miselli F, Mussolino C, Recchia A, Cathomen T, and Gonçalves MA. 2012. Differential integrity of TALE nuclease genes following adenoviral and lentiviral vector gene transfer into human cells. *Nucleic acids research*. **41**(5): e63.

Horvath P and Barrangou R. 2010. CRISPR/Cas, the immune system of bacteria and archaea. *Science*; **327**:167-170.

Hsu PD, Lander ES and Zhang F. 2014. Development and Applications of CRISPR-Cas9 for Genome Engineering. *Cell*, **157(6)**: 1262-1278.

Hubbard BP, Badran AH, Zuris JA, Guilinger JP, Davis KM, Chen L, Tsai SQ, Sander JD, Joung JK and Liu DR. 2015. Continuous directed evolution of DNA-binding proteins to improve TALEN specificity. *Nat Methods*,**12**: 939-942.

Ishino Y, Shinagawa H, Makino K, Amemura M, and Nakata A. 1987. Nucleotide Sequence of the iap Gene, Responsible for alkaline Phosphate Isozyme Conversion in Escherichia coli, and Identification of Gene Product. *Journal of Bacteriology*, **169** (**12**): 5429-5433.

Jacquier A, and Dujon B .1985. An intron-encoded protein is active in a gene conversion process that spreads an intron into a mitochondrial gene. *Cell*, **41**:383-394.

Jinek M, Chylinski K, Fonfara L, Hauer M, Daudna JA, and charpentier E. 2012. A programmable dual-RNA- guided endonucleases in adaptive bacterial immunity . *Science*, **337** (6096): 816-822.

Karvelis T, Bigelyte G, Young JK, Hou Z, Zedaveinyte R, Pociute K, Silanskas A, Venclovas C and Siksnys V. 2019. PAM recognition by miniature CRISPR-Cas14 triggers programmable double-stranded DNA cleavage. *Bio Rxiv* (*Preprint*), Doi:http://doi.org/10.1101/654897

Kim HJ, Lee HJ, Kim H, Cho SW and Kim JS. 2009. Targeted genome editing in human cells with zinc finger nucleases constructed via modular assembly. *Genome Res*, **19**: 1279-1288.

Kim Y, Kweon J, Kim A, Chon JK, Yoo JY, Kim HJ, Kim S, Lee C, Jeong E, Chung E, et al. 2013a.A library of TAL effector nucleases spanning the human genome. *Nat Biotechnol*, **31**: 251-258.

Kim YG, Cha J and Chandrasegaran S. 1996. Hybrid restriction enzymes: Zinc finger fusions to Fok I cleavage domain. *Proc Natl Acad Sci*, **93**: 1156-1160.

Liu J, Gaj T,Wallen MC and Barbas CF III. 2015. Improved cell penetrating zinc-finger nuclease proteins for precision genome engineering. *Mol Ther Nucleic Acid*,,**4**: e232.

Maeder ML, Thibodeau-Beganny S, Osiak A, Wright DA, Anthony RM, EichtingerM, Jiang T, Foley JE,Winfrey RJ, Townsend JA, et al. 2008. Rapid "open-source" engineering of customized zinc-finger nucleases for highly efficient gene modification. *Mol Cell*, **31**: 294-301.

Maggio I, Stefanucci L, Janssen JM, Liu J, Chen X,Mouly V and Goncalves MA. 2016. Selection-free gene repair after adenoviral vector transduction of designer nucleases: rescue of dystrophin synthesis in DMD muscle cell populations. *Nucleic Acids Res*, **44**: 1449-1470.

Magnenat L, Blancafort P and Barbas CF III. 2004. In vivo selection of combinatorial libraries and designed affinity maturation of polydactyl zinc finger transcription factors for ICAM-1 provides new insights into gene regulation. *J Mol Biol*, **341**: 635-649.

Mahiny AJ, Dewerth A, Mays LE, Alkhaled M, Mothes B, Malaeksefat E, Loretz B, Rottenberger J, Brosch DM, Reautschnig P, et al. 2015. In vivo genome editing using nuclease-encoding mRNA corrects SP-B deficiency. *Nat Biotechnol*, **33**: 584-586.

Mak AN, Bradley P, Cernadas RA, Bogdanove AJ and Stoddard BL. 2012. The crystal structure of TAL effector PthXo1 bound to its DNA target. *Science*, **335**: 716-719.

Makarova KS, Wolf YI, Alkhnbashi OS, Costa F, Shah SA, Saunders SJ, Barrangou R, Brouns SJ, Charpentier E and Haft D. 2015. An updated evolutionary classification of CRISPR–Cas systems. *Nat Rev Genet*, **13**:722.

Meckler JF, Bhakta MS, Kim MS, Ovadia R, Habrian CH, Zykovich A, Yu A, Lockwood SH, Morbitzer R, Elsaesser J, Lahaye T, Segal D and Baldwin EP. 2013. Quantitative analysis of TALE-DNA interactions suggests polarity effects. *Nucleic Acids Res*.; **41**(7):4118-4128.

Miller JC, Tan S, Qiao G, Barlow KA, Wang J, Xia DF, Meng X, Paschon DE, Leung E, Hinkley SJ, Dlay GP, Hua KL, Ankoudinova I, Cost GJ, Urnov FD, Zhang HS, Holmes MC, Zhang L, Gregory PD and Rebar EJ. 2011. A TALE nuclease architecture for efficient genome editing. *Nat Biotechnol*, **29 (2)**:143–148.

Miller JC, Zhang L, Xia DF, Campo JJ, Ankoudinova IV, Guschin DY, Babiarz JE, Meng X, Hinkley SJ, Lam SC, Paschan DE, Vincent AI, Dulay GP, Barlow KA, Shivak DA, Leung E, Kim JD, Amora R, Urnov FD, Gregory PD and Rebar EJ. 2015. Improved specificity of TALE-based genome editing using an expanded RVD repertoire. *Nat Methods*, **12(5)**: 465–471.

Minkenberg B, Wheatley M and Yang Y. 2017. CRISPR/Cas9-enabled multiplex genome editing and its application. In Progress in Molecular Biology and Translational Science; *Elsevier: Amsterdam, The Netherlands*, **149**: pp. 111-132.

Mohanty S, Dash A and Pradhan CK. 2019. CRISPR-Cas9 Technology: A magical tool for DNA editing, *Int J of Biosciences and Bioengineering*, **1**:005.

Mussolino C, Alzubi J, Fine EJ, Morbitzer R, Cradick TJ, Lahaye T, Bao G and Cathomen T. 2014. TALENs facilitate targeted genome editing in human cells with high specificity and low cytotoxicity. *Nucleic Acids Res*, **42**: 6762-6773.

Netter P, Petrochilo E, Slonimski PP, Bolotin-Fukuhara M, Coen D, Deutsch J and Dujon B. 1974. Mitochondrial genetics. VII. Allelism and mapping studies of ribosomal mutants resistant to chloramphenicol, erythromycin and spiramycin in *S. cerevisiae*. *Genetics*, **78**:1063-1100.

Osakabe K, Osakabe Y and Toki S. 2010. Site-directed mutagenesis in Arabidopsis using custom-designed zinc finger nucleases. *Proc Natl Acad Sci* USA, **107**:12034-12039.

Pavletich NP and Pabo CO. 1991. Zinc finger-DNA recognition: Crystal structure of a Zif268-DNA complex at 2.1 *A. Science*, **252**: 809-817.

Petolino JF, Worden A, Curlee K, Connell J, Moynahan TLS, Larsen C and Russell S. 2010. Zinc finger nuclease-mediated transgene deletion. *Plant Mol Biol*, **73**:617-628.

Rai KM, Ghose K, Rai A, Singh H, Srivastava R, and Mendu V. 2019. Genome Engineering Tools in Plant Synthetic Biology. In Current Developments in Biotechnology and Bioengineering; *Elsevier: Amsterdam, The Netherlands*, pp. 47-73.

Ran FA, P.D. Hsu PD, Wright J, Agarwala V , D.A. Scott DA, and Zhang F . 2013. Genome engineering using the CRISPR-Cas9 system. *J Nature Protocols*, **8**:2281.

Reyon D, Tsai SQ, Khayter C, Foden JA, Sander JD and Joung JK. 2012. FLASH assembly of TALENs for high-throughput genome editing. *Nat Biotechnol*, **30**: 460-465.

Schmid-Burgk JL, Schmidt T, Kaiser V, Honing K and Hornung V. 2013. A ligation-independent cloning technique for high-throughput assembly of transcription activatorlike effector genes. *Nat Biotechnol*, **31**: 76-81.

Shukla VK, Doyon Y, Miller JC, DeKelver RC, Moehle EA, Worden SE, Mitchell JC, Arnold NL, Gopalan S and Meng X. 2009. Precise genome modification in the crop species Zea mays using zinc-finger nucleases. *Nature*, **459**:437.

Silva A, Almeida B, Sampaio-Marques B, Reis MIR. et. al. 2011. Glyceraldehyde-3-phosphate dehydrogenase (GAPDH) is a specific substrate of yeast metacaspase./ *Biochimica et Biophysica Acta*, **1813,** 2044-2049.

Smith J, Bibikova M, Whitby FG, Reddy AR, Chandrasegaran S and Carroll D. 2000. Requirements for double-strand cleavage by chimeric restriction enzymes with zinc finger DNA-recognition domains. *Nucleic Acids Res*, **28**: 3361-3369.

Song G, Balakrishnan R, Binkley G, Costanzo MC, Dalusag K, Demeter J, Engel S, Hellerstedt ST, Karra K, et al. 2016. Integration of new alternative reference strain genome sequences into the Saccharomyces genome database. *Oxford University Press*, article ID baw0**74**.

Sorek R, Kunin V and Hugenholtz P. 2008. CRISPR — a widespread system that provides acquired resistance against phages in bacteria and archaea. *Nat Rev Microbiol*, **6**:181-186.

Stella S, Alcón P and Montoya GJN. 2017. Structure of the Cpf1 endonuclease R-loop complex after target DNA cleavage. *Nature*, **546**:559.

Sternberg SH, Redding S, Jinek M, Greene EC, and Doudna JA.2014. DNA interrogation by the CRISPR RNA-guided endonuclease Cas9. *J Nature*. **507**: 62.

Stoddard BL. 2005. Homing endonuclease structure and function. *Quarterly Reviews of Biophysic*, **38**: 49-95.

Stoddard BL. 2011. Homing Endonucleases: From Microbial Genetic Invaders to Reagents for Targeted DNA Modification, *Structure* **19**: 7-15.

Stoddard BL. 2014. Homing endonucleases from mobile group I introns: discovery to genome engineering. *Mobile DNA*, **5**: 7.

Streubel J, Blucher C, Landgraf A and Boch J. 2012. TAL effector RVD specificities and efficiencies. *Nat Biotechnol* 30: 593-95.

Tang X, Liu G, Zhou J, Ren Q, You Q, Tian L, Xin X, Zhong Z, Liu B and Zheng X. 2018. A large-scale whole-genome sequencing analysis reveals highly specific genome editing by both Cas9 and Cpf1 (Cas12a) nucleases in rice. *Genome Biol*. **19**: 84.

Tang X, Lowder LG, Zhang T, Malzahn AA, Zheng X, Voytas DF, Zhong Z, Chen Y, Ren Q and Li QA. 2017. CRISPR–Cpf1 system for efficient genome editing and transcriptional repression in plants. *Nat. Plants*, **3**:17018.

Urnov FD, Rebar EJ, Holmes MC, Zhang HS and Gregory PD. 2010. Genome editing with engineered zinc finger nucleases. *Nat Rev Genet*, **11**: 636–646.

Vats S, Kumawat S, Kumar V, Patil GB, Joshi T, Sonah H, Sharma TR, and Deshmukh R. 2019. Genome Editing in Plants: Exploration of Technological Advancements and Challenges, *Cells*, **8**:1386;

Wang H, La Russa M, and Qi LS. 2016. CRISPR/Cas9 in genome editing and beyond. *J Annual review of biochemistry*, **85**:227-264.

Wolfe SA, Nekludova L and PaboCO. 2000. DNA recognition by Cys2His2 zinc finger proteins. *Annu Rev Biophys Biomol Struct*, **29**: 183-212.

Xie K, Zhang J and Yang Y.2014. Genome-wide prediction of highly specific guide RNA spacers for CRISPR–Cas9-mediated genome editing in model plants and major crops. *Mol Plant*, **7**:923-926.

Xie Y, Kang R, Sun X, Zhong M, Huang J, Klionsky DJ, and Tang D. 2015. Posttranslational modification of autophagy-related proteins in macroautophagy, *Autophagy*, **11**: 28-45.

JJBS

Volume 14, Number 3, September 2021
ISSN 1995-6673
Pages 513 - 522

Jordan Journal of Biological Sciences

Comparative Metabolomics Analysis and Radical Scavenging Activity of *Saraca asoca* (Roxb.) de Wilde Flowers in Different Stages of Maturity

Anindita Hazra, Susmita Das*

Phytochemistry and Pharmacognosy Laboratory, Department of Botany, University of Calcutta, 35, Ballygunge Circular Road, Kolkata – 700019, West Bengal, India

Received: July 24, 2020; Revised: November 18, 2020; Accepted: December 10, 2020

Abstract

The flower extracts of *Saraca asoca* were evaluated in their three different phenological stages of flowering [bud (S1), mature (S2) and senescent (S3)] in terms of chemical composition and antioxidant activity. The GC/MS based fingerprinting led to identification of 85 metabolites, including 9 amino acids, 20 organic acids, 7 fatty acids, 20 sugar and sugar acids, 8 sugar alcohols, 13 phenols and phenolic acids and 8 others compounds. The three flowering stages showed prominent changes in their metabolite profile during the process of maturation of the flowering stages from bud to mature to senescence stages determined via GC/MS based metabolomics and chemometric approaches. The amounts and composition of metabolites in each stage showed statistically significant differences, which were reflected in their antioxidant capacities. The three phenological stages showed antioxidant activities in a dose dependent manner, but the senescent stage showed highest superoxide radical scavenging activity (IC_{50} = 65.17 ± 2.647 mg/ml) and metal chelating effect (6.65 ± 0.331 mg/ml) in agreement with their high content of phenolic acids. These differences were strongly reproduced in the chemometric analyses (PCA, PLS-DA and s-PLS-DA), identifying the most distinctive features of the three flowering stages. This study might be beneficial to select the most potent flowering stage for incorporation in functional food.

Keywords: *Saraca asoca*, phenological stages, flowering, antioxidant, phytochemicals, functional food

1. Introduction

Since time immemorial, plant products or their derivatives and other natural resources are beneficial for the treatment of various illnesses. Mainly fruits and vegetables provide most of the phytonutrients in human diet. But flowers can also become an important source of bioactive components and can be added in human diet. Earlier flowers were mainly eaten for their therapeutic properties rather than their nutritional features. In the present time, several metabolomics studies revealed the presence of important bioactive molecules by metabolite profiling of wild and ornamental flowers. Wild flowers can also be an important source of low cost natural antioxidants, and many edible flowers are used as food additives to enhance color, flavor, taste and fragrance to food and drinks (Kelley *et al.,* 2001; Pires *et al.,* 2018)

Saraca asoca (Roxb.) de Wilde, known as Ashoka in West Bengal, India, belongs to the family Caesalpiniaceae and is a small evergreen tree. The plant is one of the most ancient plants known, mentioned in old Indian Ayurvedic manuscripts and is geographically distributed mainly in Asia and some parts of North America (Murthy *et al.,* 2008). The medicinal properties of this plant are beneficial in several gynecological complications (Panchawat and Sisodia 2010). In India, married women are known to consume Ashoka flower buds as a ritual to protect their children and for several gynecological problems (Pradhan *et al.,* 2009).

All parts of this plant especially barks, leaves, flowers and seeds are considered useful with high medicinal impact (Shukla *et al*., 2008). The flowers are therapeutically important part as these are used in the treatment of cancer, diabetes, hemorrhagic dysentery, several uterine disorders like menorrhagia, and also used in bleeding piles, bacillary dysentery, etc. During a Bengali Hindu ceremonial known as '*Ashoka – sasthi*' the flower buds are taken orally by women. Only a few reports on phytochemical constituents of leaves and flowers of the plant have been published earlier (Pradhan *et al.,* 2010) but no detailed qualitative and quantitative phytochemical analyses are found for flowers.

The flowers of *Saraca asoca* are the important part of many Ashoka rich herbal formulations. So far, it has been reported to contain tannins, flavonoids, saracasin, saracadin, waxy substances, carbohydrates, proteins and steroids (Saha *et al.,* 2013). The presence of many fatty acids like oleic acid, palmitic acid, stearic acid, linoleic acid and linolenic acids, glucosides like quercetin-3-O-p-D-glucoside, apigenin-7-O-p-D-glucoside, pelargonidin-3,5-diglucoside and cyanidine-3,5-diglucoside, steroids such as p- and γ-sitosterols, flavonoids such as quercetin, leucocyanidin and polyphenols such as gallic acid and

* Corresponding author e-mail: susouravipar@gmail.com.

ellagic acid have been reported also (Pradhan *et al.*, 2009; Saha *et al.*, 2013; Gupta *et al.*, 2014).

Due to normal physiological processes and various xenobiotic factors by the process of membrane lipid and many other biomolecular peroxidations, Reactive Oxygen Species (ROS) like superoxide anion, hydroxyl radicals and hydrogen peroxide are generated. These ROS are associated in the etiology of several high risk ailments like cardiovascular disorders, coronary artery disease, stroke, rheumatoid arthritis, diabetes, hypertension and several types of carcinogenicity (Lefer and Granger 2000; Zahin *et al.*, 2009). Free radicals prompt oxidative damages to biomolecules. Antioxidants and free radical scavengers from natural sources exert a significant role in protecting humans from several contagious infections, stress related pathologies and degenerative disorders (Feugang *et al.*, 2006; Saha *et al.*, 2018). The adverse effects of synthetic antioxidants like BHA (Butylated hydroxyl anisole) and BHT (Butylated hydroxyl toluene) used as synthetic additives in food stuff have already been experienced by modern humans that these synthetic antioxidants induce immense toxicity, carcinogenicity and causes DNA damage and other aberrations (Rajkumar *et al.*, 2010). Recently, scientists are looking for diet derived antioxidants or naturally occurring antioxidants to replace all those synthetic antioxidants which are being restricted for their adverse impacts.

The plant metabolomics is an important tool to identify and quantify primary and secondary metabolites of natural products (Mishra *et al.*, 2015; Pandey *et al.*, 2015; Patel *et al.*, 2016). Although plant primary metabolites are indispensable to perform life functions, the production of plant secondary metabolites are influenced by genotype, phenological stages and eco-physiological conditions (Marrelli *et al.*, 2012). The phenological stage is considered as the most important determining factor of the quality and quantity of metabolites from dietary, nutritional and pharmaceutical point of view and thus holds immense importance (Marrelli *et al.*, 2012).

Saraca asoca flowers are a potent reservoir of bioactive components, which may vary through the floral developmental stages. Studying the metabolite composition of this flower developmental stage associated with specific metabolism and free radical scavenging activity would be of enormous importance. However, to the best of our knowledge, so far no such research has been done on the metabolite profiling and radical scavenging analysis with respect to the different phenological / maturation stages of *Saraca asoca* flowers from bud, to mature to senescent stages to find out the most potent floral stage to be incorporated as functional food. Moreover, the present study may also deliver an understanding of the optimisation of the procurement of *Saraca* flowers and the maximization of bioactive potentials.

2. Materials & Methods

2.1. Plant material

Saraca asoca flowers were procured from the garden of Burdwan University Campus, East Burdwan, West Bengal (23°25’N, 87°84’E), India, during the season of spring time in the month of March, 2018, with an average day temperature ranges between 27° C. to 30° C. for the three different developmental / phenological stages [bud stage: flowers with closed petal (S1), mature stage: full flowering stage, stamens are extruded and the petals are fully exposed (S2) and senescent stage : stamens dried and shrivelled, just started to develop fruit and flower near to senescence, but still attached (S3) with the plant (Figure 1)]. All the three stages of flowers were collected in ample amounts from the same species of plant and at the same season and weather pattern.

After proper taxonomic identification of the plant (Voucher No. Phytopharma 332 1a), the flower samples of S1, S2 and S3 stages were shade – dried separately and the dried samples were then powdered with an electric grinder and sieved to make fine dried homogenous powder of three different stages.

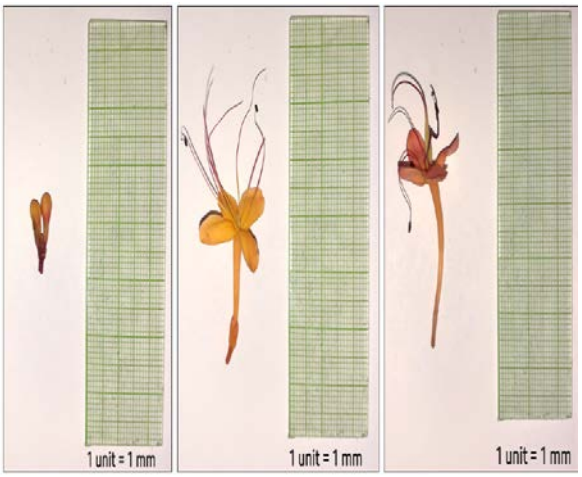

Figure 1. Flower of *Saraca asoca* in the S1, S2 and S3 stages

2.2. Chemicals

Adonitol, MOX, MSTFA, FAME standards were procured from Sigma Aldrich (St. Louis, MO); and pyridine from Merck Specialities Private Limited, India. DPPH was obtained from Sigma, USA. NBT, ferrozine were obtained from SRL PVT. Ltd., India. Methionine, riboflavin and EDTA were obtained from HiMedia Laboratories Limited. Ferric chloride, ammonium molybdate were obtained from Merck Specialities Pvt. Ltd. All the other reagents used for sample preparation were of analytical grade, and all the solvents used for GC/MS were of HPLC grade.

2.3. Preparation of extracts for the evaluation of antioxidant properties

80% methanolic extracts were prepared from the dried samples of S1, S2 and S3 stages. The samples (150 gram) were extracted by stirring with 300 ml of 80 % methanol in a water bath at 65ºC for 3 hours and subsequently after cooling, the filtrate was cold centrifuged at 10,000 rpm for 20 minutes. The combined 80% methanolic extracts were evaporated to dryness under reduced pressure. The crude extracts obtained were preserved at -20º C freezer for further study.

The dried crude extracts were re-dissolved in methanol (1 mg/ml) for evaluation of antioxidant potentiality. The final solutions were further diluted to different concentrations to determine the bioactivity for S1, S2 and S3 stages of the samples in *in vitro* assays. Each

experiment was performed thrice. The results were expressed in IC_{50} values (i.e., the concentration at which the samples showing 50 % inhibition of free radicals).

2.4. DPPH radical scavenging activity

DPPH free radical scavenging activities of S1, S2 and S3 extracts were assessed following the method described (Braca *et al.,* 2001). 0.1 ml of extract was added to 3 ml of DPPH solution (0.004% methanolic solution). After 30 minutes of incubation at room temperature, the absorbance was measured at 517 nm using a UV-VIS spectrophotometer. Lower absorbance values indicate greater free radical scavenging activity. The percentage inhibition activity of scavenging DPPH radical was calculated using the formula $[(A_0 - A_e) / A_0] \times 100$; where A_0 = absorbance of control reaction and A_e = absorbance in presence of extract. All the tests were performed in triplicates and the results were averaged.

2.5. Superoxide radical (O2-) scavenging activity

Superoxide radical scavenging activity was measured following the method of Banerjee and De (Beauchamp and Fridovich 1971; Dasgupta and De 2004) in the riboflavin-light-NBT system. The superoxide anion radicals were made in 50 mM sodium phosphate buffer (pH 7.8), 13 mM methionine, 2 µM riboflavin, 100 µM EDTA and 75 µM NBT solution and 1 ml extract of sample of different concentrations is added to the mixture. After 10 minutes of illumination from fluorescent lamp, the formation of blue formazan was measured by following the increase in absorbance at 560 nm. One set of reaction tubes was covered with aluminium foil. Similar tubes with reaction mixture were kept in the dark and served as blanks. The percentage inhibition activity of scavenging superoxide radical was calculated with the formula $[(A_0 - A_e)/ A_e] \times 100$.

2.6. Metal chelating effect (Ferrous ion)

Fe^{2+} chelating ability proves the antioxidant capacity of plant extract (Wang *et al.,* 2003). The reaction mixture containing 100 µl of the plant extract, 200 µl of 0.5 mM ferrous chloride, 200 µl of 5 mM ferrozine were incubated at 37°C for 10 minutes. After addition of 1.5 ml double distilled water to the mixture, the absorbance of the solution was taken at 562 nm where the lower absorbance indicated the stronger chelating effect.

2.7. Total antioxidant capacity (TAC)

The reaction mixture contained 0.1 ml of sample solution and 1 ml of reagent mixtures (prepared by mixing phosphate buffer, sulphuric acid and ammonium heptamolybdate in a ratio of 4:3:3) (Aguilar *et al.,* 1999). The reaction mixture was incubated at 95°C for 90 min., then the mixture was cooled to room temperature. The absorbance of the solution was measured at 695 nm against the blank. The reduction of Mo_{VI} to Mo_v by the extract and the formation of green phosphate / Mo_v complex at acidic pH were assayed. The TAC was measured from the regression equation $y = 31.54x - 0.001$ as equivalent to ascorbic acid.

3. Sample preparation for GC/MS analysis

5 mg of crude extract was dissolved in methanol: water in a ratio of 1:1. In it 20 µl of ribitol (Adonitol - Internal Standard) (0.2 mg/ ml) was added and the aliquot made thereafter was distributed into eppendorff tubes (50 µl × 4) and evaporated to dryness. The residue obtained was re-suspended in 5 µl of MOX (20 mg/ml in pyridine) and then shaken for 90 minutes at 30ºC. Then 45 µl of MSTFA was added and shaken at 37ºC for 30 minutes for trimethylsilylation of acidic protons to enhance the volatility of components. 1 µl of FAME markers (a mixture of IRI markers) was added (prepared using fatty acid methyl esters of C8, C10, C12, C16, C18, C20, C22, C24 and C26 linear chain length dissolved in chloroform). GC/MS analysis (Agilent 7890 A GC equipped with 5795 C inert MSD with Triple Axis Detector) was carried out following the method of Kind et al., 2009 (Kind *et al.,* 2009) with some modifications (Das *et al.,* 2016). Prior to injection in GC the samples were preserved at 4ºC for 10 minutes to maintain sedimentation of components.

3.1. Detection of metabolites by GC/MS

The detection of metabolites was done using DB-5-MS capillary column under the following oven temperature programme: oven ramp 60º C (1 minute hold) to 325 ºC at10 ºC /min, 10-minute hold before cool down, 37.5 minute run time. The injection temperature was set at 250º C, the MS transferline at 290º C, and the ion source at 230 ºC. Helium was used as the carrier gas at a constant flow rate of 2.5 ml / minute (carrier linear velocity 57.95 cm/sec). 1 µl of sample was injected manually via the split mode (split ratio 1:5) onto the GC column. Before analysis, the method was calibrated with the FAME standards available on the Fiehn GC/MS Metabolomics library (2008) (Agilent Chem Station, Agilent Technologies Inc., Wilmington, USA) following user's guide. AMDIS was used to deconvolute GC/MS results to identify the chromatographic peaks. Auto-tuning and tune evaluation of Mass Detector was done at least once a week.

Identification of metabolites was done by comparing the RT, RI of the metabolites and also by comparing the MS fragmentation patterns of the mass spectra with the entries of compound in Agilent Fiehn GC/MS Metabolomics library (2008) using metabolite database – AMDIS using Agilent RTL method. RT of some of the metabolites were further compared with that of the standard compounds.

3.2. Statistical analysis

Antioxidant activities were estimated in triplicates. The results were expressed as means ± standard deviations. All the statistical tests were performed at 5% significance level using Microsoft Excel 2013.

The three selected phenological stages were subjected to Multivariate Analysis to determine the differences in metabolite composition among S1, S2 and S3 stages.

To identify the statistical significance difference and to compare the dependent variables, the one-way ANOVA and a post-hoc test using Tukey's HSD were done and determined by p-values lower than 0.05. Based on the generalized logarithm transformed dataset, heat map, clustering of samples as well as metabolites were also developed utilizing squared Euclidean distance and ward linkage.

The relative response ratios of the metabolites of S1, S2 and S3 stages were subjected to Metaboanalyst 4.0. PCA,

PLS-DA and s-PLS-DA were applied as pattern recognition unsupervised classification method. The construction of the matrix for PCA included 85 variables (corresponding to the responses of metabolites) and 3 samples (corresponding to the flowering stages).

4. Results

4.1. Evaluation of antioxidant potentialities

In this investigation, the antioxidant activities of the studied flowering stages were measured and compared by DPPH, superoxide radical scavenging, metal chelation activity and TACs. All the flowering stages showed antioxidant activities. DPPH (1, 1-diphenyl-2-picrylhydrazyl) is a widely known stable radical used for the assessment of the ability of phenolic substances which can donate labile H-atom to the free radicals. In this assay, the H-donating antioxidant component reduces the DPPH to form non-radical DPPH-H (Shen *et al.*, 2010). DPPH free radical scavenging activities of extracts of S1, S2 and S3 stages of *Saraca asoca* flowers were found proportionate to the concentration of the extracts ($r > 0.9$). Activity of S1 stage was found significantly higher than S2 and S3 stages in DPPH inhibition. IC_{50} values are shown in Table 1. S1 stage (bud stage) showed the highest radical scavenging activity against DPPH (IC_{50} value = 65.82 mg/ml ± 0.614).

In this study, we have observed that the extracts of all the three stages of flowering scavenged the superoxide radical in a dose dependent manner ($r > 0.93$). IC_{50} values are presented in Table 1. The S3 stage was significantly different from S1 and S2 stages. The S3 stage (senescent stage) gave highest inhibitory activity against superoxide radical (IC_{50} value = 65.17mg/ml ± 2.647).

The metal chelation effect is based on the chelation of ferrous ions by plant extract. Ferrozine can form complexes with ferrous ions (Fe^{2+}). The formation of complex with Fe^{2+} is disrupted in presence of plant extract as chelating agent resulting in a significant decrease in the red color of the complex. Removal or reduction of iron ion from the cellular system is a promising approach to prevent oxidative stress related diseases and disorders. Fe^{2+} ion chelating property of S1, S2 and S3 stages were compared as shown in Table 1. The ferrous ion chelating property was also found greatest in S3 stage (6.65mg/ml ± 0.331).

No significant difference was estimated in TACs of the three stages of flowering (Table 1).

Table 1. Antioxidant activity of 80% methanolic extracts obtained from three stages of flowering (S1, S2 and S3) of *Saraca asoca* (Mean ± SE)

		Antioxidant assays (IC_{50}values* ± SE) mg/ml			
		DPPH radical scavenging activity	Superoxide radical scavenging activity	Metal Chelating Effect	Total Antioxidant Capacity
Flowering stage	S1 (bud stage)	65.82 ± 0.614	74.79 ± 5.258	15.161 ± 0.43	0.000305 ± 3.295E-05
	S2 (mature stage)	95.26 ± 6.225	120.61 ± 5.279	12.905 ± 0.129	0.00037 ± 7.33 E-05
	S3 (senescent stage)	71.39 ± 1.711	65.17 ± 2.647	6.65 ± 0.331	0.00041 ± 8.758 E-05
p-value**		0.0021	0.0004	5.05E-06	

* IC_{50} values correspond to the sample concentration showing 50% of inhibitory activity

**p value < 0.05 indicates that the mean value of the evaluated parameters of one flowering stage differs from the others (ANOVA post _ hoc HSD Tukey's Test were performed)

4.2. Characterization of metabolites

A total of 85 metabolites have been identified (Table 2) following GC/MS based metabolomics approach from the three phenological stages of *Saraca asoca* flowers. The metabolites identified include 9 amino acids, 20 organic acids, 7 fatty acids, 20 sugar and sugar acids, 8 sugar alcohols, 13 phenols and phenolic acids and 8 other compounds using Agilent Fiehn Metabolomics Library.

The Relative response ratios (RRR) were calculated by normalization of the peak areas of each metabolite obtained by dividing with the weight of the sample and the peak areas of the internal standard. The relative response ratios correspond with the semi-quantitative concentration of each metabolite. From the log of RRR / gram sample extracted, dendrograms (Figure 2) and heat map (Figure 3) were prepared using Metaboanalyst 4.0 software to separate the three phenological stages of flowering based on the metabolite profiling. The data were further analyzed by unsupervised PCA (figure not given) and supervised discriminant analysis (PLS-DA and s-PLS-DA). PCA, PLS-DA and s-PLS-DA (Figure 4) separated the bud, mature and senescent stages distinctly from each other.

Table 2. Tentative identification and quantification of metabolites

	Metabolites Identified	Response ratios / gram sample extract (Average ± SD)		
		S1	S2	S3
AMINO ACIDS	Aspartic acid	14.19 ± 9.05	664.23 ± 1132.05	117.91 ± 79.94
	Beta-alanine	7.09 ± 0.00	0.0028 ± 0.00	7.06 ± 5.41
	Glycine	0.85 ± 1.54	9.88 ± 18.70	0.0004 ± 0.00
	L-norleucine	0.85 ± 0.00	0.0028 ± 0.00	1.28 ± 1.57
	Phenylalanine	2.22 ± 1.56	0.0028 ± 0.00	0.0004 ± 0.00
	L-proline	6.40 ± 5.86	237.65 ± 339.94	76.18 ± 20.15
	L-serine	7.17 ± 3.14	0.0028 ± 0.00	6.88 ± 5.45
	L-threonine	4.96 ± 1.87	49.47 ± 88.52	1.13 ± 1.34
	L-valine	4.52 ± 3.87	116.93 ± 210.17	12.97 ± 1.64
ORGANIC ACID	2-isopropylmalic acid	2.54 ± 0.00	62.46 ± 102.70	30.23 ± 3.41
	cis-4-hydroxycyclohexanecarboxylic acid	0.0002 ± 0.00	0.0028 ± 0.00	3.41 ± 4.14
	Citric acid	367.70 ± 113.96	35955.53 ± 435.95	4594.03 ± 37.29
	Fumaric acid	372.74 ± 4.04	791.40 ± 12.61	403.05 ± 90.18
	Gluconic acid	37.99 ± 24.22	14898.21 ± 232.11	500.23 ± 61.07
	Glyceric acid	108.97 ± 27.93	30049.76 ± 553.35	10692.37 ± 632.23
	Glycolic acid	113.46 ± 95.74	2960.66 ± 43.34	402.53 ± 42.38
	3-hydroxy-3-methylglutaric acid (dicrotalic acid)	7.22 ± 5.94	5.45 ± 6.35	0.00042 ± 0.00
	L-(+)lactic acid	27.33 ± 37.23	4435.01 ± 72.48	57.32 ± 50.94
	D-malic acid	823.36 ± 36.14	39281.90 ± 426.14	11006.72 ± 514.28
	Maleamic acid	800.43 ± 0.00	530.02 ± 1014.19	19.84 ± 15.05
	Maleic acid	0.0002 ± 0.00	71.88 ± 143.53	123.17 ± 86.79
	Malonic acid	1.01 ± 1.17	90.34 ± 121.80	12.42 ± 9.61
	Oxalic acid	34.48 ± 3.41	3848.34 ± 64.89	25.64 ± 17.89
	Phosphoric acid	85.00 ± 67.86	14709.13 ± 171.83	3830.18 ± 24.53
	Pipecolic acid	54.56 ± 4.85	413.00 ± 778.48	22.80 ± 8.79
	Succinic acid	10.10 ± 16.04	4287.67 ± 82.60	92.19 ± 64.08
	Tartaric acid	16.33 ± 31.99	2063.14 ± 33.95	67.22 ± 78.34
	Tatronic acid	9.25 ± 0.00	0.0028 ± 0.0024	32.69 ± 3.63
FATTY ACIDS	Capric acid	1.33 ± 1.21	181.06 ± 13.77	8.31 ± 5.44
	Heptadecanoic acid	3.24 ± 2.56	214.54 ± 227.01	5.83 ± 4.19
	6-hydroxyhexanoic acid	4.01 ± 6.54	172.09 ± 200.31	32.41 ± 7.23
	Lauric acid	13.11 ± 12.13	1007.60 ± 956.41	69.64 ± 24.03
	Myristic acid	2745.90 ± 662.87	66206.58 ± 513.77	13266.21 ± 134.36
	Palmitic acid	2809.36 ± 86.32	3209.72 ± 311.04	396.27 ± 75.64
	Stearic acid	137.19 ± 76.09	6969.87 ± 70.33	327.99 ± 78.63
SUGARS and SUGAR DERIVATIVES	D-allose	152.25 ± 21.77	60214.27 ± 732.19	108.81 ± 17.89
	Fructose	2725.97 ± 103.11	12913.69 ± 73.62	6328.67 ± 51.30
	D-glucose	3644.51 ± 2697.22	44601.07 ± 55830.26	2969.58 ± 985.96
	Gluconic acid lactone	1014.15 ± 16.41	3391.20 ± 96.93	0.0004 ± 0.00
	L-gulonic acid gamma-lactone	8.88 ± 6.86	0.0028 ± 0.0024	0.0004 ± 0.00
	Lactulose	2.81 ± 0.00	955.68 ± 1226.62	0.0004 ± 0.00
	Leucrose	1.26 ± 4.41	956.76 ± 1244.68	0.0004 ± 0.0004
	Maltose	1.26 ± 0.00	555.88 ± 1055.13	119.49 ± 44.79
	D-mannose	71.71 ± 51.62	32691.94 ± 395.46	583.13 ± 80.59
	Mucic acid	75.83 ± 4.91	456.90 ± 732.69	61.88 ± 19.89
	Palatinose	8.48 ± 6.83	1823.71 ± 282.01	36.70 ± 43.48
	Ribonic acid-gamma-lactone	32.59 ± 20.42	4246.33 ± 77.22	111.17 ± 62.40
	D-saccharic acid	28.24 ± 0.00	606.34 ± 48.83	0.00042 ± 0.00043
	Sedoheptulose anhydride monohydrate	7.75 ± 10.35	2119.35 ± 54.65	0.00042 ± 0.00043
	Sophorose	14.87 ± 27.07	2665.70 ± 3691.11	0.00042 ± 0.00043
	Sucrose	68.47 ± 70.77	61392.09 ± 467.22	105.95 ± 38.64
	Tagatose	61.35 ± 0.00	390.12 ± 689.19	171.54 ± 15.11
	Talose	0.00 ± 0.00	4282.46 ± 6837.99	0.00042 ± 0.00043
	D-(+) trehalose	6.38 ± 17.94	0.0028 ± 0.00	10159.29 ± 6651.45
	turanose	17.96 ± 9.50	3457.66 ± 77.24	99.99 ± 82.40

SUGAR ALCOHOLS	Acetol	11.58	± 0.00	0.0028	± 0.00	2499.76	± 874.17
	Allo-inositol	169.24	± 70.83	29142.81	± 344.88	3177.24	± 246.06
	Galactinol	170.14	± 2.39	53.24	± 102.46	0.0004	± 0.0004
	Glycerol	0.89	± 0.00	16455.97	± 19856.48	556.60	± 234.03
	D-mannitol	2.14	± 6.31	2365.66	± 991.42	1644.39	± 181.18
	Myo-inositol	565.92	± 17.75	49024.79	± 623.02	16995.64	± 153.38
	D-sorbitol	563.78	± 0.00	0.0028	± 0.00	69.40	± 55.82
	D-threitol	0.00017	± 0.00	166.05	± 304.29	461.06	± 74.13
PHENOLS AND PHENOL DERIVATIVES	O-acetylsalisylic acid	0.00017	± 0.00	95.43	± 175.36	24.72	± 19.63
	Alizarin	1.60	± 3.55	38.14	± 49.89	0.0004	± 0.0004
	Benzoic acid	1.79	± 0.55	0.0028	± 0.00	5.85	± 1.67
	3,4-dihydroxybenzoic acid	9.44	± 9.27	0.00283	± 0.00	0.00042	± 0.00043
	Gallic acid	1297.04	± 33.74	43236.67	± 440.85	11015.00	± 68.58
	Gentisic acid	1287.79	± 0.00	135.04	± 27.75	60.16	± 85.69
	Homogentisic acid	0.0002	± 0.00	0.0028	± 0.00	1.56	± 1.13
	4-hydroxy-3-methylbenzoic acid	0.00017	± 0.00	0.00283	± 0.00	19.46	± 22.57
	2-hydroxyphenylacetic acid	0.00017	± 0.00	0.00283	± 0.00	6.35	± 7.39
	Hydroquinone	0.17	± 0.58	23.24	± 32.75	0.00042	± 0.00043
	4-isopropylbenzoic acid	0.96	± 1.11	110.88	± 163.74	5.99	± 0.97
	Shikimic acid	46.94	± 50.95	1586.94	± 2409.22	907.11	± 160.31
	4-vinylphenol	46.55	± 0.42	20.34	± 32.87	0.00042	± 0.00043
N-BASES AND OTHERS	Adenosine	4.39	± 5.74	344.05	± 55.30	0.00042	± 0.00043
	Adrenaline	4.00	± 0.00	197.65	± 34.00	0.00042	± 0.00043
	Nicotinic acid	1.77	± 6.31	232.04	± 38.78	16.62	± 4.46
	Pyrogallol	5.48	± 3.11	166.47	± 65.77	0.00042	± 0.00043
	Thymine	3.71	± 0.00	16.61	± 3.55	0.97	± 1.12
	Tyramine	66.34	± 50.16	731.81	± 83.42	106.56	± 6.33
	Uracil	67.74	± 2.31	153.56	± 184.28	14.49	± 12.20
	Urea	2.04	± 1.33	0.0028	± 0.0024	0.0004	± 0.0004

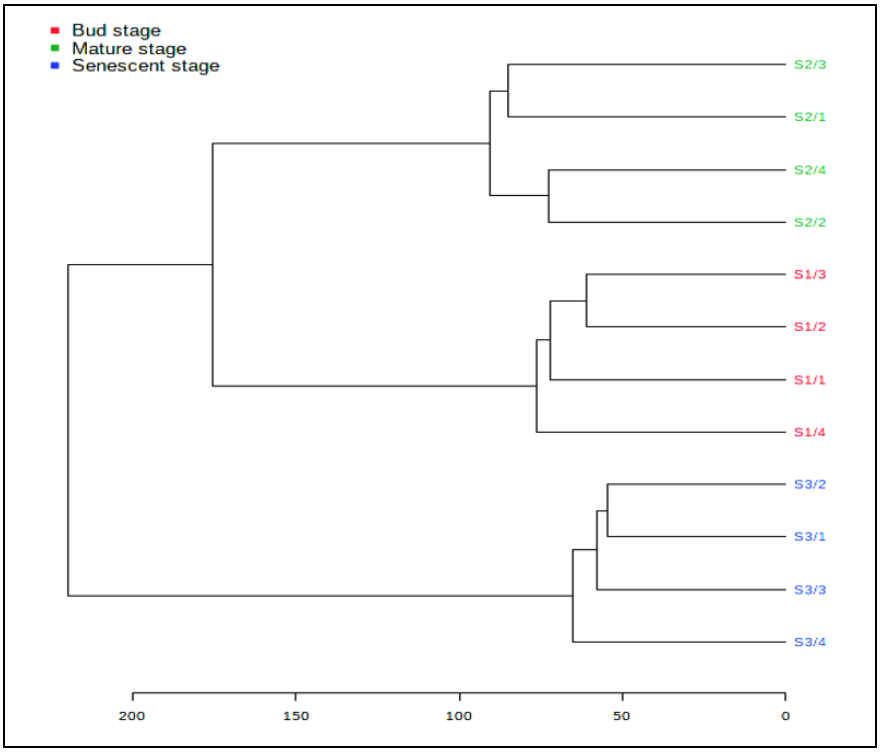

Figure 2. Dendrogram generated from log of normalised RRRs of three phenological stages of flowering of *Saraca asoca*

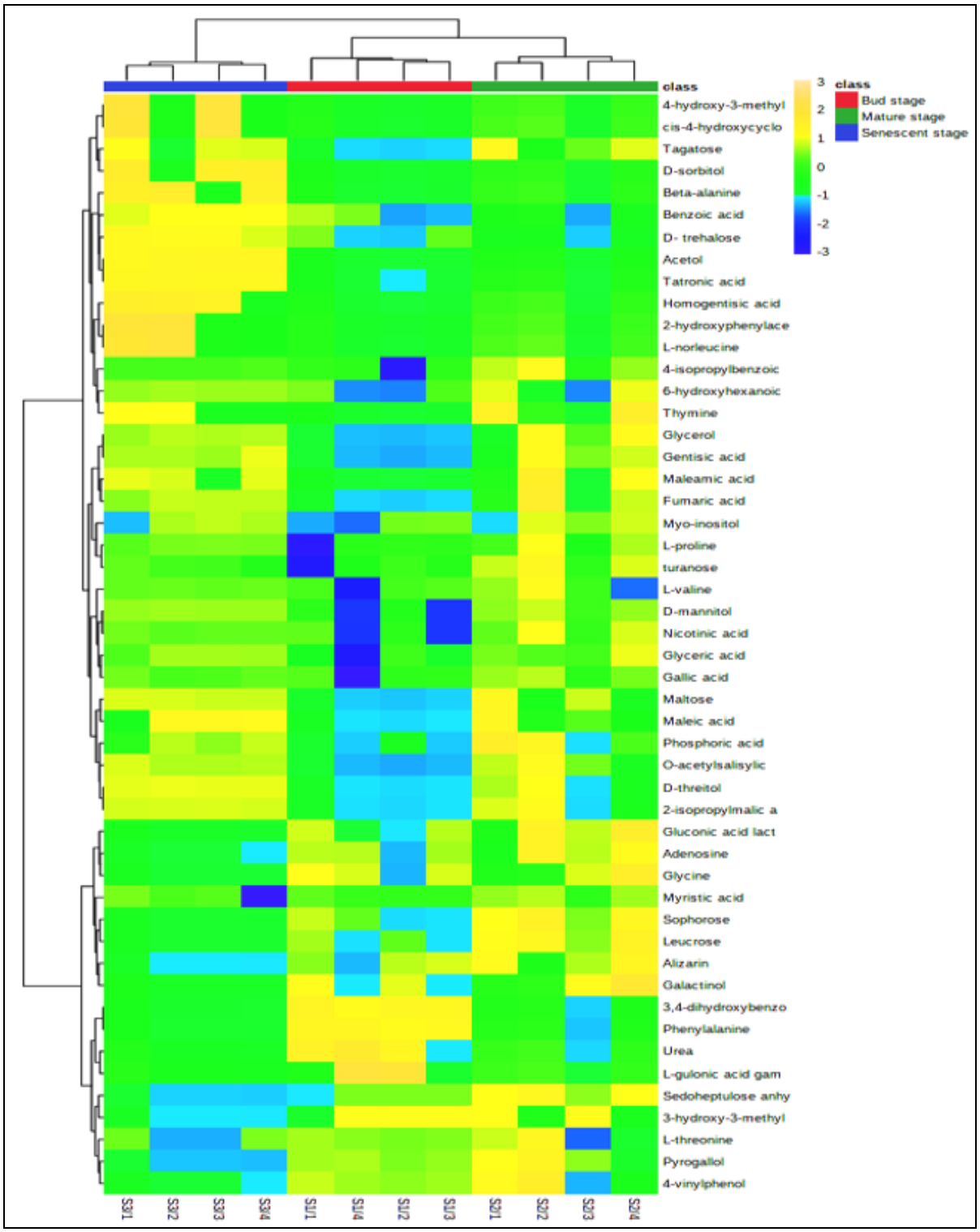

Figure 3. Heat map showing changes in relative concentration among the three phenological stages of flowering

The dendrogram (Figure 2) and the heat map (Figure 3) illustrate that the three flowering stages (Bud-S1, Mature-S2 and Senescent-S3) of *Saraca asoca* are distinctly different based on their primary and secondary metabolite compositions. In the heat map (Figure 3), the changes in relative concentration of the identified metabolites among the three stages of flowering have also been well characterized distinctly.

5. Discussion

Metabolomic approaches, utilizing GC/MS and other mass spectrometric analyses allow the single experiment profiling and semi-quantification and or quantification of numerous metabolites that are generally conserved across the kingdoms of life (Tohge and Fernie 2014). Metabolomics can take a print of any biochemical status to evaluate biochemical changes in metabolic pools (Hanhineva *et al.*, 2008; Osorio *et al.*, 2014). The large

data sets obtained in metabolomic experiments are analyzed with multivariate statistical tools in an aim to determine biological components that show differential behavior under various circumstances within a single species.

In this study among the 85 identified metabolites, important metabolites viz., the top 25 metabolites based on VIP (Variable importance projection) scores detected by PLS-DA loading plots (Figure 5) for the separation of S1, S2 and S3 stages were found: acetol, glycerol, D-threitol, maltose, tartronic acid, gentisic acid, 2-isopropyl malic acid, O-acetylsalisylic acid, D-trehalose, maleic acid, D-mannitol, tagatose, 3,4-dihydroxy benzoic acid, D-sorbitol, pyrogallol, maleamic acid, phenylalanine, glyceric acid, beta-alanine, sedoheptulose anhydride monohydrate, 3-hydroxy-3-methylglutaric acid (dicrotalic acid), 4-vinylphenol, homogentisic acid, 6-hydroxyhexanoic acid and adenosine.

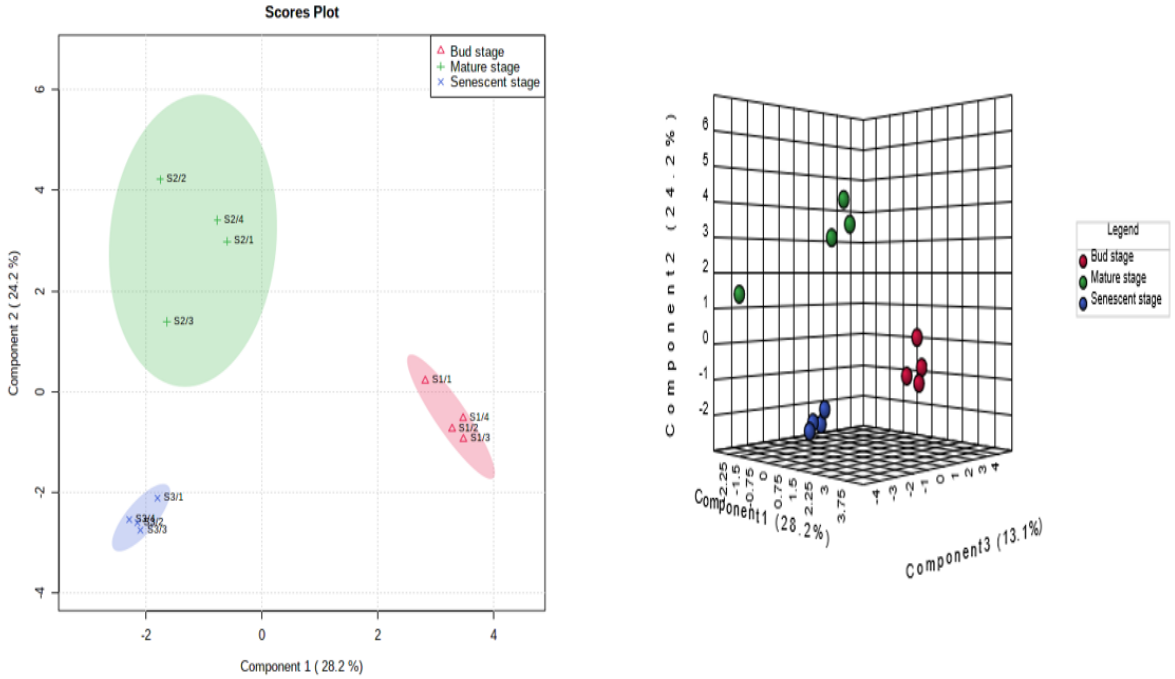

Figure 4. s-PLS-DA 2-D and 3-D scores plot indicating each flowering stage is individualized based on their metabolite profile

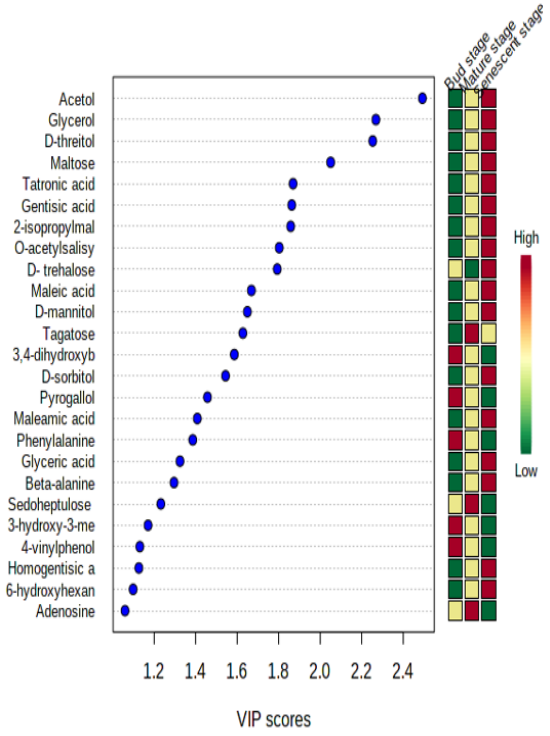

Figure 5. Loading plot in PLS-DA showing the top 25 metabolites

The bi-plot (Figure 6) of component loadings also indicates the distinct groups corresponding to each flowering stage (S1, S2 and S3) based on their different chemical profile. The flowering stage corresponding to S1 is mainly characterized by high contents of phenol derivatives like 3-hydroxy-3-methylglutaric acid (Dicrotalic acid), 3, 4-dihydroxybenzoic acid; amino acids like L-serine, phenylalanine; sugar derivative like L-gulonic acid gamma lactone and urea. On the other hand, the group corresponding to S2 is distinguished clearly by having high amounts of sugars like sophorose, leucrose, lactulose, talose, D-allose and sugar derivatives like gluconic acid lactone, sedoheptulose anhydride monohydrate, D-saccharic acid, sugar alcohols like galactinol; phenolic compounds like 4-vinylphenol, hydroquinone, pyrogallol, alizarin; organic acids like oxalic acid, tartaric acid, maleic acid and a few other compounds like adenosine, adrenaline, whereas the group corresponding to S3 is characterised and distinguished by having a large number of phenolics such as benzoic acid, gentisic acid, gallic acid, O-acetylsalicylic acid, 4-hydroxy-3-methyl benzoic acid, homogentisic acid; sugars like D-trehalose, maltose, tagatose; sugar alcohols such as acetol, D-sorbitol, glycerol, D-threitol, D-mannitol, myoinositol; organic acids like maleamic acid, tartronic acid, glyceric acid, isopropylmalic acid, acetic acid, maleic acid; amino acids such as beta-alanine, L-valine, norleucine and other compounds like nicotinic acid, thymine, etc.

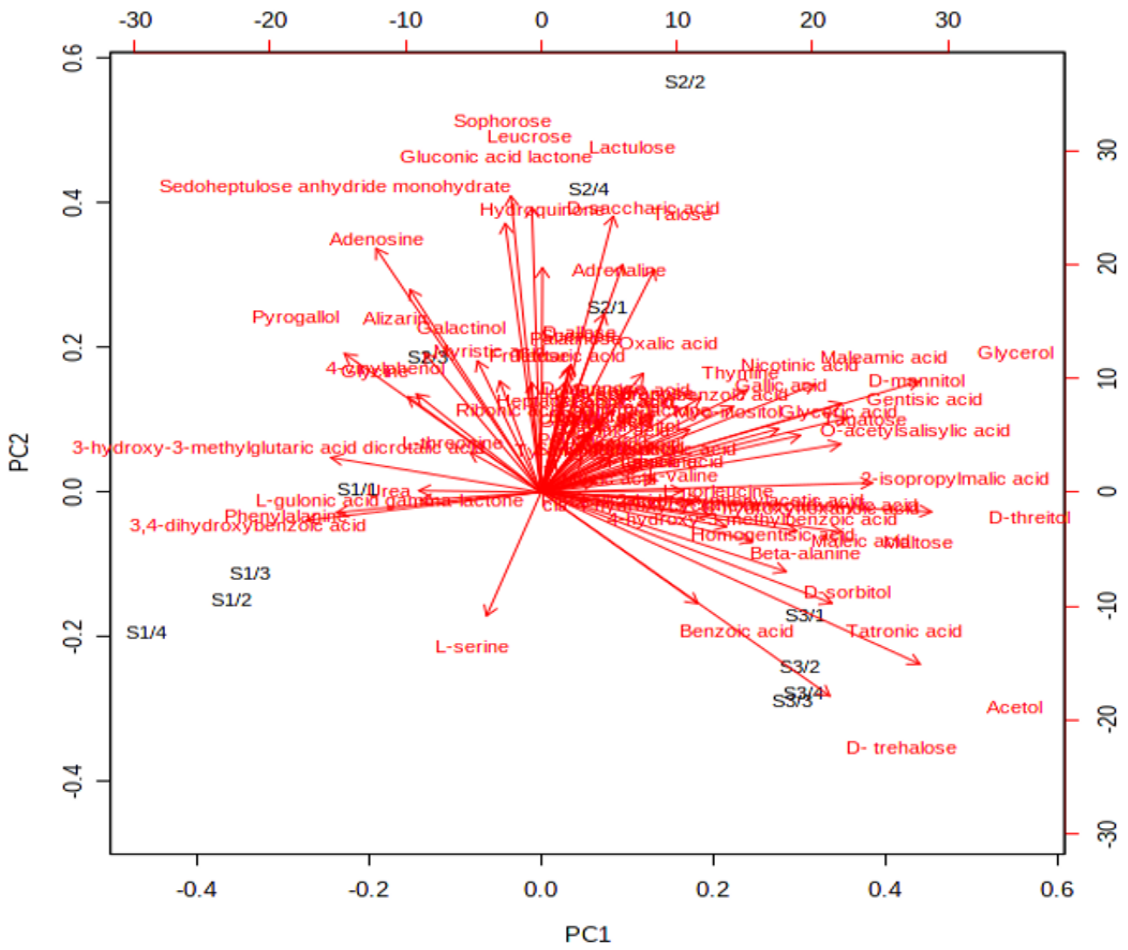

Figure 6. Biplot of component loadings using flowering stage as labelling variable

6. Conclusion

The three flowering stages showed prominent changes in their metabolite profile during the process of maturation of the flowering stages from bud to mature to senescence stages determined via GC/MS based metabolomics and chemometric approaches. The amounts and composition of metabolites in each stage showed statistically significant differences, which were reflected in their antioxidant capacities. Although all the three phenological stages showed antioxidant activities in a dose dependent manner, the senescent stage showed highest superoxide radical scavenging activity (IC_{50} = 65.17 ± 2.647 mg/ml) and metal chelating effect (IC_{50} = 6.65 ± 0.331 mg/ml) in agreement with their high content of phenolic acids. These differences were strongly reproduced in the chemometric analyses (PCA, PLS-DA and s-PLS-DA). It could also be reflected in the distribution of the biplot markers in different groups or clusters (which correspond to each phenological stage of flowering of *Saraca asoca*) with significant differences in an integrated manner. The differences detected might be beneficial for the selection of a specific flowering stage concerning its incorporation as an important source of medicine and also as a functional food.

Acknowledgements

The authors are grateful to Burdwan University, West Bengal, for granting permission to collect the samples in ample amounts. GC-MS based work was supported by DST-FIST Program, Govt. of India [Grant Number: SR/FST/LS1-459/2010], conducted in the Central Instrumentation Facility, Department of Botany, University of Calcutta, West Bengal, India.

Authors' contributions

SD and AH conceived the research project and assisted in editing; AH conducted the research, SD analyzed the results and wrote the manuscript.

Data availability

Most of the data not explicitly presented are available in the Supplementary Material. The remaining is available upon request (susouravipar@gmail.com).

Conflict of interest

The authors declare that they have no conflict of interest.

References

Aguilar Urbano M, Pineda Priego M, Prieto P. 1999. Spectrophotometric quantitation of antioxidant capacity through the formation of a phosphomolybdenum complex: specific application to the determination of vitamin E1. *Anal. Biochem*., **269 (2)**: 337-341.

Beauchamp C, Fridovich I. 1971. Superoxide dismutase: improved assays and an assay applicable to acrylamide gels. *Anal biochem*., **44 (1)**: 276-287.

Braca A, Tommasi N D, Bari L D, Pizza C, Politi M, Morelli I. 2001. Antioxidant principles from *Bauhinia terapotensis*. *J. Nat. Prod.*, **64**: 892-895.

Das S, Dutta M, Chaudhury K, De B. 2016. Metabolomic and chemometric study of *Achras sapota* L. fruit extracts for identification of metabolites contributing to the inhibition of α-amylase and α-glucosidase. *Eur Food Res Technol*., **242 (5)**: 733-743.

Dasgupta N, De B. 2004. Antioxidant activity of *Piper betle* L. leaf extract *in vitro*. *Food chem.*, **88 (2)**: 219-224.

Feugang J M, Konarski P, Zou D, Stintzing FC, Zou C. 2006. Nutritional and medicinal use of Cactus pear (*Opuntia* spp.) cladodes and fruits. *Front Biosci*., **11**, 2574-2589.

Gupta M, Sasmal S, Mukherjee A. 2014. Therapeutic effects of acetone extract of *Saraca asoca* seeds on rats with adjuvant-induced arthritis via attenuating inflammatory responses. ISRN Rheumatol. 1-12.

Hanhineva K, Rogachev I, Kokko H, Mintz-Oron S, Venger I, Karenlampi S, Aharoni A. 2008. Non-targeted analysis of spatial metabolite composition in strawberry (*Fragaria* x *ananassa*) flowers. *Phytochemistry*, **69 (13)**: 2463-2481.

Kelley K M, Behe B K, Biernbaum JA, Poff KL. 2001. Consumer preference for edible-flower color, container size, and price. *Hort Science.*, **36**: 801-804.

Kind T, Wohlgemuth G, Lee D Y, Lu Y, Palazoglu M, Shahbaz S, Fiehn O. 2009. FiehnLib: mass spectral and retention index libraries for metabolomics based on quadrupole and time-of-flight gas chromatography/mass spectrometry. *Anal. Chem*., **81**: 10038-10048.

Lefer D J, Granger DN. 2000. Oxidative stress and cardiac disease. *Am J Med*., **109 (4)**: 315-323.

Marrelli M, Menichini F, Statti GA, Bonesi M, Duez P, Menichini F, Conforti F. 2012.Changes in the phenolic and lipophilic composition, in the enzyme inhibition and antiproliferative activity of Ficus carica L. cultivar Dottato fruits during maturation. Food *Chem Toxicol*., **50 (3-4)**: 726-733.

Mishra A, Kumar A, Rajbhar N, Kumar A. 2013. Phytochemical and pharmacological importance of *Saraca indica*. *Int. J. Pharm. Chem. Sci.*, **2**: 1009-1013.

Mishra A, Patel M K, Jha B. 2015. Non-targeted metabolomics and scavenging activity of reactive oxygen species reveal the potential of *Salicornia brachiata* as a functional food. *J Funct Foods*., **13**: 21-31.

Murthy SM, Mamatha B, Shivananda TN. 2008. *Saraca asoca* – an endangered plant. *Biomed*., **3**: 224-228.

Panchawat S, Sisodia SS. 2010. In vitro antioxidant activity of *Saraca asoca* Roxb. De Wilde stem bark extracts from various extraction processes. *Asian J. Pharm. Clin. Res.*, **3 (3)**: 231-233.

Pandey S, Patel M K, Mishra A, Jha B. 2015. Physio-biochemical composition and untargeted metabolomics of cumin (*Cuminum cyminum* L.) make it promising functional food and help in mitigating salinity stress. *PLoS One.*, **10 (12)**: e0144469.

Patel MK, Mishra A, Jha B. 2016. Non-targeted metabolite profiling and scavenging activity unveil the nutraceutical potential of *Psyllium* (Plantago ovate Forsk). *Front. Plant Sci*., **7**: 431.

Pires TCSP, Dias MI, Barros L, Barreira JCM, Buelga CS, Ferreira ICFR. 2018. Incorporation of natural colorants obtained from edible flowers in yogurts. *LWT*, **97**: 668-675.

Pradhan P, Joseph L, George M, Kaushik N, Chulet R. 2010. Pharmacognostic, phytochemical and quantitative investigation of *Saraca asoca* leaves. *J. Pharm. Res.*, **3**: 776-780.

Pradhan P, Joseph L, Gupta V, Chulet R, Arya H, Verma R, Bajpai A. 2009. *Saraca asoca* (Ashoka): a review. *J. Chem. Pharm.*, **1 (1)**: 62-71.

Rajkumar V, Guha G, Kumar RA, Mathew L. 2010. Evaluation of Antioxidant Activities of *Bergenia ciliate* Rhizome. *Rec. Nat. Prod.*, **4 (1)**: 38-48.

Saha J, Mitra T, Gupta K, Mukherjee S. 2012. Phytoconstituents and HPTLC analysis in *Saraca asoca* (Roxb) Wilde. *Int. J. Pharm. Pharm. Sci*., **4 (1)**: 96-99.

Saha J, Mukherjee S, Gupta K, Gupta B. 2013. High-performance thin-layer chromatographic analysis of antioxidants present in different parts of *Saraca asoca* (Roxb.) de Wilde. *J Pharm Res.*, **7 (9)**: 798-803.

Saha S, Islam Z, Islam S, Hassan MF, Hossain MS, Islam SMS. 2018. Determination of antioxidant properties and the bioactive compounds in wheat (Triticum aestivum L.). *JJBS*, **11(3)**: 315-321.

Shen Q, Zhang B, Xu R, Wang Y, Ding X, Li P. 2010. Antioxidant activity *in vitro* of the selenium-contained protein from the Se-enriched Bifidobacterium amimalis. *Anaerobe*, **16 (4)**: 380-386.

Shukla R, Chakravarty M, Gautam MP. 2008. Indigenous medicine used for treatment of gynecological disorders by tribal of Chhattisgarh, *India*. *J. Med. Plant Res*., **2 (12)**: 356-360.

Tohge T, Fernie AR. 2014. Metabolomics-inspired insight into developmental, environmental and genetic aspects of Tomato fruit chemical compositionand quality. *Plant Cell Physiol.*, **56 (9)**: 1681-1696.

Wang L, Yen JH, Liang HL, Wu MJ. 2003. Antioxidant effect of methanol extracts from lotus plumule and blossom (*Nelumbo nucifera* Gertn.). *J Food Drug Anal.*, **11**: 60-66.

Zahin M, Aqil F, Ahmad I. 2009. The *in vitro* antioxidant activity and total phenolic content of four Indian medicinal plants. *Int. J. Pharm.*, **1**: 88-95.

JJBS

Volume 14, Number 3, September 2021
ISSN 1995-6673
Pages 523 - 527

Jordan Journal of Biological Sciences

Biocontrol of Sweet Melon Fruit Rot Caused by *Fusarium solani* using an Endophytic Fungus Isolated from the Medicinal Plant *Solenostemma arghel*

Fatma F. Abdel-Motaal[1,2,*], Noha M. Kamel[1,2], Magdi A. El-Sayed[1,3], Mohamed Abou-Ellail[4]

[1]*Botany Department, Faculty of Science, Aswan University, Aswan 81528, Egypt;*[2]*Unit of Environmental Studies and Development, Aswan University, Aswan 81528, Egypt;*[3]*Molecular Biotechnology Program, Faculty of Advanced Basic Sciences, Galala University, New Galala City, Egypt;*[4]*Department of genetics, Faculty of Agriculture and Natural Resources, Aswan University, Aswan81528, Egypt.*

Received: July 27, 2020; Revised: October 3, 2020; Accepted: November 21, 2020

Abstract

The fruit rot disease of sweet melon is responsible for serious of economic crop losses that have occurred sporadically in Aswan, Egypt recently. The symptoms appeared as water-soaking lesion which advanced to the rotting of the fruit surface. White mycelial mats with brown color inside appear on the lesion at the surface of the fruit. Disease symptoms, morphological and mycological characteristics, pathogenicity and molecular identification, indicated as *Fusarium solani*, are the disease causative. When healthy fruits of sweet melon sprayed with spore suspension of the isolated *F. solani*, the disease symptoms appeared as white spot, which enlarged and turned brown. Dual culture techniques showed that the endophytic fungi, *Aspergillus terreus*, *Fusarium solani* and *Penicillium verrucosum* isolated from the medicinal plant *Solenostemma arghel* inhibited the pathogen growth in variable levels. The extract of ethyl acetate of the endophytic fungal was found to be active against *Fusarium solani*. The ethyl acetate fractions of *Penicillium verrucosum* inhibited the pathogen growth by 47% while *A. terreus*, and *F. solani* showed inhibition percentage of 45% and 40%, respectively.

Keywords: Sweet Melon, *Fusarium solani*, fruit wilt, *Solenostemma arghel*

1. Introduction

Sweet melon, (*Cucumis melo*) is a very important fruit crop cultivated worlwide. The crop is

cultivated in Egypt for local market consumption and exportation. It is known as a very healthful fruit containing vitamins, sugars, folic acid, ascorbic acid and other health-bioactive compounds (Nuangmek *et al.,* 2019). The sweet melon is sensitive to the disease of *fusarium* rot when cultivated in the same soil without regular rotation (Soriano-Martin *et al.,* 2006). According to Nuangmek *et al.,* (2019), the disease caused by *Fusarium* species is considered the high prevalent postharvest and preharvest diseases of cucurbit fruits (melon and cucumbers). The melon disease caused by *Fusarium* species leads to serious economic losses. In addition, the plant pathogen can stay dormant in the soil for many years via the production of chlamydospores, making it very tough to be controlled (Garret, 1970). Many strategies have been used to control this severe pathogen like crop rotation strategy, but completely failed when a disease outbreak occured (Zhao *et al.,* 2011). The alternaive emerging strategy to control *Fusarium* rot disease is the biological control. Many antagonistic microorganisms and microbial endophytes have been confirmed to be effective as biocontrol agents against many plant pathogens (Bhakthavatchalu and Shivakumar, 2018; Marrez *et al.,* 2019). Many of these endophytes are capable of synthesizing antimicrobial secondary metabolites which act as biocontrol agents (Kamel *et al.,* 2020). Many studies reported that the soil incorporation with fungal antagonists results in reducing the incidence of diseases in different crops (Alwathnani and Perveen, 2012).

The purpose of our study was to isolate and identify the causal agent of the sweet melon fruit rot disease using morphological and molecular teqniques and to evaluate the efficacy of extracts of fungal endophytes isolated from the medicinal plant *Solenostemma arghel* as biocontrol to the pathogen.

2. Materials and Methods

2.1. Samples collection

In summer 2019, brown color appeared inside the fruits of the native Sweet Melon (shamam) for the first time in Upper Egypt at Aswan University farm (Aswan city, Egypt). The fruits were collected and kept in bags and then transferred immediately for pathogen isolation.

2.2. Isolation of the Pathogen from infected fruits of Sweet Melon

The skin of the sympotomatic part of infected sweet melon was firstly surface sterilized by ethanol (70%) for 1 min and NaClO (1%) for 1 min then washed four times

* Corresponding author. e-mail: fatma.fakhry@aswu.edu.eg.

with sterilized distilled water. Small parts were aseptically cut and plated on potato dextrose agar (PDA) plates for 4 days at 28 °C. Within two days, fungal mycelia were visibly grown from the fruit pieces. Using hyphal tip method for purification, a single hypha was transmitted and inoculated on fresh PDA plates then examined by microscope (Ghuffar *et al.,* 2018).

2.3. Morphological and Molecular identification

Isolated fungal species were identified morphologically based on their colonial and hyphal characteristics (Booth, 1977; Christensen and Raber, 1978; Moubasher, 1993; Raper and Fennell, 1965). The pathogen molecular identification was performed by rRNA gene sequencing. CTAB method (Gontia-Mishra *et al.,* 2014) was used to extract DNA from five days incubated cultured fungus. The partial fragment of rDNA gene was amplified by using two fungal primers ITS1 and ITS4 (Suarez *et al*., 2005). The PCR amplifications were detected by electrophoreses on 1% agarose gel. These bands were eluted and sequenced in Korea Solgent Company. NCBI Blast website was used to analyze sequences. MEGA6 software programme was used for construction of phylogenetic tree (Tamura *et al.,* 2013).

2.4. Pathogenicity test

The re-inoculation test of pathogenicity was done by the method according to Berner *et al*. (2007), the pathogen was injected on PDA media and incubated at 28 °C for 11 days. The harvested conidia were suspended in sterilized water at 1 x 10^6 Conidia/ ml, the sweet melon fruits were sprayed by the conidial suspension then covered with bags and incubated at 28°C for two weeks. In the same conditions, the control fruits were sprayed with sterile distilled water.

2.5. Selection of antagonistic isolates from Solenostemma arghel

From fungal lab collection from Faculty of Science, Aswan University, endophytic fungi isolated from the medicinal plant, *S. arghel* (*Aspergillus terreus, Fusarium solani* and *Penicillium verrucosum*) (unpublished result) were obtained. Each isolate was sub-cultured on PDA media for their cultivation and allowed to flourish at 28 °C.

2.6. In vitro screening of antagonistic fungi against sweet melon pathogen

Antagonistic effects of endophytic fungi isolated from *S. arghel* were tested *in vitro* against sweet melon pathogen by dual culture assay (Albert *et al.,* 2011). The control plates were made by culturing the pathogenic fungus against agar plug. The tests were done in four replicates and incubated at 28±2 °C and the growth diameter of tested pathogen was measured. The inhibition percentage was calculated after 7 days based on the inhibition of colony diameter:

$$\text{Inhibition (\%)} = D1\text{-}D2/D1 \times 100$$

D1: the colony diameter of the pathogen co-inoculated with agar plug (control), and D2: the pathogen colony diameter co-inoculated with fungal endophytes.

2.7. Extraction of secondary metabolites from endophytic fungi

Endophytic fungi isolated from *S. arhgel* were incubated as 6 mm disc in 1000 ml flask containing 400 ml PDA media under shaking condition (210 rpm) along 10 days. Then ethyl acetate (EtOAc) was combined with culture and left 24h under continuous shaking, and then the extract of EtOAc was separated by separating funnel and vacuum dried (Abdel-Motaal *et al.,* 2010).

2.8. Antifungal activity of endophytic fungi against sweet melon pathogen

Fungal ethyl acetate extracts were added into PDA at various concentrations (0.5, 1.0 and 2.0 mg/ml), shaken well to homogenize. The disc of mycelia (0.8 cm diameter) was transferred in the center of the plate (6.0 cm in diameter) according to the 'poisoned food method' that used to check the antimicrobial effect against the pathogen (Balouiri *et al.,* 2016). According to Singh and Tripathi, (1999), the fungal growth diameters of the treated and control plates were measured after 3 days, and the inhibition percentage was calculated. The minimum inhibitory concentration (MIC) values of each extract for fungal growth were determined in comparison with the control according to Balouiri *et al.,* (2016).

2.9. Statistical analysis

All experiments were done in triplicate. One-way analysis of variance (ANOVA) was used to analyze the obtained results with the help of Minitab 18 software (www.minitab.com). Tukey test was run to verify the significant differences between the control and treatments ($P \leq 0.05$). Values shown in the figures are the means ± standard errors (SEs).

3. Results

3.1. Examined symptoms

Sweet melon fruits showed the typical rot symptoms on the base of the fruits in which the fissures are found as white mycelia present in the epidermal tissue (Fig. 1A). A cross section through a mature lesion showed brown and spongy internal rot with a light brown halo (Fig. 1B).

3.2. Morphological characterisation of the pathogen

Colonies of the examined fungi were cottony white color (Fig 1C) with hyalline hyphae, and the mycelium became yellowish white and its reverse is yellow-brown. *Fusarium solani* has aerial hyphae that grow to form conidiophores which branch into monophialides which produce conidia. Phialids were more or less erect. The macroconidia were slightly curved; hyaline and have three septa but may have as many as 4–5. Microconidia were oval or cylindrical, hyaline, smooth and absecnce of septa, but sometimes they may have one or two. Chlamydospores also forms by *F. solani* that most usually emerged under suboptimal growth conditions (Fig. 1D, 1E, 1F, 1G). This fungus was identified as *F. solani* according to morphological characteristics, (Summerbell, 2003; Chehri *et al.,* 2015).

3.3. Molecular characterisation of sweet melon pathogen

To confirm the morphological identification, *F. solani* was exposed to a genomic DNA extraction and gene amplification. The partial 28S nrDNA gene and internal transcribed spacer region (ITS) were amplified by using primers ITS1 and ITS4 (Suarez *et al*., 2005; White *et al*., 1990). According to the NCBI-BLAST analysis, the ITS sequence showed 97–100% similarity with all *F. solani* (LC70340.1, MF359555.1, JN786598.1) in the Phylogenetic tree (Fig. 2). The ITS sequences of *F. solani* were placed in the Gen Bank database with accession number LC510255.

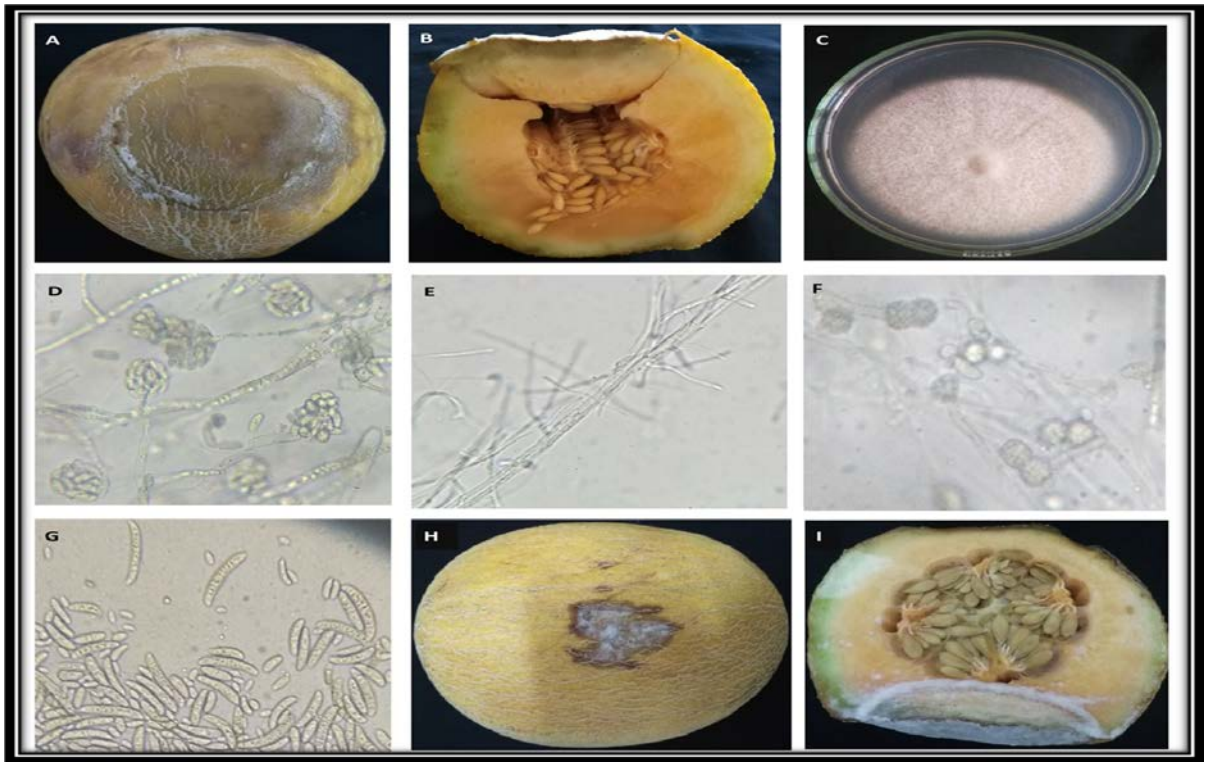

Figure 1. Fruit rot symptoms on Sweet Melon after natural infection by *Fusarium solani*. (A,B) Natural disease symptoms on Sweet Melon fruit. (C) Colony shape. (D) False head. (E) Phialids. (F) chlamydospores. (G) Macro and Micro-conidia. (H, I) Pathogenicity re-test using isolated *Fusarium solani* on Sweet Melon. (*Cucumis melo*) fruits one week after inoculation.

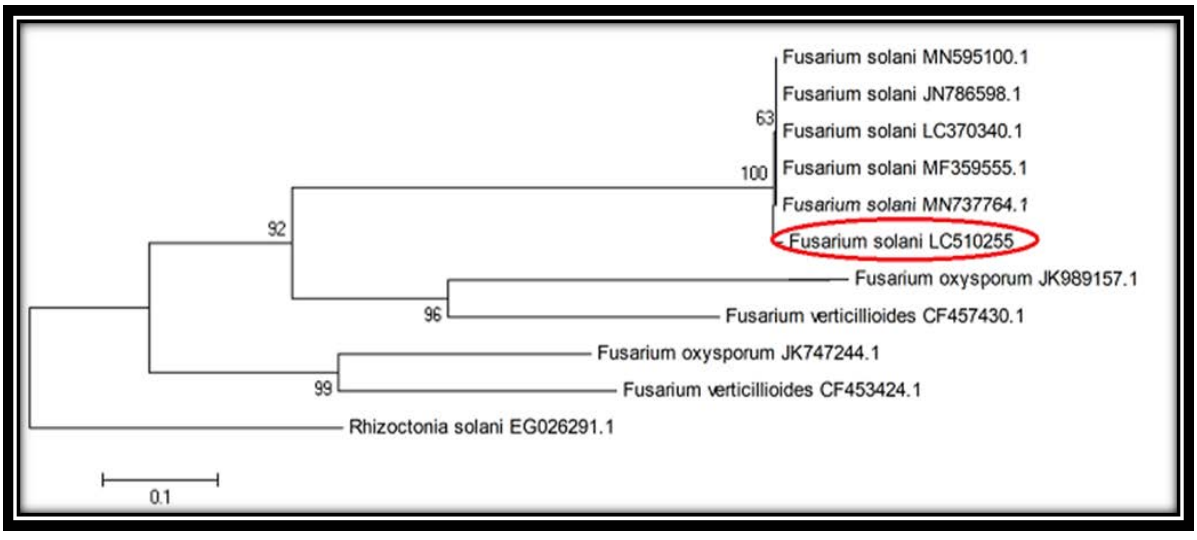

Figure 2. Phylogenetic relationships of partial sequences of rRNA gen from *Fusarium solani* fungal pathogenic and selected fungi derived from NCBI Genbank. The construction of phylogenetic tree represents Neighbor-joining method using MEGA 6 software.

3.4. Pathogenicity test

When the healthy fruits of sweet melon were sprayed with *F. solani*, the symptoms of disesae appeared after one week as a white spots, that turned to brown after two weeks (Fig. 1H, 1I) while control fruits did not show any morphological symptoms. *Fusarium solani* was reisolated from the parts of diseased fruits but not from the control fruits.

3.5. Antagonist activity of Solenostemma arghel endophytes against sweet melon pathogen

The dual culture assay demonstrated that the tested endophytic fungi obtained from *S. arghel* (*Aspergillus terreus*, *Fusarium solani* and *Penicillium verrucosum*) inhibited the growth of *F. solani* (the sweet melon pathogen). Figure (3) showed that the antagonistic isolates change the shape of phytopathogen colonies from circular as in control to elongated ellipse. In comparison with the control, the above mentioned isolates had a significant inhibition effect ($p<0.05$) on the growth of pathogen colonies. The antagonistic activity of the selected endophytic fungi showed varying degrees of inhibition against the phytopathogenic *F. solani*, the highest inhibition percentage demonstrated by *F. solani* followed by *A. terreus* and *P. verrucosum* with inhibition percentage (35%, 26.1% and 22.7%), respectively (Fig. 3).

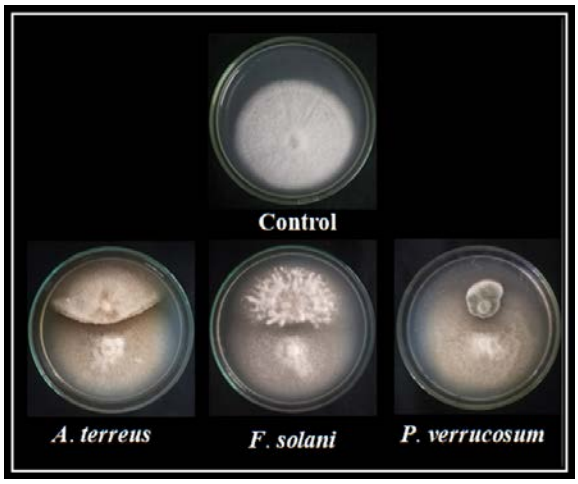

Figure 3. Antagonistic activity of *S. arghel* fungi against the pathogen *F. solani*.

3.6. Antifungal activity of endophytic fungi against sweet melon pathogen

The antifungal activities of selected endophyte had a significant efficacy against sweet melon pathogen (Fig. 4).

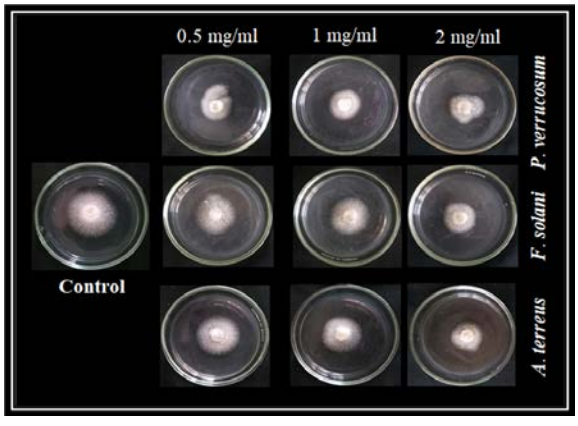

Figure 4. Antifungal activity of *S. arghel* endophytic fungal extracts against *F. solani* (the sweet melon pathogen).

The growth inhibition percentage of *F. solani* by various extract concentrations (0.5, 1.0 and 2.0 mg/ml) of *S. arghel* endophytes was determined by measuring the inhibition zones diameter. The concentrations of the selected fungal endophytes were active significantly ($p<0.05$) against the sweet melon pathogen with variable inhibitory effects. In Figure (5), *Penicillium verrucosum* produced the most active substances in the EtOAc fraction which showed the best antifungal activity at concentration 2.0 mg/ ml (MIC_{47}) and at 0.5 mg/ ml, the inhibition percentage was 41.6%. *Aspergillus terreus* and *F. solani* exhibited antifungal activity against the pathogenic fungi *F. solani* at concentration 2 mg/ml (MIC_{45}, MIC_{40}), respectively (Fig. 5).

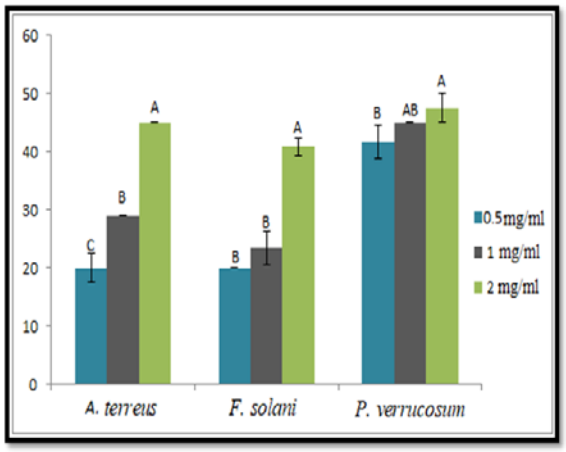

Figure 5. Histogram showing the antifungal activity of *S. arghel* endophytic fungi against *Fusarium solani*, values are mean ± stander errors (SEs) of three independent replicates (n=3). Letters a, b and c indicate significant differences $p<0.05$ (ANOVA after Tukey's test analysis).

4. Discussion

Rot disease caused by *Fusarium* species is severe for many crops. It is a very common disease of cucurbit fruits during preharvest and postharvest time according to Nuangmek *et al.*, (2019). Our results reported that *F. solani* is the causal agent of fruit rot disease to sweet melon in this study. *Fusarium solani* was reported as a predominant factor in rotting mature melon fruits under wet weather conditions in Texas (Toussoun and Snyder1961). Vast isolates of *F. solani* obtained from roots of muskmelon plants showed root-rot symptoms (Champaco, 1990). Also, other *Fusarium* species like *F. equiseti* have been recorded as a causal agent of fruit rot of cantaloupes by Kim and Kim, (2004) and *F. incaratum* caused fruit rot to muskmelon (Wonglom and Sunpapao, 2020). To reduce losses caused by *Fusarium* to sweet melon fruits, control actions are currently subjected to research. In the present study, the above-mentioned endophytic fungi considerably inhibited the growth of the phytopathogenic *Fusarium in vitro*. They were effective as biological control agents against the sweet melon pathogen. Previous researches reported that several antagonistic species have been confirmed to be effective as bio-control agents in controlled laboratory conditions (Zhao *et al.*, 2011), like *Peniciliium* species (Sabuquillo *et al.*, 2006), *Aspergillus* species (Kandhari *et al.*, 2000) and *F. solani* which isolated from cotton plants as endophytic fungi (Wei *et al.*, 2019).

Our results clearly show that *S. arghel* endophytes affected the growth of the phytopathogenic fungus *F. solani*. This inhibition is propably attributed to the secretion of phytoanticipins or other inhibitory substances produced by antagonists such as aspergillic acid and

dermadin. This inhibition differs according to the nature, quantity and quality of antibiotics/inhibitory substances (Alwathnani and Perveen, 2012). Purification of active molecules may enhance the biocontrol process through the increase in the inhibition percentage compared to the crude extract.

5. Conclusion

Fusarium solani is the causal agent of fruit rot disease of Sweet Melon. Biological control of *F. solani* by friendly endophytic fungi, *Aspergillus terreus*, *Fusarium solani* and *Penicillium verrucosum* isolated from the medicinal plant *Solenostemma arghel* inhibited the growth of the pathogen at a variable manner. These fungal endophytes can be used as biocontrol agents to supress the Fusarium pathogenicity.

References

Abdel-Motaal FF, El-Sayed M, El-Zayat S, Nassar MM and Ito S. 2010. *Choanephora* rot of floral tops of *Hyoscyamus muticus* caused by *Choanephora cucurbitarum. J Gen Plant Pathol*, **76**: 358-361.

Albert S, Chauhan D, Pandya B and Padhiar A. 2011. Screening of *Trichoderma spp*. as potential fungal partner in co-culturing with white rot fungi for efficient biopulping. *Global J Biotechnol Biochem*, **6**: 95–101.

Alwathanani AH and Perveen K. 2012. Biological control of *fusarium* wilt of tomato by antagonist fungi and cyanobacteria. Afr J, **11**: 1100–1105.

Azevedo LJ, Pereira OJ and Araujo LW. 2000. Endophytic microorganisms: a review on insect control and recent advances on tropical plants. *EJB*, **3**: 15-16.

Balouiri M, Sadiki M and Ibnsouda KS. 2016. Methods for in vitro evaluating antimicrobial activity: a review. *J Pharm Anal*, **6**: 71–79.

Berner DK, Smallwood EL, McMahon MB and Luster DG. 2007. First report of leaf spot caused by *Cladosporium herbarum* on *Centaurea solstitialis* in Greece. *Plant Dis*, **91**: 463.

Bhakthavatchalu S and Shivakumar S. 2018. The influence of physicochemical parameters on phosphate solubilization and the biocontrol traits of *Pseudomonas aeruginosa* FP6 in phosphate-deficient conditions. *Jordan J Biol Sci*, **11**:215-221**.**

Booth C. 1977. *Fusarium.* Laboratory guide to the identification of major species. *Mycologia*, **69**:1239.

Chehri K, Salleh B and Zakaria L. 2015. Morphological and Phylogenetic Analysis of *Fusarium solani* Species Complex in Malaysia. *Microb Ecol*, **69**: 457–471.

Christensen M and Raber BK. 1978. Synoptic key to *Aspergillus nidulans* group species and related *Emericella* species. *Trans Br Mycol Soc*, **71**: 177-191.

Garret SD. 1970. Pathogenic Root-Infecting Fungi. Cambridge University Press, London, UK.

Ghuffar S, Irshad G, Naz F, Rosli HB, Hyder S, Mehmood N, Zeshan MA, Mayer CG and Gleason ML. 2018. First report of two *Penicillium* spp. causing post-harvest fruit rot of grapes in Pakistan. *Plant Dis*, **104**: 1037.

Gontia-Mishra I, Tripathi N and Tiwari SA. 2014. Simple and rapid DNA extraction protocol for filamentous fungi efficient for molecular studies. *IJBT*, **13**: 536-539.

Kamel NM, Abdel-Motaal FF and El-Zayat SA. 2020. Endophytic fungi from the medicinal herb Euphorbia geniculata as a potential source for bioactive metabolites. *Arch Microbiol*, **202**: 247–255.

Kandhari J, Majumder S and Sen B. 2000. Impact of *Aspergillus niger* AN27 on growth promotion and sheath blight disease reduction in rice. *Int Rice Res Notes*, **25**: 21-22.

Kim JW and Kim HJ. 2004. *Fusarium* fruit rot of posthavest oriental melon (*Cucumis melo* L. var. makuwa Mak.) caused by *Fusarium* spp (in Korean with English summary). *Res Plant Dis*, **10**: 260–267.

Marrez DA, Abdel-Rahman GN and Salem SH. 2019. Evaluation of *Pseudomonas fluorescens* Extracts as Biocontrol Agents Against some Foodborne Microorganisms. *Jordan J Biol Sci*, **12**: 535-541.

Moubasher AH. 1993. Soil fungi in Qatar and other Arab countries.The scientific and applied research center. University of Qatar, Doha

Nuangmek W, Aiduang W, Suwannarach N, Kumla J, Kiatsiriroat T and Lumyong S. 2019. First report of fruit rot on cantaloupe caused by *Fusarium equiseti* in Thailand. *J Gen Plant Pathol*, **85**: 295–300.

Raper KB and Fennell DI. 1965. The genus *Aspergillus*. Williams & Wilkins Co, Baltimore.

Sabuquillo P, De Cal A and Melgarejo P. 2006. Biocontrol of tomato wilt by *Penicillium oxalicum* formulations in different crop conditions. *Biol Control*, **37**: 256-265.

Singh J and Tripathi NN. 1999. Inhibition of storage fungi of blackgram Vigna mungo by some essential oils. *Flavour Frag J*, **14**:1–4.

Soriano-Martın ML, Porras-Piedra A and Porras-Soriano A. 2006. Use of microwaves in the prevention of *Fusarium oxysporum* f. sp. melonis infection during the commercial production of melon plantlets. *J Crop Prot*, **25**: 52–57.

Suarez MB, Walsh K and Boonham N. 2005. Development of realtime PCR (Taq-Man) assays for the detection and quantification of *Botrytis cinerea* in planta. *Plant Physiol Bioch*, **43**: 890–899.

Summerbell R. 2003. 'Ascomycetes: *Aspergillus*, *Fusarium*, *Sporothrix*, *Piedraia*, and Their Relatives', in Pathogenic Fungi in Humans and Animals (2nd ed.), ed. D.H. Howard, New York: Marcel Dekker, pp. 361-368.

Tamura K, Stecher G, Peterson D, Filipski A, and Kumar S. 2013. MEGA6: Molecular

Evolutionary Genetics Analysis version 6.0. *Mol Biol and Evol*, **30**: 2725-2729.

Toussoun TA and Snyder WC. 1961. The pathogenicity, distribution, and control of two races of *Fusarium* (Hypomyces) *solani* f. cucurbitae. *Phytopathology*, **51**:17-22.

Wei F, Zhang Y, Shi Y, Feng H, Zhao L, Feng Z and Zhu H. 2019. Evaluation of the Biocontrol Potential of Endophytic Fungus *Fusarium solani* CEF559 against *Verticillium dahliae* in Cotton Plant. *Biomed Res Int*, **3**: 1-12.

White TJ, Bruns T, Lee S and Taylor JW. 1990. Amplifcation and direct sequencing of fungal ribosomal RNA genes for phylogenetics. PCR protocols: a guide to methods and applications. Academic Press Inc., New York, 315-322.

Wonglom P and Sunpapao A. 2020. *Fusarium incarnatum* is associated with postharvest fruit rot of muskmelon (*Cucumis melo*). *J Phytopathol*, **168**: 204–210.

Zhao Q, Dong C, Yang X, Mei X, Ran W, Shen Q and Xu Y. 2011. Biocontrol of *Fusarium* wilt disease for *Cucumis melo* melon using bio-organic fertilizer. *Appl Soil Ecol*, **47**: 67–75.

JJBS

Volume 14, Number 3, September 2021
ISSN 1995-6673
Pages 529 - 535

Jordan Journal of Biological Sciences

In vivo Anti-inflammatory Activity of Aqueous Extract of *Carthamus caeruleus L* Rhizome Against Carrageenan-Induced Inflammation in Mice

Amari Nesrine Ouda[1] , Missoun Fatiha[1,*], Mansour Sadia[1] , Sekkal Fatima Zohra[2] and Djebli Noureddine[1]

[1]*Laboratory of Pharmacognosy and Api-Phytotherapy, University of Mostaganem (UMAB), Mostaganem 27000, Algeria;*[2] *Laboratory of Biodiversity and Conservation of Water and Soil ,University of Mostaganem (UMAB), Mostaganem 27000, Algeria.*

Received: July 27, 2020; Revised: October 28, 2020; Accepted: November 12, 2020

Abstract

Carthamus caeruleus L belongs to the family Asteraceae and is reported to have anti-inflammatory, anti-burns and wound healing properties. The aim of the present study was to evaluate the anti-inflammatory activity of aqueous extract of *Carthamus caeruleus L* rhizome in mice. Carrageenan was used to induce inflammation in mice; the percentage inhibition of edema (% INH), the percentage increase in paw edema volume (% AUG) and histological study were used to evaluate the anti-inflammatory activity.

Phytochemical investigations indicate the presence of Carotenoids, flavonoids, terpenoids and steroids, tannins, saponins, coumarins, quinons, mucilage, proteins and glycosides and a very low quantity of phenolic compounds (13.08 ±0.22mg GAE/g extract) and flavonoids (5.02 ±0.55mg QE/g extract) in the rhizome of *Carthamus caeruleus L* . In acute toxicity test, the oral doses of plant extract administered to mice were not toxic. Our findings show that the treatment with aqueous extract of *Carthamus caeruleus L* presents a significant inhibitory activity in carrageenan-induced paw inflammation in group A (dose 150 mg / kg) and B (dose 300 mg / kg) compared with the standard drug Diclofenac during the whole period of experimentation; these results were confirmed by the histological study in the paws of mice. *Carthamus caeruleus L* appears to be a promising plant for further preclinical and clinical trials in inflammation.

Keywords: *Carthamus caeruleus L*, Inflammation, Carrageenan, Rhizome, Paw edema, Phytoconstituents.

1. Introduction

Inflammation is a process of immune defense of the organism in response to an aggression of exogenous origin (burn, infection, allergy, trauma) or endogenous (cancer cells or autoimmune pathologies) .The clinical symptoms of those inflammation processes are: redness, heat, swelling and pain, moreover, the function of the inflamed organ can be impaired. At the tissue level, the inflammatory response is characterized by an increase in vascular permeability, an increase in the denaturation of proteins and the alteration of cell membranes. (Winter, 1967; Roitt *et al*., 2001). Chronic inflammation is the main cause of continuing disorders, such as autoimmune diseases, allergies, metabolic syndrome, cardiovascular dysfunctions and Cancer and imposing an enormous economic burden on individuals and therefore on society (Sarkar, 2020; Bagad *et al*., 2013; Sreedam *et al.*, 2012).

Various effective anti-inflammatory drugs can reduce pain and inflammation by the inhibition of the metabolism of arachidonic acid by the isoform of the enzyme cyclooxygenase (COX-1 and/or COX-2), thereby reducing the production of prostaglandin (Payan *et al*., 1995) . Unfortunately, there are many side effects associated with the administration of nonsteroidal anti-inflammatory drugs like headache, gastric ulcer, damage of liver function (Oguntibeju *et al* ., 2018) .

Over the past decade, phytotherapy has become more important, making an impact on both health and international trade. Return to natural products is essential as it would be less toxic and equally effective (Missoun *et al.,* 2017). Algeria has a diverse climate and a large geographical location, making it a treasure trove of medicinal plants; furthermore, the trade of plants is very easy and cheap. In addition, many people are interested in having more autonomy over their medical care in Algeria.

For this reason, we have chosen for our study *Carthamus caeruleus* L .In traditional medicine, this plant is used to prepare ointment by boiling the rhizomes in water until becoming beige cream and using it against burns, inflammation and skin rejuvenation in a deep burn. GC / MS analysis made by Dahmani, *et al* (2018) indicated the presence of very interesting phytochemicals in the rhizomes of *Carthamus caeruleus L* collected from Tizi Ouzou north of Algeria, as an example: n −

* Corresponding author e-mail: fatiha.missoun@yahoo.fr.

** Abbreviation:NFκB = nuclear factor, iNOS: inducible nitric oxide synthase, NO: nitric oxide, ICAM: intercellular adhesion molecule, VCAM: vascular cell adhesion molecule, PECAM: platelet endothelial cell adhesion molecule, IL: interleukin, TNF: tumor necrosis factor, MCP: monocyte chemoattractant protein.

hexadecanoic acid (palmitic acid), mono (2-ethylhexyl) phthalate (MEHP); this molecule is known for its anti-inflammatory , antifungal, antidiabetic, antioxidant, antitumor, and antimicrobial effects. The enzyme kinetics study proved that n-hexadecanoic acid inhibits phospholipase A(2) in a competitive manner (Vasudevan *et al*., 2012).

This study focuses on the anti-inflammatory effect of *Carthamus caeruleus* L rhizome collected from Mostaganem region on mice .The inflammation process was induced by lipopolysaccharide called carrageenan and treated thereafter by *Carthamus caeruleus* L rhizome aqueous extract.

2. Materials and methods

2.1. Plant material

Carthamus caeruleus L. rhizomes were collected in August 2018 from Sidi lakhder region, Mostaganem city, west of Algeria. The samples were taken randomly and transported in black plastic bags to the laboratory. Samples were identified by Dr. Sekkal FZ, and a voucher specimen (C.C .Sidi Lakhder/2018) of the plant was kept at the Herbarium of Laboratory of Pharmacognosy & Api Phytotherapy, University of Mostaganem, Algeria, for future reference. After washing and drying, the samples were crushed and sieved to obtain a fine powder which was used for the preparation of the extracts. It has been preserved in a hermetic bottle protected from light.

Figure 1 . Photography of *Carthamus caeruleus* L .A : Stem and flower , B : Rhizome

2.2. Preliminary phytochemical screening

2.2.1. Qualitative Analysis

Colorimetric methods were carried out on the methanolic and aqueous extract and on the powdered specimens using standard procedures to identify Alkaloids, Flavonoids, Quinones, Tannins, Saponins, Coumarins, Carotenoids, Triterpenoids, Sterols, Proteins, Glycosides, Combined anthraquinones, Mucilages as described by Harborne (1998), Trease *et al* (2009), Sofowara (1993) and Ayoola *et al* (2008).

2.2.2. Quantitative Analysis : Total phenolic and flavonoid content

The total phenolic content was determined by the Folin reagent method Ciocalteu (FCR) (Mruthunjaya *et al* ., 2016). One milliliter (1 ml) of the plant methanol extract was mixed with FCR (diluted 10 times). After standing for 5 min at 22 ° C, a volume of 750 ml $NaCO_3$ was added to the mixture. The absorbance was measured at 725 nm by spectrophotometer (Shimadzu UV mini1240). The content of TPCs of each extract was estimated by comparison with the standard curve generated from gallic acid. The results were expressed in gallic acid equivalents (mg GAE / g extract).

The flavonoid content is determined using quercetin as a reference compound. One milliliter (1ml) of plant extract in methanol was mixed with 1ml chloride aluminum. The absorbance was read at 415 nm. The flavonoid content was expressed in mg quercetin / g extract. The amount of flavonoids in *Carthamus caeruleus L* extracts in quercetin equivalents (QE) was calculated by the following formula:

$$F = (A \cdot W_0) / (A_0 \cdot W)$$

Where F = flavonoid content was expressed as milligrams of QE/milligrams of plant extracts.

A = absorbtion of plant extracts solution, A_0 = absorbtion of standard quercetin solution,

W_0 = weight of standard quercetin solution in mg, W = weight of the plant extract in mg.

2.3. Experimental design

2.3.1. Plant Extract Preparation for in vivo anti-inflammatory activity

1000 mL of distilled water was added to100g of rhizome dry powder, let boiled for 60 min. The dark yellow extract was filtered by using Whatman filter paper. The filtrate was then lyophilized conserved until use for anti-inflammatory activity in mice. Yield obtained from rhizomes extraction was 15% .

2.3.2. Acute toxicity study

Acute toxicity study was assessed in mice by using an acute oral toxic class method of Organization of Economic Co-operation and Development (OECD), guidelines (OECD/OCDE, 2000) .This test consists in administering gradual doses (300 mg, 500 mg, 1000mg / kg BW) to the animals and observed for any manifestation of toxicity, increase in locomotor activity, salivation, convulsion, coma and death. These observations are made regularly up to 24 hours.

2.3.3. In vivo anti-inflammatory activity

Twenty eight healthy adult female mice NMRI weighing 33±5g were obtained from Algerian Pasteur Institute. Animals were kept in polyacrylic cages and maintained under standard housing conditions (room temperature at 25±5°C with 12:12 light: dark cycles) and water *ad libitum*. Food was provided by dry pellets. Animals were randomly divided into four groups of seven mice each. Experimental work was carried out at UMAB in accordance with the Algerian Legislation (Law Number 12−235/2012) inherent to the protection of animals designed to experimental and other scientific purposes as well as with the guidelines of the Algerian Association of Experimental Animal Sciences (AASEA).

All animals were fasted 18 h before testing. The duration of experimentation was 6 hours, with each group receiving the experimental solutions orally one hour before the injection of carrageenan as follows:

Control Carrageenan group **C** (n=7) : Physiological water NaCl (0,9%).

Standard group **St** (n=7): Was given an anti-inflammatory medicine (Diclofénac dissolved in NaCl 0,9% with concentration of 10ml/kg).

Group A (n=7): Aqueous extract of Carthamus caeruleus L (150 mg/Kg de BW dissolved in NaCl 0,9%).

Group B (n=7): Aqueous extract of *Carthamus caeruleus L* (300mg/Kg de BW dissolved in NaCl 0,9%).

One hour after the administration of the treatments, each animal in all groups received, by sub-plantar injection in the right hind paw, 0.1 ml of a 0.1% carrageenan a high-molecular-weight polysaccharide induced paw edema model (Alwashli *et al*., 2012; Bignotto *et al*., 2009) dissolved in 0.9% NaCl.

2.3.4. Evaluation of anti-inflammatory activity

a. The percentage increase in paw edema volume (% AUG)

The diameter of the paw was measured, using a digital micrometer before and after induction of inflammation at intervals of one hour for six hours . The percentage increase in paw edema volume (% AUG) was calculated for each group of mice. It is given by the following formula :

$$\%AUG = (Dn-D0) \times 100 / D0$$

Dn: Diameter of the leg the n hour after the injection of the carrageenan.

D0: Diameter of the leg before the injection of the carrageenan.

b. Calculation of the percentage inhibition of edema (% INH)

The percentage inhibition (% INH) of the edema was calculated for each group of mice treated relative to the control. It is obtained by the following formula

%INH = (% AUG control - % AUG treated)*100 / %AUG control

% INH : the percentage inhibition of edema

% AUG : The percentage increase in paw edema volume

2.4. Histopathological examination

Two mice were randomly selected from each group for histopathological investigations. Tissue samples were taken 6 hours after the induction of inflammation , legs were fixed in 10% formalin, decalcified with a decalcifying solution (980 ml of distilled water + 20 ml of nitric acid), for three hours, incorporated into paraffin and sectioned to obtain paraffin sections 4 µm thick using a slide microtome. The tissue sections obtained were collected on glass slides, dewaxed in xylene, hydrated in descending series of ethyl alcohol, stained with hematoxylin and eosin (H&E) stains, dehydrated in ascending series of ethyl alcohol, eliminated in two changes of xylene, assembled with DPX (Bancroft *et al*., 2008) then examined with optical microscope.

2.5. Statistical analysis

For numerical outcomes, one-way analysis of variance (ANOVA) with Tukey-Kramer Multiple Comparisons post tests were performed using GraphPad InStat Version 3 (GraphPad Software) and all graphs were made by utilizing Microsoft office 2007 software. The results were expressed as an average ± SEM. The values of $p < 0.05$; $p < 0.01$; $p < 0.001$ were considered significant (*), very significant (**) and highly significant (***) respectively.

3. Results

3.1. phytochemical screening

In this study, the phytochemical screening of *Carthamus caeruleus L* rhizomes extracts has shown that this herb contains : Flavonoids, carotenoids, terpenoids and steroids, tannins, saponins, combined anthraquinones, coumains, quinons, mucilage, proteins and glycosides, whereas the absence of alkaloids (table 1).

The Flavonoids and Total phenolic compound contents of *Carthamus caeruleus L* are shown in table 2. The results are expressed in milligram equivalent (standard) per gram of dry powder extract (mg standard E/g DM), using the equation of the linear regression of the calibration curve plotted from the corresponding standard (Quercetin, Gallic acid, respectively). Results show very low quantity of phenolic compounds (13.08 ±0.22mg GAE/g extract) and flavonoids (5.02 ±0.55mg QE/g extract) in the rhizome part of *Carthamus caeruleus L* .

Table 1. The results of phytochemical screening of *Carthamus caeruleus L*

Class of compounds	Test name or reagent	*C. Caeruleus* extract rhizome
Alkaloids	Mayer and Dragendorff's reagent	-
Flavonoids	Shinoda test	+
Quinones	NAOH + Extract	+++
Tannins	Ferric chloride test	+++
Saponins	Froth test	+++
Coumarins	Fluorescence test	+
Carotenoids	Carr-Price reaction	++
Triterpenoids	Salkowski's test	+++
Sterols	Libermann-Burchard test	+++
Proteins	Trichloroacetic acid test	+++
Glycosides	Legal test	+++
Combined anthraquinones	Borntrager's test	+++
Mucilages	Extract + Alcohol	+++

−Absence, +Presence in low concentration, ++Presence, +++Presence in high concentration

Table 2. Flavonoids and Total phenolic compound contents of *Carthamus caeruleus L*

Samples	**Flavonoids** (mg Quercetin equivalent/g of extract)	**Total phenolic compound** (mg Gallic acid equivalent/g of extract)
Alcoholic Extract	5.02 ±0.55	13.08 ±0.22

3.2. In vivo anti-inflammatory activity

Oral administration of the aqueous extract of rhizome of *Carthamus caeruleus L* at doses of (300 mg, 500 mg, 1000 mg) / kg BW to mice did not induce any signs of acute toxicity during the 24 h of observation.

The percentage increase in paw edema volume (%AUG) that carrageenan administration significantly increased ($p < 0.001$) the paw edema in mice in the first hour of the experiment (figure 2) .The administration of the anti-inflammatory drug Diclofenac (50 mg / kg) in the second group (St) significantly decreased the paws edema from the second hour in mice up to the fifth hour of the experiment.

Treatment with the aqueous extract of the rhizome of *Carthamus caeruleus L* (150 mg / kg) induces a significant decrease in the volume of the mice's paws edema during the second, third, fifth and sixth hours of the experiment ($P < 0.01$). (Figure 2). Treatment with dose of 300 mg / kg induces a highly significant reduction over the 6 hours compared to Carrageenan control group.

On the other hand, the results of the percentage inhibition of edema (% INH) *indicate that after* the first and second hour (Figure 3), the treatment with the oral administration of the aqueous extract of *Carthamus caeruleus L* at the dose 300 mg / kg caused a highly significant inhibitory activity in carrageenan-induced paw inflammation compared to the group treated with the extract at a dose of 150 mg / kg BW and standard group ($P < 0.001$).

Our results show that the treatment with aqueous extract of *Carthamus caeruleus L* presents an anti-inflammatory activity in group A and B compared to the standard drug Diclofenac during the whole period of experimentation.

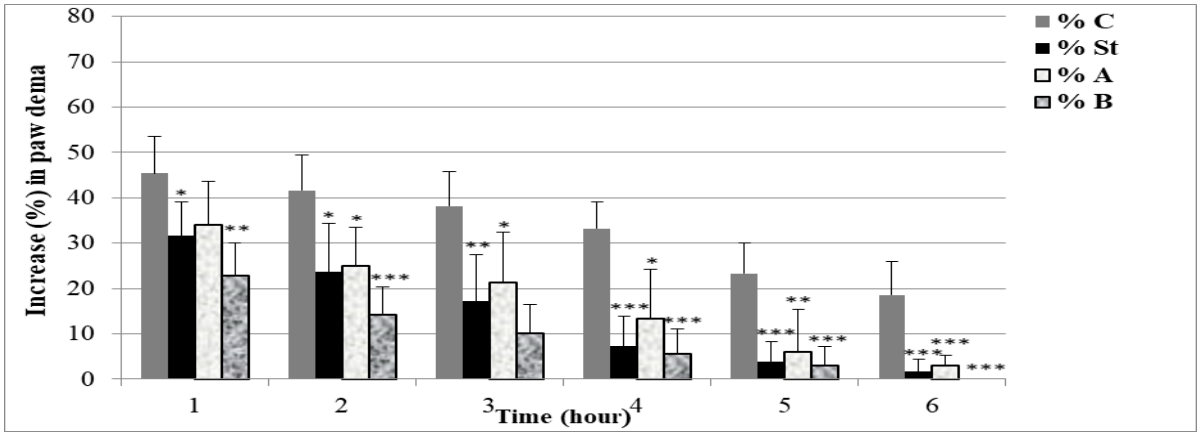

Figure 2. The percentage increase in paw edema volume (%AUG) . Mice were divided randomly into four groups: Control (C) Carrageenan group , Diclofenac (St) group (50mg/kg), *C. Caeruleus* (A) groups (150mg/kg) and *C. Caeruleus* (B) groups (300mg/kg). Results are expressed as the mean±SD (n=7 animals per group). *p<0.05, **p<0.01, ***p<0.001 were considered significant when compared with the Control carragenan group (C).

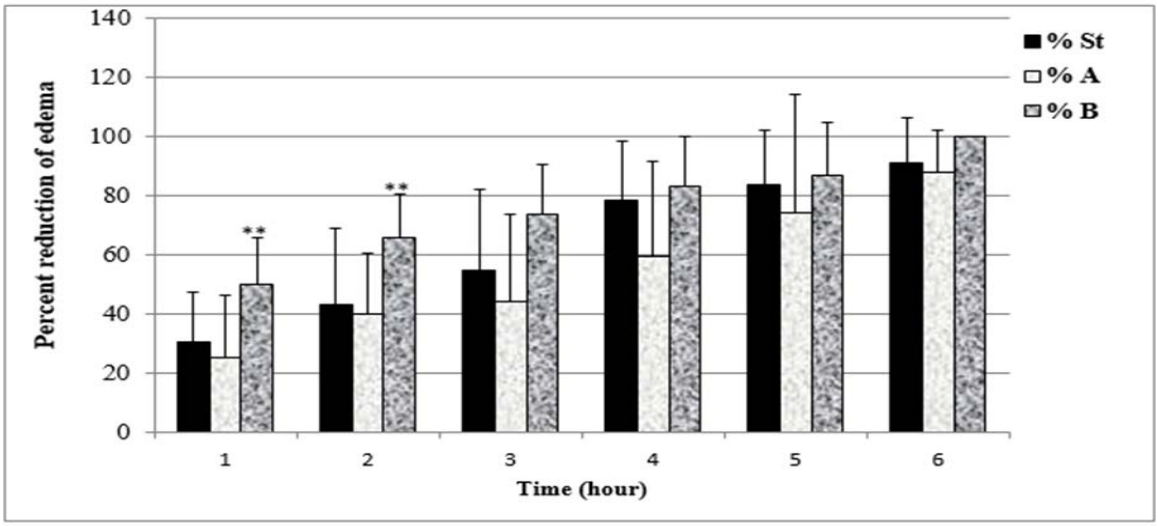

Figure 3 . Effect of *Carthamus caeruleus* on percentage inhibition of edema (% INH). Mice were divided randomly into four groups : Control carrageenan group , Diclofenac (St) group (50mg/kg), *C. Caeruleus* (A) groups (150mg/kg) and *C. Caeruleus* (B) groups (300mg/kg). Results are expressed as the mean±SD (n=7 animals per group). *p<0.05, **p<0.01, ***p<0.001 were considered significant when compared with the Standard group (St).

3.3. Histological study

The histological study in the paw tissues of control carrageenan mice showed severe acute inflammation with dense infiltration comprising of neutrophils and lymphocytes (chronic inflammatory cells). The epidermis showed sponge-like appearance. Necrosis, exudates ,polymorphic associated with edema were also noted (Figure 4) .In the group treated with Diclofenac, we noticed the disappearance of edema and tissue congestion, decrease in the intensity of the inflammatory infiltrate

were observed compared to the carrageenan control. Treatment with the aqueous extract of the rhizome of *Carthamus caeruleus L* in the doses of 150 mg / kg and 300 mg / kg reduce inflammatory response with few proliferation blood vessel and minimal number of inflammatory cells.

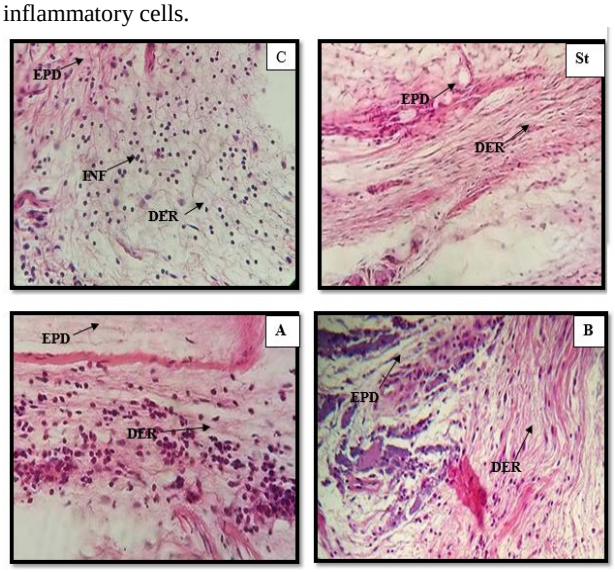

Figure 4. Photographs from the skin of mice paw tissue showing the protective effect of *Carthamus caeruleus* against carrageenan-induced inflammation. Control carrageenan (C), Diclofenac (St) group (50mg/kg), *C. Caeruleus* (A) group (150mg/kg) and *C. Caeruleus* (B) group (300mg/kg), EPD: epidermis, Der: dermis, INF →: lymphocytic infiltration. (X40)

4. Discussion

In this study, the potential anti-inflammatory effects of aqueous rhizome of *Carthamus caeruleus L* collected from Mostaganem west of Algeria were investigated using female NMRI mice as animal models, carrageenan was used to induce paw edema model . The percentage inhibition of edema (% INH), the percentage increase in paw edema volume (% AUG) and histological study were used to evaluate the anti-inflammatory activity of the test substance**.**

Our results of phytochemical screening are in the same order with the results of Dahmani *et al (*2018) and Benhamou *et al.* (2013) with *Carthamus caeruleus L* collected from Tizi Ouzou and Setif regions respectively in Algeria; they found that the rhizomes of this plant are rich in tannins, anthocyanins, flavonoids, leucoanthocyanins, saponins, terpenoids and steroids, glycosides, mucilage, and coumarins. The results show that the total polyphenols compounds in rhizome aqueous crude extract of *Carthamus caeruleus L* was low 13.08 ±0.22 mg GAE/g DM as well as flavonoids with 5.02 ±0.55 mg EQ / g DW. Our results are in the same order with the findings of Baghiani *et al.* (2010) with the same genus collected from Setif northeast of Algeria; they found 10.358 ± 0.428 mg GAE/g DM of total polyphenols compounds and 1.508 ± 0.094 mg EQ / g DW of flavonoids in crude aqueous extract of roots of *Carthamus caeruleus L* . Our results are completely different from those obtained by Dahmani (2019) with methanolique extract of rhizomes of *Carthamus caeruleus L* collected from Tizi Ouzou Northern Algeria ; they found a high total polyphenol content equal to 57,91±0.57 mg EAG/g DM. These differences in the contents of total polyphenols, flavonoids and the absence or presence of phytochemicals in different regions can be explained by experimental conditions, climatic and environmental area, genetic heritage and period and time of harvest (Atmani, 2009; Allaoui *et al*., 2016; Tinu*et al* ., 2015).

Carrageenan is a polysaccharide induced paw edema in two phases. First phase: there are incidences such as releasing of histamine, serotonin and kinins while the second phase of edema is manifested by releasing of prostaglandins, protease and lysosome. The most clinically effective anti-inflammatory drugs are effective against the second phase (Posadas *et al*., 2004). In the present study, the treatment with aqueous extract of rhizome of *Carthamus caeruleus L* shows a significant inhibitory activity in carrageenan induced paw inflammation in group A and B and it was important than Standard (Diclofenac) . The percentage inhibition of edema (% INH) was dose dependent because the percentage increase in paw edema volume (%AUG) was significantly decreased in mice treated with 300mg/kg BW than with 150mg/kg BW ; these findings suggested that rhizome of *Carthamus caeruleus L* has antagonist action against inflammation induced by carrageenan. The total inhibition of edema in group B was observed after six hours, which indicates a strong inhibitory activity of inflammation and all related appearances in tissues of epidermis and dermis. The inflammatory granuloma is a typical feature of subacute inflammatory reaction (Spector , 2004). Results in this study show a very important granuloma in histological slides of carrageenan control group, the treatment with *Carthamus caeruleus L* has shown a minimal inflammatory granuloma. Our results are in the same order with Dahmani *et al*. (2018) , Benhamou *et al*. (2013) and Benmansour *et al*. (2020) with *Carthamus caeruleus L* collected from Tizi Ouzou , Setif and Tipaza, respectively. They have shown that the rhizomes of this herb were effective against inflammation induced by carrageenan in experimental animals**.** This anti-inflammatory activity could be due to the phytochemical compounds. The anti-inflammatory activity of many phytoconstituents is manifested by their ability to inhibit the mediators of inflammation like iNOS, NO and cytokines like TNF-α, IL-1β, IL-6, IL-12, etc. The inhibition of chemokines as well as the inhibition of the activities of some enzymes responsible for inflammation like cycloxygenase-2 (COX-2), prostaglandins and leukotrienes, reduction in reactive oxygen species (ROS), regulation of enzymatic antioxidants (superoxide dismutase, catalase, etc.) and non-enzymatic (glutathione, etc.) defense systems and the inhibition of neutrophil infiltration decrease expression of cell adhesion proteins (VCAM ,ICAM, PECAM). Metallo-proteins were also tested as markers of anti-inflammatory activity. The down regulation of signaling pathways like NF- κB by the active plants compounds were also tested by many studies (Lee *et al*., 2011; Hyam *et al*., 2013 ; Wu X *et al*., 2014).

Phytochemical screening of the rhizomes of *Carthamus caeruleus L* in this study has revealed the richness of this plant in terms of phytoconstituents. The anti-inflammatory and anti-nociceptive effect of plants has been attributed to their secondary metabolites such as flavonoids, saponins, steroids, terpenoids, tannins and alkaloids (Birhane *et al*., 2020). The phytochemical studies on the rihzomes of

Algerian *Carthamus caeruleus L* with gaz chromatography coupled to the mass spectroscopy were carried out by Dahmani *et al.* (2018) and Benhamou *et al.* (2013) who showed the presence of sesquiterpenes and fatty acids such as palmitic acid and mono(2-ethylhexyl) phthalate (MEHP) and 5-(hydroxymethyl)-2-furancarboxaldehyde (5-HMF). Many pharmacological studies on active plant components showed that unsaturated fatty acids like palmitic acids are able to influence the biochemical properties of the membrane such as fluidity and permeability (Dhifi *et al*., 2013; Nasri *et al*., 2005). Xu *et al* (2007) and Oh *et al* (2012) indicated that (5−HMF) and (MEHP) had good biological activities, such as anti−inflammatory activity and antioxidant action.

5. Conclusion

Based on our findings from this study, it can be concluded that the aqueous extract of the rhizome of *Carthamus caeruleus L* collected from Mostaganem northern of Algeria was effective against inflammation caused by carrageenan and decreased the volume of edema and pain in the paws of experimental animal. The phytochemical investigation showed that the rhizomes of this plant are rich in terms of secondary metabolites. The synergistic effect of these metabolites or one of these phytoconstituents could be responsible for the anti-inflammatory activity. Hence, other researches should be made to isolate and identify the active compound responsible for this pharmacological activity.

Acknowledgement

This research was funded by the Algerian ministry of higher education and scientific research, PRFU project code “D01N01UN270120190001”.

Conflict of interest

The authors declare no conflict of interest.

References

Allaoui M, Cheriti A, Chebouat E, Dadamoussa B and Gherraf N. 2016. Comparative study of the antioxidant activity and phenols and flavonoids contents of the ethyl acetate extracts from two Saharan chenopodacea: *Haloxylon scoparium* and *Traganum nudatum* . *Algerian Journal of Arid And Environment* (AJAE)., **6(1)**:71-79.

Alwashli A, Al-sobarry M , Alnamer R , Cherrah Y and Alaoui K. 2012. Analgesic and anti-inflammatory activities of *Boswellia elongata* balf methanolic extracts, as endemic plants in Yemen, *Journal of Biologically Active Products from Nature* ., **2(2)** : 90–98.

Atmani D. 2009. Antioxidant capacity and phenol content of selected Algerian medicinal plants. *Food Chemestry*.,**112** : 303-9.

Ayoola GA, Coker HA, Adesegun SA, Adepoju-Bello AA, Obaweya KE and Atangbayila TO. 2008. Phytochemical screening and antioxidant activities of some selected medicinal plants used for malaria therapy in Southwestern Nigeria. *Tropical Journal of Pharmalogical Research*., **7(3)**:1019-1024 .

Bagad S, Joseph J A , Bhaskaran N and Agarwal, A. 2013. “Comparative evaluation of anti-inflammatory activity of curcuminoids, turmerones, and aqueous extract of Curcuma longa . *Advances in Pharmacological Sciences*., **2013(805756) :**1-7

Baghiani A, Boumerfeg S, Belkhiri F, Khennouf S, Charef S, Harzallah D, Arrar L and Mosaad A . 2010. Antioxidant and radical scavenging properties of *Carthamus caeruleus* L extracts grow wild in Algeria flora. *Comunicata Scientiae*., **1(2)**: 128-136.

Bancroft JD, Gamble M. 2008. **Theory and practice of histological techniques**, 6th Ed. Churchill Livingstone, pp .126-127.

Benhamou A and Fazouane F. 2013. Ethnobotanical study, phytochemical characterization and healing effect of *Carthamus coeruleus* L. rhizomes. *International Journal of Medicinal and Aromtic Plants.*, **3(1)** : 61-68.

Benmansour N. 2020. Study of the Anti-Inflammatory and Healing Properties of the Rhizomes of *Carthamus Caeruleus L*. (Asteraceae) Harvested in the Region of Tipaza. *Medical Technologies Journal.*,**4(1)** : 525-6.

Bignotto L, Rocha J and Sepodes B .2009. Anti-inflammatory effect of lycopene on carrageenan-induced paw oedema and hepatic ischaemia-reperfusion in the rat. *British Journal of Nutrition.*, **102(1)** : 126-133.

Birhane SW and Asres K . 2014. Evaluation of analgesic and Anti-inflammatory activities of the root extracts of *Indigofera spicata F* in mice. *Ethiopian Pharmcology J*2 ., **14** :30-65.

Dahmani MM .2019 . Evaluation de l’activité biologique des polyphénols de *Carthamus caeruleus L* (Asteraceae)., Universite de M’hamed Bouguera-Boumerdes ,Algérie.

Dahmani MM, Laoufi R, Selama O and Arab K. 2018. Gas chromatography coupled to mass spectrometry characterization, antiinflammatory effect, wound-healing potential, and hair growth-promoting activity of Algerian *Carthamus caeruleus L* (Asteraceae). *Indian Journal of Pharmacolgy* .,**50**:123-9.

Dhifi W, Jelali N, Chaabani E, Beji M, Fatnassi S and Omri S. 2013 .Chemical composition of Lentisk (*Pistacia lentiscus L*.) seed oil. *African Journal of Agricultural Research.*, **8(16)** :1395–1400.

Harborne JB. 1998. **Phytochemical methods** . A guide to modern techniques of plant analysis . 3rd ed. Chapman and Hall Int (Ed).NY, pp .49–188 .

Hyam SR, Lee IA, Gu W, Kim KA, Jeong JJ, Jang SE, Han MJ and Kim DH. 2013. Arctigenin ameliorates inflammation in-vitro and in-vivo by inhibiting the PI3K/AKT pathway and polarizing M1 macrophages to M2-like macrophages. *European Journal of Pharmacology* .,**708**: 21-9.

Lee CL, Huang CH, Wang HC, Chuang DW, Wu MJ, Wang SY, Hwang TL, Wu CC, Chen YL, Chang FR and Wu YC. 2011. First total synthesis of antrocamphin A and its analogs as anti-inflammatory and anti-platelet aggregation agents. *Organic and Biomolecular Chemistry* ., **9**: 70-3.

Missoun F, Bouabedelli F, Benhamimed E, Baghdad A and Djebli N. 2017. Phytochemical study and antibacterial activity of different extracts of *Pistacia lentiscus L* collected from Dahra Region West of Algeria . *Journal of Applied and Fundamental Sciences.*, **9(2)**: 669-648.

Mruthunjaya D , Hanumanthachar J , and Monnanda SN . 2016. Phytochemicals, Antioxidative and in vivo Hepatoprotective Potentials of Litsea floribunda (BL.) Gamble (Lauraceae) - An Endemic Tree Species of the Southern Western Ghats, India. *Jordan Journal of Biological Sciences* ., **9 (3)**. 163 – 171.

Nasri N, Khaldi A, Fady B and Triki S. 2005. Fatty acids from seeds of *Pinus pinea L*.Composition and population profiling. *Phytochemistry.*, **66(14)** :1729–1735.

OECD/OCDE. 2000. OECD Guidelines for the testing of chemicals, revised draft guidelines, **Acute Oral Toxicity Acute Toxic class methods**, **423** :1-14

Oguntibeju OO and Oluwafemi O. 2018. Medicinal plants with anti-inflammatory activities from selected countries and regions of Africa. *Journal of Inflammation Research*., **11** : 307-317.

Oh YC, Kang OH, Kim SB, Mun SH, Park CB and Kim YG . 2012. Anti−inflammatory effect of sinomenine by inhibition of pro−inflammatory mediators in PMA plus A23187−stimulated HMC−1 cells. *European Review for Medicine and Pharmacology Sciences* .,**16** :1184−91.

Payan DG, Katzung BG. 1995. Non-steroidal antiinflammatory drugs, Non-opoid Analgesics; Drugs used in Gout. **Basic and Clinical Pharmacology**. Prentice-Hall International, London, Edition 6th , pp . 536-59.

Posadas I and Inmaculada P .2004. Carrageenan-induced mouse paw edema is biphasic, age-weight dependent and displays differential nitric oxide cyclooxygenase-2 expression. *British Journal of Pharmacology* ., **(142)2** : 331-8.

Roitt I, Brostoff, J and Male D . 2001. Cell migration and Inflammation, **Immunology**. Gower Medical Publications, New York, Edition 6th, pp .47-64.

Sarkar D. 2020 . The anti-inflammatory activity of plant derived ingredients: an analytical review. *International Journal of Pharmacology Sciences & Research* .,**11(2)**: 496-06.

Sofowara A. 1993. **Medicinal plants and Traditional medicine in Africa Ibadan**. Spectrum Books Ltd, Nigeria.

Spector WG. 1969. The Granulomatous Inflammatory Exudate. *Internatinal Review and Experiemntal Patholology*., **8** :51–5.

Sreedam CD , Subrata B , Sumon R , Sajal K , Saiful I and Sitesh CB .2012. Analgesic and Anti-inflammatory Activities of Ethanolic Root Extract of Swertia chirata (Gentianaceae) . *Jordan Journal of Biological Science* .,**5(1)** : 31 – 36.

Tinu O and Kelly O. 2015. A Comparative Study of in vitro Antioxidant Activity and Phytochemical Constituents of Methanol Extract of Aframomum melegueta and Costus afer Leaves .*Jordan Journal of Biological Sciences* ., **8(4)**: 273 – 279 .

Trease GE and Evans WC . 2009. Pharmacognsy 11 th ed. Brailliar Tiridel Can, Macmillian, urinary tract infections. *Infection Disease Clin North America*., **23**: 355-385 .

Vasudevan A, Kalarickal V, Pradeep K, Ponnuraj K, Chittalakkottu S and Madathil KH.2012. Anti-Inflammatory Property of n-HexadecanoicAcid: Structural Evidence and Kinetic Assessment. *Chemical Biology and Drug Design* ., **80**: 434–439.

Winter C. A. 1967 . Nonsteroid anti-inflammatory therapy II. *Gaceta Medica de Mexico.,*

97(5): 543-50**.**

Wu X, Yang Y, Dou Y, Ye J, Bian D, Wei Z, Tong B, Kong L, Xia Y and Dai Y.2014. Arctigenin but not arctiin acts as the major effective constituent of Arctium lappa L. fruit for attenuating colonic inflammatory response induced by dextran sulfate sodium in mice. *International Immunopharmacology* ., **23**: 505-15.

Xu Q, Li YH and Lü XY. 2007.Investigation on influencing factors of 5−HMF content in schisandra. *Journal of Zhejiang University-SCIENCE B*., **8**: 439−45.

JJBS

Volume 14, Number 3, September 2021
ISSN 1995-6673
Pages 537 - 543

Jordan Journal of Biological Sciences

Histopathological Alterations in the Gills and Liver of *Clarias Gariepinus* Juveniles Exposed to Acute Concentrations of *Anogeissus Leiocarpus*

Bala Sambo Audu[1,*], Idris Audu Wakawa[2], Omirinde Jamiu Oyewole[3] and Ponwa Zingfa Changdaya[1]

[1]*Hydrobiology and Fisheries Unit, Department of Zoology, University of Jos, Jos, Nigeria;*[2] *Department of Biology, Umar Suleiman College of Education, Gashua, Yobe State, Nigeria;*[3]*Department of Anatomy, Faculty of Veterinary Medicine, University of Jos. Nigeria.*

Received: August 12, 2020; Revised: November 25, 2020; Accepted: December 12, 2020

Abstract

Over the years, people have used the stem bark extract of *Anogeissus leiocarpus* in traditional tanneries as a native agent in tendering hide and skin. The wastes from the processing plant are washed into aquatic environment and cause pollution. The acute toxicity (96hr-LC_{50}) of the aqueous crude stem extract of *A. leiocarpus* on behaviour and histopathology of gills and liver of *Clarias gariepinus* juveniles (average weight 42.00±0.05 g and average total length 27.83±0.71 cm) were investigated in a static non-renewable bioassay to ascertain its toxicity. A total of five concentrations of aqueous crude stem extract of *A. leiocarpus* (450.00, 400.00, 350.00, 300.00, and 250.00 mg/L) and a control (0.00 g/L) were used. Ten (10) juveniles were stocked in each tank with dimension of 50x30x25 cm. Of the one hundred and twenty (120) mixed sex *C. gariepinus* juveniles (in duplicate replication) used, mortalities of 100, 70, 50, 20, and 10% were recorded in concentrations 450.00, 400.00, 350.00, 300.00, and 250.00 mg/L respectively while control recorded 0% after 96 hr. The 96 hr. LC_{50} of *A. leiocarpus* on *C. gariepinus* resulted in 353.77 mg/L characterized by upper and lower confidence limits of 390.27 and 320.69 mg/L respectively. There was marked variation in the water quality parameters (total alkalinity and free carbon dioxide) in all the test tanks compared with the control. The behavioural signs exhibited by *C. gariepinus* exposed to concentrated grades of the plant material were erratic swimming, loss of stability, spiral movement, air gulping, restlessness and settling on tank bottom. Histopathological alterations such as lamellar vascular congestion, lamellar clubbing and partial to complete inter-lamellar space occlusion were recorded in the gills of *Clarias gariepinus* exposed to the graded concentrations of the extract. The liver of the catfish showed dose-related hepatic lesions such as portal congestion, periportal cellular degeneration and cellular infiltration. This study shows that 300.00 to 450.00 mg/L of *A. leiocarpus* is toxic to fish's health. Hence its indiscriminate disposal into aquatic environment should be discouraged or totally avoided to avert death of aquatic animals.

Keywords: Acute toxicity; Histopathology; *Anogeissus leiocarpus*; *Clarias gariepinus*

1. Introduction

Anogeissus leiocarpus, commonly known as African birch, is a deciduous tall plant found in the tropical Africa (Steentoft, 1988). It grows continually to attain a height of 15-18.0 m with the stem measuring about 1 m in diameter (Arbab, 2014). The bark of *A. leiocarpus* is grayish and rough while leaves are alternate, ovate to lanceolate shape with length-width dimensions of 2.0–8.0 cm and 1.3–5.0 cm respectively (Mbagwu, 2011). Small branches of *A. leiocarpus* are crushed to make dyes in tanning skin while decoction of the bark is reputed man and farm animals antihelmintics as well as potent antiprotozoans against malaria and trypanosomiasis in animals (Arbonnier, 2004; Okpekon, 2004). The sticks are chewed into fibrous brush to clean teeth by rural population in Nigeria (Rotimi, 1988).

Plants constitute an unlimited origin of a variety of biological active substances (Istvan, 2000) which have toxic effects on the aquatic biota. Artisanal fishermen use plant extract as part of their arsenal of fishing tools (Power *et al.*, 2010). Extracts of plants such as *Blighia sapda, Kigelia africana*, *Raphia, vinifera* (Omoitoyin *et al.*, 1999), *Derris elliptica, Tephrosia vogelli* (Oluwatoyin, 2011) and *Balanites aegyptiaca* (Wakawa *et al.*, 2018) have been reported to be used by fishermen as fishing tool. These plant extracts used in harvesting fish have toxic properties (Fafioye *et al.*, 2004) that paralyze or stupefy fish (Fafioye, 2011) in the aquatic environment. Examination of the phytochemicals of plants used as fish poison shows the presence of saponins, alkaloid and flavonoids (Fafioye, 2011). Others are tannins, resins, terpens, cardiac glycosides and balsam (Wakawa *et al.*, 2018). Saponins affect haematology and oxygen uptake of fish (Roy and Munshin, 1989) while alkaloid and flavonoids have anaesthetic properties on fish (Tsuchiya,

* Corresponding author e-mail: audusambo@yahoo.com.

2017). Stem bark of *A. leiocarpus* contains phytochemicals such as tannins, flavonoids, terpens and saponins with absence of alkanoids and anthraquinones (Salau *et al*., 2013). Introduction of plant extracts containing these phytochemicals could result into physiological stress in aquatic biota which could ultimately reduce aquatic productivity (Oluwatoyin, 2011) or even death.

In view of the effect of the plant extracts used in harvesting fish, many workers have assessed the acute toxicity performance of biosynthetic chemicals of plant origin to cause disease conditions in tissues/organs, serum biochemistry and haematology of different fish species. Audu *et al.* (2020) studied histopathological effects of unrefined water fractions of the foliage of *Balanites aegyptiaca* on gills, kidney and liver of *Oreochromis niloticus* fingerlings. Similarly, Audu *et al.* (2017) examined histological changes in gills and liver of *C. gariepinus* intoxicated with acute concentrated grades of *Vernonia amygdalina*. Also, Adesina *et al.* (2013) evaluated the effect of acute toxicity of *Moringa oleifera* root extract on *O. niloticus*. Nasiruddin *et al.* (2012) investigated the histological alterations in organs of *Heteropneustes fossilis* intoxicated with extracts of three dry seed, while Oluwatoyin (2011) studied the *Ipomoea aquatica* leaf extract toxic potential on histopathology of *O. niloticus*. Shahi and Singh (2011) investigated the effects of extracts of euphobious plants on serum biochemistry and haematology profiles of *Channa punctatus.* There is, however, paucity of data on acute toxicity of aqueous crude stem bark extract of *A. leiocarpus* on histopathology of *C. gariepinus* juveniles. Hence this study aimed at investigating the possibilities on behaviour and histopathology of gills and liver of *C. gariepinus* juveniles.

2. Materials and Methods

2.1. Collection and Preparation of Stem Bark of Anogeissus leiocarpus

A. leiocarpus stem bark (50 g) was collected from Hwol Yarje, Jos North Local Government, Plateau State, Nigeria. The plant was identified by a plant taxonomist as *Anogeissus leiocarpus* (DC.) Guill & Perr; voucher number=JUHN20000324, mounted and deposited in the Herbarium of Plant Science and Technology Department, University of Jos, Nigeria. The stem bark was sheared from the tree plant using an axe and shade-dried over seven days with outdoor relative humidity of 57% and ambient temperature of 28^{o}C. The dried stem bark was pulverized in the laboratory using mortar and pestle into fine particles, sieved with a meshed utensil (30μm) and stored in airtight transparent polyethene bag for subsequent use.

2.2. Laboratory Conditioning of Test Fish (Clarias gariepinus)

Outright, one hundred and twenty (120) juveniles (6-9weeks old) of *C. gariepinus* (average weight 42.00±0.05 g and average total length 27.83±0.71 cm) were procured from a private fish farm at Kangang, Dadinkowa, Jos South were moved in three aerated cellophane bags (40 juveniles per bag) to the Zoology Department (Hydrobiology and Fisheries Laboratory Unit), University of Jos and stocked using 10 round plastic tanks of 20 L capacity (10 fish/tank) each filled with 15 L of dechlorinated municipal water. Commercial diet (Multifeeds ®) was given to fish twice daily on satiation basis and water in the holding tanks was changed once daily. Fish were allowed to acclimate for two weeks during this period; fish were held under natural photo regime (12 Light: 12 Dark) (Bala *et al*., 2014).

2.3. Experimental Design

Sequel to acclimation period, fish were divided into experimental tanks which consists of twelve (12) rectangular plastic tanks (50x30x25 cm) and 120 *C. gariepinus* juveniles arranged in a randomized block design. All the tanks contained ten (10 L) liters each of chloric-free pipe borne water, with five (5) of the test tanks exposed to varying concentrations (450.00, 400.00, 350.00, 300.00 and 250.00 mg/L) of the aqueous stem bark extract of *A. leiocarpus*. Ten (10) *C. gariepinus* juveniles each were introduced into all the five (5) test and control tanks. The sixth tank served as the control and was not inoculated with the test material (0.00mg/L). The setup was replicated twice.

2.4. Acute toxicity test

Static non-renewal bioassay technique (USEPA, 1985) was used for the 96 hr. LC_{50} experiment. The aqueous stem extract was obtained by macerating two (2) grams of the finely grinded particles of stem bark of *A. leiocarpus* in distilled water for 24 hours under room (25^{o}C) condition from which graded concentrations of 450, 400, 350, 300, and 250.00 mg/L were obtained through serial dilution of the stock after range finding tests. The control tank (0.00mg/L) did not contain the test plant. The test tanks with the definitive concentrated grades of the plant extract and the control tanks were each duplicated replicated, stocked with ten (10) juveniles per tank and were devoid of artificial aeration and feeding throughout the 96 hours experiment.

2.5. Aquatic medium quality analysis

Physicochemical parameters including dissolved oxygen (DO), temperature, free carbon (iv) dioxide (CO_2), hydrogen ion concentration (pH) and total alkalinity (TA) were monitored every day as described by the American Public Health Association (APHA) (1985) techniques for water quality for fish culture throughout the experimental phase.

2.6. Histopathological Examination

Fish from each of the test concentrations (450.00.00, 400.00, 350.00, 300.00 and 250.00 mg/L) were sacrificed and dissected to excise gills and liver. Excised organs were carefully washed of blood stains and kept in specimen bottles containing 0.005L formal saline (Audu *et al*., 2017). Histopathological examinations were conducted at the central diagnostic unit of National Veterinary Research Institute (NVRI) Vom, Plateau State, Nigeria. Routine paraffin wax method and haematoxylin-eosin staining technique of tissue processing described by Drury and Wallington (1967) and Avwioro (2011) were adopted for the examinations of the excised organs (gills and liver) of *C. gariepinus* exposed to aqueous crude stem bark extract of *A. leiocarpus*.

2.7. Statistical Analyses

Water quality parameters were analysed using IBM SPSS (version 20) software. The Analysis of Variance (ANOVA) was used to establish significant differences. The Tukey test was used to separate treatment means while level of significance was determined at $\alpha_{0.05}$.

3. Results

3.1. Mean Water Quality Parameters of Tanks with Clarias gariepinus exposed to Acute Concentrations of Anogeissus leiocarpus

Water quality parameters in the 96 hr acute bioassay of *A. leiocarpus* extract on *C. gariepinus* juveniles are summarized in Table 1. Temperature, DO and pH decreased as the toxicant concentration increased while free CO_2 and TA correspondingly rose with elevated toxicant concentrations. P-value of significance ($p<0.05$) was obtained for TA and free CO_2 in the test tanks compared to the control group.

3.2. Behavioural Patterns of Clarias gariepinus Juveniles during 96 hr Acute Toxicity Test with Extract of Anogeissus leiocarpus

Fish exposed to the plant extract showed behavioural patterns such as erratic movement, loss of stability and spiral movement. Fish settled at the bottom of the tank and remained motionless for a while and sudden frequent swimming to the water surface to gulp air. After prolonged exposure (> 48 hr.) the fish skin peeled off and the fish gradually became weak, and finally death occurred. Fish was considered dead when there was permanent cessation of spontaneous movement and a failure to react to strong external stimulation probe made of glass rod. The death of the juveniles was directly concentration- dependent in relation to exposure time. At the highest plant extract concentration (400.00 mg/L), mortality was within 24 hr exposure while in the lower concentrations (300.00 and 350.00 mg/L) mortality resulted after 48 hr exposure of the juveniles to the plant extract. In the lowest concentrations (250.00 mg/L) of the plant extract, death of juveniles was recorded after 72 hr of exposure to the plant extract (Table 2).

Table 1. Mean Water Quality Parameters of Acute Bioassay of Crude Stem Bark Extracts of *Anogeissus leiocarpus* on *Clarias gariepinus* Juveniles

Water Quality Parameters	Concentration (mg/L)					
	0.00	250.00	300.00	350.00	400.00	450.00
Temp. (ºC)	25.5±0.00	24.60±0.28	24.20±0.28	24.40±0.07	24.40±0.28	24.20±0.14
DO (mg/L)	2.20±0.00	1.90±0.00	1.90±0.00	1.70±0.00	1.50±0.14	1.45±0.07
TA (mg/L)	60.50±0.00	68.85±0.07*	74.90±0.71*	85.00±12.73*	114.50±0.71*	220.10±0.14*
pH	7.35±0.07	7.20±0.00	7.25±0.07	7.20±0.00	7.20±0.07	7.10±0.14
Free CO_2 (mg/L)	34.00±0.00	49.00±0.00*	49.60±0.85*	54.30±4.94*	60.00±2.83*	68.00±0.00*

Values with Asterisks (*) in the same Row are Significantly Different Compared with the Control

TA= Total Alkalinity

Table 2. Behavioural Patterns shown by *Clarias gariepinus* Juveniles exposed to Aqueous Crude Stem Bark Extract of *A. leiocarpus*

Concentration mg/L	Behavioural Patterns	Exposure Period (Hours)		
		24	48	72
450	Erratic swimming	+++	++	+
	Loss of stability	+	+	+
	Air gulping	+++	++	++
	Spiral motion	-	+	+
	Inactivity	_	+	++
	Peeling of skin	+	++	+++
	Death	+	++	+++
400	Erratic swimming	+++	++	+
	Loss of stability	+	+	+
	Air gulping	++	++	++
	Spiral motion	-	+	+
	Inactivity	_	++	++
	Peeling of skin	_	+	+++
	Death	+	+	++
350	Erratic swimming	+	++	++
	Loss of stability	_	++	++
	Air gulping	+	+	++
	Spiral motion	-	++	++
	Inactivity	_	_	+
	Peeling of skin	_	_	+
	Death	_	_	+
300	Erratic swimming	+	++	++
	Loss of stability	_	++	++
	Air gulping	+	+	++
	Spiral motion	-	++	++
	Inactivity	_	_	+
	Peeling of skin	_	_	+
	Death	_	_	+
250	Erratic swimming	_	+	+
	Loss of stability	_	+	+
	Air gulping	_	+	+
	Spiral motion	+	+	+
	Inactivity	_	_	_
	Peeling of skin	_	_	_
	Death	_	_	_

No recorded pattern (-), slight (+), moderate (++), severe (+++)

96 hr (LC50) Acute Bioassay of Extract of Anogeissus leiocarpus on Survival of Clarias gariepinus Juveniles

The effect of 96 hr LC_{50} acute bioassay of the extract of *A. leiocarpus* on survival of *C. gariepinus* juveniles is shown in Table 3. Survivals of the juveniles depend on the concentration of the extract. The rate of survival increased with decrease in the aqueous crude stem extract concentration. Recorded mortalities were 100, 70, 50, 20 and 10% of the plant extract concentrations 450.00, 400.00, 350.00, 300.00 and 250.00 mg/L respectively. The control tank (0.00 mg/L) recorded 0% mortality.

3.3. Linear Relationship Between Mean Probit Mortality Versus Log Concentration of C. gariepinus Juveniles exposed to Extract of Anogeissus leiocarpus

Figure 1 shows the linear relationship between mean probit mortality and log concentration of *C. gariepinus* juveniles exposed to the extract of *A. leiocarpus*. The 96hr LC_{50} of *A. leiocarpus* on *C. gariepinus* resulted in 353.77 mg/L characterized by upper and lower confidence limits of 390.27 and 320.69 mg/L respectively.

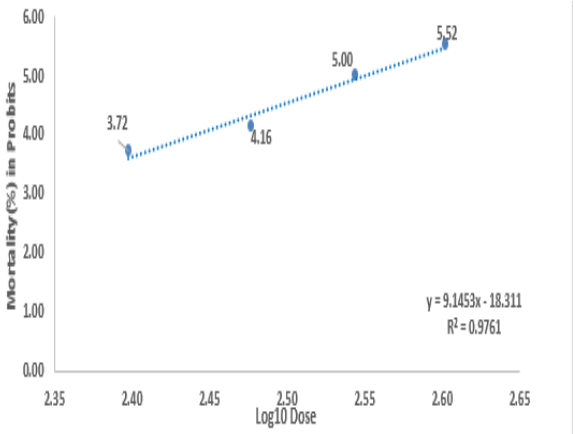

Figure 1. Linear Relationship between Mean Probit Mortality and Log Concentration of *Clarias gariepinus* Juveniles Exposed to Aqueous Crude Stem Bark Extract of *Anogeissus leiocarpus*

Table 3. Effects of Acute Bioassay of Aqueous Crude Stem Bark Extract of *A. leiocarpus* on Survival of *Clarias gariepinus* Juveniles

Conc. (mg/L)	Log Conc.	No. of fish	Mortality Time (Hours)								Total Dead	Mortality (%)	Probit Mortality
			12	24	36	48	60	72	84	96			
450.00	2.6532	10	3.50	2.50	1.50	1.00	1.00	1.00	0.50	0.00	10	100	8.7190
400.00	2.6020	10	2.00	1.50	0.50	1.50	0.50	0.50	0.00	0.50	7	70	5.5244
350.00	2.5440	10	0.00	0.00	1.00	0.50	0.50	0.50	0.00	1.00	5	50	5.0000
300.00	2.4771	10	0.00	0.00	0.00	1.50	0.00	0.00	0.00	0.50	2	20	4.1584
250.00	2.3979	10	0.00	0.00	0.00	0.00	0.00	0.50	0.5	0.00	1	10	3.1784
0.00	0.0000	10	0.00	0.00	0.00	0.00	0.00	0.00	0.00	0.00	0	0	0.0000

3.4. Histopathology of Gills of Clarias gariepinus Juveniles

Photomicrograph of effects of 96hr acute concentrations of extract of *A. leiocarpus* on gills of juveniles of *C. gariepinus* are presented in Plate 1 A-F. The gills of the control (Plate 1A) appear morphologically normal with typical structural organization of primary and secondary lamellae. There were progressive dose-dependent gill branchial-lamella injuries typified by slight (Plate 1B) to heavy vascular congestion and clubbing of the lamellae, partial to complete interlamellar space occlusion and lamellar cell hyperplasia. The gravity of the tissue distortion seemed to be more visible in the gill anatomical structure of juveniles treated with concentrations of 300.00, 350.00, 400.00, and 450.00 mg/L of the plant extract (Plates C-F). The histo-

architecture of *C. gariepinus* intoxicated with the 250.00 mg/L of the extract appeared to be normal when compared to the control.

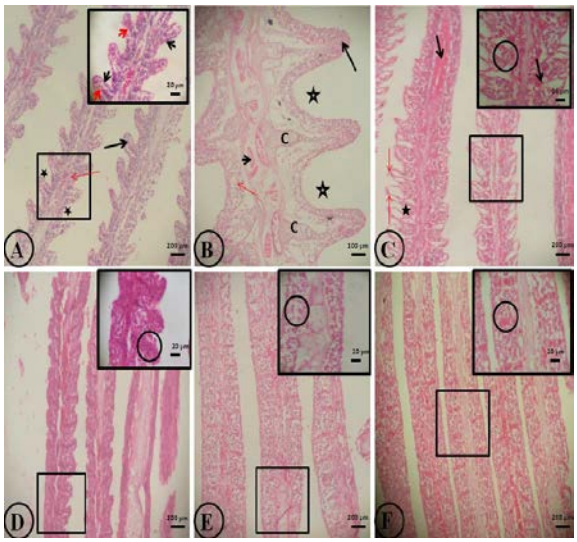

Plate 1.Light micrographs of the Gills of *Clarias gariepinus* Exposed to Acute Concentrations of Aqueous Crude Stem Bark Extract of *Anogeissus leiocarpus.* **A**. **Control (0.00 mg/L)**: normal gill parenchyma typified by occurrence of structures like primary (red arrow) and secondary lamellae (black arrow), distinct epithelial (short black arrow) and pillar cells (short red arrow) of the secondary lamellae and patent inter-lamellar space or water channel (star). **B. 250.00 mg/L**: Normal parenchyma as revealed by intact primary and secondary (red and black arrows respectively) lamellar epithelium and water channels (star) except for mild lamellar vascular congestion (short black arrow) **C. 300.00 mg/L:** Apical lamellar clubbing (red arrow), moderate lamellar cell fusion with partial to complete interlamellae space occlusion (star and circle outline (within inset) respectively), severe lamellar vascular congestion (black arrow) **D. 350.00 mg/L:** Severe hyperplastic lamellar cell with total disappearance of water channels (oval-outline)**. E. 400.00 mg/L; F. 450.00 mg/L:** Severe lamellar cell hyperplasia with complete inter-lamellar space occlusion (oval outlines within inset).

3.5. Histopathology of Liver of Clarias gariepinus Juveniles

Histopathological lesions noticed in the *C. gariepinus* liver exposed to acute concentrated grades of crude extract of *A. leiocarpus* are presented in Plate 2 A-F. The histopathological features of liver of *C. gariepinus* juveniles in the non-exposed (control) group include normal hepatic histo-architecture characterized by polyhedral outline and roundish nuclear, sinusoidal space and central veins; while, in *C. gariepinus* groups exposed to various concentrations of *A. leiocarpus*, the liver displayed increase in severity of histopathological lesions as concentration of the plant extract increased. Histopathological lesions observed in the treatment groups include moderate to severe portal congestion, periportal cellular degeneration, cellular infiltration and complete hepatocellular depletion.

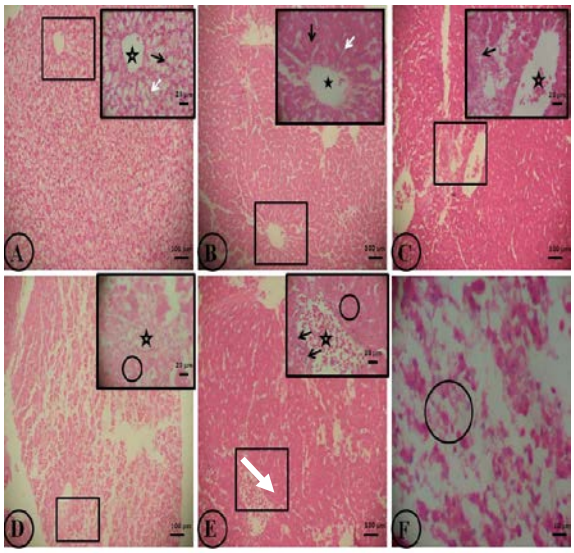

Plate 2. Light micrographs of the Liver of *Clarias gariepinus* Exposed to Acute Concentrations of Aqueous Crude Stem Bark Extract of *Anogeissus leiocarpus* **A. Control (0.00 mg/L):** normal hepatic histo-architecture as revealed by hepatocytes with typical polyhedral outline and roundish nuclear (black arrow), sinusoids space (white arrows) and central vein (star). **B. 250.00 mg/L:** no visible lesion as evidenced by liver with intact hepatocyte (black arrow), sinusoids space (white arrow) and central vein (star) **C. 300.00 mg/L**: visible lesion except for moderate sinusoidal congestion (black arrow). **D. 350.00 mg/L:** moderate portal congestion (star) and peri-portal cellular degeneration (circle outline). **E. 400.00 mg/L:** severe portal congestion (star), marked peri-portal cellular infiltration (arrow) and peri-portal cellular degeneration (circle outline) **F. 450.00 mg/L:** Severe hepato-cellular depletion (circle outline).

4. Discussion

Determination of water quality parameters in fish culture during an experiment is necessary owing to the complete dependent nature of the whole life process of fish on the quality of the immediate surroundings (Bolorunduro and Abdullahi, 1996). Water quality is determined to confirm whether it plays any role in the alterations observed during the experiment as decline in water quality influences stress and disease in fish (Devi *et al.*, 2017). The concentration-dependent decrease in DO in this study corroborates the findings of Makori *et al*. (2017). The minimum DO requirement of fish is 3.00 mg/L (Makori *et al.*, 2017); therefore, the minimum mean DO (1.45±0.07 mg/L) in this study could be attributed to the presence of the plant extract in the water (Adebola and Ayo, 2014). The pH range (7.10±0.14-7.25±0.07) in treatment tanks of this study is within the tolerable limits of catfish since the optimum pH for their survival is between 5 and 8 (Nobre *et al.*, 2014); therefore, the pH in this study could not have affected the recorded mortalities in the test animal. Similarly, the recorded temperature range (24.20±0.14-24.60±0.28 ^{o}C) in treatment tanks falls within the standard range (20-35 ^{o}C) documented by Ngugi *et al*. (2007), hence temperature could not have influenced the observed distortion in the histology of organs (gills and liver) of *C. gariepinus.* The TA which measures water productivity shows that the water tainted with the plant extract in this study is productive since the TA range (68.85±0.07-

220.10±0.14 mg/L) is within the productive (50-500 mg/L) level (Devi *et al.*, 2017).

The abnormal behavioural patterns such as erratic movement, loss of stability, spiral movement and air gulping displayed by *C. gariepinus* juveniles in the higher treatment concentrations (350.00, 400.00 and 450.00 mg/L) of the aqueous stem bark extract could be due to the fish's deliberate effort to overcome the toxic plant bioactive substances and the hypoxic condition possibly caused by the aqueous stem bark extract of *A. leiocarpus*. The manifested behavioural patterns have earlier been linked to derangement in the biochemical and nervous systems of the stressed fish (Fadina *et al*., 1991; Fafioye *et al*., 2005). In addition, the dose-related increase in the mortality rate seen in this study further established the toxic nature of *Anogeissus leiocarpus*. The trends of behavioural signs and the mortality rate shown by fish exposed to graded concentrations of *A. leiocarpus* are similar to those documented for *Trephosia vogelii* (Adewoye, 2010), *Parkia biglobosa* (Ojutiku *et al*., 2012), *Carica papaya* (Eyo *et al*., 2013), and *Vernonia amygdalina* (Audu *et al.*, 2017).

Histological distortions have been extensively optimized as biomarkers of pollutants in fish (Naeemi *et al.*, 2013). Gill of fish plays important function including respiration, osmoregulation and excretion (Camargo and Martinez, 2007; Jalaludeen *et al.*, 2012; Audu *et al.*, 2017) due to its contact with the immediate water environment (Olojo *et al.*, 2005). This proximity with the external environment predisposes it to histological damages such that the fish becomes vulnerable to respiratory and osmoregulatory difficulties (Olusegun and Adedayo, 2014) especially when toxicants enter the body and cause damage to gill membranes and affect its physiological functions (Bala and Malachy 2020). Succinctly put, fish exposed to toxicants die when their gill lamella epithelia and blood vessels are adversely affected (Hinton and Lauren, 1990).

Therefore, the observed moderate to severe gill histo-architectural alterations (lamellar vascular congestion, lamellar clubbing, partial to complete inter-lamellar space occlusion and lamellar cell hyperplasia) in this study further established the toxic potential of *A. leiocarpus* extract. The gill histopathogical profiles in this study corroborate lesions earlier reported in similar studies conducted by Camargo and Martinez (2007) in Neotropical fish caught from stream laden with toxicant and the histopathological report of Nasiruddin *et al.* (2012) on *Heteropneustes fossilis* exposed to three dried leaves extracts.

The detoxification and biotransformation processes are reputed functions of the liver which has directly placed it as most morpho-physiologically disrupted organ by contaminants in the water (Hadi and Alwan (2012). With respect to these physiological roles, the histopathological alterations (moderate to severe portal congestion, periportal cellular degeneration, cellular infiltration and complete hepatocellualar depletion) shown by *C. gariepinus* exposed to graded concentrations of *A. leiocarpus* could precipitate serious hepatic dysfunction. The dose-related disruption in the liver parenchyma of *C. gariepinus* juveniles has earlier been credited to extreme physiological activities needed by the fish to excrete the toxic substances out of its body during detoxification and biotransformation processes (Adebola and Ayo, 2014). However, further studies that will incorporate liver enzymes profiles and anti-oxidant assays will be necessary to reveal the impact of the extract (aqueous stem bark) of *A. leiocarpus* on *C. gariepinus* liver physiology.

5. Conclusion

This study has demonstrated that aqueous crude stem bark extract of *A. leiocarpus* has deleterious and piscicidal effects on *C. gariepinus* juveniles, hence its washing, processing and indiscriminate disposal into aquatic environments should be discouraged or totally avoided to preserve aquatic biodiversity and abundance particularly of fish species such as tropical freshwater African catfish *C. gariepinus*.

Acknowledgement

The authors are appreciative of the laboratory space provided by the Department of Zoology, University of Jos for the conduction of the experiment and for the expertise rendered by the technical staff of the Central Diagnostic Unit of National Veterinary Research Institute, Vom, Plateau State, Nigeria.

References

Adebola K and Ayo F. 2014. Histological changes in liver, gills and kidney of catfish (*Heterobranchus bidorsalis) e*xposed to *c*ypermethrin concentration. *Int. J Histol .Cytol.,* **1**: 31-36.

Adesina BT, Omitoyin BO, Ajani EK and Adesina OA. 2013. Acute-lethal toxicity (LC_{50}) of *Moringa oleifera* (Lam.) fresh root bark extract on *Oreochromis niloticus* juveniles under renewal toxicity exposure. *Int. J Appl. Agric. Apicu. Res.,* **1**: 182-188.

Adewoye SO. 2010. Haematological and biochemical changes in *Clarias gariepinus* exposed to *Trephosia vogelii* extract. *Adv. Appl. Sci. Res.,* **1**(1): 74 – 79.

APHA (American Public Health Association) 1985. **Standard Methods for Examination of Water and Wastewater.** Washington. USA. Pp: 258-259.

Arbab AH. 2014. Review on *Anogeissus leiocarpus* a potent African traditional drug. *Int. J Res. Pharm. Chem.,* **4**: 496-500.

Arbonnier M. 2004. **Trees, Shrubs and Lianas of West African Dry Zones**. The Netherlands: Cirad Margraf. Pp. 573.

Audu BS, Omirinde JO, Gosomji IJ and Wazhi PE. 2017. Histopathological changes in the gill and liver of *Clarias gariepinus* exposed to acute concentrations of *Vernonia amygdalina. Ani. Res. Int.,* **14**: 2576-2587.

Audu BS, Wakawa IA, Omirinde JO, Garba U and Damshit M. 2020. Histopathological alterations in organs of Nile tilapia fingerlings exposed to sublethal concentrations of aqueous crude leaves extract of desert date. *Pan Afri. J Life Sci.,* **4**: 59-67.

Bala SA, Kabir MA and Paul CO. 2014. Biochemical Parameters of Common Carp (*Cyprinus carpio*) exposed to Crude Leaf Extract of *Cannabis sativa*. *Jordan J Biol Sci.,* **7**, 147 – 151. Cite score (0.47)

Bala SA and Malachy NOA. 2020 Metabolic enzyme profile, behavioural changes and morpho physiological parameters of African catfish *Clarias gariepinus* juveniles in response to burnt waste tyres. *Comp Clin Pathol.,* **29**:787–797.

Bolorunduro PI and Abdullah AY. 1996. Water quality management in fish culture, national agricultural extension and research liaison services, Zaria, Extension Bulletin No. 98.

Camargo MMP and Martinez CBR. 2007. Histopathology of gills, kidney and liver of a neotropical fish caged in an urban stream. *Neotrop Ichthyo.*, **5**: 327-336.

Devi PA, Padmavathy P, Aanand S and Aruljothy K. 2017. Review on water quality parameters in freshwater cage fish culture. *Int. J App. Res.*, **3**: 114-120.

Drury R Wallington E. 1967. **Histological Technique**. 4th edition, Oxford University Press, USA, **pp** 279-280.

Eyo JE, Levi CA, Asogwa CN, Odii EC, Chukwuka CO, Ivoke N, Onoja US and Onyeke CC. 2013.

Toxicity and effect of Carica papaya seed aqueous extract on liver biomarkers of Clarias gariepinus. *Int. J Indig. Med. Plant.*, **46**(3): 1301 – 1307.

Fadina OO, Taiwo VO. and Ogunsanmi AO. 1991. The effects of single and repetitive oral administration

of common pesticides and alcohol on rabbits. *Trop Vet.*, **17**: 97 – 106.

Fafioye OO, Fagade S O and Adebisi AA. 2005. Toxicity of *Raphia vinifera*, P. beauv fruit extracts

on biochemical composition of Nile tilapia (*Oreochromis niloticus*, Trewavas). *Biokemistri*., **17**: 137 – 142.

Fafioye OO. 2011. Lethal and sublethal effects of plant extract on some freshwater fauna. PhD thesis, University of Ibadan, Nigeria.

Fafioye OO, Adebisis AA and Fagade SO. 2004. Toxicity of *Parkia biglobosa* (locust bean) and *Raphia vinifera* extracts on *Clarias gariepinus* juveniles. *Afri. J Biotech.*, **3**: 627-630.

Hadi AA and Alwan SF. 2012. Histopathological changes in gills, liver and kidney of fresh water fish, *Tilapia zillii*, exposed to aluminium. *Int. J Pharm Life Sci.*. **3**: 2071-2051.

Istvan U. 2000. Semi-natural products and related substances as alleged botanical pesticides. *Pest Manage. Sci.*, **56**: 703-705.

Jalaludeen MD, Arunachalam M, Raja M, Nandagopal Bhat SA, Sundar S and Palannimuthu D. 2012. Histopathology of the gill, liver and kidney tissues of the freshwater fish *Tilapia mossambica* exposed to cadmium sulphate. *Int. J Adv. Biol. Res.*, 2: 572-578.

Hinton DE and Laurén DJ. 1990. Liver structural alterations accompanying chronic toxicity in fishes: Potential Biomarkers of Exposure. In: McCarthy JF and Shugart LR (Eds.). **Biomarkers of Environmental Contamination**, Boca Raton: Lewis Publishers. **pp**. 51-65.

Makori AJ, Aboum PO, Kapiyo R, Ayona DN and Dida GO. 2017. Effects of water physico- chemical parameters on tilapia (*Oreochromis niloticus*) growth in earthen ponds in Teso North Sub-county, Busia county. *Fish. Aqua. Sci.*, **20**: 2-10.

Mbagwu ES. 2011. Acute toxicity of *Persea americana* crude seed extracts on the physiology and histopathology of *Clarias gariepinus* fingerlings under laboratory conditions. BSc project, University of Jos, Jos, Nigeria.

Naeemi A, Jamili S, Shabanipour N, Mashinchian A and Shariati FS. 2013. Histopathological changes of gill, liver, and kidney in *Caspian kutum* exposed to linear alkylbenzene. *Iran J Fish. Sci.*, **12**: 887-897.

Nasiruddin M, Azadi MA and Jahan A. 2012. Histopathological changes in gill, liver and intestine of *Heteropneustes* fossilis (bloch) treated with three dry seed extracts. *J Asia Soc Bangladash Sci.*, **38:** 217-226.

Ngugi CC, James RB, and Bethuel OO. 2007. **A New Guide to Fish Farming in Kenya**, Oregon State University, USA. 95pp.

Nobre MKB, Lima FRS and Magalhaes FB.2014. Alternative liming blends for fish culture. *Acta Sci. Ani. Sci.*, **36**: 11-16.

Ojutiku, RO, Avbarefe EP, Kolo RJ and Asuwaju FP. 2012. Toxicity of *Parkia biglobosa* pod

extract on *Clarias gariepinus* juveniles. *Int. J Fish. Aquac.*, **4**(7): 133 – 138.

Okpekon T. 2004. Antiparasitic activities of medicinal plants used in Ivory Coast. J Ethnopharm., 90: 91-97.

Olojo EAA, Olurin KB, Mbaka G and Oluwemimo AD. 2005. Histopathology of Gills and Liver Tissues of the African Catfish (*Clarias gariepinus*) exposed to Lead. *Afri. J Biotech*., **4**: 117-122.

Olusegun AA and Adedayo OO. 2014. Haematological responses, serum biochemistry and histology of *Clarias gariepinus* (Burchell, 1822) exposed to sublethal concentrations of cold water fresh root bark extracts of *Plumbago zeylanica* (leadwort). *J. Aqua. Res. Dev.*, **5**: 282-288.

Oluwatoyin AS. 2011. Histopathology of Nile tilapia (*Oreochromis niloticus*) juveniles exposed to aqueous and ethanolic extracts of *Ipomoea aquatic* leaf. *Int. J Fish. Aquac.*, **3**: 244-257.

Omoitoyin BO, Ogunsami AO and Adesina BT. 1999. Studies on acute toxicity of piscidal plants extract on tilapia (*Sarotherodon galliceus*) fingerlings. *Tropic J Ani. Sci.*, **2:** 191-197.

Power DM, Fuentes J, Harrison AP. 2010. "A noninvasive monitoring device for anaesthetics in fish" *Dove press*, http://www.dovepress.com (May 5, 2014).

Rotimi VO. 1988. Activities of Nigerian chewing stick extracts against *Bacteroides gingivalis* and *Bacteroides melaninogenicus. Antimicrob Agents Chemothera.*, **32**: 598-600.

Roy RK and Munshin DJ. 1989. Effects of saponin extracts in oxygen uptake and haematology of air brcathing climbina perch (*Anabastes titutdines*) (Bloch) *J Fresh Water Biol.*, **1:** 167-172.

Salau AK, Yakubu MT, Oladiji AT, 2013. Cytotoxic activity of aqueous extracts of Anogeissus leiocarpus and Terminalia avicennioides root barks against ehrlich ascites carcinoma cells. Indian J Pharm., 45: 381-385.

Shahi J and Singh A. 2011. Effect of bioactive compounds extracted from euphorbious plants on haematological and biochemical parameters of *Channa punctatus. Rev Inst. Med. Tropic. Sao Paulo.*, **53:** 259-263.

Steentoft M. 1988. **Flowering plants in West Africa**. Cambridge University Press. London UK. Pp234.

Tsuchiya H. 2017. Analgestic agents of plant origin. A review of phytochemicals with anaesthetic activity. *Molecules.*, **22**: 1369-1402.

USEPA 1985. Disciplinary Review Ecological Effects Profile. US Environmental Protection Agency, Office of Pesticide Programs, 401 M St. S.W., Washington DC 20460, USA.

Wakawa AI, Audu BS, Sulaiman Y. 2018. Phytochemistry and proximate composition of root, stem bark, leaf and fruit of desert date, *Balanites aegyptiaca, J. Phytopharm. Pharmacog. Phytomed. Res.*, **7**: 464-470.

JJBS

Volume 14, Number 3, September 2021
ISSN 1995-6673
Pages 545 - 549

Jordan Journal of Biological Sciences

The Effects of Olive Mill Wastewater on Soil Microbial Populations

Laith N. AL-Eitan[1,2,], Rami Q. Alkhatib[1,2], Bayen S. Mahawreh[1], Amneh H. Tarkhan[1], Hanan I. Malkawi[3], and Munir J. Rusan[4]*

[1]Department of Applied Biological Sciences, Jordan University of Science and Technology, Irbid 22110, Jordan;[2]Department of Biotechnology and Genetic Engineering, Jordan University of Science and Technology, Irbid 22110, Jordan;[3]Department of Biological Sciences, Yarmouk University, Irbid 21163, Jordan;[4]Department of Natural Resources and Environment, Jordan University of Science and Technology, Irbid 22110, Jordan

Received: August 31, 2020; Revised: November 11, 2020; Accepted: November 24, 2020

Abstract

Olive mill wastewater (OMW) is a common pollutant in Jordan due to the large number of olive mills and the importance of the olive oil industry in the country. In this study, the effects of OMW and fertilizer on soil microbial populations were examined by counting the number of microbial colonies on each plate after respective treatments with water, OMW, and fertilizer. Colonies were identified based on macroscopic and microscopic examination as well as a range of biochemical tests. After treatment with OMW, a significant increase was exhibited in the *Bacillus* (*p*-value of 0.011 in clay) and *Yeast* (*p*-values of 0.001 in clay and 0.037 in sand) populations. In contrast, *Staphylococcus*, *Streptomyces (p*-values of 0.034 in clay and 0.016 in sand) and Mold (*p*-value of 0.013 in sand) exhibited population decreases. Our results showed that OMW significantly affects natural soil microbial populations, which is an important finding as most of the OMW in Jordan is disposed of in a way that exposes it to the soil. This study illustrated that OMW has a potential to be recycled and utilized as an antibacterial agent. Further studies should be conducted using molecular PCR analysis in order to accurately determine the species of each studied microorganism.

Keywords: olive mill wastewater; soil microbes; fertilizer; Jordan.

1. Introduction

Olive and olive oil production is of particular importance to the economic sectors of Jordan in particular and Mediterranean countries as a whole (Rusan *et al*., 2015). However, the olive oil industry generates a large amount of toxic drainage known as olive mill wastewater (OMW), the latter of which is characterized by an acidic pH as well as a high content of organic compounds and polyphenols (Ribeiro *et al*., 2018). The disposal of untreated OMW poses a number of threats to both environmental and public health, and its management is a source of considerable problems for most of the Mediterranean region (Ioannou-Ttofa *et al*., 2017). OMW has phytotoxic and inhibitory effects on plant growth, acts as an anti-bacterial agent, and contains compounds that are toxic to non-bacterial microorganisms, all of which result in an altered state of soil microbial diversity (Mekki *et al*., 2013; Ntougias *et al*., 2013; Rusan *et al*., 2016). Therefore, OMW can neither be disposed of directly into the environment nor into the sewage systems, and several different OMW management, treatment, and valorization strategies have been proposed (Souilem *et al*., 2017).

Jordan's eastern Mediterranean climate makes it particularly suited for the cultivation of olive trees, which hold great cultural, religious, and economic importance for the Jordanian people (Al Ganideh and Good, 2016). In fact, Jordan is a major exporter of olives and olive oil, and olive trees cover 73% of the agricultural land occupied by fruit trees (El Hanandeh and Gharaibeh, 2016). As a result, nearly 180,000 families are supported by the farming of 20 million olive trees, and the annual income from olive oil production is approximately 100 million Jordanian dinars (*The Jordan Times*, 2015). More than 70% of the Jordanian olive oil processing industry utilizes three-phase oil mills (86 out of a total of 118 oil mills as of 2011), while the remaining 30% consists of two-phase oil mills (20%) and traditional press mills (10%) (Qdais and Alshraideh, 2016). Three-phase oil mills produce large amounts of OMW, a pulp-like substance called olive cake, and a substantial amount of wastewater from washing the olives prior to extraction (Dourou *et al*., 2016).

Several studies have been conducted concerning OMW itself as well as its management and disposal in Jordan and abroad. OMW can be treated in jet-loop (JACTO) reactors in order to reduce its chemical oxygen demand (COD) and total phenol content by 85% and 80%, respectively (Ribeiro *et al*., 2018; Khoufi *et al*., 2015). Furthermore, the simple act of diluting OMW with water was reported to eliminate its phytotoxic effects on plant growth (Rusan and Malkawi, 2016). In addition, biodegradation of OMW by various types of thermophilic bacteria is another potential treatment strategy that is under investigation (Al-Qodah *et al*., 2015). Moreover, volcanic tuff treated with nitric acid was found to reduce the COD and total phenol content of OMW by 14% and 21%, respectively (Azzam, 2018). Likewise, natural Jordanian clay that was subject to calcination and acid treatment reduced the COD of OMW by up to 50% (Azzam *et al*., 2015). Lastly, the use of OMW as a fertilizer was found to enhance plant growth, but such growth was lower than that obtained by

* Corresponding author e-mail: lneitan@just.edu.jo.

conventional fertilizer and potable water (Rusan *et al*., 2015; Barbera *et al*., 2013).

Since OMW has been investigated in the context of plant growth and fertilization, it is important to also consider how OMW application might affect the microbial diversity of the soil it is being applied to. It has previously been found that olive washing conditions and the resulting OMW can affect the growth of certain fungal species in Jordan's environment (Massadeh *et al*., 2010; Al-Ameiri *et al*., 2015). Therefore, the main aim of this study is to investigate the impact of raw OMW on various soil microbiota obtained from local sources, specifically in comparison with fertilizer and water treatments.

2. Materials and methods

2.1. Field and soil sampling

Two types of soil samples were used in this study: clay and sand. Soil samples were collected from an on-campus site at Jordan University of Science and Technology, while raw OMW was collected from local olive mills in Irbid, Jordan. A greenhouse experiment was conducted to evaluate the effects of three treatments (tap water (W), tap water and fertilizer (W+F), and raw OMW) on the microbiota populations of clay and sand.

A total of 18 pots were filled with 5 kg of air-dried silty clay loam (n=9) or 5 kg of air-dried sandy loam (n=9), so that each treatment was replicated three times in a randomized complete block design. Three corn seeds were planted in each pot, after which the soil moisture was brought up to the field capacity water content. The amount of water required to bring the sand to field capacity was 900 cm^3, while the amount required for the clay was 1,500 cm^3. Afterwards, all the pots were watered periodically to keep the soil moisture level at field capacity. Irrigation solution was added three times per week depending on the losses of soil moisture by evapotranspiration, the latter of which was determined by the periodic weighing of the pots. Pretreatment characteristics of the soil and irrigation solutions are summarized in **Tables 1** and **2**, respectively. After 8 weeks of growth, the plants were harvested, and representative soil samples were taken from each pot after thoroughly mixing the soil.

Table 1. Characteristics of soil samples.

Parameters	**Units**	**Sand**	**Clay**
pH*	-	7.8	8.18
Electrical conductivity*	dS/m	1.2	0.61
Calcium carbonate ($CaCO_3$)	%	27.1	15.3
Cation exchange capacity (CEC)	cmol/kg	24.1	34.3
Organic matter	%	1.01	0.72
Texture Class	-	Sandy loam	Silty clay loam

*of 1:1 soil:water suspension

Table 2. Characteristics of irrigation water and olive mill wastewater (OMW).

Parameters	Units	Water	Raw OMW	Treated OMW
pH	-	7.8	4.7	6.2
Electrical conductivity	dS/m	0.6	7.6	5.1
Total suspended solids (TSS)	mg/l	10	1236	-
Total polyphenol content	mg/l	0.98	1666	700

2.2. Treatment of soil

Soil samples were sieved and dried, and 1g of each sample was mixed with 99 mL of sterile distilled water and placed in a reciprocal shaker to be shaken for three hours at 120 rpm. Each sample was properly diluted, and 0.1 mL was inoculated on nutrient agar (for general bacteria, *Bacillus* spp, and *Staphylococcus* spp), oatmeal agar (for *Streptomyces* spp), malt extract agar (for yeast), and potato dextrose agar (for molds).

2.3. Culturing of microorganisms

Inoculated plates were placed in an incubator at 37ºC for incubation. The general bacterial, *Bacillus* and *Staphylococcus* colonies were counted after an incubation period of 24 hours, while the *Streptomyces*, yeast and mold plates required 4 days of incubation before their colonies were counted. There were two types of colonies on the nutrient agar plate, and they were separated into two groups depending on their morphology (**Table 3**).

Table 3. Colony morphology, microscopic examination and biochemical tests.

Biochemical test	Type 1 (*Staphylococcus*)	Type 2 (*Bacillus*)
Colony morphology	White, round	Large, flat, white, smooth, non-pigment producer
Gram staining	Gram-positive	Gram-positive
Shape of cell	Cocci	Long rod
Arrangement of cells	In clusters	In chains
Endospore staining	Non-spore former	-
Catalase	-ve	-
Benzidine	-ve	-
Nitrate red	-ve	-
Motility	-ve	-

2.4. Microbial parameters

In this study, the main parameters were the colony counts, macroscopic and microscopic examination, and a series of biochemical tests.

2.4.1. Colony counts

The main parameter used for observing the effect of each treatment on soil microbial populations was the colony count, which was carried out via a Quebec colony counter. The colony count is a basic microbiological technique that attempts to quantify the amount of bacterial growth in terms of number of colonies. Therefore, this technique is useful in the present study as it provides a

quantitative means of measuring the effects of the various treatments on each bacterial population.

2.4.2. Macroscopic and microscopic examination

As there were two types of colonies on the nutrient agar plates, further examination was necessary to identify each genus. Macroscopically, it was found that Type 1 (*Staphylococcus*) microorganisms had a white and round appearance, while Type 2 (*Bacillus*) microorganisms had a large, flat, white and smooth surface with no pigment production. Upon microscopic examination, Type 1 (*Staphylococcus*) microorganisms had a cocci shape and were arranged in clusters, while Type 2 (*Bacillus*) microorganisms appeared as long rods that were linked together to form chains.

2.4.3. Biochemical tests

Several biochemical tests were employed in order to further ascertain the identities of the microorganisms. The first biochemical test was the basic Gram stain procedure in order to determine whether the cell was Gram-positive or Gram-negative. Afterwards, a series of biochemical tests were applied to the Group 1 (*Staphylococcus*) microorganisms in order to fully confirm their identity. These included the catalase, benzidine, nitrate red, and motility tests.

2.4.4. Statistical analysis

The data was analyzed by one-way ANOVA using IBM SPSS. Levene's test was first applied in order to test homogeneity of variance, and the post-hoc tests consisted of Tukey's test (for equal variances) and Games-Howell test (for unequal variances). All statistical analyses were conducted using SPSS statistical package 19.0 (SPSS Corp., USA).

3. Results

The application of OMW resulted in an increase in the general bacterial count compared with the application of fertilizer. *Bacillus* populations were the highest after OMW application and increased substantially after treatment with OMW in both clay and sand. The lower population was observed in sand. Like *Bacillus*, yeast populations were highest after OMW application in both sand and clay. However, yeast populations were much higher in clay compared to sand. On the other hand, the *Streptomyces*, *Staphylococcus*, and mold populations were the lowest after OMW application, as they decreased substantially after treatment in both clay and sand. The lower populations were observed in sand (**Figure 1**).

Table 4 shows statistical comparisons between the different types of treatments. There was a significant effect of the treatments on *Bacillus* populations in clay [F (2, 6) = 10.388, p = 0.011]. The Tukey post hoc test indicates that the mean for the OMW treatment (M = 20.3 x 10^5, SD = 75.2 x 10^5) differs significantly from the mean for no treatment (M = 8 x 10^5, SD = 2 x 10^5). Moreover, the treatments also had a significant effect on *Streptomyces* populations in clay [F (2, 6) = 6.288, p = 0.034]. The Tukey post hoc test indicates that the mean for the OMW treatment (M = 36.7 x 10^5, SD = 15.2 x 10^5) differs significantly from the mean for the fertilizer treatment (M = 11.6 x 10^6, SD = 2.1 x 10^6). A significant result was also observed for *Streptomyces* populations in sand [F (2, 6) = 8.988, p = 0.016].

There was a significant effect of the treatments on mold populations in sand [F (2, 6) = 9.653, p = 0.013]. The Tukey post hoc test indicates that the mean for the OMW treatment (M = 10 x 10^3, SD = 2 x 10^3) differs significantly from the mean for the fertilizer treatment (M = 50 x 10^3, SD = 17.3 x 10^3) and the no treatment (M = 40 x 10^3, SD = 10 x 10^3) groups. There was a significant effect of the treatments on yeast populations in clay [F (2, 6) = 34.543, p = 0.001]. The Tukey post hoc test indicates that the mean for the OMW treatment (M = 24 x 10^4, SD = 5.57 x 10^4) differs significantly from the mean for the fertilizer treatment (M = 50 x 10^3, SD = 17.3 x 10^3) and the no treatment (M = 30 x 10^3, SD = 10 x 10^3) groups. For yeast populations in sand, a significant effect was also shown [F (2, 6) = 6.000, p = 0.037]. The Tukey post hoc test did not indicate which groups showed the significant difference.

Table 4: Statistical comparisons between microbiota in the two types of soil.

	Type of soil	Mean Square	Sum of Squares	F	*P-value*
Bacillus	Clay	1.754 x 10^{12}	3.509 x 10^{12}	10.388	**0.011 ***
	Sand	4.878 x 10^{11}	9.756 x 10^{11}	2.851	0.135
Staphylococcus	Clay	2.413 x 10^{12}	4.827 x 10^{12}	3.899	0.082
	Sand	6.544 x 10^{11}	1.309 x 10^{11}	4.007	0.078
Streptomyces	Clay	5.782 x 10^{13}	1.156 x 10^{14}	6.288	**0.034 ***
	Sand	4.219 x 10^{13}	8.439 x 10^{13}	8.988	**0.016 ***
Mold	Clay	25.2 x 10^7	50.5 x 10^7	1.857	0.236
	Sand	13 x 10^8	26 x 10^8	9.653	**0.013 ***
Yeast	Clay	40.3 x 10^9	80.6 x 10^9	34.543	**0.001 ***
	Sand	16 x 10^8	32 x 10^8	6.000	**0.037 ***

***significant at p<0.05 at 2 df

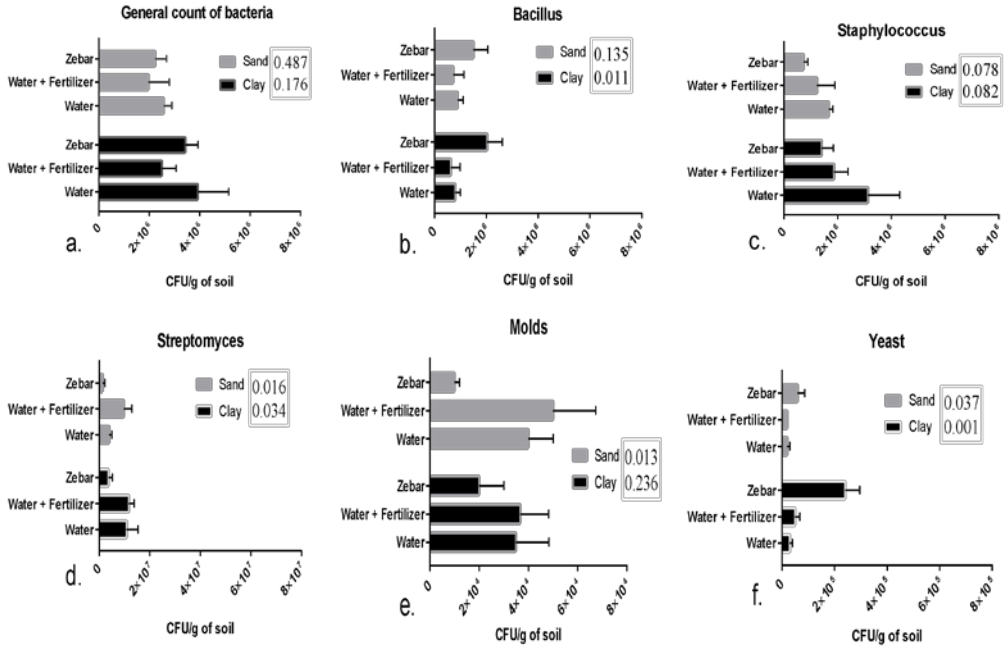

Figure 1: Graphical representation of colony counts (values in the legend represent the p-values): **a**. Applying raw OMW (zebar) resulted in an increase in the general count of bacteria in both sand and clay **b**. *Bacillus* populations exhibited increases in both sand and clay after application with OMW, with p-values of 0.135 and 0.011, respectively **c**. while *Staphylococcus* populations decreased to almost half after OMW application, their p-values in sand (0.078) and clay (0.082) were not significant **d.** *Streptomyces* populations decreased substantially after OMW treatment, with p-values of 0.016 in sand and 0.034 in clay that were statistically significant **e.** Mold populations were also reduced after being treated with OMW, with p-values of 0.013 in sand and 0.236 in clay **f.** Yeast populations (like *Bacillus*) increased significantly after application of OMW, and the p-values in sand 0.037 and in clay 0.001 reflected this significance.

4. Discussion

The olive oil industry is predominant in Jordan and other Mediterranean countries, making the safe disposal of any waste and harmful by-products of the utmost environmental importance. As a consequence of the OMW's high phenolic composition, it has a significant antimicrobial effect on several types of native soil microorganisms. In Jordan, oil mills are prohibited from the direct disposal of OMW, and they cannot discharge the OMW into municipal wastewater treatment systems (Rusan *et al*., 2015). Instead, raw OMW is disposed of at specified dumping sites and their surrounding areas (Rusan and Malkawi, 2016). Therefore, the aim of the present study was to investigate the effects of raw OMW on native soil microbiota sourced from local sites.

The fact that OMW is generally detrimental to the microbial populations of soil was corroborated by the results obtained in this study, which showed that general bacterial populations decreased after exposure to raw OMW (Ntougias *et al*., 2013). Moreover, the application of OMW resulted in a major reduction of *Staphylococcus* and *Streptomyces* populations in both clay and sand, which agreed with previously published results (Tafesh *et al*., 2011). In contrast, the *Bacillus* population flourished in the presence of OMW, which could be explained by the fact that *Streptomyces* produces toxic substances that diminish *Bacillus* growth (de Lima Procópio *et al*., 2012). Correspondingly, one study reported that OMW sustained indigenous populations of *Bacillus*, while another found that OMW was conducive to *Bacillus* growth by protecting it from UV radiation (Yangui *et al*., 2008; Jallouli *et al*., 2014).

In terms of molds, our findings showed that the application of OMW led to an overall decrease in mold populations. Similarly, the application of OMW to fruit infected with gray mold as well as plum tree orchards led to a significant decrease in fungal formation (Saadi *et al*., 2007; Vagelas *et al*., 2009). Several types of molds, namely *Alternaria*, *Colletotrichum*, *Sclerotium*, and *Rosellinia*, species were strongly inhibited by the application of OMW (Cibelli *et al*., 2017). In contrast, the spreading of OMW to a field of olive trees led to an almost 5-fold increase in arbuscular mycorrhizal fungi, which caused the fungal-bacterial ratio to increase from 0.23 to 1.11 (Mechri *et al*., 2008). Concerning yeast, our findings show that yeast populations grew substantially when treated with OMW, with increases of 700% and 200% in clay and sand, respectively. Few studies about the effects of OMW on yeast were reported. However, the role of various yeast strains in the biodegradation of OMW phenols has been previously confirmed (Jarboui *et al*., 2012; Bevilacqua *et al*., 2013).

There are several limitations of the present study. Firstly, the populations of microorganisms were not measured before treatment, a step that is required to fully understand the anti-microbial effects of OMW. Secondly, representative soil sampling after plant harvest may have missed root-associated bacteria, i.e., rhizobacteria, which might also be affected by OMW.

In the present study, Jordanian OMW is suggested to unequally impact the growth of a variety of microorganisms depending on the type of soil. While *Bacillus* spp and yeast flourished under OMW treatment, *Staphylococcus* spp, *Streptomyces* spp, mold, and the general bacteria all exhibited decreases in colony counts. More research is needed to elucidate this difference in bacterial response, and future studies could further analyze OMW's antimicrobial effects in order to utilize it as a possible disinfectant. In addition, molecular PCR analysis could also be employed in order to determine the exact species of each microorganism that was studied.

Acknowledgements

This work was prepared within the framework of the project titled "Mediterranean Cooperation in the Treatment and Valorisation of OMW (MEDOLICO)", which was funded by the European Union under the ″ENPI Cross-Border Cooperation Mediterranean Sea Basin Programme″ . The total budget for MEDOLICO was 1.9 million Euros, and it was co-financed by the European Neighborhood and Partnership Instrument (90%) and the national funds of the countries participating in the project (10%).

References

'Jordan among world's top 10 producers of olive, olive oil'. 2015. *The Jordan Times*. Available at: http://www.jordantimes.com/news/local/jordan-among-world%E2%80%99s-top-10-producers-olive-olive-oil%E2%80%99 (Accessed: 9 August 2021).

Al Ganideh SF and Good LK. 2016. Nothing Tastes as Local: Jordanians' Perceptions of Buying Domestic Olive Oil. *J Food Prod Mark.*, **22(2)**: 168–190.

Al-Ameiri NS, Karajeh MR and Qaraleh SY. 2015. Molds Associated with Olive Fruits Infested with Olive Fruit Fly (Bactrocera oleae) and their Effects on Oil Quality. *Jordan J Biol Sci.*, **8(3)**: 217–220.

Al-Qodah Z, Al-Shannag M, Bani-Melhem K, Assirey E, Alananbeh K and Bouqellah N. 2015. Biodegradation of olive mills wastewater using thermophilic bacteria. *Desalin Water Treat.*, **56(7)**: 1908–1917.

Azzam MOJ, Al-Gharabli SI and Al-Harahsheh MS. 2015. Olive mills wastewater treatment using local natural Jordanian clay. *Desalin Water Treat.*, **53(3)**: 627–636.

Azzam MOJ. 2018. Olive mills wastewater treatment using mixed adsorbents of volcanic tuff, natural clay and charcoal. *J Environ Chem Eng.*, **6(2)**: 2126–2136.

Barbera AC, Maucieri C, Cavallaro V, Ioppolo A and Spagna G. 2013. Effects of spreading olive mill wastewater on soil properties and crops, a review. *Agric Water Manag.*, **119**: 43–53.

Bevilacqua A, Petruzzi L, Corbo MR and Sinigaglia M. 2013. Bioremediation of Olive Mill Wastewater by Yeasts – A Review of the Criteria for the Selection of Promising Strains. In: Patil YB and Rao P (Eds.), **Applied Bioremediation - Active and Passive Approaches**. InTechOpen, UK.

Cibelli F, Bevilacqua A, Raimondo ML, Campaniello D, Carlucci A, Ciccarone C, Sinigaglia M and Corbo MR. 2017. Evaluation of Fungal Growth on Olive-Mill Wastewaters Treated at High Temperature and by High-Pressure Homogenization. *Front Microbiol.*, **8**: 2515.

de Lima Procópio RE, da Silva IR, Martins MK, de Azevedo JL and de Araújo JM. 2012. Antibiotics produced by Streptomyces. *Brazilian J Infect Dis.*, **16(5)**: 466–471.

Dourou M, Kancelista A, Juszczyk P, Sarris D, Bellou S, Triantaphyllidou IE, Rywinska A, Papanikolaou S and Aggelis G. 2016. Bioconversion of olive mill wastewater into high-added value products. *J Clean Prod.*, **139**: 957–969.

El Hanandeh A and Gharaibeh MA. 2016. Environmental efficiency of olive oil production by small and micro-scale farmers in northern Jordan: Life cycle assessment. *Agric Syst.*, **148**: 169–177.

Ioannou-Ttofa L, Michael-Kordatou I, Fattas SC, Eusebio A, Ribeiro B, Rusan M, Amer ARB, Zuraiqi S, Waismand M, Linder C, Wiesman Z, Gilron J and Fatta-Kassinos D. 2017. Treatment efficiency and economic feasibility of biological oxidation, membrane filtration and separation processes, and advanced oxidation for the purification and valorization of olive mill wastewater. *Water Res.* **114**: 1–13.

Jallouli W, Sellami S, Sellami M and Tounsi S. 2014. Efficacy of olive mill wastewater for protecting *Bacillus thuringiensis* formulation from UV radiations. *Acta Trop.*, **140**: 19–25.

Jarboui R, Baati H, Fetoui F, Gargouri A, Gharsallah N and Ammar E. 2012. Yeast performance in wastewater treatment: case study of *Rhodotorula mucilaginosa*. *Environ Technol.*, **33(7–9)**: 951–960.

Khoufi S, Louhichi A and Sayadi S. 2015. Optimization of anaerobic co-digestion of olive mill wastewater and liquid poultry manure in batch condition and semi-continuous jet-loop reactor. *Bioresour Technol.*, **182**: 67–74.

Massadeh MI, Fraij A and Fandi K. 2010. Effect of Carbon Sources on the Extracellular Lignocellulolytic Enzymetic System of Pleurotus Sajor-Caju. *Jordan J Biol Sci.*, **3(2)**: 51–54.

Mechri B, Ben Mariem F, Baham M, Ben Elhadj S and Hammami M. 2008. Change in soil properties and the soil microbial community following land spreading of olive mill wastewater affects olive trees key physiological parameters and the abundance of arbuscular mycorrhizal fungi. *Soil Biol Biochem.*, **40(1)**: 152–161.

Mekki A, Dhouib A and Sayadi S. 2013. Review: Effects of olive mill wastewater application on soil properties and plants growth. *Int J Recycl Org Waste Agric.*, **2(15)**: 1–7.

Ntougias S, Bourtzis K and Tsiamis G. 2013. The microbiology of olive mill wastes. *Biomed Res Int.*, **2013**: 784591.

Qdais HA and Alshraideh H. 2016. Selection of management option for solid waste from olive oil industry using the analytical hierarchy process. *J Mater Cycles Waste Manag.*, **18**: 177–185.

Ribeiro B, Torrado I, Di Berardino S, Paixão SM, Rusan MJ, Bani Amer A, Zuraiqi S and Eusébio A. 2018. Jet-loop reactor with cross-flow ultrafiltration membrane system for treatment of olive mill wastewater. *Water Pract Technol.* **13(2)**: 247–256.

Rusan MJM and Malkawi HI. 2016. Dilution of olive mill wastewater (OMW) eliminates its phytotoxicity and enhances plant growth and soil fertility. *Desalin Water Treat.*, **57(57)**: 1–9.

Rusan MJM, Albalasmeh AA and Malkawi HI. 2016. Treated Olive Mill Wastewater Effects on Soil Properties and Plant Growth. *Water Air Soil Pollut.*, **227**: 135.

Rusan MJM, Albalasmeh AA, Zuraiqi S and Bashabsheh M. 2015. Evaluation of phytotoxicity effect of olive mill wastewater treated by different technologies on seed germination of barley (Hordeum vulgare L.). *Environ Sci Pollut Res.*, **22(12)**: 9127–9135.

Saadi I, Laor Y, Raviv M and Medina S. 2007. Land spreading of olive mill wastewater: Effects on soil microbial activity and potential phytotoxicity. *Chemosphere*, **66(1)**: 75–83.

Souilem S, El-Abbassi A, Kiai H, Hafidi A and Sayadi S. 2017. Olive oil production sector: environmental effects and sustainability challenges. In: Galanakis CM (Ed.), **Olive Mill Waste**. Academic Press, USA, pp. 1–28.

Tafesh A, Najami N, Jadoun J, Halahlih F, Riepl H and Azaizeh H. 2011. Synergistic antibacterial effects of polyphenolic compounds from olive mill wastewater. *Evid Based Complement Alternat Med.* **2011**: 431021.

Vagelas I, Papachatzis A, Kalorizou H and Wogiatzi E. 2009. Biological Control of *Botrytis* Fruit Rot (*Gray Mold*) on Strawberry and Red Pepper Fruits by Olive Oil Mill Wastewater. *Biotechnol Biotechnol Equip.*, **23(4)**: 1489–1491.

Yangui T, Rhouma A, Gargouri K, Triki MA and Bouzid J. 2008. Efficacy of olive mill waste water and its derivatives in the suppression of crown gall disease of bitter almond. *Eur J Plant Pathol.*, **122**: 495–504.

JJBS

Volume 14, Number 3, September 2021
ISSN 1995-6673
Pages 551 - 558

Jordan Journal of Biological Sciences

Chemical Analysis, Antioxidant, Anti-Alzheimer and Anti-Diabetic Effect of Two Endemic Plants from Algeria: *Lavandula antineae* and *Thymus algeriensis*

Benabdallah Fatima Zohra [1, 2,*], Zellagui Amar [2], Bensouici Chawki [3]

[1]*Sciences of nature and life Faculty, University of Ferhat Abbas Setif 1, El Bez 1900, Algeria,* [2]*Laboratory of Biomolecules and Plant Breeding, Life Science and Nature Department, exact science, Life science and nature Faculty, Larbi Ben Mhidi University, Constantine road 04000 Oum El Bouaghi, Algeria,*[3]*Biotechnology Research Center, Ali Mendjli New Town UV 03 BP E73 Constantine, 25000, Algeria.*

Received: September 3, 2020; Revised: November 21, 2020; Accepted: December 5, 2020

Abstract

The purpose of the present work is searching for new sources of bioactive molecules from plants to use them in treating or controlling some health problems. The methanolic extracts of two endemic species in Algeria *Lavandula antineae* (very few studies on its biological effects) and *Thymus algeriensis* were analyzed by HPLC/UV then tested for their antioxidant effect by the DPPH and ABTS scavenging radical tests, FRAP test and CUPRAC test. The inhibitory power of these same extracts on acetylcholinesterase, butyrylcholinesterase and α-glucosidase was also evaluated. Phenolic acids and flavonoids were found in common in both extracts as 3-hydroxy-4-méthoxycinnamic acid, and quercetin. The results showed considerable antioxidant effects for both plants with minimal IC_{50} values equal to 10.77±1.14 µg/ml for *L. antineae* and 11.73±0.20 µg/ml for *T. algeriensis*. The minimal value of $PR_{0.5}$ was recorded with *L. antineae* (10.57± 0.38 µg/ml) after the BHA. The two species are shown to be effective on acetylcholinesterase especially *T. algeriensis*. *L. antineae* exhibited a high inhibitory power against butyrylcholinesterase with 20.84±9.74 µg/ml IC_{50} value. The same plant showed more effective than Galantamine in inhibiting α-glucosidase with 168.61±7.60 µg/ml IC_{50} value. Interesting results were given by methanolic extract of both plants, which can be exploited in medicine and pharmaceutical domains as natural treatments for diseases like Alzheimer and diabetes type 2.

Keywords: *Lavandula antineae, Thymus algeriensis,* methanolic extract, HPLC/UV, antioxidant activity, enzymes inhibitory.

1. Introduction

Oxidative stress can be defined as an imbalance between reactive oxygen species (free radicals) and antioxidant systems (Ichai *et al*., 2011). The uncontrolled formation of reactive oxygen species will often have serious consequences for the body (Pelletier *et al*., 2004). In several serious diseases, notably those linked to aging, oxidative stress is the original triggering factor; this is the case of cancers, ocular pathologies, diabetes and neurodegenerative diseases like Alzheimer's disease (Favier, 2006). That is why many studies are focusing on searching molecules with antioxidant potential. Indeed, the use of plant extracts and their derived phytochemicals, particularly phenolic compounds, has a probable future for controlling various pathologies. Their capacity to scavenge free radicals can entitle them to promote health effects (Payan, 2004; Subhashini *et al*., 2011; Mukherjee *et al*., 2018; Simonovic *et al*., 2019).

In Algeria, a diverse plant flora can be found, including endemic plants with medicinal proprieties such as *L. antineae* and *T. algeriensis* (Lamiaceae family) (Ozenda, 2004). The genus *Lavandula* is known for its medicinal and ornamental effects; it has a high antioxidant activity (Zuzarte *et al*., 2011; Nikolic *et al*., 2014; Ceylan *et al*., 2015). Thyme has been utilized since ancient times for its pharmacological proprieties (Goatez and Guédira, 2012), especially *Thymus algeriensis* which has antioxidant potential and can act as inhibitors of free radical or scavengers (Delgado *et al*., 2014; Guesmi *et al*., 2014).

Our work aims is to analyze the chemical composition of the methanolic extracts of *Lavandula antineae* and *Thymus algeriensis* searching for some phenolic compounds, and in order to seek new natural bioactive molecules sources, we have tested the tow extracts *in vitro* for their antioxidant activity and their inhibitory capacity against certain enzymes involved in several diseases like acetylcholinesterase, butyrylcholinesterase known by their relation with Alzheimer's disease and the digestive enzyme α-glucosidase linked with diabetes type 2.

2. Material And Methods

2.1. Material

2.1.1. Plant material

Lavandula antineae identification was done in the arid regions scientific and technical research center (CRSTRA)-Biskra, while *Thymus algeriensis* was identified in Bellezma National Park of Batna. Desert lavender was harvested from Biskra during the flowering

* Corresponding author e-mail: univ07@outlook.fr

cycle starting at the end of February to early of April. The sampling of *Thymus algeriensis* from Batna was carried out in April. For further preparation of methanolic extracts, aerial sections, precisely leaves and stems, have been dried outdoors and in shade.

2.2. Methods

2.2.1. Methanolic extract preparation

A test sample of 2.5 g of leaf powder was macerated in 25 ml of 80% methanol. Then the macerate was filtered and the solvent was evaporated under reduced pressure at a rotary evaporator at 40-50 °C to dryness. The extract was kept at 4 °C (Falleh *et al*., 2008).

2.2.2. Analysis of the methanolic extract by High Performance Liquid Chromatography (HPLC/UV)

The samples were diluted in methanol and then filtered by 0.45 µm syringe filters. Twenty available standards (phenolic compounds), in fine quantities, have been diluted in methanol. Twenty microliters aliquot of each sample was introduced in the HPLC system combined with a UV-Vis detector at room temperature and with a steady flow rate of 1.0 ml per ml. Compound identification in each sample was established on differences between the retention times of the components determined and the retention times of the standards.

2.2.3. Antioxidant activity in vitro

2.2.3.1. DPPH free radical scavenging test

The antioxidant test by scavenging DPPH radical was conducted in accordance with Bougandoura and Bendimerad (2013) protocol. Fifty microliters of each extract was added to 2 ml DPPH methanolic solution (0.025 g/l). At the same time by combining fifty microliters of the solvent (methanol) with 2 ml of the DPPH methanolic solution, a negative control was prepared. For each concentration, a blank was made and the absorbance was read at 515 nm after 30 min incubation time in the darkness and ambient temperature. BHA and BHT presented the positive control.

2.2.3.2. ABTS free radical scavenging test

ABTS was dissolved in twice-distilled water to obtain a concentration of 7 mM. The cation (ABTS $^{\bullet +}$) was made by reacting solutions of ABTS stock and $K_2S_2O_8$ (2.45 mM) in the presence of K_3PO_4 buffer solution. The mixture was incubated in the darkness for 12-16 hours before use at ambient temperature. Absorbance reading was taken at 734 nm. BHT and BHA solutions were prepared at different concentrations and tested as positive controls (Re *et al*., 1998). The results for DPPH scavenging and ABTS scavenging tests are indicated as an inhibition percentage (I %).

I% = [(Abs control - Abs test) / Abs control] x 100.

2.2.3.3. Iron reduction test: FRAP (Ferric Reducing Antioxidant Power)

Methanolic extract was dissolved in 2.5 ml of Na_3PO_4 buffer at pH 6.6 and 2.5 ml of 1% $C_6N_6FeK_3$ at different concentrations. The mixture was incubated at 50 °C for twenty minutes. After 2.5 ml of trichloroacetic solution (10%) was put, the mixture underwent centrifugation for 10 min at 3000 g. The surnatant (2.5 ml) was added and agitated with 0.5 ml (0.1 percent) of $FeCl_3$ and 2.5 ml of distilled water. Absorption was measured at 700 nm. For BHA and BHT, the same test was performed (Ferreira *et al*., 2007).

2.2.3.4. Cupric ion reduction CUPRAC (Cupric ion Reducing Antioxidant Capacity)

The method followed was reported by Apak *et al*. (2004), fifty microliters of Cu (II) (10 mM), fifty microliters of the neocuproin (7,5 mM), sixty microliters of the NH_4Ac buffer (1 M, pH = 7), and forty microliters of each plant's methanol at a variety of concentrations. After one hour, absorption was registered at 450 nm.

The reducing power at absorbance value 0.5 (PR0.5) was calculated for both tests FRAP and CUPRAC.

2.2.4. Anti-enzymatic activity in vitro

2.2.4.1. Anti-Alzheimer activity (inhibition of acetylcholinesterase and butyrylcholinesterase)

The spectrophotometric approach was followed by testing extracts' ability to inhibit acetylcholinesterase (AChE) and butyrylcholinesterase (BChE) enzymes (Ellman *et al*., 1961). The buffer was made up of 150 µl of Na_3PO_4 at pH 8.0 (100 mm), 10 µl of the solution to test were dissolved into ethanol at various concentration and the amount of 20 µl AChE (5.32 per 10^{-3} U) or BChE (6.85 per 10^{-3} U) was added and incubated at 25 °C for 15 minutes, and then 10 µl DTNB (0.5 mM) had been applied. Then the reaction was initiated by the inclusion of 20 µl of acetylthiocholine iodide at 0.71 mM concentration or butyrylthiocholine chloride at 0.2 mM concentration. Absorbance was read at 412 nm. AChE or BChE inhibition was determined by comparing enzyme activity without extract and its activity in the presence of extract in the following formula:

I (%) = (E - S) / E x 100

E: Enzyme activity without extract S: the enzyme activity in the presence of the extract. The reference compound was galantamine.

2.2.4.2. Inhibition of α-glucosidase

The inhibitory action of α-glucosidase has been carried out respecting Palanisamy *et al*. (2011) method with few modifications. Fifty microliters of the solution to test was mixed with 50 µl of 4-Nitrophenyl α-D-glucopyranoside (5 mM) and 100 µl of the enzyme, the mixture was incubated for 15 minutes at 37 °C. A blank was made for each sample. Absorption was read at 405 nm (0 min and 15 min). Acarbose was used in this experiment as a standard. α-glucosidase's inhibitory function has been demonstrated as follows:

% inhibition = (Abs extract-Abs blank) / Abs control x 100

Control: Enzyme + Substrate + Solvent of the extract.

2.3. Statistical analysis

Each test was done in triplicate; the comparison of means was carried out by ANOVA one way with the Tukey test where the difference was considered significant to a degree ≤ 0.05. For these purposes, the SPSS Statistics version 25 program was used.

3. Results

3.1. Analysis by HPLC

In a time interval between 3 min and 42 min, peaks were marked on the chromatographic profile of the extract

of *Lavandula antineae* (Figure 01); a dominant component of the plant extract with a percentage of 67.2% was detected at a retention time of 24.4 min, followed by two other components with the following percentages: 8.8% and 4.4%. Their retention times were 32.7 min and 27.4 min, respectively. Many peaks were observed, in a time interval of 3 min to 60 min, on the chromatographic profile of *Thymus algeriensis* extract. Three phenolic components were revealed constituting more than 50% of the total extract, with percentages of 26.4%, 17.3% and 8.2%; their corresponding retention times were, respectively, 32.8 min, 36.4 min and 40.0 min (Figure 2).

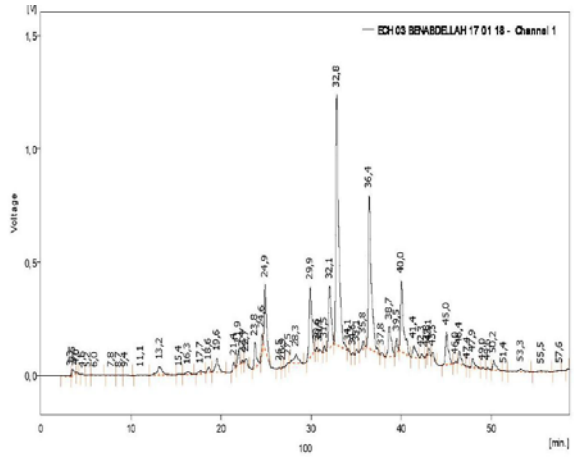

Figure 1. Chromatogram of methanolic extract of *L. antineae*

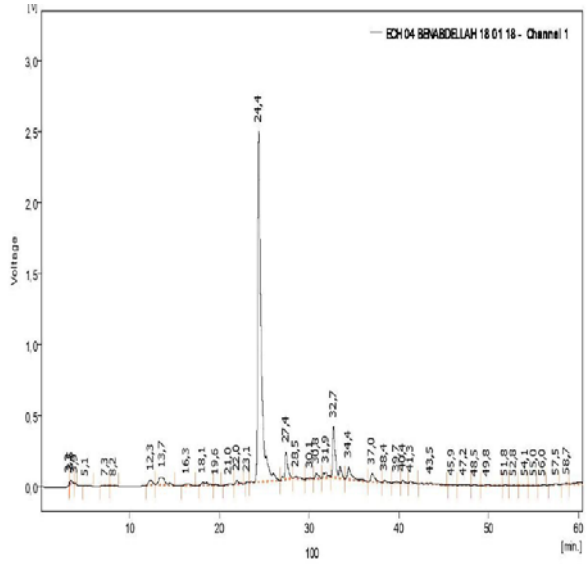

Figure 2. Chromatogram of methanolic extract of *T. algeriensis*

Table 1. Identified components by HPLC/UV in methanolic extract of *L. antineae* and *T. algeriensis*

Plant Composant	Retention time (min)	*L. antineae* (%)	*T. algeriensis* (%)
3-hydroxy-4-méthoxycinnamic acid	28.287	0.5	1.5
Ferulic acid	26.56	-	0.1
Gallic acid	6.543	0.1	-
Anisic acid	33.037	-	26.4
Salicylic acid	30.747	0.9	0.2
Syringic acid	21.967	0.7	1
Trans-2.3-diméthoxycinnamic acid	39.28	-	0.9
Trans-cinnamic acid	25.173	-	5.4
Vanillic acid	22.623	0.3	0.2
Catechin	21.553	0.7	0.5
Epicatechin	22.503	-	0.1
Euleropein	32.367	-	6.1
Kaempferol	41.103	0.4	1.5
Myricetin	34.27	3	0.2
Quercetin	36.85	1.7	17.3
Rutin	30.687	-	0.2

3.2. Results of the antioxidant activity

3.2.1. Result of DPPH radical scavenging test

An almost similar and more powerful antioxidant power than BHT was noted for *L. antineae* and *T. algeriensis*, their IC_{50} values were 18.59 ± 0.07 and 18.40 ± 0.42 µg/ml respectively (Table 02). The inhibition percentages took their maximum values at the 400 µg/ml concentrations: 90.26 ± 0.99 µg/ml for *T. algeriensis* and 88.54 ± 0.23 µg/ml for *L. antineae*.

3.2.2. Result of ABTS radical scavenging test

L. antineae presented inhibition percentage greater than 90% from the concentration of 50 µg/ml. Considerable values was recorded for the methnolic extract of *T. algeriensis* from the concentration of 50 µg/ml. *T. algeriensis* and *L. antineae* showed close IC_{50} values, 11.73 ± 0.20 and 10.77 ± 1.14 µg/ml, respectively (Table 03). Their antioxidant capacity was lower than that of BHT and BHA.

Table 2. Percentages of DPPH inhibition by *L. antineae* and *T. algeriensis* methanolic extracts, BHA, BHT and the corresponding IC_{50}

Plant/Standard	Inhibition %							
	6.25 µg/ml	12.5 µg/ml	25 µg/ml	50 µg/ml	100 µg/ml	200 µg/ml	400 µg/ml	IC_{50} µg/ml
L. antineae [a]	19.03±1.86	35.87±1.18	68.39±1.32	87.07±0.13	87.86±0.07	88.27±0.20	88.54±0.23	18.59±0.07
T. algeriensis [a]	22.23±2.58	35.50±1.70	66.92±3.39	87.71±0.11	88.42±0.47	89.66±0.17	90.26±0.99	18.40±0.42
BHA [a]	36.46±2.45	59.63±1.50	78.91±0.77	83.11±0.46	84.21±0.50	85.31±0.35	85.91±0.50	10.03±0.84
BHT [a]	18.55±2.46	32.60±3.72	53.80±2.58	74.97±2.14	83.41±0.86	84.59±0.46	85.76±0.91	23.54±1.83

Values indicated are means ± SD of three measurements $p \leq 0.05$. a: subset determined by the tukey test

Table 3. Percentages of ABTS inhibition by *L. antineae* and *T. algeriensis* methanolic extracts BHA, BHT and the corresponding IC_{50}.

Plant/Standard	Inhibition %							
	6.25 µg/ml	12.5 µg/ml	25 µg/ml	50 µg/ml	100 µg/ml	200 µg/ml	400 µg/ml	IC_{50} µg/ml
L. antineae [b]	29.73±3.63	60.38±3.78	88.44±0.69	92.01±0.20	92.70±0.10	92.81±0.10	92.87±0.20	10.77±1.14
T. algeriensis [ab]	29.96±0.75	55.20±0.85	84.93±1.25	92.01±0.26	92.58±0.35	92.93±0.17	92.98±0.10	11.73±0.20
BHA [b]	93.50±0.09	93.55±0.09	93.60±0.16	93.60±0.95	94.17±0.90	95.37±2.63	95.42±2.69	1.81±0.10
BHT [ab]	61.38±0.57	62.02±3.82	76.50±1.40	82.55±1.04	88.60±2.66	90.38±0.67	95.83±0.15	1.29±0.30

Values indicated are means ± SD of three measurements $p \leq 0.05$. a, b: subsets determined by the tukey test

3.2.3. Result of the FRAP test

In regard to *L. antineae* extract, from the 50 µg/ml concentration, the absorbance values were marked by a significant increase, up to the value of 1600 µg/ml where the absorbance approached the value of 3. This increase was greater than that produced by BHA and BHT (Figure 03 a).

From the concentration of 25 µg/ml, *T. algeriensis* had absorbance values considerably higher than the values obtained with BHA and BHT (Figure 03 b). A more interesting increase was detected from 400 µg/ml. The $PR_{0.5}$ of the two plants was determined at lower values than the values obtained with BHA and BHT (Table 04).

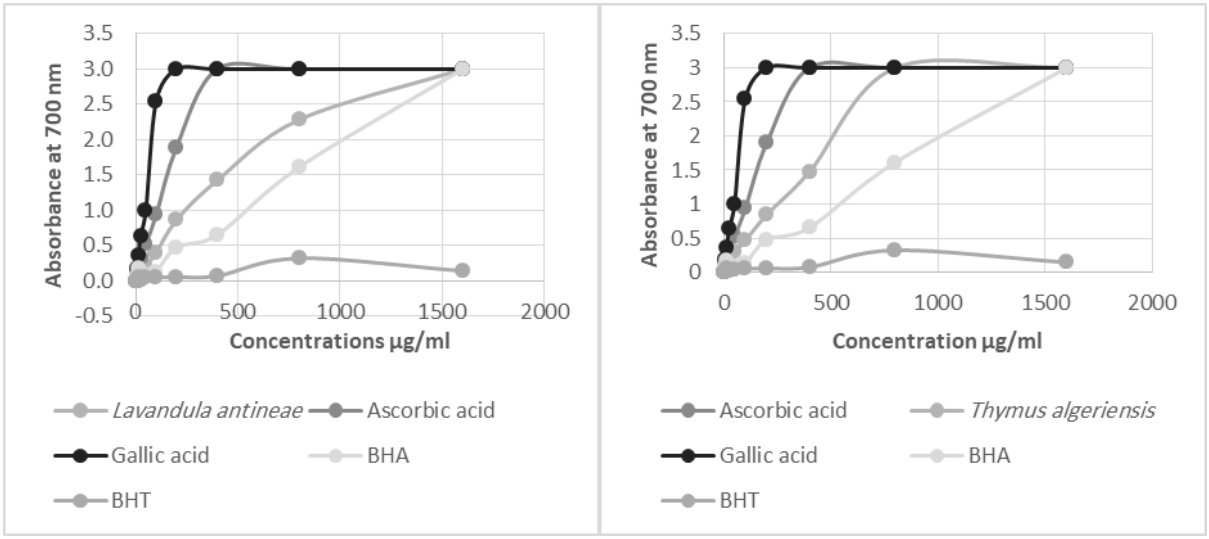

(a) (b)

Figure 3. Antioxidant activity of *L. antineae* methanolic extract (a) and *T. algeriensis* methanolic extract (b) obtained by FRAP test

Table 4. $PR_{0.5}$ obtained by FRAP test for *L. antineae*, *T. algeriensis*, BHA and BHT (µg/ml)

Plant/Standard	$PR_{0.5}$
L. antineae [ab]	155.733±0.196
T. algeriensis [ab]	147.44±0.191
BHA [a b]	464±0.007
BHT [a]	7566.66±0.0007

Values indicated are means ± SD of three measurements $p \leq 0.05$.
a: subset determined by the tukey test

3.2.4. Result of copper reduction test (CUPRAC)

The methanolic extract of *L. antineae* had a considerable reducing power (Figure 04 a), the absorbance values were marked by a strong increase with all the concentrations tested. By comparing it with BHA and BHT, the extract of *L. antineae* was less efficient than BHA, with an absorbance of 2.53 ± 0.19 at 100 µg/ml concentration and more effective than BHT. The $PR_{0.5}$ of the extract was determined to be 10.57± 0.3 µg/ml (Table 5).

The methanolic extract of *T. algeriensis* exhibited remarkable reducing power; its effect was more powerful than BHT at concentrations above 200 µg/ml. At concentrations over 400 µg/ml, the plant extract exhibited a performance close to that of BHA (Figure 04 b). The $PR_{0.5}$ of the studied extract was determined to be 25.04 ± 0.86 µg/ml (Table 05).

(a) (b)

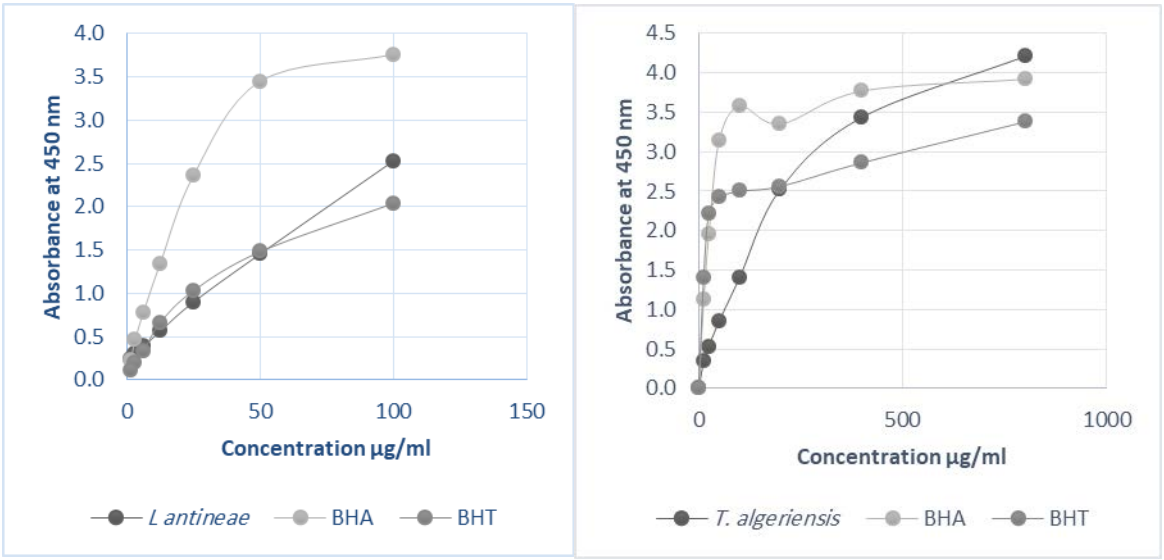

Figure 04 Antioxidant activity of *L. antineae* methanolic extract (a) and *T. algeriensis* methanolic extract (b) obtained by CUPRAC test

Table 5. $PR_{0.5}$ obtained by CURAC test for *L. antineae* and *T. algeriensis* methanolic extracts, BHA and BHT (µg/ml)

Plant/Standard	$PR_{0.5}$
L. antineae [ab]	10.57± 0.38
T. algeriensis [a]	25.04± 0.86
BHA [b]	3.64±0.19
BHT [ab]	9.62±0.87

Values indicated are means ± SD of three measurements $p \leq 0.05$. a, b: subsets determined by the tukey test

3.3. Result of the anti-enzymatic activity

3.3.1. Result of the anti-Alzheimer's activity

Anticholinesterase: An interesting anti-cholinesterase activity was provided by the methanolic extract of *T. algeriensis*. The increase in inhibition percentages was remarkably noted with the increase in concentrations (Figure 05 b). The percentage of inhibition exceeded 50% and the IC_{50} of the extract was deduced to a value of 154.47 ± 3.55 µg/ml at the concentration 200 µg/ml (Table 06). *L. antineae* showed an inhibitory effect on acetylcholinesterase which increased slowly by increasing concentrations (Figure 05 a). The inhibition percentages did not exceed the value of 20% until the concentration exceeded the value of 200 µg/ml. The IC_{50} have been estimated at values greater than 200 µg/ml (Table 6).

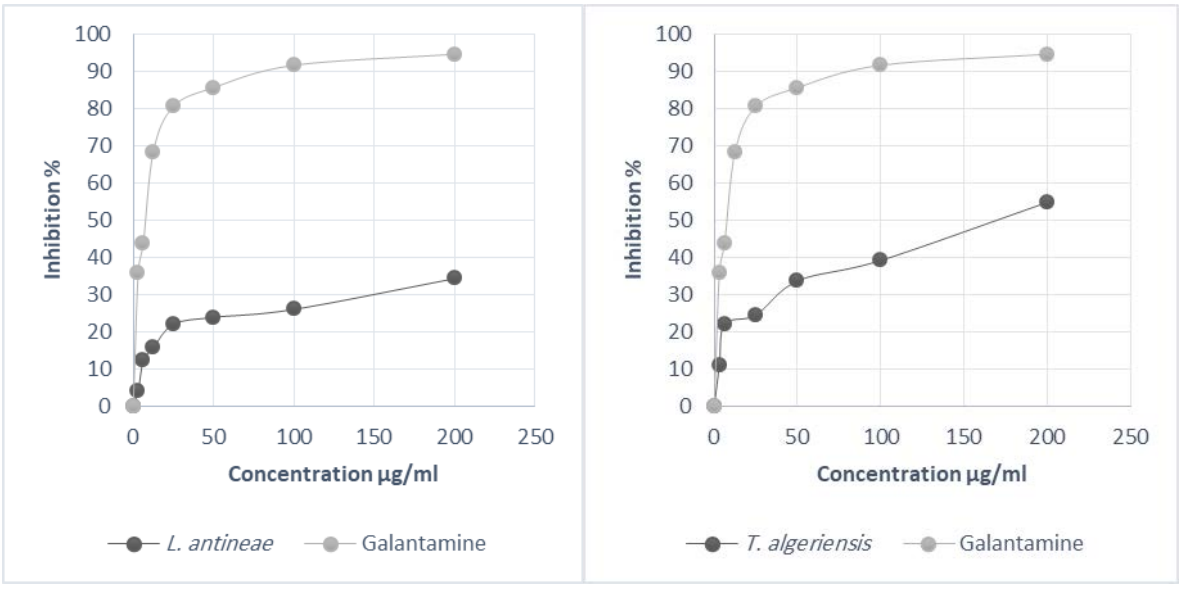

(a) (b)

Figure 05. Anticholinesterase activity of *L. antineae* methanolic extract of (a) and *T. algeriensis* methanolic extract (b)

Antibutyrylcholinesterase: A marked increase was recorded in the percentages of inhibition obtained with methanolic extract of *L. antineae*. Even at low concentrations (3.125, 6.25 and 12.25 µg/ml), this increase

was more considerable than the increase achieved by galantamine. In concentration value equal to100 µg/ml, A small variation was observed between the plant extract and the galantamine performances (Figure 06 a). The IC_{50} was determined to be 20.84 ± 9.74 µg/ml, while galantamine was denoted by an IC_{50} equal to 34.75 ± 1.99 µg/ml (Table 07), which may be translated by a promising effectiveness of the plant for the fight against Alzheimer's disease.

The methanolic extract of *T. algeriensis* was characterized by an interesting IC_{50} which equals the value of 161.53 ± 22.65 µg/ml (Table 07). The inhibition percentages increased proportionally with the concentrations. From 25 µg/ml concentration value, the difference in performance of the extract compared to the standard became significantly high (Figure 06 b).

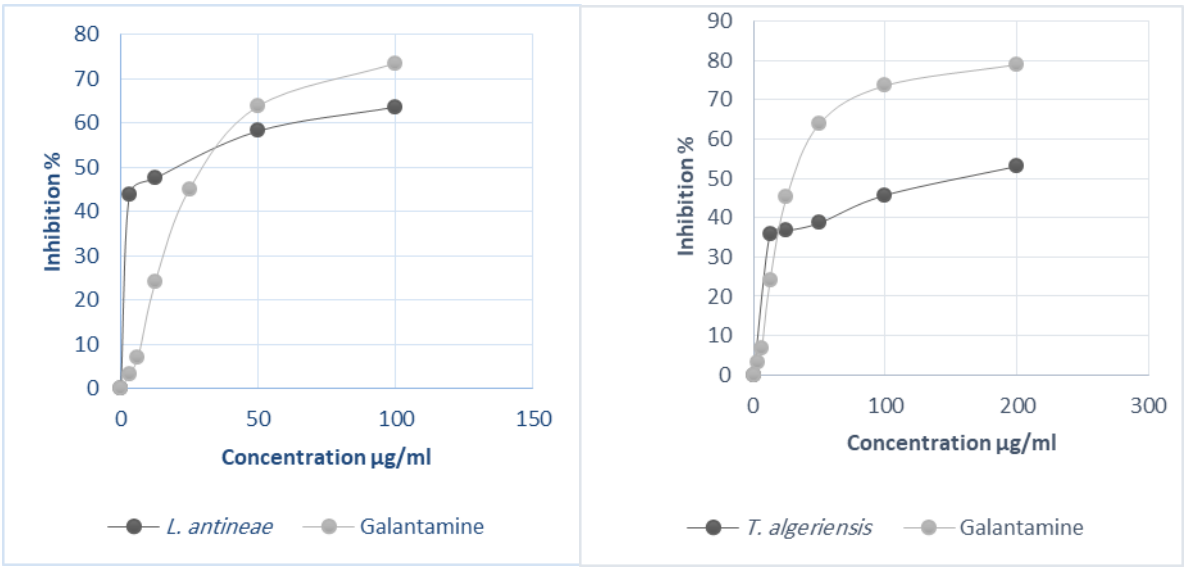

(a) (b)

Figure 6. Antibutyrylcholinesterase activity of *L. antineae* methanolic extract (a) and *T. algeriensis* methanolic extract (b)

Table 6. IC_{50} of anticholinesterase activity of *L. antineae*, *T. algeriensis*, and galantamine.

Plant/Standard	IC50 (µg/ml)
L. antineae [ab]	>200
T. algeriensis [b]	154.47±3.55
Galantamine [c]	6.27±1.15

Values indicated are means ± SD of three measurements $p \leq 0.05$.
a, b, c: subsets determined by the tukey test

Table 7. IC_{50} of ntibutyrylcholinesterase activity of *L. antineae*, *T. algeriensis* and galantamine

Plant/Standard	IC_{50} (µg/ml)
L. antineae [a]	20.84±9.74
T. algeriensis [a]	161.53±22.65
Galantamine [a]	34.75±1.99

Values indicated are means ± SD of three measurements $p \leq 0.05$.
a: subset determined by the tukey test

3.3.2. Result of the α-glucosidase inhibition test

The methanolic extract of *L. antineae* showed significant inhibitory activity against α-glucosidase enzyme; the IC_{50} was estimated at a value equal to 168. 61 ± 7.60 µg/ml (Table 08). Galantamine gave an IC_{50} value equal to 275.43 ± 1.59 µg/ml; therefore, *L. antineae* gave promising effect for the inhibition of one of enzymes involved in diabetes types 2 disease. The methanolic extract of *T. algeriensis* did not show any inhibitory effect on α-glucosidase for all the tested concentrations.

Table 8. Inhibition activity of α-glucosidase by methanolic extracts of *L. antineae*, *T. algeriensis* and acarbose

	Inhibiton %								
Plant/Standard	3.125 µg/ml	6.25µg/ml	12.5µg/ml	25µg/ml	50µg/ml	100µg/ml	200µg/ml	800µg/ml	IC_{50} (µg/ml)
L. antineae [a]	NT	NT	0.00±0.0	0.00±0.0	12.815±3.41	48.079±1.62	53899±2.21	63.702±0.0	168.61±7.60
T. algeriensis	No activity								
Acarbose a	78.125µg/ml	156. 5µg/ml	312.5µg/ml	625 µg/ml	1250 µg/ml	2500µg/ml	5000µg/ml	IC_{50} (µg/ml)	
	27.43±2.18	38.91±3.20	54.86±1.79	67.29±2.63	80.19±1.66	85.54±0.45	91.05±0.72	275.43±1.59	

NT: Not tested. Values expressed are means ± SD of three measurements $p \leq 0.05$. a: subset determined by the tukey test.

4. Discussion

The chemical composition of *L. antineae* extracts has not been studied before. The majority of research was carried out on other species of the same genus, notably *L. angustifolia*. Extracts from the latter were shown to be rich in caffeic acid, rosmarinic acid, and 4-hydroxybenzoic acid (Turgut *et al*., 2017); we did not mark their presence in our extract (Table 1). A study by Boutaoui *et al*. (2018) has demonstrated the presence of ferulic acid and catechin in the ethanolic extract of *T. algeriensis.* We have also found the same components but in few percentages (Table 01).

L. antineae extract has provided an antioxidant effect greater than *L. dentatae* (Bouzidi *et al*., 2018); the latest one was marked by IC_{50} values ranging from 0.33 to 1.84 mg/ml which were obtained by methanolic extracts from various plant parts. Most studies of antioxidant activity by the DPPH scavenging test, which are carried out on species of the genus *Lavandula*, are carried out on essential oils. Their results show a strong antioxidant activity (Mohammedi and Atik, 2012; Bettaieb Rebey *et al*., 2012; El Hamdaoui *et al*., 2018). By comparing the results of these studies and the result in our work, we can attribute to the methanolic extract of *L. antineae* a remarkable antioxidant capacity. Khled Khoudja *et al.* (2014) found an IC_{50} of the methanolic extract of *T. algeriensis* equal to 179 ± 0.012 µg/ml, a value significantly higher than that obtained in our results. In another study carried out on methanolic extract of the same plant, IC_{50} was estimated at a value of 7 ± 0.02 µg/ml (Megdiche-Ksouri *et al*., 2015). Our results do not agree with the results obtained by Guesmi *et al*. (2014) who found that BHT exerted a more powerful antioxidant activity than methanolic extract of *T. algeriensis*. This difference in anti-free radical power within the same species can be attributed to several factors. Several studies have shown that water addition at low rates to the solvent ameliorates the extraction of powerful antioxidants (Turkmen *et al*., 2006; Zhao and Zhao, 2013). Different origins of the same species can also influence antioxidant potential (Bettaieb Rebey *et al*., 2012).

In our study, the methanolic extract of *T. algeriensis* exhibited a greater AChE inhibitory effect than the effect which was given by the ethanolic extracts of six other species of *Thymus*, namely *T. longicaulis, T. serpyllum* subsp. *Serpyllum, T. pulegioides, T. striatus, T. praecox* subsp. *polytrichus* and *T. vulgaris* where the IC_{50} values took between 656.06 and 837.96 *µ*g/ml (Kindl *et al*., 2015). Our extract seems to be more effective than the leaves essential oils of the same plant which provided an IC_{50} value equal to 98.84 ± 1.81 µg/ml (Bendjabeur *et al*., 2018). A study by Bendjabeur *et al*. (2018), which was done to evaluate the inhibitory effect of *T. algeriensis* against butyrylcholinesterase, has found that essential oils extracted from the leaves provided a slightly lower IC_{50} value than our extract and which equal to124.09 ± 2.84 µg/ml. Even at a concentration equivalent to 1 mg/ml, ethanolic extracts of *L. angustifolia* and *L. pedunculata* established an inhibition of AChE less than the inhibition provided by *L. antineae*, with inhibition percentages equal to 28.4 ± 3.8 and 42.0 ± 16.8% (Ferreira *et al*., 2007). Plants can be regarded as good bioactive compound sources with an ability of inhibiting enzymes such as AChE and BChE (Murray *et al*., 2013). Many secondary metabolites as terpenes, quinones, alcaloids and phenols were shown very effective to inhibit α-glucosidase enzyme and can be clinically developed for treating diabetes type 2 (Yin *et al*., 2014).

5. Conclusion

HPLC/UV analysis revealed the common existence of quercetin, 3-hydroxy-4-methoxycinnamic acid, salicylic acid, syringic acid, Kaempferol and myricetin in the methanolic extract of the two plants. *L. antineae* presented an interesting antioxidant activity and a very promising inhibitory power of butyrylcholinesterase and α-glucosidase which is more effective than the standards used, hence the possibility of its use for the treatment of Alzheimer's disease and type 2 diabetes. *T. algeriensis* was also marked by an appreciable antioxidant activity and an ability to inhibit cholinesterase and butyrylcholinesterase. The potential involvement of natural antioxidants in the replacement of conventional treatments for several diseases, such as age-related diseases, could be significant and should be elucidated in long-term clinical trials.

Acknowledgements

The authors thank the MESRS (Ministry of Higher Education and Scientific Research of Algeria) for its partial funding.

Conflict Of Interest

The authors proclaim no conflict of interest.

References

Apak R, Guclu K, Ozyurek M and Karademir SE. 2004. Novel total antioxidant capacity index for dietary polyphenols and vitamins C and E, Using their cupric ion reducing capability in the presence ofneocuproine: CUPRAC Method. *J Agric Food Chem.*, **52**: 7970-7981.

Bendjabeur S, Benchabane O, Bensouici C, Hazzit M, Baaliouamer A and Bitam A. 2018. Antioxidant and anticholinesterase activity of essential oils and ethanol extracts of *Thymus algeriensis* and *Teucrium polium* from Algeria. *J Food Meas Charact.*, **12**: 2278-2288.

Bettaieb Rebey I, Bourgou S, Ben Slimen Debez I, Jabri Karoui I, Hamrouni Sellami I, Msaada K, Limam F and Marzouk B. 2012. Effects of Extraction Solvents and Provenances on Phenolic Contents and Antioxidant Activities of Cumin (*Cuminum cyminum* L.) Seeds. *Food Bioprocess Technol.*, **5** : 2827-2836.

Bougandoura N and Bendimerad N. 2013. Evaluation de l'activité antioxydante des extraits aqueux et méthanolique de *Satureja calamintha ssp.Nepeta* (L.) Briq. *NATEC.*, **09**: 14-19.

Boutaoui N, Zaiter L, Benayache F, Benayache S,,Carradori S, Cesa S, Giusti AM, Campestre C, Menghini L, Innosa D and Locatelli M. 2018.IQualitative and quantitative phytochemical analysis of different extracts from *Thymus algeriensis* aerial parts. *Molecules*, **23**: 1-11.

Bouzidi MA, Dif MM, Chihaoui G, Taïbi S and Toumi-benali F. 2018. First determination of polyphenols content, antioxidant activity and soil characterization of *Lavandula dentata* L. from Oran region. *PCBSJ.*, **12 (2)**: 117-124.

Ceylan Y, Usta K, Usta A, Maltas E and Yildiz S.2015. Evaluation of Antioxidant Activity, Phytochemicals and ESR Analysis of *Lavandula Stoechas*. *Acta Phys Pol A*., **128**: 483-487.

Delgado T, Marinero P, Asensio S, Manzanera MC, Asensio C, Herrero B, Pereira JA and Ramalhosa E. 2014. Antioxidant activity of twenty wild Spanish *Thymus mastichina* L. populations and its relation with their chemical composition. *LWT - Food Sci Technol.*, **57**: 412-418.

El Hamdaoui A, Msanda F, Boubaker H, Leach D, Bombarda I, Vanloot P, El Aouad N, Abbad A, Boudyach EH, Achemchem F, Elmoslih A, Ait Ben Aoumar A and El Mousadik A. 2018. Essential oil composition, antioxidant and antibacterial activities of wild and cultivated *Lavandula mairei Humbert*. *Biochem Syst Ecol*., **76**: 1-7.

Ellman GL, Courtney KD, Andres V, Featherstone RM. 1961. A new and rapid colorimetric determination of acteylcholinesterase activity. *Biochem Pharmacol.*, **7**: 88-95.

Falleh H, Ksouri R, Chaieb K, Karray Bouraoui N, Trabelsi N, Boulaaba M and Abdelly C. 2008. Phenolic composition of *Cynara cardunculus* L. organs, and their biological activities. *CR Biol.*, **331(5)** : 372-9.

Favier A. 2006. Stress oxydant et pathologies humaines. *Ann pharm fr.*, **64(6)**: 390-396.

Ferreira ICFR, Baptista P, Vilas-Boas M and Barros L. 2007. Free-radical scavenging capacity and reducing power of wild edible mushrooms from northeast Portugal: Individual cap and stipe activity. *Food Chem.*, **100**: 1511-1516.

Goatez P and Guédira K. 2012. **Phytothérapie anti-infectieuse**, Springer Science and Business Media, Paris.

Guesmi F, Ben Farhat M, Mejri M and Landoulsi A. 2014. *In-vitro* assessment of antioxidant and antimicrobial activities of methanol extracts and essential oil of *Thymus hirtus* sp. *algeriensis*. *Lipids Health Dis.*, **13**: 114.

Ichai C. Quintar H and Orban JC. 2011. **Désordres métaboliques et réanimation *: de la physiopathologie au traitement,*** Springer, France.

Khled khoudja N, Boulekbache-Makhlouf L and Madani K. 2014. Antioxidant capacity of crude extracts and their solvent fractions of selected Algerian Lamiaceae. *Ind Crop Prod.*, **52**:177-182.

Kindl M, Blazekovic B, Bucar F and Vladimir-Knezevic S. 2015. Antioxidant and Anticholinesterase Potential of Six *Thymus* Species. *Evid-Based Complementary Altern Med.*, 1-10.

Megdiche Ksouri W, Saada M, Soumaya B, Snoussi M, Zaouali Y and Ksouri R. 2015. Potential use of wild *Thymus algeriensis* and *Thymus capitatus* as source of antioxidant and antimicrobial agents. *J new sci*., **23 (4)** : 1046-1056.

Mohammedi Z and Atik F. 2012. Pouvoir antifongique et antioxydant de l'huile essentielle de *Lavandula stoechas* L. *NATEC.*, **06** : 34-39.

Mukherjee PK, Biswas R, Sharma A, Banerjee S, Biswas S and Katiyar CK. 2018. Validation of medicinal herbs for anti-tyrosinase potential. *J Herb Med.*, **14**: 1-16.

Murraya AP, Faraonia MB, Castroa MJ, Alza NP and Cavallaro V. 2013. Natural AChE Inhibitors from Plants and their Contribution to Alzheimer's disease Therapy. *Curr Neuropharmacol.*, **11**: 388-413.

Nikolic M, clija J G, Ferreira ICFR, Calhelha RC, Fernandes A, Markovi T, Giweli A andSoković M. 2014. Chemical composition, antimicrobial, antioxidant and antitumoractivity of *Thymus serpyllum* L., *Thymus algeriensis* Boiss. and Reut. and *Thymus vulgaris* L. essential oils. *Ind Crop Prod.*, **52**: 183-190.

Ozenda P. 2004. **Flore du Sahara**, CNRS, Paris.

Palanisamy UD, Ling LT, Manaharan T and Appleton D. 2011. Rapid isolation of geraniin from Nephelium lappaceum rind waste and its anti-hyperglycemic activity. *Food Chem*., **127**: 21-27.

Payan F. 2004. Structural basis for the inhibition of mammalian and insect α-amylases by plant protein inhibitors. *BBA-Proteins and Proteomics.*, **1696 (2)**: 171-180.

Pelletier E, Campbell PGC and Denizeau F. 2004. **Écotoxicologie Moléculaire: Principes Fondamentaux et Perspectives de Développement**, PUQ.

Re R, Pellegrini N, Proteggente A, Pannala A, Yang M and Rice-Evans C. 1998. Antioxidant activity applying an improved ABTS radical cation decolorization assay. *Free Radical Bio Med.*, **26 (9)**: 1231-1237.

Simonovic M, Simonovic BR, Ostojic S, Pezo L, Micic D, Nemanj Stanisavljevi and Pejin B. 2019. A contribution to the estimation of berry fruits quality. *Sci Hortic*., **258**: 1-6.

Subhashini N, Nagarajan G and Kavimani S. 2011. In vitro antioxidant and anticholinesterase activities of *Garcinia combolia*. *Int J Pharm.*, **3(3)**: 129-132.

Turgut AC, Emen FM, Canbay HSER, Demirdöğen ÇN, Kılıç D and Yeşilkaynak T. 2017. Chemical Characterization of *Lavandula angustifolia* Mill. as a Phytocosmetic Species and Investigation of its Antimicrobial Effect in Cosmetic Products. *JOTCSA.*, **4(1)**: 283-298.

Turkmen N, Sari F and Velioglu Y S. 2006. Effect of extraction solvents on concentration and antioxidant activity of black and black mate polyphenols determined by ferrous tartrate and Folin-Ciocalteu methods. *Food Chem.*, **99**: 838-841.

Yin Z, Zhang W, Feng F, Zhang Y and Kang W. 2014 α-Glucosidase inhibitors isolated from medicinal plants. *FSHW.*, **3**: 136–174

Zhao Y and Zhao B. 2013. Oxidative stress and the pathogenesis of Alzheimer's disease. Oxid *Med Cell Longev.*, 1-10.

Zuzarte M, Gonc alves MJ, Cavaleiro C, Canhoto J, Vale-Silva L, Silva MJ, Pinto E and Salgueiro L. 2011. Chemical composition and antifungal activity of the essential oils of *Lavandula viridis*. *J Med Microbiol.*, **60**: 612–618.

JJBS

Volume 14, Number 3, September 2021
ISSN 1995-6673
Pages 559 - 564

Jordan Journal of Biological Sciences

Employment of Somatic Embryogenesis as a Tool for Rescuing Imperiled *Narcissus tazetta* L. Growing Wild in Jordanian Environment.

Tamara M. Al-Zghoul[1], Rida A. Shibli[1,*], Tamara S. Qudah[2], Reham W. Tahtamouni[3], Nasab Rawshdeh[4]

[1]Department of Horticulture and Agronomy, Faculty of Agriculture, University of Jordan, Amman, Jordan,[2]Hamdi Mango Center for Scientific Research (HMCSR), University of Jordan, Amman, Jordan, [3] Department of Biotechnology, Faculty of Agricultural technology, Al Balqa- Applied University, Salt, Jordan.[4]National Center for Agricultural Research and Extension (NCARE).

Received: September 3, 2020; Revised: November 4, 2020; Accepted: November 24, 2020

Abstract

Somatic embryogenesis was used as a tool for micropropagation of wild *Narcissus tazetta* plants exposing to overcollection and rapidly changed environmental conditions. In the growth regulators experiment, somatic embryogenesis was successfully induced in all treatments except for explants grown in the control treatment (Murashig and Skoog (MS) hormone-free medium). Meanwhile, the highest value for the number of somatic embryos/ callus segment (441) was obtained into MS media supplemented with 0.2 mg l^{-1} 6-(gamma, gamma- Dimethylallylamino) purine (2iP) under dark conditions. Moreover, sucrose at 30g L^{-1} was the best sugar source resulting in higher number of somatic embryos compared to the other sugar treatments. The highest shoot development rate from somatic embryos was (191.99/ non-embryonic calli segment) recorded in cultures grown on MS media plus 0.5 mg l^{-1} 2iP. Maximum bulbet size (1.6 cm diameter) was recorded in plantlets kept onto hormone-free MS hormone free media for 6 weeks before acclimatization, while less durations resulted in smaller bulbet size. Well developed *in vitro* plantlets were acclimatized successfully with high survival percentage of (95%). The acclimatized plants were normal and did not show any morphological abnormalities.

Keywords: Callus, Embryogenesis, *Narcissus tazetta*, Somatic embryo.

1. Introduction

Narcissus tazetta is a wild ornamental plant that grows naturally in the hills and mountainous rocky grounds of Jordan. It is known by the local community as (Narjes Baladi). It has an important ornamental value due to its white-cream with orange crown flowers and its distinctive odor (Al-Eisawi, 1998). In addition, many wild plants in Jordan had been reported for their medicinal activities (Alenizi *et al*., 2020; Al Qudah, 2020; Tahtamouni *et al*., 2016). Also, *Narcissus tazetta* was reported recently in many research articles as a natural source of galantamine (GAL) which has been prescribed for treatment of Alzheimer's disease (Bores and Kosley, 1996; Khonakdari *et al*., 2020). Because of overexploitation through uprooting and continuous removal of the plants, natural habitat destruction, climate change, and increasing demands on this plant for both ornamental and medicinal values (Alenizi *et al*., 2020), the wild *N. tazetta* populations in Jordan are exposed to extinction (RBG, 2016). Propagation of this valuable genetic resource is imperative for its survival and continuity. Unfortunately, *N. tazetta* propagation through vegetative methods by chipping and twin scales is not efficient due to its slow propagation (Stone, 1973; Stone *et al*., 1977). Propagation of *N. tazetta* can help in conserving this valuable plant from extinction. In vitro development techniques including somatic embryogenesis are important and easy methods of vegetative multiplication, and they have the advantage of rapid multiplication (Shibli *et al*., 2012). High numbers of genetically uniform plants can be cultured from a single plant by using those techniques (Al Qudah *et al*., 2011; Shibli *et al*., 2018). Somatic embryogenesis is one of the basic tools widely used in plant biotechnology and *in vitro* development research. It is useful for micropropagation and production of transgenic plants, which can be used for producing fully transformed plants after mutagenesis or gene transfer (Mostafa *et al*. 2010). Somatic embryos can be produced in high frequencies, but maturation and plant development are still a difficult task, requiring optimization of medium and environmental conditions (Kumar *et al*., 2013; Shibli *et al*., 2012). In reviewing the literature, until now, there were no reports on the in vitro development via somatic embryogenesis of the valuable wild Jordanian *N. tazzeta* L. Thus, this study was carried out to develop a protocol for in vitro massive propagation via somatic embryogenesis and ex vitro acclimatization of *N. tazetta* L, hoping that this approach might contribute to its sustainability.

* Corresponding author e-mail: r.shibli@ju.edu.jo.

2. Materials and methods

2.1. Plant material

Bulbs of *Narcissus tazetta* L. were collected from Ajloun- Kufranja during December of 2014 (N 32.25006°, E 35,652336°) at 210 m above sea level (Fig. 1). The experiments were held at the plant biotechnology laboratories at Hamdi Mango Center/ Faculty of Agriculture, The University of Jordan, (Amman-Jordan).

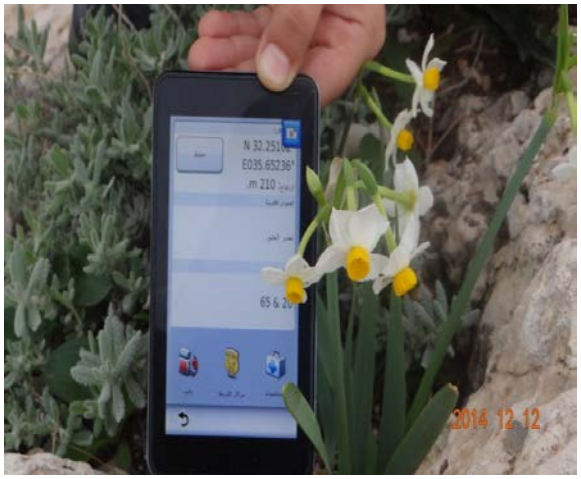

Figure 1. N. tazetta flowering plant in the wild at Ajloun-Kufranja during December, 2014 (N 32.25006°, E 35,652336°) at 210 m above sea level.

2.2. Callus and Embryos induction

To induce callus and embryos formation, sterilized segments of inner bulb scales of *Narcissus tazetta* were grown on (Murashig and Skoog, 1962) (MS) media premix (Duchefa Biochemiea: Murashige and Skoog media plus vitamins; Duchefa-Postbus 809,2003 RV Haarlem, Netherlands) supplemented with different concentrations (0.5, 1.0 or 2.0 mg/L) of 6-Benzylaminopurine (BAP) plus 0.1, 0.4, 1.0, 2.0 mg/L of 1-Naphthaleneacetic acid (NAA) or 2,4-Dichlorophenoxyacetic acid (2,4-D). Next, the inner bulb scales were transferred to the growth room which consisted of the following physical conditions (the growth room temperature was 24±1°C under a 16/8 (light/dark) and 45–50 µmol / m^2s irradiance or to full dark conditions) and maintained for five weeks. Data was taken for callus formation percentage in each treatment. Data showed that 1.0 mg l^{-1} of (BAP) with 2.0 mg l^{-1} (2,4-D) (Figure 2) was found to be the best formula for callus initiation (data is still under publication).

Next, different embryos induction media with different types and levels of growth regulators or carbon sources (sugars) were investigated. In the first experiment, different concentrations (0.0, 0.2, 0.5, 1.0, 1.5 or 2.0 mg/ L) of growth regulators; (2iP, BAP, or Kinetin (KIN) were used. In the second experiment, different sugar types (sucrose, glucose or fructose) and levels (0, 10, 30, 40, 50 g/L) were added to MS callus induction media which contained 1.0 mg l-1 of (BAP) plus 2.0 mg l-1 (2,4-D). Each treatment in both experiments was replicated five (Petri dishes), each with 4 callus segments (250 mg). Cultures were maintained in dark undergrowth room conditions where growth room temperature was 24 ± 1°C while petri dish relative humidity was 90%.

Data were collected after one month for callus fresh weight and number of embryos produced per each callus segment and number of regenerated shoots per non-each embryonic calli segment.

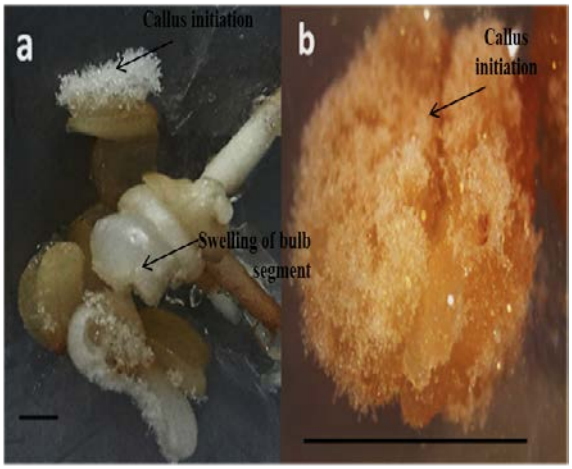

Figure 2. a) Start of callus initiation and swelling of *N. tazetta* explants cultured on MS media supplemented with 1.0 mg/L BAP and 2.0 2,4-D, and maintained under dark for 5 weeks. b) Callus initiation of *N. tazetta* explants cultured on MS media supplemented with 1.0 mg/L BAP and 2.0 2,4-D, and maintained under dark for 7 weeks. Scale bar = 1.0 cm.

2.3. Shoot development from embryos

Shoot development from the obtained embryos was experimented using MS media supplemented with (0.0, 0.2, 0.5, 1.0, 1.5, 2.0 mg l-1) of different growth regulators; (2iP, BAP, or KIN) plus 30 g sucrose. However, to induce shoot development, cultures were transferred from dark into a daily regime of 24±1°C under a 16/8 (light/dark) photoperiod of 45–50 µmol/ m2s irradiance. Numbers of regenerated shoots per segment of callus were recorded, and the percentage of germinated embryos was calculated. The regenerated shoots were subcultured into MS hormone-free media in 250 ml Erlenmeyer flasks. After rooting, developed plants were ready for acclimatization.

2.4. Acclimatization

Before acclimatization, *in vitro* produced planlets were maintained in MS hormone-free media for (2, 4 and 6 weeks) to increase bublet size before being transferred to greenhouse conditions, as increasing bublet size would increase survival chances for the plantlets during acclimatization *Ex vitro* acclimatization was performed for plantlets with well-developed roots. The plantlets were taken out form the flasks then the agar was washed away from the roots under running tap water, then the plantlets were cultured into sterilized plastic cups (5×5 cm) containing sterilized growing medium (peat: perlite mixture). Each cup was irrigated with distilled water every 3 days for 6 weeks. The potted plantlets were initially maintained inside the culture room conditions for 6 weeks and later transferred to green house (33 ±1°C) conditions for 8 weeks, and data were recorded for survival rate.

All conducted treatments were arranged in a completely randomized design (CRD). Data were statistically analyzed using SPSS, and analysis of variance (ANOVA) was used to analyze the obtained results; means

were separated with a probability level of 0.05 according to Tukey's honestly significant difference (HSD) test.

3. Result and discussion

3.1. Effect of plant growth regulators on somatic embryos

Embryo induction was observed after three weeks of inoculation of *N. tazetta* calli under concentrations of BAP and 2iP, while it took four weeks for embryos to appear in callus grown in KIN enriched media, while calli grown in the control treatment turned into brown and died. Using 2iP at 0.2 mg.l^{-1} was significantly the most effective treatment as it resulted in the highest values of callus weight (1818.25 mg), the number of somatic embryos (441.03/callus segment) and the number of regenerated shoots per non-embryonic calli (6.5) (Table 1, Figure 3). Meanwhile, high concentrations of 2iP had affected adversely callus growth, number of somatic embryos and regenerated shoots. Using 2iP for embryogenesis was reported in another study about *Iris nigricans* micropropagation, where embryos were successfully obtained in a medium supplemented with 1.0 mg l^{-1} 2iP as it yielded 2,686 embryos/g callus (Shibli and Ajlouni 2000). Similarly, Duquenne *et al*. (2006) in his study about "Zantedeschia hybrids reported that somatic embryos were regenerated into plantlets when cultured on MS medium supplemented with 1.0 mg l^{-1} 2iP. Meanwhile, our data showed that (KIN) at all used levels gave the least numbers of somatic embryos compared to the other plant growth regulators tested (Table 1). This result agrees with Shibli *et al.*, (2012), who found that KIN was the least effective cytokinin for the production of embryogenic callus of *Arum palaseitinum.*

Table 1: Effect plant growth regulators type and level on embryonic callus weight, the approximate number of somatic embryos/ callus segment and the number of regenerated shoots per non-embryonic calli of *N. tazetta* cultured on MS media in dark at growth room conditions for 4 weeks.

Growth regulator (mg/L)	Embryonic callus weight (mg)	Approximate number of somatic embryos/callus segment	Number of regenerated shoots/ nonembryonic calli segment
BAP			
C^{x}	0.0 d ^{z}	0.0 d	0.0 a
0.2	1010 ab	262.6 ab	1.2 a
0.5	1256 a	326.56 a	1.8 a
1.0	710 c	184.6 c	0.8 a
1.5	730 bc	189.8 bc	1.4 a
2.0	546 c	141.96 c	1.8 a
2iP			
C^{x}	0.0 d^{z}	0.0 d	0.0 c
0.2	1818.25 a	441.03 a	6.5 a
0.5	1195.8 b	298.95 b	4.4 b
1.0	1201.60 b	300.4 b	1.6 c
1.5	952.50 bc	238.125 bc	1.33 c
2.0	669.4 c	167.35 c	1.0 c
KIN			
C^{x}	0.0 c^{z}	0.0 c	0.0 b
0.2	558.75 b	55.875 b	0.0 b
0.5	754 ab	82.94 ab	2.4 ab
1.0	670 ab	87.10 ab	0.4 b
1.5	825 ab	90.75 a	3.4 a
2.0	900 a	99.0 a	1.6 ab

^{x} Control treatment represents hormone-free MS media. Each plant growth regulator was analyzed separately.^{z} Means within columns having different letters are significantly different according to Tukey HSD at P≤0.05.

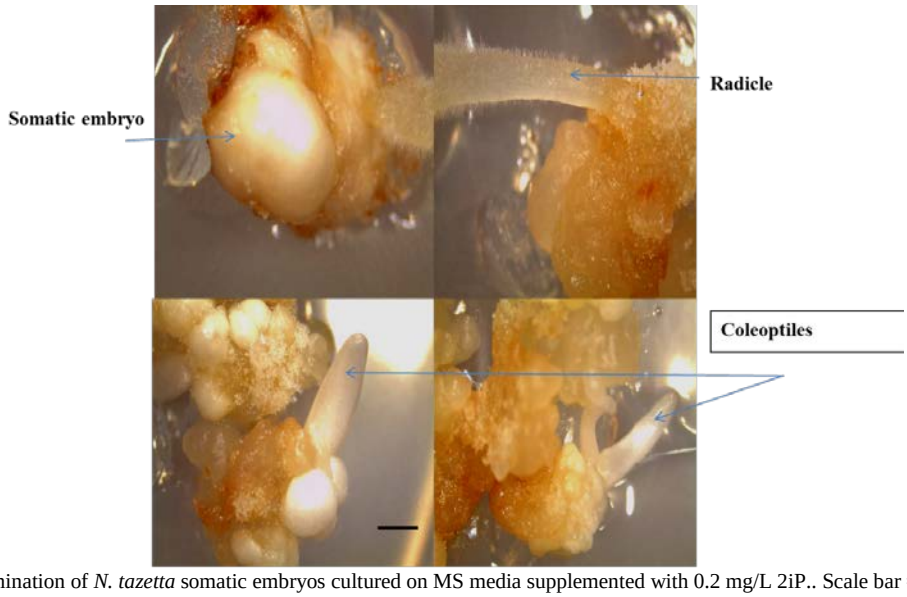

Figure 3. Germination of *N. tazetta* somatic embryos cultured on MS media supplemented with 0.2 mg/L 2iP.. Scale bar = 0.50 cm.

3.2. The effect of different carbon sources on somatic embryos

Our data revealed that sucrose at the level of 3% w/v was the best carbon source for N. *tazetta* when compared to fructose and glucose (Table 2). Meanwhile, 4% sucrose resulted in direct development of small bulblets and was not efficient for embryogenesis. On the other hand, glucose and fructose were not effective as a carbon source for embryos expression most callus formed became black with time and died (Table, 2). Sucrose was reported as the

best as a carbon source for micropropagation in many plant species, as it is the most popular carbohydrate in the plant phloem (Murashige & Skoog, 1962; Ahmad *et al*., 2007; Tahtamouni *et al*., 2016). Furthermore, in a study about strawberry, 6% sucrose was found superior not only for giving optimum embryo induction of embryonic culture but also a uniform embryo developmental stages compared to the other tested sugars (glucose and fructose), (Gerdakaneh *et al*., 2009).

Table 2. Effect of carbon sources and levels on embryonic callus weight, number of somatic embryos, and number of regenerated shoots from non-embryonic calli of *N. tazetta* calli cultured on MS media supplemented with 0.2 mg l^{-1} 2iP in dark at growth room conditions for 4 weeks.

Carbon source (g/L)	Embryonic callus weight (mg)	Approximate number of somatic embryos/callus segment	Number of regenerated shoots/ non-embryonic calli segment
Sucrose			
C[x]	0.0* c[z]	0.0 c	0.0 c
10	558.00 b	14.2 bc	3.20 ab
30	1818.25 a	441.03 a	6.5 a
40	520 b	39.8 b	4.4 a
50	520 b	16.7 bc	1.4 ab
Fructose			
C[x]	0.0 b[z]	0.0 b	0.0 a
10	483 a	7.7 a	0.4 a
30	446 a	0.0 b	0.0 a
40	465 a	0.0 b	0.0 a
50	473.6 a	0.0 b	0.0 a
Glucose			
C[x]	0.0 c[z]	0.0 b	0.0 a
10	289 b	0.0 b	0.2 a
30	381 b	13.5 a	0.8 a
40	625 a	2.2 b	0.0 a
50	289 b	0.8 b	0.0 a

[x] Control treatment represents sugar free MS media + 0.2 mg l^{-1} 2iP. Each sugar type was analyzed separately. [z] Means within columns having different letters are significantly different according to Tukey HSD at P≤0.05.

3.3. Shoot developmentdevelopment from embryos

The embryos started to germinate and developed into plantlets with shoots and roots after the subculture of embryonic callus into light conditions(Figure 4). Table 3 showed that 2iP at 0.5 mg.l^{-1} gave significantly the highest number of germinated shoots (191.99) and germination percentage (45.76 %) over the other concentrations or other plant growth regulators, while in BAP treatments, the highest number of germinated shoots (42.28) and germination percentage (16.3%) were obtained on MS media supplemented with 0.2 mg l^{-1}. Our data agree with, Lokhande *et al.* (2010) fiding on *Sesuvium portulacastrum* as the highest number of shoots, average shoot elongation, and percent shoot development per explant were observed on MS medium supplemented with 8.0 mg l^{-1} 2iP followed by 4.50 mg l^{-1} BAP. Moreover, *Zantedeschia* hybrids somatic embryos developed into plantlets on basal media supplemented with 1.0 mg l^{-1} 2iP (Duquenne *et al.*, 2006). On the other hand, Shibli *et al.*, (2012) reported that the highest number of regenerated shoots from somatic embryos of *A. palaestinum* was achieved on MS media supplemented with 2.0 mg l^{-1} BAP

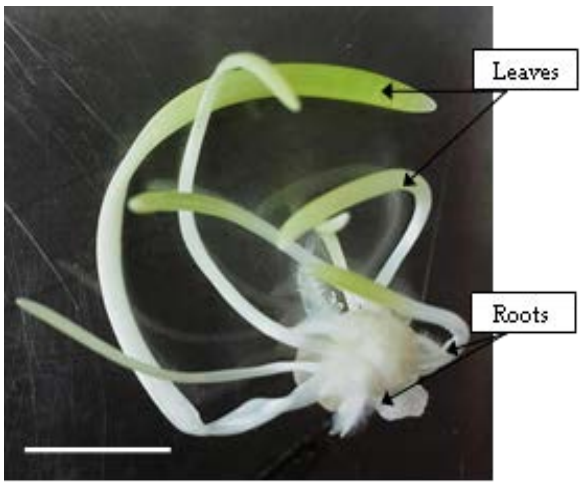

Figure 4. Regenerated *N. tazetta* plantlet from somatic embryos cultured on MS media supplemented with 0.5 mg/L of 2iP, and maintained under growth room conditions of 24±1°C under a 16/8 (light/dark) photoperiod of 45–50 µmol/ m2s irradiance and flask relative humidity of 90% for 4 weeks. Scale bar = 1.0 cm.

Table 3: Effect of plant growth regulators type and level on the number of germinated shoots from somatic embryos and germination percentage of *N. tazetta* somatic embryos cultured on MS media for 4 weeks.

Growth regulator (mg/L)	Number of germinated shoots from somatic embryos	Germination percentage of somatic embryos % (Number of germinated shoots/number of somatic embryos %)
BAP		
C[x]	0.0 c	0.0 d
0.2	42.28 a	16.3 a
0.5	16.02 b	4.95 b
1.0	5.28 c	2.76 bcd
1.5	3.56 c	1.84 cd
2	5.11 c	3.36 bc
2iP		
C[x]	0.0 c	0.0 d
0.2	78.95 b	29.44 b
0.5	191.99 a	45.76 a
1.0	51.24 b	16.32 c
1.5	11.95 c	5.12 d
2	5.30 c	3.20 d
KIN		
C[x]	0.0 c	0.0 c
0.2	0.0 c	0.0 c
0.5	10.90a	9.532ab
1.0	3.72 ab	3.70 bc
1.5	13.08 a	12.00 a
2	5.08 ab	5.08 abc

[x] Control represents free hormone MS media supplemented with 30 g/L sucrose. Each plant growth regulator was analyzed separately. [z]Means within columns having different letters are significantly different according to Tukey HSD at P≤0.05.

3.4 Ex Vitro Acclimatization

Our results showed that the period of incubating the plantlets on hormone-free MS media plus 30 g sucrose before acclimatization had positively affected bulb size measured after 5 weeks in the greenhouse conditions. Most plantlents incubated for 2 weeks in hormone-free MS media produced bulblets with approximately 0.5 - 0.6 cm in diameter and produced only a single leaf, while those inculcated for 4 weeks produced bulblets with 0.9 - 1.1 cm in diameter and 2 leaves. On the other hand plantlets inoculated for 6weeks produced bulblets with 1.4 - 1.6 cm in diameter and 3 leaves (Figure 5).

Meanwhile, most *in vitro* produced plants of *N. tazetta* L. showed excellent survival rate of 95% in growth room and 100% in the greenhouse. The acclimatized plants were normal and did not show any morphological abnormalities (Figure 6).

Figure 5. a) Bulblet of *N. tazetta* inculcated for 2 weeks on hormone-free MS media with approximately 0.5 cm diameter and single leaf. b) Bulblet of *N. tazetta* inculcated for 4 weeks on hormone-free MS media with approximately 1.0 cm diameter and two leaves. c) Bulblet of *N. tazetta* plant inculcated for 6 weeks on hormone-free MS media with approximately 1.6 cm diameter and three leaves. Scale bar = 1.0 cm.

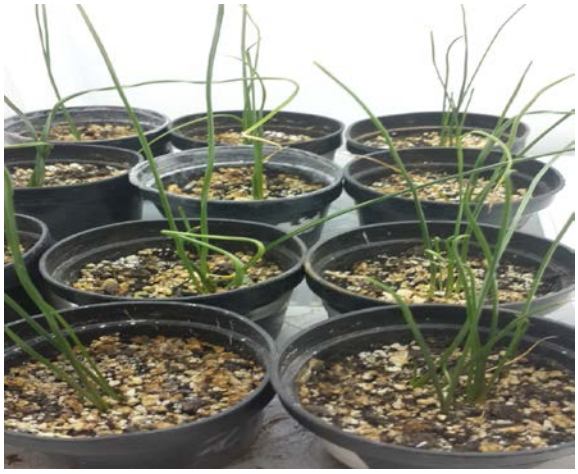

Figure 6. Successful acclimatization of *N. tazetta* plants maintained for 5 weeks on 1:1 peat perlite medium under greenhouse conditions and irrigated with tap water every 3 days with a 95% survival rate.

4. Conclusion

The current protocol could represent a successful tool for rapid micropropagation of *N. tazetta* via somatic embryogenesis using MS media + 0.2 mg/L2iP + 30 g sucrose. Meanwhile, adding 0.5 mg/L 2iP + 30 g sucrose to the culture media was required for maximum shoot development from the resulting embryos. This protocol could be applied commercially to produce a high number of plants with high survival rates. Further studies can be done to produce flowering size bulbs that can flower in the current or next season. Also, more research can be conducted to induce production of medicinally important secondary metabolites including galantamine (GAL) in *N. tazetta* plant cells *in vitro*.

5. References

Ahmad T., Abbasi, N. A., Hafiz, I. A. and Ali, A. 2007. Comparison of sucrose and sorbitol as main carbon energy sources in micropropagation of peach rootstock GF-677. Pakistan Journal of Botany, **39(4)**: 1269–1275.

Al-Eisawi, D. M. 1998. Field guide to wild flower of Jordan and neighboring countries. Al-Rai, Amman, 296.

Alenizi A., Shibli R., Tahtamouni R., Al-Qudah T. S. 2020. *In Vitro* Propagation and Enhancement of Quercetins and Isorhamnetin Production in Wild *Paronychia argentea* L. *Jordan Journal Pharmaceutical Sciences*, **13(1)**: 65-75

Al-Qudah, T.S.; (2020). Discovering antimicrobial powers of some herbs used by Bedouin in the Jordanian Petra. Eco. Env. & Cons., **26 (1).** 433-440.

Al-Qudah T. S, R.A. Shibli, and F. Q. Alali. 2011. In vitro propagation and secondary metabolites production in wild germander (*Teucrium polium* L.). In Vitro Cellular and Developmental Biology – Plant. **47**: 496-505.

Bores, G., Kosley, R. 1996. Galanthamine derivatives for the treatment of Alzheimer's disease. *Drugs Future*, **21(6)**:621–635).

Duquenne, B., Eeckhaut, T., Werbrouck, S., Van Huylenbroeck, J. 2006. *In vitro* somatic embryogenesis and plant development in Zantedeschia hybrids. *Plant Cell, Tissue and Organ Culture*, **87 (3)**: 329-331.

Gerdakaneh, M., Mozafari, A. A., Khalighi, A. 2009. The Effects of Carbohydrate Source and Concentration on Somatic Embryogenesis of Strawberry (*Fragaria x ananassa Duch*.). *American-Eurasian Journal of Agricultural & Environmental Sciences*, **6(1)**: 76–80.

Khonakdari, M. R.; Rezadoost, H. Heydari, R.,Mirjalili, M. H. 2020. Effect of photoperiod and plant growth regulators on in vitro mass bulblet proliferation of *Narcissus tazzeta* L. (*Amaryllidaceae*), a potential source of galantamine. *Plant Cell, Tissue and Organ Culture*, **142**:187–199.

Kumar, M., Singh, H., Shukla, A. K., Verma, P. C., Singh, P. K. 2013. Induction and establishment of somatic embryogenesis in elite Indian cotton cultivar (*Gossypium hirsutum* L. cv Khandwa-2). *Plant Signaling and Behavior*, **8(10)**: 1-10.

Lokhande, V. H., Nikam, T. D., Ghane, S. G., Suprasanna, P. 2010. *In vitro* culture, plant regeneration and clonal behaviour of *Sesuvium portulacastrum* (L.) a prospective halophyte. *Physiology and Molecular Biology of Plants*, **16(2)**: 187–193.

Mostafa, S. E. Karam, N. S. Shibli, R. A. Alali, F.Q. 2010. Micropropagation and production of arbutin in oriental strawberry tree (*Arbutus andrachne* L.). *Plant Cell, Tissue and Organ Culture*, **103**:111–121.

Murashige, T., Skoog, F. 1962. A revised medium for rapid growth and bio assays with tobacco tissue cultures. *Physiologia Plantarum*, **15(3)**: 473–497.

RBG. Royal botanic garden. 2016. Jordanian habitats and flora. http://royalbotanicgarden.org/plants/narcissus-tazetta.

Shibli, R. A., and Ajlouni, M. M. 2000. Somatic embryogenesis in the endemic black iris. *Plant Cell, Tissue and Organ Culture*, **61(1)**: 15–21.

Shibli, R. A., Duwayri, M., Sawwan, J., Shatnawi, M., Al-Qudah, T. S. 2012. Regeneration via somatic embryogenesis of the endangered wild arum (*Arum palaestinum*). *In vitro Cell. Dev. Biol.-Plant*. **48**: 335-340.

Shibli, R. A., Sharaf, S. A., Kasrawi, M. A., and Al-Qudah, T. S. 2018. *In Vitro* Multiplication of the White Wormwood, Artemisia herba-alba asso. *Jordan Journal of Biological Sciences*, **11(3)**: 265 271.

Stone, O. M. 1973. The elimination of viruses from Narcissus tazetta cv. Grand Soleil d'Or, and rapid multiplication of virus-free clones. *Annals of Applied Biology*, **73(1)**: 45–52.

Stone, O. M., Brunt, A. A., and Hollings, M. 1977. Methods, logistics and problems in the production, distribution and use of virus-free clones of *Narcissus tazetta* cv. Grand Soleil d'Or. *Ann. Rep. Glasshouse Crops Res. Inst*.

Tahtamouni, R., Shibli, R., Al-Abdallat, A.,Al-Qudah, T. 2016. Analysis of growth, oil yield, and carvacrol in Thymbra spicata L. after slow-growth conservation. *Turkish Journal of Agriculture and Forestry*, **40(2)**: 213-221

JJBS

Volume 14, Number 3, September 2021
ISSN 1995-6673
Pages 565 - 570

Jordan Journal of Biological Sciences

Regulation of Leaves Senescence by Virus-Induced Gene Silencing (VIGS) Modus Operandi in Arabidopsis

Allah Jurio Khaskheli[1,2,*], Muhammad Ibrahim Khaskheli[3], Muharam Ali[2], Li Zhang[1], Asad Ali Khaskheli[4] Hai Qing Liu[1], Muhammad Azeem Khaskheli[5], Syad Zakir Hussain Shah[2]

[1]Institute of Cell Biology, School of Life Sciences, Lanzhou University, Cheng Guan, Lanzhou-730000, Gansu, P.R. China;[2]Department of Biotechnology, Faculty of Crop Production, Sindh Agriculture University, Tandojam-70060, Pakistan;[3]Department of Plant Protection, Faculty of Crop Protection, Sindh Agriculture University Tandojam- 70060, Pakistan;[4]Department of Animal Nutrition, Shaheed Benazir Bhutto University of Veterinary & Animal Sciences, Sakrand, Pakistan;[5]Department of Plant Pathology, Sindh Agriculture University Tandojam- 70060, Pakistan

Received: October 27, 2020; Revised: December 3, 2020; Accepted: December 5, 2020

Abstract

The final leaf developmental stage starts with nutrients salvage and ends at cells' death, whereby leaf yellowing is the first noticeable event during senescence. Yellowing of leaves starts at the margins and progresses to the interior of the leaves' blade. In this regard, there are only a few factors that are being demonstrated in involving the regulation of cell death by evaluating the leaf senescence appearances of knocking of mutants and identifying downstream target genes. Thus, the current research aimed to evaluate the efficiency of Virus-Induced Gene Silencing (VIGS) and its functional analysis for a potential regulation of leaves senescence in Arabidopsis. In the present study, the silencing of the plant by *VIGS* technique caused a narrative phenotype with a high level of transcript levels. Nevertheless, the phenotype is exemplified with a smaller size compared to the wild type (WT) with smaller roots, leaves, and overall plant bodies. Interestingly, the *vector (VG)-silenced* plants showed intense yellowing of leaves developed at the bottom regions along with a smaller number of tillers from the base of the plants. Moreover, we also tested leaves of age-dependent silenced Arabidopsis plants and observed a reduction in size and number of leaf cells compared to that of non-silenced (WT) control plants. To understand the advanced regulatory molecular mechanisms, the efficiency of vector infection has been confirmed through changes that happened via the measurement of ion seepage and decreasing content of chlorophyll, measurement of SAG12, and PAGs gene expressions. In conclusion, *VIGS* approach play a critical role in leaves senescence.

Keywords: Arabidopsis, Chlorophyll, Senescence, Silencing, VIGS.

1. Introduction

Aging is a complex and highly regulated process involving the decay mechanism of photosynthesis, cessation of chloroplasts, and the degradation of biomolecules such as proteins, nucleic acids, and lipids (Al-Shomali *et al*., 2017). The first visible event during aging so far is that the leaves turn yellow (Quirino *et al*., 2000). The leaf senescence is a comprehensive response of leaf cells. It provides information about plant age, internal, and environmental indicators. Integrating the internal and external plant environment in given ecological zone help the plant in adapting aging process (Odiyi and Eniola, 2015).

There are various abiotic and biotic factors influencing the leaf senescence (Lim *et al*., 2007). However, knocking out genes is also important in the aging of any plant organ, such as fruits, flowers, and leaves (Chen *et al*., 2002; Guo *et al*., 2004). Therefore, in this study, we hypothesized and planned to observe the role of (*VIGS-vectors*) activity in the senescence of leaves. Given to that, Programmed Cells Death is a positively active process involving the distinct expression of thousands of genes (Hee *et al*., 2010). Through genome-wide analysis of gene expression changes, several Arabidopsis genes encoding transcription factors can be identified (Harb *et al*., 2020). However, only a few factors are being demonstrated in involving the regulation of cell death by evaluating the leaf senescence appearances of knocking of mutants and by identifying downstream target genes (Balazadeh *et al*., 2008; Buchanan-Wollaston *et al*., 2005; Lin and Wu, 2004). In the present study, we focused on the manifold roles of *VG vector* relationships in regulating the cells' death of plants. Nevertheless, the transcriptional factors family gene regulates cell death by different hormonal stress, environmental strain, and their role in retrograde signaling (Ryu *et al*., 2004). This emergent complexity needs to be discussed first to explore the commercialization of plants and understand the controlled molecular mechanism involved in it. Detailed studies of SAGs identities and its expression indicate that regulation of leaf senescence is a complex process (Orzaez *et al*., 2006); however, in the Arabidopsis, the age of even a single leaf plays an

* Corresponding author e-mail: aajkhaskheli2012@gmail.com.

important role in discovering leaf durability (Liu *et al*., 2004; Lu *et al*., 2003).

In the present study, we investigated the VIGS method in Arabidopsis, which relates to leaf senescence. Further, we hypothesized that vectors (VG) either function only in plant leaves or in other organs and plant growth behaviors. Therefore, we assumed that the vector (VG) could be tested in the leaf senescence method compared to other organs of the Arabidopsis plant. Also, we have evaluated various aspects of the vector (VG) promoting leaf senescence and demonstrated that vector (VG) continues to promote leaf senescence.

2. Materials and methods

2.1. Plant materials and growth circumstance

The seeds of the Arabidopsis plant were sterilized first with 10% of Sodium Hypochlorite solution by proper shaking approximately for 20-30min. After that, under the Laminar Air Flow Cabinet, seeds were rinsed with sterilized distilled water about 8-10 times. Then seeds were grown on MS-basal medium under 4°C for 2-3 days and kept for two weeks at 25°C. Seedlings were then transferred to soil media and infiltrated with vector solutions. The phenotypic observations have been made at two days interval of treatment (Guo *et al*., 2004).

2.2. Vector construction and transformation

Vector was constructed in advance. The two weeks old seedlings of wild type Arabidopsis were infected with *vector (VG)* and *vector (C)* using vacuum infiltration method. Following infection, the seedlings were grown in soil media. After two weeks, seedlings were transferred to soil media. The samples were collected for DNA isolation to confirm the efficiency of vector transformation (Tanaka and Makino, 2009).

2.3. Phenotypic examination yellowish discoloration

Regular examinations were made every two days to characteristically check the yellowing of the leaves. However, in experiments with Arabidopsis mutant studies, leaf yellowing may have started at the tip, petiole side, and mid of the leaf (Hee *et al*., 2010).

2.4. Ion leakage measurement

The infected plants were collected at every week's interval after infiltrations. Collected leaves were boiled into hot water and then suspended solution was checked through the instruments. Further, the infected leaves of plants were then suspended into measuring solution and observed the ion leakage measurement by leakage activity through instruments as recommended by (Ryu *et al*., 2004).

2.5. Measurement of chlorophyll content

For measuring the leaves' senescence activity, measurement of chlorophyll content is very important. The content of chlorophyll was measured according to the method recommended by (Lu *et al*., 2003). The fresh plants materials were routed and chopped to small pieces. 0.5 g sample was measured through an analytical weight balance. The material was standardized by adding 100ml of 80% acetone. The mixture was homogenized, and the extract was separated. The extract was examined on the spectrophotometer for chlorophyll content.

2.6. Extraction of total DNA and Polymerase Chain Reaction

Arabidopsis affected leaves were subjected to total DNA extraction. Solution 2 X CTAB (10 ml) was preheated in a water bath at a temperature of 65-70°C. 5g of leaves was frozen in liquid nitrogen and, thereafter, the pulverized powder was transferred to a pre-heated solution (50 ml). The test tube containing 10 ml of the 2XCTAB solution was centrifuged. Besides, CIA liquid was added, incubated at 37 °C and shacked at 120 rpm for 20 minutes. Slowly, precipitation buffer was added and shacked gently for 15-20 times until the DNA completely precipitated. Pre-cooled ethanol (-20°C) was transferred and immersed in the following ethanol solution: 70% ethanol, 7 minutes, 100% ethanol, and 5 minutes. For PCR analysis, the kit manufacturer's procedure was followed. 1 µg of total DNA was used. The specific primers used are listed in Table 1. The PCR reaction was performed for 30 minutes at 94°C for 5 minutes, the 30s at 94 °C, 30s at 55 °C, and at 72°C for 30 minutes. The PCR products were then estranged on 1.0% agarose gel. Alpha Ease FC-2200 software (Alpha Innotech, USA, version 3.2.1) was used to enumerate the absolute transcript values from the PCR.

2.7. Statistical analysis

Statistical analysis was performed on the obtained results according to the analysis of variance (ANOVA) technique. Treatments were compared using the least significant difference (LSD) at the 5% probability level. All calculations and statistical analyses were performed using the student software package 8.1.

3. Results

3.1. VIGS plays a significant role in promoting the leaves senescence

In our study, virus-induced gene silencing has been proved as an exceptional source of rapid advances in the field of genetics (Tripathi and Tuteja, 2007). The TRV can infect the different plant organs including carpopodia (Liu *et al*., 2002; Dinesh-Kumar *et al*., 2003), leaves (Fu *et al*., 2005), fruits (Lu *et al*., 2003), and roots (Orzaez *et al*., 2006) by agro-injection, agro-drench, agro-infiltration, and vacuum infiltration methods. In present study, we infected the Arabidopsis plant with investigated *Vector (VG)* efficiency in concern to senescence approaches by vacuum infiltrations method. The vacuum infiltration method was designed, whereby infected leaves were kept at 8°C for three days. Vector infected Arabidopsis leaves were subjected to phenotypic analysis every alternate day during the study period. Slightly, yellowish discoloration of leaves was seen at the start in all silenced leaves and non-silenced leaves (Wild type). After 10 days of infiltration the *vector (VG)* leaves were flattering to yellow faded instead of *the vector (C)* (control) and wild type (Figure 5). For confirming the efficiency and effectiveness of *vector (VG)*, the changes occurred due to *vector (VG)* expression (Figure 3); ion leakage measurement; chlorophyll content, and SAG12 expression as the markers for senescence progression, were calculated. Significant difference (Figure 3) was noticed between *vector (VG)* and *vector (c).* Similarly, increased ionic leakage and SAG12 expression, decreased chlorophyll concentration were seen during

senescence of leaves and the whole plants, which proved that *vector (VG)* played a critical role in leaves senescenc.

3.2. Quantity of chlorophyll content highly reduced in vector (VG) infected plants

Photosynthesis is a multi-stage process which plays a significant role in the growth and development of plant (Ayumi and Amane, 2009). In present study, we investigated chlorophyll concentrations in *vector (VG)* and *vector (C)* infected leaves of Arabidopsis. It has been significantly proved that *vector (VG)* had affected the concentration of chlorophyll content (Figure 6a). The chlorophyll concentration remarkably decreased in *vector (VG)* leaves of Arabidopsis (Figure 6a) compared to non-silencing *vector (C)*, where chlorophyll concentration remained consistent. For further confirmation of these alternations, the expression of the PAG gene concerning to SAG12 gene was tested. The findings were confirmed by noticing slightly lower expression of PAGs and significantly higher expression of SAG12 in the *vector (VG)* (Figure 6c) compared to higher PAGs and lower SAG12 expression in the non-silenced *vector (C)*.

3.3. VIGS implicating in the reduction of cells enlargement

We further investigated that *vector (VG)* either affected the cell size enlargement or cell size reduction. We tested age-dependent leaves of the vector (*VG*) silenced Arabidopsis plants. We categorized leaves as young leaves, mature leaves, partial senesced leaves, and fully senesced leaves. It was found that from beginning, when the leaves are becoming mature, had reduced size and as well as decreased the number of cells (Figure 7b) in *vector (VG)* leaves compared to that of non-silenced leaves vector (C) control. Regardless of Arabidopsis, the phenotype of plants is also differentiated with a persistently smaller size compared to that of non-silenced (vector C) and as well as wild type (WT). More interestingly, these features have given an image to the novelty of phenotype in the shape of more yellowing of leaves in silencing plants compared to the wild type (Figure 5). Further, we observed that *vector (VG)* suppressed to phenotype is responsible for the repression of cells and resulted in decreasing the size and structure of the overall plant body (Figure 7d). Therefore, *vector (VG)* was plausible as a strong sensitive transcription factor that was responsible for some key functions during the cellular behavior of plant structure.

3.4. Method infiltrating by seed significantly affect the growth behaviors of Arabidopsis plant

Further, we had investigated the silencing approach by the seed infiltration method in Arabidopsis. Only a few reports have been illustrated about the silencing approach by seed infiltration methods as well as young seedlings of Arabidopsis till to date. There are a few studies on silencing approaches by VIGS application to seedlings and seeds in the premature growing stage (Nagamatsu *et al*., 2007). It is very challenging to inoculate (VIGS) vectors and induce infection in very young seedlings and through seeds as well. Thus, we tried to inoculate the infection by these two novel infiltration methods in Arabidopsis and we found amazing results. For the seeds' infiltration method, we sterilized wild-type Arabidopsis seeds with 10% sodium hypochlorite for 20 min with continuous shakings. After that, sterilized seeds were infiltrated under vacuum infiltration with the solution containing *vector (C)* and *vector (VG)* at equal OD of 2.0, and kept infected seeds for about 1 hour at 8°C. After that, we grown the seeds on two different types of culture media containing MS-Basal supplemented with 25ng of specific antibiotics and MS-basal media. Silenced seeds grew well on both antibiotic supplemented and MS-basal media (Figure 2a). After the seeds were cultured on media, the plants were placed at 4°C for about three days and then kept at 25°C for further growth. The *vector (VG)* showed better germination rate at the supplementation of antibiotics (Figure 2a). Moreover, the length of roots and leaves were remarkably suppressed in *vector (VG)* plants compared to *vector (C)* and wild type plants (Figure 4c, e). The phenotypes were measured after two weeks grown in the soil. The *vector (VG)* showed completely different phenotypes with a smaller size of whole plants, and the rate of growth was slightly slower compared to that of *vector (C)* and wild type (Figure 4d).

4. Discussion

It has been cited that VIGS is a valuable tool for functional analysis of genes in plants (Burch-Smith *et al*., 2004). The VIGS stimulated the knock-down/silencing of a particular gene expression by using a viral vector carrying a fragment of the target gene. Most of VIGS vectors were utilized for gene silencing in plant growth stages, such as leaves. On the other hand, several VIGS vectors were successfully induced in the reproductive organs, including flowers (Fu *et al*., 2005; Nagamatsu *et al*., 2007; Ayumi and Amane, 2009), and fruits (Lim *et al*., 2003; Andersson *et al*., 2004). In present study, we applied VIGS techniques through the infiltrating *vector (VG)* for leaves senescence. The VIGS techniques was found better approach for testing functional analysis to the silencing of *the vector (VG)* in the senescence of leaves. Moreover, the method proposed for the way to infiltration of Arabidopsis concluded that the entire aging process was comparable and provided a suitable experimental system. Thus, we also applied and followed the way with minor modification and used leaves, whole plants, whereby we found novel results.

4.1. VIGS induced at early stages leaf senescence

It is well understood that leaf senescence is a heritably controlled developmental process that ultimately leads to cell death. Obviously, under normal growth conditions, young leaves do not senesce. Perhaps, senescence inhibitors can effectively inhibit senescence during early leaf development and activate activators of the leaves age (Peitao *et al*., 2014). Interestingly, the role of the carrier (VG) was significantly different in Arabidopsis leaves. The overall observation of the silent leaves of Arabidopsis was analyzed, and it was shown that during the whole experiment, the vector (VG) and vector (C) and wild type leaves showed slightly yellow leaves at the beginning of infiltration. Later, the vector (VG) leaves turned yellow to fade, instead of the vector (C) and wild type. This view shows that the efficiency and effectiveness of the vector (VG) are more important. Although changes were assessed by measuring ion leakage activity, the expressions of chlorophyll, SAG12, and PRGs genes were used as markers of aging progress. We found that there are significant differences compared to the vector (VG) and

the vector (C). Similarly, the increased ionic leakage and SAG12 expression contrasted with the decreased chlorophyll concentration observed during leaf senescence, and the whole plant vector (VG) also played a key role in leaf senescence. Like our findings few others reported that by transferring nutrients from senescent leaves and carefully adjusting leaf senescence to maximize the plant's adaptability, the differential expression of many genes should be used to precisely control its occurrence, progress, and completion. Recent applications of genomics technology have enabled the isolation of a class of genes, so-called senescence-associated genes (SAG), whose expression is increased in senescent leaves (Zentgraf *et al*., 2004; Fu *et al*., 2006).

4.2. VIGS play a critical role in stimulating the instigation of leaf senescence

The effects of the vector (VG) on leaf senescence were noted by comparison of the yellowish discoloration level of the vector (VG) with non-silent vector (C) and wild type during the age-related leaf senescence in Arabidopsis. On the 15th day after infiltration, the leaves started to turn yellow in the vector (VG), but the vector (C) infected and wild-type leaves remained green (Figure 1a). The vector (VG) remained silent 25-30 days after infiltration, and those leaves turned completely yellow and revealed the signs of death. On the other hand, the vector (C) and wild-type leaves upheld their integrity and revealed only slight yellowish discoloration (Figure 5). For authenticity, leaf aging symptoms were further investigated, and typical senescence-related physiological markers were measured including photosynthesis-related gene expression, senescence-related genes expression (SAG12), and chlorophyll concentration (Figure 6b). After 3 weeks of infiltration, the chlorophyll content of the vector (C) and wild-type leaves began to decrease, while the silent leaves of the vector (VG) had lost 45-50% of chlorophyll content (Figure 6a). To be sure, similar findings have been reported concerning their acceleration, induction, and onset of leaf senescence, photosynthetic activity to reduce chlorophyll content in silenced plants (Al-Gabbiesh *et al*., 2015; Del *et al*., 2008). Besides, we reviewed that plant transcription factors of other gene families often have similar functions. For example, (NAC) and (WRKY) family genes are well-known aging-related transcription factors (Fu *et al*., 2006). More than 20% of the 109 (NAC) family genes in Arabidopsis are specifically induced during development-triggered senescence (Buchanan-Wollaston *et al*., 2003). Combining all these observations, the general findings suggest that the vector (VG) can play an amazing regulatory role in the initiation of leaf senescence, and as a transcription factor, it may control senescence by activating or inhibiting genes involved in the process by transcription.

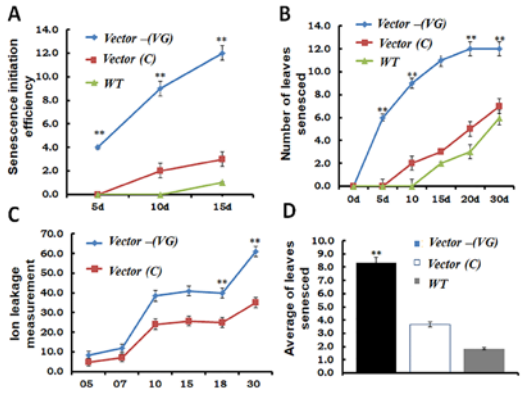

Figure 1. *VIGS* inducing leaves senescence. Senescence initiation efficiency **(A)**, number of leaves senesced after infiltration **(B)**, measuring of ion leakage after different time intervals **(C)**, middling mean of overall senesced leaves of Arabidopsis **(D)**. Asterisks denote statistically significant differences using student's *t*-test (P<0.05, P<0.01). Error bar represent the SD of the average from three different biological replicates.

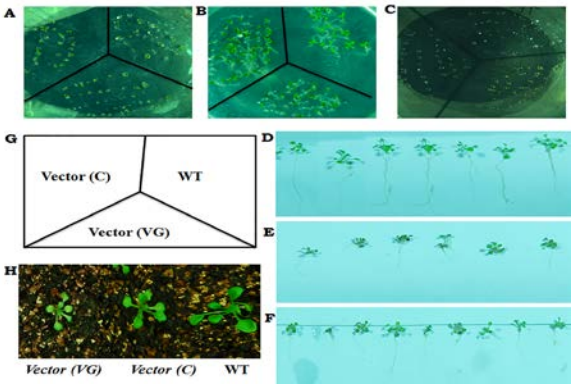

Figure 2. Virus Induced Gene Silencing by seed infiltration method. Germination percentage of *vector (VG*), *vector (C)* and WT at MS-basal media **(A, B)**, Survival rate of *vector (VG*), *vector (C)* and WT seeds in supplementation of antibody **(C)**, Wild-type of two weeks old rooted seedlings **(D)**, *vector (C)* two weeks old rooted seedlings **(E)**, *vector (VG)* two weeks old rooted seedlings **(F)**, illustration of preparing plates **(G)**, seedlings grow into soil and after 10 days *vector (VG)* showed remarkably low sized plant compare to that of wild type and *vector (C)* and showed slight light color of leaves **(H)**. Data are the average of three different biological replicates.

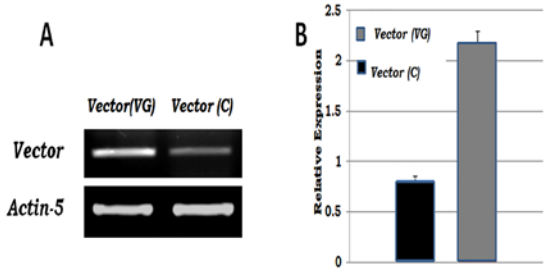

Figure 3. Relative expression level of *vector (VG*) affecting senescence in Arabidopsis. Qualitative expression measured by the PCR **(A)**, PCR analysis of *vector (VG)* and *vector (C)* **(B)**. Asterisks denote statistically significant differences using student's *t*-test (P<0.05, P<0.01). Error bar represent the SD of the average from three different biological replicates.

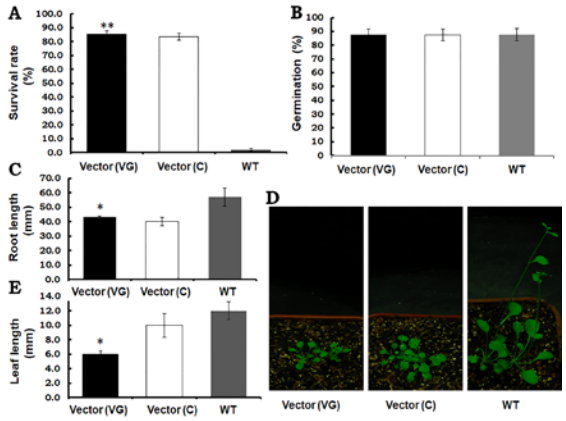

Figure 4. Effect of *vector (VG)* on growth behavior of Arabidopsis. Survival rate at supplementation media **(A)**, Germination percentage at basal media **(B)**, root length observed after germination **(C)**, growth behaviors of Arabidopsis suppressed by *vector (VG*), *vector (C)* and wild type **(D)**, leaves length measurement **(E)**. Asterisks denote statistically significant differences using student's *t*-test (P<0.05, P<0.01). Error bar represent the SD of the average from three different biological replicates.

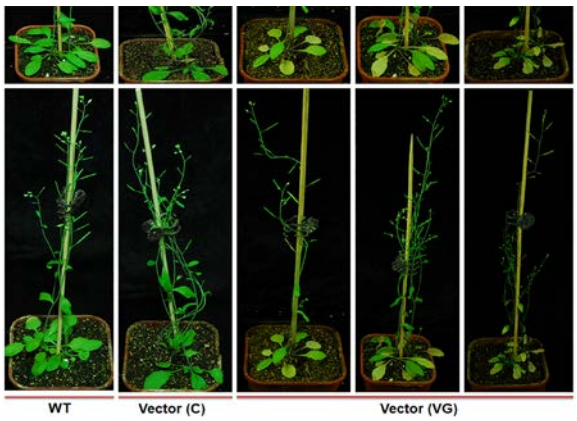

Figure 5. Phenotypic analysis of *vector (VG)* associated mutant lines of Arabidopsis. Data are the average of three different biological replicates.

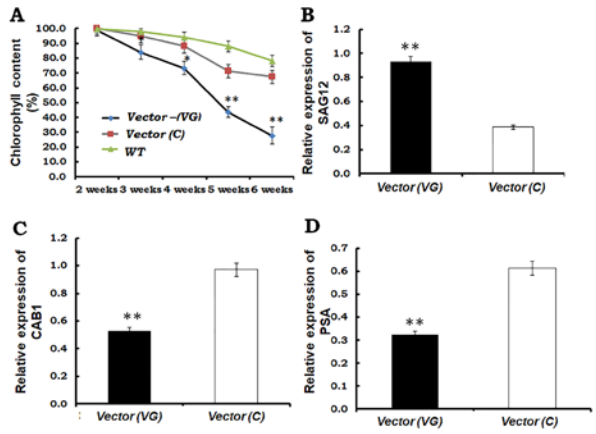

Figure 6. Expression pattern analysis with different marker genes and chlorophyll reduction in *vector (VG)* of Arabidopsis leaves. Chlorophyll content measurement (A), Relative expression analysis of SAG12 as senescence marker gene (B), Relative expression analysis of PSA as photosynthetic associated gene (C), Relative expression analysis of CAB1 as chlorophyll relating gene (D). Asterisks denote statistically significant differences using student's *t*-test (P<0.05, P<0.01). Error bar represent the SD of the average from three different biological replicates.

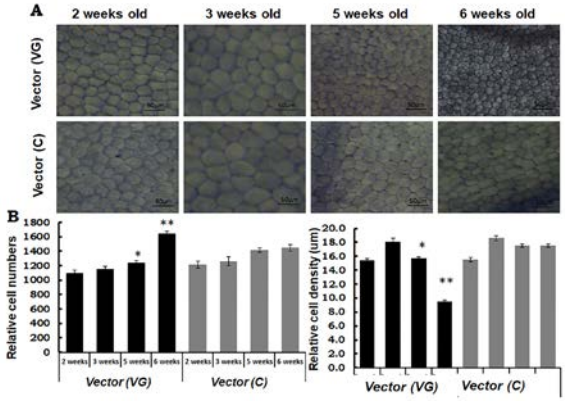

Figure 7. Effect of *vector (VG)* on cells sized reduction. Microscopic examination of leaves cells on different time intervals **(A)**, Relative cells number and cell density observations **(B).** Asterisks denote statistically significant differences using student's *t*-test (P<0.05, P<0.01). Error bar represent the SD of the average from three different biological replicates.

Acknowledgment

We would like to thank the School of Life Sciences, Lanzhou University, Gansu Province, P.R. China for providing research opportunity. We are also thankful to the Department of Biotechnology, Sindh Agriculture University, Tandojam, Pakistan which providing additional research resources for doing current research.

Conflict of interest

All authors declare that no conflict of interest exist.

References

Al-Shomali I, Sadder MT and Ateyyeha A. 2017. Culture Media Comparative Assessment of Common Fig (Ficus carica L.) and Carryover Effect. *Jordan J Biol Sci*., **10(1):** 13-18.

Al-Gabbiesh A, Kleinwächter M and Selmar D. 2015. Influencing the contents of secondary metabolites in spice and medicinal plants by deliberately applying drought stress during their cultivation. *Jordan J Biol Sci*., **147(3379):** 1-10.

Andersson A, Keskitalo J and Sjödin A. 2004. A transcriptional timetable of autumn senescence. *Genome Bio*., **5:** 24-30.

Ayumi T and Amane M. 2009 Photosynthetic Research in Plant Science. *P Cell Phys*., **50:** 681-683.

Balazadeh S, Rian DM, Pacho O and Mueller-Roeber B. 2008. Transcription factors regulating leaf senescence in Arabidopsis thaliana. *P Bio*., **10:** 63-75.

Buchanan-Wollaston V, Page T and Harrison E. 2005. Comparative transcriptome analysis reveals significant differences in gene expression and signaling pathways between developmental and dark/starvation-induced senescence in Arabidopsis. *The P J*., **42:** 567-585.

Buchanan-Wollaston V, Earl S, Harrison E, Mathas E, Navabpour S, Page T and Pink T. 2003. The molecular analysis of leaf senescence: a genomics approach. *P Biotech J*., **1:** 3-22.

Buchanan-Wollaston V, Page T and Harrison E. 2005. Comparative transcriptome analysis reveals significant differences in gene expression and signaling pathways between developmental and dark/starvation-induced senescence in Arabidopsis. *The P J*., **42:** 567-585.

Burch-Smith TM, Anderson JC, Martin GB and Dinesh-Kumar SP. 2004. Applications and advantages of virus-induced gene silencing for gene function studies in plants. *The P J*., **39:** 734-746.

Chen JC, Jiang CZ, Gookin TE, Hunter DA, Clark DG and Reid MS. 2004. Chalcone synthase as a reporter in virus-induced gene silencing studies of flower senescence. *P Mol Bio.*, **55:** 521-530.

Chen W, Provart NJ and Glazebrook J. 2002. Expression profile matrix of Arabidopsis transcription factor genes suggests their putative functions in response to environmental stresses. *The P Cell*., **14:** 559-574.

Del RA, del CR, López MG, Rivera-Bustamante RF and Ochoa-Alejo N. 2008. Virus-induced silencing of Comt, pAmt and Kas genes results in a reduction of capsaicinoid accumulation in chili pepper fruits. *Planta*., **227:** 681-695.

Dinesh-Kumar SP, Anandalakshmi R, Marathe R, Schiff M and Liu Y. 2003. Virus-induced gene silencing. *Methods Mol Bio*., **236:** 287-294.

Fu DQ, Zhu BZ, Zhu HL, Jiang WB and Luo YB. 2005. Virus-induced gene silencing in tomato fruit. *P J*., **43:** 299-308.

Fu DQ, Zhu BZ, Zhu HL, Zhang HX, Xie YH, Jiang WB, Zhao XD and Luo YB. 2006. Enhancement of virus-induced gene silencing in tomato by low temperature and low humidity. *Mol Cells*., **21:** 153-160.

Guo Y, Cai Z and Gan S. 2004 Transcriptome of Arabidopsis leaf senescence. *P Cell & En*., **27:** 521-549.

Harb AM, AL-Hadid KJ and Sharab AS. 2020. Molecular and Biochemical Changes of Indole-3-Acetic Acid in the Expanding Leaves of Barley (Hordeum vulgare L.) under Salinity Stress. *Jordan J Biol Sci*., **13(1):** 93-100.

Hashem HA and El-Sherif NA. 2019. Exogenous Jasmonic Acid Induces Lead Stress Tolerance in Kidney Bean (Phaseolus vulgaris L.) by Changing Amino Acid Profile and Stimulating Antioxidant Defense System. *Jordan J Biol Sci*., **12(3):** 345-353.

Hee K, Junyoung K, Jeongsik K, Ung L, In-Ja S, Jin HK, Hyo-Yeon L, Hong GN and Pyung OL. 2010. The RAV1 transcription factor positively regulates leaf senescence in Arabidopsis. *J Exp Bot*., **14:** 3947-3957.

Lim PO, Woo HR and Nam HG. 2003. Molecular genetics of leaf senescence in Arabidopsis. *Trends P Sci*., **8:** 272-278.

Lim PO, Kim HJ and Nam HG. 2007. Leaf senescence. *Ann Rev P Bio*., **58:** 115-136.

Lin JF and Wu SH. 2004. Molecular events in senescing Arabidopsis leaves. *The P J*., **39:** 612-628.

Lin Z, Hong Y, Yin M, Li C, Zhang K and Grierson D. 2008. A tomato HD-Zip homeobox protein, LeHB-1, plays an important role in floral organogenesis and ripening. *P J*., **55:** 301-310.

Liu Y, Nakayama N, Schiff M, Litt A, Irish VF and Dinesh-Kumar SP. 2004. Virus induced gene silencing of a DEFICIENS ortholog in Nicotiana benthamiana. *P. Mol Bio*., **54:** 701-711.

Liu Y, Schiff M and Dinesh-Kumar SP. 2002a. Virus-induced gene silencing in tomato. *P J*., **31:** 777-786.

Lu R, Malcuit I, Moffett P, Ruiz MT, Peart J, Wu AJ, Rathjen JP, Bendahmane A, Day L and Baulcombe DC. 2003. High throughput virus-induced gene silencing implicates heat shock protein in plant disease resistance. *EMBO J*., **22:** 5690-5699.

Lu R, Martin-Hernandez AM, Peart JR, Malcuit I and Baulcombe DC. 2003a. Virus-induced gene silencing in plants. *Methods*., **30:** 296-303.

Nagamatsu A, Masuta C, Senda M, Matsuura H, Kasai A, Hong JS, Kitamura K, Abe J and Kanazawa A. 2007. Functional analysis of soybean genes involved in flavonoid biosynthesis by virus-induced gene silencing. *P Biotech J*., **5:** 778-790.

Odiyi BO and Eniola AO. 2015. The Effect of simulated acid rain on plant growth component of Cowpea (Vigna unguiculata) L. Walps. *Jordan J Biol Sci*., **147(3379):** 1-4.

Orzaez D, Mirabel S, Wieland WH and Granell A. 2006. Agroinjection of tomato fruits. A tool for rapid functional analysis of transgenes directly in fruit. *P Phys*., **140:** 3-11.

Peitao L, Changqing Z, Jitao L, Xiaowei L, Guimei J, Xinqiang J, Muhammad AK, Liangsheng W, Bo H and Junping G. 2014. RhHB1 mediates the antagonism of gibberellins to ABA and ethylene during rose (Rosa hybrida) petal senescence. *The P J*., **78:** 578-590.

Quirino BF, Noh YS, Himelblau E and Amasino RM. 2000. Molecular aspects of leaf senescence. *Trends in P Sci*., **5:** 278-282.

Robertson D. 2004. VIGS vectors for gene silencing: many targets, many tools. *Ann Rev P Bio*., **55:** 495-519.

Ryu CM, Anand A, Kang L and Mysore KS. 2004. Agrodrench: a novel and effective agroinoculation method for virus-induced gene. *P Cell Rep*., **31:** 1713-1722.

Tanaka A and Makino A. 2009. Photosynthetic research in plant science. *P Cell Phys*., **50(13):** 681-683.

Tripathi S and Tuteja N. 2007. Integrated signaling in flower senescence: an overview. *P Sig Behav*., **2:** 437-445.

Zentgraf U, Jobst J, Kolb D and Rentsch D. 2004. Senescence-related gene expression profiles of rosette leaves of *Arabidopsis thaliana*: leaf age versus plant age. *P Bio*., **6:** 178-183.

JJBS

Jordan Journal of Biological Sciences

Volume 14, Number 3, September 2021
ISSN 1995-6673
Pages 571 - 579

Environmental Disparity Index (EDI): The New Measurement to Assess Indonesia Environmental Conditions for Supporting Sustainable Development

Fitri Hariyanti[1,2,*], Bekti Indasari[2], Almasdi Syahza[1], Zulkarnain[1], Nofrizal[1]

[1]*Riau University, Pekanbaru, Riau, Indonesia 28293;* [2]*BPS-Statistics of Riau Province, Pekanbaru, Riau, Indonesia 28131*

Received: February 27, 2021; Revised: May 25, 2021; Accepted: June 22, 2021

Abstract

Countries in the world including Indonesia agreed to continue development by carrying out the concept of Sustainable Development Goals. Many environmental problems that occur in Indonesia and the world are the result of activities carried out by companies and by households. These cause a development system that is needed not only to pay attention to economic and social aspects but also to environmental aspects. To know about the success of development in the environmental field, a disparity analysis is needed to be done by measuring the gap in environmental conditions between provinces in Indonesia using the Environmental Disparity Index. This analysis was constructed using six dimensions based on the Framework for Development of Environment Statistics (FDES) 2013 which include environmental conditions and quality; natural resources and their use; residuals; extreme events and disasters, human settlements and environmental health; environmental protection, management, and engagement. The method used in this analysis was through the taxonomic method approach and factor analysis. The results of the analysis showed that there were significant disparities between provinces in Indonesia in the five dimensions of the environment. This was because each province had different component strengths depending on the character and potential of each region. West Papua was the province with the best environmental conditions, while the province with the worst environmental conditions was Jakarta. The impact of uneven development between Western Indonesia and Eastern Indonesia also affected the environmental conditions in the two regions. The environment of Eastern Indonesia was still better than Western Indonesia. The recommendations that need to be taken: reducing carbon dioxide emissions; enforcing environmental laws; harnessing natural resources for sustainable development; improving the lives of the poor; protection and environmental management on a serious and consistent basis by the government.

Keywords: Development, Disaster, Disparity, Environment, Residue, Resources

1. Introduction

Countries in the world, including Indonesia, have agreed to continue development by carrying out the concept of Sustainable Development Goals with the principle of meeting current needs without sacrificing the needs of future generations. To achieve comprehensive sustainability, it is necessary to integrate the three pillars of development, namely sustainability in the social, economic, and environmental aspects that integrate and strengthen one another (Purvis *et al*., 2019). For this reason, these three aspects must be integrated into the planning and implementation of development to achieve sustainable development which in addition to protecting the environment/ecology from destruction or quality degradation can also maintain social justice without sacrificing the needs of economic development (BAPPENAS, 2010).

Many environmental problems that occur in Indonesia and the world are a result of activities carried out by companies and by households. Besides, the lack of public awareness can further exacerbate environmental problems. These cause a development system that is needed not only to pay attention to economic and social aspects but also to environmental aspects. In other words, a system that carries the concept of sustainable development is needed. One of the environmental problems in Indonesia is caused by the existence of large-scale industries. The research in Bangladesh shows that the lack of environmental responsiveness in several large-scale industries (include the tannery, pulp & paper, fertilizer, textile and cement industries) has a major impact on human health and the environment. Besides, it also generates extraordinary socio-ecological problems and creates huge social costs (Hoque *et al*., 2018).

Another example, the dairy industry will produce milk waste. This waste is one of the significant wastes source of water pollution (Senousy & Ellatif, 2020). Likewise, such fragile desert ecosystems are subjected to severe human activities (e.g. establishment of new urban settlements, road construction, construction of summer resorts along the coast, and significant uncontrolled grazing) contributed to land degradation, destruction of natural vegetation, loss of special resources, habitats and bidoversity (Salama *et al*., 2019). Another environmental issue is the management

* Corresponding author e-mail: fhariyanti@bps.go.id.

of household waste. Management of waste sorting for households will help recover recyclable materials and can reduce the amount of waste in landfills (Maskey, 2018). There are many other environmental problems currently occurring in Indonesia.

To realize sustainable development, a development plan is needed that pays attention to the optimization of natural resources and their use. This as much as possible can prevent environmental damage and increase the carrying capacity of the environment. Besides, in order to evaluate the success of pro-environmental development both national and provincial levels, it is necessary to have an accurate measuring and reporting tool of an environmental parameter so that it can be compared, understood and replicated (Both *et al*., 2015). As well as being able to know the environmental conditions of the area accurately so that it can be used as a reference to increase environmental awareness. Therefore, it becomes a very important aspect.

Starting from the framework of the United Nation-Framework for the Development of Environment Statistics (UN-FDES), Indonesia and the Asian Development Bank (ADB) developed the Indonesian-Framework for the Development of Environment Statistics (IFDES) which include environmental conditions and quality; natural resources and their use; residuals; extreme events and disasters, human settlements and environmental health; environmental protection, management, and engagement (BPS, 2017). The six dimensions can be used as a measuring tool to know environmental conditions in Indonesia. In contrast to the new version of the Environmental Quality Index which combines the Air Pollutant Standard Index, Water Quality Index, Forest Cover Index, Biodiversity Index, Public Health Index, and Environmental Health Index as a basis for environmental quality assessment (Yuwono, 2012).

This study aims to determine environmental disparities in the provinces in Indonesia and also to know the Environmental Disparity Index (EDI) for each dimension (environmental conditions and quality; natural resources and their use; residuals; extreme events and disasters, human settlements and environmental health; environmental protection, management, and engagement) for each province in Indonesia. The benefits of this research study can be a reference for developing an environmental system to increase public awareness.

2. Materials And Methods

2.1. Data Source

This study is macro analysis at the provincial level, so an Environmental Disparity Index (EDI) will be obtained between provinces. In this paper, the source that will be used as a reference is national data. One limitation of the study is that several measuring variables that use different data years, but for each of the same measuring variables in different provinces use the same data year. In general, EDI is compiled using 2018 data, so the results described are close to those conditions of 2018.

2.2. Conceptual Framework

An analysis of environmental disparities was constructed using six dimensions, where each dimension consists of several measuring variables/indicators. The six dimensions used are Environmental Conditions and Quality; Natural Resources and their Use; Residuals; Extreme Events and Disasters, Human Settlements and Environmental Health; Environmental Protection, Management, and Engagement. Before variables are used to determine environmental disparity, variable selection is first carried out through the validity and reliability test and factor analysis. Based on this description, the research framework is described as follows:

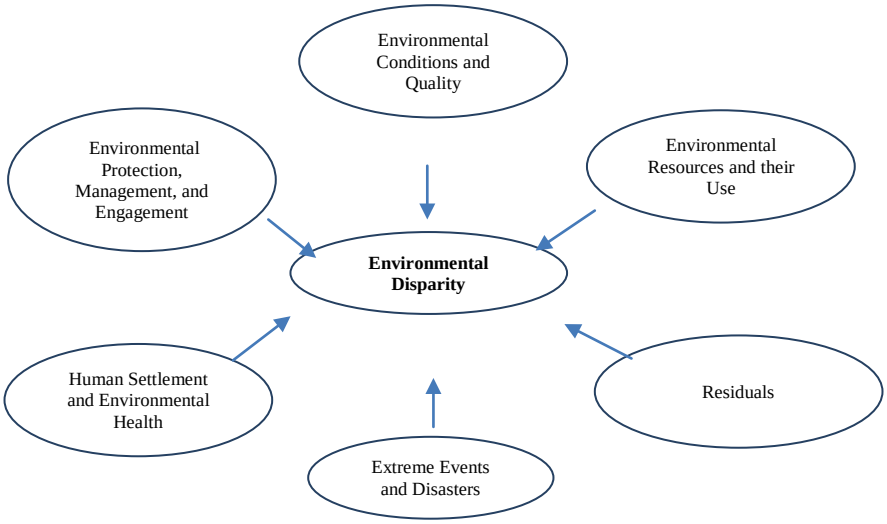

Figure 1. Conceptual Framework

2.3. Variable Selection

2.3.1. Test Validity

Validity is used to test the accuracy or correctness of the variables as a measuring tool for research. In other words, this test aims to assess whether the variables used are appropriate to measure the problem in a study. In this case, validity test aims to determine whether the variable/indicator used as a measure of environmental disparities is appropriate. To test the validity, the correlation coefficient is calculated between the candidate variables and the validator, using the Spearman Rank Correlation Coefficient.

Table 1. Number of Valid Variables for Each Dimension

Dimension	Number of valid variables
Environmental Conditions and Quality	-
Natural Resources and their Use	12
Residuals	7
Extreme Events and Disasters	6
Human Settlement and Environmental Health	14
Environmental Protection, Management, and Engagement	6

The variables used for the validity test are 74 variables. This analysis uses a 90% confidence level. Based on the results of the validity test, it is known that there are 29 invalid variables which cannot be used for further analysis.

2.3.2. Test Reliability

In addition to being valid for measuring disparity, some selected variables are also expected to make a large contribution to the reliability of the measure both jointly and individually. Reliability refers to how consistently a test measures a characteristic. The ideal size sought is a measure of high reliability, involving a few variables, and each variable has a significant contribution to the reliability of the size. The reliability level of a measure involving *k* variables is calculated using the Cronbach's alpha formula (Carmines & Zeller, 1979).

Table 2. The Results of Reliability Test

Dimension	Cronbach's Alpha
Environmental Conditions and Quality	-
Natural Resources and their Use	0.688
Residuals	0.900
Extreme Events and Disasters	0.800
Human Settlement and Environmental Health	0.722
Environmental Protection, Management, and Engagement	0.774

Cronbach's Alpha is a measure of reliability that has values ranging from zero to one (Hair Jr *et al*., 2010). The minimum reliability level of Cronbach's Alpha is 0.60 (Ursachi *et al*., 2015). Based on the test results, the Cronbach Alpha value for each dimension is greater than 0.60, which means that all dimensions in this study have met the reliable requirements.

2.3.3. Composite Index Calculation

This analysis was built using the taxonomic method approach which used to rank a group of countries, regions, or spatial units based on certain measures related to various socio-economic conditions of each country, region, or spatial unit. This method was originally proposed by Polish mathematicians under the leadership of Florek in 1952. In 1967, Hellwig proposed the method to UNESCO for international comparisons of economic and social development of countries in the world. Then in 1970 this method was used by Harbison, Maruhnik, and Resnik to make a study of the development of various countries (Arief, 2006).

The taxonomic method aims to determine a composite index (composite index) of various sizes, then based on the composite index a spatial unit ranking is made. Concerning the development input disparity analysis, the calculation of the composite index is based on several variables that have passed the validity and reliability tests.

3. Results And Discussion

In this study, variables that measured environmental disparity conditions were initially assessed based on concepts/definitions, theoretical studies, and data availability. The results of variable detection at this early stage obtained 74 variables selected as candidates to measure environmental disparity. Then all the candidate variables were further selected through validity, reliability and factor analysis. Based on these considerations, the study of environmental disparity was measured using 45 variables that passed the test and formed into five dimensions: Natural Resources and their Use; Residuals; Extreme Events and Disasters, Human Settlements and Environmental Health; Environmental Protection, Management, and Engagement. The results of the calculation of the Environmental Disparity Index (EDI) per dimension for each province in Indonesia were presented in Table 3.

Table 3. The Environmental Disparity Index (EDI) per Dimension for Each Province in Indonesia

Province	Natural Resources and their Use	Residuals	Extreme Events and Disasters	Human Settlement and Environmental Health	Environmental Protection, Management and Engagement	Total
Aceh	47.08	87.11	63.02	80.82	23.19	60.24
North Sumatera	53.57	70.29	79.69	69.51	37.41	62.09
West Sumatera	47.12	88.76	87.39	75.13	23.34	64.35
Riau	33.20	86.18	87.81	79.30	29.91	63.28
Jambi	43.40	86.00	93.35	77.51	31.69	66.39
South Sumatera	51.14	80.73	89.05	77.30	38.42	67.33
Bengkulu	42.07	95.15	97.70	74.59	21.46	66.19
Lampung	63.07	82.44	91.47	74.08	28.15	67.84
Bangka Belitung Islands	42.07	96.64	82.44	73.08	13.91	61.64
Riau Islands	42.87	95.74	98.76	82.09	15.43	66.98
Jakarta	42.61	46.65	89.05	44.07	20.31	48.54
West Java	62.54	52.73	35.77	53.79	46.85	50.34

Table 3. cont.

Province	Natural Resources and their Use	Residuals	Extreme Events and Disasters	Human Settlement and Environmental Health	Environmental Protection, Management and Engagement	Total
Central Java	72.27	47.14	33.50	65.83	77.01	59.15
Yogyakarta	50.48	86.28	86.60	74.67	19.65	63.53
East Java	69.50	31.66	42.28	59.21	61.55	52.84
Banten	46.67	82.03	89.05	68.74	19.17	61.13
Bali	45.36	83.66	87.41	82.87	22.04	64.27
West Nusa Tenggara	46.58	87.33	75.01	81.22	21.29	62.29
East Nusa Tenggara	46.98	90.45	78.43	82.36	21.93	64.03
West Kalimantan	44.68	88.20	79.74	71.49	34.11	63.64
Central Kalimantan	38.18	94.11	87.80	71.24	19.53	62.17
South Kalimantan	39.00	88.26	88.38	74.83	45.51	67.20
East Kalimantan	42.66	86.56	91.67	77.04	22.86	64.16
North Kalimantan	38.32	100.00	99.71	82.19	12.20	66.48
North Sulawesi	44.67	93.65	96.52	81.49	16.65	66.60
Central Sulawesi	46.29	91.45	91.00	83.12	21.40	66.65
South Sulawesi	51.13	75.42	83.23	81.97	30.16	64.38
Southest Sulawesi	42.16	93.67	95.00	85.87	18.27	66.99
Gorontalo	44.37	96.78	96.12	84.92	14.60	67.36
West Sulawesi	49.63	98.52	98.60	80.83	17.90	69.10
Maluku	44.47	97.55	98.67	86.00	21.78	69.69
North Maluku	39.27	99.01	96.94	84.05	14.41	66.74
West Papua	48.80	99.44	98.61	88.36	15.53	70.15
Papua	29.13	95.75	91.46	80.83	20.99	63.63

3.1. Environmental Disparity per Dimension

3.1.1. Natural Resources and their Use

Indonesia was located on the equator and had a tropical climate. This country also had a lot of potential natural resources including soil resources at the bottom layer (minerals and energy), land resources, biological resources, and water resources. These could be used as a driving force for development. These natural resources could be classified as renewable and non-renewable**.** Natural resources were important capital in the development process and were used as input in the process of production and consumption of human activities such as the provision of housing, food, health, transportation, infrastructure, and so on.

As a rich country in natural resources, it was very important to know the extent to which these natural resources could play a role in the development process both at the national level and in each province. Therefore, information regarding its availability and use was very important for policymakers to make decisions and to maintain their sustainability. The difference in potential natural resources and their use in each province was what causes disparities in the environment in the dimensions of natural resources and their use.

By using the taxonomic method, the value of the Environmental Disparity Index (EDI) in dimensions of natural resources and their use was obtained. EDI value of 34 provinces are divided into five radii, where each radius represents the level of environmental disparity between provinces. Provinces that were in the same radius can be known they have gaps in environmental conditions that were not too large. Otherwise, if the two provinces were in different radius then it could be known they had a greater gap in environmental conditions.

Based on the results of the EDI analysis, it was known that the disparity measure for this dimension was in the range of 0.00 to 0.50 which was divided into 5 radii. Central Java, East Java, Lampung, and West Java were in the first radius with a range of 0.00-0.10. The first radius indicated the highest rank of this dimension. Meanwhile, the province with the lowest rank in the dimension of natural resource and its use was Papua. Papua is in the fifth radius with a range of 0.40-0.50. Besides, the development measured for this dimension in 28 provinces was spread over a radius range of 0.10-0.50.

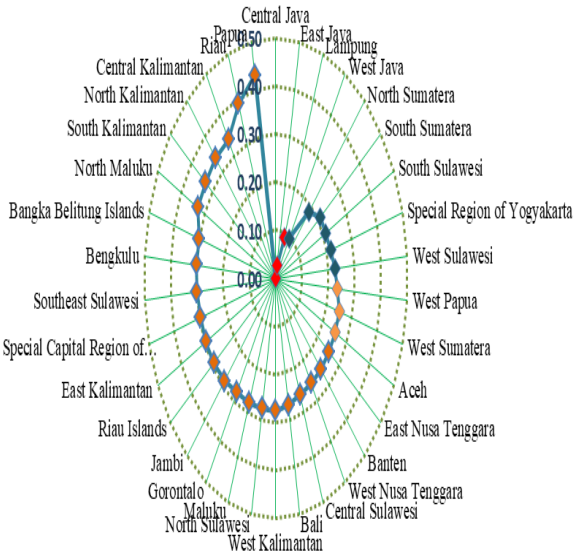

Figure 2. The Measure of Environmental Conditions and EDI Ranking Based on the Dimension of Natural Resource and Its Use in 2018

Figure 2 explained that Papua and Riau were in the lowest rank for the measure of environmental conditions based on the dimension of natural resource and its use. For Riau, this indicated high natural resource ownership and extensive forest ownership, but there was a lot of deforestation and fire on these forest lands. Papua, in particular, had a very high forest area, but the use of agricultural food crops was still very low. The four provinces that ranked the best in terms of potential environmental conditions were Central Java, East Java, Lampung, and West Java, respectively. These four provinces were seen as the top provinces in terms of the potential for land use for food crop agriculture coupled with the absence of deforestation activities on forest land.

3.1.2. Residuals

Various human activities could generate residues, for example from simple things such as breathing, eating, cooking, using vehicles, and other activities. All of these activities generated residues that were released through the production and consumption processes into the environment, either directly released or collected, processed before disposal, recycled or reused. The resulting residues could be harmful or harmless. Harmful residues could increase greenhouse gases which currently became one of the world's discussion topics.

Greenhouse Gases were gases in the atmosphere that caused global warming and climate change. In Presidential Regulation No. 71 of 2011 concerning the National Greenhouse Gas Inventory, there were several types that classified as GHG, such as carbon dioxide (CO_2), methane (CH_4), and nitrogen oxides (N_2O), sulfur hexafluoride (SF_6), perfluorocarbons (PFCS), and hydrofluorocarbons (HFCS). CO_2, CH_4, and N_2O had important roles as major contributors to climate change because they were included in long-lived greenhouse gases (WMO, 2014).

In this section, the gap between provinces that occured in the residual dimension would be measured using 7 indicators that had passed the variable selection. Before being used to calculate the composite disparity index, there were 10 variables based on similarities in measuring the environmental conditions of the residual dimensions. Furthermore, EDI and ranking of each province were calculated with the taxonomic method, the results of which were shown in Figure 3.

From Figure 3, it was known that by using the ideal value as a reference, the environmental disparity measure of residual dimensions could be grouped in 5 radii. About this grouping, there were 15 provinces located in the first radius with the best rank being North Kalimantan. Meanwhile, there was one province located in radius 5 and the lowest is East Java. The results of the provincial grouping in the residual dimensions indicated that provinces which were in the same radius tended to have the potential to produce residues that are almost the same when compared to provinces located in different radius. So the gap between provinces which are within the same radius is relatively low.

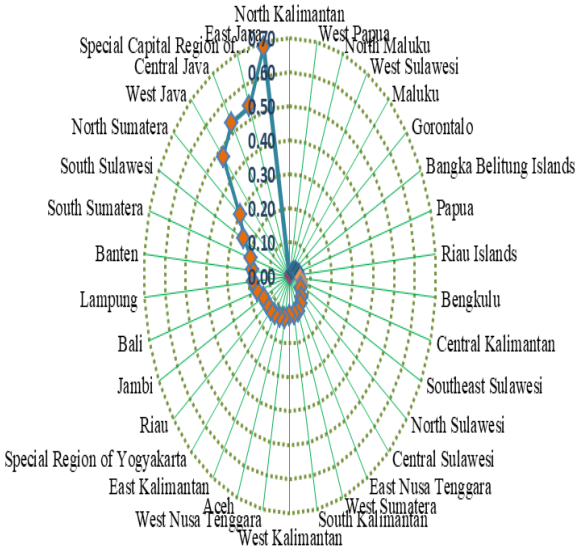

Figure 3. The Measure of Environmental Conditions And EDI Ranking Based on the Dimension of Residue in 2018

East Java and Jakarta were in the last radius which showed that two provinces had the greatest potential in producing residuals. It happened because both were big provinces in Indonesia that produced a lot of emissions from households, gasoline, diesel, motorized vehicles. Especially for East Java coupled with CH_4 emissions from livestock. Meanwhile, North Kalimantan as a newly formed province had the lowest potential to produce residues. The residual gap between East Java and North Kalimantan was estimated to be proportional to the environmental disparity measure difference of the two provinces.

3.1.3. Extreme Events and Disasters

One of the factors that could disrupt environmental balance was extreme events and natural disasters. Coupled with destructive human behavior and activities could increase the frequency and severity that occurred; for example illegal logging could cause floods, landslides, and drought. Disasters could cause a lot of loss both in terms of casualties and material as well as infrastructure damage because natural disasters usually came suddenly or through a gradual process (Fillah *et al*., 2016).

Preparedness and alertness in dealing with the threat of disaster are vital for a country. For this reason, precise and

accurate data or information were important to increase awareness and anticipation so that the impacts resulting from disasters could be reduced. As a Non-Departmental Government Institution, the National Disaster Management Agency had the task of assisting the President in carrying out disaster management. From this institution, the types of natural disasters can be identified and mapped based on the number and type that frequently occur.

In this section, disparity of extreme events and disasters will be explained through 6 measuring variables as mentioned in Table 1. From Figure 4, it could be explained that the disparity measure for this dimension could be grouped into 5 radii, where each radius used an interval of 0.15. The results showed that provinces within the same tended to have almost the same potential for extreme events and natural disasters, so the gap between environmental conditions for this dimension tended to be the same. Central Java was the province with the most landslides and floods, and the number of victims and physical damage due to disasters was also the highest compared to other provinces. This was what caused Central Java to be an area with the highest potential for extreme events and disasters.

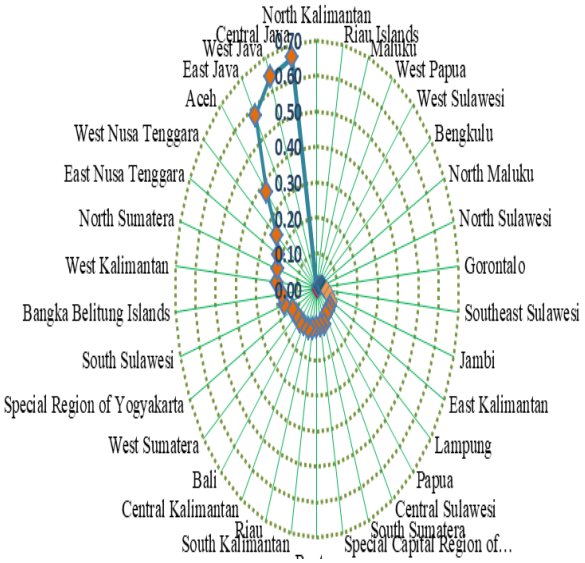

Figure 4. The Measure of Environmental Conditions and EDI Ranking Based on the Dimension of Extreme Events and Disasters in 2018.

3.1.4. Human Settlement and Environmental Health

The Framework for Development of Environment Statistics (FDES) 2013 explained that residential settlements could differ from small rural areas and urban or metropolitan cities. Besides, the addition of the population also presented its challenges to changing environmental conditions. Activities that were carried out continuously in settlements could cause environmental changes that could damage existing resources. The ability of the environment to cope with impacts caused by residential activities could affect the health of residents and the surrounding environment. Various efforts could be made to improve the health of settlements and the environment by providing waste disposal, providing infrastructure for water supply and sanitation, planning land used wisely, providing clean and safe transportation, ecosystem health, etc.

Based on the report of the United Nations (UN) by the titled "Urban and Rural Areas 2014," it was mentioned that the world population would increase to 8.42 billion people in 2030 from the number of 7.24 billion people in 2014. The number would continue to grow to 9.55 billion in 2050. Based on estimates, more world population lived in urban areas than in rural areas. There was 53.6 percent in 2014 to 60.0 percent in 2030 and 66.4 percent in 2050. The same trend of population development also happened in Indonesia. The results of population projections made by Statistics Indonesia (BPS), the population of Indonesia in 2025 would rise to 284.83 million from 238.52 million in 2010. This number would continue to increase to 305.65 million by 2035. Based on projections, more Indonesia's population would live in urban areas than in rural areas at 63.4 percent in 2030 and 66.6 percent in 2035 (BPS, 2017).

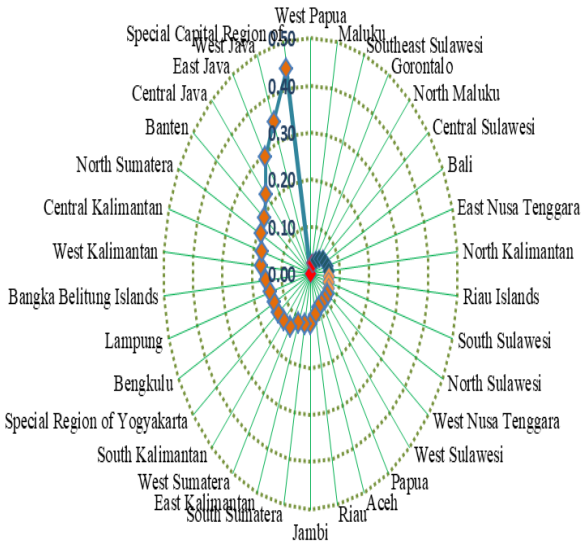

Figure 5. The Measure of Environmental Conditions and EDI Ranking Based on the Dimension Of Settlement and Environmental Health in 2018.

This increase in population would affect the availability of adequate basic needs in each province. Access to basic needs such as access to drinking water, sanitation, garbage/ waste disposal, and access to energy sources could have a positive impact on health, well-being, and environmental quality. So the existence of this access is important to determine the policy of a region.

Furthermore, by observing the EDI ranking for the dimensions of settlement and environmental health, it could be seen that 3 provinces ranking as the best EDI in a row are West Papua, Maluku, and Southeast Sulawesi, while the 3 provinces that had lowest rank, respectively are Jakarta, West Java, and East Java. If explored further, the superiority of West Papua in this dimension was due to the relatively low number and population density. Likewise, the percentage of villages according to water, air, and soil pollution is also relatively low. Meanwhile, the disparity in dimensions of settlements and environmental health in Jakarta was due to a large number of population and high population density. Furthermore, the percentage of households based on improved drinking water sources and access to proper sanitation services was also very low, coupled with the very high percentage of regions according to water pollution and air pollution.

3.1.5. Environmental Protection, Management and Engagement

The protection and management of natural resources is an activity that aimed to preserve and maintain the stock of natural resources. Natural resource management activities included the management of energy and mineral resources, wood resources, aquatic resources, other biological resources, water resources, research and development activities for resource management, and other resource management activities (BPS, 2017).

In Indonesia, the Ministry of Environment and Forestry had the task of organizing government affairs in the field of environment and forestry to assist the President in organizing state government. One of the functions established by the Ministry of Environment and Forestry was to implement policies in the field of sustaining the establishment of forest areas and the environment in a sustainable manner, managing conservation of natural resources and their ecosystems, enhancing the carrying capacity of watersheds and protection forests, managing sustainable production forests, increasing power primary industry competitiveness of forest products, improvement of the quality of environmental functions, control of pollution and environmental damage, control of climate change, control of forest and land fires, social forestry and environmental partnerships, as well as reduction of disturbances, threats, and violations of laws in the field of environment and forestry (BPS, 2017).

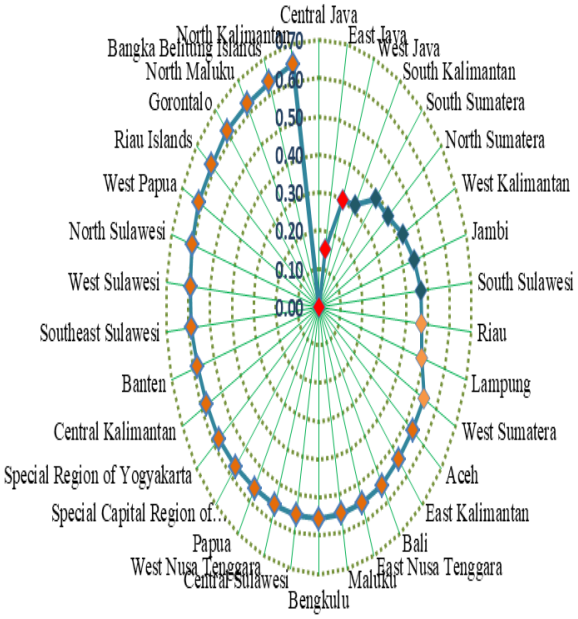

Figure 6. The Measure of Environmental Conditions and EDI Ranking Basedon the Dimension of Environmental Protection, Management, and Engagement in 2018

The best province for this dimension was Central Java. If explored further, then the superiority of Central Java in this dimension was due to the many environmental institutions, a large number of forestry extension workers both civil servants, private and non-governmental organizations. As well as supported by the number of schools that received an appreciation for successfully carrying out the environmental care and culture movement (i.e. *Adiwiyata*). Meanwhile, North Kalimantan is the province with the lowest rank in Indonesia. This is because it has the fewest environmental institutions and the number of forestry extension workers (both civil servants, private and non-governmental organizations).

3.2. Environmental Disparity for All Dimensions

The overall dimensions referred were a combination of the dimensions used to calculate the Environmental Disparity Index (EDI), there were Natural Resources and their Use; Residuals; Extreme Events and Disasters, Human Settlements and Environmental Health; Environmental Protection, Management, and Engagement. This measure seen from the composite index was recalculated with each dimension as input. Each province had different dimension strengths. For example, Central Java had a superior dimension on natural resources and their use as well as participation, management, and environmental protection, while West Papua had a superior dimension on residue as well as settlements and environmental health. These strengths complement each other to describe environmental conditions. After weighting for all dimensions, the top 3 best provinces were West Papua (1), Maluku (2), and West Sulawesi (3). Whereas the 3 provinces with the lowest index were East Java (32), West Java (33), and Jakarta (34).

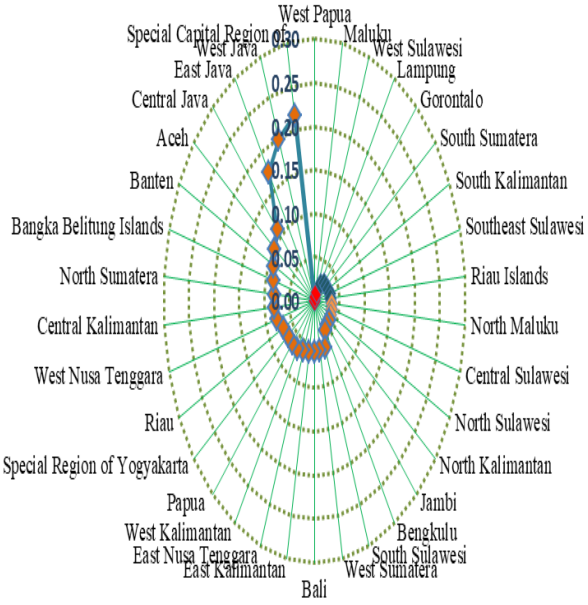

Figure 7. The Measure of Environmental Conditions and EDI Ranking for All Dimensions in 2018

Based on the previous analysis, West Papua had the strength that is the basis for its environmental conditions, such as the low residue generated, fairly good settlement and health conditions, and the occurrence of extreme events and disasters that were not so high. Meanwhile, the dimension of natural resources and their use were relatively low. This was because despite having a high area of land and forest land, the use was still considered low. Jakarta was the province with the lowest IDE value. This was because Jakarta had weaknesses in almost all dimensions, although in some dimensions it was not the lowest. The fundamental flaw in Jakarta is being the largest residue-producing province. Likewise, for the dimensions of settlement and environmental health, Jakarta has the lowest score. This is because it has the highest population density, which causes the lack of access to basic facilities such as drinking water and sanitation services.

3.3. Environmental Disparity by Region

The terms of Western Indonesia and Eastern Indonesia began since the formation of the State Policy Guidelines in 1993, and it turned out that until now the term regional division was still often used. The Western Indonesia consisted of Java, Sumatra, Kalimantan, and Bali. Whereas Eastern Indonesia consisted of Sulawesi, Maluku, Papua, West Nusa Tenggara, and East Nusa Tenggara. There was a difference between Western Indonesia and Eastern Indonesia in terms of development. When viewed further, the population of Western Indonesia was much greater so that the real economic activities that were in line with market mechanisms were also higher in this region. Eastern Indonesia had a larger area and had a wealth of natural resources that was very much so it was very ironic if Eastern Indonesia must continue to face the backward development and low welfare of its people.

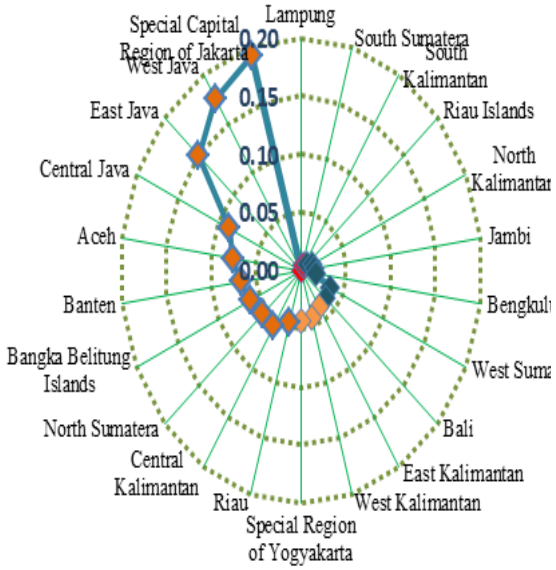

Figure 8. Western Indonesia

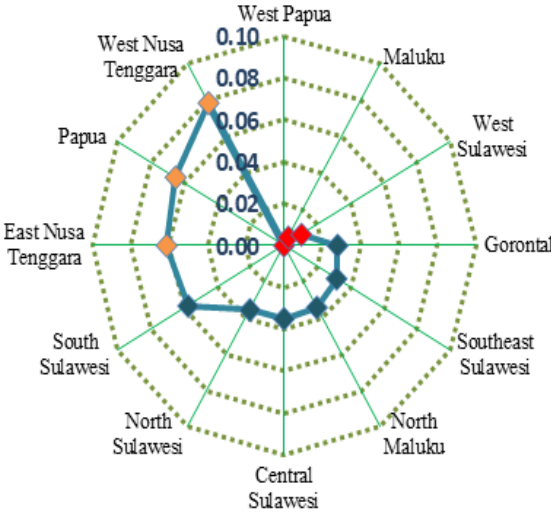

Figure 9. Eastern Indonesia

Based on Figure 8 and Figure 9 it could be seen that for Western Indonesia, Lampung and South Sumatra were the two provinces with the best Environmental Disparity Index (EDI), while the provinces with the lowest EDI were Jakarta and West Java. For the eastern part of Indonesia, West Papua was the province with the highest EDI, while the West Nusa Tenggara was province with the lowest EDI for this region.

The impact of uneven development between Western Indonesia and Eastern Indonesia also affected the environmental conditions in the two regions. The environment of Eastern Indonesia was still better than Western Indonesia because the residuals generated from community activities and economic activities were still low, the number of extreme events and natural disasters was also lower, and also the condition of settlements and environmental health was better. To overcome the gap between Western Indonesia and Eastern Indonesia, the government paid attention and made a priority for Eastern Indonesia's development. Various efforts were made to increase development in Eastern Indonesia so that it would not be left behind.

4. Conclusion

Differences in potential human resources and activities that occur in each province in Indonesia cause environmental disparities. To accurately know the local environmental conditions and that can be used as a reference to increase public awareness, a measuring tool is needed, namely the Environmental Disparity Index (EDI). The Environmental Disparity Index is divided into five dimensions: Natural Resources and their Use; Residuals; Extreme Events and Disasters, Human Settlements and Environmental Health; Environmental Protection, Management, and Engagement.

In all dimensions, West Papua has the strengths that are the basis for its environmental conditions, namely the low residue generated, the relatively good settlement and health conditions, and the occurrence of extreme events and natural disasters that are not so high. Meanwhile, the dimensions of natural resources and their use in this province are relatively low. This is because despite having a high area of land and forest land, the use side is still considered low, while Jakarta is a province with the lowest EDI value. This is because Jakarta is the largest producer of residues compared to other provinces. Likewise, for the dimensions of settlement and health, this province has the lowest value because the number and level of population density are the highest, which causes access to basic facilities to be as low as access to drinking water sources and proper sanitation services.

If differentiated by region, for the Western Indonesia, Lampung and South Sumatra are the two provinces with the best Environmental Disparity Index (EDI), while the provinces with the lowest EDI are Jakarta and West Java. For Eastern Indonesia, West Papua is the province with the highest EDI, while the West Nusa Tenggara is the province with the lowest EDI for this region.

Recommendations that can be given from the results of the analysis are the reduction of residues such as carbon dioxide emissions from burning fossil fuels and switching to environmentally friendly energy sources; enforcing rules and sanctions in violation of environmental laws; sustainable use of natural resources; improving the standard of living of the poor so that they can obtain a better social, economic and environmental life. The seriousness of the government is important in the management and protection of the environment both through increasing the government budget and the active role in protecting the environment.

Reference

Arief S. 2006. **Metodologi Penelitian Ekonomi (Metode Taksonomik)**. UI-Press, Depok.

BAPPENAS. 2010. **Laporan Pencapaian Tujuan Pembangunan Milenium Indonesia**. Bappenas, Jakarta.

Both AJ, Benjamin L, Franklin J, Holroyd G, Incoll LD, Lefsurd MG and Pitkin G. 2015. Guidelines for measuring and reporting environmental parameters for experiments in greenhouses. *Plant Methods*., **11**: 43.

BPS. 2017. **Statistik Lingkungan Hidup Indonesia 2016**. BPS, Jakarta.

Carmines EG and Zeller RA. 1979. **Reliability and Validity Assessment**. Sage Publications, California.

Fillah AS, Ishartono I and Fedryansyah M. 2016. Program penanggulangan bencana oleh Disaster Management Center (DMC) Dompet Dhuafa. Prosiding Penelitian & Pengabdian Kepada Masyarakat. Universitas Padjadjaran. Sumedang, Indonesia.

Hair Jr JF, Black WC, Babin BJ and Anderson RE. 2010. **Multivariate Data Analysis**, seventh ed. Pearson, London.

Hoque ASMM, Siddiqui BA, Awang ZB and Baharu SMAT. 2018. Exploratory factor analysis of entrepreneurial orientation in the context of Bangladeshi Small and Medium Enterprises (SMEs). *Eur J Manage Mark Stud.*, **3(2):** 81-94.

Maskey B. 2018. Determinants of household waste segregation in Gorkha Municipality, Nepal. *J Sustainable Dev*., **11(1):** 1-12.

Purvis B, Mao Y and Robinson D. 2019. Three pillars of sustainability: In search of conceptual origins. *Sustainability Sci*., **14(3):** 681-695.

Salama FM, El-Ghani MMA, El-Tayeh NA, Amro AM, Gaafar AA and El-Galil AAEA. 2019. Assessing the role of environmental gradients on the phytodiversity in Kharga Oasis of Western Desert, Egypt. *Jordan J Biol Sci*., **12(4):** 421-434.

Senousy HH and Ellatif SA. 2020. Mixotrophic cultivation of *Coccomyxa subellipsoidea* microalga on industrial dairy wastewater as an innovative method for biodiesel lipids production. *Jordan J Biol Sci.*, **13(1):** 47-54.

Ursachi G, Horodnic IA and Zait A. 2015. How reliable are measurement scales? External factors with indirect influence on reliability estimators. *Procedia Econ Finance*., **20**: 679-686.

WMO. 2014. **El Nino/Shouthern Oscillation**. Chairperson, Geneva.

Yuwono AS. 2012. Indeks Kualitas Lingkungan Hidup (IKLH) versi baru sebagai dasar implementasi analisis risiko lingkungan. Prosiding Seminar Nasional. Institut Pertanian Bogor. Bogor, Indonesia.

JJBS

Volume 14, Number 3, September 2021
ISSN 1995-6673
Pages 581 - 586

Jordan Journal of Biological Sciences

Driving Factor of Consumer Preferences for Food and Beverages Product Enriched with Green Tea Powder

Lucyana Trimo[1,*], Yosini Deliana[1], Sri Fatimah[1],Mai Fernando Nainggolan[1], Mohamad Djali[2]

[1]*Department of Agricultural Socio-Economics, Faculty of Agriculture, UNPAD;*[2]*Department of Food Industry Technology, Faculty of Agricultural Science Technology, UNPAD*

Received: February 27, 2021; Revised: May 18, 2021; Accepted: July 19, 2021

Abstract

In general, people have known tea as a refreshing and healthy beverage product. Green tea powder is one of the raw materials for the meter industry which contains a lot of polyphenols and antioxidants beneficial for health. The purpose of this study was to evaluate consumer preferences for a variety of food and beverage products containing green tea powder. The research method used is a positive approach and descriptive statistics. Primary data and information were collected from 200 respondents through a survey using well-structured questionnaires and interviews. Organoleptic test (hedonic or preference test) is a technique used in testing the acceptability of various food and beverage products. The hedonic scale is used to determine the level of preference, which is then analyzed using the same multi-attribute ideal number as the Semantic Differential Method. The results showed that 53% of respondents liked the taste of products enriched with green tea powder. Tea lattes, cupcakes, and layer cakes are products that are not favored. They have a preference value of 1.79, 1.48, 1.48, respectively. This means that the product has a dislike attribute, especially in taste, while bread is the most preferred product with a preference value of 0.31. In increasing consumer preferences for food and beverage products enriched with green tea powder, there are at least four development priorities that must be carried out, namely determining the right combination of product composition, improving texture, competitive prices, being more attractive and good, environmentally friendly packaging, create the uniqueness of product.
.

Keywords: green tea powder, driving factor, food and beverages product, product improvement

1. Introduction

People in Indonesia have recognized tea as a refreshing and healthy drink in various forms (i.e. black tea, green tea, Oolong tea, fragrant tea and white tea, which are very popular lately). Globally, tea itself is no longer a food ingredient that is processed only for beverages, but has become an ingredient (intermediate product) that can be added to various food and beverage products, cosmetics, and biopharmaceuticals. In line with Hugard Patil (2017), consumers around the world are increasingly paying attention to the nutrition, health, and quality of their tea products. Environmental and health awareness is increasingly reflected through increasing consumer interest in the consumption of branded tea. Oikarinen et al. (1998) in Hasan (2020) stated that skin therapy is through combination therapy such as the use of moisturizers, antibiotics, antihistamines, and corticosteroids to treat skin inflammation to improve the function of the changed skin barrier and reduce tingling.

Every change in people's lifestyle will require a lot of practicality. Besides being valuable, green tea powder is also a practical product that can be used as a raw material for mixed foods and beverages that have market prospects, both locally and abroad. Basically, to produce green tea powder does not require complicated technology, and this technology has been available in Indonesia for ten years. Making green tea powder can be done simply through the process of steaming, drying, particle size reduction, and sifting until it reaches a certain particle size according to market needs.

Global consumers are increasingly paying attention to the nutrition, health, and quality of Green Tea Powder Products (Indrani and Mohanapriya, 2018). This statement is in line with Arifin, B., Suprihatini, R. (2013) almost 80 percent of the world's tea consumption is black tea but in recent years the interest in green tea has increased. Consumers are beginning to understand that their food choices can affect their health, and then they pay more attention to the health benefits of food in their efforts to maintain a healthy lifestyle (Goetzke et al., 2014 cit. Yang, J. M., Lee, J, 2020).

Green tea powder in Indonesia is defined as a dry powder produced by the processing of shoots and young leaves from the tea plant (*Camellia sinensis*) without going through a fermentation process (BSNI, 1998). Variation foods and beverage product enriched with green tea powder have been produced and widely used in West Java include: chocolate, pastries, cake, drinks, milk, and others.

* Corresponding author e-mail: lucy.trimo@gmail.com; lucyana.trimo@unpad.ac.id.

The green tea had many health benefits; for example, the antioxidants lowered the risk of cancer, diabetes and obesity, etc. Mostafa (2014) says that the tea supported with catechin, drunk for many weeks, may be beneficial for people suffering from moderate diabetes or hyperlipidemia, reducing its complications such as liver and kidney disorders. The type of tea powder that is widely used in the food and beverage industry is green tea powder. The use of green tea powder has some benefits, especially on health. Raharjo et al. (2020) showed that the addition of green tea powder to wheat bread had a significant effect on increasing antioxidant activity. In line with the increasing attention of consumers towards healthy products, the preference of consumers to buy food and beverage containing green tea powder is also increased. The purpose of this study is to determine how consumers respond to food and beverages enriched with green tea powder, formulate marketing strategies, and develop the tea powder market. These findings have important implications for manufacturers, marketers and retailers in food and beverages product enriched with green tea powder, especially in Bandung city.

2. Research Methods

The research method used to evaluate consumer preferences for a variety of food and beverage products containing green tea powder was a positive approach and descriptive statistics. The research location was the city of Bandung which is considered as one of the world's creative cities famous for its food and beverages, apart from being the center of culinary tourism in West Java Province. Primary data and secondary data were used in this study. The method used in primary data collection was a descriptive survey using a well-structured questionnaire and interviews with 200 selected respondents. Respondents were selected using accidental sampling technique. The primary data collected were consumer characteristics, types of food and beverage products containing green tea powder purchased, consumer responses and opinions on the purchased product. Secondary data was collected from various sources, including the Central Statistics Agency, the Ministry of Trade, the Ministry of Industry, and the Central Statistics Agency for West Java. Testing the consumer's acceptability of various food and beverage products enriched with green tea powder was carried out using organoleptic tests. The organoleptic test carried out in this study was the hedonic test (preference test). In this test, researchers were asked to express their personal responses about their likes or dislikes and their level of preference for fineness, particle size, taste, aroma, shape and color, and price attributes. This level of preference is called the hedonic scale (Choi et al., 2002). The hedonic scale is then converted into a numerical scale with numerical quality according to the level of preference (Rahmi et al, 2013). The hedonic scale used was 1-5, with 1 = very like, 2 = like, 3 = neutral, 4 = dislike, and 5= very dislike (Singh-Ackbarali and Maharaj, 2014).

The applied method is used to determine the attitudes of potential consumers towards tea powder products which are symbolically formulated as follows:

$$AB = \sum Wi \mid Ii - Ji \mid$$

Where AB is the respondent's attitude towards the product enriched with green tea powder, W_i is the importance of attribute ***i*** to the product enriched with green tea powder, and I_i is Ideal performance required by consumers in attribute ***I,*** J_i is trust regarding the actual performance of existing products and samples of products.

Numerical linear scale used are :
$0 \leq Ab < x$: very good
$x \leq Ab < 2x$: good
$2x \leq Ab < 3x$: neutral
$3x \leq Ab < 4x$: bad
$4x \leq Ab < 5x$: very bad

3. Results and Discussion

3.1. Characteristics of Consumers

The characteristics of consumers West Java Typical food and beverages enriched with green tea powder can be seen from their age, education, and type of work. When viewed from the age distribution of consumption of typical foods and beverages of West Java made from green tea powder, most of them are under the age of 31-49 years (83%) with the range between 19-50 years old. This shows that they are in the productive age group and live in urban areas which usually have a high desire to always try new things.

The level of education also influences consumer choices in choosing food and beverage. Education describes how a person's knowledge about an object or phenomenon and can provide information for the person concerned. Furthermore, knowledge can be obtained through experience or interaction with other people. Experience provides an understanding of an object. The results of interactions with other people create a form of communication that contains messages, for example knowledge. Related to this research, education can influence a person in determining their choice of West Java food and beverages product made from green tea powder.

From the results of the study, it was found that 50 percent of education consumers were undergraduates. This is understandable because they generally live-in urban areas, have higher education and income, and have more opportunities and options to sample new foods and drinks. In addition, the ease and availability of new food and beverages are widely circulated in urban areas; in other words, urban areas, especially Bandung City, are one of the culinary centers in West Java. In the city of Bandung, there are many foods and beverages that have various innovations in taste, shape and size, as well as packaging. The high level of education possessed by consumers will affect the way of thinking in choosing the available food and drinks. Several factors that can influence them in choice include: taste, price, uniqueness of a product, packaging, convenience/availability, prestige, health, environmental considerations, and others. In addition, their average occupations are: self-employed, student, civil servant, pharmacist, designer, and civil servant, with these livelihoods representing different levels of income. The level of consumer income varies, causing different types of food and beverages purchased, depending on the level of income.

3.2. Consumer Preference on West Java Type of Foods and Beverages Products Enriched with Green Tea Powder

The types of food product they like are: bakpia, pukis, block cake, mocha, brownies, chocolate, cake, martabak, donuts, banana nuggets, ice cream, cubit cakes, and toast, while the preferred green tea flavor drinks are: matcha, green tea milk, thai tea, greentea latte. Some of the foods that have been consumed by consumers and their opinions on these foods can be seen in Table 1(a&b). Most consumers (97 percent) stated that Foods that are mixed with green tea have a fresh taste, are fragrant, and reduce sweetness, especially for chocolate, spongecake and dodol.

From the survey results on the taste preferences of culinary foods and typical souvenirs of West Java, it turns out that people in West Java prefer the taste of tea, so this is a potential for West Java as a center for tea producers in Indonesia and also to be able to develop a typical food and beverage industry made from tea. This is supported by a statement from Shen et.al. (2014) that the addition of green tea powder to these foods does not reduce the liking value based on sensory tests. The preference of consumers for the taste of food and souvenirs typical of West Java who like food and drinks with the taste of tea reached 53% of respondents; the rest of respondents (47%) still prefer non-tea flavors for various reasons as the price is more expensive, the size is smaller, and the texture is still not soft. For the typical West Java cake made with tea, it turns out that the cubit cake with green tea flavor is the most favorite choice in West Java (36%), followed by brownies as a second choice (19%). Lapis Bogor and green tea flavored bread each only occupy the favorite choices by 14% of all respondents, and other types of cakes by 17%.

Consumer responses to green tea flavored mixed food and beverage are quite diverse. They expressed their liking for the product with various responses, that is: 1) delicious and fresh, 2) distinctive and unique taste, 3) add flavor, 4) the fragrance enhances the taste, 5) and beneficial for health. Furthermore, the response of consumers who stated that they did not like food and beverage mixed with green tea flavors, stated: 1) it caused an unpleasant taste, 2) the taste was less familiar, 3) did not like the smell, 3) it tasted strange, 4) did not like being mixed, 5) did not like the taste of green tea, and 6) Not all foods are suitable to be combined with green tea.

Table 1a. Consumer Opinion on Food Product Enriched with Green Tea Powder

Kind of product	Consumer response
Cake	
Cubit	The taste is delicious, the soft texture is unique and varied
Bakpia	Different and distinctive taste
Pisang	The texture is soft and the taste is good
Bread	The taste is delicious
Pocky*	Aroma smell is good and taste is delicious
Malkist*	The taste is delicious
Kue balok	It's a good mix, good created menu, and good smells
Dorayaki	The taste is delicious
Donat	Appropiate combined of green tea taste
Spongecake	
Bolu susu	Delicious, because the taste of green tea is stronger
Amanda*	Soft texture and not too sweet (relative sweet), unique and distinctive taste
Bandung Makuta	Savory taste and delicious
Cakenian	Unique and delicious and more fragrant, the green tea taste is not bitter
Brownis kukus	Delicious, the aroma of green tea causing a fresh taste
Sangkuriang*	Green tea is soft, a perfect blend of cheese and green tea is
Coccolate	
Kit Kat*	The chocolate taste less sweet, a mix of creamy chocolate and a distinctive matcha aroma, the right combination
Silverqueen*	The green tea tastes just right, neither too bitter nor too sweet
Cadburry*	The chocolate taste is soft because it is mixed with green tea, and reduces the sweetness
Delvi*	Even though the tastes is bitter, but it still delicious
Royce almond matcha*	Delicious and not too sweet
Hersey*	The taste is different from other product
Dodol	The taste is unique and the sweet taste is reduces

Note: * = trade name (brand name)

Food mixed with green tea powder, according to some consumers (53 percent), has a fresh and fragrant taste and reduces sweetness, especially for the *cubit* cake, brownies, and Bogor layers cake. Furthermore, they also argue that beverage mixed with green tea can provide a refreshing taste and reduce sweetness (especially for dairy products), give a fragrant and healthy smell. Favorite beverages are: matcha, green milk tea, *thai tea*, green tea latte. In addition, they also rated not delicious taste to some types of drinks mixed with green tea, that are: coffee (strange taste), *bandrek* (strange taste), *bajigur* (strange taste), original green tea (it tastes bitter), and ocha (it tastes so bitter).

Table 1b. Consumer Opinion on Food and Beverages Enriched with Green Tea Powder

Product Type	Consumer Opinion
Gomilk	Makes the sweet taste less dominant
Chocolatos green tea	Nice and fragrant taste and sweet taste is not too dominant
Milk	The taste of milk is reduced if you add green tea to make it more delicious, refreshing. It tastes good when bought warm, the taste is more varied, and is a great combination, between milk and green tea
Green tea latte	The taste is not too sweet, fresh and smells like tea
Thai tea green tea	Tea mixed with milk is delicious, refreshing, fragrant and delicious
Matcha latte	It's fresh, sweet, perfectly bitter, themixture of milk and green tea is a perfect match
Green tea	The taste is unique and very refreshing
Pure Green tea	Can lower cholesterol levels and smell good
Green tea frappucino	Green tea taste decreased and less fresh
Bajigur	The distinctive taste and aroma is lost.
Bandrek	The distinctive taste and aroma is lost.

Furthermore, most consumers (76 percent) stated that drinks mixed with green tea can provide a refreshing taste and reduce sweetness (especially for dairy products), provide a fragrant and healthy aroma. The rest (24 percent) stated that coffee, *bandrek* and *bajigur* mixed with green tea tasted bad and strange.

Based on the description above, it can be concluded that product innovation among food and beverage producers has a different uniqueness and taste. However, it was found that 24 percent of consumers showed that mixed drinks with green tea powder did not always taste good and fresh, for example: coffee (strange taste), *bandrek* (strange taste), *bajigur* (strange taste), original green tea (it tastes bitter), and ocha (it tastes bitter). Generally, the consumer stated that the distinctive taste and aroma of *Bajigur* and *Bandrek* is lost. In addition, consumers also stated that foods and drinks with too much green tea taste will cause the bitter of green tea taste in product. Based on research of Phongnarisorn et al. (2018), it can be seen that matcha green tea powder (MGTP) is made with finely ground green tea leaves that are rich in phytochemicals, most particularly catechins. Catechins are the main polyphenols found in green tea. The content of catechins is what causes food and drinks to be fresh as well as the Acute Metabolic Response.

In order to improve food and beverage products typical of West Java made from tea as a favorite food in West Java and to support the tourism industry, there are several suggestions from respondents for improvement the quality of food and beverages product enriched with green tea powder. Consumer suggestions to food and beverages product enriched with green tea powder can be seen in the following figure 1:

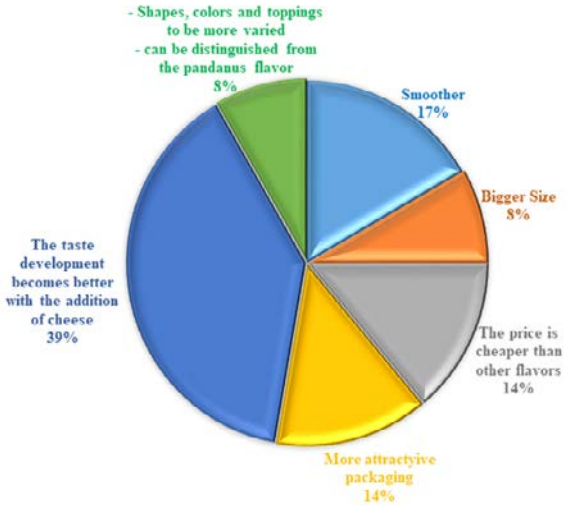

Figure 1. Consumers Suggestions for improvement of West Java typical food and beverages enriched with green tea powder

The first priority suggestion is to improve the taste to make it better, that is by reducing the bitterness and it should be for food combined with cheese (39%) to make it savorer and more delicious. The second and third places are texture refinement to make it softer and tastier, as well as the price attribute. Yang and Lee (2020) stated it is important that new products have competitive sensory quality and that production is economically viable for the local community. This improvement product is very important, because the design of the innovated product has powerful impact on consumer attention (Mahir, 2020)

The price of green tea-flavored cakes is more expensive than other cake flavors because it will cause them to be unable to compete in the market with other food products that are not made from green tea. According to Kiranmayi (2017), the price plays an important factor for the customer. The customer prefers to shop the product with cheap prices. The price and promotion have the strongest impact on consumer acceptance and buying decisions (Melovic et al., 2020). According to Hugar and Patil (2017), discounts and gifts given, such as buy one get one, greatly influenced the consumer preferences. The final consumers' opinion regarding food and beverage products is that the packaging and presentation of the taste of the product are made more attractive and varied. In addition, consumers also want packaging that is environmentally friendly, such as paper bags (easy to recycle), unique shapes, and clear images or photos of green tea (leaves and powder) on the label. Availability of Food and Beverages Products Enriched with Green Tea Powder

Availability and convenience for consumers to get food made from green tea powder are crucial for consumers to buy it. Furthermore, for novice consumers this convenience will encourage them to be willing and interested to try it. The above conditions are shown by the results of this study that more than half of the consumers studied (58.20 percent) stated that it was easy to obtain food made from green tea powder in Bandung. Furthermore, they also stated that there are various kinds of food made from green tea powder both in form and taste. They can easily find places to buy green tea powder at: UKM exhibition stands, cafes, shops, canteens, stalls,

and also in mini markets or super-markets around Bandung.

The marketing strategies like product, price, promotion, place, process, people and physical evidence play a significant role in assuring a success and sizable profits for the companies. On the other hand, customers face several problems such as delay in product supplies, unfair and discriminated prices, and lack of information about expired and obsolete products, deceptive advertisements, raising customer complaints, unsociable approach of sales force, reduced sales after service, etc. These problems potent to increase customer's dissatisfaction..

3.3. Preference of West Java Typical Food Products Based on Green Tea Powder from the producer Side

The results of the analysis of the preferences for food and beverage products containing green tea powder in terms of food and beverage producers, namely by using the multi-attribute ideal number which are similar to the Semantic Differential method (Kotler, 1993) seen in Table 2. In Table 2, it can be seen that the attributes of food and beverages that have the highest weight are taste criteria, which are then followed respectively by aroma and particle fineness criteria. Furthermore, price is the attribute with the lowest level of importance (rank five). This result is in line with Chueamchaitrakun et al. (2018), that Indonesian people considered color, flavor and taste as key attributes affecting purchase.

Table 2. The Results Preference Analysis of Food and Beverages Product Contain Green Tea Powder

Attributes	Weight	Ideal	Brownies	Bread	Layer Cake	*Cubit* Cake	Coffee	Tea Latte
Particle size fineness	0,13	5	4	5	4	3	4	3
Taste	0,31	5	3	4	2	3	4	3
Aroma	0,25	5	5	5	4	3	4	3
Shape and Color	0,24	5	5	5	4	4	4	3
Price	0,07	3	4	3	4	5	3	4
Value of product attitude			0,68	0,31	1,48	1,48	0,93	1,79
Product Refinement Priorities			4	5	2	2	3	1

Based on the Semantic Differential method, if the calculation results obtained are closer to zero then closer to ideal preference. This means that refinement of particle size attribute, taste, aroma, color, and price are getting closer to zero, the food and beverages products based on green tea flour are increasingly accepted and liked by consumers. Meanwhile, the value of the tea latte showed that it was far above zero, that is 1.79, and it was far from the ideal value. This condition is also experienced by *kue cubit* and *lapis bogor*, which have the same value, 1.48. Only bread has a value close to zero, that is 0.31. It means that only bread which has high preference and great demand and purchased by consumers, then followed by brownies which have value of 0.68. The ranking order for product refinement to fulfil the needs of the food and beverage producers, starting from priorities requiring immediate improvement, was the tea latte, lapis Bogor and pinch cake, coffee; brownish, and bread.

Food and beverage producer also must prioritize these four criteria (taste, aroma, shape and color, and particle fineness) because they can affect the quality of their products. This is not a difficult thing because food and beverage producers are always accustomed to pursuing consumer tastes and needs. This result corresponds to Mahir (2020), i.e. that the design of the innovated product has powerful impact on consumer attention

4. Conclusions And Suggestions

The results showed that respondents (53%) preferred the taste of green tea. Green tea-based product of foods and beverages that were preferred by consumers are *cubit* cakes, brownies, Bogor layers cake, bread, and others. Consumers' favorite beverages are matcha, green tea milk, and green tea latte, while favorite food are bread and brownies. In innovating to produce products that have a unique taste and are different from others, food and beverage producers often forget the local specialties, such as *Bandrek* and *Bajigur*.. The distinctive taste and aroma of *Bajigur* and *Bandrek* is lost. In addition, consumers also claim that foods and drinks that taste too much of green tea will cause a bitter taste of green tea to appear.

In order to increase the consumer preferences on foods and beverages product enriched with green tea powder-based, food and beverages manufacturer must improve the product, especially in 1) the combination must be right so that the bitterness is lost, 2) texture of food product become more softer and tastier, 3) the price of green tea flavored cakes is cheaper than non-tea taste, 4) the packaging views more attractive and good looking, 5) use environmentally friendly packaging, 6) create the uniqueness of product.

Acknowledgments

Finally, we would like to thank the DRPMI (Directorate of Research and Community Service for Innovation) Padjadjaran University for funding and supporting us in conducting this research, through the ALG (Academic Leadership Grant) scheme with contract number 1427 / UN6.3.1/ LT / 2020, and also I would like to thank to the anonymous reviewers who have offered helpful suggestions.

References

Rahmi, A, Susi, Agustina L. 2013. Anlisi tingkat kesukaan konsumen, penetapan umur simpad, nanalisia kelayakan usaha dodol pisang awa. Ziraa'ah., **37(2):** 26-32.

Arifin, B., Suprihatini, R. 2013. Rapid Appraisal of Indonesian Tea Value Chains. Research Report prepared for the World Bank.

BSNI (Badan Standar Nasional Indoneia). 1998. Standard of Green tea powder, SNI-01-4453-1998.

Campbell, E.L., Chebib, M., Johnston, G.A. 2004. The dietary flavonoids apigenin and (-)-epigallocatechin gallate enhance the positive modulation by diazepam of the activation by GABA of recombinant GABA(A) receptors. Biochem. Pharmacol.**(68):** 1631-1638.

Choi, J.Y., Park, C.S. Kim, D.J., Cho, M.H., . Jin, B.K, Pie. J.E., Chung, W.G. 2002.Prevention of nitric oxide-mediated 1-methyl-4-phenyl-1, 2,3,6 tetrahydro-pyridineinduced Parkinson's disease in mice by tea phenolic epigallocatechin 3-gallate. Neurotoxicology; **23**: 367-374.

Chueamchaitrakun, P., Adawiyah D. R, Prinyawiwatkul, W. 2018. Understanding Indonesian People: Consumer Acceptance and Emotions Study of Green Tea Products from Thailand. CAST, **18 (1):** 37-44.

Engel, J.F., Blackwell, R.D, Miniard, P.W. 1990. Consumer Behavior, Sixth Edition. The Dryden Press. Illinois. 789 pp

Frei, B., Higdon, J.V. 2003. Antioxidant activity of tea polyphenols in vivo: evidence from animal studies. J. Nutr**.(133):**3275S-3284S.

Hantraye, P., Brouillet, E. Ferrante, R., Palfi, S., R. Dolan, R.T. Matthews, R.T., Beal, M.F.. 1996. Inhibition of neuronal nitric oxide synthase prevents MPTP-induced parkinsonism in baboons. Nat. Med. **2**: 1017–1021.

Hara, Y. 2001. Green tea : health benefits and applications. Marcel Dekker, Inc.New York.. pp

Hassan, S.M.A. 2020. Anti-inflammatory and Anti-proliferative Activity of Coconut Oil against Adverse Effects of UVB on Skin of Albino Mice. Jordan Journal of Biological Sciences (JJBS). **15(3):** 295 – 303

Ho, C.T., Lin, J.K., Shahidi, F.. 2008. Tea and tea products : chemistry and health-promoting properties. Boca Raton, Florida: CRC Press. .

Hugar, G., Patil**,** M. R. 2017.Customer Behavior Analysis towards Select Fast Moving Consumer Goods with Special Reference to Branded Tea Powder Products: Empirical Study from Mumbai City. Imperial Journal of Interdisciplinary Research (IJIR) Vol-3, Issue-1: 1226-1236.

Indrani, G, Mohanapriya, T..2018. A Study on Customers Perception and Satisfaction towards Green Tea with Special Reference to Coimbotore City. International Journal of Business and Management Invention (IJBMI) .,**7(3)** : 25-28

Kimura, K.,. Ozeki, M., Juneja, L.R., Ohira, H. 2007.L-Theanine reduces psychological and physiological stress responses. Biol. Psychol. **(74)**: 39-45.

Kiranmayi, N. 2017. Factors Affecting the Consumer Behavior with Reference to Select FMCG Retail Outlets. International Journal of Creative Research Thoughts(IJCRT): 32-334.

Kotler, P. 1993. ManajemenPemasaran. Analisa, Perencanaan, Implementasi, dan Pengendalian. Terjemahan A. Zakaria Afiff. Lembaga Penerbit Fakultas Ekonomi Universitas Indonesia.

Lu, T.M,.,.Lee, C.C., Mau, J. L., Lin. S.D. 2010. Quality and antioxidant property of green tea sponge cake. Food Chemistry. **119(3):** 1090–1095.

Maeda-Yamamoto, M., Ema, K., Tokuda, Y., Monobe, M., Tachibana, H. Sameshima, Y., Kuriyama, S. 2014. Effect of green tea powder (*Camellia sinensis*L. cv.Benifuuki) particle size on o-methylated EGCG absorption in rats; The Kakegawa Study. Cytotechnology: 171–179.

Mahir, A. M.. 2020. The Impact of Product Innovation on Consumer Behavior in Food Sector of Azerbaijan. Dissertant of Baku Engineering University. No. **12**: 203-207.

McKinley, H., Jamieson, M. 2009. Handbook of green tea and health research. New York: Nova Science Publishers, Inc.

Melovic, B., Cirovic, D., Dudic,V, Vulic, T. B, Gregus, M. 2020. The Analysis of Marketing Factors Influencing Consumers' Preferences and Acceptance of Organic Food Products—Recommendations for the Optimization of the Offer in a Developing Market. *Foods* 2020, *9*, **259**: 1-23

Mostafa, U. El-Sayed. 2014. Sciences Effect of Green Tea and Green Tea Rich with Catechin on Blood Glucose Levels, Serum Lipid Profile and Liver and Kidney Functions in Diabetic Rats. Jordan Journal of Biological (JJBS). 7(1): 7 – 12. Phongnarisorn, B., Orfila, C., Holmes, M., Marshall, L. J.2018. Enrichment of Biscuits with Matcha Green Tea Powder: Its Impact on Consumer Acceptability and Acute Metabolic Response. Foods. 7, 17: pp. 15

PPTK. 2008. PetunjukTeknisPengolahanTeh. Bandung: Pusat Penelitian The dan Kina.

Rahardjo, M., Wahyu, F. D., Nadia, T. 2020. Karakteristik Fisik, Sensori, Serta Aktivitas Antioksidan Roti Gandum dengan Tambahan Serbuk Teh Hijau. Jurnal Pangan dan Agroindustri. **8(1):** 47-55

Shen, X. J., Han, J.Y. , Ryu, G. H. 2014. Effects of the addition of green tea powder on the quality and antioxidant properties of vacuum-puffed and deep-fried Yukwa (rice snacks). LWT - Food Science and Technology 2014.; **55(1):** 362–367.

Singh-Ackbarali, D., Maharaj, R. 214. Sensory Evaluation as a Tool in Determining Acceptability of Innovative Products Developed by Undergraduate Students in Food Science and Technology at The University of Trinidad and Tobago. Journal of Curriculum and Teaching., **3(1)**: 10-27.

Yang, J. M., Lee, J. 2020. Consumer perception and liking, and sensory characteristics of blended teas. Food Sci Biotechnol. **29(1):** 63–74.

JJBS

Volume 14, Number 3, September 2021
ISSN 1995-6673
Pages 587 - 592

Jordan Journal of Biological Sciences

Biological Traits of Azotobacter Isolated from Marginal Soils and their Resistance to Tetracycline

Reginawanti Hindersah[1,*], Priyanka Asmiran[2], Etty Pratiwi[3], Tualar Simarmata[1]

[1]*Faculty of Agriculture Universitas Padjadjaran Jalan Raya Bandung-Sumedang Km. 21, Jatinangor, Sumedang 45363, Indonesia;*
[2]*Graduated from Soil Science Master Program, Faculty of Agriculture, Universitas Padjadjaran, Indonesia;*[3]*Soil Research Institute, Jalan Tentara Pelajar 12, Bogor 16114, Indonesia;*

Received: February 27, 2021; Revised: May 26, 2021; Accepted: July 19, 2021

Abstract

Multiple stress in soil due to abiotic and biotic stressor are the constraints of plant production. Human activity contributes to soil abiotic stress such as salt and heavy metal accumulation, and biotic stress cause by soil tetracycline contamination from manure. Nitrogen-fixing Azotobacter enable to increase plant growth and perform the biological activities in stressed soil. The objective of laboratory experiment was to determine the plant growth-related properties of some strain of Azotobacter isolated from saline and mercury-contaminated soil. Five isolates of Azotobacter were grown in liquid medium prior to nitrate, phytohormones, organic acids, and phosphatase analysis. All isolates were then tested for their susceptibility of tetracycline. Based on antibiotic resistance test, two Azotobacter isolates were further assessed for their ability to proliferate and produce exopolysaccharide in tetracycline-contaminated broth. The results verified that the five Azotobacter isolates produced different amounts of important metabolites for plant growth. Azotobacter c2a9 and K4 isolated from mercury- and salt-contaminated soil can respectively proliferate in the liquid culture with 5 mg/L-87.5 mg/L tetracycline. In the presence of 100 mg/L tetracycline, their growth was limited but they still produced low concentration of exopolysaccharides. This experiment suggested that Azotobacter has a potency to improve plant growth in the multiple-stressed soil.

Keywords: Azotobacter, Cell viability, Mercury contaminated soil, Metabolites, Saline soil, Tetracycline

1. Introduction

Soil is a natural reservoir of antibiotic since certain soil microbes produce antibiotic as defense mechanisms to other microbial attack (Massadeh and Mahmoud, 2019). Bacteria and fungi in soil are reported to produce antibiotic-like compounds and antibiotics such as streptomycin, and tetracycline (Al-Saraireh et al., 2015; Chandra and Kumar, 2017). Handling the livestock's health with antibiotics and then adding their manure in agricultural soil can increase antibiotic content in soil (Cycoń *et al*., 2019). Soil antibiotic residue due to frequent use of manure in agriculture can cause biotic stress to soil microbes as well as plants.

Tetracyclines are a broad-spectrum antibiotic frequently used for veterinary practice due to their low cost (Granados-Chinchilla and Rodríguez, 2017). A total of 93 countries used tetracycline commonly for animals compared to another antimicrobial agents (OIE, 2020). The concentrations of tetracycline in pig and poultry manure were ranging from a few of mg/kg to hundreds of mg/kg (Ghirardini *et al*. 2020). Tetracyclines contamination in soil may induce soil microbial resistant (Wepking *et al*., 2017). The presence of tetracycline in soil is reported to affect the seedling appearance and metabolic activities due to chlorophyll degradation (Margas *et al*., 2019). Despite the risk of antibiotic increment in soil, manure amendments are always recommended to increase the soil health and crop production of marginal soil in tropics.

Abiotic and biotic stress in soil reduces plant productivity and limits soil microbial activity in maintaining soil nutrient cycles. Soil stress induced by escalated concentration of metallic ions, salts and antibiotics disturbs microbial metabolism and hence their proliferation and function. Nowadays, plant growth promoting rhizobacteria (PGPR) is progressively used as a biofertilizer in sustainable agriculture. The application of PGPR in marginal soils might decrease the ability of microbes to multiply and their function related to their biological characteristics. Introduction of multiple-stress resistance PGPR has a potency to overcome those issues.

The Azotobacter is well known PGPR widely used as biofertilizer for food crops production. The mechanisms by which Azotobacter induce plant growth and productivity are nitrogen (N) fixation; phytohormones, organic acids and exopolysaccharides (EPS) production; and phosphate solubilizing. Inoculation of Azotobacter on important food crops are reported to increase N content in soil and plant growth (Kurrey *et al*., 2018; Hindersah *et al*., 2018; Mahato and Kafle, 2018; Suárez-Moreno *et al*., 2019).

Researchers reported the ability of Azotobacter to produce phytohormones Indole Acetic Acid (IAA) and Cytokinines (CKs) in liquid culture (Viscardi *et al*., 2016; Chobotarov *et al*., 2017; Hindersah *et al*., 2020). The CKs include zeatin, zeatin-riboside dan zeatin glucose also detected in nanoparticle solid-based inoculant (Chobotarov

* Corresponding author e-mail: reginawanti@unpad.ac.id.

et al., 2017). The Azotobacter produces low-molecular weight organic acids for releasing phosphate ions from insoluble inorganic phosphor (Nosrati *et al*., 2014; El-Badry *et al*., 2016). However, the organic acid profile of Azotobacter has not been studied intensively.

The resistance of Azotobacter to mercury (Hg) and salinity has been documented. In the presence of 100, 1,000 and 1,200 mg/L Cadmium (Cd), Chromium (Cr) and Nickel (Ni), *A. chroococcum* CAZ3 produced certain metabolites to avoid cell damage (Rizvi *et al*., 2019). At least four Azotobacter isolates withstand high temperatures and low pH (5-5.5) were able to grow on media containing 2% of NaCl. Azotobacter S2 was resistant to 3.4 % NaCl but their growth was limited compared with the growth in the liquid media with 1.7% (Hindersah *et al*., 2019).

Naturally, Azotobacter synthesize EPS on cell wall surface to protect nitrogenase from oxygen during nitrogen fixation. The EPS is a major mechanism by which bacteria adapt to the presence of cationic metal in their surroundings (Gupta and Diwan, 2017; Ventorino *et al*., 2019; Abd El-Ghany *et al*., 2020). The mechanisms of bacterial resistance to tetracycline (drug) may be native to the microorganisms (Reygaert, 2018). The EPS play a significant role in formation of biofilms which induce the tolerance to antibiotics and other external stress (Sharma *et al*., 2019) to benefit the agriculture in contaminated soil.

The inoculation of Azotobacter in marginal soils with multiple stress might reduce their viability, and their natural function related to plant growth promotion. So that introduced Azotobacter have to be resistance to soil stress. The objective of this laboratory experiment was to verify the plant growth-related properties of some strains of mercury- and saline-resistance Azotobacter; and their ability to proliferate and produce EPS in tetracycline-contaminated broth.

2. Materials and Methodes

The research was conducted on February 2018 to July 2018 in Soil Biology Laboratory of Faculty of Agriculture, Universitas Padjadjaran, West Java, Indonesia. All Azotobacter isolates belong to Soil Biology Laboratory. The Azotobacter bd3a and Azotobacter c2a9 were isolated from mercury-contaminated gold tailing at Buru Regency, Maluku Province, Indonesia. The Azotobacter K4 and Azotobacter S2 were isolated from saline soil (EC 4 ds/cm) of paddy field in Karawang Regency, West Java, Indonesia. The control isolate, *A. chroococcum* BT1, was isolated from corn rhizosphere grown in uncontaminated Inceptisols soil. In vitro experiment consisted of four sub process (Figure 1). Five Azotobacter isolates were tested in the 1st to 3rd experiment.

The 4th experiment was carried out for two Azotobacter isolates selected from tetracycline resistance test. The 1st - 3rd experiments were setup in completely block design with five replications. Analysis of variances ($p \leq 0.05$) were performed to verify the effect of treatments on the parameters. The 4th experiment was performed in triplicate without analysis of variance.

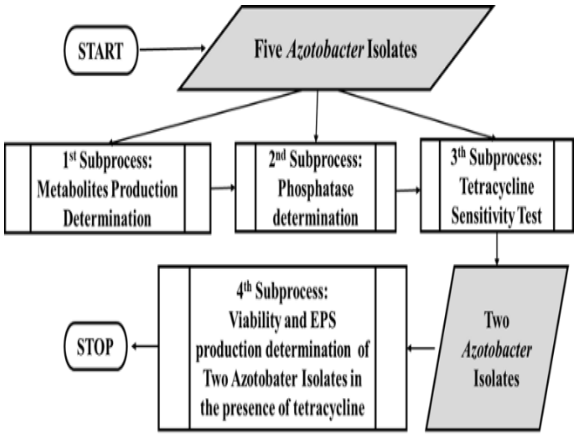

Figure 1. The process of laboratory experiment by using five isolates of N-fixing Azotobacter

2.1. Determination of nitrate, phytohormones and organic acid production

Each isolate was cultured in individual 100-mL Erlenmeyer contained 50 mL of N-free Asbhy's mannitol broth (Mannitol 20 g, Dipotassium phosphate 0.2 g, Magnesium sulfate 0.2 g, Sodium chloride 0.2 g, Potassium sulfate 0.1 g, Calcium carbonate 5 g). The culture then incubated for 72 hours at room temperature (24-27 ^{0}C) on the 115-rpm gyratory shaker.

At the end of incubation, Azotobacter liquid culture was centrifuged 10,000 rpm at 4 ^{0}C for 10 minutes. Supernatants were collected for metabolites measurement. Nitrate quantification was carried out by using Kjeldahl Methods (AOAC, 2012; Sáez-Plaza *et al*., 2013). The presence of phytohormones IAA was determined by spectrophotometer at 510 nm after mixing 1 mL supernatant with 4 mL Salkowski reagents (Rahman *et al*., 2010). Supernatant was extracted with ethyl acetate (Hussain and Hasnain, 2009) prior to zeatin and kinetin quantification by using phase reserved High Performance Liquid Chromatograph at the wave lengths of 254 nm and 270 nm, respectively.

Organic acids in the supernatant were analyzed by using phase reserved. Supernatant was filtered using 0.2 µm Whatman paper number 1. The five organic acid standards and samples were injected into C18 column in isocratic conditions with 50 mM Potassium dihydrogen phosphate as mobile phase. The measurement of organic acids was carried out at a wavelength of 210 nm.

2.2. Determination of Soluble phosphate and phosphatase activity

Azotobacter isolates were grown in Pikovskaya broth (Yeast extract 0.5 g, Dextrose 10 g; Tricalcium phosphate 5.0 g, Ammonium sulfate 0.5 g, Sodium chloride 0.2 g, Magnesium sulfate 0.1 g, Mangan (II) sulfate 0.0001 g, Ferrous sulfate 0.0001g) for 5 days at room temperature at shaking period of 115 rpm. The soluble phosphate was then determined by spectrophotometer at 880 nm (Behera *et al*., 2017). Azotobacter were grown in Pikovskaya broth for 3 days at room temperature prior to acid phosphatase activity measurement. The supernatant of bacterial culture was mixed with Disodium p-nitrophenyl phosphate (tetrahydrate). Phosphatase activity was defined based on the concentration of p-nitrophenol at 420 nm using UV–Vis spectrophotometer (Behera *et al.*, 2017).

2.3. Tetracycline resistance test

Tetracycline resistance assay for five Azotobacter isolates was performed with five antibiotic concentrations included 15, 20, 50, 100 and 1,000 mg/L by using the disk diffusion susceptibility method (Jorgensen and Turnidge, 2015). A total of 1 mL liquid mother culture of Azotobacter was spread evenly on the surface of Ashby's plate agar and left 10 minutes at room temperature. Sterilized filter papers were impregnated with each antibiotic solution and placed on the surface of plate agar. The control treatment was sterilized water. All plates were incubated for 5 days at 30 ^{0}C prior to measure the inhibition zone around the antibiotic disk.

2.4. Cell viability and exopolysaccharides production in the presence of tetracycline

Based on the third experiment, plate agar of Azotobacter c2a9 and Azotobacter K4 showed smaller halo zone around paper disk dipped on 100 mg/L and 1,000 mg tetracycline compared with another isolates. Both isolates were then used in the last experiment to test their viability and EPS production in the presence of 50 mg/L -100 mg/L tetracycline. A total of 1% Azotobacter c2a9 and Azotobacter K4 pure liquid culture were inoculated separately into 50 mL Ashby broth contained 50, 62.5, 75, 87.5 and 100 mg/L tetracycline. All cultures were incubated on the gyratory shaker for 72 h at room temperature. Every experimental unit was carried out in triplicate. Asbhy's broth for the control treatments received no tetracycline. Population of Azotobacter was determined by serial dilution plate method (Pal *et al*., 2017). Exopolysaccharides content in liquid culture were determined by gravimetric method after extracted the EPS from supernatant by cold acetone (Hindersah *et al*., 2017)

2.5. Data analysis

The data of 1^{st,} 2nd and 3rd trial were subjected to analysis of variance (F test at p≤0.05). If the sum square of treatments was significant for measured parameters than Duncan multiple range tests were performed at p≤ 0.05.

3. Results

In Table 1 – Table 4, numbers in a column followed by the same letter were not significantly different based on Duncan's multiple range test (P≤0.05). Data depicted in Table 5 were not subjected to statistical analysis.

3.1. Plant growth promoting related biological traits

All isolates provided nitrate and produced IAA as well as zeatin, but they did not produce kinetin in Ashby's broth at 72 h after inoculation (Table 1). Duncan's test showed that nitrate content in the culture of all isolates was not significantly different. The IAA content in the bacterial supernatant significantly determined by the isolate but zeatin production by all isolates was not significantly different. In general, Azotobacter isolated from marginal soil demonstrated high IAA production compared with BT1 isolated from rhizosphere of maize grown in uncontaminated soil. The Azotobacter bd3a isolated from Hg-contaminated gold tailing produced highest IAA. Nonetheless, Azotobacter K4 isolated from saline soil produced lower IAA concentration than *A. chroococcum* BT1. All Azotobacter isolates released the same amount of zeatin.

Various composition of organic acids released by different isolates was shown after 72 h incubation (Table 2). The result showed that there was no significant difference in the concentration of maleic acid produced by the bacteria, but their oxalic and lactic acid production were different. Only Azotobacter bd3a and K4 excreted tartaric-acid into the broth. However, no acetic-acid was found in all culture. The Azotobacter BT1 (bacterial control) produced highest oxalic acid but lowest lactic acid compared with the Azotobacter isolated from contaminated sites. The acidity (pH) of every broth culture were decreased from 7 before trial to about 6 (data were not presented).

Table 1. Nitrate and phytohormones content in N-free liquid culture of five different isolates of Azotobacter

Azotobacter isolates	NO_3^- (mg/L)	IAA (mg/L)	Zeatin (mg/L)
BT1	123.4 a	9.0 a	0.151 a
bd3a	103.6 a	32.5 c	0.148 a
c2a9	118.4 a	20.2 b	0.143 a
K4	88.8 a	6.5 a	0.156 a
S2	108.6 a	23.4 b	0.155 a

Table 2. Organic acid production by five different isolates of Azotobacter in N-free liquid culture

Azotobacter isolates	Organic acids (mg/L)			
	Oxalic	Maleic	Lactic	Tartaric[a]
BT1	51.8 b	0.16 a	6.6 a	nd[b]
bd3a	14.6 a	0.15 a	11.7 b	1.4
c2a9	17.6 a	0.15 a	7.6 a	nd
K4	15.9 a	0.15 a	10.5 b	3.9
S2	14.3 a	0.15 a	11.8 b	nd

[a]Statistical analysis has not been performed on tartaric acid trait due to incomplete data, [b]nd, not detected

Available phosphate production and phosphatase activity depend on Azotobacter isolates (Table 3). Azotobacter c2a9 and Azotobacter S2 demonstrated the highest ability to produce soluble phosphate in liquid culture although it was not significantly different with the control (BT1). The higher phosphatase activity was shown by BT1 as well as c2a9 and S2 isolated from mercury-contaminated and saline soil, respectively.

Table 3. Soluble phosphate and phosphatase activity of Azotobacter isolates in Pikovskaya broth with calcium phosphate

Azotobacter isolates	Soluble phosphate (mg/L)	Phosphatase activity (Unit/mL)
BT1	0.24 c	0.62 c
bd3a	0.05 a	0.14 a
c2a9	0.31 c	0.78 c
K4	0.16 b	0.41 b
S2	0.34 c	0.87 c

3.2. Azotobacter Resistance to Tetracycline

Tetracycline assay showed that Azotobacter proliferation was repressed in the presence of higher concentration of tetracycline. Azotobacter isolate influenced the diameter of inhabition zone (Table 4). The absence of clear zones surrounding disk paper of 15 mg/L tetracycline indicated that all isolates were resistance to the tetracycline ≤ 15 mg/L. The halo zone measurement demonstrated that Azotobacter BT1, bd3a, c2a9 and K4 enabled to proliferate in the presence of 20 mg/L and 50 mg/L without being inhibited by tetracycline. The Azotobacter K4 was the most resistant to 100 mg/L tetracycline compared with other isolates from marginal soil. All isolates included BT1 (control) were susceptible to 1,000 mg/L tetracycline. Table 4 showed that Azotobacter c2a9 and K4 were more resistant to higher concentration of tetracycline than other isolates.

Table 4. Zone inhibition diameter around disk paper of different concentration of tetracycline on Azotobacter

Azotobacter isolates	Diameter of halo zone (cm) for each tetracycline concentration (mg/L)					
	C[a]	15	20	50	100	1,000
BT1	0	0	0	0	0.00 a	2.76 b
bd3a	0	0	0	0	0.67 ab	2.46 b
c2a9	0	0	0	0	0.56 ab	2.43 b
K4	0	0	0	0	0.26 a	1.73 a
S2	0	0	0.56	0.86	1.16 b	2.53 b

[a]Control without tetracycline

3.3. Cell viability and EPS production in the presence of tetracycline.

Based on the third experiment, Azotobacter c2a9 and K4 (Fig 2) were more resistant to tetracycline. Nonetheless, a higher amount of tetracycline decreased the population of both isolates (Table 5). A clear reduction of c2a9 population was only shown in the presence of 87.5 and 100 mg/L of tetracycline; meanwhile, 50-100 mg/L tetracycline reduced the growth of K4. Table 5 showed that in the presence of tetracycline, the EPS content in liquid culture of c2a9 and K4 was lower than the control. A decreased amount of EPS of both isolates was related to the increase in tetracycline concentration.

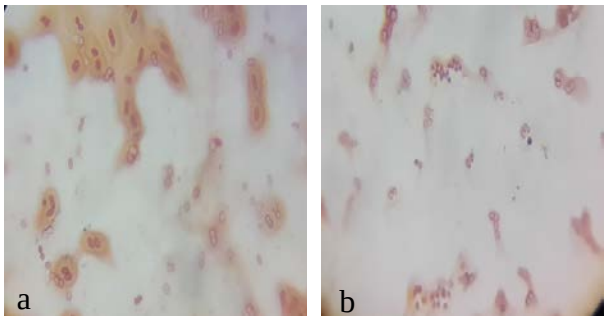

Figure 2. Cell morphology of cocci Gram-negative Azotobacter c2a9 (a) and K4 (b)

Table 5. Azotobacter count in N-free broth of c2a9 and K4 isolates contaminated with tetracycline.

Tetracycline (mg/L)	Bacterial Population (log_{10} of cfu/mL)		EPS (mg/L)	
	c2a9	K4	c2a9	K4
0	5.48	5.48	34.4	29.7
50	5.42	0.00	27.1	25.7
62.5	5.23	1.00	21.8	22.7
75	5.32	0.00	17.3	20.7
87.5	2.78	0.00	15.3	13.8
100	0.00[a]	0.00[a]	9.07	5.72

Value is an average of three replications. [a]The colonies did not grow in plate agar with the culture from 10^{-2} dilution.

4. Discussion

The research confirmed that five Azotobacter isolates had a plant growth promoting related traits. The first experiment verified the presence of nitrate in cell-free supernatant extracted from N-free liquid culture that proved the N fixation occurred in N-free broth. The presence of IAA and Zeatin in liquid culture verified that synthesis of phytohormones by bacteria was taken place in diazotrophic condition. Phytohormones released by Azotobacter were depending on the isolates. The five isolates produced 9.0-32.5 IAA, the high IAA production were shown by isolates bd3a (32.5 mg/L) and S2 (23.4 mg/L).

The result demonstrated that IAA released by bd3a was more or less equal to IAA production by *A. chroococcum* 67B and 76, which were 28 mg/L and 34 mg/L respectively. The lower phytohormones production has been shown by *A. chroococcum* and *A. vinelandii* that only produce 0.52 mg/L and 0.82 mg/L of IAA (Hindersah *et al*., 2020). A significant amount of organic acids was detected in liquid culture of Azotobacter and hence reduced the culture pH from neutral to slightly neutral. Despite of the prominent role of organic acid to provide P for plant through P solubilizing, the research about organic acid production by Azotobacter is still limited. Moreover, all isolates demonstrated the ability to produce soluble P and phosphatase activity.

This experiment showed that all Azotobacter isolates produced soluble phosphate in Pikovskaya broth due to calcium phosphate solubilizing by organic acid. The phosphatase activity proved the ability of Azotobacter to carry out organic P mineralization catalyzed by phosphatase to produce available P. The result agrees with the ability of some Azotobacter isolates that have phosphate solubilizing index ranging from 1.2 to 3.5 during 7-day incubation (Nosrati *et al*., 2014). More recent research demonstrated that *A. vinelandii* reach maximum phosphate solubilizing (25.3%) in the presence of inorganic phosphate after 3 days by lowering the pH of Pikovskaya broth (El-Badry *et al*., 2016). The decrease of pH is caused by organic acid production by five Azotobacter isolates in our finding.

The growth of Azotobacter isolated from marginal soil was inhibited by higher concentration of tetracycline. The experiment showed that all Azotobacter isolates were susceptible to 100 and 1,000 mg/L tetracycline but the halo

zone around Azotobacter c2a9 and K4 colonies was lower compared with other isolates. The Azotobacter K4 was more susceptible to tetracycline compared with c2a9. In the last experiment, Azotobacter c2a9 and K4 released 34.4 mg/L and 29.7 mg/L respectively in broth without tetracycline. Slight reduction of EPS production in broth with 62.5 mg/L and 50 mg/L verified their resistance to tetracycline. However, both isolates did not show resistance to high levels of tetracycline due to cell growth restriction. The increase of EPS by Azotobacter c2a9 and K4 in the presence of tetracycline might be related to bacterial protection against antibiotic by biofilm formation since EPS is a key element of biofilm extracellular matrix (Abebe, 2020).

Tetracycline is a broad-spectrum antibiotic; their targets are membrane system of Gram positive and negative bacteria. The resistance of Azotobacter to tetracycline is important for maintaining their proliferation and function include nitrogen fixation, as well as phytohormones, organic acids and EPS production. Some strains of *A. chroococcum* are resistant to 10 µg/ml of ampicillin, chloramphenicol, erythromycin, kanamycin, rifampicin, streptomycin, tetracycline and trimethoprim has been reported (Sindu *et al*., 1989).

Azotobacter might have a resilience for adapting to multitude environmental threats, including the presence of mercury, salt and tetracycline molecule. This intrinsic adaptation can maintain Azotobacter existence in plant-rhizobacteria interaction that is very important for cycling the essential macronutrient nitrogen and promoting plant growth as well.

5. Conclusion

The Azotobacter isolated from marginal soil produced some important metabolites for improving plant growth. The available N (nitrate) was found in N-free broth after Azotobacter inoculation that showed bacterial ability to fix nitrogen. Every Azotobcter isolates produce IAA and Zeatin as well. The bacteria produce organic acid which might be related to their properties in P solubilizing. Azotobacter c2a9 and K4 isolated from Hg-contaminated and saline soil respectively have the ability to proliferate in the presence of less than 87.5 mg/L tetracycline. They also produce EPS in liquid media with tetracycline up to 100 mg/L although the EPS content is reduced significantly at higher concentration of tetracycline. The results verified that Azotobacter c2a9 and K4 isolated from abiotic stressed soil have the resistance to 87.5 mg/L tetracycline.

Acknowledgements

For the most part, this research was funded by Academic Leadership Grant of Universitas Padjadjaran. Isolation of Azotobacter from Hg-contaminated tailing and their resistance to Hg was funded by former Maluku Corner of Universitas Padjadjaran. The first author thanks the Head of Microbiology Laboratory at Soil Research Institute, Ministry of Agriculture in Bogor.

References

Abebe GM. 2020. The role of bacterial biofilm in antibiotic resistance and food contamination. *Int J Microbiol*., **2020**: 1705814.

Abd El-Ghany MF and Attia M. 2020. Effect of exopolysaccharide-producing bacteria and melatonin on faba bean production in saline and non-saline soil. *Agronomy*, **10(3)**: 316.

Al-Saraireh A, Al-Zereini WA and Tarawneh KA. 2015. Antimicrobial activity of secondary metabolites from a soil *Bacillus* sp. 7B1 Isolated from South Al-Karak, Jordan. *Jordan J Biol Sci*., **8(2)**:127 – 132.

AOAC. 2012. **Official Methods of Analysis**, 19th edition. Association of Official Analytical Chemist, Washington DC, USA.

Behera BC, Yadav H, Singh SK, Mishra RR, Sethi BK, Dutta SK and Thatoi HN. 2017. Phosphate solubilization and acid phosphatase activity of *Serratia* sp. isolated from mangrove soil of Mahanadi river delta, Odisha, *India J Genet En Biotechnol*., **15**: 169–178.

Chandra N and Kumar S. 2017. Antibiotics producing soil microorganisms. In Hasmi et al. (Eds). **Antibiotics and Antibiotics Resistance Genes in Soils: Monitoring, Toxicity, Risk Assessment and Management**. Springer International Publishing AG, Switzerland, pp 1–18.

Chobotarov A, Volkogon M and VoytenkoL IK. 2017. Accumulation of phytohormones by soil bacteria azotobacter vinelandii and Bacillus subtilis under the influence of nanomaterials. *J Microbiol Biotechnol food Sci*., **7(3)**: 271-274.

Chun JA, Lim C, Kim D and Kim JS. 2018. Assessing impacts of climate change and sea-level rise on seawater intrusion in a coastal aquifer. *Water*, **10**: 357.

Cycoń M, Mrozik A and Piotrowska-Seget Z. 2019. Antibiotics in the soil environment—degradation and their impact on microbial activity and diversity. *Front Microbiol*., **10**: 338.

El-Badry MA, Elbarbary TA, Ibrahim IA and Abdel-Fatah YM. 2016. *Azotobacter vinelandii* Evaluation and optimization of Abu Tartur Egyptian phosphate ore dissolution. *Saudi J Pathol Microbiol.*, **1(3)**: 80–93.

Ghirardini A, Grillini V and Verlicchi P. 2020. A review of the occurrence of selected micropollutants and microorganisms in di_erent raw and treated manure-environmental risk due to antibiotics after application to soil. *Sc Total Environ.*, **707**: 136118.

Granados-Chinchilla F and Rodríguez C. 2017. Tetracyclines in food and feeding stuffs: from regulation to analytical methods, bacterial resistance, and environmental and health implications. *J Anal Methods Chem.*, **2017**: 315497.

Gupta P and Diwan B. 2017. Bacterial exopolysaccharide mediated heavy metal removal: a review on biosynthesis, mechanism and remediation strategies. *Biotechnol Rep.*, **13**: 58–71.

Hindersah R, Mulyani O and Osok R. 2017. Proliferation and exopolysaccharide production of Azotobacter in the presence of mercury. *Biodiv*., **8(1)**: 21-26.

Hindersah R, Sulaksana DA and Herdiyantoro D. 2018. Perubahan kadar N tersedia dan populasi Azotobacter di rizosfer sorgum (*Sorghum bicolor* L.) yang ditanam di dua ordo tanah dengan inokulasi *Azotobacter* sp. *Agrologia*, **3(1):** 10-17. In Indonesian, abstract in English.

Hindersah R, Suryatmana P, Setiawati MR, Fitriatin BN, Nurbaity A and Simarmata T. 2019. Salinity resistance of Azotobacter isolated from saline soil in West Java. In Sayyed, RZ (Eds). **Plant Growth Promoting Rhizobacteria (PGPR): Prospects for Sustainable Agriculture**. Springer, Singapore, pp 323–334.

Hindersah R, Setiawati MR, Asmiran P and Fitriatin BN. 2020. Formulation of Bacillus and Azotobacter consortia in liquid cultures: preliminary research on microbes-coated urea. *Int J Agric Syst.*, **8(1)**: 1–10.

Hussain A and Hasnain S. 2009. Cytokinin production by some bacteria: its impact on cell division in cucumber cotyledons. *African J Microbiol Res.*, **3(11)**: 704-712.

Jorgensen JH and Turnidge JD. 2015. Susceptibility test methods: dilution and disk diffusion methods. In Jorgensen JH *et al*. (Eds). **Manual of Clinical Microbiology** 11th Edition. American Society of Microbiology. pp 1253–1273.

Kurrey DK, Sharma R, Lahre MK and Kurrey RL. 2018. Effect of Azotobacter on physio-chemical characteristics of soil in onion field. *The Pharma Innov J.*, **7(2)**: 108-113

Mahato S and Kafle A. 2018. Comparative study of Azotobacter with or without other fertilizers on growth and yield of wheat in Western hills of Nepal. *Ann Agrar Sci*., **16(3)**: 250–256.

Margas M, Piotrowicz-Cieślak AI, Michalczyk DJ and Głowacka K. 2019. A Strong Impact of Soil Tetracycline on Physiology and Biochemistry of Pea Seedlings. *Scientifica*, **2019**: 3164706.

Massadeh MI and Mahmoud SM. 2019. Antibacterial activities of soil bacteria isolated from Hashemite University area in Jordan. *Jordan J Biol Sci.*, **12(4)**: 503 – 511.

Nag NK, Dash B, Gupta SB, Khokher D and Soni R. 2018. Evaluation of stress tolerance of Azotobacter isolates. *Biologija*, **64(1)**: 82–93.

Nosrati R, Owlia P, Saderi H, Rasooli I and Ali Malboobi M. 2014. Phosphate solubilization characteristics of efficient nitrogen fixing soil Azotobacter strains. *Iran J Microbiol.*, **6(4)**: 285–95.

OIE. 2020. **OIE Annual Report on Antimicrobial Agents Intended for Use in Animals: Better Understanding of the Global Situation,** fourth rep. World Organization for Animal Health (OIE), Paris.

Pal P, Khatun N and Banerjee SK. 2017. Potential screening of Azotobacter from soil. *Int J Adv Res*., **5(3):**24-31.

Rahman A, Sitepu I R, Tang S-Y and Hashidoko Y. 2010. Salkowski's reagent test as a primary screening index for functionalities of rhizobacteria isolated from wild dipterocarp saplings growing naturally on medium-strongly acidic tropical peat soil. *Biosci Biotechnol Biochem.*, **74(11)**: 2202–2208.

Reygaert WC. 2018. An overview of the antimicrobial resistance mechanisms of bacteria. *AIMS Microbiol.*, **4(3)**: 482–501.

Rizvi A, Ahmed B, Zaidi A and Khan MS. 2019. Bioreduction of toxicity influenced by bioactive molecules secreted under metal stress by *Azotobacter chroococcum*. *Ecotoxicol.*, **28(1)**: 302–22.

Sáez-Plaza P, Michałowski T, Navas MJ, Asuero AG and Wybraniec S. 2013. An overview of the Kjeldahl method of nitrogen determination. Part I. Early history, chemistry of the procedure, and titrimetric Finish. *Crit Rev Anal Chem.*, **43(4):** 178–223.

Sharma D, Misba L and Khan AU. 2019. Antibiotics versus biofilm: an emerging battleground in microbial communities. *Antimicrob Resist Infect Control*, **8**: 76.

Sindhu SS, Grover V, Narula N and Lakshminarayana K. 1989. Occurrence of multiple antibiotic resistance in *Azotobacter chroococcum*. *Zentralbl Mikrobiol.*, **144(2)**: 97-101.

Suárez-Moreno ZR, Vinchira-Villarraga DM, Vergara-Morales DI, Castellanos L, Ramos FA, Guarnaccia C, Degrassi G, Venturi V and Moreno-Sarmiento N. 2019. Plant-growth promotion and biocontrol properties of three *Streptomyces* spp. isolates to control bacterial rice pathogens. *Front Microbiol*., **10**: 290.

Ventorino V, Nicolaus B, Di Donato P, Pagliano G, Poli A, Robertiello A, Iavarone V and Pepe O. 2019. Bioprospecting of exopolysaccharide-producing bacteria from different natural ecosystems for biopolymer synthesis from vinasse. *Chem Biol Technol Agric.*, **6**: 18.

Viscardi S, Ventorino V, Duran P, Maggio A, De Pascale S, Mora ML and Pepe O. 2016. Assessment of plant growth promoting activities and abiotic stress tolerance of *Azotobacter chroococcum* strains for a potential use in sustainable agriculture. *J Soil Sci plant Nutr.*, **16(3)**: 848–63.

Wepking C, Avera B, Badgley B, Barrett J E, Franklin J, Knowlton K F, Ray P P, Smitherman C and Strickland MS. 2017. Exposure to dairy manure leads to greater antibiotic resistance and increased mass-specific respiration in soil microbial communities. *Proc Royal Soc B.*, **284(1851)**: 20162233.

JJBS

Volume 14, Number 3, September 2021
ISSN 1995-6673
Pages 593 - 599

Jordan Journal of Biological Sciences

Microbes-Coated Urea for Reducing Urea Dose of Strawberry Early Growth in Soilless Media

Reginawanti Hindersah[1,*], Indyra Rahmadina[2], Betty Natalie Fitriatin[3], Mieke Rochimi Setiawati[2], Diky Indrawibawa[3]

[1]*Faculty of Agriculture, Universitas Padjadjaran, Jalan. Raya Bandung-Sumedang Km. 21, Jatinangor, Sumedang 45363, Indonesia*
[2]*Graduated from Agrotechnology Undergraduate Program, Faculty of Agriculture, Universitas Padjadjaran, Indonesia*
[3]*Bumi Agrotechnology Farm, Kp. Kebon Cau, Jalan Mekartani, Kertawangi Village, Cisarua District, Bandung Barat Regency, Indonesia*

Received: February 27, 2021; Revised: May 17, 2021; Accepted: July 19, 2021

Abstract

Strawberry is a high-value fruit in Indonesia. During the growth phase for transplant production, farmers applied conventional urea that is easy to volatile and leach. Coated Urea has proven to reduce nitrogen (N) losses from urea fertilizer. Microbial-coated urea application is a reliable way to limit the loss of N from urea and at the same time increase the use of biofertilizer. Azotobacter and Bacillus are widely used as a biofertilizer formulation. This experimental objective was to determine the effect of two formulations and doses of urea coated with solid organic inoculant of Azotobacter and Bacillus on the growth parameters of strawberry seedling as well as reducing urea fertilizer. The green house experiment was carried out in randomized completely block design (RCBD) with five treatments and five replications. One-month old strawberry cv Festival seedlings were grown in coco peat based organic substrate. The seedlings were treated with four combinations of two doses and formulation of microbial coated urea (MCU). Control seedlings received a dose of conventional prilled urea. The results showed that MCU affected root dry weight, root volume, root to shoot ratio, SPAD value, and N uptake but did not significantly affect shoot parameters compared to controls. The best composition of urea coated material was compost-based inoculant enriched with 5% zeolite and 5% liquid inoculant. Moreover, this experiment explained that microbial-coated urea might replace 50% of conventional urea.

Keyword: Bacteria coated Urea, *Azotobacter* sp., *Bacillus* sp., Zeolite, Fertilizers doses, Strawberry growth

1. Introduction

Strawberries (Fragaria × Ananassa Duch) grow well in Indonesian mountainous area with good physical soil properties. Farmers in high land Bandung and Bandung Barat Regency cultivate the strawberries since decade ago with significant economic benefit. Strawberry productivity and quality in Indonesian high land are limited by the nutrients management. In general, farmers propagate the strawberry from runner, well known as stolon, that grow above the ground. The new clone will grow and can be separated from the mother plant once the stolon roots touch the soil.

Some strawberry producers have carried out strawberry nurseries to produce strawberry using soilless growth media composed of coco peat and manure (Ameri *et al*., 2012; Raja *et al*., 2018). Compared to soil, this medium contains only a few nutrients but its physical properties are good for rooting. Farmers in Bandung Regency applied chemical fertilizer, urea and NPK compound as well, to provide nutrient during bare-root strawberry transplant production.

The disadvantage of using urea is ammonia volatilization at high temperatures environment (Fan *et al*., 2011; Jadon *et al.,* 2018). Increasing temperature from 20 to 30 °C enhanced NH_3 volatilization with higher loss recorded in sandy soil than loamy soil (Fan *et al*., 2011). Urea can be easily leaching from root zone since the precipitation is higher over the water holding capacity (Burger and Jackson, 2003; Wang *et al*., 2015). To overcome the constraints, coated urea has been recommended as a reliable way to slow and control N release from urea (Bibi *et al*., 2016). Ground application of neem-and oleoresin-coated urea reported to reduce the ammonia volatilization and nitrate leaching significantly (Jadon *et al*., 2018).

We have limited information about fertilizer/urea coated with beneficial microbes. Researchers have shown the effectivity of microbes-coated urea (MCU) to reduce the level of chlorinated pesticide and the persistent organic pollutant in soil (Wahyuni *et al*., 2016). Ahmad *et al* (2017) stated that bacterial-impregnated ammonium phosphate enhancing nitrogen (N) and phosphorus (P) use efficiency of wheat. Coating urea with soil beneficial microbes such as the N-fixing *Azotobacter* and the phosphate solubilizing *Bacillus* is also a way to enhance the beneficial microbe application. *Azotobacter* and *Bacillus* are the active ingredients of biofertilizer suggested to provide nutrients and ensure plant growth through N fixation and phosphate solubilization respectively (Rubio *et al*., 2013; Saeid *et al*., 2018). Both

* Corresponding author e-mail: reginawanti@unpad.ac.id.

rhizobacteria produced phytohormones of auxins cytokinins, gibberellins (Fitriatin *et al*. 2020; Hindersah *et al*., 2019; Hindersah *et al*. 2020a) which is beneficial to stimulate root and subsequent plant growth (Bhattacharyya and Jha. 2012). The *Azotobacter* and *Bacillus* form cysts and spores (Rodriguez-Salazar *et al.*, 2017; Tan and Rammurthi, 2014) as a response to drought stress. However, farmers in Indonesia are rarely including the biofertilizer in their nutrient management since the labor cost will increase when the biofertilizer is applied separately from the urea. Coating urea with the microbes might overcome this constraint.

Nitrogen and P are essential macronutrients and determine plant productivity. The advantage of N-fixer Azotobacter and P-solubilizer Bacillus inoculation in strawberry cultivation have been documented to increase significant growth and yield in field and greenhouse as well (Mishra and Tripathi, 2011; Shternshis *et al.*, 2015; Reddy and Goyal, 2021). Moreover, Bacillus can control the diseases and induce plant resistance to the strawberry diseases (Shternshis *et al*., 2015; Wei *et al*., 2016).

We have already developed a mixed liquid biofertilizer containing *A. chroococcum, A. vinelandii, B. subtilis* and *B. megaterium* with the equal composition to maintain each bacterial population up 10^8 CFU/ml (Hindersah *et al*., 2020b). For coating the urea, a solid inoculant is needed to avoid direct intact with urea and ensure the bacterial viability since the water content of urea is as low as 0.5%.

Based on previous research, an effective carrier for maintaining the population of both microbes was 200-mesh compost enriched with 100-mesh zeolite at 15% moisture content (Hindersah *et al.*, 2020a). The level zeolite and liquid inoculant in solid inoculant formultion is also essential prior to urea coating. Furthermore, compost-based solid inoculant with 5% Zeolite + 5% Liquid as well as 1% zeolite and 10% liquid Inoculant supported Azotobacter and Bacillus count at 10^9 and 10^{11} CFU/g respectively during 4 weeks of storage (Hindersah *et al*., 2021). In the formulation described above, the molecule structure of zeolites functions in adsorbing water (Tatlier *et al*, 2018) to maintain low water content in carrier and further coated urea fertilizer.

Biofertilizers are now integrated in horticultural crops production for decreasing the level of chemical fertilizer and increasing the soil health. However, the price of microbial-coated urea might be higher over the conventional urea. The use of coated urea will be efficient for high value horticultural products such as strawberry in Bandung Regency, and then research to optimize the application of these newer coated urea is needed. The effectiveness of the urea coated with Azotobacter-Bacillus consortium on the growth of strawberry seedlings, especially the morphological parameters, needs to be verified prior to the wider use by the farmers. The objective of this greenhouse experiment was to determine the effect of solid inoculant-coated urea on the growth properties of strawberry seedlings grown in soilless media for 4 weeks during bare-roots strawberry seedling production.

2. Material and Methods

Greenhouse trials were conducted from October 2019 to March 2020 at Bumi Agrotechnology Farm in Cisarua, Bandung Barat Regency at the altitude of 1,225 m above sea level. The location situated in tropics with average annual temperature 17-26^{o}C and humidity 70-90%. Urea was coated with solid inoculant of N-fixing *A. vinelandii* and *A. chrococcum*, and phosphate-solubilizing *B. subtilis* and *B. megaterium* consortia developed by the Soil Biology Laboratory Faculty of Agriculture, Universitas Padjadjaran. Liquid inoculant of all bacteria was prepared in molasses based broth enriched with N source (Hindersah *et al*., 2020b). The Azotobacter and Bacillus produced phytohormone of indole acetic acid (IAA), cytokinins (CK) and gibberellins (GA) in the in-vitro test (Hindersah *et al*., 2020b). The seedlings of strawberry cv. Festival were provided by Bumi Agrotechnology Farm. Four-week old daughter plants of strawberry growing on the tip of stolon have been separated from the mother plant at planting time (Fig 1).

Figure 1. One-month old strawberry seedlings before being cutting from the mother plant and transplant.

2.1. Experimental Establishment

The experiment was setup in completely randomized block design with 5 treatments consisting of 4 combinations of doses and composition of MCU and one control treatment (Fig 2); all treatments were replicated 5 times. Based on previous experiment, two best formulations of solid bacterial inoculant for coating the urea are:

1. 200-mesh cow manure compost enriched with 5% of 100-mesh zeolite and 5% of mixed liquid Inoculant of *Bacillus* and *Azotobacter* (composition I) and
2. 200-mesh cow manure compost enriched with 1% zeolite + 10% liquid inoculant (composition II).

The MCU treatments were the combination of each formula with full and half application doses, so that we have 4 combination treatments of Microbial coated urea (MCU). The doses of MCU were based on the recommended urea dose for strawberry released by Indonesian Agricultural Research and Development Institute, i.e. 200 kg/ha equal to 2 g/plant. Plant with full and half doses received 1 g and 2 g of urea respectively. The control treatment was 2 g of conventional prilled urea.

The 14-cm height of strawberry seedling cv Festival with 5 leaves and 18-20 cm in crown diameter were grown in the substrate contained mixed of coco peat, chicken and sheep manure at volume ratio of 8:2:1. The substrates were

average in N (0.57%), and very low in P_2O_5 (0.035 mg/kg) and K_2O (0.26 mg/100 g) with the C/N 39.74. The media were put in 40x40 cm polyethylene bag and placed in the greenhouse for a week prior to transplant with two strawberry seedlings. One week after transplanting, strawberry seedlings received the MCU that incorporated with the first two 2-cm depth at 10 cm next to the base crown. Inorganic NPK fertilizer (16:16:16) at the rate of 2 g/plant (Palupi *et al*., 2017) was applied two weeks after planting to all treatments. The fertilizer was placing on the circle about 10 cm away from the base crown and covering with the growth medium.

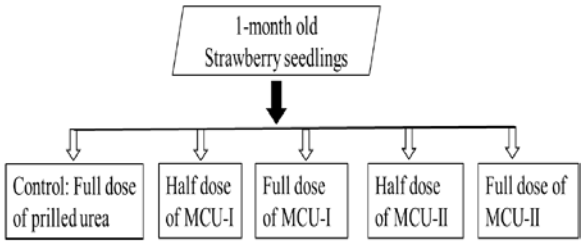

Figure 2. The experimental treatments of microbial coated urea (MCU) application in strawberry seedlings cultivation

2.2. Parameters Measurement

All plants were maintained in the greenhouse for 4 weeks. The data of plant height, root length, crown diameter, root dry weight, root volume, shoot dry weight, root to shoot ratio, chlorophyll unit, as well as N content and N uptake of shoot were taken at the end of trial. Nitrogen uptake represent their accumulation in crops as well as N availability in soil (Gastal and Lemaire, 2002). Root and shoot biomass were dried separately in oven at 70 ^{0}C for two days until constant weight prior to dry weight measurement. Root volume was determined by Water Displacement Method (Pang et al., 2011); roots were immersed in 100 mL water in graduated cylinder with 0.1 ml accuracy measurement. The water volume increment after root immersion was suggested as the roots volume. The crown (thickened stem) diameter of strawberry seedlings was measured from the upper end of the crown using a caliper with 0.1 ml accuracy.

Chlorophyll value of strawberry foliage were estimated using a Soil Plant Analysis Development (SPAD-502) chlorophyll meter (Güler et al., 2006) for the six points in five leaves below the fully opening leaves on the top of shoot. The N content of shoots was analyzed by Kjeldahl Method based on Association of Official Analytical Chemists (AOAC) methods for proximate analysis (AOAC, 2012). The N uptake of shoots was calculated by multiplying the N content of shoot with the shoot dry weight.

2.3. Statistical Analysis

All data were subjected to analysis of variance (F test with $p \leq 0.05$) to verify the significant of sum square on the parameters. The Duncan's multiple range test ($p \leq 0.05$) was then performed when F test was significant. The data were analyzed with IBM SPSS statistics version 25 (Mustafa and Hayder, 2021)

3. Results

MCU-I refers to coated urea with compost-based biofertilizer formulated enriched with 5% zeolite enrichment and inoculated with 5% mixed Azotobacter-Bacillus liquid Inoculant, whereas MCU-II is coated urea with compost-based biofertilizer with 1% zeolite and 10% liquid inoculant.

3.1. Root Parameters

The different dose of MCU integrated with different composition of solid inoculant for coating the urea has not affected the roots length but some treatments increased root dry weight and volume as compared with the control (Table 1). Strawberry seedling received 1 g of urea coated with solid inoculant contained 5% zeolite and 5% liquid inoculant (MCU-I) have highest root dry weight compared to the control and other treatments after 4 weeks in soilless substrate. The root volume of seedling received 1 g urea coated with solid inoculant contained 1% zeolite and 10% liquid inoculant (MCU-II) was higher than other treatments but their root dry weight was slightly lower than seedling with 1 g MCU-I.

Table 1. The effect of dose and microbes-coated urea on roots length dry weight and volume of four-week old strawberry grown in the greenhouse.

Coated Urea Treatments	Root Parameters		
	Lenght (cm)	Dry weight (g)	Volume (ml)
2 g of Prilled Urea (control)	25.3 a	2.7 b	103.2 c
1 g of Microbial Coated Urea -I[a]	25.8 a	5.7 a	110.5 b
2 g of Microbial Coated Urea -I	25.0 a	5.1 a	109.3 b
1 g of Microbial Coated Urea -II[b]	25.2 a	4.4 ab	114.2 a
2 g of Microbial Coated Urea -II	27.8 a	2.9 b	107.5 b

Numbers followed by the same letter didn't significantly differ based on Least Significant Test ($p<0.05$). aCoated urea with compost-based biofertilizer contained 5% zeolite + 5% liquid inoculant; bCoated urea with compost-based biofertilizer contained 1% zeolite + 10% liquid inoculant.

3.2. Shoot Parameters

The results verified that the dose of urea coated with different composition of solid bacterial inoculant has not affected all measured shoot parameter (Table 2). However, reducing the dose of MCU to 50% resulted in equal shoot height and dry weight as well as crown diameter.

Tabel 2. The effect of dose and microbes-coated urea on shoot height and dry weight, and crown diameter of four-week old strawberry grown in the greenhouse

Coated Urea Treatments	Shoot Parameters		
	Dry Weight (gr)	Height (cm)	Crown Diameter (cm)
2 g of Prilled Urea (control)	2.7 a	22.2 a	2.4 a
1 g of Microbial Coated Urea -I[a]	3.1 a	21.3 a	2.4 a
2 g of Microbial Coated Urea -I	2.5 a	20.5 a	2.9 a
1 g of Microbial Coated Urea -II[b]	2.6 a	20.6 a	2.4 a
2 g of Microbial Coated Urea -II	2.8 a	20.2 a	2.5 a

Numbers followed by the same letter didn't significantly differ based on Least Significant Test ($p<0.05$). [a]Coated urea with compost-based biofertilizer contained 5% zeolite + 5% liquid inoculant; [b]Coated urea with compost-based biofertilizer contained 1% zeolite + 10% liquid inoculant.

3.3. Root to shoot ratio

The ratios of root to shoot dry weight (R/S) of strawberry were significantly different among the treatments. Application of 1 g of MCU-I clearly resulted in higher R/S of the plant (Table 3). The R/S mostly > 1 revealed that the root growth was more rigorous than shoot growth. Nonetheless, seedlings treated with either recommended-dose urea or 2 g of MCU-II have R/S <1.

Tabel 3. Change in root to shoot ratio of 4-week old strawberry in the greenhouse after different dose and microbes-coated urea application

Coated Urea Treatments	Root to Shoot Ratio
2 g of Prilled Urea (control)	0.96 c
1 g of Microbial Coated Urea-I[a]	2.53 a
2 g of Microbial Coated Urea-I	1.86 b
1 g of Microbial Coated Urea -II[b]	1.74 b
2 g of Microbial Coated Urea -II	0.94 c

Numbers followed by the same letter didn't significantly differ based on Least Significant Test ($p<0.05$). [a]Coated urea with compost-based biofertilizer contained 5% zeolite + 5% liquid inoculant; [b]Coated urea with compost-based biofertilizer contained 1% zeolite + 10% liquid inoculant.

3.4. Chlorophyll content and N uptake

Chlorophyll unit, percentage of N in shoot and N uptake (mg/plant) of strawberry shoot were influenced by MCU doses and types (Table 4). The result showed that 2 g of MCU-II and 1 g of MCU-I increased the SPAD value compared to the control treatment. The plants treated with 2 g of MCU had the highest SPAD value.

Tabel 4. The effect of dose and microbes-coated urea on SPAD value, and N content and N uptake of 4-week old strawberry shoots

Coated Urea Treatments	SPAD value	Shoot N content (%)	Shoot N uptake (g/plant)
2 g of Urea (control)	26.1 c	2.38 b	0.07 b
1 g of Microbial Coated Urea -I[a]	25.9 cd	2.47 a	0.06 b
2 g of Microbial Coated Urea -I	29.1 b	2.41 a	0.09 a
1 g of Microbial Coated Urea -II[b]	24.8 d	2.19 c	0.07 b
2 g of Microbial Coated Urea -II	31.1 a	2.23 b	0.07 b

Numbers followed by the same letter didn't significantly differ based on Least Significant Test ($p<0.05$). [a]Coated urea with compost-based biofertilizer contained 5% zeolite + 5% liquid inoculant; [b]Coated urea with compost-based biofertilizer contained 1% zeolite + 10% liquid inoculant.

4. Discussion

The experiment found that the effect of MCU was mostly significant for root growth compared to the shoots. Increased root dry weight of MCU-treated plants compared to the control plants was possibly caused by root volume increment. Both Bacillus and Azotobacter produce phytohormones IAA, GA and CK (Hindersah et al., 2020a) which stimulate root growth. Plant treated with lower doses of MCU-I showed the intensive rooting compared to the control or higher doses of MCU.

Phytohormones play a central role on root growth. Plant has endogenous phytohormones, then the balance composition of the three phytohormones associated with well performance of shoot and root growth. Small quantities of IAA produced by soil microbes have been reported to increase root but high concentration inhibit root elongation (Kurepin et al., 2014). The better root growth might relate to the ability of all bacteria to synthesize the CK and GA. The CK is involved in the regulation of many processes in plant development (Kulaeva et al., 2002). The IAA positively interacts with GA in growth regulation, in which the concentration of GA is enhanced in the presence of IAA. The GA also plays an essential role in the normal development of roots, keeping the root long and slender (Tanimoto, 2005). In common, normal roots enable to uptake the water and nutrients optimally.

The MCU supports root growth indicated by higher R/S (Table 3) due to available N slow released from urea and Azotobacter as well. The effect of MCU on the delay of N release has not been yet reported, but coating the urea is already known as controlled-released way to slow down the N release (Bibi *et al., 2016*). The main ingredients of solid inoculant in this experiment were composted cow waste. Organic matter in the surface of urea has a function to prevent high temperature exposure to urea and hence reduce the ammonia volatilization. Microbial solid inoculant can minimize direct contact of water to urea and further reduce nitrate leaving the root zone. This agrees with the reduction of 27.5% in ammonia volatilization and 18.3% in nitrate leaching of neem-coated urea (Jadon *et al*., 2018).

The coco peat-based growth substrate used in this experiment contained average level of total N due to enrichment with animal manure, but Shanmugasundaram *et al*. (2013) state that coco peat contains very low N, P and potassium (K); then N, P and K supplement is considered to be applied. However, mixing coco peat in organic media enables improving the physical properties of the potted substrate and hence supports root growth in limited area of a pot (Singh *et al*., 2016). The good physical properties induce the growth of rhizobacteria utilized in coating the urea. Low N in coco peat induce nitrogenase activity to fix the dinitrogen (N_2) since the abundance of N limited the N fixation (Hoffman et al. 2014). On the other hand, high porosity of coco peat-based substrate cause urea leaching when excessive watering had taken place (Burger and Jackson, 2003; Wang *et al*., 2015).

Strawberry shoot parameters did not influence by MCU at any doses and composition compared to the control. The duration of our experiment was only one month since after that the seedling will be transplanted for strawberry production. A one-month experiment might be too short to demonstrate the effect of MCU on shoot parameters**.** Contrary to our results, positive effect of urea application combined with biofertilizer on plant height was reported for potted and hydroponic strawberry during 60-120 days (Rueda et al., 2016; Beer et al., 2017; Reddy and Goyal, 2020). In their study, application of biofertilizers and N fertilizer increased the plant height, plant spread, number of leaves per plant and crown diameter significantly. Our

results indicated that the reduced dose of MCU maintains the crown diameter. In strawberry, crown as well as roots have an important role as carbohydrate reserve (Menzel and Smith, 2012). The crown size clearly affected strawberry yield under Florida conditions in two-year consecutive seasons (Torres-Quezada et al., 2015). Our strawberry seedling will be utilized in strawberry production; the crown size >10 mm ensures total fruit number compared to < 10 mm (Torres-Quezada et al., 2015).

Only half and full doses of MCU-I increased shoot N content compared to control plant but SPAD value of full dose MCU treatment was higher than the control (Table 4). The Azotobacter fix N_2 to ammonia which is then nitrify to nitrate by nitrifying bacteria (Fiencke et al. 2005). Mostly terrestrial plant uptake the nitrate as N source in the metabolisms (Chapin et al., 2002); with involving of specific transporter of nitrate, NRT (Nacry *et al*., 2013). Highest N content usually related to chlorophyll-a since the chlorophyll-a is substituted tetrapyrrole that contained four N atoms (Berg et al, 2002). The chlorophyll is a central photoreceptor for electron transport in photoautotrophic metabolisms (Berg et al, 2002) in order to generate the energy for plant growth. High N content of shoot of strawberry with MCU-I was due to constant supply on N and phosphate from rhizobacteria for roots uptake. Reducing urea fertilizer to 50% in lower dose of MCU-I apparently induced N fixation that needs a lot of ATP molecules since nitrogenase is sensitive to high available N of substrate (Hoffman et al., 2014). The presence of available P by phosphate solubilizing Bacillus may contribute the P supply for ATP formation. Both Bacillus species in this experiment produced extracellular phosphatase (Hindersah et al., 2020b) as a prominent mechanism to solubilize the organic P in growth substrate (Guang *et al.*, 2008; Ambreen *et al*.,2020).

Although the strawberry has grown only for a month, Our experiment showed that half dose of MCU resulted in the similar value of root and shoot parameter (Table 1 and Table 2). This indicated that urea fertilizer dose can be saved up to 50%. Delaying N released from coated urea might lead to increase the N efficiency used from fertilizer based on shoot N uptake (Mesquita et al., 2017).

The result showed that seedlings received half dose MCU-I and half dose of MCU-II have higher R/S at early growth compared to the control. Biofertilizer application integrated with urea play a significant role to increase strawberry rooting compared to the control**.** In early vegetative, good rooting and crown size of bare roots strawberry transplant plant ensure the strawberry biomass due to optimal N uptake (Tagliavini *et al*., 2005; Cocco *et al*., 2011). In Bandung Regency, the first harvest of strawberry fruit is commonly no later than 10 weeks after transplanting the bare-root strawberry transplant.

In general, lower doses of MCU-I was more effective to replace conventional urea in early growth of strawberry. The MCU was the urea coated with solid inoculant with compost as the main ingredients of carrier enriched with zeolite. The MCU-I contained 5% zeolite while the MCU-II contained only 1 % zeolite. Higher content of zeolite in coating material of MCU-I can protect the urea from the humidity as well as slower urea hydrolysis and N release to soil. However, the result indicated that the N uptake of one individual plant was very low compared to applied urea and NPK fertilizer. This verifiy that N use efficiency (NUE) by seedling in soilless substrate might be low. Further experiment is needed to assess the NUE value.

Strawberry is an important horticultural product of Bandung and Bandung Barat Regency. Nowadays, the strawberry productivity is not as high as years before due to fertilization and seedling problem. The results of this greenhouse trial are the first information concerning the response of strawberry seedlings to reduced dose of chemical fertilizer application in Indonesia. However, next experiment is needed to verify the long-term effect of MCU doses and application method on NUE and plant growth during strawberry transplant production.

5. Conclusion

Urea fertilizer coated with solid biofertilizer composed of composted manure, 5% zeolite and 5% liquid bacterial inoculant increased root volume, root dry weight, root to shoot ratio and shoot N content significantly, but only full dose of that MCU formulation increased shoot N uptake and SPAD value. Compared to the control, MCU at any dose and formulation did not affect crown diameter, root length, plant height and shoot dry weight at 4 weeks after planting. The effect of urea coated with solid inoculant of Azotobacter and Bacillus was mostly increased root parameters compared to the shoots. However, MCU application resulted in > 20 mm of crown diameter which ensures the growth of transplant in strawberry production. Utilizing half dose of urea fertilizer coated with composted manure with 5% zeolite and 5% liquid inoculant is considered resulted in the increment of certain growth parameter of strawberry seeding until 4 weeks after treatment compared to a dose of conventional. This result indicated that utilizing microbial coated urea might lower the doses of urea applications up to 50%.

Acknowledgement

The research was funded by Directorate General of Higher Education, Ministry of Education and Culture, Republic of Indonesia, in 2020.

References

Ahmad S, Imran M, Hussain S, Mahmood S, Hussain A and Hasnain M. 2017. Bacterial impregnation of mineral fertilizers improves yield and nutrient use efficiency of wheat. *J Sci Food Agric*., **97(11)**:3685-3690.

Ambreen A, Yasmin A and Aziz S. 2020. Isolation and characterization of organophosphorus phosphatases from *Bacillus thuringiensis* MB497 capable of degrading Chlorpyrifos, Triazophos and Dimethoate. *Heliyon*, **6(7)**: e04221.

Ameri A, Tehranifar A, Davarynejad GH and Shoor M. 2012. Effect of substrate and cultivar on growth characteristic of strawberry in soilless culture system. *J Biol Environ Sci*, 6(17):181-188.

AOAC. (2012). **Official Methods of Analysis**, 19th ed. Association of official analytical chemist, Washington D.C., USA.

Bhattacharyya PN and Jha D.K. 2012. Plant growth-promoting rhizobacteria (PGPR): emergence in agriculture. *World J Microbiol Biotechnol.*, **28**:1327–1350.

Bibi S, Saifullah, Naeem A and Dahlawi S. 2016. Environmental impacts of nitrogen use in agriculture, nitrate leaching and

mitigation strategies. In: Hakeem KR et al. (Eds.), Soil Science: **Agricultural and environmental prospectives**. Springer International Publishing, Switzerland, pp. 131-157.

Beer B, Kumar S, Gupta AK, Syamal MM. 2017. Effect of organic, inorganic and bio-fertilizer on growth, flowering, yield and quality of strawberry (Fragaria × Ananassa Duch.) cv. Chandler. *Int J Curr Microbiol App Sci.*, **6(5**):2932-2939.

Berg JM, Tymoczko JL and Stryer L.2002. **Biochemistry**. 5th ed. W H Freeman, New York

Burger M and Jackson LE. 2003. Microbial immobilization of ammonium and nitrate in relation to ammonification and nitrification rates in organic and conventional cropping systems. *Soil Biol Biochem.*, **35(1**):29-36.

Chapin FS, Matson PA and Mooney HA. 2002. Terrestrial plant nutrient use. In: **Principles of terrestrial ecosystem ecology**. Springer, New York, NY. pp. 176-196

Cocco C, Andriolo JL, Cardoso FL, Erpen L and Schmitt OJ. 2011. Crown size and transplant type on the strawberry yield. *Sci. Agric*., **68(4)**:489-493.

Fan XH, Li YC and Alva AK. 2011. Effects of temperature and soil type on ammonia volatilization from slow-release nitrogen fertilizers. *Comm Soil Sci Pl Anal*., **42(10):**1111-1122.

Fiencke, C., Spieck, E., &Bock, E. (2005). Nitrifying Bacteria. In: Werner D and Newton WE (Eds.). **Nitrogen fixation in Agriculture, Forestry, Ecology, and the Environment**. Springer, Netherlands, pp 255-276.

Fitriatin BN, Fauziah D, Fitriani FN, Ningtyas DN, Suryatmana P, Hindersah R, Setiawati MR and Simarmata T. 2020. Biochemical activity and bioassay on maize seedling of selected indigenous phosphate-solubilizing bacteria isolated from the acid soil ecosystem. *Open Agric*., **5(1)**:300–304.

Gastal,G G. Lemaire. 2002. N uptake and distribution in crops: an agronomical and ecophysiological perspective. *J Exp Bot.*, **53(370**): 789–799.

Guang-Can TAO, Shu-Jun T, Miao-Ying CAI and Guang-Hui XIE. 2008. Phosphate-solubilizing and mineralizing abilities of bacteria isolated from soils. *Pedosphere*, **18**:515–523.

Güler S, Macit I, Koç A and Ibrikci H. 2006. Estimating Leaf nitrogen status of strawberry by using Chlophyll meter reading. *J Biol Sci*., **6(6)**:1011-1016.

Hindersah R, Setiawati MR, Fitriatin BN, Suryatmana P and Asmiran P. 2019. Chemical characteristics of organic-based liquid inoculant of *Bacillus* spp. *IOP Conf Ser: Earth Environ Sci.*, **393**:012005.

Hindersah R, Setiawati MR, Fitriatin BN, Rahmadina I and Risanti RR. 2020a. Organic carrier-based inoculant of Bacillus and Azotobacter consortium. *Test Engineer Manag*, **82**:7464 – 7470.

Hindersah R, Setiawati MR, Asmiran P and Fitriatin BN. 2020b. Formulation of Bacillus and Azotobacter consortia in liquid cultures: preliminary research on microbes-coated urea. *Int J Agric Sys.*, **8(1)**:1-10.

Hindersah R, Rahmadina I, Harryanto R, Suryatmana P and Arifin M. Bacillus and Azotobacter counts in solid biofertilizer with different concentration of zeolite and liquid inoculant. *IOP Conf. Series: Earth and Environ Sci*., **667(2021)**: 012010.

Hoffman BM, Lukoyanov D, Yang Z-Y, Dean DR and Seefeldt LC. 2014. Mechanism of nitrogen fixation by nitrogenase: the next stage. *Chem Rev*., **114(8)**: 4041–4062.

Jadon P, Selladurai R, Yadav SS, Coumar MV, Dotaniya ML, Singh AK, Bhadouriya J and Kund S. 2018. Volatilization and leaching losses of nitrogen from different coated urea fertilizers. *J Soil Sci Pl Nutr.*, **18(4)**:1036-1047.

Kulaeva ON and Kusnetsov VV. 2002. Recent advances and horizons of the cytokinin studying. *Russ. J Plant Physiol.*, **49**:561–575.

Kurepin LV, Zaman M and Pharis RP. 2014. Phytohormonal basis for the plant growth promoting action of naturally occurring biostimulators. *J Sci Food Agric.*, **94(9)**:1715-22.

Mishra AN and Tripathi VK. 2011. Influence of different levels of Azotobacter, PSB alone and in combination on vegetative growth, flowering, yield and quality of strawberry cv. Chandler. *Int J Appl Agric Res.*, **6(3)**:203-210.

Menzell CM and Smith, L. Relationship between the levels of non-structural carbohydrates, digging date, nursery-growing environment, and chilling in strawberry transplants in a subtropical environment. *Hort Sci.*, **47(4)**: 459-464, 2012.

Mesquita GL, Zambrosi FCB, Cantarella H. 2017. A practical approach for assessing the efficiency of coated urea on controlling nitrogen availability. *Bragantia*, **76(2)**: p.311-317.

Mustafa HM and Hayder G. 2021. Performance of *Salvinia molesta* plants in tertiary treatment of domestic wastewater. *Helycon*, **7(2021)**: e06040.

Nacry P Bouguyon E Gojon A . 2013. Nitrogen acquisition by roots: physiological and developmental mechanisms ensuring plant adaptation to a fluctuating resource. *Pl Soil*, **370**: 1–29.

Palupi NE, Aji TG, Kurnilasari D dan Sutopo. 2017. Efektivitas Dosis Dan Aplikasi Pupuk Npk Majemuk Pada Fase Vegetatif Pada Tanaman Strawberry (Fragaria x ananassa Duchesne). *Agrisaintifika*, **1(2)**:109-116. In Indonesian, abstract in English.

Pang W, Crow WT, Luc JW, McSorley R, Giblin-Davis RM, Kenworthy KE and Kruse JK. Comparison of water displacement and WinRHIZO software for plant root parameter assessment. *Pl Dis*, **95(10):**1308-1310.

Raja WH, Kumawat KL, Sharma OC, Sharma A, Mir JI, Nabi SUN, Lal S and Qureshi I. 2018. Effect of different substrates on growth and quality of strawberry cv. chandler in soilless culture. *The Pharma Innov J.*, **7(12)**: 449-453.

Reddy GC and Goyal RK. 2020. Growth, yield and quality of strawberry as affected by fertilizer N rate and biofertilizers inoculation under greenhouse conditions. *J Pl Nutr.*, **44(1)**:46-58.

Rodriguez-Salazar J, Moreno S and Espín G. 2017. LEA Proteins are involved in cyst desiccation resistance and other abiotic stresses in Azotobacter vinelandii. *Cell Stress Chaperon*, **22**: 397–408.

Rubio EJ, Montecchia MS, Tosi M, Cassán FD, Perticari A and Correa OS. 2013. Genotypic characterization of Azotobacteria isolated from Argentinean soils and plant-growth-promoting traits of selected strains with prospects for biofertilizer production. *Sci World J.*, **2013**: 519603.

Saeid A, Prochownik E and Dobrowolska-Iwanek J. 2018. Phosphorus solubilization by Bacillus Species. *Molecules*, 23:2897.

Shanmugasundaram R, Jeyalakshmi T, Mohan SS, Saravanan M, Goparaju A and Murthy PB. 2013. Coco peat - An alternative artificial soil ingredient for the earthworm toxicity testing. *J Toxicol Environ Health Sci.*, **6(1)**:5-12.

Shternshis MV, Belyaev AA, Shpatova TV and Lelyak AA. 2015. Influence of Bacillus spp. on strawberry gray-mold causing agent and host plant resistance to disease. *Contemp Probl Ecol.*, **8**:390–396.

Singh S, Dubey RK, Kukal SS. 2016. Nitrogen supplemented cocopeat-based organic wastes as potting media mixtures for the growth and flowering of chrysanthemum. *J Comm Soil Sci Pl Anal.*, **47(16)**: 1856-1865.

Rueda D, Valencia G, Soria N, Rueda BR, Manjunatha B, Kundapur RR and Selvanayagam M. 2016. Effect of *Azospirillum* spp. and *Azotobacter* spp. on the growth and yield of strawberry (*Fragaria vesca*) in hydroponic system under different nitrogen levels. *J Appl Pharma Sci.*, **6(1)**:048-054.

Tan IS and Ramamurthi KS. 2014. Spore formation in *Bacillus subtilis*. *Environ Microbiol Repos.*, **6(3)**: 212–225.

Tanimoto E. 2005. Regulation of root growth by plant hormones—roles for auxin and gibberellin. *Crit Rev Pl Sci.*, **24(4)**: 249-265.

Tagliavini M, Baldi E, Lucci P, Antonelli M, Sorrenti G, Baruzzi G and Faedi W. 2005. Dynamics of nutrients uptake by strawberry plants (Fragaria × Ananassa Dutch.) grown in soil and soilless culture. *Euro J Agron.*, **23(1)**:15-25.

Tatlier M, Munz G and Henning SK. 2018. Relation of water adsorption capacities of zeolites with their structural properties. *Micropor Mesopor Mat*, 264:(70-75).

Torres-Quezada EA, Zotarelli L, Whitaker VM, Santos BM and Hernandez-Ochoa I. Initial crown diameter of strawberry bare-root transplants affects early and total fruit yield. *Hort Technol.*, **25(2)**:203-208.

Wahyuni S, Indratin, Sulaeman E and Ardiwinata AN. 2016. Activated carbon coated urea enriched with microbial consortia accelerates the decrease of heptachlor insecticide residue in paddy fields. *Informatika Pertanian*, **25(2)**:155–162. In Indonesian, abstract in English.

Wang B, Lai T, Huang Q-W, Yang X-M and Shen Q-R. 2009. Effect of N fertilizers on root growth and endogenous hormones in strawberry. *Pedosphere*, **19(1)**:86-95.

Wang H, Gao J-e, Li X-h, Zhang S-l and Wang H-j. 2015. Nitrate accumulation and leaching in surface and ground water based on simulated rainfall experiments. *PLoS ONE*, **10(8)**: e0136274.

Wei F, Hu X and Xub X. 2016. Dispersal of *Bacillus subtilis* and its effect on strawberry phyllosphere microbiota under open field and protection conditions. *Sci Rep.*, **6**: 22611.

JJBS

Volume 14, Number 3, September 2021
ISSN 1995-6673
Pages 601 - 605

Jordan Journal of Biological Sciences

The Role of Rhizobacterial Inoculum and Formulated Soil Amendment in Improving Soil Chemical-Biological Properties, Chlorophyll Content and Agronomic Efficiency of Maize under Marginal Soils

Betty Natalie Fitriatin[1,*], Debora Dellaocto Melati Ambarita[2], Mieke Rochimi Setiawati[1] and Tualar Simarmata[1]

[1]*Department of Soil Sciences and Land Resouces, Agriculture Faculty, Universitas Padjadjaran. Jatinangor 45363-West Java – Indonesia;*
[2]*Postgraduate of Soil Science, Agriculture Faculty, Universitas Padjadjaran. Jatinangor 45363-West Java – Indonesia*

Received: February 27, 2021; Revised: May 17, 2021; Accepted: July 19, 2021

Abstract

Intensively use of chemical fertilizers accelerates organic matter and soil health degradation. Consequently, the soil capacity in providing the essential nutrient is decreasing significantly. The research was conducted to investigate the contribution of selected rhizobacteria inoculant as biofertilizers and formulated soil amendment (FSA) for enhancing the soil organic carbon, abundance of nitrogen fixer bacteria (NFB), phosphate solubilizing bacteria (PSB), chlorophyll content and yield of maize in marginal soils. The experiment was arranged as Randomized Complete Blocks Design (RCBD) consisting of two factors and provide with three replications. The first factor were biofertilizers (consortia of PSB and N-fixing bacteria combined with formulated soil amendment (compost 50%, biochar 20%, humid acid 1%, guano 9%) and the second factor were the rate of N,P fertilizers100%, 80%, 60%, 40% recommended doses (138; 110.4; 82.8; 55.2 kg ha^{-1} N and 36; 28.8; 21.6; 14.4 kg ha^{-1} P). The results revealed that application of biofertilizers and FSA increased soil C-org, population of PSB and N-fixing bacteria, chlorophyll leaves and yield of maize were increased significantly. The highest population of PSB and N-fixing bacteria, chlorophyll leaves and yield of maize were obtained by application of 1.200 g ha-^{1} of biofertilizers and 2 t ha^{-1} of organic FSA. The application of biofertilizers and FSA with 60-100% NP fertilizer could increase maize yields. Additionally, fertilizers efficiency was increased by 40 %. This finding recommends the use of 1200 g of biofertilizers inoculant and 2 t of FSA ~~to~~ improved the soil properties and increased the maize productivity on marginal soils.

Keywords: N-fixer, organic carbon, P-solubilizer, fertilizers efficiency

1. Introduction

Concern for environmental pollution due to the use of various chemicals especially inorganic fertilizers and synthetic pesticides as well as health and environmental reasons makes sustainable agriculture one of the alternatives of modern agriculture. One effective step that can be developed in sustainable agriculture is the use of microbes that are useful in facilitating or increasing the availability of soil nutrients or known as biofertilizers (Macik *et al*., 2020). Microbes which are commonly used as an active ingredient in biological fertilizers are nitrogen-fixing bacteria, phosphate solubilizing microbes, mycorrhizae, and phytohormone-producing bacteria (Wahane *et al.*, 2020).

Beneficial microbe that has a role to facilitate available phosphate is phosphate-solubilizing microbes (PSM). These microbes are able to improve plant growth and increase soil P availability (Jayakumara *et al.*, 2019; Wu *et al*., 2019) and produce phosphatase enzyme (Chen and Liu, 2019) and produce phytohormone (Fitriatin *et al*., 2020).

Some bacteria can convert atmospheric nitrogen into ammonia in symbiosis with plants or without symbiosis. Gentili and Jumpponen (2006) reported that *Azotobacter* sp. and *Azospirillum* sp. are non-symbiotic and free-living bacteria that play a role in N fixation. Steenhoudt and Vanderleyden (2000) stated that *Azospirillum* is the best genus from Plant Growth-Promoting Rhizobacteria (PGPR) genera group because its interactions with several plant roots are able to fix nitrogen and produce plant growth hormones.

Biofertilizers play an important role to sustainably increase land productivity and influence plant growth and yield positively (Itelima *et al*. 2018). Fitriatin *et al*. (2019) reported that the application of biofertilizers that contain consortium of phosphate-solubilizing microbes and nitrogen-fixing bacteria increase soil nitrogen and P availability. The application of biofertilizers and organic ameliorants is a step to reduce soil damage due to excessive use of inorganic fertilizers. The use of organic fertilizers is expected to supplement the use of chemical

* Corresponding author e-mail: betty.natalie@unpad.ac.id.

fertilizers. More research is needed to know more about the impact of biofertilizers which contain phosphate-solubilizing microbes and nitrogen-fixing bacteria with formulated soil amendment in increasing soil carbon, population of PSM, chlorophyll content and yield of maize.

2. Materials and Method

The field experiment was conducted at Horticultural Seed Development Centre and Various Plants Pasir Banteng, Sumedang, West Java on Inceptisols. A composite sample was taken from the field from depth 0-30 cm for physical and chemical analysis of the soil. The physic-chemical properties of the soil are as follows: texture dusty clay; pH 5.95; C_{org} 2.3%; N_{total} 0.21%; C/N 10; P_2O_5 HCl 25% 60.75 mg $100g^{-1}$; P_2O_5 (Bray) 11.36 ppm; and CEC 23.61 $cmol.kg^{-1}$.

The experiment was laid out in Randomized Complete Blocks Design (RCBD) consisting of two factors and three replications (The plot size was 3m × 1.5m with inter row spacing of 75 cm and intra row spacing of 25 cm). The first factors were biofertilizers and formulated soil amendment (FSA) (control; biofertilizers; FSA ; and biofertilizers + FSA). Biofertilizers with a peat base material carrier contain N-fixer bacteria (*Azotobacter chroococcum*, and *Azospirillum* sp.) and phosphate solubilizing bacteria (*Bulkholderia vietnamiensi* and *Enterobacter ludwigii)*. These bacteria were selected in isolation from several ecosystems including rice rhizosphere, peanut rhizosphere and sweet potato rhizosphere. *Azotobacter* and *Azospirillum* were cultured on JNFb media while *Enterobacter* and *Bulkholderia* were cultured on Pikovskaya media. Formulated soil amendment contains mixture of compost 50%, biochar 20%, humid acid 1%, and guano 9%. The second factor was the rate of NP fertilizers 100%, 80%, 60%, 40% recommended doses (138; 110.4; 82.8; 55.2 kg ha^{-1} N and 36; 28.8; 21.6; 14.4 kg ha^{-1} P) with Urea (46% N) and single super phosphate (36% P) which is applied around the planting hole. Maize seeds used BISI 2 with a germination rate of more than 85%.

2.1 Data collection

Soil Organic Carbon (SOC)

Was determined by oxidimetric titration Walkley and Black method (Nelson and Sommers 1982).

The number of bacterial population

Nitrogen fixing bacteria and phosphate solubilizing bacteria population were determined by serial dilution plate count technique (Zhang *et al*. 2012).

Content of chlorophyll

Chlorophyll content of leaf was measured by using Soil Plant Analysis Development (SPAD) meter (SPAD 502, Minolta, Japan). Five plants were randomly selected from each plot to measure chlorophyll content.

Grain yield

To calculate grain yield by using given formula:

$$Gr\,(Kg\,ha-1) = \frac{yield\ plot\ at\ 14\%\ moisture\ (Kg)}{plot\ size\ in\ m\,2}\ x\ 10000\ m2 \quad (1)$$

Agronomic efficiency

Agronomic efficiency was calculated by equation below (Zemichael *et al*. 2017):

$$AE\ (kg\ kg-1) = \frac{Gf\ -\ Gu}{Na} \quad (2)$$

If: Gf: the grain yield in the fertilized plot (Kg).

Gu: the grain yield in the un fertilized plot (Kg).

Na: the quantity of nutrient applied (Kg).

Data were processed using DSAASTAT (Dipartimento in the Scienze Agrarie ed Ambientali Statistic) and Duncan's multiple range test with a 95% confidence level to determine differences in mean values between treatments.

3. Results

3.1 Soil Organic Carbon

The soil organic C content of the soil was measured at the end of the vegetative phase. The experimental results show that there was no interaction between biofertilizers and FSA with NP fertilizers (Table 1).

Table 1. Soil organic carbon as affected by biofertilizers, FSA and N, P fertilizers

Treatments	Soil Organic C (%)
Biofertilizers and formulated soil amendment (FSA)	
- Control	3.80 a
- Biofertilizers	3.83 a
- FSA	4.12 b
- Biofertilizers + FSA	4.31 b
N, P Fertilizers	
100%	4.01 a
- 80%	4.02 a
- 60%	4.19 a
- 40%	3.84 a

Note: Numbers followed by the same letter are not significantly different according to Duncan's test at 5% significance level

Biofertilizers did not significantly increase soil organic carbon. Different results are shown by the treatment of FSA which was able to increase soil organic carbon significantly. The combination treatment of biofertilizers and FSA increased soil organic carbon up to 13.4% compared to control.

3.2 Chlorophyll content

The statistical analysis showed the interaction between biofertilizers and FSA with NP fertilizer on chlorophyll content of maize leaves (Table 2). In general, the application of biofertilizers and FSA at various doses of NP fertilizers increased the chlorophyll content. The combination of biofertilizers and FSA at various doses of NP fertilizers higher chlorophyll content compared to the treatment of only biofertilizers or FSA. Chlorophyll content tends to be higher in the treatment of high NP fertilizer doses. The treatment of 100% NP fertilizers and

the combination of biofertilizers and FSA gives the highest C soil content (39.47).

Table 2. Chlorophyll content of maize leaves (SPAD)

Treatments	N, P Fertilizers			
	100%	80%	60%	40%
control	32.83 a (d)	31.87 a (c)	30.73 b (b)	28.90 a (a)
Biofertilizers	38.90 c (c)	31.80 a (b)	29.47 a (a)	29.77 ab (a)
FSA	35.07 b (c)	31.73 a (b)	30.30 ab (a)	29.50 ab (a)
Biofertilizers + FSA	39.47 c (d)	34.37 b (c)	32.20 c (b)	30.20 b (a)

Note: Numbers followed by the same letter are not significantly different according to Duncan's test at 5% significance level. Letters in parentheses are read horizontally. Letters without brackets are read vertically

3.3 Soil microbe population

Beneficial soil microbe populations measured were PSB and N-fixer bacteria at the end of vegetative period. The PSB population ranges between 2.7-57.55 x 10^7 colony forming unit (CFU) g^{-1} (Table 3).

The results of statistical analysis show a significant interaction between biofertilizers and FSA with NP fertilizer on PSB population. Biofertilizers and FSA increased population of PSB at various doses of NP fertilizers. Application of 80-100% NP fertilizers and the combination of biofertilizers and FSA provide a better influence on the PSB population (55.9-57.55 x 10^7 CFU g^{-1}).

Table 3. Population of phosphate solubilizing bacteria (10^7 CFU g^{-1})

Treatments	N,P Fertilizer s			
	100%	80%	60%	40%
Control	20. 67 a (a)	22.00 a (a)	21.67 a (a)	20.67 a (a)
Biofertilizers	52.25 b (c)	51.10 c (bc)	48.50 c (a)	48.81 c (ab)
FSA	27.35 c (b)	26.33 b (b)	24.73 b (ab)	23.63 b (a)
Biofertilizers + FSA	57.55 d (c)	55.90 d (c)	50.43 c (b)	47.18 c (a)

The population of N-fixing bacteria was affected by the application of biofertilizers and FSA at several doses of N and P fertilizers. The statistical analysis shows a significant interaction between biofertilizers and FSA with NP fertilizer on N-fixing bacteria population.

Application of 80-100% NP fertilizers and the combination of biofertilizers and FSA provided a better influence on the population of (N-fixing bacteria (47.37 x 10^7 CFU g^{-1}). Fertilizing low-dose NP tended to give a lower population number of N fixing bacteria compared to other treatments (Table 4).

Table 4. Population of N-fixing bacteria (10^6 CFU g^{-1})

Treatments	N,P Fertilizer s			
	100%	80%	60%	40%
control	12.45 a (a)	12.17 a (a)	10.83 a (a)	11.933 a (a)
Biofertilizers	25.18 b (a)	26.37 b (a)	22.933 c (a)	23.77 b (a)
FSA	16.92 a (a)	16.9 a (a)	15.78 b (a)	19.78 b (a)
Biofertilizers + FSA	47.37 c (d)	33.63 c (c)	28.17 c (b)	22.38 b (a)

3.4 Agronomic efficiency

Agronomic efficiency (AE) is calculated in units of yield increase per treatments of NP fertilizer applied. It more closely reflects the direct production impact of an applied inorganic fertilizer. The result showed that there was a significant effect of biofertilizers and FSA application and also application of inorganic fertilizers on yield of maize.

Biofertilizers application with 40% NP fertilizers increased grain yield of maize up to 5.28 Kg Kg $^{-1.}$ Furthermore, increasing the dosage of NP fertilizer to 80%, the application of biofertilizers decreased the yield to 0.86 Kg Kg $^{-1}$ (Table 5). Application of FSA with 40% NP fertilizers increased grain yield up to 6.22 Kg Kg^{-1}. However, the combination of biofertilizers and FSA applications with 100%, 80% and 60% NP fertilizer increased grain yield of maize by 5.40, 4.20, 2.16 Kg Kg $^{-1}$, respectively.

Table 5. Agronomic efficiency of NP fertilizers application on maize

Treatment	Grain yield of maize (Kg ha^{-1})	Agronomic efficiency (Kg Kg $^{-1}$)
Control (100% NP fertilizer)	2844	-
80% NP fertilizer	2660	1.32
60% NP fertilizer	2456	3.71
40% NP fertilizer	2237	8.72
Biofertilizers + 100% NP fertilizer	3447	3.46
Biofertilizers + 80% NP fertilizer	2965	0.86
Biofertilizers + 60% NP fertilizer	2672	1.64
Biofertilizers + 40% NP fertilizer	2476	5.28
FSA + 100% NP fertilizer	3044	1.14
FSA + 80% NP fertilizer	2860	0.11
FSA + 60% NP fertilizer	2545	2.86
FSA + 40% NP fertilizer	2411	6.22
Biofertilizers and FSA + 100% NP fertilizer	3785	5.40
Biofertilizers and FSA + 80% NP fertilizer	3430	4.20
Biofertilizers and FSA + 60% NP fertilizer	3070	2.16
Biofertilizers and FSA + 40% NP fertilizer	2715	1.85

4. Discussion

In general, the treatment of biofertilizers and FSA can significantly increase soil organic carbon, chlorophyll content, and PSB population. This shows that the biofertilizers will have an optimal effect if there is an energy source for growth obtained from FSA. This proves that biofertilizers is more effective to promote plant growth when combined with FSA. Application of biofertilizers combined with FSA increases the soil organic carbon. The soil amendment used consists of materials which are rich in organic carbon such as compost with raw materials of bagasse, biochar, dolomite, hemic acid and guano which can increase the organic carbon content *in* the soil.

The application of biofertilizers can also help increase organic carbon by the decomposition process carried out by bacteria. Therefore, soil amendment and biofertilizers can increase the organic carbon content higher than other treatments. Compost and biochar are the source of carbon and energy for microbes in biological fertilizer. In this atudy, the compost has a C/N ratio of 23. This is supported by the results of research by Husna *et al*. (2019) showing the highest viability of phosphate solubilizing microorganisms in biochar carriers.

Increasing soil organic carbon greatly affects soil health (Tully and McAskill, 2020). The organic carbon can affect soil structure, aeration, and water holding capacity (Colombi *et al.*, 2019). These soil properties can support plants to produce in the soil. Provision of soil amendment and biofertilizers can increase organic carbon in the soil. Provision of soil amendment and P solubilizing microbes and N fixers can increase organic carbon by up to 75% in the soil after three years of application (Debska *et al*., 2016). The application of soil amendment and biofertilizers can increase organic carbon and affect other chemical properties that can support soil health.

The advantages of biofertilizers include reducing the use of chemical fertilizers and environmental pollution, increasing the availability of nutrients and enhancing plant growth, and improve the physical, chemical and biological properties of the soil (Wahane *et al*., 2020). Yasmin *et al.* (2020) reported that beneficial microbes application increased yield and available nutrient (N,P,K) and reduced the nitrogen fertilizer rate. Furthermore, Albdaiwi *et al.* (2019) stated that some microbes as Plant Growth-Promoting Rhizobacteria (PGPR) increase nutrient availability, yield of crops and substitute to chemical fertilizers. The formulated soil amendment is a source of energy for soil macro and microbes. Addition of soil amendment will increase microbiological activities and populations, especially those related to the decomposition and mineralization of organic matter (Stevenson, 1986).

Application of biofertilizers resulted in considerable increase in the chlorophyll content of maize plant leaf tissue. In this study, biofertilizers which contain phosphate solubilizing bacteria and N-fixing bacteria improved the growth of maize and increased chlorophyll content of maize plant leaf tissue. Khan (2018) observed chlorophyll content increases with biofertilizers application. The application of biofertilizers has been reported to improve the soil health and escalate the efficiency of applied fertilizers (Simarmata *et al*.. 2017).

Chlorophyll content is one of the parameters for plants to grow well. Chlorophyll is a green pigment in plants playing a role in the photosynthesis process of plants (Li *et al*., 2018). Chlorophyll is formed from several nutrients, so if the plant does not get the optimum nutrient, the chlorophyll content in the plant is not optimal. Table 2 shows that the application of biofertilizers and ameliorants combined with 100% of the recommended dosage of inorganic fertilizers can increase the chlorophyll content higher than other treatments. This could be due to the 100% dose of inorganic fertilizer affecting the chlorophyll content of leaves. The availability of nutrients in the soil, especially the essential nutrients N, P and K can increase chlorophyll content in plants (Eisvand *et al*., 2018).

The higher the supply of nitrogen into plants, the higher the chlorophyll content of plants in the leaves so that the photosynthesis process is faster (Bassi *et al*., 2018). The N element received by plants is obtained from the application of inorganic fertilizers which are not reduced from the recommended dosage and the use of N-fixing bacteria.

Table 4 shows that biofertilizers and FSA combined with inorganic fertilizers 100% of the recommended dosage resulting in the highest of PSB population compared to other treatments. The biofertilizers in this study contained PSB (*Bulkhoderia vietnamiensi* and *Enterobacter ludwigii*). The increase of PSB population was accompanied by soil amendment applied to the soil which can be a source of energy for bacteria to reproduce. The provision of ameliorants also increased PSB population because it helped bacteria grow and get a source of energy.

The increase in the population of N-fixing bacteria was caused by the application of biofertilizers and soil amendment. The biofertilizers used in this study contained N-fixing microorganisms, namely *Azotobacter chroococcum* and *Azospirillum* sp. However, increasing the N,P fertilizer will inhibited the N-fixing bacteria. Increasing population of N-fixing bacteria improves soil health and increases plant productivity (Tahat *et al*., 2020).

Based on the measurement of agronomic efficiency, the application of biofertilizers and FSA with 60-100% NP fertilizer could increase maize yields. 100 % of the N, P fertilizer will inhibit the N-fixation bacteria. In addition, the combination of biofertilizers and FSA application increased fertilizers efficiency by 40%. This is in line with research by Cisse *et al*. (2019) that application of 20 kg ha^{-1} biofertilizer reduced at least 50% of the NPK fertilization.

5. Conclusion

Application of biofertilizers (N-fixer bacteria *Azotobacter chroococcum*, and *Azospirillum* sp. and phosphate solubilizing bacteria *Bulkholderia vietnamiensi* and *Enterobacter ludwigii*) and formulated soil amendment (mixture of compost 50%, biochar 20%, humid acid 1%, and guano 9%) can significantly increase soil organic carbon, chlorophyll content, PSB population and yield of maize. The highest population of PSB and N-fixing bacteria, chlorophyll leaves and yield of maize were obtained by application of 1.200 g ha^{-1} of biofertilizers and 2 t ha^{-1} of formulated soil amendment. Additionally, fertilizers efficiency was increased by 40 %.

Acknowledgment

We are grateful to staff Laboratory of Soil Biology Faculty of Agriculture, Universitas Padjadjaran and staff Horticultural Seed Development Center and Various Plants Pasir Banteng, Sumedang-West Java for their supporting and valuable advice of this work.

Funding

This research was funded by Academic Leadership Grant (ALG) Universitas Padjadjaran.

References

Albdaiwi RN, Khyami-Horani H and Ayad JY. 2019. Plant growth-promoting rhizobacteria: an emerging method for the enhancement of wheat tolerance against salinity stress-(Review). *Jordan J Biol Sci*., **12 (5):** 525 – 534.

Bassi D, Menossi M and Mattiello L. 2018. Nitrogen supply influences photosynthesis establishment along the sugarcane leaf. *Sci Rep.*, **8(1) :**1-13.

Chen Q and Liu S. 2019. Identification and characterization of the phosphate-solubilizing bacterium *Pantoea* sp. S32 in reclamation soil in Shanxi, China. *Front Microbiol*., **(10)** Article 2171.

Cisse A, Arshad A, Wang X, Yattara F, and Hu Y. 2019. Contrasting impacts of long-term application of biofertilizers and organic manure on grain yield of winter wheat in north china plain. *Agronomy*., **9(6):** 312.

Colombi T, Walder F, Büchi L, Sommer M, Liu K, Six J, van der Heijden MGA, Charles R and Keller T. 2019. On-farm study reveals positive relationship between gas transport capacity and organic carbon content in arable soil. *SOIL*, **5**: 91–105,

Debska B, Dlugozs J and Piotrowska-Dlugozs A. 2016. The impact of a bio-fertilizer on the soil organic matter status and carbon sequestration—results from a field-scale study. *J Soil Sediments*., **16 (10):** 2335-2343.

Eisvand HR, Kamael H, and Nazarian F. 2018. Chlorophyll fluorescence, yield components of bread wheat affected by phosphate bio-fertilizer, zinc and boron under late-season heat stress. *Photosynthetica.*, **56 (4):** 1287-1296.

Fitriatin BN, Silpanus R, Sofyan ET, Yuniarti A, and Turmuktini T. 2019. Effect of microbial fertilizers and dosage of NPK on growth and yield of upland rice (Oryza sativa L.). *Int. j. environ. agric. Biotech.*, **4 (4):** 899-902.

Fitriatin BN, Fauziah D, Fitriani FN, Ningtyas DN, Suryatmana P, Hindersah R, Setiawati MR and Simarmata T. 2020. Biochemical activity and bioassay on maize seedling of selected indigenous phosphate-solubilizing bacteria isolated from the acid soil ecosystem. *Open Agric*., **5:** 300–304.

Gentili F and Jumpponen A. 2006. Potential and possible uses of bacterial and fungal Biofertilizers. In: Handbook of Microbial Biofertilizers. Haworth Press, Technology & Enginering, New York, pp 1-28.

Husna N, Budianta D, Munandar, and Napoleon A. 2019. Evaluation of several biochar types as inoculant carrier for indigenous phosphate solubilizing microorganism from acid sulphate soil. *J Ecol. Eng.*, **20 (6):** 1–8.

Itelima JU, Bang WJ, Sila MD, Onyimba IA, and Egbere OJ. 2018. Bio- fertilizers as key player in enhancing soil fertility and crop productivity: A review. *Direct Res. J. Agric. and Food Sci*., **6 (3) :**73-83.

Jayakumara N, Paulraja P, Sajeesha P, Sajnaa K, and Zinneera A. 2019. Application of native phosphate solubilizing bacteria for the use of cheap organic and inorganic phosphate source in agricultura practise of Capsicum annum (Chili) - A pilot scale field study. *Mater. Today: Proc.*, **16 :**1630–1639. Available online at www.sciencedirect.com

Khan HI. 2018. Appraisal of biofertilizers in rice: to supplement inorganic chemical fertilizer. *Rice Sci.*, **25(6):** 357−362. Available online at www.sciencedirect.com

Li Y, He N, Hou J, Xu L, Liu C, Zhang J, Wang Q, Zhang X, and Wu X. 2018. Factors influencing leaf chlorophyll content in natural forests at the Biome scale. *Front. Ecol. Evol*., **6:** article 64.

Macik M, Gryta A, and Frąc M. 2020. Biofertilizers in Agriculture: An overview on concepts, strategies and effect on soil microorganisms. *Adv. Agron.*, **162:** 31-87.

Nelson D W, Sommers L E. 1982. Total carbon, organic carbon, and organic matter. In: Page A L, Miller R H, Keeney D R, eds., Methods of Soil Analysis. Part 2. Chemical and Microbiolobical Properties. Soil Science Society of America, American Society of Agronomy, Madison, WI. USA. pp. 539–594.

Simarmata T, Hersanti, Turmuktini T, Fitriatin, BN, Setiawati MR and Purwanto. 2017. Application of bioameliorant and biofertilizers to increase the soil health and rice productivity. *HAYATI J. Biosci*., **23 (4):** 181-184.

Steenhoudt O. and Vanderleyden J. 2000. *Azospirillum*, a free-living nitrogen-fixing bacterium closely associated with grasses: genetic, biochemical and ecological aspects. *FEMS Microbiol. Rev.*, **24:** 487–506.

Stevenson FJ. 1986. Cycles of Soil Carbon, Nitrogen, Phosphorus, Sulfur, Micronutrient. A Wiley-Inetrscience Publication John Wiley & Sons.

Tahat, MM, Alananbeh KM, Othman YA, and Leskovar DI. 2020. Soil health and sustainable agriculture. *Sustainability.*, **12(12):** 4859.

Tully KL and McAskill C. 2020. Promoting soil health in organically managed systems: a review. *Org. Agric*., **10(3):** 339–358.

Wahane MR, Meshram NA, More SS and Khobragade NH. 2020. Biofertilizer and their role in sustainable agriculture-A review. *J. Pharm. Innov*., **9(7):** 127-130.

Wu F, Li J, Chen Y, Zhang L, Zhang Y, Wang S, Shi X, Li L and Liang J. 2019. Effects of phosphate solubilizing bacteria on the growth, photosynthesis, and nutrient uptake of Camellia oleifera Abel. *Forests*., **10 (4) :** 348-357

Yasmin F, Othman R and Maziz MNH. 2020. Yield and nutrient content of sweet potato in response of Plant Growth-Promoting Rhizobacteria (PGPR) inoculation and N fertilization. *Jordan J Biol Sci.*, **13 (1) :** 117-122.

Zemichael B, Dechassa, N and AbayF. 2017. Yield and nutrient use efficiency of bread wheat (Triticum aestivum L.) as influenced by time and rate of nitrogen application in Enderta, Tigray, Northern Ethiopia. *Open Agric.*, **2(1)**: 611-624.

Zhang J, Liu J Y, Meng L Y, Ma Z Y, Tang X Y, Cao Y Y and Sun L .2012. Isolation and characterization of plant growth-promoting rhizobacteria from wheat roots by wheat germ agglutinin labeled with fluorescein isothiocyanate. *J. Microbiol.*, **50 (2):** 191–198.

JJBS

Volume 14, Number 3, September 2021
ISSN 1995-6673
Pages 607 - 611

Jordan Journal of Biological Sciences

Efficacy of Combining Hyaluronic Acid and Platelet-Rich Fibrin in Diabetic Foot Ulcer

Ronald W. Kartika[1], Idrus Alwi [2], Em Yunir[2], Sarwono Waspadji[2], Franciscus D. Suyatna[3] ,Saptawati Bardosono[4], Suzzana Immanuel[5] , Saleha Sungkar[6], Jusuf Rachmat [7], Todung Silalahi[8] , Mirta Hediyati Reksodiputro [9,*]

[1]Doctoral Program in Medical Science Faculty of Medicine Universitas Indonesia, Department of Thoracic , Cardiac and Vascular Surgery , Faculty of Medicine Krida Wacana Christian University; [2]Department of Internal Medicine, Faculty of Medicine Universitas Indonesia – Cipto Mangunkusumo Hospital, Jakarta, Indonesia ;[3]Department of Clinical Pharmacology, Faculty of Medicine Universitas Indonesia; [4]Department of Clinical Nutrition , Faculty of Medicine Universitas Indonesia, Jakarta, Indonesia [5]Department of Clinical Pathology, Faculty of Medicine Universitas Indonesia – Cipto Mangunkusumo Hospital, Jakarta, Indonesia;[6]Department of Parasitology , Faculty of Medicine Universitas Indonesia, Jakarta, Indonesia;[7]Department of Thoracic Cardiac and Vascular Surgery , Faculty of Medicine Universitas Indonesia, Jakarta, Indonesia;[8]Department of Internal Medicine, Faculty of Medicine Krida Wacana Christian University , Jakarta, Indonesia;[9]Department of Otorhinolaryngology, Facial Plastic Reconstructive Division, Faculty of Medicine, Universitas Indonesia, Cipto Mangunkusumo Hospital, Jakarta, Indonesia.

Received: March 3, 2021; Revised: May 2, 2021; Accepted: July 19, 2021

Abstract

Objectives: A chronic complication of type-2 diabetes mellitus (DMT-2) is Diabetic Foot Ulcer (DFU). The main treatment used in DFU is wound cleansing, followed by dressing the wound as a local control to increase tissue granulation and epithelialization. This study aims to compare the efficacy of the combination of Hyaluronic Acid with Platelet Rich Fibrin (HAPRF) and Platelet Rich Fibrin alone in DFU.

Methods: We conducted a randomized controlled trial from July 2019 to April 2020. The study was approved by the Ethics Committee of the Faculty of Medicine of Universitas Indonesia ID 0855 / UN2.F1 / ETIK / 2018. Informed consent was obtained from the patients.

This was a randomized clinical study to compare the efficacy of HAPRF and PRF in DFU one week post debridement. Twenty DFU samples were collected divided into 2 treatment groups: topical treatment using HAPRF compare with PRF alone. Assessment for wounds improvement was recorded using a digital camera 48 mega pixel with an accuracy of 0.1% on day-0, 3, 7, and 14. The results of the wound photographs were processed using ImageJ software. The granulation area (GA) and wound area (WA) were evaluated by IBM SPSS software v.20. The general data description was presented in median (range) value and parameter's differences were conducted using Mann–Whitney test

Results: The two treatment groups showed insignificant difference in characteristics between both group before intervention. The mean granulation width after two weeks of use HAPRF was 97.4% and PRF was 81.9%. Statistical analysis using Mann Whitney test showed granulation area of HAPRF group was significantly different compared with PRF group on day-3($p=0.047$) , day-7 ($p = 0.004$) and day-14 ($p < 0.001$). At the end of the wound healing process, the HAPRF group was significantly different compared with PRF group on Δ day $0-3$ ($p=0.048$), Δ day $0-7$ ($p = 0.039$), and Δ day $0-14$ ($p = 0.023$).

Conclusions: HAPRF improves wound healing rate through increasing granulation tissue and epithelialization compared with PRF only in diabetic foot ulcer after 2 weeks post debridement compared to PRF.

Keywords: Diabetic ulcer, *Hyaluronic Acid, Platelet Rich Fibrin,* Granulation Area, Delta Wound Area

1. Introduction

Diabetic foot ulcer (DFU) is one of diabetes mellitus type-2 (T2DM) complications causing tissue damage that is difficult to heal. In the last decade, diabetic ulcer became serious problem, in both the medical and economic fields, and estimated around 15% offering in DMT2. This situation will increase morbidity and mortality (Amstrong D, 2017)

Standardized therapy previously used for diabetic ulcer includes optimal blood glucose levels control, debridement sharply, offloading/pressure reduction, antibiotic infection controlled, ischemic correction, and wound dressing (Abott CA, 2002).

Chronic wound healing processes such as DFU are different from acute wounds and require more complex management. The moist atmosphere in DFU increases the rate of granulation formation and epithelialization as well wound repair (Jeffcoate WJ et al. 2018) The principle of

* Corresponding author e-mail: citamirta@yahoo.com.

treating wounds with moist was introduced in 1960, and since then much research was carried out by applying the gel on chronic wound treatment (Mill et al. 2014). The Hyaluronic Acid (HA) compound will bind to the extracellular matrix tissue which can help the wound healing process, and support tissue regeneration. HA has been used for a long time in ophthalmology connective tissue diseases, joints inflammatory and rheumatoid arthritis (Price RD et al. 2005).

Previous studies on the use of HA for acute wound care showed faster healing process. Meanwhile for chronic wound such as DFU, there was not much evidence to support this (Kartika et al, 2020). Platelet Rich Fibrin (PRF) contained source of growth factor (GF) obtained alpha granule (Reksodiputro, 2018). Another study states that hyaluronic acid (HA) is a biopolymer contained in the extracellular matrix of the bone, cartilage and skin tissue. Accordingly, HA and platelet concentrate are involved in the pathophysiology underlying wound healing. The aim of this study was to evaluate the clinical efficacy by measuring the development of ulcer area as well as looking at the safety by looking epithelialization signs from HA+PRF and PRF alone in the treatment of Diabetic Foot Ulcer. Research on the use of HA+PRF combination to treat diabetic ulcers has not been fully reported (Shi, 2018).

2. Methods

This study had been approved by The Institutional Board of the Faculty of Medicine Universitas, Indonesia (No. 0855/UN2.F1/ETIK/2018). This open-label randomized controlled trial was conducted at Koja District Hospital and Gatot Soebroto Hospital from July 2019 to April 2020.

2.1. Study Subjects

DFU subjects age >18 years old, suffer chronic wound (more than 4 weeks) on lower limbs. Wagner-2 criteria, and ulcer size <40 cm^2 were recruited and randomly assigned for HA+ PRF group, PRF group and control group. Subjects including International Working Group on the Diabetic Foot (IWGDF) score infection > 2 (moderate- high infection) , platelet level < 150 $10^3/\mu L$, Hemoglobin A1C (HbA1c) >12.0%, impaired kidney function hemophilia, sickle cell anemia, leukemia, peripheral arterial disease, or with incomplete data were excluded. On day-0, day-3 and day-7, fluid samples were collected using cotton swabs and photographs were taken. The examination was performed at the Integrated Laboratory, Faculty of Medicine, Universitas Indonesia.

2.2. PRF and HA+PRF Production

To generate PRF and HA+PRF, from the blood peripheral collection and proceed to produce platelet rich fibrin (PRF), each patient had around 20 cc cubit vein from each patient's arm without anticoagulant tube and centrifuge 200G around 8 minutes. We separated fibrin and buffy coat by sterile scissor and applied the fibrin to the wound (Dohan, 2009). In HAPRF group, process continued to make homogenous HA+PRF by adding HA 0.075% to PRF with comparison 0.6 cc: 1 cc use vortex machine. Every three days, the same protocol was used, and a picture was taken to evaluate wound assessment.

2.3. Application of PRF or HA+PRF in DFU

The wound was first cleaned and debrided. Assessment for Wound Area (WA) and Granulation Area (GA) were made before any fibrin gel application, recorded as day-0. After the assessment, 1 mL of fibrin gel (HA+PRF, or PRF alone) was applied topically on the wound area of 10 cm^2. A sterile gauze was then applied to cover the wound as a secondary dressing to maintain moisture. The treatments were applied for 3 times on day-0, 3 and 7. After day-7, only a standard NaCl 0.9% therapy was given to the subjects until day-14

2.4. Assessment for Wounds Improvement

The wound's area improvement was recorded using a digital camera, 48 mega pixels with an accuracy of 0.1% on day-0, 3, 7, and 14. The results of the wound photographs were processed using Image-J (National Institutes of Health, Bethesda, MD, USA), and the GI was evaluated. GI was counted as the ratio between granulation area to wound area, in percent.

2.5. Statistical Analysis

IBM SPSS software v.20 (IBM Coorporation, Armonk, NY, USA) was used for all statistical analysis. Statistical significance was determined at the 5% level. The general data description was presented in mean±SD and the median (range) value. The parameter's differences were conducted using Mann–Whitney u test and independent t-test and the graphs created using GraphPath7 software.

3. Results

We got around 25 DFU patients, meanwhile only 20 subjects got included in this study in which 8 (40%) were male and 12 were (60%) female. Twenty subjects with DFU were involved in this study. The subjects were randomly divided into two groups according to fibrin gel applied (HAPRF and PRF alone). HAPRF group had five women and five men, while the PRF group had six women and four men. The subjects' characteristics were already presented in our previous publication (Kartika, 2020). There were no significance differences between the two groups' characteristics.

The effect of topical therapy of both groups was evaluated during two weeks after treatment by measuring the width of granulation tissue. Table 1 shows that there was a significant increase in granulation tissue area in HAPRF group compared with PRF alone in day- 3 (p= 0.047), day-7 (p = 0.004) and day-14 (p< 0.001) Furthermore, Accordingly, Figure 1 shows the increase of granulation area in HAPRF compared with PRF in day-3, day-7 and day-14.

Table 1. Mean Presentation of Granulation Area Based on Intervention

Intervention	HAPRF	PRF	p- value
Day-0	42.1 (18.4–57.8)	34.8 (14.1–58.9)	0.921
Day-3	62.2 (33.6–81.3)	47.7 (28.3–73.0)	0.047*
Day-7	78.9.1(90.8–65.8)	64.6 (37.2–69.9)	0.004**
Day-14	97.7 (89.4–99.6)	79.2(46.0.4–81.9)	<0.001***

*Data median (min-max), Mann Whitney test

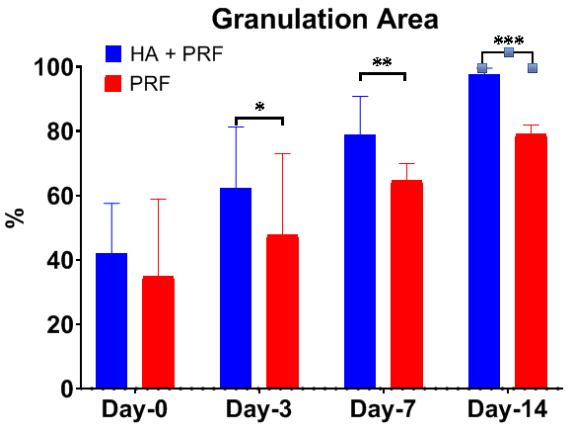

Figure 1. The increasing of granulation area between HAPRF and PRF

Furthermore, this study examined epithelialization growth by measuring wound area in day-3 until day -14. Table 2 shows that in the HAPRF group there was a significant reduction in wound area compared to PRF alone in day-3 (0.049), day-7 (p = 0.039) dan day-14 (p = 0.025)

Table 2. Mean of Wound Area (WA) between the intervention

Intervention	HA+PRF (n = 10)	PRF (n = 10)	p-value
Before*	31.9 (21.9–39.9)	32.7 (29.3–9.7)	0.848
Day-3*	21.7 (15.6–31.2)	30.4 (21.4–6.5)	0.049
Day-7 **	14.9 (8.6–16.3)	21.6 (24.4–5.6)	0.039
Day-14 ***	8.1(6.6–11.6)	15.6 (19.0–3.0)	0.025
Δ day 0−3	-10.2(-6.3 − -8.7)	-2.3 (-7.9 − -3.2)	0.048
Δ day 0−7	-17.9(-13.3 − -5.9)	-11.1(-4.9 – -24.1)	0.039
Δ day 0−14	-23.8(-15.3 − -23.6)	-17.1(-10.3 − -6.7)	0.023

* Data median (min-maks), Mann Whitney test

There is a decrease of wound area measurement in the wounds that use HA+PRF as topical therapy in DFU (Figure 2). Figure 3 shows the DFU which use topical HA+PRF has wound measurement smaller than the use of topical PRF only.

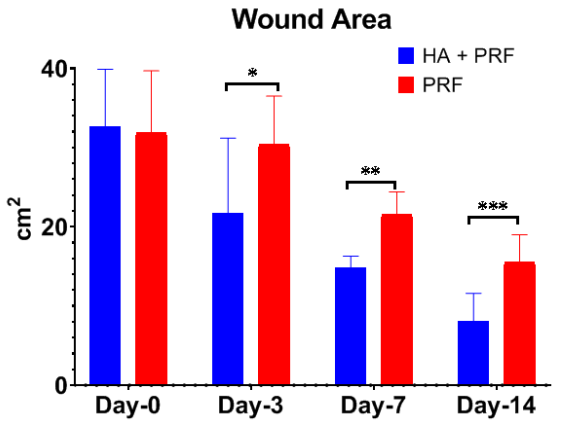

Figure 2. Mean of Wound Area (WA) showed the decrease of wound area between HAPRF vs PRF

Figure 3. HA+PRF topical in DFU (Before and after treatment)

4. Discussion

In the last decade, diabetic foot ulcers have been a serious problem because chronic wound care is needed with many complications that arise. About 16 million people in the US have T2DM, of which 15% have complications of DFU, while 12% of them undergo amputation. According Mill Jr 2014, the process of healing chronic wounds such as diabetic foot ulcers is more complicated so additional therapy may be considered as the therapy of choice. Topical therapy requirements must be able to protect the DFU surface from infection contamination and keep the wound moist so that it can produce faster granulation and epthelialization (Shi , 2018).

In presentation of granulation tissue, it was found that in the HAPRF group, there was an increase of granulation tissue formation in day-7 (83.1%) and day-14 (97.4%). In the PRF group, there was also an increase in the granulation tissue formation in day-7 (68.3%) and day-14 (81.9%). There was a significant difference in the granulation tissue formation in HAPRF group compared with PRF only in day-3 , day=7 and day-14 ($p < 0.05$, Mann Whitney test).

In this study, there were many growth factors trapped in HAPRF compared to PRF alone. Although in PRF alone, there were concentrates of immune and platelet growth factors trapped in the fibrin membrane that induce healing and immunity, but with the addition of HA, there would be an induction effect of growth factor from platelet alpha granules as an anti-inflammatory. It would increase the granulation tissue formation in DFU healing adan induce tissue response growth and tissue regeneration. Many biologically active substances are contained in platelet concentrates and affect tissue repair mechanisms such as cell proliferation, differentiation, and chemotaxis. In addition, there was also an increase in intracellular matrix deposition, angiogenesis substance, immune modulation, antimicrobial activity, and wound tissue remodeling (Sudmann EA 2014).

Platelet-rich fibrin supports three key wound healing mechanisms of "angiogenesis", "immunity", and "epithelial proliferation", and thus implies their use to protect open wounds and promote healing (Pochini, 2016).

PRF releases any many growth factors namely Transformation Growth Factor β- 1 (TGF β-1), Platelet Derivate Growth Factor-AB (PDGF-AB), Vascular Endothelial Growth Factor (VEGF), and other important angiogenesis factor such as matrix cellular glycoproteins Thrombospondin-1 for 7 days (Dohan, 2009). It is believed that GF is contained in platelets concentration seven times higher compared with non-diabetic patients. In addition, PRF also contains EGF, FGF, and three important pro inflammatory cytokines such as IL-6, IL-1β and TNF-α. PRF's has ability to promote rapid angiogenesis and remodeling of wound tissue which is easier to adhere to connective tissue (Pochini, 2016).

However, in T2DM patients, the platelet quality is reported to be greatly decreased due to the state of chronic hyperglycemia. The additional HA in PRF might increase growth factor release in HAPRF compared with PRF alone. Ilio K, (2016) reported that HA can induce the release of growth factor from PRP in cases of genu osteoarthritisc

In HAPRF group, there is more increase of epithelialization tissue compared with PRF alone (Anderegg 2014). Therefore, the addition of HA, a matrix of extracellular components, known as anti-inflammatory, will control inflammation biomolecularly in the HAPRF combination (Azyenela R, 2015). HAPRF will make a moist environment in the DFU; it will support tissue regeneration. The combination of HA and GF contained in PRP has been published several times in various fields, both for the treatment of skin aging and cases of osteoarthritis . The combination of HA and PRP can reduce proinflammatory cytokines and increase the proliferation of articular chondrocytes and chondrogenic differentiation through the Erk1 / pathway. Meanwhile in PRP though Smad2 / 3 pathway. The clinical application of a mixture of PRP and HA may be more effective than PRP or HA alone for tissue regeneration (Longitti, 2014).

HA scaffolding is used in tissue reconstruction techniques to provide a three-dimensional template for enhancing cell growth and GF supply. Delayed wound healing can be due to both reduced and excessive inflammation. Hyaluronic acid (hyaluronan, HA) is a large glycosaminoglycan and an essential extracellular component of skin. It is active throughout the entire process of wound healing being involved in proliferation, migration, and tissue remodeling. The combination of HA filler and Platelet concentrate can provide a synergistic effect, because HA acts as a scaffold and PRP induces collagen which is needed for wound repair (Chen WY,1999). There is a failure of chronic wound healing in T2DM patients and reduction of fibroblast function (Azyenela Rika, 2016). Fibroblasts have decreased ability to proliferate and synthesize collagen and do not respond to the transforming growth factor1 (TGF-1). Platelet derived growth factor (PDGF) derived from platelet rich fibrin (PRF) lysates can restore TGF-β receptor expression. Increasing the mechanical strength of the extracellular matrix with the addition of hyaluronic acid (HA) can improve TGF-beta signaling to trigger fibroblasts in wound epithelialization (Sundmann, 2014).

Longinotti, 2014 uses a combination of Platelet-Rich Plasma (PRP) and HA for treating open tendon wounds. In this study, HA synergized with PRP promoted rapid renovation and better healing, and a significant reduction in pain relief. Mateial HA has acts as an anti-inflammatory via tissue barrier by scavenging reactive oxygen species and inhibiting the inflammatory cell-derived serine proteinase. In addition, HA also has anti-edematous effect related to the osmotic HA buffer capacity(Chen et al, 1999).

Afat et al., (2017) reported that the combination of AH with L-PRF reduces edema after oral surgery for molar teeth 3. The HAPRF has a mechanism to reduce edema by means of HA affecting three main receptors in modulation of tissue regeneration, namely migration, proliferation and activation of keratinocyte cells (CD44). HAPRF also restores epidermal, fibroblast migration, controls inflammation, neoangiogenesis and promotes ECM deposits such as collagen fibers which contribute to wound healing (Price, 2005).

HA and PRF also work together to reduce inflammation due to chronic hyperglycaemia in diabetic patients (Sangameswaran, 2010).

That is to propose that mechanism of HAPRF in increased granulation tissue and epithelialization also reduces the inflammation. Due to decreased inflammation and wound repair, the combination HAPRF can indirectly reduce pain (Sreedam, 2012) (Figure 4).

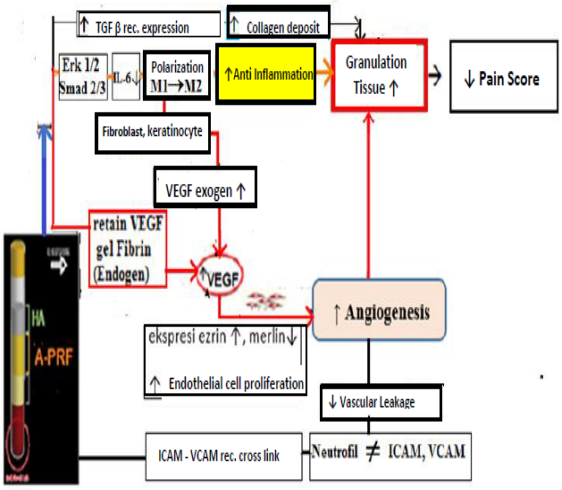

Figure 4. The proposed mechanism of HAPRF increases granulation tissue in DFU healing

5. Conclusion

Combination of HAPRF increase granulation tissue and epithelialization level on day-3 and day-7 significantly compared with PRF alone. It could also promote wound healing process in DFU by increasing angiogenesis, anti-inflammatory and reduce pain. This would provide a new simple and cheap modality treatment for diabetic wounds in clinical practice.

Acknowledge

This study was a dissertation for a Program in Doctoral Medical Science Universitas Indonesia

Conflict of Interest

This study was funded by Universitas Indonesia, Jakarta.

References

Armstrong DG et al .2017. Diabetic foot ulcers and their recurrence. N Engl J Med ,**1(376):**2367–75

Jeffcoate WJ et al.2018. Current challenges and opportunities in the prevention and management of diabetic foot ulcers. Diabetes Care , **41(1)** :645–52

Abbott CA et al.2002. North-West Diabetes Foot Care Study. The North-West Diabetes Foot Care Study: incidence of, and risk factors for, new diabetic foot ulceration in a community-based patient cohort. Diabet Med ,**19**:377–84

Mills JL Sr et al. 2014.The Society for Vascular Surgery Lower Extremity Threatened Limb Classification System: risk stratification based on wound, ischemia, and foot infection (WIfI). J Vasc Surg , **59**:220–34.e1–e2

Armstrong DG and Mills JL. 2013. Juggling risk to reduce amputations: the three-ring circus of infection, ischemia and tissue loss-dominant conditions. Wound Medicine ,**1**:13–14

Deng C et al.2017.Wound Repair Regen. Extracellular matrix/stromal vascular fraction gel conditioned medium accelerates wound healing in a murine model **,25(6)**:923−32. doi: 10.1111/wrr.12602.

Price RD.2005. The role of hyaluronic acid in wound healing: assessment of clinical evidence. Am J Clin Dermatol, **6(6):**393−402.

Reksodiputro MH et al.2018. Platelet-rich fibrin enhances wound epithelialization in the skin graft donor site. J. Phys. Conf. Ser.**2(3):**211−19

Pochini A et al.2016. Analysis of cytokine profile and growth factors in platelet-rich plasma obtained by open systems and commercial columns. Einstein (Sao Paulo), 14(3): 391–97.

Shi G et al.2018. Involvement of growth factors in diabetes mellitus and its complications: A general review, Biomed & Pharmacother, **101(1):** 510−27

Voigt J and Driver VR.2012.Hyaluronic acid derivatives and their healing effect on burns, epithelial surgical wounds, and chronic wounds: a systematic review and meta-analysis of randomized controlled trials. Wound Repair Regen,**20(3):**317−31.

Dohan Ehrenfest DM.2009. Slow release of growth factors and thrombospondins-1 in Choukroun's platelet-rich fibrin (PRF): a gold standard to achieve for all surgical platelet concentrates technologies. Growth factors , **27**: 63−9

Ilio K.2016. Hyaloronic acid induces the release of growth factors from platelet rich plasma. Asia Pac J Sports Med Arthrosc Rehabil Technol, **4**: 27−32.

Anderegg U et al.2014. More than just a filler – the role of hyaluronan for skin homeostasis. Experimental Dermatology, **23(5):** 295−303

Azyenela R.2016. Efek Penambahan Asam Hialuronat Pada Lisat Platelet Rich Fibrin Terhadap Perbaikan Aktivitas Selular Fibroblas Tua, Gadjah Mada University Press,

Sundman EA *et al*. 2014.The anti-inflammatory and matrix restorative mechanisms of platelet-rich plasma in osteoarthritis. *Am. J. Sports. Med,***42(1),** 35–41

Kartika RW, Alwi I, Suyatna FD, Yunir E, Waspadji S, Immanuel Suzzanna, et al. 2020.The Use of Image Processing in the Evaluation of Diabetic Foot Ulcer Granulation after Treatment with Advanced-Platelet Rich Fibrin + Hyaluronic Acid. Sys Rev Pharm., **11(12):**519-526.

Longinotti C et al .2014. The use of hyaluronic acid based dressings to treat burns: A review. Burns Trauma , 2:162−74

Chen WY and Abatangelo G , 1999. Functions of hyaluronan in wound repair. Wound Repair Regen ,**7**:79-89

Afat IM et al .2018. Effects of leukocyte- and platelet-rich fibrin alone and combined with hyaluronic acid on pain, edema, and trismus after surgical extraction of impacted mandibular third molars. J Oral Maxillofac Surg,**76(5):**926−32

Sangameswaran B and Ilango K.2010. Evaluation Anti-hyperglycemic and antihyperlipidaemic activities of Andrographis leneata Nees on Stertpzotocin induced diabetic Rats, JJBS, **3(3):**83-86

Sreedam Chandra Das et al .2012. Analgesic and Anti-inflammatory Activities of Ethanolic Root Extract of Swertia chirata (Gentianaceae), **5 (1):**31-36

Pastar I, Stojadinovic O, Yin NC, et al. Epithelialization in wound healing: a comprehensive review. *Adv Wound Care (New Rochelle).* 2014;**3**:445–464.

JJBS

Volume 14, Number 3, September 2021
ISSN 1995-6673
Pages 613 - 620

Jordan Journal of Biological Sciences

Healthy-Smart Concept as Standard Design of Kitchen Waste Biogas Digester for Urban Households

Roy Hendroko Setyobudi[1,2,3,*], Erkata Yandri[1,2], Manar Fayiz Mousa Atoum[4], Syukri Muhammad Nur[1,2], Ivar Zekker[5], Rinaldi Idroes[6], Trina Ekawati Tallei[7], Praptiningsih Gamawati Adinurani[8], Zane Vincēviča-Gaile[9], Wahyu Widodo[3], Lili Zalizar[3], Nguyen Van Minh[10], Herry Susanto[1,2], Rangga Kala Mahaswa[11], Yogo Adhi Nugroho[12], Satriyo Krido Wahono[13], and Zahriah Zahriah[14]

[1]Graduate School of Renewable Energy, Darma Persada University, Jl. Radin Inten 2, Pondok Kelapa, East Jakarta 13450, Indonesia; [2]Center of Renewable Energy Studies, Darma Persada University, East Jakarta 13450; [3]Department of Agriculture Science, Postgraduate Program, University of Muhammadiyah Malang, Jl. Raya Tlogomas No. 246, Malang, 65145, East Java,Indonesia; [4]Department of Medical Laboratory Sciences. The Hashemite University, PO Box 330127, 13133 Zarqa, Jordan; [5]Institute of Chemistry, University of Tartu, Ravila 14a, 50411 Tartu, Estonia; [6]Department of Chemistry, Faculty of Mathematics and Natural Sciences, Universitas Syiah Kuala, Kopelma Darussalam, Banda Aceh 23111, Naggroe Aceh Darussalam, Indonesia; [7]Department of Biology, Faculty of Mathematics and Natural Sciences, University of Sam Ratulangi, Kampus UNSRAT Bahu, Manado 95115, North Sulawesi, Indonesia; [8]Department of Agrotechnology, Merdeka University of Madiun, Jl. Serayu No.79, Madiun 63133, East Java, Indonesia; [9]Department of Environmental Science, University of Latvia, Jelgavas Street 1, Room 302, Riga LV-1004, Latvia; [10]Faculty of Agriculture and Forestry, Tay Nguyen University, 567 Le Duan St. Buon Ma Thuot City, Dak Lak Province, Vietnam, 63100; [11]Faculty of Philosophy, Universitas Gadjah Mada, Jl. Olahraga, Caturtunggal, Depok, Sleman,Yogyakarta 55281 – Special Region, Indonesia; [12] IPB University, Bogor, and Data Processing, Rumah Paper – Editage Services, Jl. Tokala No.1, Malang 65146, East Java, Indonesia; [13]Research Division for Natural Product Technology – Indonesian Institute of Sciences, Jl. Jogja - Wonosari, km 31.5, Gunung Kidul, Special Region Yogyakarta 55861, Indonesia; [14]Department of Architecture and Planning, Faculty of Engineering, Universitas Syiah Kuala, Kopelma Darussalam, Banda Aceh 23111, Naggroe Aceh Darussalam, Indonesia

Received: June 22, 2021; Revised: August 15, 2021; Accepted: August 23, 2021

Abstract

This paper aims to analyse the healthy-smart concept as a standard design of kitchen waste biogas for urban people. The anaerobic digester (AD) is designed for family size. The planned vertical digester is a one-stage- semi-continuous type because this AD type is easy to operate in urban areas. Kitchen waste or food waste can be generalized as all bio-materials produced from kitchen activities (including vegetables, fruits, bread, rice, coffee ground, tea leaves, etc). The biggest problem with household waste is the non-uniformity of feedstock entering the digester biogas. Five steps will be carried out: to establish technical standards in designing kitchen waste; to calculate the biogas potential from kitchen waste; to simulate the methane demand and generation profile; to calculate the geometry of the biogas digester; and to analyse the operation parameter for gas production into the healthy-smart concept. With a simple simulation of two people in the household for 1 d, the results show that biogas produced from kitchen waste is sufficient for cooking purposes. For the healthy-smart concept of biogas production, some operation parameters must be considered, such as; pH, alkalinity, temperature, volatile fatty acid concentration, volatile solids, and C/N ratio. The results can be used in overcoming the urban household waste and also as a reference in sustainable urban planning.

Keywords: Biodegradation, Circulair economy, Eco-friendly technology, Green energy, Methane capture, Municipal solid waste, Waste management, Welfare improvement

1. Introduction

The demand for renewable energy is increasing along with emission reduction campaigns by the use of fossil energy (Nizami *et al.*, 2020; Owusu and Asumadu-Sarkodie, 2016). Every alternative deserves to be explored regardless of scale so long as source availability exists. Countries like China, India, Indonesia, Pakistan, which have a big population, produce biomass energy sources from inhabitant activities (Abbasi and Abbasi, 2010; Helwani *et al*., 2020; Khan and Khan, 2020). Humans produce organic waste daily. In this case, organic waste is waste that can be converted into energy, such as agricultural waste, household kitchen waste, human waste (excreta disposal from septic tanks), animal waste, and so on (Adinurani *et al*., 2018; Herry, *et al.*, 2020; Heryadi *et al*., 2018; Heryadi *et al*., 2019a; Heryadi *et al*., 2019b, Leela *et al*., 2018; Prabowo *et al*., 2017; Syaifudin *et al*., 2018a; Syaifudin *et al*., 2018b; Setyobudi *et al*, 2012a; Setyobudi *et al*, 2012b; Setyobudi *et al*., 2018; Setyobudi *et al*., 2019). The term household kitchen waste is not limited to civilian household kitchen waste but includes food waste generated by hotel kitchens, restaurants, and

* Corresponding author e-mail: roy_hendroko@hotmail.com

also the waste food from supermarkets (Ramadhita *et al*., 2021). Kitchen waste or food waste can be generalized as all bio-materials produced from kitchen activities (which include: vegetables, fruits, remains of food such as gravy, oils, bones, fish remains, bread, rice, coffee filters, coffee ground, tea bags, and tea leaves, etc. The Ministry of National Development Planning (Indonesian: *Kementerian Perencanaan Pembangunan Nasional Republik Indonesia*) (abbreviated Bappenas) states that food waste in Indonesia is 112×10^6 t yr^{-1} (Hidayat, 2021).

Anaerobic digester (AD) is one technology used to digest organic waste and produce energy as renewable energy (Adinurani *et al*., 2017; Yusuf *et al*., 2020). AD can be developed from small to large sizes for cooking or energy generation purpose. AD for cooking purposes is very popular for the rural people in China, Bangladesh, India, Indonesia, and Nepal. Mostly, the digester is supplied with animal dung, such as cow manure, chicken manure, and pig manure. On the contrary, AD is not so popular for urban people. Urban people may think of AD as dirty, impractical, and low technology for rural people.

AD can also be fed with organic waste that is generated greatly in an urban household. In other words, to supply the energy for cooking in an urban household, AD can be applied to produce biogas. One of the major components of organic waste in municipal solid waste (MSW) is household kitchen waste. But, this waste is non-uniformity that allows process instability in AD (Adinurani *et al*, 2017; Setyobudi, *et al*, 2015).

Based on studies from Shenzhen, family size and household income levels are the main factors affecting the production of household kitchen waste (Zhang *et al*., 2018). Compared to wind and solar energy (Hendroko *et al*., 2013; Slorach *et al*., 2019), the electrical energy produced from AD requires lower energy. AD also has the potential to reduce toxicity, heavy metals, and pathogen. Unfortunately, AD has a higher global warming potential, mainly for methane capture. Biodegradation in AD is eco-friendly technology for welfare improvement through a circular economy because AD produces solid and liquid organic fertilizers (Setyobudi *et al*, 2012a; Setyobudi *et al*, 2012b).

For urban households, we focus on the healthy-smart concept as the standard design of kitchen waste. That means that it has to meet several criteria such as: being odorless or non-pollutive to the air; the effluent liquid waste is non-pollutive to the surrounding water-source and soil; the gas can be used safely for cooking without leaking; no remaining waste in the process (all must be processed); modular systems for ease of installation, operation, and maintenance. We determined the digester was a one-stage- semi-continuous type with multiple feedstocks (household kitchen waste mixed with excreta disposal from septic tanks). However, this design can be changed to two stages if there are processing difficulties due to the diversity of feedstocks.

The process of methane with AD is explained in Figure 1. While acting on biodegradable materials in an anaerobic condition, the bacteria methanogenic can produce a mixture of gas, called biogas. The composition of biogas contains 50 % to 60 % CH_4, 38 % to 48 % CO_2, and the rest 2 % (H_2, H_2S, etc.). To facilitate the conversion process, there are two key groups of bacteria (Khalid *et al.,* 2011; Setyobudi *et al.,* 2015). Group 1 acts as the fermenting bacteria. It uses extracellular enzymes. It works as successive fermentation of the hydrolyzed products. Through hydrolysis, it transforms the organic material into short-chain fatty acids. Alcohol, CO_2, and H_2 are the other products of the fermentation process. The organic materials are transformed into advantageous ingredients for the bacteria during the process of hydrolysis. Group 2 acts as the acidogenic bacteria. It burns the short-chain fatty acids under the forming of H_2, formic acid, acetic acid, and CO_2. During the transformation processes, there are two additional groups of bacterias. Group 3 acts as the methanogen bacteria. It transforms the CH_3COOH, H_2, and CO_2 into CH_4. From the metabolism, it benefits more energy at high hydrogen concentrations. Group 4 acts as the homoacetogens bacteria. Under the production of CH_3COOH, it agitates a wide range of ingredients. Group 5 acts as the acetic acid oxidizers bacteria. If the H_2 is detached at the same time by other processes, it will oxidize the CH_3COOH to H_2 and CO_2. The hydrolysing process becomes gradual when the biomaterial accommodates a high quantity of cellulose. The intensification of acetic acid plays a meaningful role in AD to produce CH_4 and CO_2 (Setyobudi *et al.,* 2013).

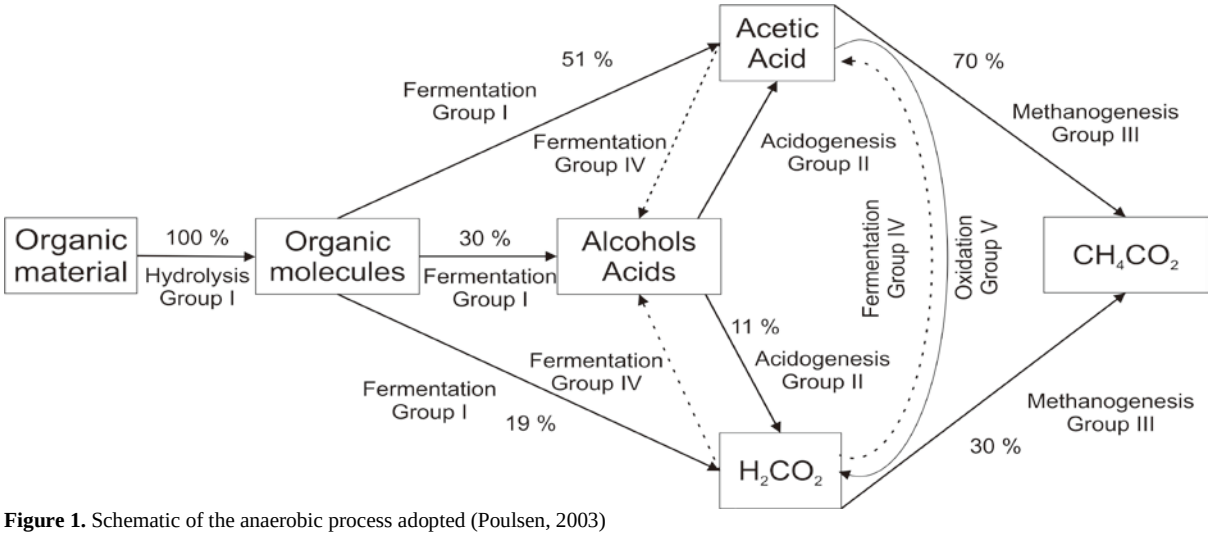

Figure 1. Schematic of the anaerobic process adopted (Poulsen, 2003)

A feasibility study of kitchen waste for biogas plants as an alternative energy source contributing around 50 % of total solid waste in urban areas has been carried out by Hanafi *et al*., in 2016. As a feasible solution for low organic load and a decentralized strategy to improve MSW management, Muñoz (2019) suggested anaerobic digester food waste at psychrophilic temperatures. Alexander *et al*. (2019) analysed the domestic urban biogas digester to accomplish the brine decarbonisation of the system of energy. Tasnim *et al*. (2017) suggested combining cow manure with kitchen waste and other waste materials such as sewage. Rianawati *et al*. (2018) suggested the household scale biogas digester as the most feasible to be implemented due to the small amount of waste needed. Oguntoke *et al*. (2019) classified the positive proportions of bio-digestible waste based on the family size and income level of households in a city in Nigeria. Nwaigwe *et al*. (2018) estimated the potential of 0.7 kg household wastes per person per day generated in Johannesburg, South Africa. Gandhi *et al*. (2019) reported a lot of food waste from the different classes of hotels in Jaipur, India. Gaballah *et al*. (2020) reported that solar energy can be integrated with biogas digester to accomplish the ideal temperature for biogas production. Amir *et al*. (2016) studied some technical failures of AD to produce biogas due to the compliance of people. Curry and Pillay (2012) investigated the analysis of production with molecular formula and computer simulation for the AD model. Gebreegziabher *et al*. (2014) reviewed the potential, opportunities, challenges, and demanding conditions for the success of biogas in urban applications. Kjerstadius *et al*. (2015) studied how biogas production can increase more than 70 % compared with a conventional system with the source control systems. Igoni *et al*. (2008) synthesised the key issues design of a high-performance AD. Apte *et al*. (2013) identified the potential of biogas production based on the kitchen waste survey from several cities. Kayhanian and Hardy (1994) investigated the methane production rate as the contrary comparable to the moderate size of feedstock, the ratio of C/N organic, and the retention times. Clercq *et al*. (2016) reported the previous project of urban AD with food waste facing similar operational issues in China. Setyobudi *et al* (2012a), Setyobudi *et al*. (2012b), and Herry *et al*. (2020) showed impacts one-stage, and two-stage AD in the circular economy on household scale biorefinery. Akkoli *et al*. (2015) created a more cost-effective, eco-friendly organic processing facility to generate biogas.

Based on the literature review above, there have been many studies with various topics related to biogas in urban areas. However, it seems that there is no clear healthy-smart concept for the standard design of kitchen waste biogas digesters for urban households. The purpose of this study is to analyse the healthy-smart concept as the standard design of kitchen waste biogas digesters for urban households. The digester is designed as family size, as one of the efforts in realizing national energy security, (Yandri *et al*., 2017; Yandri *et al*., 2020). Other goals to be achieved with AD are suppressing global warning, welfare improvement with a circular economy, and improving human health in urban areas (Herry *et al*., 2020; Setyobudi *et al*., 2012a; Setyobudi *et al*., 2012b).

2. Materials and Methods

To achieve the objectives of this study, five steps were carried out, as follows; *First*, establishing the technical standards in designing kitchen waste biogas digesters for urban households. The standard becomes a reference in subsequent calculations. *Second*, calculating the biogas potential from kitchen waste with AD. The composition of typical waste organic matter is

$$C_aH_bO_cN_d + \left(\frac{4a-b-2c+3d}{4}\right)H_2O \rightarrow \rightarrow \left(\frac{4a+b-2c-3d}{8}\right)CH_4 + \left(\frac{4a-b+2c+3d}{8}\right)CO_2 + dNH_3 \quad (1)$$

Under standard conditions (0 ^oC, 1 atm), the specific theoretical methane yield (B_{th}), Nm^3 CH_4 per ton volatile solids (VS), defined as agitation loss at 55 ^oC);

$$B_{th} = 22.4\frac{\left(\frac{4a+b-2c-3d}{8}\right)}{12a+b+16c+14d} \quad (2)$$

Under anaerobic conditions, Lignin is formed from parts of organic material that cannot be broken down. The estimation of Biodegradable fraction (*BF*) for lignin content LC;

$$BF = 0.83 - 0.028LC \quad (3)$$

The formulation as a function of design for methane yield (B) per mass of COP or VS input;

$$B = \frac{B_0 S_0}{HRT}\left(1 - \frac{K}{HRT\mu_m - 1 + K}\right) \quad (4)$$

where: B_0 *is* the ultimate methane yield can be found by plotting the steady-state methane production against *1/HRT* for different levels of *HRT* (hydraulic retention time) for a given constant temperature and extend the plot to infinity (*1/HRT = 0*). The input biodegradable substrate concentration, S_0, in terms of chemical oxygen demand (COD):

$$S_0 = \frac{Dry\ Matter \times (1 - Inert\ solids)}{Vol_{input}} \times BF \quad (5)$$

where; S_e = input biodegradable effluent substrate concentration S_e has relation with S_o

$$S_e = (1 - VS_{design}) \times S_0 \quad (6)$$

where; μ_m is the optimum growth rate of the bacteria in the biogas digester, can be estimated;

$$\mu_m = 0.013T - 0.129 \quad (7)$$

where; *T and K are* the temperature [^oC] and the dimensionless kinetic parameter, respectively. The degree of digestion is controlled by HRT, as the reactor volume V_f is divided by input volumetric flow rate Q.

$$HRT = \frac{V_d}{Q} \quad (8)$$

Third, simulating the methane demand and generation profile for a household. The aim was to determine the potential kitchen waste generated and gas requirements in an urban household with several family members. *Fourth*, calculating the geometry of the biogas digester which be used to estimate the exact area requirement and

appropriate location for the biogas digester. *Fifth*, analysing the operation parameter for gas production into a healthy-smart concept, included site location, operational parameters, construction, effluent treatment, utilization: single/hybrid.

For analysis, there were some estimations and assumptions. The purposes were to know how much biogas demand and also how much kitchen waste will be generated for this family. The digestion processes determined the control of temperature. The mesophilic processes (30 ^{o}C to 40 ^{o}C) were operated by the experienced AD. Recently, thermophilic processes (50 ^{o}C to 60 ^{o}C) have become more common to use. Table 1 was used to estimate the chemical composition of input organic matter.

Table 1. Standard design for biogas digester

	Parameter	Unit	Value
Kitchen Waste	Estimate inert solid of dry weight	[%]	1
	The estimated water content of input weight	[%]	80
	The design water content of input weight	[%]	90
	Design dry matter weight	[%]	10
	Design biodegradable VS reduction eff.	[%]	80
Household	Biogas consumption for cooking	[Nm^3/person d^{-1}]	1
	Design cooking behaviour	[times d^{-1}]	80
	Person supplied per unit digester	[persons/digester]	90
	Number of person per household	[person]	4
	Kitchen waste generation per person (wet)	[kg/person d^{-1}]	1

3. Results

To know how much biogas can be produced from kitchen waste, some calculations were done to find several parameters. Using Table 1, the other parameters were calculated. Methane potential from kitchen waste was calculated using some steps. There were specified references to explain the chemical composition of the food waste. In this case, its chemical composition was considered so close to kitchen waste.

Table 2 used the weight percentage of organic atoms data for food waste. The chemical composition of kitchen waste was calculated by assuming it as food waste. The CH_4 yield kg^{-1} of biodegradable VS degraded in the digester was calculated from Equation (1) and Equation (2).

Table 2. Design biogas potential from kitchen waste

Description	Unit	Calculation	Equation
Total Solid (TS) of actual input weight	kg d^{-1}	0.8	
Water Content (WC) of actual input weight	kg d^{-1}	3.2	
Water Content (WC)	kg d^{-1}	7.2	
Volume input after dilution	m^3 d^{-1}	0.008	
Constant mass flow rate, m (kg s^{-1}) during 24 h	kg s^{-1}	9.26×10^{-5}	
Biodegradable Factor *(BF)*	kg m^{-3}	0.819	Eq.(3)
Input biodegradable substrate concentration S_o	kg m^{-3}	81.061	Eq.(5)
Input biodegradable effluent substrate concentration S_e	kg m^{-3}	16.212	Eq.(6)
Hydraulic Retention Time (HRT)	D	16	Eq.(8)
Methane yield kg^{-1} of biodegradable vol. solids B_{th}	Nm^3 kg^{-1} × VS	0.507	Eq.(2)
	Nm^3 d^{-1}	0.329	
	Nm^3 h^{-1}	0.014	
	Nm^3	0.4113	

Methane content in biogas was approximately 60 % of the total biogas volume. For initial estimation, the digester was designed for two persons. The needs of biogas for two persons must be supplied by the digester. Two persons also can produce 4 kg of kitchen waste (wet) to supply to the digester. This was the reason to make the digester small, easy to maintain, less space, and modular system. member of the family has also increased. Methane demand for a household that must be produced per digester was calculated as;

$$B_{design} = 0.25\ Nm^3/person/d \times 60\,\% \times 2\ person = 0.3\ Nm^3/d \quad (9)$$

So, for one-time cooking, methane consumed by one person ($B_{con,\ person}$) was described in Equation (10).

$$B_{cons.person} = \frac{0.25\ Nm^3/d}{3\ cooking/d} \times 60\,\% = 0.05\ Nm^3/d \quad (10)$$

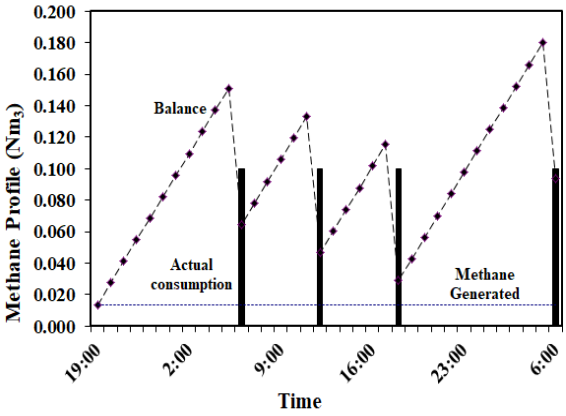

Figure 2. Methane generation and consumption profile vs time

Methane demand and generation profile was plotted by using data from the previous calculation as shown in Figure 2. The standard methane demand for cooking per person per day was 0.05 Nm^3 [3], which means 0.10 Nm^3 for two persons. Methane generated per hour by digester from the previous calculation was 0.014 Nm^3. The total volume of the digester geometry:

$$V_{tot} = V_f + V_s + V_g \quad (11)$$

where: V_{tot} is the total digester volume, V_f is the fermentation chamber volume, V_s is the sludge chamber volume (assumed 5 % of V_f), V_g is the gas chamber volume (6 h to stored hourly biogas production from 18.00 to 06.00). The digester height was calculated as a cylinder. The design radius geometry of the cylinder was 0.25 m. Then, the digester height was also calculated, as shown in Table 3.

Table 3. Geometrical summary of the digester

Item	Volume (m^3)		Height (m)	
Fermentation chamber	V_f	0.128	H_f	0.620
Gas chamber	V_g	0.140	H_g	0.033
Sludge chamber	V_s	0.006	H_s	0.699
Digester chamber	V_{tot}	0.274	H_{tot}	1.352

For the healthy-smart concept biogas production, some operation parameters must be considered, such as pH, temperature, alkalinity, volatile fatty acid (VFA) concentration, volatile solids, C/N ratio. Table 4 shows a summary of operational control for gas production. All parameters must be controlled by a computer-based instrument in real-time to produce optimal biogas with safe operation. For this reason, the control value of these parameters must be known by reference to existing standards, which must be ensured during the initial biogas digester testing.

Table 4. Summary of operational for gas production

Parameters	Controlled items	Optimum values
pH	Acid concentration vs buffer materials	refer to standard and testing
Temperature	Medium or high temperature	refer to standard and testing
Alkalinity	Acid concentration vs bicarbonate & fatty acid	refer to standard and testing
VFA	degradation of organic material into acetate and hydrogen	refer to standard and testing
VS	The degradation efficiency of output to input	refer to standard and testing
C/N	The amount of carbon and nitrogen	refer to standard and testing

4. Discussion

Based on what has been analysed so far, two things need to be discussed. The first issue concerns the design and operational parameters, which were very important to be understood and anticipated from the beginning. This means that, from the initial design stage, the cost, performance, and failure of biogas can be anticipated. The organic material will not be fully degraded if the HRT is too short, resulting in low gas yields and possible inhibition of the process. If the HRT is shorter than their rate of multiplication, this results in a washout of the methanogenic bacteria. The main contribution failures of biogas digester were caused by some factors, such as the unrealistic assumptions on bio-waste quantity quality, unsuitable AD designs and overestimation of economic returns from biogas, underestimation of the complex bio-waste supply chain (Breitenmoser *et al*., 2019). The second issue concerns the layout area of urban households. Households in large cities are generally located in densely populated areas with small layouts. For this reason, the location of the biogas digester must be determined using certain analysis to minimize the environmental and social impact (Akther *et al*., 2019). Both points must strongly adopt the defined healthy-smart concept.

This research discussed the concept of healthy-smart kitchen waste biogas digesters ideas for urban households. Our results are very useful in overcoming the problem of urban household waste that is used as a source of biogas energy. The results can also be contributed as a reference in sustainable urban planning, as well as the hi-tech cookstove concept (Yandri *et al*., 2021). This concept can also be applied in other urban buildings, such as offices or campuses as a complement to green buildings and industries with energy efficiency (Purba *et al*., 2021; Yandri *et al*., 2020). For future research directions, the healthy-smart concept design of the kitchen biogas digester needs to be developed. It has to be complemented with the other studies, such as: how to analyse in detail the potential of biogas from a variety of kitchen waste materials in different cities, how to design an appropriate electronic or mechanical control system so that biogas digester operates with healthy and optimal conditions, and also how to get greener by utilizing renewable energy as energy mix from solar energy such as photovoltaic (PV) module (Faturachman *et al*., 2021; Suherman and Astuty,

2020), or hybrid photovoltaic-thermal (PVT) collector to produce electricity and heat (Yandri, 2019). The initial target of implementation should be focused on established urban households, or hotel management that is considered more adaptable to the operating/technical system as required by advanced biogas technology.

However, the authors plan further studies on possible process instability in AD due to feedstock non-uniformity. Therefore, this follow-up study will expand the AD design by implementing a two-stage modification as has been carried out by Adinurani *et al.* (2017) and Setyobudi *et al*. (2015).

5. Conclusion

Kitchen waste as a source of urban waste can be processed by every household into biogas with biogas digester technology with a healthy-smart design concept. This design is very important in controlling the material to produce optimal biogas without causing effects on the environment, such as air and water pollution. Based on a simple simulation for two people in the household, the biogas produced from kitchen waste biogas digester is sufficient for a day's cooking purposes. With a vertical design, the total volume and height of a digester unit are 0.274 m^3 and 1.352 m, respectively. If the need for biogas increases as the number of families increases, then the next units can be connected in parallel. For the healthy-smart concept biogas production, some operation parameters must be controlled properly, such as pH, alkalinity, temperature, volatile fatty acid (VFA) concentration, volatile solids, and C/N ratio. The results can be used in overcoming the problem of urban household waste that is used as a source of biogas energy, can also be contributed as a reference in sustainable urban planning.

Acknowledgment

Yogo Adhi Nugroho, one of the authors of this article, passed away on June 30, 2021, after a fight against COVID-19. We sincerely appreciate his enthusiasm and dedication to the writing of this manuscript. May his soul rest in peace.

References

Abbasi T and Abbasi SA. 2010. Biomass energy and the environmental impacts associated with its production and utilization. *Renew. Sust. Energ. Rev.* **14(3)**: 919–937.

Adinurani PG, Setyobudi RH, Nindita A, Wahono SK, Maizirwan M, Sasmito A, Nugroho YA, and Liwang T. 2015. Characterization of *Jatropha curcas* Linn. capsule husk as feedstock for anaerobic digestion. *Energy Procedia* **65**:264–273.

Adinurani PG, Setyobudi RH, Wahono SK, Mel M, Nindita A, Purbajanti E, Harsono SS, Malala AR, Nelwan LO, and Sasmito A. 2017. Ballast weight review of capsule husk *Jatropha curcas* Linn. on acid fermentation first stage in two-phase anaerobic digestion. *Proc. Pakistan Acad. Sci. B Life Environ. Sci*. **54(1)**: 47–57.

Akkoli KM, Dodamani BM, Jagadeesh A, and Ravi C. 2015. Design and construction of food waste biogas plant for hostel mess. *Int. J. Sci. Res.* **3(03)**: 101–104.

Akther A, Ahamed T, Noguchi R, Genkawa T, and Takigawa T. 2019. Site suitability analysis of biogas digester plant for municipal waste using GIS and multi-criteria analysis. *Asia-Pacific J. Reg. Sci*. **3(1)**:61–93.

Alexander S, Harris P, and McCabe BK. 2019. Biogas in the suburbs: An untapped source of clean energy? *J. Clean. Prod.* **215**: 1025–1035.

Amir E, Hophmayer-Tokich S, and Kurnani TBA. 2016. Socio-economic considerations of converting food waste into biogas on a household level in Indonesia: The case of the city of Bandung. *Recycling* **1**: 61–88.

Apte A, Cheernam V, Kamat M, Kamat S, Kashikar P, and Jeswani H. 2013. Potential of using kitchen waste in a biogas plant. *Int. J. Environ. Sci.* **4(4)**: 370–374.

Breitenmoser L, Gross T, Huesch R, Rau J, Dhar H, Kumar S, Hugi C, and Wintgens T. 2019. Anaerobic digestion of biowastes in India: Opportunities, challenges and research needs. *J. Environ. Manage*. **236**:396–412.

Curry N and Pillay P. 2012. Biogas prediction and design of a food waste to energy system for the urban environment. *J. Renew. Energy* **41**: 200–209.

De Clercq D, Wen Z, Fan F, and Caicedo L. 2016. Biomethane production potential from restaurant food waste in megacities and project level bottlenecks: A case study in Beijing. *Renew. Sustain. Energy Rev.* **59**: 1676–1685.

Faturachman D, Yandri E, Tri Pujiastuti E, Anne O, Setyobudi RH, Yani Y, Susanto H, Purba W, and Wahono SK. 2021. Techno-economic analysis of photovoltaic utilization for lighting and cooling system of ferry Ro/ro ship 500 GT. *E3S Web Conf.* **226(00012)**: 1–10.

Gaballah ES, Abdelkader TK, Luo S, Yuan Q, and El-Fatah Abomohra A. 2020. Enhancement of biogas production by integrated solar heating system: A pilot study using tubular digester. *Energy* **193(116758)**: 1–11.

Gandhi P, Kumar S, Paritosh K, Pareek N, and Vivekanand V. 2019. Hotel generated food waste and its biogas potential: A case study of Jaipur city, India. *Waste and Biomass Valorization.* **10(6)**:1459–68.

Gebreegziabher Z, Naik L, Melamu R, and Balana BB. 2014. Prospects and challenges for urban application of biogas installations in Sub-Saharan Africa. *J. Biomass Bioenergy* **70**: 130–140.

Hanafi BM, Bhattacharjee L, Rahman SMR, and Basit MA. 2016. Application of kitchen waste in biogas system: a solution for solid waste management in Chittagong. In: *Proceedings of 3rd International Conference on Advances in Civil Engineering* p. 21–23.

Helwani Z, Fatra W, Fernando AQ, Idroes GM, and Idroes R. 2020. Torrefaction of empty fruit bunches: Evaluation of fuel characteristics using response surface methodology. *IOP Conf. Ser.: Mater. Sci. Eng.* **845(1)**: 1–10.

Hendroko R, Liwang T, Adinurani PG, Nelwan LO, Sakri Y, and Wahono SK. 2013. The modification for increasing productivity at hydrolysis reactor with *Jatropha curcas* Linn. capsule husk as bio-methane feedstocks at two-stage digestion. *Energy Procedia* **32**:47–54.

Herry S., Roy H.S., Didik S., Syukri M.N, Erkata Y., Herianto H., Yahya J., Wahono S.K., Praptiningsih G. A. ,Yanuar N. and Abubakar Y. 2020. Development of the biogas-energized livestock feed making machine for breeders. E3S Web Conf., **188 (00010):** 1–13.

Heryadi R, Uyun AS, Yandri E, Nur SM, Abdullah K, and Anne. O. 2019a. Biomass to methanol plant based on gasification of palm empty fruit bunch. *IOP Conf. Ser. Earth Environ. Sci.* **293(012036)**: 1–10.

Heryadi R, Uyun AS, Yandri E, Nur SM, and Abdullah K. 2018. Palm empty fruit bunch gasification simulation in circulating fluidized bed gasifier. *E3S Web Conf.* **67**: 1–10.

Heryadi R, Uyun AS, Yandri E, Nur SM, and Abdullah K. 2019b. Single-stage dimethyl ether plant model based on gasification of palm empty fruit bunch. *IOP Conf. Ser.: Mater. Sci. Eng.* **532(012009)**: 1–9.

Hidayat AAN. 2021. Bapenas: without policy intervention, food waste is 112 million tons per year. *Tempo.Co*. June 9, 2021 [Internet] https://bisnis.tempo.co/read/1470633/bappenas-tanpa-intervensi-kebijakan-sampah-makanan-112-juta-ton-per-tahun (Accessed on June 20, 2021).

Igoni AH, Ayotamuno MJ, Eze CL, and Ogaji SOT. 2008. Designs of anaerobic digesters for producing biogas from municipal solid waste. *Applied Energy* **85(6)**: 430–438.

Kayhanian M and Hardy S. 1994. The impact of four design parameters on the performance of a high - solids anaerobic digestion of municipal solid waste for fuel gas production. *Environ. Technol.*, **15(6)**:557–567.

Khalid A, Arshad M, Anjum M, Mahmood T, and Dawson L. 2011. The anaerobic digestion of solid organic waste. *Waste Manag*. **31(8)**: 1737–1744.

Khan M and Khan H. 2020. Choice of alternative energy sources of farm households for cooking in rural areas of Peshawar. *Sarhad J. Agric*. **36(1)**: 367–374.

Kjerstadius H, Haghighatafshar S, and Davidsson A. 2015. Potential for nutrient recovery and biogas production from blackwater, food waste and greywater in urban source control systems. *Environ. Technol.* **36(13)**: 1707–1720.

Leela D, Nur SM, Yandri E, and Ariati R. 2018. Performance of palm oil mill effluent (POME) as biodiesel source based on different ponds. *E3S Web Conf.* **67(02038)**: 1–9.

Muñoz P. 2019. Assessment of batch and semi-continuous anaerobic digestion of food waste at psychrophilic range at different food waste to inoculum ratios and organic loading rates. *Waste and Biomass Valorization* **10**: 2119–2128.

Nizami A, Ali J, and Zulfiqar M. 2020. Climate change is real and relevant for sustainable development, an empirical evidence on scenarios from North-West Pakistan. *Sarhad J. Agric.* **36(1)**: 42–69.

Nwaigwe KN, Agarwal A, and Anyanwu EE. 2018. Biogas potentials evaluation of household wastes in Johannesburg metropolitan area using the automatic methane potential test system (Ampts) II. In *ASME 2018 12th International Conference on Energy Sustainability collocated with the ASME 2018 Power Conference and the ASME 2018 Nuclear Forum.* American Society of Mechanical Engineers Digital Collection, p. 1–7.

Oguntoke O, Amaefuna BA, Nwosisi MC, Oyedepo SA, and Oyatogun MO. 2019. Quantification of biodegradable household solid waste for biogas production and the challenges of waste sorting in Abeokuta Metropolis, Nigeria. *Int. J. Energy Water Resour*. **3**: 253–261.

Owusu PA and Asumadu-Sarkodie S. 2016. A review of renewable energy sources, sustainability issues and climate change mitigation. *Cogent*. *Eng*. **3(1)**: 1–15.

Poulsen TG. 2003. **Anaerobic Digestion – Solid Waste Management**. Aalborg University, Denmark.

Prabowo B, Yan M, Syamsiro M, Setyobudi RH, and Biddinika MK. 2017. State of the art of global dimethyl ether production and it's potential application in Indonesia. *Proc. Pakistan Acad. Sci. B. Life Environ. Sci*, **54(1)**: 29–39.

Purba W, Yandri E, Setyobudi RH, Susanto H, Wahono SK, Siregar K, Nugroho YA, Yaro A, Abdullah K, Jani Y, and Faturahman D. 2021. Potentials of gas emission reduction (GHG) by the glass sheet industry through energy conservation. *E3S Web Conf.* **226(00047)**: 1–12.

Ramadhita AN, Ekayani M, and Suharti S. 2021. Do hotel restaurant consumers know the issue of food waste? *Jurnal Ilmu Keluarga & Konsumen* **14(1)**: 88–100.

Rianawati E, Damanhuri E, Handajani M, and Padmi T. 2018. Comparison of household and communal biogas digester performance to treat kitchen waste, case study: Bandung city, Indonesia. *E3S Web Conf.* **73**: 1–4.

Setyobudi, R.H., Tony L., Salafudin, Praptiningsih G.A, Leopold O.N., Yohannes S and Wahono S.K. 2012a. Synergy of bio-methane made from *Jatropha curcas* L. waste, and food in the implementation of sustainable food home area program. Prosiding Simposium dan Seminar Bersama PERAGI-PERHORTI-PERIPI-HIGI, Bogor, Indonesia, pp. 437–443.

Setyobudi R.H., Tony L., Salafudin, Leopold O.N. and Wahono S.K. 2012b. Household scale biorefinery: Integration of renewable energy - biogas and food. Seminar Hasil Penelitian Semester Ganjil 2011/2012, Lembaga Penelitian, Pemberdayaan Masyarakat dan Kemitraan Universitas Darma Persada, Jakarta, Indonesia. pp. 1–13.

Setyobudi RH, Sasmito A, Adinurani PG, Nindita A, Yudhanto AS, Nugroho YA, Liwang T, and Mel M. 2015. The study of slurry recirculation to increase biogas productivity from *Jatropha curcas* Linn. capsule husk in two-phase digestion. *Energy Procedia* **65**: 300–308.

Setyobudi RH, Wahono SK, Adinurani PG, Wahyudi, Widodo W, Mel M, Nugroho YA, Prabowo B, and Liwang T. 2018. Characterisation of arabica coffee pulp - hay from Kintamani-Bali as prospective biogas feedstocks. *MATEC Web Conf.* **164(01039)**: 1–13..

Setyobudi RH, Wahyudi A, Wahono SK, Adinurani PG, Salundik S, and Liwang T. 2013. Bio-refinery study in the crude Jatropha oil process: Co-digestion sludge of crude Jatropha oil and capsule husk *Jatropha curcas* Linn. as biogas feedstock. *Int. J. Technol.* **4(3)**: 202–208.

Setyobudi RH, Zalizar L, Wahono SK, Widodo W, Wahyudi A, Mel M, Prabowo B, Jani Y, Nugroho YA, Liwang T, and Zaebudin A. 2019. Prospect of Fe non-heme on coffee flour made from solid coffee waste: Mini review. *IOP Conf. Ser. Earth Environ. Sci.*, **293(012035)**: 1–24.

Slorach PC, Jeswani HK, Cuéllar-Franca R, Azapagic A. 2019. Environmental sustainability of anaerobic digestion of household food waste. *J. Environ. Manage*. **236**:798–814.

Suherman E and Astuty EY. 2020. Designing a solar power plant model as an energy mix at Darma Persada University. *J. Phys. Conf.* **1469(012103)**: 1–6.

Syaifudin N, Nurkholis, Handika R, and Setyobudi RH. 2018a. Formulating interest subsidy program to support the development of electricity generation from Palm Oil Mill Effluent (POME) biomass: An Indonesian case study. *MATEC Web Conf.* **164(01033)**:1–9.

Syaifudin N, Nurkholis, Handika R, and Setyobudi RH. 2018b. The importance of credit program scheme on waste to energy program in Indonesia: Case study on tofu industry. *MATEC Web Conf.* **164(01032)**:1–10.

Tasnim F, Iqbal SA, and Chowdhury AR. 2017. Biogas production from anaerobic co-digestion of cow manure with kitchen waste and water hyacinth. *Renewable Energy* **109**: 434–439.

Yandri E, Ariati R, and Ibrahim RF. 2017. Improving energy security model through detailing renewable and energy efficiency indicators: A concept for manufacture industry. In: *Proceedings of the SIGER 2017 Universitas Lampung*, p. 9.

Yandri E, Ariati R, Uyun AS, and Setyobudi RH. 2020. Potential energy efficiency and solar energy applications in a small industrial laundry: A practical study of energy audit. *E3S Web Conf.* **190(00008)**: 1–9.

Yandri E, Novianto B, Fridolini F, Setyobudi RH, Wibowo H, Wahono SK, Abdullah K, Purba W, and Nugroho YA. 2021. The technical design concept of Hi-Tech cook stove for urban communities using non-wood agricultural waste as fuel sources. *E3S Web Conf.* **226(00015)**: 1–9.

Yandri E, Setyobudi RH, Susanto H, Abdullah K, Nugroho YA, Wahono SK, Wijayanto F, and Nurdiansyah Y. 2020. Conceptualizing Indonesia's ICT-based energy security tracking system with detailed indicators from smart city extension. *E3S Web Conf.* **188(00007)**: 1–7.

Yandri E. 2019. Development and experiment on the performance of polymeric hybrid Photovoltaic Thermal (PVT) collector with halogen solar simulator. *Sol. Energy Mater. Sol. Cells.* **201(110066)**: 1–11..

Yusuf I, Arzai KI, and Dayyab AS. 2020. Evaluation of pre-treatment methods and anaerobic co-digestions of recalcitrant melanised chicken feather wastes with other wastes for improved methane and electrical energy production. *Jordan J. Biol. Sci.* **13(4):** 413–418.

Zhang H, Duan H, Andric JM, Song M, and Yang B. 2018. Characterization of household food waste and strategies for its reduction: A Shenzhen City case study. *J. Waste Manag.* **78**: 426–433.

Subscription

Jordan Journal of Biological Sciences

An International Peer – Reviewed Research Journal

Published by the Deanship of Scientific Research, The Hashemite University, Zarqa, Jordan

Name: ..... الاسم:

Specialty: ..... التخصص:

Address: ..... العنوان:

P.O. Box: ..... صندوق البريد:

City &Postal Code:..... المدينة: الرمز البريدي:

Country: ..... الدولة:

Phone: ..... رقم الهاتف

Fax No.: ..... رقم الفاكس:

E-mail: ..... البريد الإلكتروني:

Method of payment: ..... طريقة الدفع:

Amount Enclosed: ..... المبلغ المرفق:

Signature: ..... التوقيع:

Cheque should be paid to Deanship of Research and Graduate Studies – The Hashemite University.

I would like to subscribe to the Journal

For

- ☐ One year
- ☐ Two years
- ☐ Three years

One Year Subscription Rates

	Inside Jordan	Outside Jordan
Individuals	JD10	$70
Students	JD5	$35
Institutions	JD 20	$90

Correspondence

Subscriptions and sales:

The Hashemite University
P.O. Box 330127-Zarqa 13115 – Jordan
Telephone: 00 962 5 3903333
Fax no. : 0096253903349
E. mail: jjbs@hu.edu.jo

المجلة الأردنية للعلوم الحياتية
Jordan Journal of Biological Sciences (JJBS)

http://jjbs.hu.edu.jo

المجلة الأردنية للعلوم الحياتية: مجلة علمية عالمية محكمة ومفهرسة ومصنفة، تصدرعن الجامعة الهاشمية وبدعم من صندوق دعم البحث العلمي والإبتكار – وزراة التعليم العالي والبحث العلمي.

ترسل البحوث الى العنوان التالي:

رئيس تحرير المجلة الأردنية للعلوم الحياتية
الجامعة الهاشمية
ص.ب , 330127 , الزرقاء, 13115 , الأردن
هاتف: 0096253903333
E-mail: jjbs@hu.edu.jo, Website: www.jjbs.hu.edu.jo

المملكة الأردنية الهاشمية

المجلة الأردنية

للعلوم الحياتية

مجلة علمية عالمية محكمة

تصدر بدعم من صندوق دعم البحث العلمي و الابتكار

http://jjbs.hu.edu.jo/